Gabriela Guillena
Diego J. Ramón   *Editors*

Hydrogen Transfer Reactions

Reductions and Beyond

Springer

Topics in Current Chemistry Collections

Aims and Scope

The series Topics in Current Chemistry Collections presents critical reviews from the journal Topics in Current Chemistry organized in topical volumes. The scope of coverage is all areas of chemical science including the interfaces with related disciplines such as biology, medicine and materials science.

The goal of each thematic volume is to give the non-specialist reader, whether in academia or industry, a comprehensive insight into an area where new research is emerging which is of interest to a larger scientific audience.

Each review within the volume critically surveys one aspect of that topic and places it within the context of the volume as a whole. The most significant developments of the last 5 to 10 years are presented using selected examples to illustrate the principles discussed. The coverage is not intended to be an exhaustive summary of the field or include large quantities of data, but should rather be conceptual, concentrating on the methodological thinking that will allow the non-specialist reader to understand the information presented.

Contributions also offer an outlook on potential future developments in the field.

More information about this series at http://www.springer.com/series/14181

Gabriela Guillena • Diego J. Ramón
Editors

Hydrogen Transfer Reactions

Reductions and Beyond

With contributions from

Laina M. Geary • Gabriela Guillena • Raquel P. Herrera
Robert R. Knowles • Michael J. Krische • Xiantao Ma
David C. Miller • Yasushi Obora • Susumu Oda • Felix Perez
Franc Požgan • Diego J. Ramón • Bogdan Štefane
Chenliang Su • Kyle T. Tarantino • Liang Wang • Martin Wills
Jian Xiao • Qing Xu

Springer

Editors
Gabriela Guillena
Facultad de Ciencias
Universidad de Alicante
Alicante, Spain

Diego J. Ramón
Facultad de Ciencias
Universidad de Alicante
Alicante, Spain

Contents

CrossMark

EDITORIAL

Gabriela Guillena[1] · Diego J. Ramón[1]

"The two most common elements in the universe are Hydrogen and stupidity"
Harlan Ellison (Science Fiction writer) [1].

This book is concerned with one of the most common elements in the universe: Hydrogen. The organic chemistry of the hydrogen transfer process dates back to the mid-nineteenth and the early twentieth centuries, and it arises from the investigations of core organic scientists, such as Cannizzaro (1853), Tishchenko (1908), Guerbet (1909), Meerwein (1925), Ponndorf (1926), Verley (1925), and Oppenauer (1937), amongst others. Due to its long history, it could be assumed that no further development can be done in this field. However, the hydrogen transfer process is a very active research field, open currently to new discoveries, and constantly growing. The processes, being sustainable and both environmentally benign and non-hazardous, compared to other alternative processes, foreshadow a promising future. The authors of the different chapters are active researchers in the field, allowing the reader to be introduced easily and quickly into a specific area. Similarly, their experience teaches us about mature areas as well as those areas that are in their early development or in aspects that have not yet been resolved, and unapproachable issues.

In this volume, we aim to give insights for different aspects of the hydrogen transfer processes. Each chapter provides a short overview of the context and subsequent developments of their respective transformations.

✉ Gabriela Guillena
  Gabriela.Guillena@ua.es

✉ Diego J. Ramón
  djramon@ua.es

[1] Departamento de Química Orgánica, Facultad de Ciencias, Instituto de Síntesis Orgánica (ISO), Universidad de Alicante, Apdo. 99, E-03080 Alicante, Spain

Prof. Požgan and Štefane describe the metal-catalyzed transfer hydrogenation of ketones, introducing the classic, while also assessing the newest ones, capable of performing this enantioselective reduction with high efficiency. Meanwhile, Prof. Wills did the corresponding transfer of hydrogen to imines, pointing up the industrial synthesis of several drugs. Prof. Herrera ends this initial series devoted to different aspects of the Meerwein-Ponndorf-Verley reaction, with a chapter dedicated to organocatalytic versions of this process. Although this last approach has not yet achieved the versatility and wide scope reached by metal-catalyzed versions, they are complementary and in some cases, at the industrial level, can become competitive.

Prof. Knowles et al. describe the unconventional redox process in which both proton and electron are exchanged, usually in a concerted elementary step. The proton-coupled electron transfer is presented not as central biological catalytic processes but as the organic transformation possibilities. The hydrogen transfer processes are not only used in functional redox processes. Prof. Xiao et al. present the [1,n]-hydrogen transfer/cyclization as a powerful tool in the construction of five- and six-membered hetereo- and carbocycles, in which the formation of a carbon–carbon bond is fundamental. The role of the heteroatom, as well as the minimum requirements for the success of the processes is highlighted throughout.

The last chapters of this book deals with the *hydrogen autotransfer* processes, also called borrowing hydrogen or a self-supplying system for active hydrogen. In these reactions, the catalyst must transform one starting material, usually an alcohol or amine, into the real electrophilic reagent by abstraction of hydrogen (*mono-activation*). Prof. Obora describes the utilization of this strategy for the alkylation of carbon-nucleophiles, such as ketones, esters, amides, nitriles, alcohols, and heterocycles. Meanwhile, Prof Xu et al. present a similar process involving nitrogen-nucleophiles, such as ammonia, amines, and amides. Lastly, Prof. Krische et al. assess a new version of the hydrogen autotransfer in which not only the abstraction of hydrogen takes place but also the in situ formed hydride catalyst must react with another starting material to form the real nucleophilic reagent (*di-activation*), paying special attention to ruthenium catalysts.

Just taking a quick look at the different chapters, one can realize which areas of each field are mature and which can evolve immediately. Although it is very difficult to venture a general trend for the whole area, we could emphasize that there is not a truly enantioselective version for the mono-activated hydrogen autotransfer reaction. The use of first-row transition metals is almost an unexplored "Blue Ocean", in all aspects. Furthermore, the possible impact of green neoteric solvents, including deep eutectic mixtures, supercritical fluids, and bio-based solvents, on the hydrogen transfer process is definitely unknown.

Finally, as editors, we would like to thank all the contributors, as well as the reviewers, for their participation in this project and for their patience throughout the entire process.

April, 2016

Gabriela Guillena

Diego J. Ramón

Reference

1. Balachandran M (2009) Quotations for all occasions. Emerald Publisher, Egmore, p 115

CrossMark

Metal-Catalysed Transfer Hydrogenation of Ketones

Bogdan Štefane[1] · Franc Požgan[1]

Abstract   We highlight recent developments of catalytic transfer hydrogenation of ketones promoted by transition metals, while placing it within its historical context. Since optically active secondary alcohols are important building blocks in fine chemicals synthesis, the focus of this review is devoted to chiral catalyst types which are capable of inducing high stereoselectivities. Ruthenium complexes still represent the largest part of the catalysts, but other metals (e.g. Fe) are rapidly penetrating this field. While homogeneous transfer hydrogenation catalysts in some cases approach enzymatic performance, the interest in heterogeneous catalysts is constantly growing because of their reusability. Despite excellent activity, selectivity and compatibility of metal complexes with a variety of functional groups, no universal catalysts exist. Development of future catalyst systems is directed towards reaching as high as possible activity with low catalyst loadings, using "greener" conditions, and being able to operate under mild conditions and in a highly selective manner for a broad range of substrates.

Keywords   Ketones · Asymmetric transfer hydrogenation · Chiral metal catalysts · Recyclable catalysts · Transfer hydrogenation in water

---

✉ Franc Požgan
  franc.pozgan@fkkt.uni-lj.si

[1] Faculty of Chemistry and Chemical Technology, University of Ljubljana, Večna pot 113, 1000 Ljubljana, Slovenia

1   ⊘ Springer

1 Introduction

Metal-catalysed hydrogenations without doubt represent a powerful and practical method for the reduction of ketones to produce the corresponding secondary alcohols, which are valuable building blocks in the pharmaceutical, perfume and agrochemical industries [1–5]. While H_2-hydrogenation is a clean reaction and proceeds with complete atom efficiency, transfer hydrogenation (TH) has become more popular, since it avoids the use of hazardous molecular hydrogen and the need for high-pressure equipment [6–9]. In a typical transfer hydrogenation process, the metal catalyst is able to abstract a hydride and a proton from the hydrogen donor and deliver them to the carbonyl moiety of the ketone. Moreover, a number of cheap chemicals can be used as hydrogen donors, propan-2-ol [10] and formic acid/triethylamine mixture (FA-TEA) [11] being the most representative. Propan-2-ol is a particularly appropriate choice from an environmental point of view and many metal catalysts survive long enough even in refluxing 2-propanol. However, it should be used together with a strong base (typically alkoxide or hydroxide) which is needed for the transformation of a metal complex to an active catalyst, but, disadvantageously, the base can sometimes also cause undesired reactions. A major drawback of using *i*-PrOH is the reaction reversibility, and therefore it is used either in a large excess also acting as a solvent or acetone is distilled off throughout the reaction to shift the equilibrium towards the secondary alcohol formation. In contrast, formic acid does not suffer from equilibrium problems as it is oxidised to carbon dioxide, but it can be used in combination with a narrow range of complexes which do not undergo rapid decomposition under these conditions. Alternative alcoholic media that have recently been explored as hydrogen donors are ethanol [12], glycerol [13] and 1,4-butanediol [14], the latter necessarily not being used in a large excess as it irreversibly forms butyrolactone after two consecutive hydrogen transfers. Particularly interesting is the use of glycerol due to its renewable origin (by-product of biodiesel production) and interesting physicochemical properties such as high polarity, low toxicity and low flammability. In comparison to alcohols, dimethylamine–borane adduct acts irreversibly as a hydrogen donor [15]. Sodium hypophosphite has also been used as an efficient reducing agent in the TH of aliphatic and aromatic ketones in the presence of the [RuCl$_2$(*p*-cymene)]$_2$ complex [16].

Transfer hydrogenation of ketones has its origin in Meerwein–Pondorf–Verley reduction which appeared in the mid-1920s, where the use of stoichometric aluminium isopropoxide allowed for hydrogen transfer from propan-2-ol to a ketone [17–19], and was later introduced in its asymmetric version by Doering and Young

M = main group metal, *e.g.* **Al**
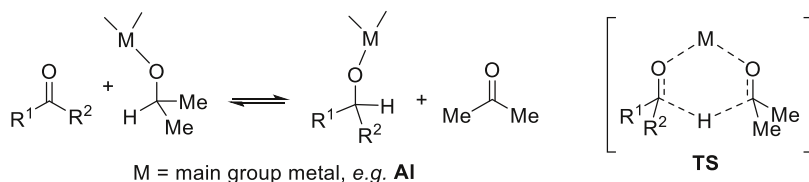
Fig. 1 Meerwein–Pondorf–Verley reduction of ketones

[20] (Fig. 1). At that time, the degree of enantioselection was very low, but the results strongly suggested that hydrogen transfer proceeded via a six-membered transition state, **TS**, as depicted in Fig. 1.

There are several metals capable of mediating the hydride transfer from the donor to the substrate. While main-group metals, like aluminium, were previously used in stoichiometric reaction, today's powerful catalysts are based on transition metals. Catalytic reactions have a clear advantage over stoichiometric ones from both economic and environmental points of view. Among the first examples of transition-metal-catalysed TH of ketones was the employment of an iridium-containing catalyst for the reduction of cyclohexanones in aqueous propan-2-ol [21, 22]. Later, Sasson and Blum [23] observed the formation of an alcohol product from saturated ketone and 1-phenylethanol in the presence of $RuCl_2(PPh_3)_3$ as catalyst, while Chowdhury and Bäckvall [24] reported that the addition of a small amount of NaOH base dramatically enhanced the TH rate of ketones in the presence of $RuCl_2(PPh_3)_3$ with propan-2-ol. In 1986, Shvo et al. [25] reported on the synthesis of ruthenium complex **1** which was originally very efficient in hydrogenation reaction, and, subsequently, many applications in hydrogen transfer reactions have been reported [26] (Fig. 2). This so-called Shvo's complex was the first reported example of ligand–metal bifunctional catalysts, the nomenclature later introduced by Noyori for powerful chiral ruthenium hydrogenation catalysts. The dinuclear complex **1** dissociates on heating into 18-electron complex **1'**, which is an active reducing agent, and highly reactive 16-electron species **1''**, which upon dehydrogenation of
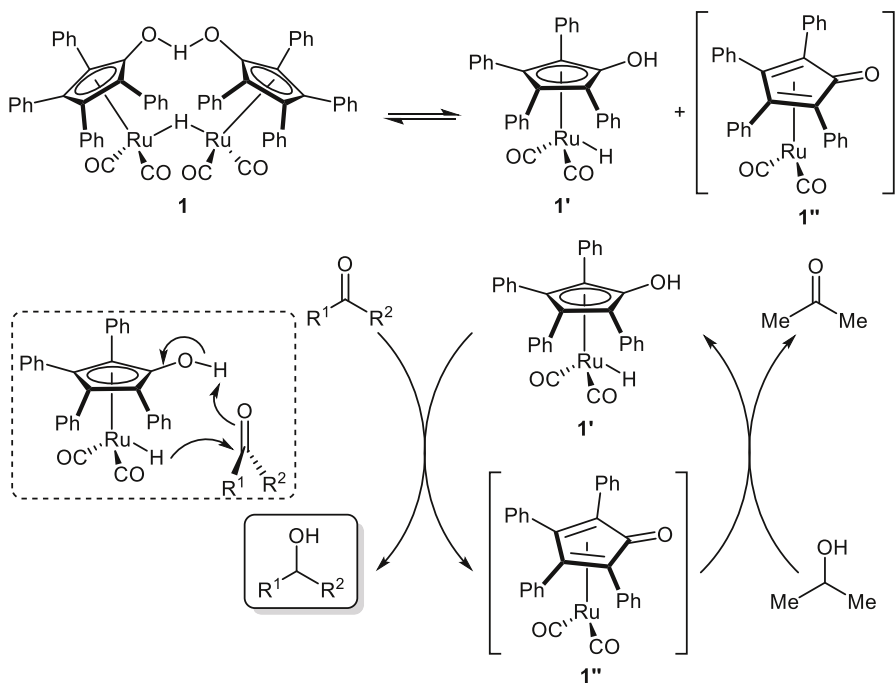
Fig. 2 Transfer of hydrogen mediated by Shvo's catalyst

propan-2-ol regenerates an active TH catalyst. In the hydrogenation of ketones, simultaneous transfer of hydride from the ruthenium centre and proton from the hydroxycyclopentadienyl ligand occurs.

Ru-indenyl systems have also been extensively studied in hydrogen transfer reactions, and the complex **2** [27] surpassed the catalytic activity of Shvo's catalyst **1** in the reduction of benzophenone with a i-PrOH/KHMDS system (TOF 190 vs. 54 h^{-1}). A simple bipyridyl dicationic complex **3** also displayed a very high activity in the reduction of acetophenones, acetonaphtone, and benzophenone (TOF for acetophenone 150,000 h^{-1}) in the presence of t-BuOK in i-PrOH [28]. Interestingly, the triazole-based scorpionate ligand **4** has been reported to be an effective catalyst for TH of acetophenone under base-free conditions suggesting that de-coordinated triazole is involved as base [29]. Tridentate dipyrazolyl-pyridine *NNN* ligands associated with the Ru–phosphane complex formed highly efficient catalyst precursors for the TH of 4′-substituted acetophenones [30]. It was observed that steric hindrance at the 5-position of the pyrazole rings in **5b** led to a pronounced increase in catalytic activity. For example, a total conversion for reduction of acetophenone with i-PrOH/KOH was obtained in 10 min at 0.5 mol% loading of the catalyst **5b**, while the catalyst **5a** delivered the same outcome in 80 min.

Zhao et al. [31] reported that TH (i-PrOH/i-PrOK) of *ortho-*, *meta-* and *para-* substituted acetophenones using 0.2 mol% of the Ru(II) complex **6** proceeded at room temperature in air reaching TOFs up to 59,400 h^{-1}. For instance, acetophenone was reduced within 1 min at room temperature, while lowering the catalyst loading down to 0.05 mol% necessitated refluxing propan-2-ol for the completion of the reaction within only 0.5 min. The same research group reported the use of another unsymmetrical complex, **7**, with an imino coordinating arm in TH of acetophenones in refluxing propan-2-ol, but it did not surpass the catalytic activity of the complex **6** [32]. The presence of a second pyrazole ring with an N–H functionality in the complex **8**, on the other hand, led to an exceptionally high catalytic activity in the TH of aromatic (acetophenones, 2-acetylnaphthalene, benzophenone, 3-pyridyl phenyl ketone) and aliphatic (cyclopentanone, cyclohexanone, octan-2-one) ketones reaching TOF of 720,000 h^{-1} in the best case [33]. In contrast, the symmetrical nature of the dipyrazolyl-pyridine ligand without an N–H structural element in the complex **9** led to a diminished catalytic activity with TOFs of up to 5940 h^{-1} [34]. Interestingly, slightly different attachments of pyrazole rings through the carbon atoms onto the pyridine ring in the pincer-type complex **10** led to increased TOF values by a magnitude of approximately 9 for the most reactive ketone substrates if compared to the catalyst **9** [35]. An *NNC* ligand constitutes yet another type of unsymmetrical Ru(II) complex **11** which was applied for the TH of a variety of ketone substrates, such as substituted acetophenones, and aliphatic cyclic and acyclic ketones [36]. In most cases, the conversions reached more than 98 % within 1 min (TOFs up to 178,200 h^{-1}) at 0.1 mol% catalyst loading in propan-2-ol at reflux in the presence of i-PrOK. Not only the above-mentioned complexes with *NNN*-type ligands but also ruthenium pincer complex **12** with the *ONO* ligand exhibited excellent catalytic activity in TH reactions [37]. The reduction reactions were carried out in propan-2-ol in the presence of a weak base, Cs$_2$CO$_3$. With 1 mol% of **12**, an excellent yield was obtained for acetophenone reduction after

18 h, and reducing the loading to 0.0001 mol% still resulted in an acceptable 59 % yield demonstrating a high 590,000 TON value.

2 Transfer Hydrogenation Catalysed by Platinum Group Metals

Although the above-mentioned complexes (Fig. 3) act as remarkably active catalysts in TH of ketones, they deliver racemic secondary alcohols as products. However, the focus of this review is rather on asymmetric versions of the TH using chiral metal catalysts. In-depth mechanistic discussions have been intentionally omitted as they are reviewed elsewhere [38, 39].

Since many biologically interesting compounds are constituted of optically active secondary alcohols (or their derivatives), asymmetric transfer hydrogenation (ATH) of prochiral ketones is a practical and powerful method for their production. There are in principle two approaches to achieve a certain degree of stereoselectivity: either (1) well-defined molecular chiral organometallic complexes (isolated or generated in situ) are used as catalysts—homogenous catalysis, or (2) solid-supported metal catalysts modified with chiral ligands are employed—heterogeneous catalysis.

Although THs using homogenous catalysts suffer from catalyst separation, molecular catalysts offer an extraordinary variability in the structure, which is virtually endless. Their reactivity, stereoselectivity and chemoselectivity can be finely tuned by changing the bulkiness, chirality and electronic properties of the auxiliaries on the metal centre of the catalyst.
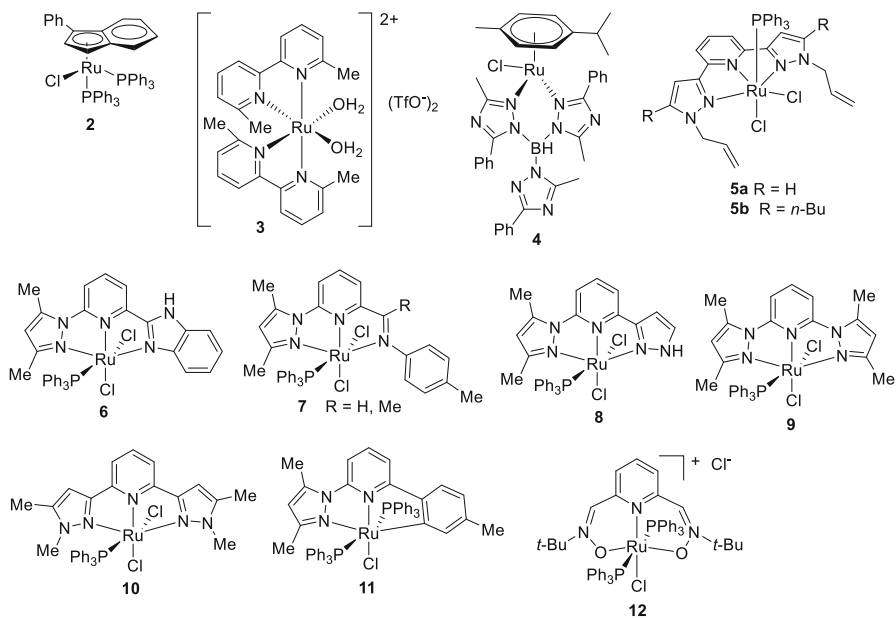
Fig. 3 Selected powerful transfer hydrogenation catalysts

2.1 Homogenous Asymmetric Catalysis

2.1.1 Ruthenium Catalysts

Ruthenium complexes bearing chiral ligands are predominant catalysts for ATH enjoying an excellent performance and a cost advantage relative to other hydrogenation metals such as rhodium. Following the discovery of efficient ruthenium catalysts for asymmetric H_2-hydrogenation, in 1995, Noyori and co-workers introduced a prototype of chiral (arene)Ru(II) catalysts of type **13** bearing *N*-sulfonylated 1,2-diamines (e.g. TsDPEN = *N*-(*p*-toluenesulfonyl)-1,2-diphenylethylenediamine (**14**) as privilege ligand) as chiral ligands for the highly enantioselective ATH of (hetero)aromatic ketones in *i*-PrOH/base [40], or in FA-TEA as reductant systems (Fig. 4) [11]. These newly developed bifunctional catalysts acted with the cooperation of the metal and N–H moiety to deliver hydrogen atoms from the hydrogen donor molecule to a ketone. In addition to *N*-sulfonylated 1,2-diamines, β-amino alcohol ligands such as **15** [41] and **16** [42] were also found to exhibit an excellent metal–ligand cooperating effect while operating in basic propan-2-ol.

Detailed experimental and theoretical investigations [43–49] revealed that chloro-ruthenium precursor **A** generates an amidoruthenium complex **B** which readily dehydrogenates propan-2-ol to produce hydrido complex **C**. Then, this hydride **C** transfers two hydrogen atoms to a ketone substrate through the cyclic, six-membered, transition state **TS**. In this so-called outer-sphere mechanism, H^+ and H^- equivalents are transferred in a concerted manner without direct coordination of ketone to metal (Fig. 5). This unique concept of bifunctional catalysis explained high rates and excellent stereoselectivities of TH reactions, because they proceed through a tight-fitting assembly of catalyst and ketone substrate (**TS** in Fig. 5). However, very recently, a revised version of the catalytic cycle of the ATH catalysed by RuH[(*R*,*R*)-XCH(Ph)NH$_2$](η^6-arene) (X = NTs, O) with *i*-PrOH as the hydrogen donor was proposed on the basis of quantum chemical calculations by including solvation effects that change the mechanism from a three-bond, slightly asynchronous, concerted reaction in the gas phase to a two-step (enantio-determining hydride transfer and proton transfer) process in solution [50].
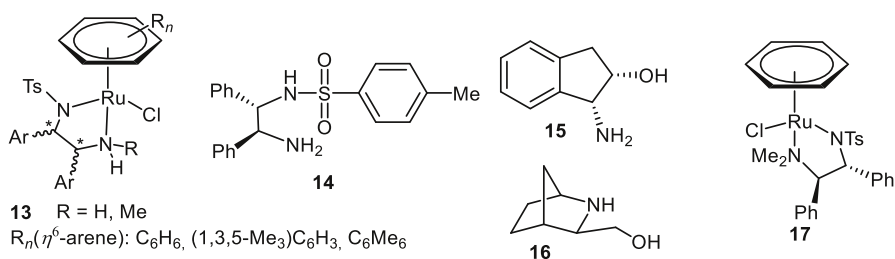
Fig. 4 Bifunctional (arene)Ru(II) catalyst systems
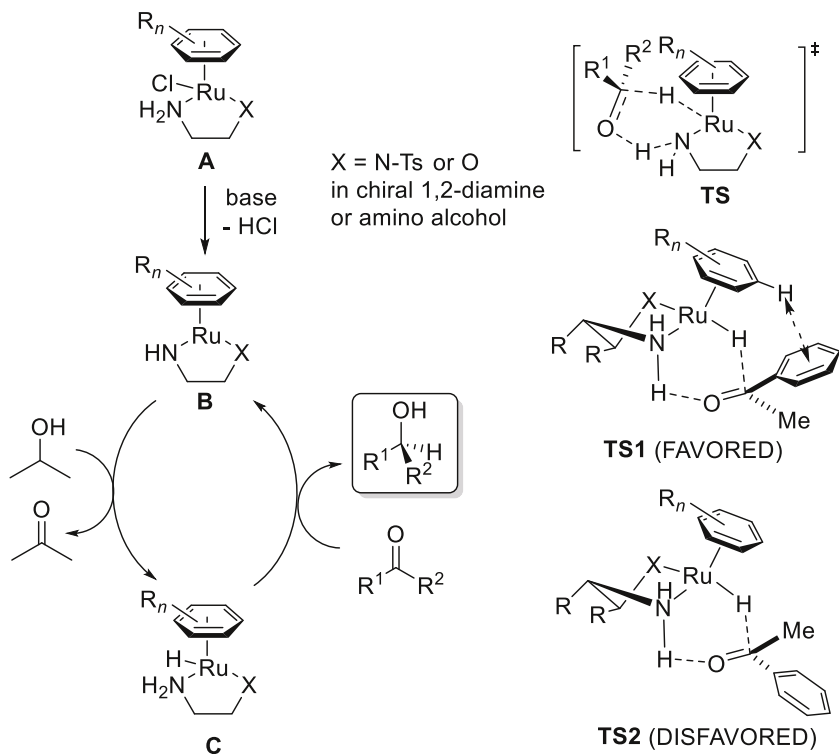
Fig. 5 Simplified mechanism of the ATH catalysed by the (arene)Ru(II) complex

The concerted transfer of hydrogen atoms suggests the importance of the N–H bond in Ru-TsDPEN complexes. Indeed, it has been reported that *N*-methylated and *N,N'*-dimethylated TsDPEN derivatives constitute poor catalysts for the ATH reactions in the case of ruthenium bearing a mesitylene group [11]. However, when an η^6-benzene ring was incorporated as an arene group, *N*-monoalkylated TsDPEN-containing complexes gave good results [51]. A recent study revealed that the presence of the N–H functionality is essential for the transfer of hydrogen to ketones in the reduction step, since, when using catalyst **17** featuring no N–H bond (Fig. 4), acetophenone was reduced in only 1.7 % conversion after 6 days [52].

The enantioselectivity in the TH of prochiral aryl ketones catalysed by (arene)Ru(II) complexes depends not only on the chiral nature of the amine ligand but also on the edge-face C–H/π interaction which stabilises the electron-rich (usually aromatic) ring of a substrate in a specific orientation as presented with **TS1** (Fig. 5) [43]. This interaction may explain why aryl ketones usually give better *ee* values than simple unfunctionalised alkyl–alkyl ketones.

After the milestone discovery of bifunctional catalysts reported by Noyori and co-workers, a large number of related or novel ligands and catalysts for the ATH of prochiral ketones have been developed that display a broad substrate scope and provide optically active alcohols in a high enantiomeric purity [9, 53, 54].

Considering the fact, that chiral vicinal diamines (for example, 1,2-diphenylethylenediamine (DPEN) derivatives) are privilege ligands in ruthenium-catalysed ATH inducing excellent stereoselectivities, their synthesis is highly desired from inexpensive naturally occurring molecules. In this regard, (R)-(+)-limonene served as a chiral backbone for the synthesis of a series of N-tosylated diamines, and their catalytic utility was evaluated in the ATH of ring-substituted acetophenones [55, 56]. As can be concluded from the results for the ATH of acetophenone, the stereochemistry of the limonene-derived diamine incorporated in Ru complexes **18–23** plays a crucial role in asymmetric induction (table in Fig. 6).

There is a continuing search for stable catalysts that will not degrade easily during the hydrogenation process, thus making it possible to execute as many catalytic cycles as possible. Wills and co-workers prepared "tethered" Ru(II) catalysts **24** in which the 1,2-diamine ligand is covalently linked to the η^6-arene ring thus benefiting from increased stability due to the "three-point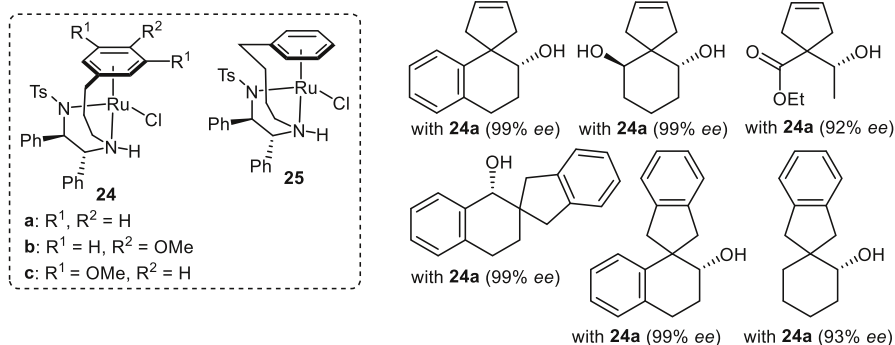" attachment of the ligand to the metal (Fig. 7) [57]. The complex **24a** with three carbon tethers has been successfully used in the reduction of α,α-disubstituted ketones containing an aromatic ring or alkene moiety, the interaction of which with η^6-arene appears to be responsible for attaining high *ee* values of the corresponding alcohols. It has also been demonstrated that the tether length and the η^6-arene substitution pattern have a significant effect on the activity of tethered catalysts, the four-carbon-tethered complex **25** with a 0.5-mol% loading being the most active in the ATH of acetophenone, achieving full reduction within 75 min while operating in the FA-TEA system [58].

The tethered catalyst **24a** proved to be superior over its untethered version **26** in the reduction of functionalised acetylenic ketones **27** with FA-TEA as hydrogen donor (Fig. 8) [59]. High enantioselectivity and substituent tolerance of these ketones indicate that the alkyne group has a dominating stereo-controlling effect through C–H/π interaction. Additionally, an efficient dynamic kinetic resolution was observed with substrates **27** favouring the *syn* products. The table in Fig. 8 shows selected examples of the reduction of acetylenic β-keto esters.

cat.	time	conv. (%)	ee (%)
18	20 d	45	9 (S)
19	32 h	100	92 (R)
20	20 d	44	17 (R)
21	42 h	100	93 (R)
22	96 h	10	60 (S)
23	96 h	21	37 (S)
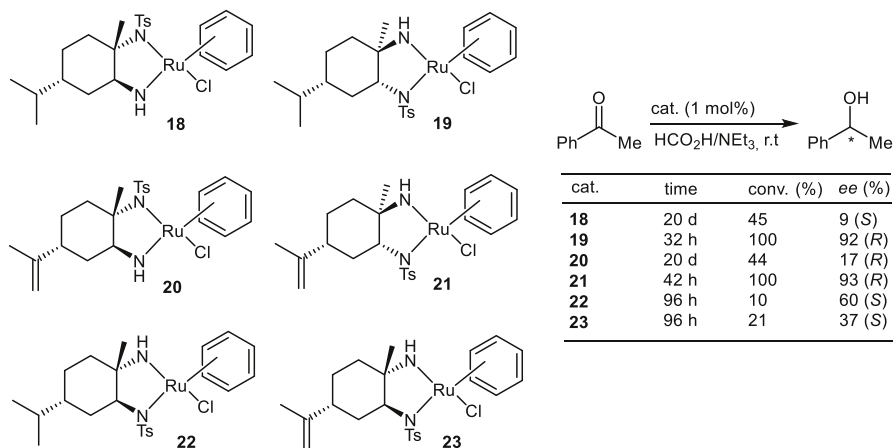
Fig. 6 Limonene-derived ligands in ruthenium ATH catalysis

Fig. 7 Alcohols formed by the reduction of α,α-disubstituted ketones using tethered Ru complexes
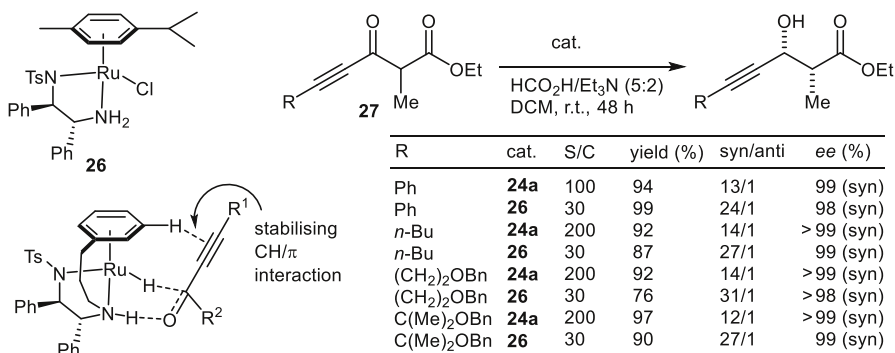
Fig. 8 Tethered Ru complex in the reduction of acetylenic ketones
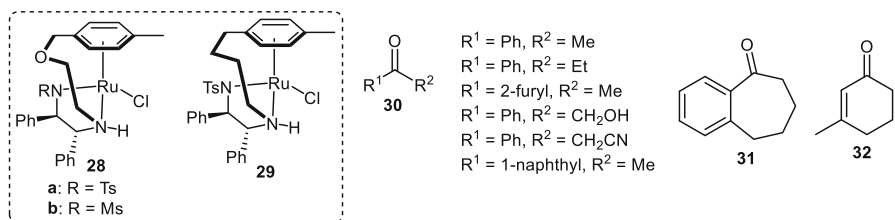
Fig. 9 Versatile tethered Ru(II) complexes

Ikariya and co-workers reported on the synthesis of the oxo-tethered Ru(II) complexes **28** that exhibited an excellent catalytic performance in the ATH of structurally different ketones **30–32** under neutral conditions, without any co-catalysts (Fig. 9) [60]. For example, by using **28a** in an S/C ratio of 40,000, acetophenone was hydrogenated in a 75 % yield after 72 h in FA-TEA, while the Wills-type four-carbon-tethered complex **29** provided only a 15 % yield under

otherwise identical conditions. The origin of the improved catalytic performance of the oxo-tethered catalysts **28** might be ascribed, on the one hand, to the delicate electronic tuning of the cooperating ligands (arene moiety with CH_2O unit), and, on the other hand, to the enhanced electron density of the secondary amino unit in the TsDPEN-derived ligand.

A potential limitation of the untethered complexes such as **26** is also the inversion of the configuration at the ruthenium centre during the catalytic cycle, which could result in the diminished stereoselectivity of the ATH process. Thus, the hydride (from hydrogen donor) can be added from either face to a 16-electron amido intermediate **B** (see Fig. 5) in the catalytic cycle. Linking the ligand to the arene ring allows the ligand to be "held over" to one side thus preventing the catalyst diastereomer interchange, yet the linkage being sufficiently long so that the 16-electron amido species **33** could be formed. Such a restriction of the chiral space could also render the catalysts more sensitive to ketones with groups of different sizes, e.g. alkyl alkyl ketones. Although "ether-linked" catalysts **34–36** prepared by Wills' group were able to promote the ATH of acetophenone and cyclohexyl methyl ketone, the corresponding alcohols were obtained in low *ee* values, but nevertheless opened up possibilities for finding new, effective and selective catalysts (Fig. 10) [61].

Another type of *ansa*-Ru(II) complex **37**, in which a DPEN-SO$_2$N(Me)- $(CH_2)_2(\eta^6$-*p*-Tol) ligand possessing an *N,C*-(*N*-ethylene-*N*-methyl-sulfamoyl) linkage is introduced, was generated in situ as reported by Kišić et al. [62]. This complex exhibited excellent catalytic efficiency in the reduction of 1-naphthyl ketones (in open air), since, by employing S/C ratios of 1000 enantioselectivities, up to >99 % coupled with 100 % conversions were attained. The same research group prepared a series of (*S,S*)-DPEN-SO$_2$N(Me)(CH$_2$)n(η^6-aryl)-based *ansa*-Ru(II) complexes in which the carbon ansa-bridge and the anchored η^6-aryl para-end substituent were systematically varied [63]. Among them, the complexes **38** and **39** demonstrated the highest catalytic species longevity in the ATH of a broad spectrum of aryl ketones in FA-TEA medium at temperatures 40 or 60 °C. Thus, these complexes displayed excellent efficiency against several alkyl aryl ketones, such as ring-substituted acetophenones, 1′- and 2′-acetonaphthones, benzofused cyclic ketones, and α-substituted acetophenones, furnishing the corresponding alcohols in full conversions and in average *ee*s of 95 % (>99.9 % *ee* for α-tetralone and 1-acetylnaphthalene) in 1–20 h (Fig. 11). The exception was the flat 1-acenaphthenone which was reduced in the presence of **38** and **39** with lower, 86 and 72 %,
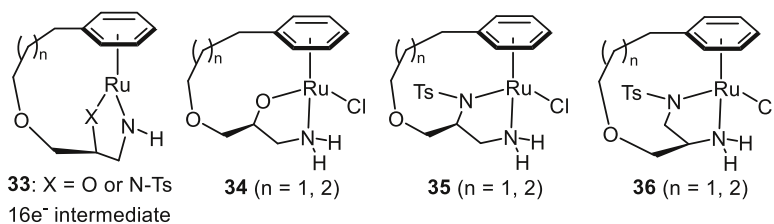
Fig. 10 Ether-linked Ru(II) complexes
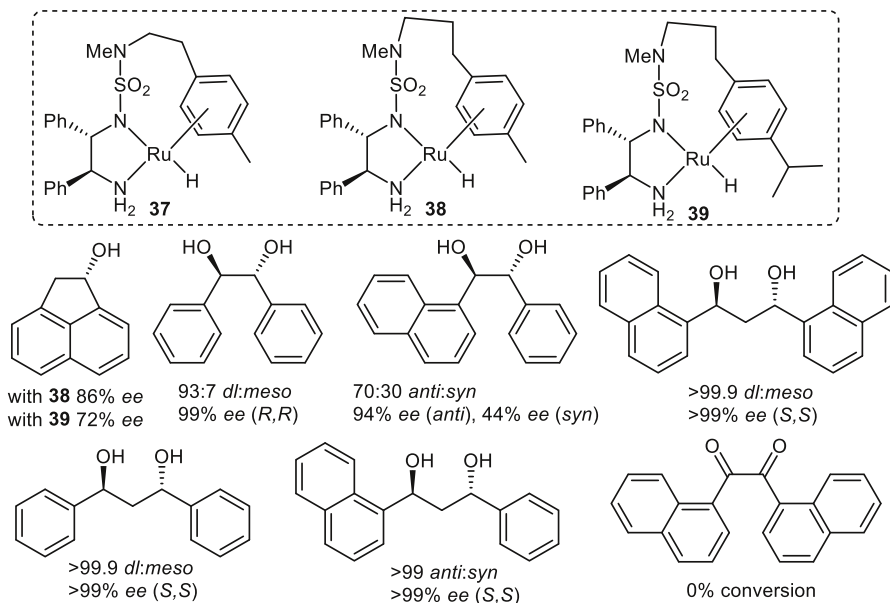
Fig. 11 *Ansa*-Ru(II) complexes in reduction of diketones

ee, respectively. Furthermore, the complex **38** exhibited exceptional stereoselectivity in the reduction of 1,3-diketones. The investigated 1,2-diketones were also successfully reduced in the presence of **38** though with decreased diastereoselectivity in comparison to 1,3-diketones. However, di(α-naphthyl)ethandione was totally inert under the applied reaction conditions, which could be ascribed to the non-co-planarity of the carbonyl groups with the naphthyl rings.

The importance of the N–H bond in the diamine ligand involved in the ketone reduction transition state has also been demonstrated by using tethered complexes **40** and **41** (Fig. 12) [52]. These complexes are lacking an unsubstituted N–H group and, consequently, low conversions and *ee* values were observed in the ATH of acetophenone. For comparison, the non-*N*-methylated analogue of **40**, i.e. the complex **24a**, gave 1-phenylethanol with 96 % *ee* and a 100 % conversion in <3 h [64].

Simple chiral *N*-tosylated 1,3-diamines **42–45** were used in Ru(II)-catalysed TH of acetophenone and other aryl ketones [65]. The highest *ee* obtained was 56 % with the ligand **42** bearing one chiral centre, while two chiral-centre ligands **44** and **45** were even less effective. A lower optical induction of 1,3-diamines when compared to 1,2-diamines could stem from better flexibility of the chelating ring of the Ru centre with 1,3-diamines, thus consequently enhancing the number of possible diastereomeric transition states with ketones.

Following Noyori's success in using chiral β-amino alcohols as ligands with arene-ruthenium(II) precursors [66], (*S*)-lactic acid and mandelic acid-based β-amino alcohol ligands **46** and **47** were employed in the Ru-catalysed ATH of various ketones (4-substituted acetophenones, 2-acetyl-6-methoxynaphthalene,
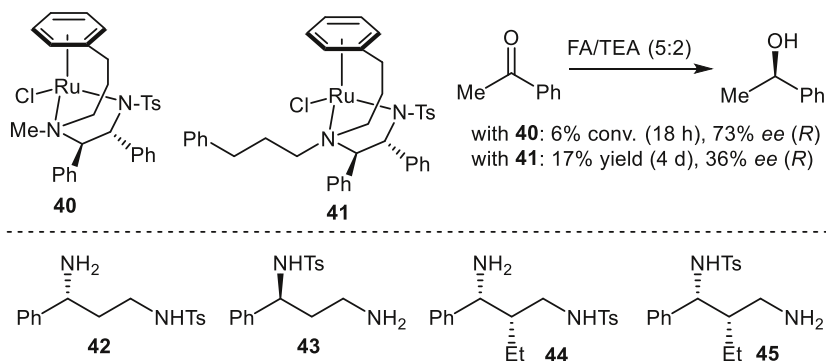
Fig. 12 (*N,N*-disubstituted-*N′*-Ts-DPEN)–Ru(II) complexes and 1,3-diamines as poor ATH catalyst systems

3-acetylpyridine) giving satisfactory conversions and moderate enantioselectivities (40–87 % *ee*) [67]. The highest *ee* (87 %) for the reduction of acetophenone with *i*-PrOH/KOH was obtained by using a (*p*-cymene)Ru–**47** catalyst system, indicating that the chiral centre attached to the –OH group is more important in deciding stereoselectivity than an additional chiral centre attached to –N as in the ligands **46**.

Interestingly, the use of the amino alcohol ligand **48** with an amino group incorporated in the cyclic structure and containing a bulky phenyl group at C-1 of tetrahydroisoquinoline together with the Ru(II) precursor gave rise to a catalyst that induced good enantioselectivity of 94 % in the ATH of acetophenone [68]. The screening of 4-substituted acetophenones as well as 1-indanone using the same catalyst system rendered alcohols with lower *ee*s. It was also observed that the stereochemistry at C-1 has an important role in catalyst stereoselectivity since, with the opposite C-1 isomer of **48**, a racemic mixture of alcohol product was obtained in the ATH of acetophenone.

A small family of chiral amino alcohol ligands **49** and **50** was prepared from inexpensive (*S*)-α-phenylethylamine and employed in the Ru-catalysed ATH of various aromatic alkyl ketones (*o*- and *p*-substituted acetophenones, propiophenone, butyrophenone, isobutyrophenone) [69]. In comparison with commonly used β-amino alcohol-based ligands, these new ligands possess a 1,4-amino alcohol structural motif. Ligand-screening in the ATH of acetophenone revealed that the less sterically demanding ligand **49** tended to give higher enantioselectivities than ligands **50** (92 % *ee* with **49** vs. 54–69 % *ee* with **50**).

Isosorbide, a renewable and commercially available carbohydrate derived from D-sorbitol served as a chiral substituent in the β-amino alcohol ligands **51** and **52** which were evaluated for the metal-catalysed enantioselective reduction of aromatic ketones [70]. The best result for [Ru(*p*-cymene)Cl₂]₂-catalysed reduction of acetophenone with *i*-PrOH/*t*-BuOK was obtained in the presence of the ligand **51** (94 % conversion and 91 % *ee* for (*R*)-1-phenylethanol), while a slightly different position of a chiral centre on the hydroxyethylamino moiety as in the ligand **52** led to a drastic drop of activity and enantioselectivity (28 % conversion, and 47 % *ee*

for (S)-1-phenylethanol). The importance of an isosorbide scaffold in these novel ligands was demonstrated by applying an unsubstituted chiral amino alcohol **53** which gave very poor enantiomeric excess in the ATH of acetophenone under otherwise identical conditions.

A family of stereodefined amino alcohol ligands **54**, in which the alkoxy and amino substituents were varied, was derived from enantiomerically pure phenyl-glycidol and evaluated in Ru-catalysed ATH of aryl alkyl ketones with propan-2-ol as the hydrogen source [71]. Although satisfactory conversions were obtained in the ATH of acetophenone, the *ee* values were rather low (23–72 %) (Fig. 13).

An interesting example of a chiral biopolymer-derived ligand was demonstrated by employment of pivaloyl functionalised chitosan together with a ruthenium complex for the TH reaction [72]. Although only moderate *ee*s (around 60 %) were observed in hydrogenation with *i*-PrOH/*i*-PrONa in methanol, the use of natural molecules as chiral supports can be of interest in the development of sustainable technologies for the synthesis of fine chemicals.

In the search for new ATH catalysts, the tridentate diamino ligands **55–56** containing a 1,2,3-triazole donor group were evaluated in conjunction with the Ru$_3$(CO)$_{12}$ complex in the ATH of ring-substituted acetophenones (Fig. 14) [73]. *N*-tosylated ligands **55c** and **56b** gave the best enantioselectivities together with high conversions. Employment of either **57** or **58** in the ATH of acetophenone resulted in <5 % conversion, which again indicates that an N–H group is essential for the formation of an active catalyst. On the other hand, the importance of an active role of a triazole ring in Ru-catalysed TH was demonstrated by using the ligands **59** and **60** with which only a trace reduction of acetophenone was observed. Of note, hydrogenations in the presence of these triazole ligands proceeded without the need for a base, which is promising for the reduction of base-sensitive substrates. Moreover, sterically more hindered *ortho*-substituted acetophenones can be reduced in the presence of the Ru–**56b** system with excellent conversions reaching *ee*s up to 85 %.

On the basis of the above-mentioned results, and by analogy with the well-established bifunctional (arene)Ru(II)-TsDPEN ATH catalysts, the mechanism of catalysis by the Ru$_3$(CO)$_{12}$–**56b** system was proposed, as depicted in Fig. 15. Thus, the ligand **56b** may form an active catalyst species via the fragmentation of the
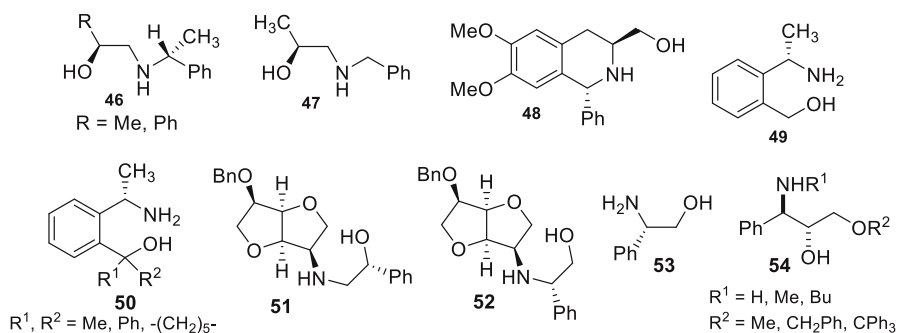
Fig. 13 Selected amino alcohol-derived ATH ligands

L	conv (%)	ee (%)
55a	12	3
55b	98	78
55c	94	80
56a	97	76
56b	97	92
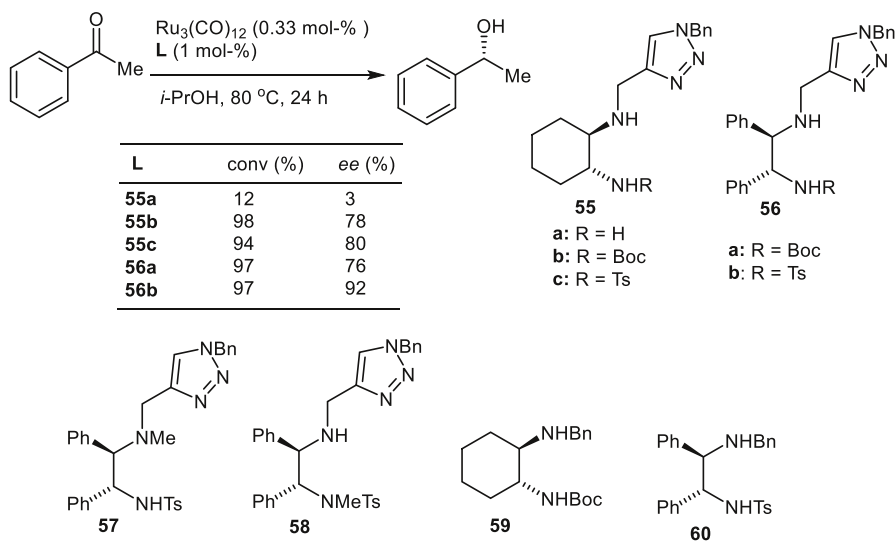
Fig. 14 1,2,3-Triazole-containing 1,2-diamino ligands
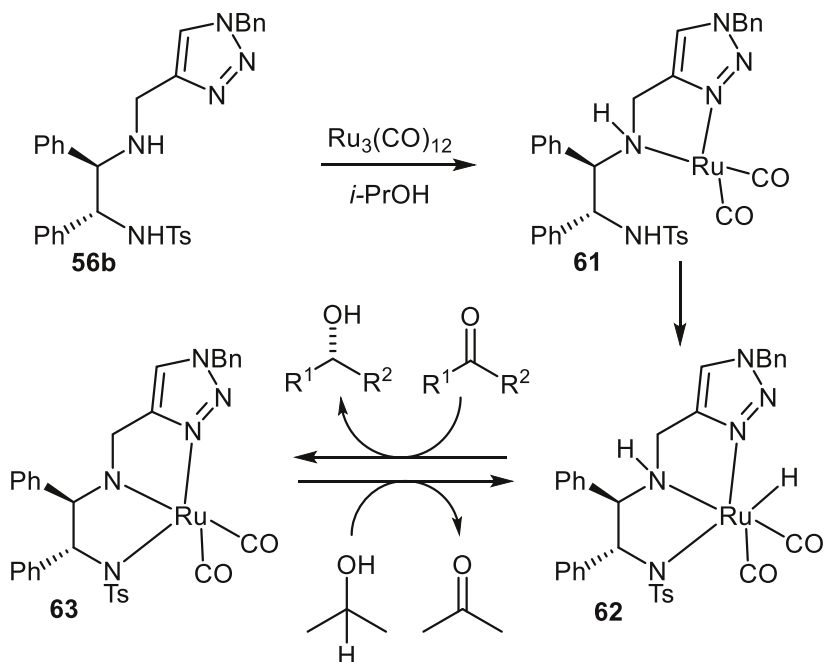
Fig. 15 Hydrogen transfer with the triazole-Ru catalyst

$Ru_3(CO)_{12}$ complex to give a bidentate complex **61**. Then, by the insertion of Ru into the N–H(Ts) bond, the Ru-hydride **62** is formed, which is capable of transferring two hydrogen atoms to a ketone substrate to give the species **63**. This

species then reacts with *i*-PrOH as the hydrogen donor to complete a catalytic cycle by regenerating **62**.

The promising ATH results of the use of the triazole ring incorporated in the TsDPEN-derived ligands inspired the same research group to consider pyridine as an alternative donor. Thus, the ligands **64–65** were successfully (conversions and *ee*s in average 90 %) employed together with Ru₃(CO)₁₂ in the ATH of ring-substituted acetophenones and aromatic bicyclic ketones in *i*-PrOH at 80 °C for 48 h [74]. On the other hand, acetylcyclohexane was reduced at a lower rate compared to aryl ketones, and additionally the enantiomeric excess was significantly lower with either ligand **64** or **65**. Here again, tosylated ligands **64** and **65** generally gave better results in the ATH of acetophenone than the Boc-protected ligand *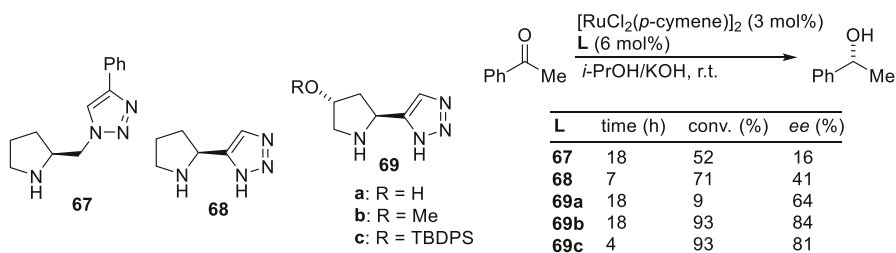*66**. These pyridine-containing ruthenium catalyst systems turned out to be in general less productive than the above-mentioned triazole ones (see Fig. 14), since, with 2 mol% of catalyst Ru–(**64** or **65**), a 97 % conversion of acetophenone was attained after 48 h, while 1 mol% of Ru–**56** gave the same result in 24 h (Fig. 16).

Taking into account that triazoles can be easily installed in a controlled manner on virtually every organic molecule, this offers great opportunities for new ligand designs. In this regard, enantiomerically pure pyrrolidine-triazole ligands were derived from L-proline and L-*trans*-4-hydroxyproline as readily accessible chiral backbones [75]. Ligands **67** and **68** in conjunction with [RuCl₂(*p*-cymene)]₂ constitute active though low-stereoinducing catalysts for TH of acetophenone with the *i*-PrOH/KOH system; ligand **68** displayed enhanced efficiency in comparison with **67**, most probably due to a free triazole N–H group (Fig. 17). Interestingly, improved catalytic behaviour was achieved by installing a second chiral centre into the pyrrolidine ring. The presence of a free hydroxyl group in ligand **69a**, although being far from the catalytic metal centre already caused a 23 % increase in the *ee* value compared to the ligand **68**. Introduction of the bulkier *tert*-butyldiphenylsilyl group (TBDPS) resulted in a strong increase of activity and enantioselectivity of the catalyst derived from the ligand **69c**. The methoxy group in the ligand **69b** was also shown to be beneficial, although a longer reaction time was required for the same outcome. The ATH of acetophenones with different substitution patterns on the phenyl ring in the presence of the [Ru(II)–**69c**] complex furnished good conversions
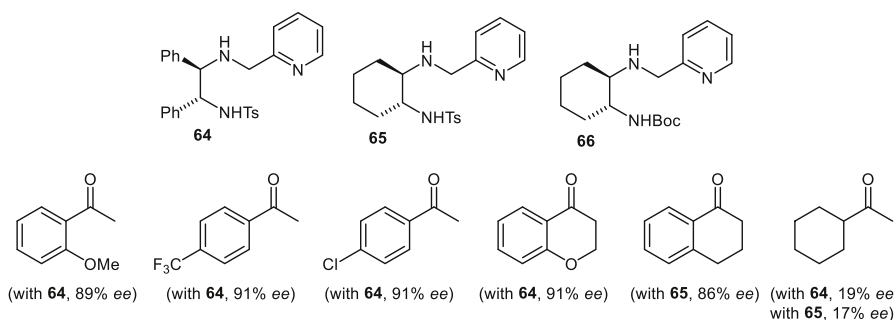
Fig. 16 Pyridine-containing 1,2-diamine ligands

Fig. 17 L-proline-derived triazole ligands

L	time (h)	conv. (%)	ee (%)
67	18	52	16
68	7	71	41
69a	18	9	64
69b	18	93	84
69c	4	93	81
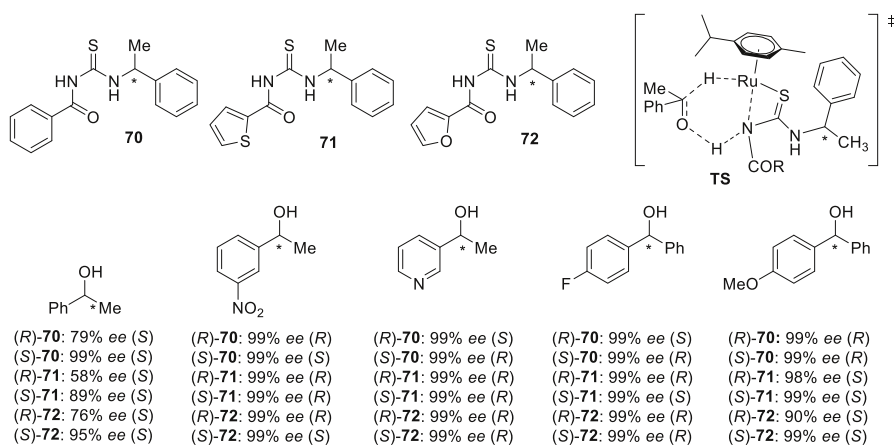
Fig. 18 Thiourea-Ru(II)-catalysed ATH

(R)-70: 79% ee (S)	(R)-70: 99% ee (R)
(S)-70: 99% ee (S)	(S)-70: 99% ee (S)
(R)-71: 58% ee (S)	(R)-71: 99% ee (R)
(S)-71: 89% ee (S)	(S)-71: 99% ee (R)
(R)-72: 76% ee (S)	(R)-72: 99% ee (R)
(S)-72: 95% ee (S)	(S)-72: 99% ee (S)

and moderate to good ees (around 70 %), while for 1-tetralone and 1-chromanone, high ees (94 and 99 %) were observed.

Simple acylthiourea ligands **70–72** were prepared from (S)- or (R)-1-phenylethylamine and used as another type of non-tosylated chiral ligands in well-defined (p-cymene)Ru(II) complexes for the ATH of selected aryl ketones (Fig. 18) [76]. Generally, high conversions and excellent enantioselectivities were achieved with 0.5 mol% of Ru(II) complexes with ligands **70–72** in the i-PrOH/KOH hydrogenation system after 24 h. In the solid state, these complexes have bound ligands **70–72** monodentately via the sulfur atom to the Ru(II) centre, and most probably act as bifunctional Noyori's catalysts through a six-membered transition state, **TS**, as depicted in Fig. 18.

It was first discovered by Noyori that an N–H functionality has a remarkable enhancing effect on the catalyst activity (the "NH effect") by facilitating the formation of a coordinatively unsaturated 16-electron Ru(II) intermediate **B** under basic conditions from the catalyst precursor, which is then transformed into the catalytically active Ru–hydride species [45] (see Fig. 5). Indeed, the Ru(II) complex **73** containing a chiral 1H-pyrazolyl-pyridyl-oxazoline NNN ligand exhibited higher
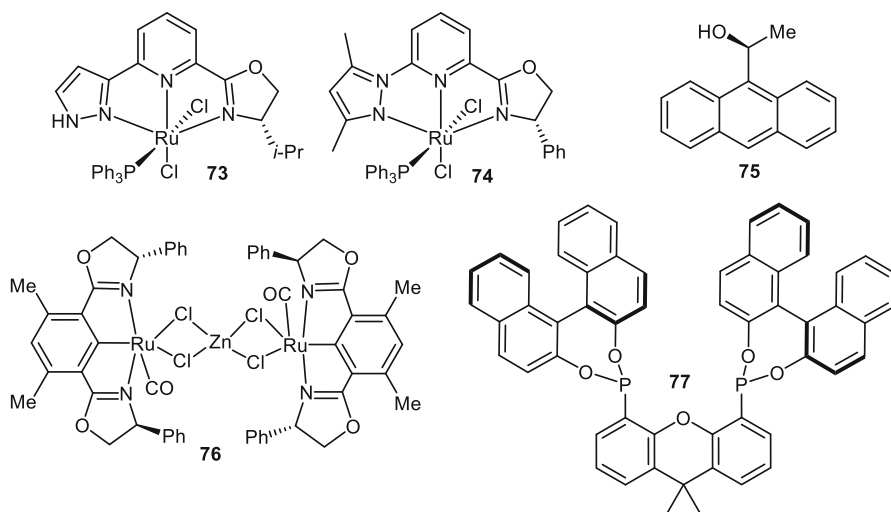
Fig. 19 NH-containing versus no NH-containing catalyst systems

catalytic activity than complex **74** featuring no N–H group (Fig. 19) [77]. Thus, the complex **73** (0.3 mol%) reached a 96 % conversion and 93 % *ee* in the reduction of acetophenone within 8 min at 40 °C, whereas the complex **74** delivered the corresponding alcohol in 98 % yield with 36 % *ee* within 60 min.

The unique phenomenon of an enhancement of the enantioselectivity was recently demonstrated by using the chiral bulky alcohol (*S*)-1-(9-anthra-cenyl)ethanol (**75**) as an additive in the ATH of 4′-phenylacetophenone with the phosphorous-free organoruthenium catalyst **76** [78]. The chiral BINOL-derived ligand **77** in combination with [RuCl$_2$(*p*-cymene)]$_2$ complex constitutes a ruthenium catalyst system solely composed of a phosphorous donor for the efficient ATH (*i*-PrOH/*t*-BuOK) of a variety of alkyl–aryl (93–99 % *ee*) and alkyl–alkyl (76–99 % *ee*) ketones, although the *ee* values were lower for the latter [79]. Interestingly, both **76** and Ru(II)–**77** catalyst systems work well and deliver excellent enantio-selectivities of the chiral secondary alcohols despite the lack of ligands containing an N–H moiety (Fig. 19).

Another type of ligand lacking a basic NH group, for example **78**, is based on a combination of *N*-Boc-protected α-amino acids and β-amino alcohols. These pseudo-dipeptide ligands have shown a high enantioselectivity (typically >99 *ee*) in the Ru-catalysed ATH of aryl ketones (ring-substituted acetophenones, 4-chro-manone, propiophenone, isobutyrophenone) [80]. It was found that the addition of LiCl in a *i*-PrOH/THF mixture led to significant rate enhancement and improved selectivity of the hydrogen transfer. On the basis of kinetic observations, the authors suggested a non-classical bimetallic hydrogen-transfer mechanism, in which the bifunctional catalyst mediates the transfer of a hydride and the lithium ion (instead of a proton as in generally accepted outer-sphere mechanism; see Fig. 5) between the hydrogen donor and the substrate through a tight transition state **TS** (Fig. 20). It
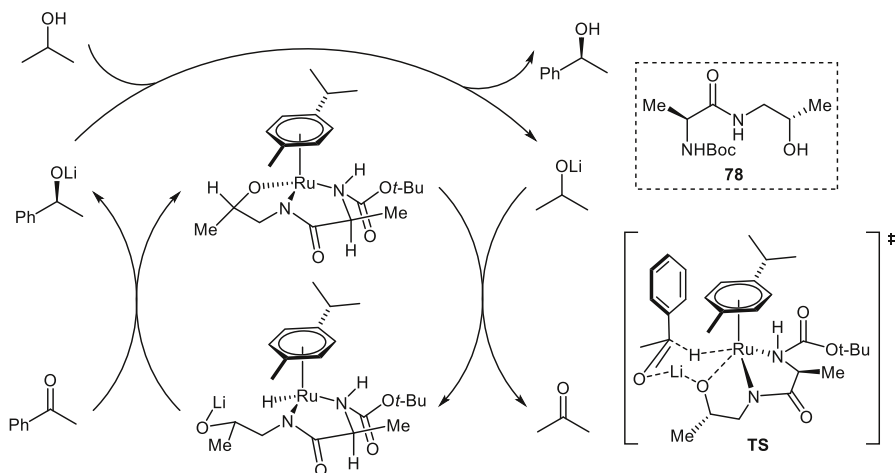
Fig. 20 Li$^+$-enhanced ATH catalysed with Ru–(α-amino acid (hydroxyalkyl)amide)

79: R = H, Me, Ph, *i*-Pr, *t*-Bu, Bn   **80**: R = H, *i*-Pr   **81**
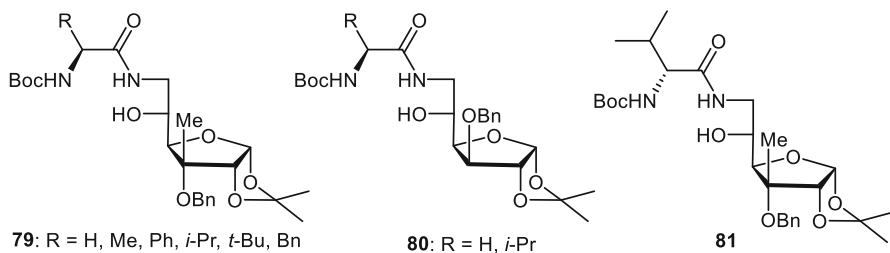
Fig. 21 Pseudo-dipeptide furanoside ligands

was subsequently reported that such a catalyst system also works well using ethanol as the hydrogen donor [81].

Similarly, the Adolfsson's and Diéguez's groups designed another class of pseudo-dipeptide ligands **79–81** containing a carbohydrate amino alcohol unit and various *N*-Boc-protected α-amino acids (Fig. 21) [82]. They were evaluated together with 0.25 mol% [RuCl$_2$(*p*-cymene)]$_2$ to catalyse the reduction of selected aryl alkyl ketones with (THF:*i*-PrOH = 1:1)/*i*-PrONa in the presence of LiCl. Interestingly, all the ligands **79** regardless the amino acid substituent R, and ligands **80** with the opposite configuration at C-3 of the furanoside moiety, exhibited >99 % *ee*s in the reduction of acetophenone. Since, with the use of ligands **79** and **80** where R=H, the obtained *ee* values were also excellent, it is suggested that the enantioselectivity is exclusively controlled by the sugar moiety which enables the use of inexpensive achiral or racemic α-amino acids. In contrast, changing the configuration of the α-amino acid moiety in the ligand **81** almost completely inhibited the catalytic activity. Although the catalyst systems Ru-(**79–81**) displayed an excellent catalytic behaviour to give exclusive access to the (*S*)-secondary alcohols, they were ineffective in the reduction of industrially important

	PP	Ar	R
82	(R,S)-Josiphos	Ph	Me
83	(R,S)-Josiphos	Ph	Ph
84	(S,R)-Josiphos	Ph	t-Bu
85	(S,R)-Josiphos*	4-MeO-3,5-Me$_2$C$_6$H$_2$	Me
86	(S,R)-Josiphos*	4-MeO-3,5-Me$_2$C$_6$H$_2$	t-Bu

87: R = Ph, Me, t-Bu (RPyme)

**88**: Ar = 4-MeO-3,5-Me$_2$C$_6$H$_2$
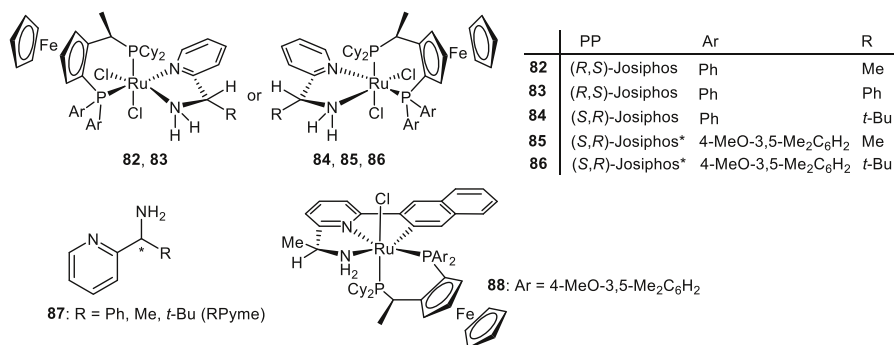
Fig. 22 Highly active Ru(II)–ferrocenyl catalysts

heteroaromatic ketones, acetylpyridines and acetylthiophenes (conversions below 1 %).

The discovery of new classes of TH catalysts that deviate from the Noyori-type **13** may represent a good opportunity to reduce virtually every type of ketone substrate with high productivity and selectivity. Baratta et al. [83] reported on the preparation of catalysts **82–86** from the ruthenium precursor [RuCl$_2$(PPh$_3$)$_3$], chiral diphosphane (Josiphos) and chiral 1-substituted-1-(pyridin-2-yl)methanamines (RPyme) **87** (Fig. 22). These complexes catalysed the TH (i-PrOH/i-PrONa) of methyl aryl ketones with very high TOF (up to 70,000 h^{-1}) and displayed a high level of asymmetric induction (ees in the range of 95–99 %). Even though the racemic mixtures of the RPyme ligands **87** were employed, single-diastereomer complexes **82–86** were obtained, thus avoiding the necessity of using both ligands in enantiopure form. The X-ray analysis of the complexes **82** and **83** revealed that only the appropriate enantiomer of the RPyme ligand incorporates into the complexes **82–86**.

The same research group further explored the utility of pyridine ligands in combination with phosphino-ferrocenyl ligands, and designed chiral pincer ligands of the *CNN* type [84]. They were used in Ru-catalysed asymmetric reduction, either in situ or in preformed complexes. Among tested ligands, the 2-naphthyl-containing ligand in the complex **88** gave the best result in terms of activity and enantioselectivity (average ee >95 %) for acetophenones, acetylnaphtahlenes, and acetylpyridines (Fig. 22). For example, acetophenone was reduced using only 0.005 mol% of complex **88** in basic propan-2-ol to (R)-1-phenylethanol with 92 % ee and TOF = 1.2×10^5 h^{-1}. The high productivity of these complexes most probably arises from the presence of the σ Ru–carbon bond, which prevents ligand dissociation and consequently catalyst deactivation.

A series of chiral ferrocenyl-based ligands **89–92** containing an oxazoline ring were prepared and incorporated into [RuCl$_2$(PPh$_3$)(P-oxazoline)] complexes, which were screened in asymmetric TH (Fig. 23) [85]. The reactions were accomplished with S/C/i-PrONa ratio 200:1:4 in propan-2-ol at room temperature. With the model substrate acetophenone, the best result was achieved with the use of the complex
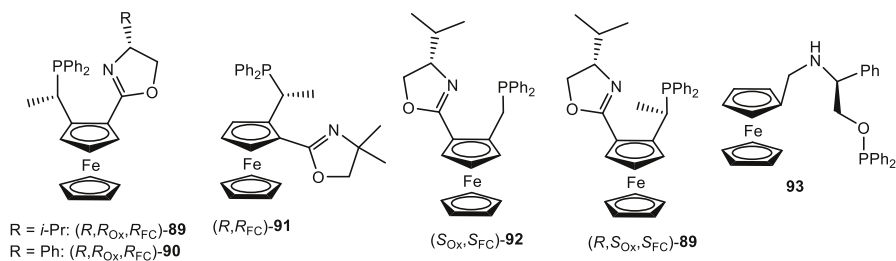
Fig. 23 Ferrocene-based phosphorous ligands

[RuCl$_2$(PPh$_3$)((R,R$_{Ox}$,R$_{FC}$)-**89**))] giving an (S)-alcohol in high 98 % *ee* and quantitative conversion within only 10 min. Removal of one stereogenic centre as in the ligands (R,R$_{FC}$)-**91** and (R,S$_{FC}$)-**92** resulted in slightly lower *ee* values (95 and 93 %). On the other hand, the use of the diastereomeric complex [RuCl$_2$(PPh$_3$) ((R,S$_{Ox}$,S$_{FC}$)-**89**))] led to a dramatic reduction in the product *ee* (41 %). Although investigated phosphino-ferrocenyl oxazoline ligands in general exhibited high activity and stereoselectivity (95 % *ee* on average) in the Ru-catalysed ATH for a wide range of prochiral ketones (2- and 4-substituted acetophenones, ethyl phenyl ketone, benzyl phenyl ketone, 1-tetralone, acetylferrocene, *tert*-butyl methyl ketone), the product's enantiomeric excess was significantly dependent on the reaction time due to product racemisation.

While ferrocenyl-phosphine ligands work well in metal-catalysed ATH, the analogous phosphinites can provide different chemical, electronic and structural properties due to an often stronger metal-phosphorous bond if compared to related phosphines. In this regard, the phosphinite ligands based on the ferrocenyl moiety containing a stereogenic centre have been screened in Ru(II)-catalysed ATH of aromatic ketones with propan-2-ol as the hydrogen source [86]. While the reduction of acetophenone in the presence of the complex [Ru(II)–**93**] and applying S/C/ NaOH 100:1:5 was sluggish at room temperature, it was enormously accelerated in refluxing propan-2-ol, thus reaching nearly quantitative conversion and a 95 % *ee* in 20 min. Although, in general, phosphinite-ferrocene-based ligands did not overpass the efficiency of the above-mentioned phosphine-ferrocene ligands in the ruthenium ATH catalysis, they offer a great opportunity for further investigation due to their outstanding air stability and ease of preparation.

2.1.2 Iridium Catalysts

The catalysts based on ruthenium undoubtedly have priority in the TH reactions of ketones due to their excellent, sometimes approaching enzyme-like, efficiencies, selectivities, and their rich chemistry which allows the introduction of diverse types of chiral ligands. However, the possibility of using other platinum-group metal catalysts have been demonstrated as a valid alternative to ruthenium systems. Since the first reports of Ir-based ATH of ketones, for example by Graziani and co-workers in 1982 [87], interest in iridium catalysts, which have often been successfully used in TH of olefins, has been growing [88].

Recently, an interesting bidentate ligand with a chiral sulfinyl group used for iridium(I) catalysis was reported. A wide range of structurally different ketone substrates were reduced in the presence of [IrCl(COE)$_2$]$_2$-**94** in propan-2-ol at room temperature [89]. Of note, without any cooperation of other chiral centres, encouraging *ee*s and conversions were achieved. Surprisingly, with ligand **95** possessing a phosphino moiety, disappointing results were obtained, suggesting that a pyridine donor in this particular case provides a more suitable coordination mode than a phosphorous one.

A tridentate phosphine-diamine ligand **96** together with [IrCl(COD)]$_2$ constituted an efficient catalyst system for TH of cycloalkyl and saturated heterocyclic ketones with propan-2-ol at room temperature [90]. For instance, cyclohexyl phenyl ketone was reduced using 0.1 mol% of the in situ-formed iridium catalyst reaching a 94 % conversion in 30 min and giving the corresponding alcohol in 95 % *ee*.

C_2-symmetric chiral multidentate ligands **97** derived from commercially available (1*R*,2*R*)-diaminocyclohexane were employed in iridium-catalysed ATH in basic propan-2-ol (Fig. 24) [91]. Despite more coordination sites in these aminophosphine ligands in comparison with simple *NNP*-ligands like **96**, only moderate *ee*s but still good conversions were observed in the ATH of aromatic ketones, the best *ee* value of 80 % being for propiophenone with **97a** ligand. *N*-Boc-protected ligand **97b** on the other hand exhibited low activity, producing (*R*)-1-phenylpropan-1-ol with only12 % yield and 63 % *ee*. The latter result indicated that a free amino group in the ligand **97a** is responsible for the good activity as well as enantioselectivity possibly by stabilising a catalytic transition state.

Xie and co-workers developed chiral spiro iridium catalysts (*S*)-**98** containing a tridentate spiro pyridyl-aminophosphine ligand and investigated its use in ATH (Fig. 25) [92]. These catalysts operated very efficiently in ethanol as a hydrogen donor, and afforded high yields and *ee* values in the reduction of acetophenone (93–98 % *ee*). Furthermore, a variety of alkyl aryl ketones were hydrogenated with catalyst (*S*)-**98a** with excellent enantioselectivities (90–98 % *ee*). However, the catalyst (*S*)-**98a** was less efficient in the hydrogenation of cyclohexyl methyl ketone and *tert*-butyl methyl ketone, providing the corresponding aliphatic alcohols with moderate enantioselectivities of 83 and 80 % *ee*, respectively.
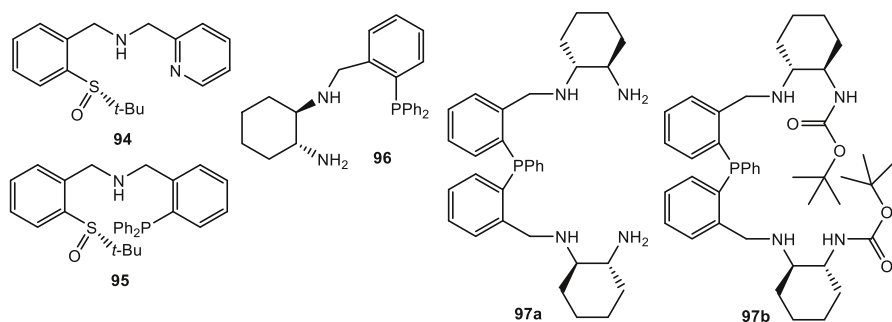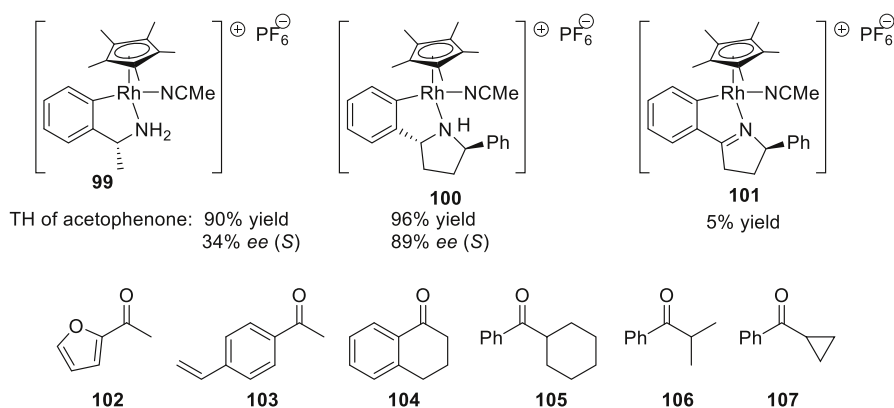

Fig. 24 Multidentate nitrogen-phosphorous ligands for iridium ATH
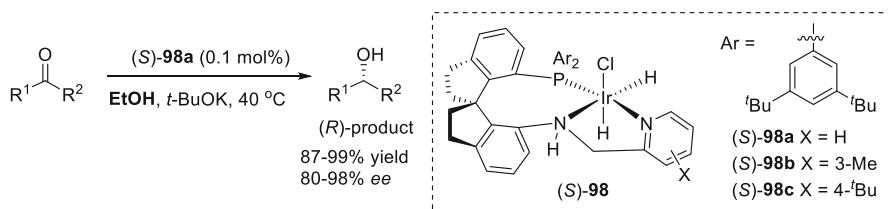
**Fig. 25** ATH with Ir catalysts containing spiro ligands

Fig. 26 Cyclometalated Rh(III) catalysts

2.1.3 Rhodium Catalyts

Since simple ketones typically coordinate more weakly to metals than olefins, many Rh-phosphane complexes may show poor activity for the hydrogenation of simple ketones. However, the catalytic properties of cyclometalated half-sandwich Rh(III) complexes **99–101**, isolated or prepared in situ from metal precursors and optically pure secondary amines, were evaluated, among which the complex **100** showed the highest productivity in the reduction of acetophenone with a *i*-PrOH/*t*-BuOK reductant system (Fig. 26) [93]. The complex **99** afforded good yield of alcohol products from acetophenone, but the enantioselectivity was low, while the cyclometalated imine **101** was almost inactive. The rhodacycle **100**, which was formed in situ, efficiently catalysed the reduction of substrates **102** (92 % *ee*), **103** (93 % *ee*) and **104** (91 % *ee*), with substrate **103** showing total chemoselectivity. For substrates **105**, **106** and **107**, however, lower *ee* values were observed (≤85 %).

Adolfsson's and Diéguez's groups synthesised a library of furanoside pseudo-dipeptide ligands **108** and **109** and the thioamide ligands **110** and **111** from inexpensive natural chiral feedstocks, D-xylose or D-glucose and α-amino acids, and
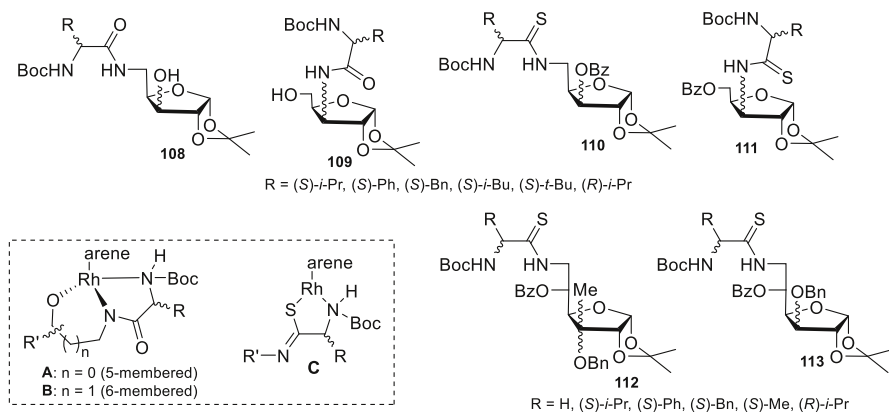
Fig. 27 Furanoside ligands for Rh catalysts

evaluated them in rhodium-catalysed (and ruthenium) ATH in *i*-PrOH/THF under basic conditions (Fig. 27) [94]. While with the pseudo-dipeptide ligands **108** and **109** conversions and enantio-selectivities in the reduction of acetophenone were low (up to 14 % conversion; up to 18 % *ee*), the use of the thioamide ligands **110** and **111** provided high enantio-selectivities for a broad range of aryl alkyl ketones (*ee* values up to 99 %). The differences in the catalytic performances using these pseudo-dipeptide ligands may be explained by the formation of less-favoured, six-membered chelate **B** from **108** and **109** (Fig. 27), which would consequently result in a more rapid catalyst decomposition in comparison with the more stable, five-membered chelate intermediate **A** formed, for example, from **79** (see Fig. 21). On the other hand, due to the bidentate coordination of the thioamide ligands **110** and **111** (the hydroxyl group is benzylated to prevent its coordination to the metal centre), a more stable, five-membered, intermediate **C** would not degrade easily, thus enabling an increased activity and a high enantioselectivity (Fig. 27).

Similarly, related pyranoside-based α-amino acid thioamide ligands **114–116** were prepared and tested in ATH (in *i*-PrOH/THF) in the presence of Ru or Rh catalyst precursor [95]. Both activity and enantioselectivity were best when thioamide ligands and Rh catalyst precursor [RhCl$_2$Cp*]$_2$ were used, and surpassed the efficiency of that previously reported [96], yet another type of furanoside thioamide ligands **112** and **113**. Investigation of the effect of the ligand parameters revealed that catalytic performance is mainly affected by the substituents/configurations at the thioamide moiety and the position of the thioamide group. The highest enantioselectivities were obtained with the thioamide ligands **114** and **115** with bulky isopropyl groups, while higher steric congestion exerted by using the ligand **116** led to lower catalytic activity in the reduction of acetophenone. Moreover, both enantiomers of the alcohol product were achieved in excellent enantioselectivity by simply changing the configuration of the thioamide group. The catalyst system Rh–**114** proved to be very compatible with aryl fluoroalkyl ketones which are hard to reduce in high enantioselectivities using TH. Interestingly, heteroaromatic ketones which are a more challenging class of substrates were
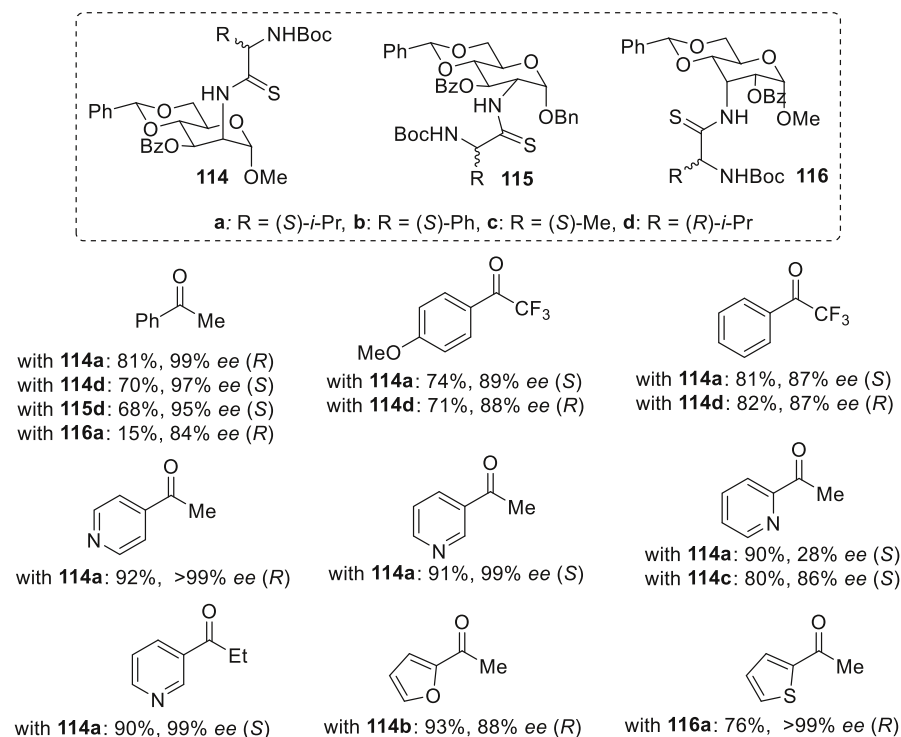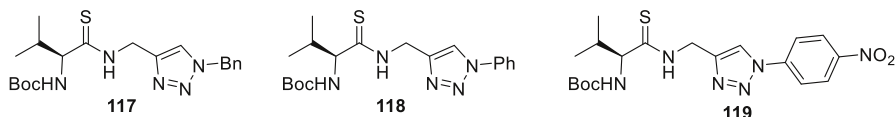
Fig. 28 Pyranoside ligands for Rh catalysts

smoothly reduced using the ligands **114–116** and excellent *ee* values were obtained (Fig. 28).

To further explore the existence of modular ligand building blocks, the amino acid thioamides functionalised with 1,2,3-triazoles were used as ligands to in situ form reduction catalysts from the complex [RhCl₂Cp*]₂ in the presence of sodium isopropoxide and lithium chloride (Fig. 29) [97]. The catalytic activity of such catalyst systems was evaluated in the ATH of *ortho*-, *meta*- and *para*-substituted acetophenones, 2-acetylnaphthalene and propiophenone. Among tested ligands, varying the substituents at the α-carbon and triazole N-1, the ligands **117–119** exerted the best *ee* values. While the conversions reached nearly 90 % after 2 h at ambient temperature, the enantioselectivities of the products were only moderate to good, and clearly inferior in comparison to reactions catalysed by Rh complexes combined with the above-mentioned furanoside-thioamide ligands **110** or **111**. It is worth mentioning that enantioselectivity of the alcohol products in most reactions decreased with prolonged reaction time, indicating that equilibrium between starting materials and products was reached, while conversions normally increased.

While there are usually chiral phosphane and chiral amine ligands incorporated in the metal complexes used in asymmetric TH, chiral *N*-heterocyclic carbenes (NHC) have attracted increasing attention as they have been proven as efficient

Fig. 29 Triazole-thioamide ligands for Rh-catalysed ATH

salt	conv. (%)	ee (%)
120	0	0
121	15	nd
122 (R = Me)	90	80
122 (R = Bu)	90	46
122 (R = Ph)	0	0
122 (R = Bn)	0	0
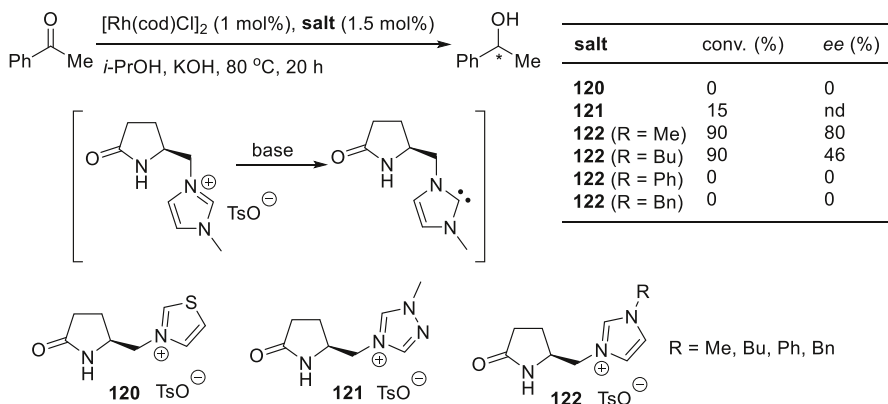
Fig. 30 *N*-heterocyclic carbenes as ATH ligands

ligands in homogenous catalysis. Because of the strong metal–NHC bond and high σ-donating ability of NHC ligands, in many cases they show higher thermal stability and activity than their phosphane counterparts. Thiazolium, 1,2,4-triazolium and imidazolium salts **120–122** derived from (*S*)-pyroglutamic acid deprotonated in basic propan-2-ol to form NHCs for ligation to Rh to in situ form the ATH catalysts [98]. Among them, only imidazolium salt **122**, having a methyl group, as carbene precursor gave satisfactory results in the reduction of substituted acetophenones (see table in Fig. 30 for the reduction of acetophenone as an example). Although the yields and *ee*s were quite modest with respect to what can be achieved with well-developed ATH catalysts, the chiral NHCs offer a great opportunity for ligand design and the discovery of new efficient catalyst systems.

As already mentioned, Ru-tethered complexes (like **24**) usually exhibited higher efficiency in ATH than the original Noyori's Ru(II)-TsDPEN catalysts (like **26**). Rhodium versions of tethered complexes were also prepared and extensively studied in TH of ketones by Wills and co-workers. They reported the use of the first tethered amino alcohol-Rh(III) catalyst **123** in ATH which, however, did not remain stable under reduction conditions (basic *i*-PrOH) [99]. Replacing the amino alcohol with TsDPEN linked to an arene ring resulted in complex **124** which proved to be a very effective catalyst in ATH and demonstrated improved activity over its untethered version [100]. It is noteworthy that, using the catalyst **124**, α-tetralone was reduced with 99.9 % *ee* which was the highest enantioselectivity reported for this substrate. Even though Ru(II) catalysts are more economical and more versatile
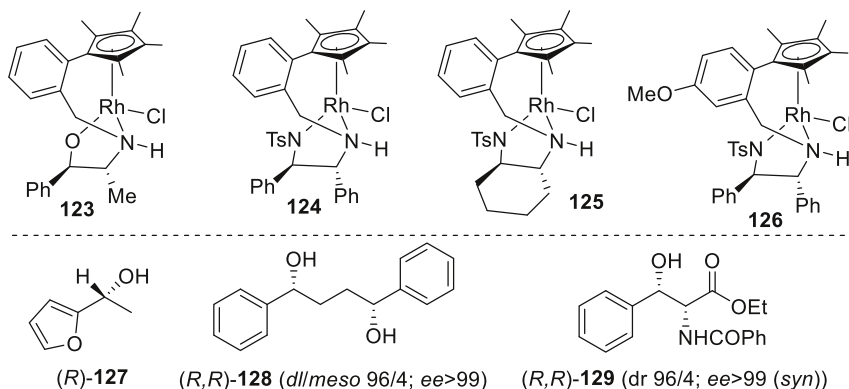
Fig. 31 Powerful tethered rhodium catalysts

than the isoelectronic Rh(III) catalysts, Rh-catalysts can be superior in some cases. For example, the reduction of α-chloroacetophenone in the presence of Ru complex **26** furnished the corresponding alcohol in 36 % yield and 91 % *ee* after 24 h (FA-TEA system) [101], while, using the complex **124** in the same reductant system, a 100 % conversion was achieved after only 2 h associated with 99.6 % *ee* of the corresponding alcohol. Activity of Rh-tethered catalysts was further improved by simply changing the monotosylated diamine. Thus, the complex **125** with (1*R*,2*R*)-*N*-*p*-tosyl-1,2-cyclohexanediamine proved to be an excellent catalyst for the reduction of a wide range of ketones in FA-TEA medium [102]. The reductions can be completed within times as short as 30 min and, in the majority of cases, the *ee*s values of the alcohol products were over 90 %. Importantly, in many cases, the *ee*s were higher than those observed with complex **124**. Not only α-substituted ketones are highly compatible with catalyst **125** but heterocyclic ketones also proved to be excellent substrates. Interestingly, the alcohol product (*R*)-**127** was obtained in the very high *ee* of 98 % with only 100 ppm of catalyst **125** in formate-water as hydrogen donor, though the complete conversion was reached after 7 days.

The Rh complex **126**, as an analogue of **124**, bearing a methoxy group on the tethering phenyl ring was used in the ATH of a series of ketones in the FE-TEA system [103]. Of note, by using catalyst **126**, the 1,4-diol (*R*,*R*)-**128** was prepared with an excellent *dl/meso* ratio and *ee* value. The ATH of α-amido β-keto ester associated to a dynamic kinetic resolution process delivered the corresponding 1,2-amino alcohol (*R*,*R*)-**129** with good diastereoselectivity and high enantiomeric excess (Fig. 31).

2.2 Heterogeneous Asymmetric Catalysis

While transition metal complexes (mostly of Ru, Rh and Ir) have been widely studied in homogenous TH of ketones, much less attention has been devoted to the hydrogen transfer reduction of carbonyl compounds under heterogeneous conditions. Generally, homogeneous catalysts are far more active and selective than

heterogeneous ones, but they also have some disadvantages which limit their possible implementation at the production level:

1. difficult separation of the catalyst from the product,
2. difficult recycling of the catalyst,
3. limited stability under certain reaction conditions,
4. most of the hydrogenations do not proceed without the use of expensive ligands (especially in ATH).

For these reasons, heterogeneously catalysed TH has recently been brought to the attention of many scientists as a comparative or complementary methodology to the homogeneous version.

Since optically active secondary alcohols represent valuable organic compounds, here again, selected examples of heterogeneous catalyst systems employed in the asymmetric TH of prochiral ketones will be presented. In principle, there are two general types of chiral heterogeneous catalysts: immobilised molecular metal catalysts on a variety of organic and inorganic materials on the one hand, and chirally modified supported metals on the other hand. While chirally modified metals (mostly Pt) have often been employed in the hydrogenation of ketones with molecular hydrogen [104], their use in TH is rather scarce. As an example found in the literature, Raney nickel modified with (R,R')-tartaric acid afforded secondary alcohols with low optical yield in the presence of propan-2-ol as the hydrogen source [105].

In many examples of TH reactions performed under heterogeneous conditions, which are mentioned below, water was used as solvent, not only contributing to greener processes but, more importantly, the ketone reduction rates and selectivities can also be improved in water medium.

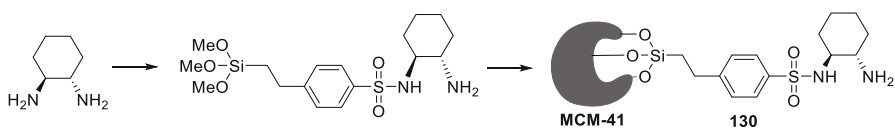### 2.2.1 Immobilisation of Catalysts

The immobilisation of homogeneous chiral catalysts onto solid supports is especially of interest from an industrial point of view, and can be achieved by employing strategies based on the ion–pair interaction or covalent binding of catalysts onto organic support, inorganic matrices, dendrimers, ionic liquids, and hybrid organic–inorganic composites. Such heterogenised homogeneous chiral catalysts have been designed as alternative systems for more effective and sustainable processes. Thus, attaching of metal complexes on a solid support provides an improvement of their stability under catalytic conditions, and also unique activity arising from their coordination on the surface of a chosen support. Normally, the materials used for immobilising molecular catalysts are mesoporous silica, magnetic materials, organic polymers, zeolites, or high surface area carbon. In obtaining a heterogeneous chiral metal catalyst, either supported chiral ligand is first formed and then coordinated with metal, or preformed optically active ruthenium complex is directly attached onto a solid support. Besides easy recovery of the expensive transition metal species and their reusability, immobilisation

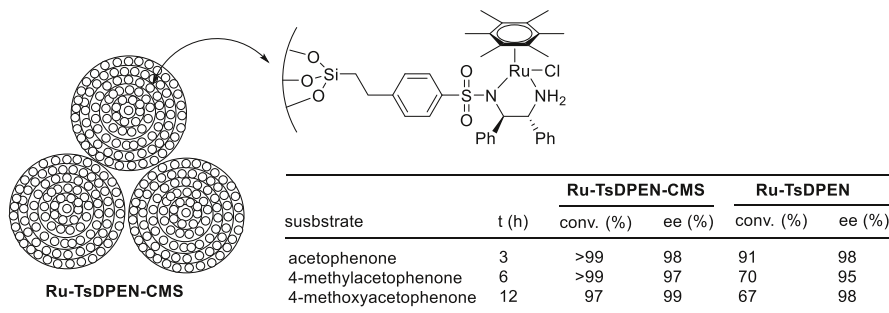should also allow to mitigate or supress contamination of hydrogenation products with toxic metals (like Ru).

2.2.1.1 Inorganic Supports Considering high activity and selectivity of the Noyori–Ikariya type homogeneous hydrogenation catalysts (for example, **26**), a very important effort has been devoted to the development of their immobilised versions. In this regard, mesoporous silica materials with regular pore arrangement and suitable pore diameter allow the assembley of well-defined active species within the inorganic material. In general, immobilisation of chiral metal complexes within mesoporous silica material can be achieved through a postgrafting (a postsynthesis method), a postmodification (an in situ coordination method), or a co-condensation strategy (a direct synthesis method).

The immobilisation of *N*-(*p*-toluensulfonyl)-1,2-diaminocyclohexane onto meso-porous MCM-41 silica was performed in two steps to obtain a chiral polyligand **130** which was subsequently treated with the $[RuCl_2(p\text{-cymene})]_2$ complex (Fig. 32) [106]. Thus, prepared heterogeneous Noyori–Ikariya type Ru catalyst (1 mol% of Ru complex and 1.7 mol% of chiral ligand) catalysed the ATH of acetophenone in the presence of HCO_2Na in pure water to give the corresponding alcohol in an 85 % yield and 86 % *ee* in 15 h. The ATH was then extended to other aromatic ketones, and the best result was obtained for α-tetralone (94 % *ee*). This catalyst could be recycled and used four times in the ATH of acetophenone without significant loss of stereoselectivity (86 % *ee* for the 1st cycle, 78 % *ee* for the 4th cycle).
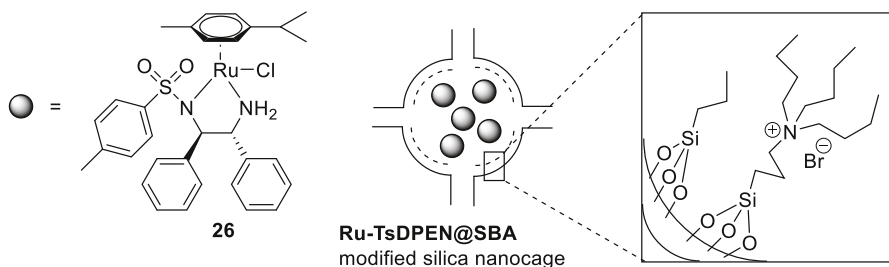
Three-dimensional flower-like mesoporous silica has some advantages over traditional ones (like MCM-41) as it possesses a short nanochanel of nanopore and a special cavum in the form of a flower, which offers easy diffusion of substrates, thus accelerating the reaction rate. The cooperative assembly between tetraethoxysilane and optically active 4-((trimethoxysilyl)ethyl)phenylsulfonyl-1,2-diphenylethylene-diamine using cetyltriethylammonium bromide (CTAB) as a structure-directing template afforded TsDPEN-functionalised chrysanthemum-like mesoporous silica (CMS) [107]. Complexation with $[RuCl_2(C_6Me_6)]_2$ gave a chiral Ru-TsDPEN-CMS catalyst, which displayed enhanced catalytic activity and enantioselectivity relative to the homogeneous counterpart in the ATH of selected ring-substituted acetophe-nones in water with HCO_2Na (Fig. 33). Almost quantitative conversions and *ee* values in the range 94–99 % were obtained in the reduction of ethyl phenyl ketone, benzyl phenyl ketone, benzyl, 1-indanone, 1-tetralone, ethyl benzoylacetate and 2-acetylfuran. Importantly, this novel heterogeneous catalyst can be easily recovered and reused at least ten times without affecting its catalytic efficiency. The remarkably high stability and reusability of the catalyst can be ascribed to

Fig. 32 Generation of polyligand at mesoporous silica

susbstrate	t (h)	Ru-TsDPEN-CMS		Ru-TsDPEN	
		conv. (%)	ee (%)	conv. (%)	ee (%)
acetophenone	3	>99	98	91	98
4-methylacetophenone	6	>99	97	70	95
4-methoxyacetophenone	12	97	99	67	98

Ru-TsDPEN-CMS

**Fig. 33** Three-dimensional silica-supported Ru catalyst

Fig. 34 Silica nanocages in ruthenium ATH

immobilisation of active catalytic centres via strong covalent bonding within the silicate network.

The catalytic efficiency of solid catalysts may be improved by tuning the microenvironment of self-assembled nanocapsules, thus changing the diffusion rates of the reactants during the catalytic process. Li and Yang reported that the catalytic activity of the Ru complex **26** encapsulated in the nanocage of mesoporous silica SBA-16 in water depended on the employment of silylation agents with different hydrophobic/hydrophilic properties for adjusting the nanocage microenvironment (Fig. 34) [108]. They observed that the catalytic performance of Ru-TsDPEN@SBA with a hydrophilic tributylpropylammonium groups-modified nanocage is about ten times higher than in the case of nanocages modified by hydrophobic propyl groups.

During the past few years, molecular imprinting of supported metal complexes has been applied for the preparation of selective heterogeneous catalysts by providing a shape-selective reaction space, also contributing to the stabilisation of an active metal species by surface matrix overlayers [109]. In this regard, a molecularly imprinted Ru catalyst on a SiO_2 surface stacked with organic polymer was prepared by (*R*)-1-(*o*-fluorophenyl)ethanol (**132**) as a template and tested in the ATH of *o*-fluoroacetophenone in water (Fig. 35) [110]. It was observed that ATH on the molecularly imprinted Ru catalyst with the polymer overlayers of 2 nm obtained by photopolymerisation of acrylate oligomer and 2-hydroxyethyl methacrylate gave better enantioselectivity than the homogeneous version **131** (81 % *ee* vs. 91 % *ee*).
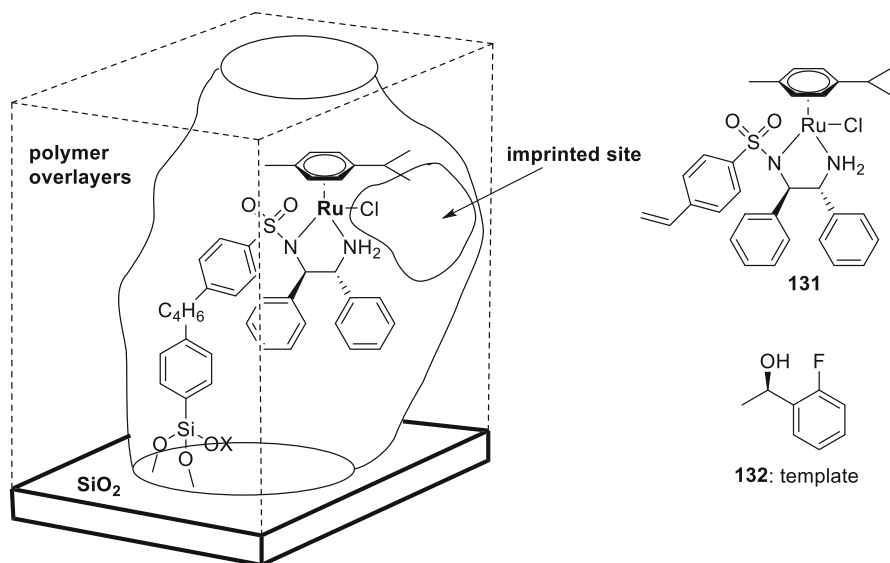
Fig. 35 Molecularly imprinted Ru ATH catalyst

A chiral Cp*Rh-TsDPEN complex was assembled within the core of core–shell-structured mesoporous silica spheres (CSSMSS) and showed excellent catalytic performance and high recyclability in the ATH of aromatic ketones in water [111]. Functionalised CSSMSS was prepared via co-condensation of $Si(OEt)_4$ and functionalised organosilane **133** in the presence of cetyltriethylammonium chloride (CTAC) acting as structure-directed template and potential phase transfer catalyst (Fig. 36). In these CSSMSS as a novel type of silica-based materials, the core assembles chiral Rh functionalities while the shell prevents the leaching of metal complexes thus assuring high recyclability. In general, excellent conversions and high enantioselctivities were obtained in the ATH of all the tested ketones (*m*- and *p*-substituted acetophenones, 2-acetylnaphthalene). For instance, acetophenone was reduced with more than 99 % conversion to give (*S*)-1-phenyl-1-ethanol with 97 % *ee* value. The high catalytic activity of this heterogeneous catalyst can be attributed to the phase transfer function of CTAC in a biphasic reaction system, and highly dispersive active Rh centres. This catalyst showed high recyclability—it could be simply recovered via centrifugation and reused in hydrogenation of acetophenone in 12 consecutive runs without obvious decrease of conversions and *ee* values.

Similarly, chiral Cp*Rh-TsDPEN was incorporated within flower-like mesoporous silica through the assembling of chiral 4-((trimethoxysilyl)ethyl)phenylsulfonyl-1,2-diphenylethylenediamine (**133**) and $Si(OEt)_4$ under a cooperative dual-template approach followed by complexation with the Rh complex in the presence of surfactant cetyltrimethylammonium bromide [112]. The obtained bifunctionalised solid catalyst showed excellent catalytic efficiency in the ATH of aromatic ketones in aqueous medium. The residual surfactant within the silicate network acted as a phase transfer catalyst thus enhancing the catalytic activity, while well-
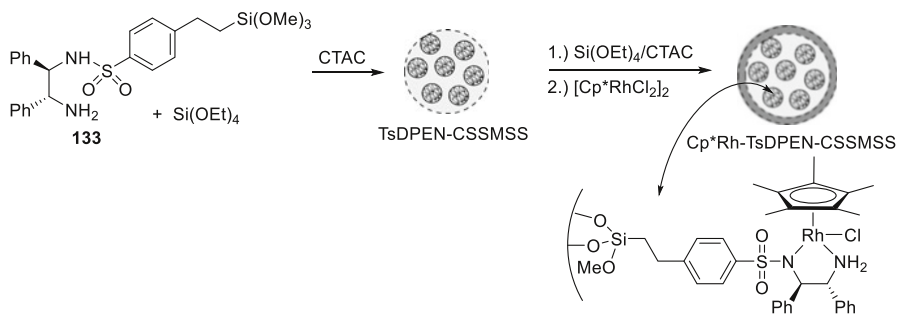
**Fig. 36** Core–shell-structured mesoporous silica-supported Rh catalyst
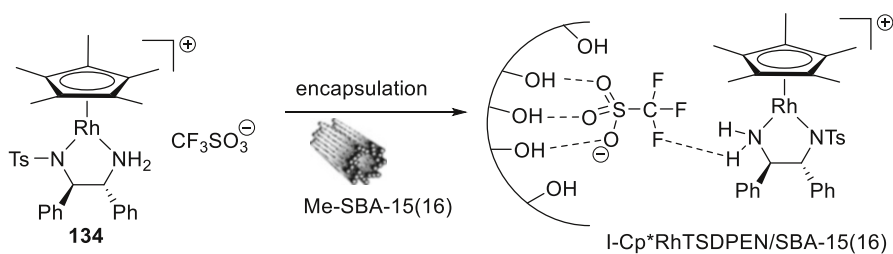
**Fig. 37** Ion–pair interactions as a catalyst-immobilising strategy

defined single-site chiral Rh functionalities could maintain high enantioselectivity. Additionally, this catalyst can be recovered and reused repeatedly ten times without serious deterioration of catalytic performance.

Xu et al. [113] have developed heterogeneous cationic chiral Rh catalysts by utilising ion–pair interactions as an immobilising strategy. The homogeneous cationic complex **134** was entrapped within mesoporous silica Me-SBA-15 or Me-SBA-16 and used in ultra-sound-promoted ATH of various aromatic ketones (ring-substituted acetophenones and acetylnaphthalenes) in water with HCO$_2$Na (Fig. 37). In comparison to the neutral Cp*Rh-TSDPEN version (as depicted in Fig. 36), the cationic version showed higher initial activity while ultra-sound irradiation could significantly enhance the reaction rate. They also showed that the catalyst with the chiral Rh functionality entrapped within Me-SBA-16 could be reused nine times without significantly affecting the enantioselectivity.

A series of chiral heterogeneous Rh catalysts **136–139** have been prepared via immobilisation of TsDPEN-based Rh complexes within mesoporous silicate networks by applying postgrafting, postmodification, and co-condensation strategies, and then tested in the ATH of aromatic ketones in water (Fig. 38) [114]. It was found that different immobilisation strategies led to different catalytic behaviour and recyclability of the prepared catalysts. Notably, the direct anchoring of Cp*Rh-TsDPEN functionalities on the surface of SBA-15 (catalysts **136** and **137**) kept the original chiral microenvironment and consequently resulted in as high a catalytic
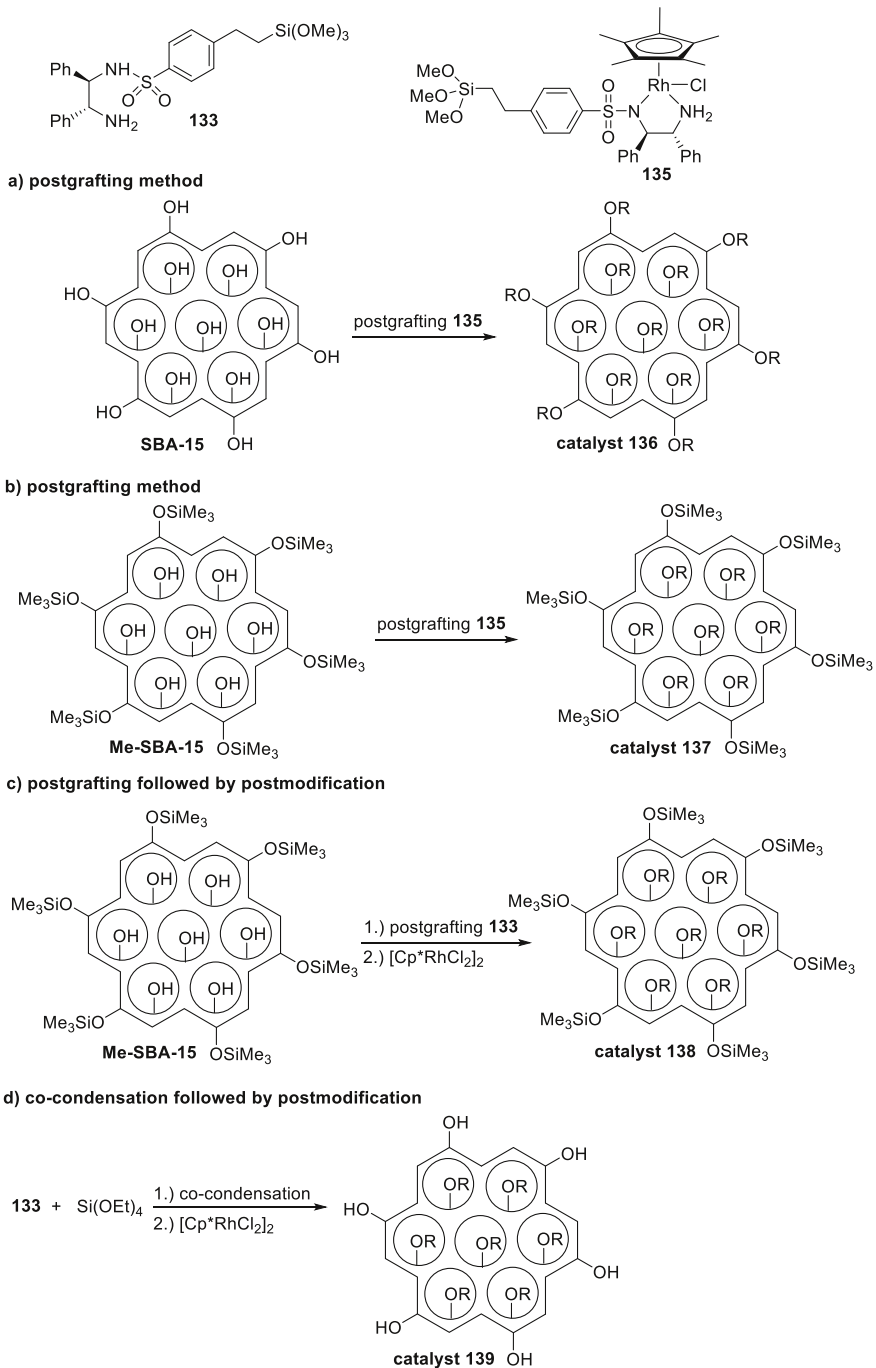
Fig. 38 Different immobilisation strategies for the preparation of silica-supported Rh catalysts
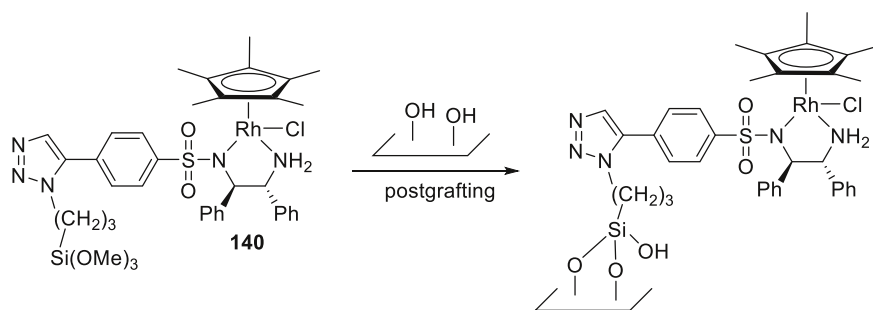
Fig. 39 Glass-supported Rh catalyst

efficiency as their homogeneous counterpart. The catalyst **139** prepared by a co-condensation strategy (immobilisation of Cp*RhTsDPEN functionalities within the silicate network forming uniformly distributed active species) presented a slightly higher catalytic efficiency than catalyst **138** derived from a postmodification method (the log-jam of Cp*RhTsDPEN functionalities near the nanopore mouth results in a disorderly distribution of active species) suggesting that the distribution of active centres plays an important role in enantioselective performance. The catalyst **139** also has the highest recyclability compared to **136–138**.

Very recently, a unique example of heterogeneous chiral Rh catalyst has emerged, in which the Rh complex **140** was immobilised at the surface of glass plates as solid support, and used in the ATH of aromatic ketones in aqueous medium [115]. Although conversions and *ee* values reached around 90 %, the recyclability of this catalyst was poor, since the conversion for the reduction of acetophenone decreased rapidly from 99 to 25 % in the 2nd cycle (Fig. 39).

Regarding a long history of cinchona alkaloids in asymmetric synthesis, Shen et al. [116] attached 9-amino *epi*-cinchonine **141** on the surface of mesoporous silica SBA-15. The hydrogenation catalyst **142** was then prepared in situ by mixing the cinchonine-modified silica and [Ir(COD)Cl]$_2$, and used for the reduction of substituted acetophenones in *i*-PrOH as hydrogen donor. Although the enantioselectivity was moderate (but still higher for acetophenone than with homogeneous analogue), the catalyst can be easily regenerated by solvent washing, while Ir leaching during four runs of the catalyst was <0.1 %. Similarly, 9-amino *epi*-cinchonine was anchored onto the external surface-passivated SBA-15 [117]. After complexing with [Ir(COD)Cl]$_2$, the in situ-obtained heterogeneous catalyst **143** delivered higher *ee* values in the ATH in *i*-PrOH for all tested ketones compared with the catalysts based on calcinated SBA-15 and its homogeneous counterpart (Fig. 40).

2.2.1.2 Hybrid Inorganic–Organic Supports   In order to ensure optimal diffusion of reactants and products in THs catalysed by solid catalysts in a HCO$_2$Na–H$_2$O reductant system, the surface properties of the catalysts are of great importance. For shortening the diffusion rates and preventing the leaching of catalytic species, the catalysts based on core–shell organic polymer–inorganic hybrid nanospheres were
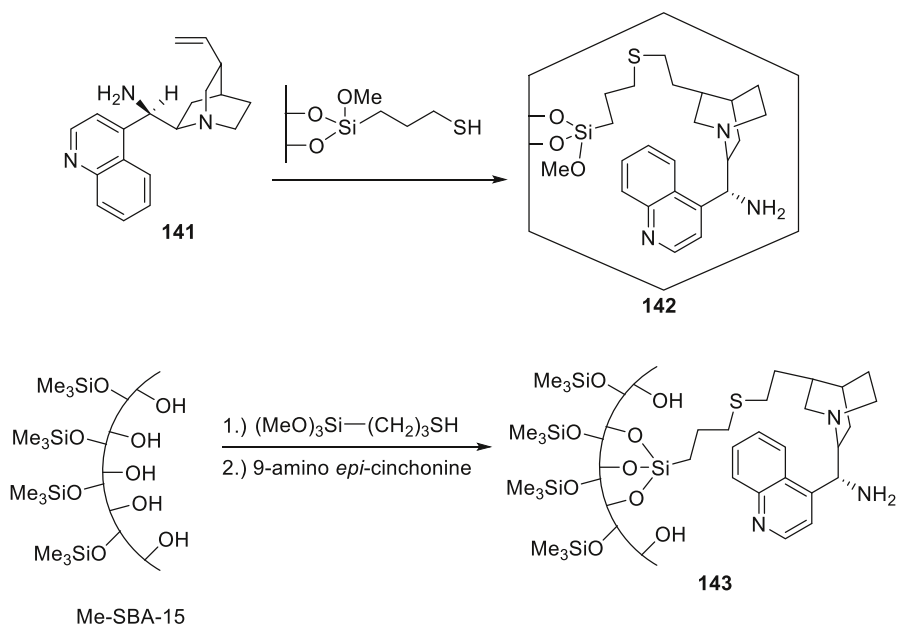
Fig. 40 Cinchonine-derived silica-supported ligands for Ir(I) ATH catalysts

designed. A chiral ligand, based on TsDPEN-polystyrene nanoparticles as the core and poly(methyl acrylate) (PMA) incorporated into the mesoporous silica network as the shell, was prepared in the presence of surfactant CTAB, then coordinated to Ru and used in situ as the catalyst in the ATH of acetophenone and simple aromatic ketones [118].

Yang and co-workers reported the immobilisation of Rh-TsDPEN by forming a polymer@silica composite catalyst [119]. A chiral monomer (1*R*,2*R*)-*N*-(4-vinyl-benzenesulfonyl)-1,2-diphenylethane-1,2-diamine was in situ-polymerised with divinylbenzene in the nanocages of mesoporous silica (FDU-12), and coordinated with a metal precursor. This chiral catalyst could efficiently catalyse the aqueous ATH of ketones to afford higher TOFs than homogeneous Rh-TsDPEN (585 vs. 340 h^{-1} for the reduction of acetophenone). Thus, the solid composite with hydrophilic outer (arising from silica) and hydrophobic inner surfaces (arising from the organic polymer) provides a suitable microenvironment for hydrophilic and hydrophobic reactants, and facilitates the mass transfer of ketone substrates in water.

Unlike inorganosilicate materials, periodic mesoporous organosilicas (PMO) possess a highly hydrophobic inner surface, which may facilitate reactions in a two-phase catalytic system, thus promoting organic transformations in water. In this regard, organosilica-bridged PMOs were prepared by the immobilisation of Cp*Rh-TSDPEN within their silicate network to afford chiral heterogeneous catalysts for aqueous ATH of aromatic ketones (Fig. 41) [120]. The ethylene-bridged PMO catalyst exhibited excellent catalytic activity and high enantioselectivity, which can
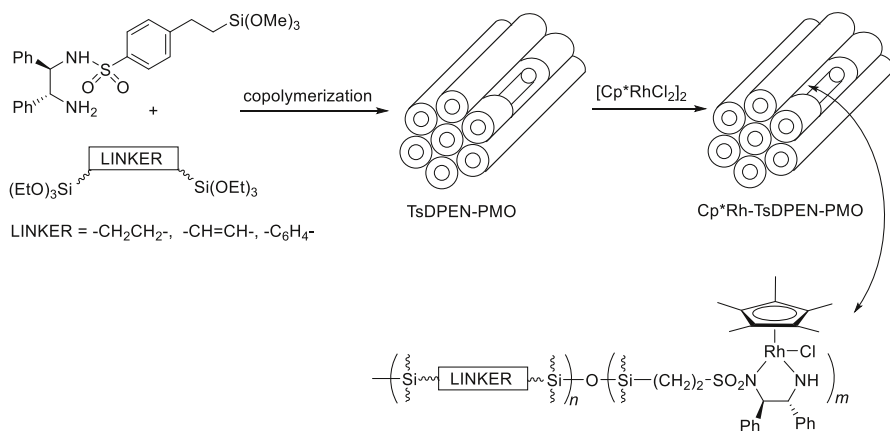
**Fig. 41** Organosilicas-supported-Rh ATH catalysts

be attributed to its hydrophobicity, and to the confined nature of the chiral organorhodium catalytic sites. This catalyst also showed a high reusability as it retained its catalytic activity after 12 cycles; for acetophenone, the *ee* value dropped from 95 to 92.2 % over 12 runs, while conversion remained unchanged (99.9 %).

In heterogeneous catalysts, the tailored and pillared cavity is an essential property as it enables the movement of reactants to inner catalytic sites. The mass transfer of reactants and products inside the pores is mainly influenced by the interaction of the internal walls of the channel with organic molecules, and can consequently be controlled by the difference in polarities. To ensure such properties, anchored ruthenium hybrid zirconium phosphate–phosphonates coated with hydrophobic linear double-stranded polystyrene over the inner surface of the Zr layers were prepared by the "first complexation of Ru and then molding of inorganic backbone" method, and used as the catalyst in the ATH of *o*-, *m*- and *p*-substituted acetophenones (Fig. 42) [121]. This catalyst showed good catalytic activity and enantioselectivity (73.6–95.6 % *ee*s) in the aqueous reduction with FA-TEA as the hydrogen donor, and could retain its catalytic properties after five runs in the case of acetophenone.

2.2.1.3 Organic Supports   From the viewpoint of green chemistry, it is worthwhile to develop water-soluble catalysts that can simplify purification and be reused without significant loss of activity. The poly(ethylene gylycol)-supported chiral ruthenium catalyst Ru-PTsDPEN **144** was found to be highly productive in the ATH of various ketones (acetophenones, acetonaphthones, 2-acetylfuran, 1-indanone, 1-tetralone) (Fig. 43) [122]. With this catalyst, the reactions were notably faster in aqueous NaHCOO than in FA-TEA azeotrope. This catalyst system is also very efficient in terms of recyclability, as it can be simply separated by precipitation and reused more than ten times with no loss in enantioselectivity, demonstrating its high stability in water.
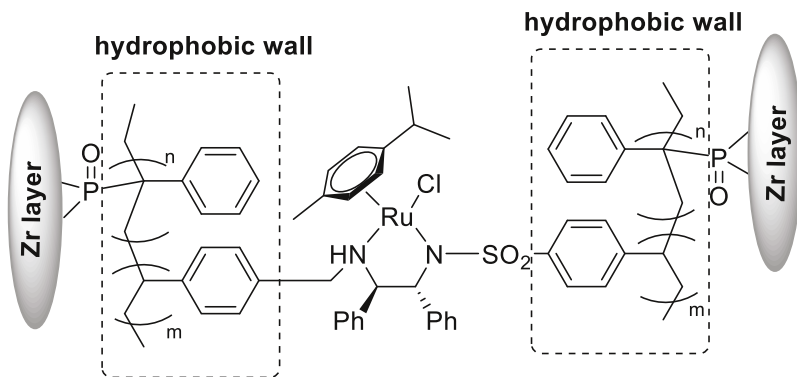
Fig. 42 Zirconium–polystyrene support for Ru catalyst
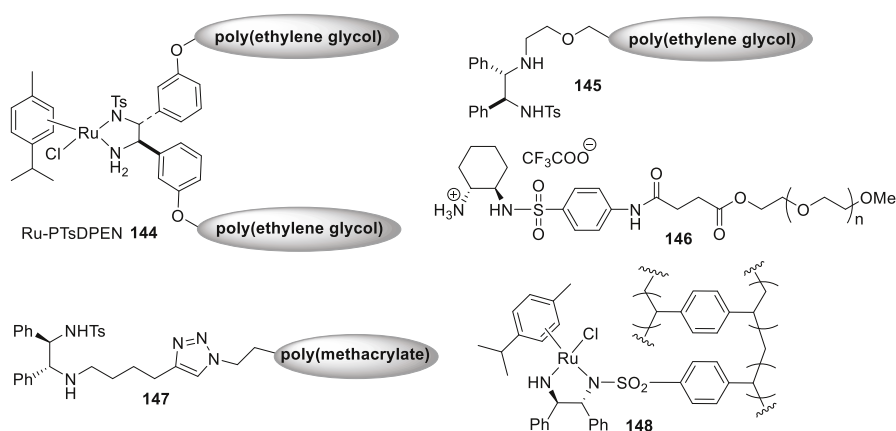
Fig. 43 Selected organic polymer-supported ligands and complexes

TsDPEN was attached to the poly(ethylene glycol) via its amino nitrogen to obtain the chiral-supported ligand **145** for Ru-catalysed ATH in aqueous NaHCOO (Fig. 43) [123]. More than 99 % conversions were obtained in the reduction of acetophenone and ring-substituted analogues, as well as for 2-acetylfuran and propiophenone. More than 90 % *ee*s were observed for the majority of products, while hydrogenation of 1-indanone and 1-tetralone delivered excellent *ee* values of 99 %. Similarly, poly(ethylene glycol)-supported chiral monosulfonamide **146** was synthesised from (*R*,*R*)-1,2-diaminocyclohexane and acted as a good ligand to in situ-form water-soluble Ru catalyst for TH in water using HCO_2Na as a reductant (Fig. 43) [124].

TsDPEN ligand was also immobilised onto soluble polymer supports obtained by copolymerisation of methyl methacrylate and 2-hydroxyethyl methacrylate, using click chemistry between the azide present on the polymer and the terminal alkyne as a part of a TsDPEN derivative (Fig. 43) [125]. The triazole-containing polyligand

147 and the Ru(II) complex constitute a good catalyst for ketone hydrogenation with FA-TEA azeotrope. For instance, the acetophenone reduction proceeded with 98 % conversion and furnished the alcohol product with 94 % *ee*. Unfortunately, the activity of the already utilised catalyst recycled from the aqueous solution by precipitation was very poor (20 % conversion after 48 h).

The performance of heterogeneous catalysts is usually lower than that of homogeneous chiral catalysts, because of their lower interaction or poorer wettability of catalytically active sites with reactant molecules. To increase the wettability, phase transfer catalysts are sometimes introduced into the H$_2$O–oil–solid system. Xiao's group reported on an elegant solution to circumvent this disadvantage of heterogeneous catalysts by demonstrating a superhydrophobic and mesoporous Ru chiral catalyst **148** synthesised by co-polymerisation of *N-p*-styrenesulfonyl-1,2-diphenylethylenediamine with divinylbenzene, followed by coordination of Ru species (Fig. 43) [126]. The catalytic performance of this superhydrophobic catalyst was evaluated in the hydrogenation of acetophenone with aqueous HCO$_2$Na, and turned out to be higher (full conversion, 94 % *ee* in 1.5 h at 40 °C) than that of the homogeneous analogue (81 % conversion, 95.1 % *ee* in 1.5 h at 40 °C), and even of Ru-TsDPEN in nanocages (>99 % conversion, 92 % *ee* in 2.5 h at 40 °C) [108], one of the best heterogeneous catalysts in the aqueous ATH reactions. Superior catalytic performance of porous copolymer Ru-TsDPEN catalyst is related to good enrichment of the reactants in the catalyst and easy transfer of the product from the catalyst into the water phase due to its superhydrophobicity.

Another organic polymer-supported version of the Noyori–Ikariya catalyst has been developed by attaching enantiomerically pure C_2-symmetrical 1,2-diamines on chlorosulfonylated polystyrene under conditions preferentially leading to monosulfonylation (Fig. 44) [127]. The obtained chiral functional resins were converted to the Ru(II) catalyst **149** and used in the TH of alkyl aryl ketones with FA-TEA azeotrope. Due to a high functionalisation level of catalytic resin, excellent activities and enantioselectivities were obtained with an S/C ratio as high as 150; the mean *ee* value of the resulting alcohols was 95 %, while conversions mostly reached 99 %.

Dimroth et al. [128] succeeded in immobilising a tethered Rh(III)-TsDPEN catalyst on hyperbranched polyglycerol (hPG), which is a suitable support due to its solubility in various solvents, high chemical stability, and weak coordination to
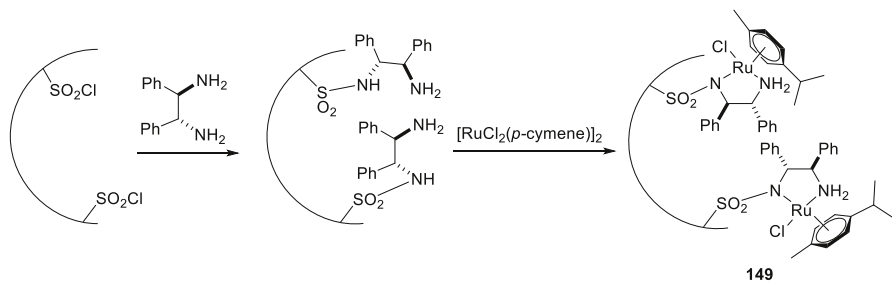
**Fig. 44** Polystyrene-supported Ru ATH catalyst
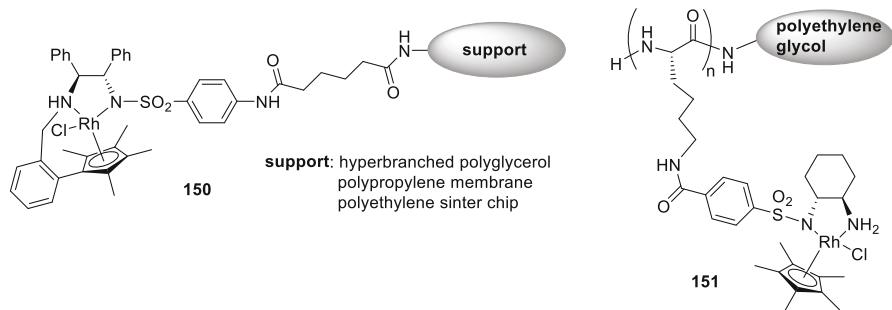
Fig. 45 Organic polymer-supported Rh catalysts

metals. A modified TsDPEN ligand was attached via amide coupling to hPG containing amino residues, and complexation with RhCl$_3$ furnished soluble hPG-supported Rh(III) complex **150** (Fig. 45). This supported catalyst showed the best performance for acetophenones, 2-acetonaphthone and propiophenone resulting in quantitative conversions and over 95 % *ee* values after 6–18 h in the aqueous hydrogen donor system (HCO$_2$Na/water). Despite its excellent catalytic activity and enantioselectivity, soluble-supported Rh catalyst could be recycled only two times. To improve the reusability, a tethered Rh complex was anchored onto polymeric chips (polypropylene- and polyethylene-based) to give a solid polymer-supported catalyst. With this catalyst, a successful recycling was achieved in a water/HCO$_2$Na/HCO$_2$H system keeping the enantioselectivity constantly high at 98 % *ee* for at least seven runs in the ATH of acetophenone.

The use of micellar systems is a convenient method to facilitate the reactions of usually hydrophobic organic molecules in water, but catalyst leaching can diminish their usage. To avoid metal leaching by stabilising micellar catalysts, a chiral 1,2-diaminocyclohexane ligand was covalently attached to the block copolymer, followed by complexation with a Rh(III) precursor to obtain an amphiphilic block polypeptide-based heterogeneous catalyst [129]. The obtained Rh-containing copolymer **151** forms micelles in water, and catalyses TH of acetophenone with HCO$_2$Na at room temperature and low loading (1 mol%), and also provides high recyclability.

2.2.1.4 Dendritic Catalyst Systems Dendritic catalysts have received special attention since they combine the advantages of both homogeneous and heterogeneous catalysts, but normally cannot outperform other types of immobilised catalysts, such as on silica or organic polymer supports with respect to reusability and catalytic activity. However, Wang's group reported on a highly efficient fluorinated dendritic chiral Ru-TsDPEN complex for the ATH in aqueous medium [130]. This catalyst was prepared in situ from the chiral ligand **152** and Ru(II) precursor, and could be easily separated via the solvent precipitation method and reused more than 26 times without significant deterioration of enantioselectivity as well as activity. This unprecedented recyclability can be ascribed to the presence of fluorine atoms which contribute to scaffold rigidity and chemical resistance (Fig. 46).
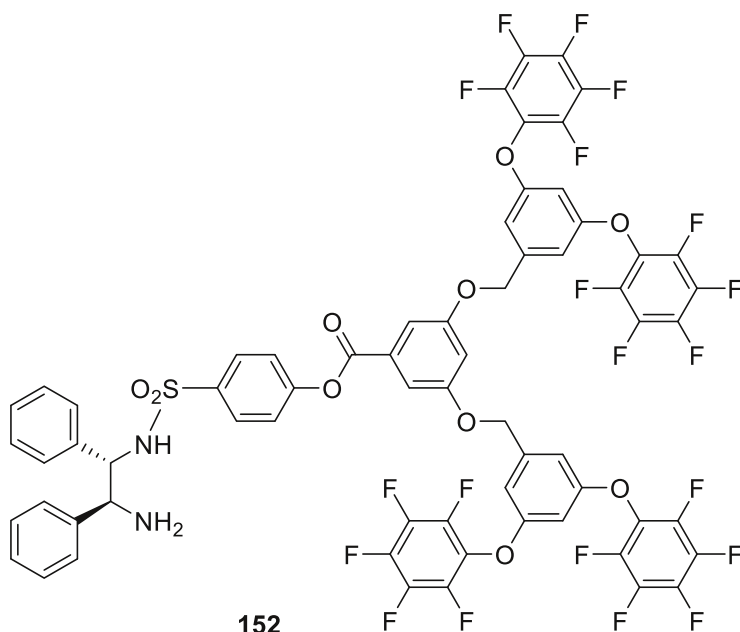
Fig. 46 Dendritic fluorinated ATH ligand

Even though self-assemblies of chirally-functionalised silanes have dominated the preparation of heterogeneous catalysts, their uncontrollable hydrolysis and sometimes complicated compatibility of functionalities result in random anchoring of chiral functionalities within frameworks. Octavinylsilsesquioxane **153** with site-directing vinyl groups was used to construct polyhedral oligomeric silsesquioxane (POSS) frameworks bearing (*R,R*)-TsDPEN as chiral functionality [131]. Complexation with [Cp*RhCl$_2$]$_2$ afforded the heterogeneous catalyst **154** which displayed excellent catalytic activity in aqueous ATH of aromatic ketones with almost quantitative conversions and high (over 90 %) *ee* values. For example, acetophenone was reduced with obviously higher conversion when compared to homogeneous Cp*Rh-TsDPEN (>99 % vs. 88 %), while enantioselectivity remained unchanged. It is worth noting that this heterogeneous catalyst could be recovered easily via nanofiltration and reused in 12 consecutive hydrogenations of acetophenone without obviously affecting enantioselectivity (Fig. 47).

2.2.1.5 Magnetic Nanoparticle Catalysts The anchoring of homogeneous chiral catalysts on magnetic nanoparticles has attracted much attention due to the easy recovery of formed catalysts via an external magnetic field. Despite this advantage, the magnetic aggregation and magnetic loss still hinder a real practical application. In early studies, chiral amino alcohol ligands immobilised on cobalt nanoparticles induced comparable conversions and enantioselectivities to amino alcohols in
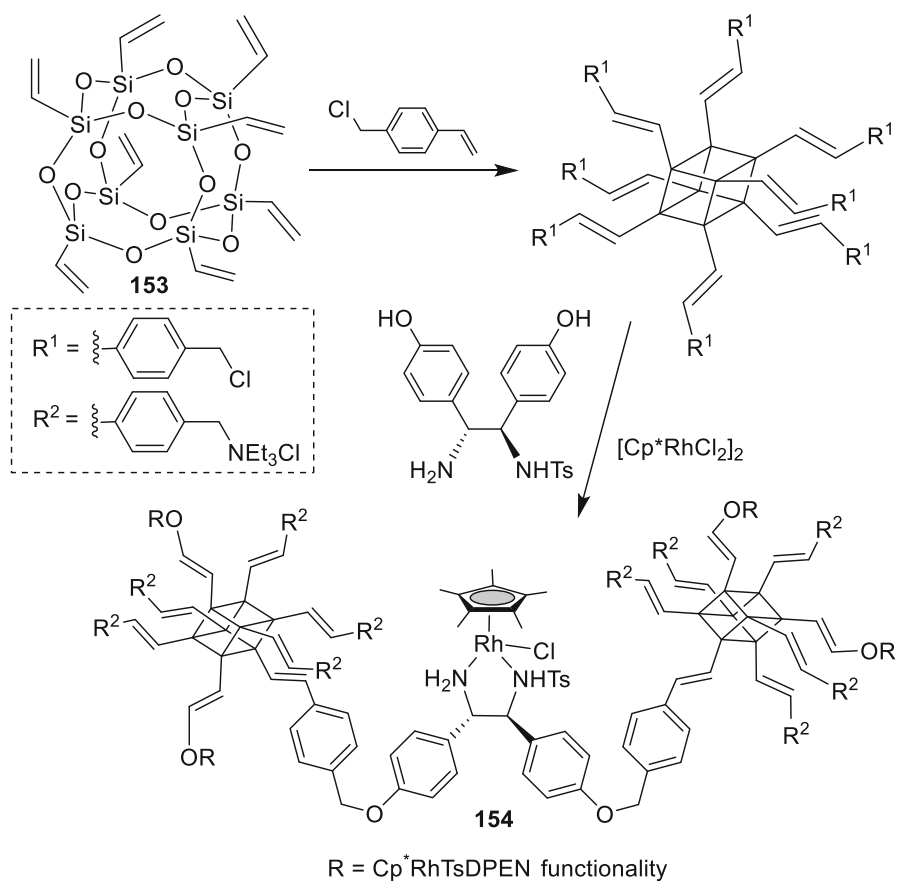
Fig. 47 Polyhedral oligomeric silsesquioxane Rh catalyst

monomeric form in Ru-catalysed ATH of acetophenone, yet benefiting from easy magnetic separation [132].

Phenylene-coated Rh-functionalised magnetic nanoparticles **155** were developed to catalyse TH of ketones in water [133]. First, a phenylene layer was coated onto Fe_3O_4 by co-condensation of (S,S)-4-(trimethoxysilyl)ethyl)phenylsulfonyl-1,2-diphenylethylenediamine and 1,4-bis(triethoxysilyl)benzene by using CTAB as a template, then $[Cp*RhCl_2]_2$ was coordinated. This catalyst exhibited high reaction rates and delivered on average 95 % ee of the resulting chiral alcohols in TH of selected ketone substrates in a H_2O/HCO_2Na system. The catalyst can be recovered by using a small magnet and can be reused in ten consecutive reductions without loss of its catalytic activity (Fig. 48).

In another approach, Fe_3O_4 magnetic nanoparticles were first coated with SiO_2, onto which TsDPEN-derived chiral ligand was grafted [134]. The catalyst was then obtained via direct complexing with $[Cp*RhCl_2]_2$. In general, high conversions and enantioselectivities were obtained in aqueous ATH of the tested ketones. For
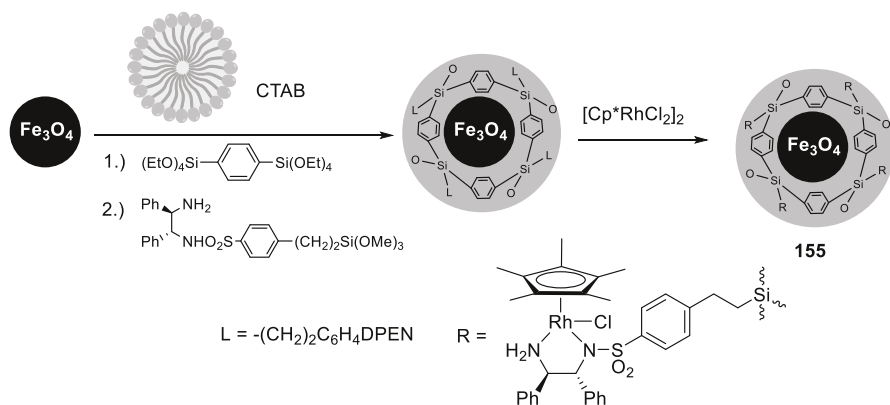
Fig. 48 Silicon-organic layer-coated magnetite Rh nanoparticle catalyst

instance, acetophenone was reduced in a 97.2 % conversion, delivering the corresponding alcohol in 97.7 % *ee* within only 1 h reaction time. The high activity of this catalyst could be due to the high dispersion of rhodium centres on the outer surface of the nanoparticles, while the high enantioselectivity may arise from the preserved homogeneous microenvironment after immobilising of the chiral ligand. This magnetic catalyst also exhibited high reusability.

Another magnetically recoverable catalytic silica microreactors **156** were prepared and tested in the ATH of ketones in aqueous medium [135]. Magnetite nanoparticles were coated with shells synthesised via co-polymerisation of $Si(OEt)_4$ and the Ru-TsDPEN complex **157** functionalised with a trimethoxysilane group. The transport of the hydrophobic reactants from the water medium to an entrapped catalyst in a sol–gel matrix was ensured by the surfactant CTAC. Under these conditions, ring-substituted acetophenones were almost quantitatively reduced with HCO_2Na giving the corresponding alcohols in over 90 % *ee*s within 24 h (Fig. 49).

3 Transfer Hydrogenation Catalysed by Other Metals

An impressive success in replacing the rare elements such as ruthenium, rhodium, and iridium in TH catalysis with Earth-abundant metals was made in the last decade. Among them, iron substitutes appeared as an important alternative. There are precedents of using iron catalysts in TH of ketones. Bianchini and Graziani reported in 1993 that the dihydrogen isostructural complexes of type *cis*-$[MH(H_2)\{P(CH_2\text{-}CH_2PPh_2)_3\}]BPh_4$ (M = Fe, Ru, Os) catalyse the transfer of hydrogen from cyclopentanol to benzylideneacetone to produce allylic alcohol with excellent chemoselectivity [136]. Beller and co-workers [137] used a catalyst precursor generated in situ-reacting $Fe_3(CO)_{12}$ with different porphyrin compounds for the TH of ketones. The reduction was performed in isopropanol at the temperature of 100 °C. The aryl ketones ($MeCOC_6H_4$-2-OMe, $MeCOC_6H_4$-4-Cl, and $EtCOPh$) were reduced with conversions of over 90 %. Structurally defined and more active
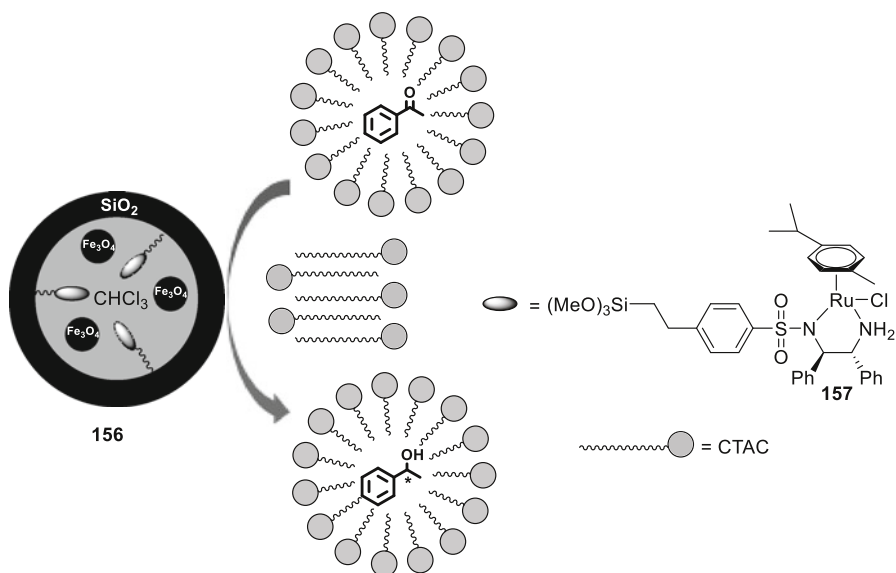
Fig. 49 Magnetite-silica microreactors containing Ru catalytic sites
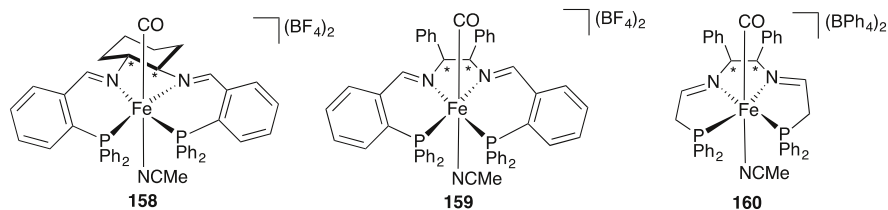
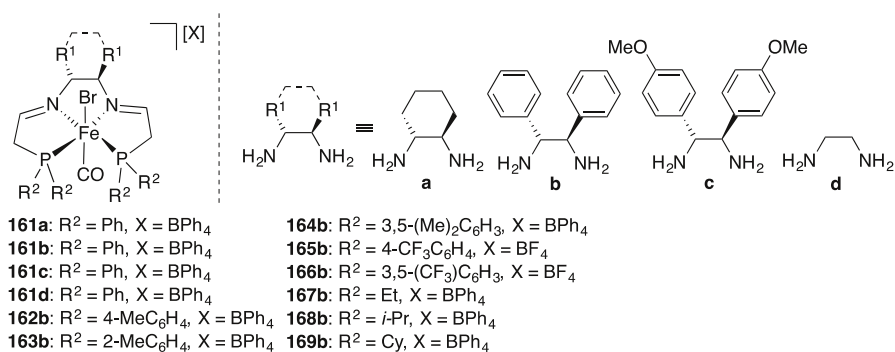**Fig. 50** First (**158** and **159**) and second (**160**) generation iron(II) ATH catalysts

iron-based TH catalysts, *trans*-[Fe(CO)(MeCN)(*PNNP*)]$^{2+}$ were designed by Morris et al. [138–141] (Fig. 50). The precatalysts were prepared by reacting the *trans*-[Fe(MeCN)$_2$(*PNNP*)]$^{2+}$ complex with carbon monoxide in acetone.

When the carbonyl complexes **158–160** are activated by *t*-BuOK in *i*-PrOH, they are surprisingly active catalysts for TH of ketones at room temperature. For example, complexes **158** and **159** (6,5,6-*PNNP* type of complexes) display comparable TOF (900 h^{-1}) in reducing of acetophenone while **160** (5,5,5-*PNNP* complex) is about 4 times more reactive. Concerning the enantioselectivity of the complexes, it increases in the order **158** < **159** < **160**, with **160** providing excellent results for a wide range of ketone substrates. In a series of phenyl alkyl ketones (PhCOR), the rate of reduction decreases in the order Me > Et > *i*-Pr > -*t*Bu, while the *ee* increases in the opposite order. The substitution pattern evidently suggests that increasing the electrophilicity of the carbon of the ketone facilitates the limiting step of the catalytic cycle. The catalyst **160** also shows the highest chemoselectivity towards the reduction of the carbonyl group in cases of reducing the α,β-unsaturated
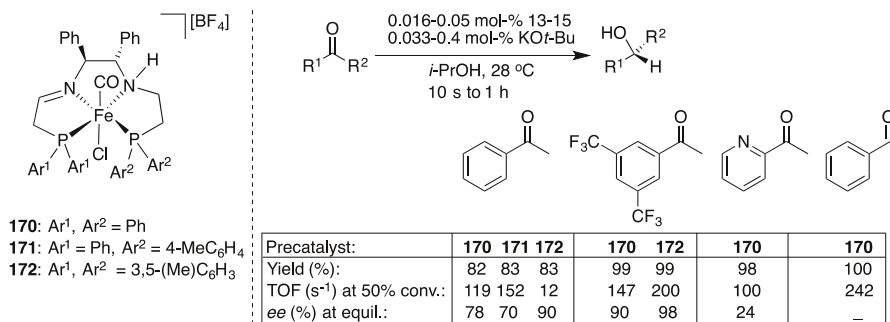
ketones. It was also proposed that higher *ee* values produced by catalysts **159** and **160** are due to the conformation characteristics of their ring system backbone, relative to that of **158**, the latter having the flat, equatorial and stereochemically less favourable cyclohexane moiety. Subsequently, detailed investigations of the 6,5,6-*PNNP* systems (complexes **158** and **159**; Fig. 50) revealed that the active catalytic species were iron(0) nanoparticles [142].

The second generation the 5,5,5-*PNNP* complex **160** was further modified and the derivatives examined in the ATH reactions of ketones. The catalytic activity of the complex **161b** (Fig. 51) versus **160** was determined to be virtually the same within the experimental error, indicating that there is no significant effect of the ligand in the *trans* position (acetonitrile vs. bromide ligand) relative to the carbonyl. The incorporation of different amines into the backbone of the ligand of complexes **161a–d** influences both the steric and electronic properties of the complexes. However, precatalysts **161a–d** show similar high activity in the ATH reaction of acetophenone (TOF ranging from 2.1×10^3 to 2.0×10^4 h^{-1}) and *ee*s 60 % for **161a** and 81 % for **161b** and **161c** using very low catalyst loadings (0.016 mol% relative to the substrate) [143]. In order to study the electronic and steric effects of the *trans*-CO/Br *PNNP* type of iron(II) complexes the *orto*- and *para*-substituted phenyl groups were introduced into the phosphorus donors (examples **162b–166b**) while the (*S,S*)-1,2-diphenylethylenediamine moiety was retained. Among them, only **162b** and **164b** were active catalysts in the ATH experiments reducing acetophenone to the corresponding alcohol; **164b** had too much steric crowding around the iron centre, while **165b** and **166b** were too electron-poor and were inactive in ATH. The precatalyst **162b** showed increased activity and comparable enantioselectivity to the precatalyst **160**, while **164b** produced more enanto-enriched (*R*)-1-phenylethanol with an *ee* of 90 % [144]. The complexes having alkyl substituents (*i*-Pr and Cy) on a phosphorus donor (**168b** and **169b**) were completely inactive in the ATH of acetophenone as a model substrate [145]; however, complex **167b** (Et substituent on phosphorus) reduced acetophenone with TOF of 2300 h^{-1}. It should be pointed out that the iron(II) carbonyl complexes are not active for ATH by themselves; a strong base, such as *t*-BuOK, is required to generate an active catalyst species [138, 139, 141, 145]. This is in general quite typical for ATH

Fig. 51 Second generation iron(II) ATH catalysts

| Precatalyst:	170	171	172	170	172	170	170
Yield (%):	82	83	83	99	99	98	100
TOF (s⁻¹) at 50% conv.:	119	152	12	147	200	100	242
ee (%) at equil.:	78	70	90	90	98	24	–

Fig. 52 Third generation iron(II) ATH catalysts

reactions and there are a plethora of similar reports in the literature [9]. The third generation iron(II) carbonyl 5,5,5-*PNNP* amine-imine diphosphine complexes **170**–**172** (Fig. 52) were designed based on detailed mechanistic investigations and investigations into the nature of the base activation of iron(II) carbonyl complexes of the second generation [146, 147], affording even more reactive catalytic species [148–150].

The ATH of (hetero)aryl ketones applying complexes **170**–**172** gave moderate to high enantioselectivities (24–98 % *ee*) with TOF as high as 242 s^{-1}. The precatalyst **171**, with *para*-tolyl substituent on a phosphorus donor, gave the highest TOF of 152 s^{-1} in reducing acetophenone, while the complex **172** displayed the best enantioselectivity (90 % *ee*; Fig. 52). A particularly interesting substrate is 3,5-bis(trifluoromethyl)acetophenone, which was reduced with TOF of 200 s^{-1} and *ee* of 98 % using the precatalyst **172** yielding the corresponding (*R*)-alcohol, which is an intermediate for the synthesis of Aprepitant, a neurokinin antagonist [151]. This highly active precatalysts exceeded the TOF demonstrated by ruthenium-based and osmium-based (*R*,*S*)-Josiphos catalysts, as well as a ruthenium *PNHNHP* complex, which possessed TOF of 89 and 92 s^{-1}, respectively, at a temperature of 60 °C [84, 152].

It was proposed that the use of a more sterically hindered phosphine, such as a dicyclohexylphosphino group on the ligand, may improve the enantioselectivity of the third generation of iron(II) complexes. The unsymmetrically substituted *PNHNP* complex **173** (Fig. 53) was synthesised by applying the templated ligand synthesis approach [153]. Precatalyst **173** was tested in the ATH of C=O bonds and gave TON up to 4300 and an enantiomeric excess up to 99 %. Comparing the activity of precatalyst **173** with the diphenylphosphino analogue **170** (Fig. 52) in the ATH of ketones, it was found that the enantioselectivity using this system was increased at the expense of the catalytic activity.

The catalytic mechanism of the ATH of ketones using Fe(II)-complex **170** was clarified by the spectroscopic detection of Fe(II)-amide and Fe(II)-hydride intermediates (Fig. 54). The reaction of complex **170** with two equivalents of *t*-BuOK generates a mixture of amido-enamido isomers **170a** which are highly active species for ATH. The amine-enamido-hydride complex **170b** is formed upon the
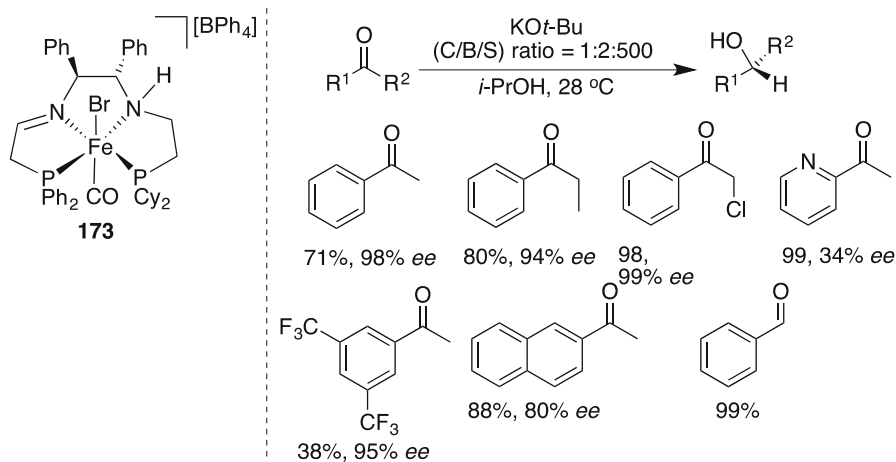
Fig. 53 An unsymmetrical $N(NH)P_2$ Fe(II) catalyst for the ATH of ketones
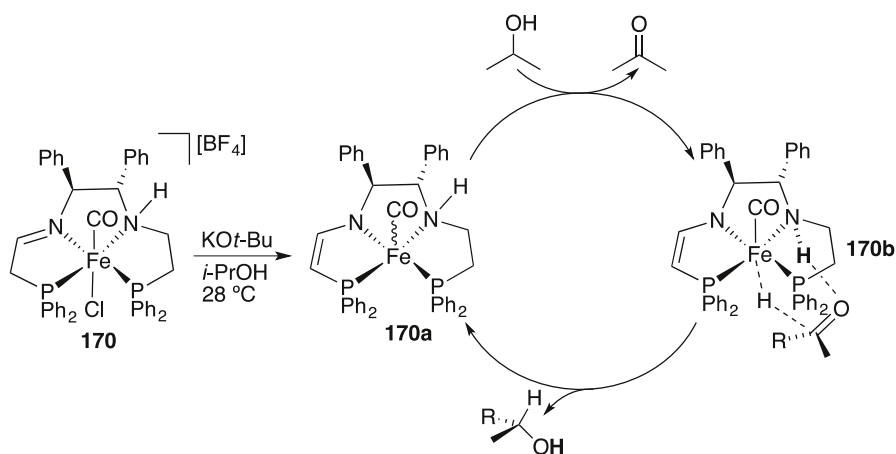
Fig. 54 Proposed mechanism of Fe(II)-catalysed ATH of ketones

reaction of **170a** with propan-2-ol enabling hydride transfer to the ketone hydrogen-bonded to the N–H with the larger group of the ketone (R is aryl) oriented to the less bulky diamine ligand moiety of the catalyst [148].

Recently, iron(II) complexes with chiral N_2P_2 and N_2P_4 macrocyclic ligands were introduced by Mazzetti and Gao for applications in ATH catalysis. In 2004, Gao and co-workers reported the ATH of ketones with the catalysts in situ generated from iron(II) complexes and chiral *PNNP* ligands [154], ligands that were later incorporated into the well-defined Fe-*PNNP* complexes by Morris et al., vide supra. The 22-membered macrocycles **174** and **175** (Fig. 55) synthesised by Gao et al. were used to in situ generate precatalysts from different iron sources (e.g.
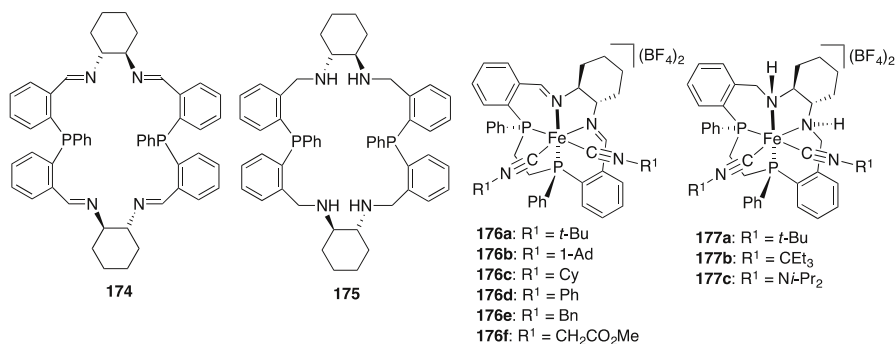
**Fig. 55** P_2N_2 and $(NH)_2P_2$-type macrocyclic Fe(II) ATH catalysts

Fe$_3$(CO)$_{12}$, [Et$_3$NH][HFe$_3$(CO)$_{11}$], and [PPN][HFe$_3$(CO)$_{11}$]). The combination of **175** and Fe$_3$(CO)$_{12}$ turned out to be the most successful in the ATH of aromatic ketones yielding the corresponding chiral alcohols in excellent yields and *ee*s up to 99 % [155]. The resulting catalytic system was, in the asymmetric hydrogenation of ketones, later found to be heterogeneous [156]. The well-defined isonitrile iron(II) complexes **176a–f** were successfully prepared from diacetonitrile analogues of which *tert*-butyl isocyanide derivative **176a** was found to be the most active and selective one. The precatalyst **176a** enabled the ATH of a variety of aryl alkyl ketones (e.g. acetophenone: 93 %, 84 % *ee*; 4-methylacetophenone: 85 %, 79 % *ee*; 3-methylacetophenone: 91 %, 86 % *ee*; 2-methoxyacetophenone: 95 %, 82 % *ee*; 3-chloroacetophenone: 98 %, 78 % *ee*; 1-acetonaphthone: 86 %, 91 % *ee*; ethylphenylketone: 74 %, 85 % *ee*, and indanone: 69 %, 44 % *ee*) in *i*-PrOH/*t*-BuONa at 75 °C. As in the examples of Morris's second generation iron(II) 5,5,5-*PNNP* precatalysts, vide supra, in the case of the complex **176a** both imine functionalities are also reduced during catalysis to amino functionalities. Therefore, the corresponding derivatives **177a–c** bearing diamino macrocyclic ligands (Fig. 55) were explored. The complexes **177a–c** are highly active and enantioselective precatalysts in the ATH of a broad scope of ketones in basic *i*-PrOH [157].

The significant influence of the isonitrile substituents on the enantioselectivity was noticed. The precatalyst **177a** gave (S)-1-phenyletan-1-ol with 96 % *ee* and 80 % yield in 1 h. Catalysts **177b** and **177c** were found to be superior over **177a** producing the same alcohol in a better yield and *ee*. Periodical sampling of the crude reaction mixture revealed that *ee* erosion was negligible while conversion is approaching equilibrium. Ketones with larger aryl groups (1- and 2-acetonaphthone) were reduced by **177c** in high yields and *ee*s. The catalyst **177b** gave the trifluoromethyl-substituted alcohols, which are important synthons for fungicides [158, 159] and NK1 antagonists [151], in quantitative yields and *ee*s of 96 and 98 %, respectively (Fig. 56). Although pyridyl or thiophenyl substituted ketones tend to coordinate to the metal centre causing poisoning, catalyst **177b** hydrogenated acyl pyridines rapidly and with high *ee*s.

Chiral bis(isonitrile) ligands and their iron(II) complexes (Fig. 57) were introduced by Reiser et al. [160] and were tested as precatalysts for the ATH of
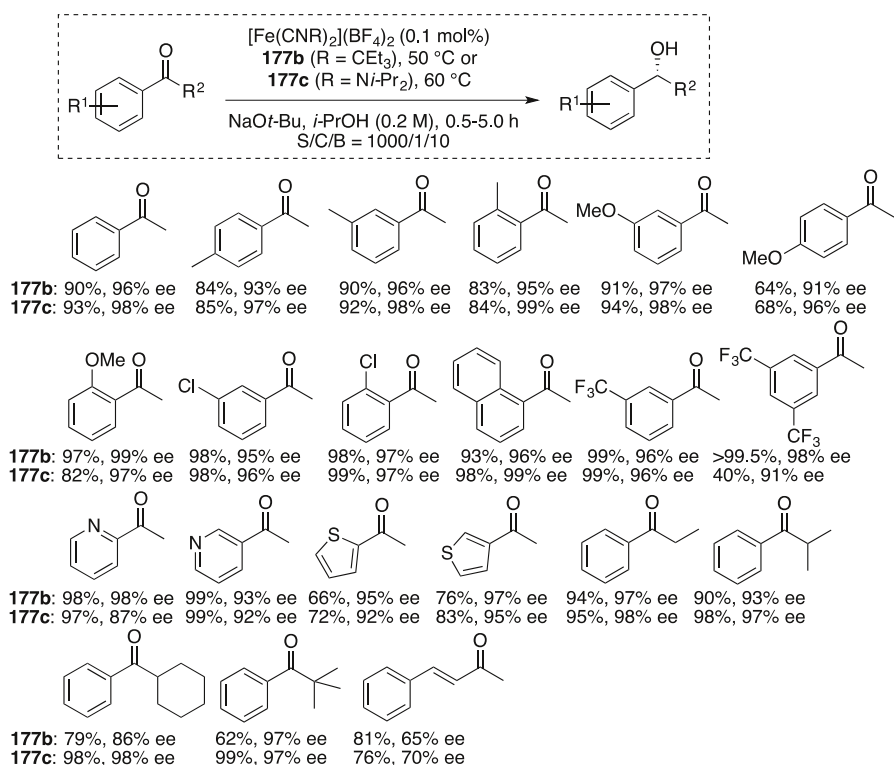
Fig. 56 Selected examples of highly enantioselective TH of ketones with **177b** and **177c**
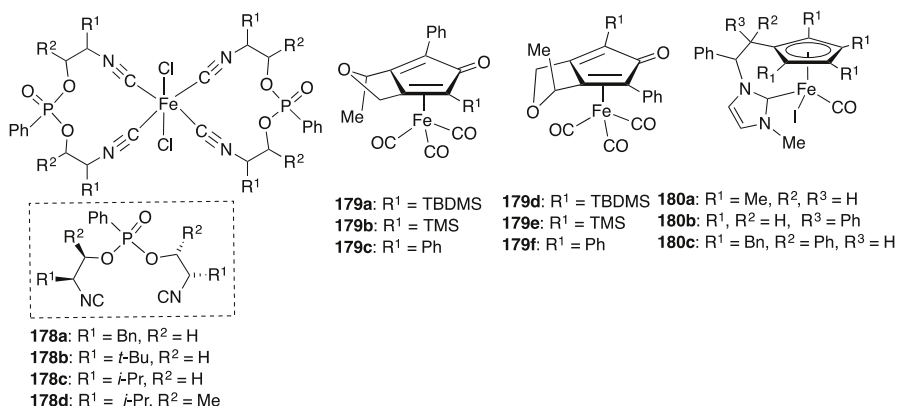
Fig. 57 Iron(II) isonitrile, cyclone, and carbene complexes for the TH catalysis

ketones. The complex **178b** was found to be the most active in the ATH of substituted phenyl alkyl ketones producing the corresponding alcohols in 50–99 % conversions and *ee*s up to 67 %. The same catalyst was also used to reduce

heteroaromatic ketones in good yields and generally moderate *ee*s. Iron(II) complexes with cyclone ligands **179a** and **179d** were proved to be of low activity; however, complexes **179b**, **179c** and **179e**, **179f** (Fig. 57), enantiomerically pure diastereoisomers, were found to be more effective ATH precatalysts in HCO_2H/ Et_3N 5:2 mixture as a hydrogen donor, giving almost complete transformation of acetophenone in 48–96 h at 40 °C to the corresponding (*R*) alcohol with low *ee*s [161]. Preliminary studies of the catalytic activity of achiral novel *N*-heterocyclic carbene ligated iron(II) complexes **180a–c** were carried out to explore their potential in the reduction of organic molecules. The catalytic (1 mol% loading) TH of ketones (acetophenone, cyclohexanone, and benzophenone) was carried out in propan-2-ol. All complexes catalysed the TH at 80 °C converting the tested ketones to the corresponding alcohols in good (80–100 %) yields [162].

Catalytic transfer hydrogenation (CTH) of substituted aldehydes and ketones was studied, using Fe(II)-phthalocyanine (Fe-Pc) homogeneous and heterogeneous (Fe-Pc/Al_2O_3) catalysts and *i*-PrOH as the hydrogen source [163]. The homogeneous catalytic system (Fe-Pc) produced moderate to excellent conversions for the various simple aldehydes and ketones (acetophenone 96 %, 4-Me-acetophenone 86 %, 4-MeO-acetophenone 63 %, and 3,5-di-MeO-acetophenone 42 %). The heterogenised version (Fe-Pc/Al_2O_3) provided similar conversions as under homogeneous conditions, allowing easy separation of the catalyst and its reusability.

Regarding osmium, catalytic TH of ketones have been reported for [Os(CO)HX(PR$_3$)$_n$] (X = Cl, H; *n* = 2, 3) and related complexes [164, 165], as well as for [OsCl(amino acids)(arene)]-type complexes [166]. A highly enantioselective example of ATH of several ketones (up to 92 % *ee*) was reported with the system generated in situ from [Os(cymene)Cl$_2$]$_2$ and (1*R*,2*S*)-(+)-*cis*-1-amino-2-indanol [167]. With the catalyst generated in situ from [OsCl$_2$(PPh$_3$)$_3$], (*R*,*S*)-Josiphos and 1-(pyridine-2-yl)methanamine ligands, efficient ATH of methyl aryl ketones (up to 96 % *ee*) and good rates of reduction have been observed [168].

In recent years, several structurally different osmium(II) ATH precatalysts have been developed, including those containing L-α-amino carboxylates, pybox ligands, monophosphinite-inositol complexes [169], and pincer complexes. Many of those reduce ketones with high enantioselectivities at very low loadings.

Synthetically readily accessible, robust, organo-osmium ATH catalysts were most recently developed by Wills and co-workers [170]. The complexes **181** (Fig. 58) are osmium analogues of Noyori-type catalysts synthesised by a
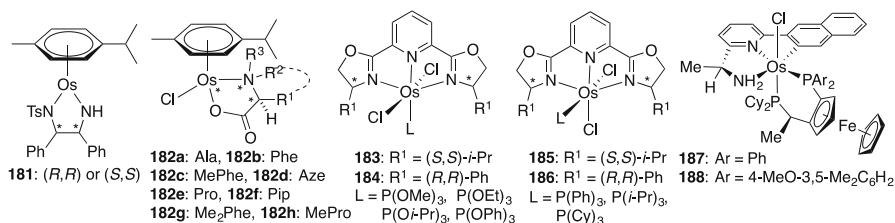
Fig. 58 Osmium(II) catalyst for ATH of ketones

microwave method, combining the dimer $[OsCl_2(\eta^6\text{-}p\text{-cymene})]_2$ with chiral diamines, (1R,2R)-(H)TsDPEN or (1S,2S)-(H)TsDPEN. When tested for the ATH of acetophenone-derived substrates, a (R,R)-configuration of the precatalyst established the reduction on the Re-face of ketone functionality, while a (S,S)-analogue was selective for the Si-face, producing the corresponding alcohols in high yields and ees up to 98 %. Among the L-α-amino carboxylates complexes **182** (Fig. 58), the proline derivative and its cationic trimer were found to be the most active providing the chiral alcohols in moderate ees [171]. Concerning the pybox complexes, the i-Pr-pybox osmium derivatives **183** and **185** displayed higher efficiency than the corresponding Ph-pybox precatalysts **184** and **186** [172]. This is in sharp contrast to the results obtained by analogous ruthenium–pybox complexes for which the Ph–pybox complexes are the most active precatalysts [173]. A pincer-type osmium system **188** [84] enabled the ATH of simple alkyl aryl ketones and acetylpyridines with TOF between $0.51\text{–}9.0 \times 10^5$ h^{-1} with good yields (up to 99 %) and ees ranging from 91 to 99 %, producing the corresponding (R)-alcohols.

Although there have been some successful examples of iron complexes as catalysts for TH and ATH of ketones, other first-row transition metals, such as Ni and Co complexes, are still rare. Nickel has been used for TH either under homogeneous [174, 175] or heterogeneous conditions [176–178], mostly for aromatic carbonyl substrates. A heterogeneous Ni/CeO_2 catalytic system for TH of ketones was recently introduced by Shimisu et al. [179], enabling the TH of a variety of aliphatic and (hetero)aromatic ketones in excellent yields. Gao et al. developed an asymmetric version of a nickel precatalyst with (S,S)-PNNP ligands for the ATH of ketones. This catalyst enabled good conversions of simple aryl alkyl ketones to the corresponding chiral alcohols with moderate enantioselectivity [180]. A cobalt complex of structure $[(PNHPCy)Co(CH_2SiMe_3)]BAr_4$ was shown to be an active precatalyst for TH of a variety of ketones [181]. The cobalt complex was a viable precatalyst for the TH of aromatic ketones bearing electron-donating or electron-withdrawing substituents. Aliphatic ketones were efficiently reduced using a similar procedure, with 2-hexanol being obtained in 95 % yield at 80 °C. For conjugated substrates, such as trans-4-phenyl-3-buten-2-on or cinnamaldehyde, TH with i-PrOH resulted in the complete reduction of both functionalities, C=C and C=O bonds. There is a recent example of a $CpMo(PMe_3)_3H$ complex capable of effecting TH of carbonyl compounds, namely RCHO (R = Me, i-Pr), RC(O)Me (R = Me, i-Pr, t-Bu, Ph), and Ph_2CO, using formic acid as the reducing reagent [182]. These investigations demonstrate that molybdenum hydride compounds may have potential regarding TH reactions using formic acid.

4 Green Approach to Transfer Hydrogenation

4.1 Catalysis in Water

The interest in green chemistry tools has become increasingly significant because of many potential advantages. The rise of green chemistry has also drawn attention to synthetic procedures that promote atom economy and the use of nontoxic reagents

and solvents. In this regard, ATH has developed to the stage where green solvents such as water or, e.g., glycerol become solvents of choice. In the last decade, numbers of Ru, Rh, and Ir homogeneous and heterogeneous catalysts for ATH in water have been developed. The first transition-metal-catalysed TH in water was described by Bényei and Joó using water-soluble monosulfonated triphenylphosphine ligand to achieve the reduction of aldehydes [183]. Wu and Xiao developed efficient and selective catalytic systems for TH and ATH of carbonyl compounds in water [184, 185]. During the application of a poly(ethylene glycol) (PEG)-supported Ru(II) complex, it was noted that catalyst recycling via solvent extraction of the chiral alcohol product was very efficient when water was present as the co-solvent [122, 186]. This observation encouraged researchers to examine the behaviour of sulfonamide ligands in acetophenone reduction by HCO_2Na in water. The reduction was significantly faster than in an organic solvent and provided excellent enantioselectivities [187]. The catalysts were in general generated from the ligands and the metal precursor ($[RuCl_2(p\text{-cymene})]_2$) in water without adding base. These precatalysts showed varying solubilities in water and in general they showed higher solubility in ketones and alcohols. Monosulfonated diamines **189–192** (Fig. 59) all performed the ATH of ketones in water efficiently, with high conversions and *ee*s up to 99 %, which were reached in short reaction times [188–190]. The ligands **189** and **192** were found to be superior under the given reaction conditions concerning enantioselectivity. In comparison with ATH in the azeotropic mixture of HCO_2H/NEt_3 with or without water, ATH in aqueous HCO_2Na is much faster [187, 188]. It was clearly shown that the pH of the solution plays an important role and is critical to the reaction rate and enantioselectivity. Thus, efficient ATH can be achieved with HCO_2H/NEt_3 in water, provided that the ratio of HCO_2H to NEt_3 is controlled in such a way that the pH is close to neutral [188]. β-Amino alcohol ligands were believed to be unsuitable for ATH in the presence of formic acid [191]; however, simple β-amino alcohol ligands **193–195** (Fig. 59) catalyse the ATH of acetophenones by HCO_2Na or HCO_2H/NEt_3 in water [192], albeit with slow rates and lower enantioselectivities than those obtained by diamine ligands.

An accurate computational study of the role of water in the TH of formaldehyde with a Ru(II)-based catalyst using a water-specific model suggests that the reaction
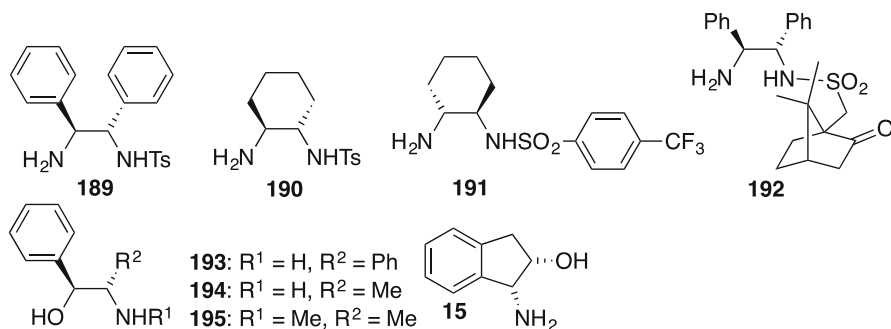
**Fig. 59** Ligands used in Ru(II)-catalysed ATH in water
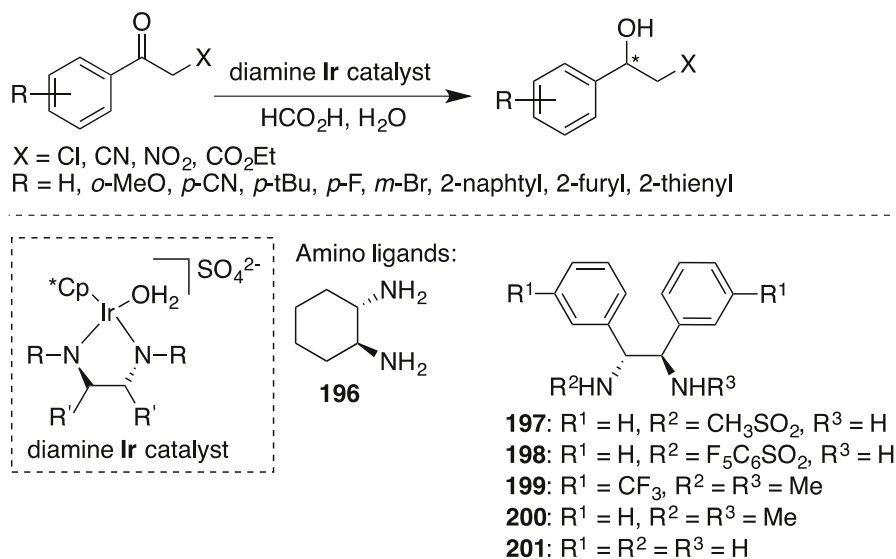
Fig. 60 Ir(III) moisture- and air-stable aqua complexes for ATH of ketones

mechanism in aqueous solution is considerably different from that in the gas phase or in methanol solution [193]. In aqueous solution, a concerted transition state is observed, though only the hydride is transferred at this point, whereas the proton transfer happens later by a water molecule instead of involving the catalyst.

Carreira et al. introduced a series of aqua Ir(III) moisture and air stable complexes with outstanding performance in the ATH of prochiral ketones in water (Fig. 60). The complexes **196–201** were readily synthesised from the Ir(III) trihydrate precursor [Cp*Ir(H$_2$O)$_3$]SO$_4$ in water/methanol medium at room temperature. The ligands **198** [194] and **199** [195] were found to be highly reactive in the ATH of α-substituted ketones, leading to excellent enantioselectivities (up to 99 % ee) of the corresponding alcohol products. Additionally, pH-independent ATH of β-keto esters in water with formic acid was achieved by applying the catalyst **197**, which was found to be superior to its fluorinated N-sulfonyl counterparts **198** and **199** [196]. The reaction tolerates substrates with both electron-donating and -withdrawing substituents in the *para-* and *meta-*positions; however, the *orto-*substituents significantly reduced enantioselectivity [e.g. ethyl (R)-3-hydroxy-3-(4-nitrophenyl)propanoate was obtained in 99 % yield and 87 % ee].

Recently, it has been shown by Xiao et al. that cyclometalated iridium(III) complexes can be "switched on" by controlling the solution pH to function as catalysts for the TH of carbonyl compounds in water using formate as the hydrogen source. Substituted benzophenones as well as alkyl aryl and dialkyl ketones were reduced in high yields (79–99 %) using 0.05 mol% of catalyst **202** (Fig. 61) [197]. Catalysts **203** and **204** were examined in the chemoselective TH of various α-substituted ketones, keto esters, and α,β-unsaturated aldehydes in water [198]. It was clearly shown that the pH of the reaction solution plays the crucial role, and pH
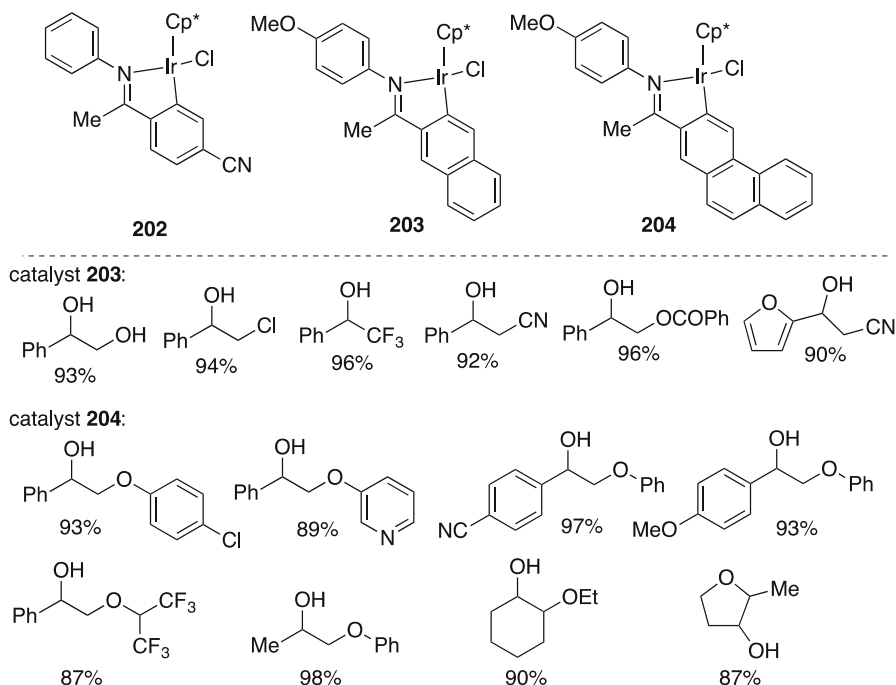
Fig. 61 Ir(III) metalacyclic complexes as TH catalysts

4.5 was found to be optimal. A wide range of β-keto esters and ethyl 2-oxopropanoate, ethyl 2-oxopropanoate, and ethyl 2-oxo-2-phenylacetate were chemoselectively reduced in high yields (91–96 %) to the corresponding α- and β-hydroxyesters applying 0.1 mol% of the catalyst **3**. With the cyclometalated complex **203**, which is slightly more active than **204** (Fig. 61), α-substituted acetophenones were reduced in high yields to the corresponding benzyl alcohols. The Ir(III) catalyst **3** was still capable (0.01 mol% loading) of reducing all types of β-aryl ketone aryl ethers; however, neither electron-withdrawing substituents nor electron-donating groups on the aryl ring of either ketones and ethers significantly affected the productivity and selectivity of the catalyst.

To unreveal some limitations concerning the solubility, catalytic activity and/or selectivity on going from an organic solvent to water as a reaction media, several water-soluble ligands/catalysts have been explored in recent years. Simple chiral *N*-tosylated diaminoligands were synthesised and used in Ru(II)-, Rh(III)-, and Ir(III)-catalysed TH of ketones. Ligands **205** and **206** (Fig. 62) exhibited excellent catalytic activity in the case of enantioselective reduction of ketones and imines; however, both ligands failed to be efficiently reused [199]. The cationic diguanidinium ligand **206** was explored in combination with Rh(III), Ir(III), and Ru(II) metal complexes to form precatalysts in water. The Rh(III) in situ-formed precatalyst exhibited the best reactivity and enantioselectivitiy in an aqueous solution of sodium formate at 28 °C [200]. A range of aromatic ketones, particularly
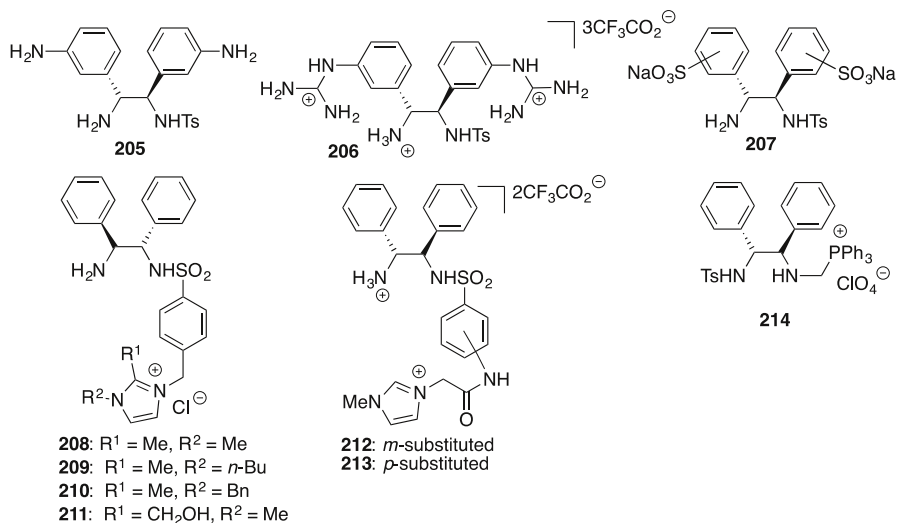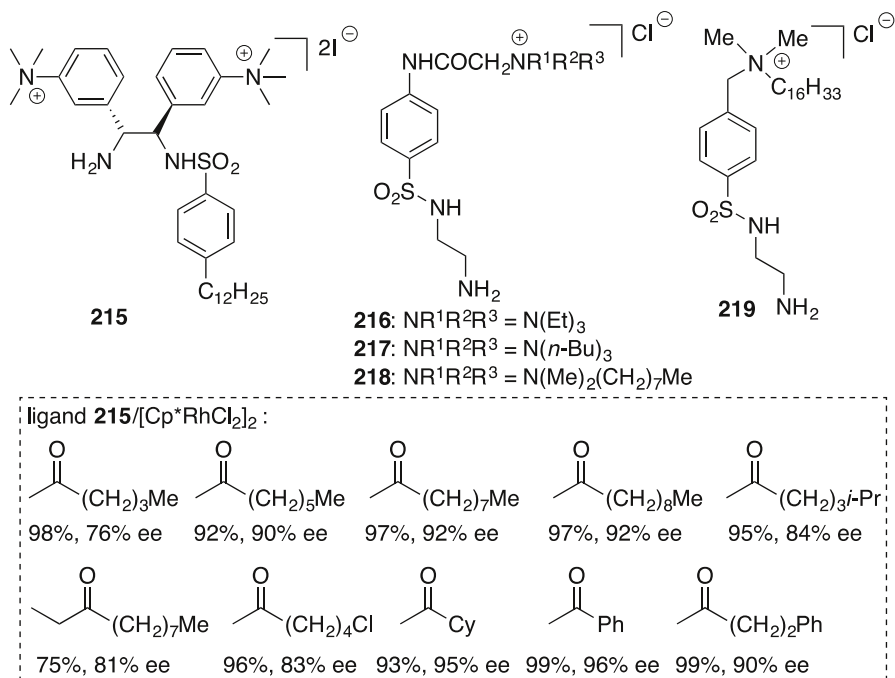
**Fig. 62** Water-soluble ligands in ATH of ketones

α-bromomethylaromatic ketones, were efficiently converted to the corresponding alcohols employing disulfonated water-soluble ligands of type **207** and $NaHCO_2$ as the hydrogen source [201, 202]. Considerable enhancement of activity was noticed in the presence of the cationic surfactants, cetyltrimethylamonium bromide (CTAB) and cetylpyridine bromide (CPB). When CPB was used as a surfactant, the water-soluble ligands **207** could be recycled 21 times without loss of high conversion and enantioselectivity. The imidazolium ion-tethered TsDPEN ligands **208–213** (Fig. 62) were used in Rh(III)- and Ru(II)-catalysed ATH of ketones in water. Ligand **211** was found to form an efficient ATH precatalyst in combination with $[Cp*RhCl_2]_2$ and $NaHCO_2$ as a hydride donor in water. Acetophenones with electron-donating groups at the C-3 and C-4 positions gave the highest *ee* values of 97–98 % with relatively low reaction rates; on the other hand, electron-withdrawing substituents at C-4 and C-3, C-5-disubstituted analogues gave the corresponding chiral alcohols in slightly lower *ee*s with high reaction rates and conversions. C-2 substituted acetophenones resulted in low *ee* values (67–73 %) [203]. Analogous water-soluble ligands **212** and **213** formed active water-soluble precatalysts when combined with $[RuCl_2(p\text{-cymene})]_2$ in water. The catalytic system showed high catalytic activity and excellent enantioselectivities (85–98 % *ee*) for 4-substituted acetophenones [204]. Wills et al. prepared triazole-functionalised TsDPEN derivatives on a soluble polymer support [125]. The best catalyst of the series reduced acetophenone in 24 h at 40 °C with 94 % *ee*. Tetraarylphosphonium (TAP) salts have been reported as solubility-control groups for reagents, ligands, and catalysts. This technology has also been applied for the ATH of prochiral ketones. Adolfsson reported on a lipophilic Rh catalyst which reduced aryl alkyl ketones with high enantioselectivity (up to 97 %) in water in the presence of sodium dodecylsulfonate [205]. A Noyori–Ikariya TAP-supported recyclable catalyst was

explored by Charette et al. for ATH applications in water [206]. The ligand **214** (Fig. 62) was readily synthesised via a three-step synthetic procedure starting from 4-bromobenzaldehyde. A precatalyst was formed in situ before catalysis with 0.6 equiv. [RuCl$_2$(*p*-cymene)]$_2$ in water at 40 °C and a mixture of HCO$_2$H and Et$_3$N in the ratio 1.2:1, as optimum, was used as the hydrogen source. The catalytic system enabled the reduction of acetophenone in 3 h with complete conversion and *ee* of 95.7 %. Interestingly, 1′-indanone, acethyltiophene and tetralone provided the best enantioselectivities with 96.8, 95.5 and 98.1 %, respectively. However, the catalyst was found to have limited recyclability.

Only a few examples of surface-active catalysts that can promote aqueous TH by improving both the catalytic reaction and the mass transfer between the reagents have been described. An amphiphilic-polymer-based iridium catalytic system that can assemble at the interface of emulsion droplets showed a significant acceleration rate in the ATH of aldehydes in water [207]. Recently, Deng et al. described TsDPEN-based chiral surfactant-type ligands **215** (Fig. 63) in micellar rhodium catalysis, with higher *ee* values in ATH of the plethora of aryl, alkyl, and dialkyl ketones compared to nonmicellar analogues [208]. Additionally, two types of 2-aminoethyl(*p*-tosyl)amide ligands with Et$_3$N, OctMe$_2$N, and Bu$_3$N substituents were investigated [209, 210]. The precatalyst were generated in situ by reacting ligands **216–218** with [RuCl$_2$(*p*-cymene)]$_2$ or [(Cp*)IrCl$_2$]$_2$ in neat water at 80 °C for 1 h. Various aldehydes, including electron-deficient and electron-rich, were

Fig. 63 Surfactant-type ligands in ATH of ketones
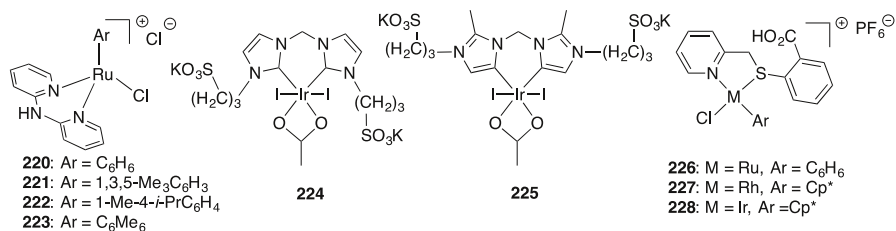
Fig. 64 Well-defined achiral water soluble Ru, Rh, and Ir complexes

reduced with high conversions and chemoselectivity using HCO_2Na in water. The ligand **219** containing the trialkyl ammonium group (Fig. 63) was used to synthesise Ru(II) and Rh(III) water-soluble catalysts for the water-phase TH of acetophenone as a model substrate. The Ru(II) and Rh(III) complexes with **219** ligand form micelles and are densely adsorbed at the water–substrate interface, where they strongly enhance the rate of TH of ketones with formate in water compared to analogues with shorter alkyl chains [211].

Several well-defined achiral water-soluble Ru, Rh, and Ir complexes were prepared and their potential in the TH reaction of carbonyls in water was explored. Dipyridylamine ruthenium complexes **220–223** (Fig. 64) were found to successfully reduce acetophenone in a water solution of HCO_2H and $NaHCO_3$ at 65 °C. The best results were obtained at pH 3.8 for equimolar ratio $HCO_2H/NaHCO_3$ (5 equiv. excess to the substrate). The reactivity of chloro complexes **220–223** depends on the nature of the ancillary arene ligand among which the catalyst **222** was found to be the most reactive, enabling the reduction of aryl ketones with good to excellent conversions [212]. Iridium and ruthenium *N*-heterocyclic carbene complexes have been tested in the TH of several carbonyl substrates using glycerol as solvent and hydrogen donor. The Ir(III) complexes **224** and **225** were the most efficient due to their solubility in the reaction media [213]. The half-sandwich Ru, Rh, and Ir complexes **227** and **228** (Fig. 64) were also found to be successful catalysts for TH in water/glycerol reaction medium. The complexes are water soluble due to the presence of a carboxylic functional group, and they efficiently catalyse pH-independent TH of standard aromatic ketones to the corresponding alcohols [214].

4.2 Catalysis in Ionic Liquids

Ionic liquids (ILs) have attracted considerable attention as environmentally benign reaction media. By the proper variation of their anionic and cationic parts, their physical properties, such as vapour pressure, thermal stability, and solvation strength, can easily be fine-tuned [215]. Although, the ILs are widely used as environmentally benign solvents in high-pressure catalysis, there are only a few examples of their application in TH reactions of carbonyls. Berthold et al. [216] first reported the application of ILs as reaction media for TH of ketones and their α,β-unsaturated derivatives. Hermecz et al. reported the reduction of chalchone and α,β-unsaturated carbonyl derivatives by using $[ClRh(PPh_3)_3]$ and $[Rh(cod)Cl]_2$

complexes in imidazolium, ammonium, and phosphonium containing ILs. Outstanding chemoselectivities depending on the nature of the anions of ILs provided the corresponding ketones with excellent yields and TOF of 2.5–20 h^{-1} at 90 °C [217]. Recyclable ruthenium catalysts prepared from ionic chiral aminosulfonamide ligands **212** and **213** (Fig. 62), which were used in the ATH of prochiral ketones in water, were also tested in [bmim][PF$_6$] ionic liquid. The catalytic system provided excellent conversions and high enantioselectivities of simple acetophenones. The presence of the IL enables the catalyst to be readily removed from the product by extraction into a low polarity solvent and reused several times [218]. Recently, several different γ-valerolactone-based IL were investigated as alternative reaction media for TH of ketones, facilitating good conversions of substituted acetophenones (60–99 %) and simple aliphatic ketones (96–99 %) to the corresponding alcohols [219].

Another approach in the application of ILs in TH reactions is to incorporate an ionic liquid structural framework into the ligand structure aiming for better catalyst selectivity and especially for efficient catalyst recovery. (Arene)Ru(II) complexes based on IL phosphinite ligands **229a–d** (Fig. 65) were prepared and tested in TH of various ketones in propan-2-ol [220]. The catalyst enabled good conversions of substituted acetophenones (95–99 %) and simple aliphatic ketones (e.g. cyclohexanone, cyclopentanone, 4-methylpentan-2-one, and dielhylketone) in *i*-PrOH at 80 °C. Sulfonated chiral diamine ligand anion-based functionalised IL has recently been reported for ATH of acetophenones in a HCO$_2$H/Et$_3$N azeotrope mixture at 40 °C providing the corresponding chiral alcohols in 86–96 % *ees* [221]. The catalyst could be recycled five times without major loss of activity and enantioselectivity. Hydrophilic coordinating chiral IL with an amino alcohol substructure **230–232** (Fig. 65) offers an attractive alternative to conventional ligands in ATH. When employed as a source of chirality in ATH of prochiral
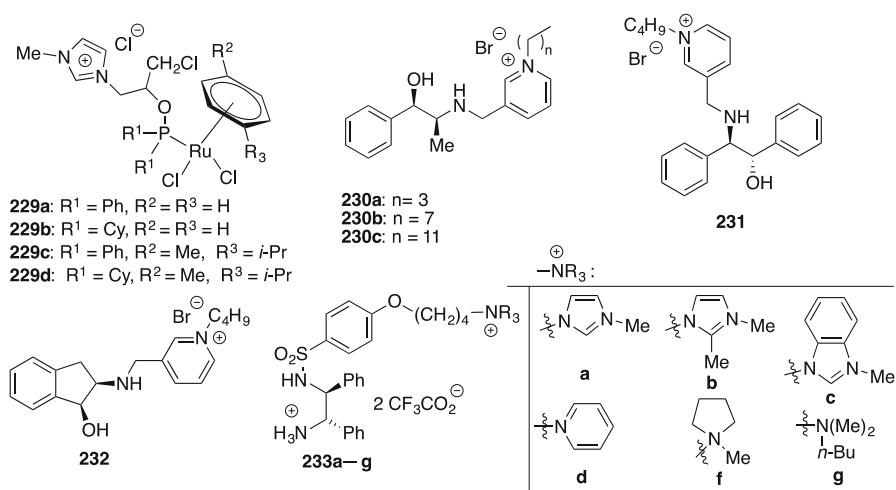

Fig. 65 Ionic liquid type of ligands for the ATH of ketones

ketones, the chiral IL **230–232** provided reasonable yields and *ee*s (e.g. acetophenone 97 and 75 % *ee*, propiophenone 30 and 65 % *ee*, 1-indanone 71 and 85 % *ee*, 1-acetonaphtone 85 and 71 % *ee*) [222]. A (*S,S*)-DPEN chiral ligand was connected to quaternary ammonium functional groups in order to improve the interaction of the Ru(II) precatalyst in IL as the medium for ATH of ketones. Among a variety of TsDPEN derivatives **233a–g** (Fig. 65) with attached different ionic moieties, **233a**, having an imidazolium group, showed the best results in using HCO_2H/Et_3N as the hydrogen source and [bmim][PF$_6$] IL as the reaction medium [223].

5 Practical Applications of Asymmetric Transfer Hydrogenations

Catalytic TH of ketones, in particular asymmetric versions, has been at the forefront of research due to the importance of optically active alcohols as intermediates for pharmaceuticals and agrochemicals. In this context, the seminal research of Noyori on ATH mediated by *N*-sulfonated diamine-η^6-arene ruthenium catalysts represents a breakthrough, changing ATH into a viable, efficient, and cost-effective technology. Among the most outstanding advances, in terms of molar substrate to catalyst ratio (S/C), are the tethered catalysts of type **234** (Fig. 66) introduced by Wills and Ikariya. Another advance in the field of TH includes the development of ruthenium catalysts containing monoanionic meridional *NNC*-ligands (e.g. complex **235**; Fig. 66), characterised by TOF over 10^5 h^{-1} and S/C 20,000.

However, industrially, the most widely applied ATH catalysts are Noyori-type catalysts such as **26**. An asymmetric and cost-effective route to (+)-erythro Mefloquine·HCl, the single enantiomer of the commercially available racemate used for the treatment of malaria, was developed by Bryant et al., starting from pyridyl quinolinyl ketone using catalyst (*S,S*)-**26** (Fig. 66) [224]. The corresponding alcohol, which was later determined to be (*S*)-(+)-**237** [225, 226], was obtained in 91 % yield and 98 % *ee* (Fig. 67, reaction 1). Okano et al. developed ATH of 3-trifluoromethylacetophenone applying (*S,S*)-**26** as an ATH precatalyst to produce (*S*)-1-(3-trifluoromethylphenyl)ethanol **238** (Fig. 67, reaction 2) (99 %, 93 % *ee*) as a key intermediate for the synthesis of a wide-spectrum agricultural fungicide, (*S*)-MA20565 [159]. The robust nature of this particular process was demonstrated by pilot plant validation on a 100-kg scale (91 % *ee*, 98 % yield). Merck used a Ru-(1*S*,2*R*)-1-amino-2-indanol-catalysed ATH to obtain the (*R*)-alcohol intermediate
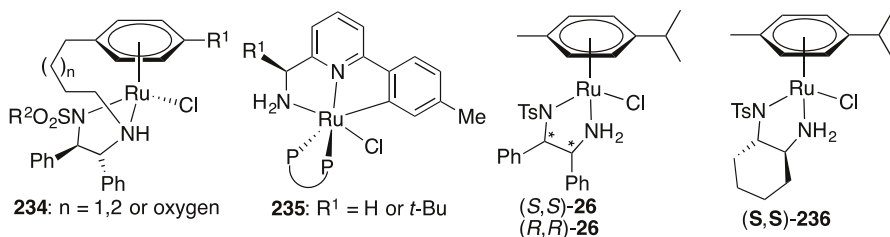
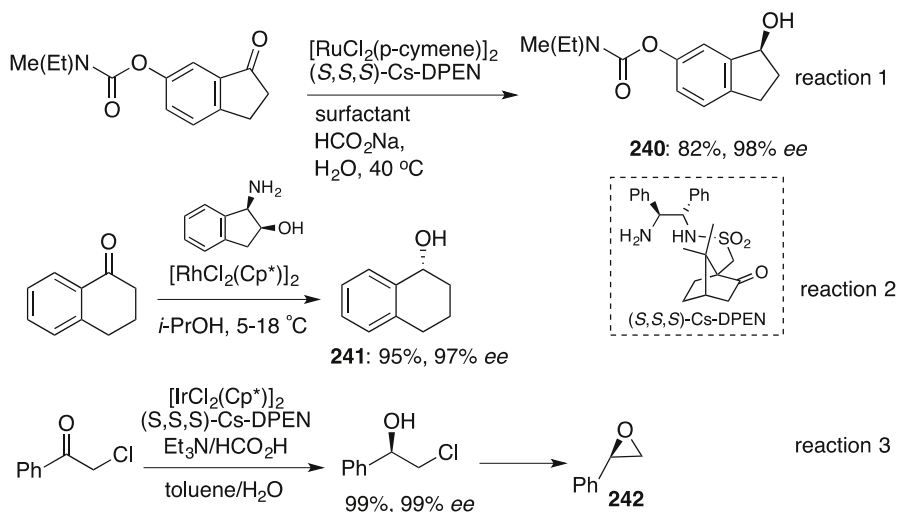**Fig. 66** Industrially most applicable ATH catalysts
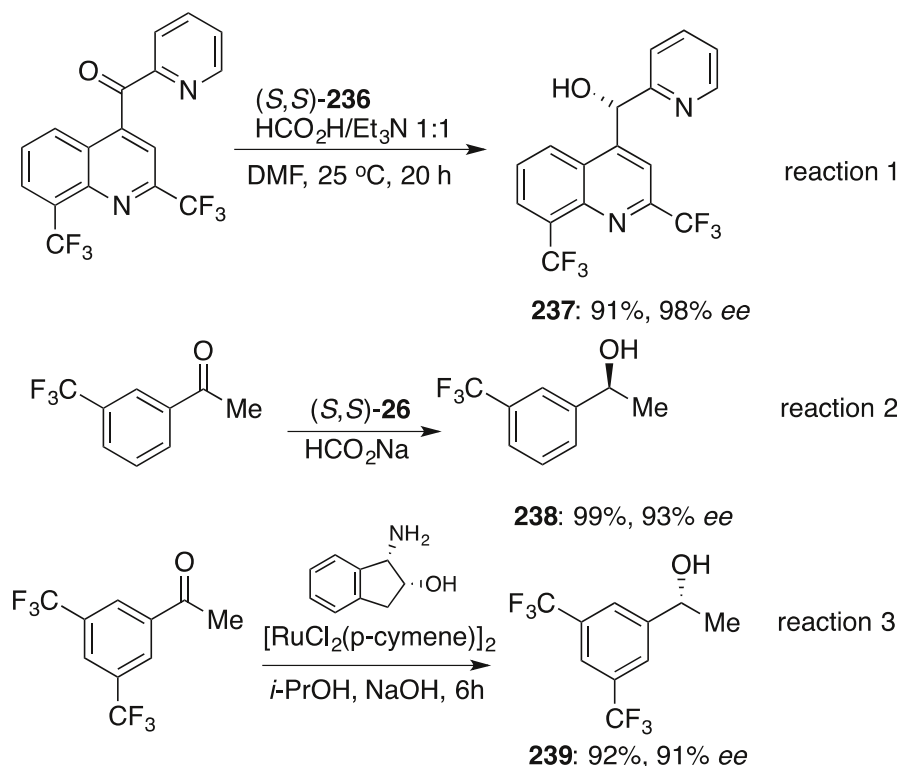
Fig. 67 Industrial applications of the ATH for the synthesis of enantio-enriched alcohol intermediates

for Aprepitant (an NK-1 receptor antagonist) in 92 % yield and 91 % *ee* (Fig. 67, reaction 3) [151, 227]. In comparison, asymmetric reduction of the 1-(3,5-bis(trifluoromethyl)phenyl)ethan-1-one with oxazaborolidine-catalysed borane reduction [(S)-Me-CBS/BH$_3$·PhNEt$_2$] gave the product in 97 % yield and 95 % *ee* [151]. Avecia also has an ATH process for the same compound using Cp*RhCl(TSDPEN) as catalyst and Et$_3$N/HCO$_2$H as hydrogen donor for 100-kg-scale production of **238**, an intermediate for Vestipitant, another NK1-receptor antagonist [228].

An intermediate for the synthesis of the Alzheimer's drug, Ladostigil (TV3326), was produced by applying (S,S)-TsDPEN or (S,S,S)-Cs-DPEN RuCl(p-cymene) precatalysts and the HCO$_2$Na/H$_2$O system as the hydrogen donor (Fig. 68, reaction 1). The corresponding (S)-derivative of 2,3-dihydro-1*H*-inden-1-ol **240** was obtained under optimised reaction conditions in 82 % yield and 98 % *ee* [229]. Two more industrial examples of ATH processes deserve attention. The first is the rhodium-catalysed synthesis of (R)-tetralol (**241**) (Fig. 68, reaction 2) [228]. To achieve the best yield and enantioselectivity, the researchers investigated ways to remove acetone, the by-product that causes the reverse reaction. By running the reaction under reduced pressure (1–1.5 kPa) and maintaining the concentration of

Fig. 68 Industrial applications of the ATH for the synthesis of enantio-enriched alcohol intermediates

the reaction mixture constant, the researchers were able to produce (*R*)-tetralol in 95 and 97 % *ee*. The second example is the multi-hundred-kilogram-scale production of styrene oxide (**242**) [228]. In this case, the catalyst **26** was investigated, and high enantioselectivity was observed (95 % *ee*), but the catalytic activity was not high enough (S/C = 100, 60 % conversion after 16 h) to be economically feasible. Alternatively, Rh and Ir catalysts were proven to be more effective. The iridium precatalyst Cp*IrCl[(*S,S,S*)-Cs-DPEN] enabled the full conversion of the starting material with a substrate to catalyst ratio of 1000 and with >99 % *ee* (Fig. 68, reaction 3).

An additional example of ATH of ketones in industrial processes is the total synthesis of the drug, Dorzolamide·HCl, indicated for the treatment of high intraocular pressure. A Ru(II)-catalysed ATH process has been developed by ZaCh System-Zambon Chemicals [230]. The complex (*S,S*)-**26** (Fig. 66) efficiently controls the stereoselectivity affording the (*S,S*)-hydroxy sulfone with high selectivity (98 % *de* and 99.9 % *ee* after isolation) (Fig. 69).

Recently, ATH methodology was applied for the asymmetric reduction of achiral purine derivatives to attain chiral acyclonucleosides, important intermediates for the synthesis of Tenofovir and its analogues. Purine derivatives were reduced using an in situ-generated catalytic system form, [RuCl$_2$(C$_6$H$_6$)]$_2$ complex, and chiral prolinol derivative **244** as a ligand. Intermediate (*R*)-1-(6-amino-9*H*-purin-9-yl)propan-2-ol (**245**) was obtained in good yield and 93 % *ee* (Fig. 70) [231].

High-throughput, multi-dimensional substrate–catalyst screening was described by Adolfsson et al. for the ATH of heteroaryl alkyl ketones. The evaluated ruthenium and rhodium precatalysts were derived from a library of modular amino acid-based ligands. The results of screening were used as a key step in the formal synthesis of the antidepressant drugs, (*R*)-Fluoxetine and (*S*)-Duloxetine. The ATH
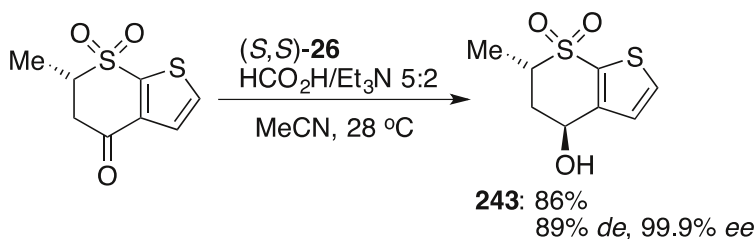
Fig. 69 Application of the ATH in the synthesis of Dorzolamide·HCl
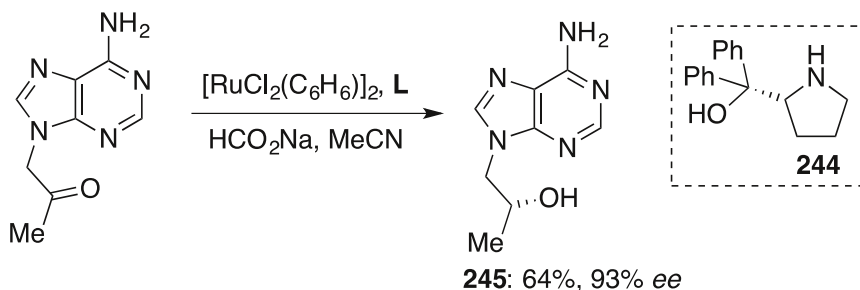
**Fig. 70** Application of the ATH in the synthesis of Tenofovir and its analogues
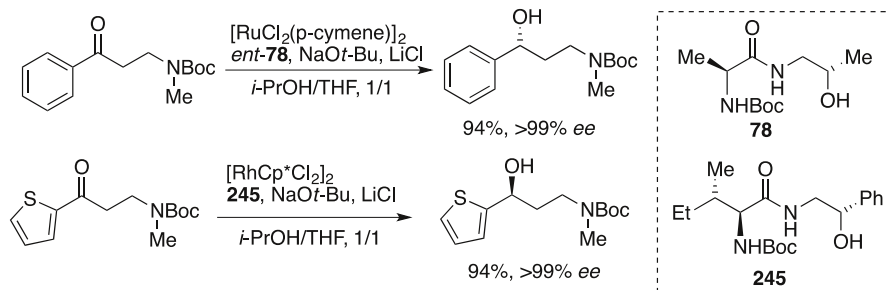
Fig. 71 ATH approach to (*R*)-Fluoxetine and (*S*)-Duloxetine intermediates

with the optimised precatalysts (ruthenium and rhodium) resulted in excellent enantioselectivities (>99 % *ee*) of 1,3-amino alcohol intermediates (Fig. 71) [232].

Most recently, Komiyama et al. [233] applied an oxo-tethered ruthenium(II) complex for an efficient and scalable enantioselective synthesis of the intermediate for a β2-adrenergic receptor antagonist. The intermediate, (*R*)-2-amino-1-oxyethyl-1,2-dihydroquinolin-2-one derivative, was obtained with 71 % yield and 98.6 % *ee* on large-scale production.

Asymmetric TH of ketones is often applied as a key synthetic step in the synthesis of chiral natural products or valuable small-molecule inhibitors of enzymes. Recent selected examples of natural products and small-molecule
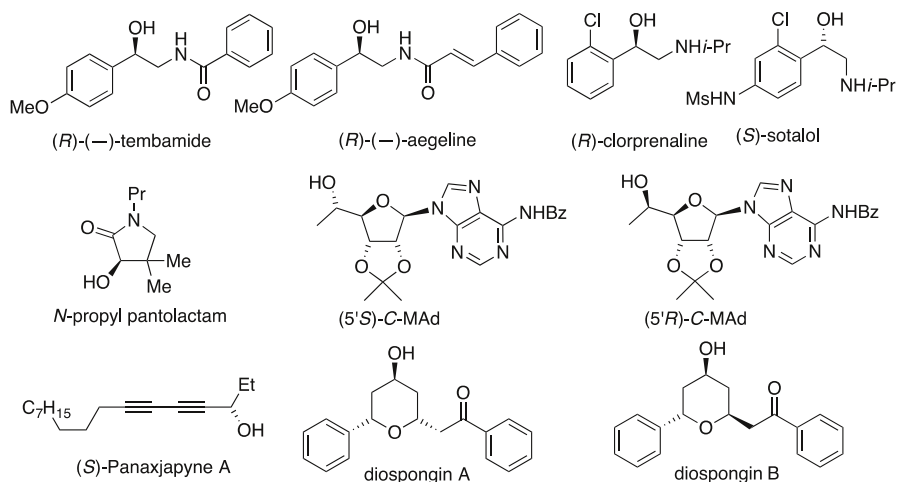
Fig. 72 Selected examples of chiral natural products or valuable small-molecule inhibitors in which the ATH was a key synthetic step

inhibitors are shown in Fig. 72, in which ATH of ketones was successfully applied, enabling the synthesis of the corresponding enantio-enriched alcohols. (*R*)-Tembamide and (*R*)-Aegeline, natural products isolated from *Fagara hyemalis* and *Aegele marmelos*, respectively, were obtained in *ee* > 99 % using (*S,S*)-**236** ruthenium complex [234]. The ruthenium precatalyst (*S,S,S*)-Cs-DPEN was used by Li et al. to synthesise (*R*)-2-chloro-1-(2-chlorophenyl)ethanol (93 % yield and 99.7 *ee*) and (*S*)-2-bromo-1-(4-nitrophenyl)ethanol (88 % yield and 93 % *ee*) as intermediates for the synthesis of (*R*)-Clorprenaline and (*S*)-Sotalol [235]. The Noyori–Ikariya precatalysts, Ru-TsDPEN (*S,S*)-**26** or (*R,R*)-**26** in combination with HCO$_2$H/Hünig's base were used for the ATH of *N*-substituted α-ketopantolactam. *N*-Propyl pantolactam was successfully prepared at a 2-kg scale with excellent chemical yield and chiral purity (95 % *ee*) (Fig. 72) [236]. (5′*S*)- and (5′*R*)-C-Methyladenosines, which are precursors for the important structural probes in molecular biology and enzymology, were synthesised by ATH from corresponding methyl ketones. The corresponding products (5′*S*)-C-MAd and (5′*R*)-C-MAd (Fig. 72) were obtained in high diastereomeric ratio [(5′*S*)/(5′*R*) = 95:5 from (*S,S*)-**26** and (5′*R*)/(5′*S*) = 8:92 from (*R,R*)-**26**] replacing the HCO$_2$H/Et$_3$N system with aqueous HCO$_2$Na as a stoichiometric reductant [237]. Total synthesis of diospongins A and B and their enantiomers was achieved by applying an asymmetric hetero-Diels–Alder reaction followed by ATH of the corresponding ketones [238]. Recently, it was demonstrated that ATH using (*S,S*)-**234** or (*S,S*)-**26** ruthenium precatalysts could be successfully applied for the asymmetric reduction of diynones to approach enantio-enriched diynols in high conversions and *ee*s up to 97 %. The methodology was demonstrated by the total synthesis of (*S*)-panaxjapyne A, which was obtained in 96 % *ee* [239].

6 Conclusions

We have discussed the transition-metal-catalysed TH of ketones, with emphasis on asymmetric versions which provide optically active secondary alcohols. Because of a plethora of TH metal catalyst systems, only prominent and interesting examples which have been found in the literature over the past decade are given. Among the most active and selective, yet numerous, catalysts are still those based on ruthenium, approaching the enzymatic performance in some cases, and delivering the chiral secondary alcohols in near-quantitative *ee*s. In this regard, Nojoyri and Ikariya were the pioneers who introduced their powerful bifunctional (arene)(diamine)ruthenium catalysts. However, there are two negative aspects of using ruthenium, its high price and toxicity, which reduce its attractiveness for future use, and at the same time demand the development of new catalysts to replace the precious metals. Here, iron stands out, since it is a cheap and ubiquitous metal, and its traces in final chemical products are not as serious a problem as traces of ruthenium. To date, the only iron catalysts that can challenge platinum metal ATH catalysts on both activity and selectivity were developed by Morris and Mezzetti. On the other hand, nickel and cobalt complexes, being capable of performing efficient TH of ketones, are still rare, and therefore the research interest in developing catalyst systems based on other metals is highly desirable. As a consequence of increasing interest for ''greener'' processes, the development of catalytic systems that can operate in water has been of great importance. While there is limited solubility of catalysts and organic substrates in water, the enhancement of hydrogenation rates and selectivities can be observed in selected examples by using micellar systems. Ionic liquids as solvents for THs also contribute to user-friendly applications because of their non-volatility, non-flammabiltiy and low toxicity. Since asymmetric TH catalysts use optically pure ligands to efficiently induce stereochemistry of the secondary alcohol products, the high price can be the limiting factor of their mass use. Here, naturally occurring compounds, for example sugars and amino acids, can serve as cheap and structurally different chiral backbones for more economical ligand production. While homogeneous TH is still prevalent exhibiting excellent activity and stereoselectivity, the interest in heterogeneous catalysis is constantly growing. Heterogeneous catalysts offer much better reusability; however, they can usually not compete with *ee*s obtained by homogeneous analogues, and, additionally, the substrate scope is still narrow. Although there are a great many catalytic systems based on platinum metals that are very active and can produce secondary alcohols in high stereoselectivity, when looking towards industrial applications and specific substrate characteristics there is always the need to develop novel catalyst systems or fine-tune existing ones.

References

1. Blaser HU, Malan C, Pugin B, Spindler F, Steiner H, Studer M (2003) Adv Synth Catal 345:103
2. Ohkuma T (2010) Proc Jpn Acad B 86:202

3. Arai N, Ohkuma T (2011) In: Molander GA (ed) Science of synthesis: stereoselective synthesis, vol 2. Thieme, Stuttgart, pp 9–57
4. Noyori R, Ohkuma T (2001) Angew Chem Int Ed 40:40
5. Klingler FD (2007) Acc Chem Res 40:1367
6. Palmer MJ, Wills M (1999) Tetrahedron Asymmetry 10:2045
7. Ikariya T, Blacker AJ (2007) Acc Chem Res 40:1300
8. Václavík J, Kačer P, Kuzma M, Červený L (2011) Molecules 16:5460
9. Gladiali S, Alberico E (2006) Chem Soc Rev 35:226
10. Hashiguchi S, Fujii A, Haack KJ, Matsumura K, Ikariya T, Noyori R (1997) Angew Chem Int Ed 36:288
11. Fujii A, Hashiguchi S, Uematsu N, Ikariya T, Noyori R (1996) J Am Chem Soc 118:2521
12. Zweifel T, Naubron JV, Büttner T, Ott T, Grützmacher H (2008) Angew Chem Int Ed 47:3245
13. Sharma AK, Joshi H, Sharma KN, Gupta PL, Singh AK (2014) Organometallics 33:3629
14. Maytum HC, Tavassoli B, Williams JMJ (2007) Org Lett 9:4387
15. Nixon TD, Whittlesey MK, Williams JMJ (2011) Tetrahedron Lett 52:6652
16. Guyon C, Métay E, Duguet N, Lemaire M (2013) Eur J Org Chem 5439
17. Schmidt R, Meerwein H (1925) Justus Liebigs Ann Chem 444:221
18. Verley A (1925) Bull Soc Fr 37:537
19. Ponndorf W (1926) Angew Chem 39:138
20. Doering WE, Young RW (1950) J Am Chem Soc 72:631
21. Haddad YMY, Henbest HB, Husbands J, Mitchell TRB (1964) Proc Chem Soc Lond 361
22. Henbest HB, Mitchell TRB (1970) J Chem Soc C 785
23. Sasson Y, Blum J (1975) J Org Chem 40:1887
24. Chowdhury RL, Bäckvall JE (1991) J Chem Soc Chem Commun 1063
25. Shvo Y, Czarkie D, Rahamim Y, Chodosh DF (1986) J Am Chem Soc 108:7400
26. Conley BL, Pennington-Boggio MK, Boz E, Williams TJ (2010) Chem Rev 110:2294
27. Manzini S, Blanco CAU, Nolan SP (2012) Adv Synth Catal 354:3036
28. Liu PN, Ju KD, Lau CP (2011) Adv Synth Catal 353:275
29. Kumar M, DePasquale J, White NJ, Zeller M, Papish ET (2013) Organometallics 32:2135
30. Ghoochany LT, Farsadpour S, Sun Y, Thiel WR (2011) Eur J Inorg Chem 3431
31. Zhao M, Yu Z, Yan S, Li Y (2009) Tetrahedron Lett 50:4624–4628
32. Zhao M, Yu Z, Yan S, Li Y (2009) J Organomet Chem 694:3068
33. Jin W, Wang L, Yu Z (2012) Organometallics 31:5664
34. Deng H, Yu Z, Dong J, Wu S (2005) Organometallics 24:4110
35. Zhu Z, Zhang J, Fu H, Yuan M, Zheng X, Chen H, Li R (2014) RSC Adv 4:52734
36. Du W, Wang L, Wu P, Yu Z (2012) Chem Eur J 18:11550
37. Zhang Y, Li X, Hong SH (2010) Adv Synth Catal 352:1779
38. Clapham SE, Hadzovic A, Morris RH (2004) Coord Chem Rev 248:2201
39. Samec JSM, Bäckvall JE, Andersson PG, Brandt P (2006) Chem Soc Rev 35:237
40. Hashiguchi S, Fujii A, Takehara J, Ikariya T, Noyori R (1995) J Am Chem Soc 117:7562
41. Palmer M, Walsgrove T, Wills M (1997) J Org Chem 62:5226
42. Alonso DA, Guijarro D, Pinho P, Temme O, Andersson PG (1998) J Org Chem 63:2749
43. Yamakawa M, Yamada I, Noyori R (2001) Angew Chem Int Ed 40:2818
44. Noyori R, Yamakawa M, Hashiguchi S (2001) J Org Chem 66:7931
45. Yamakawa M, Ito H, Noyori R (2000) J Am Chem Soc 122:1466
46. Alonso DA, Brandt P, Nordin SJM, Andersson PG (1999) J Am Chem Soc 121:9580
47. Brandt P, Roth P, Andersson PG (2004) J Org Chem 69:4885
48. Casey CP, Johnson JB (2003) J Org Chem 68:1998
49. Pàmies O, Bäckvall JE (2001) Chem Eur J 7:5052
50. Dub PA, Ikariya T (2013) J Am Chem Soc 135:2604
51. Martins JED, Clarkson GJ, Wills M (2009) Org Lett 11:847
52. Soni R, Cheung FK, Clarkson GC, Martins JED, Graham MA, Wills M (2011) Org Biomol Chem 9:3290
53. Baratta W, Rigo P (2008) Eur J Inorg Chem 4041
54. Everaere K, Mortreux A, Carpentier JF (2003) Adv Synth Catal 345:67
55. Roszkowski P, Maurin JK, Czarnocki Z (2012) Tetrahedron Asymmetry 23:1106
56. Roszkowski P, Maurin JK, Czarnocki Z (2013) Tetrahedron Asymmetry 24:643
57. Soni R, Collinson JM, Clarkson GC, Wills M (2011) Org Lett 13:4304

Ⓐ Springer

58. Cheung FK, Lin C, Minissi F, Crivillé AL, Graham MA, Fox DJ, Wills M (2007) Org Lett 9:4659
59. Fang Z, Wills M (2013) J Org Chem 78:8594
60. Touge T, Hakamata T, Nara H, Kobayashi T, Sayo N, Saito T, Kayaki Y, Ikariya T (2011) J Am Chem Soc 133:14960
61. Cheung FK, Graham MA, Minissi F, Wills M (2007) Organometallics 26:5346
62. Kišić A, Stephan M, Mohar B (2013) Org Lett 15:1614
63. Kišić A, Stephan M, Mohar B (2014) Adv Synth Catal 356:3193
64. Hayes AM, Morris DJ, Clarkson GJ, Wills M (2005) J Am Chem Soc 127:7318
65. Facchetti G, Gandolfi R, Fusé M, Zerla D, Cesarotti E, Pellizzoni M, Rimoldi I (2015) New J Chem 39:3792
66. Takehara J, Hashiguchi S, Fujii A, Inoue S, Ikariya T, Noyori R (1996) Chem Commun 233
67. Deshpande SH, Kelkar AA, Gonnade RG, Shingote SK, Chaudhari RV (2010) Catal Lett 138:231
68. Chakka SK, Andersson PG, Maguire GEM, Kruger HG, Govender T (2010) Eur J Org Chem 972
69. Han ML, Hu XP, Huang JD, Chen LG, Zheng Z (2011) Tetrahedron Asymmetry 22:222
70. Huynh KD, Ibrahim H, Kolodziej E, Toffano M, Vo-Thanh G (2011) New J Chem 35:2622
71. Pastó M, Riera A, Pericàs MA (2002) Eur J Org Chem 2337
72. Babin M, Clément R, Gagnon J, Fontaine FG (2012) New J Chem 36:1548
73. Johnson TC, Totty WG, Wills M (2012) Org Lett 14:5230
74. Darwish MO, Wallace A, Clarkson GJ, Wills M (2013) Tetrahedron Lett 54:4250
75. Cambeiro XC, Pericàs MA (2011) Adv Synth Catal 353:113
76. Sheeba MM, Tamizh M, Farruiga LJ, Endo A, Karvembu R (2014) Organometallics 33:540
77. Ye W, Zhao M, Yu Z (2012) Chem Eur J 18:10843
78. Ito J, Teshima T, Nishiyama H (2012) Chem Commun 48:1105
79. Reetz MT, Li X (2006) J Am Chem Soc 128:1044
80. Wettergren J, Buitrago E, Ryberg P, Adolfsson H (2009) Chem Eur J 15:5709
81. Lundberg H, Adolfsson H (2011) Tetrahedron Lett 52:2754
82. Coll M, Pàmies O, Adolfsson H, Diéguez M (2011) Chem Commun 47:12188
83. Baratta W, Chelucci G, Herdtweck E, Magnolia S, Siega K, Rigo P (2007) Angew Chem Int Ed 46:7651
84. Baratta W, Benedetti F, Del Zotto A, Fanfoni L, Felluga F, Magnolia S, Putignano E, Rigo P (2010) Organometallics 29:3563
85. Zirakzadeh A, Schuecker R, Gorgas N, Mereiter K, Spindler F, Weissensteiner W (2012) Organometallics 31:4241
86. Işık U, Aydemir M, Meriç N, Durap F, Kayan C, Temel H, Baysal A (2013) J Mol Catal A 379:225
87. Spogliarich R, Zassinovich G, Kaspar J, Graziani M (1982) J Mol Catal 16:359
88. Malacea R, Poli R, Manoury E (2010) Coord Chem Rev 254:729
89. Tang L, Wang Q, Wang J, Lin Z, Wang X, Cun L, Yuan W, Zhu J, Lia J, Deng J (2012) Tetrahedron Lett 53:3839
90. Fuentes JA, Carpenter I, Kann N, Clarke ML (2013) Chem Commun 49:10245
91. Xu YQ, Yu SL, Li YY, Dong ZR, Gao JX (2013) Chin Chem Lett 24:527
92. Liu WP, Yuan ML, Yang XH, Li K, Xie JH, Zhou QL (2015) Chem Commun 51:6123
93. Pannetier N, Sortais JB, Issenhuth JT, Barloy L, Sirlin C, Holuigue A, Lefort L, Panella L, de Vries JG, Pfeffer M (2011) Adv Synth Catal 353:2844
94. Coll M, Ahlford K, Pàmies O, Adolfsson H, Diéguez M (2012) Adv Synth Catal 354:415
95. Coll M, Pàmies O, Diéguez M (2014) Adv Synth Catal 356:2293
96. Coll M, Pàmies O, Adolfsson H, Diéguez M (2013) ChemCatChem 5:3821
97. Tinnis F, Adolfsson H (2010) Org Biomol Chem 8:4536
98. Aupoix A, Bournaud C, Vo-Thanh G (2011) Eur J Org Chem 2772
99. Cross DJ, Houson I, Kawamoto AM, Wills M (2004) Tetrahedron Lett 45:843
100. Matharu DS, Morris DJ, Kawamoto AM, Clarkson GJ, Wills M (2005) Org Lett 7:5489
101. Hamada T, Torii T, Izawa K, Ikariya T (2004) Tetrahedron 60:7411
102. Matharu DS, Morris DJ, Clarkson GJ, Wills M (2006) Chem Commun 3232
103. Echeverria PG, Férard C, Phansavath P, Ratovelomanana-Vidal V (2015) Catal Commun 62:95
104. Baiker A (2015) Chem Soc Rev 44:7449
105. Boerner A, Krause HW, Kortus K (1988) React Kinet Catal Lett 36:103
106. Sarkar SM, Yusoff MM, Rahman ML (2015) J Chin Chem Soc 62:177
107. Liu R, Cheng T, Kong L, Chen C, Liu G, Li H (2013) J Catal 307:55
108. Bai S, Yang H, Wang P, Gao J, Li B, Yang Q, Li C (2010) Chem Commun 46:8145

109. Lettau K, Warsinke A, Katterle M, Danielsson B, Scheller FW (2006) Angew Chem Int Ed 45:6986
110. Weng Z, Muratsugu S, Ishiguro N, Ohkoshi S, Tada M (2011) Dalton Trans 40:2338
111. Zhang H, Jin R, Yao H, Tang S, Zhuang J, Liu G, Li H (2012) Chem Commun 48:7874
112. Gao F, Jin R, Zhang D, Liang Q, Ye Q, Liu G (2013) Green Chem 15:2208
113. Xu Y, Cheng T, Long J, Liu K, Qian Q, Gao F, Liu G, Li H (2012) Adv Synth Catal 354:3250
114. Long J, Liu G, Cheng T, Yao H, Qian Q, Zhuang J, Gao F, Li H (2013) J Catal 298:41
115. Cheng TY, Zhuang JL, Yao H, Zhang HS, Liu GH (2014) Chin Chem Lett 25:613
116. Shen Y, Chen Q, Lou LL, Yu K, Ding F, Liu S (2010) Catal Lett 137:104
117. Lou LL, Du H, Shen Y, Yu K, Yu W, Chen Q, Liu S (2014) Microporous Mesoporous Mater 187:94
118. Wei J, Zhang X, Zhang X, Zhao Y, Li R, Yang Q (2014) ChemCatChem 6:1368
119. Zhang X, Zhao Y, Peng J, Yang Q (2015) Green Chem 17:1899
120. Liu R, Jin R, Kong L, Wang J, Chen C, Cheng T, Liu G (2013) Chem Asian J 8:3108
121. Wang R, Wan J, Ma X, Xu X, Liu L (2013) Dalton Trans 42:6513
122. Li X, Wu X, Chen W, Hancock FE, King F, Xiao J (2004) Org Lett 6:3321
123. Shan W, Meng F, Wu Y, Mao F, Li X (2011) J Organomet Chem 696:1687
124. Zhou Z, Ma Q (2011) Appl Organomet Chem 25:233
125. Zammit CM, Wills M (2013) Tetrahedron Asymmetry 24:844
126. Sun Q, Jin Y, Zhu L, Wang L, Meng X, Xiao FS (2013) Nano Today 8:342
127. Marcos R, Jimeno C, Pericàs MA (2011) Adv Synth Catal 353:1345
128. Dimroth J, Keilitz J, Schedler U, Schomäcker R, Haag R (2010) Adv Synth Catal 352:2497
129. Elias S, Goren K, Vigalok A (2012) Synlett 23:2619
130. Wang W, Wang Q (2010) Chem Commun 46:4616
131. Tang S, Jin R, Zhang H, Yao H, Zhuang J, Liu G, Li H (2012) Chem Commun 48:6286
132. Michalek F, Lagunas A, Jimeno C, Pericàs MA (2008) J Mater Chem 18:4692
133. Gao X, Liu R, Zhang D, Wu M, Cheng T, Liu G (2014) Chem Eur J 20:1515
134. Sun Y, Liu G, Gu H, Huang T, Zhang Y, Li H (2011) Chem Commun 47:2583
135. Zoabi A, Omar S, Abu-Reziq R (2015) Eur J Inorg Chem 2101
136. Bianchini C, Farnetti E, Graziani M, Peruzzini M, Polo A (1993) Organometallics 12:3753
137. Enthaler S, Erre G, Tse MK, Junge K, Beller M (2006) Tetrahedron Lett 47:8095
138. Sui-Seng C, Freutel F, Lough AJ, Morris RH (2008) Angew Chem Int Ed 47:940
139. Mikhailine AA, Lough AJ, Morris RH (2009) J Am Chem Soc 131:1394
140. Meyer N, Lough AJ, Morris RH (2009) Chem Eur J 15:5605
141. Sui-Seng C, Haque FN, Hadzovic A, Pütz AM, Reuss V, Meyer N, Lough AJ, Zimmer-De Iuliis RH, Morris RH (2009) Inorg Chem 48:735
142. Sonnenberg JF, Coombs N, Dube PA, Morris RH (2012) J Am Chem Soc 134:5893
143. Mikhailine AA, Morris RH (2010) Inorg Chem 49:11039
144. Sues PE, Lough AJ, Morris RH (2011) Organometallics 30:4418
145. Lagaditis PO, Lough AJ, Morris RH (2010) Inorg Chem 49:10057
146. Lagaditis PO, Lough AJ, Morris RM (2011) J Am Chem Soc 133:9662
147. Mikhailine AA, Maishan MI, Lough AJ, Morris RH (2012) J Am Chem Soc 134:12266
148. Zuo W, Lough AJ, Li YF, Morris RH (2013) Science 342:1080
149. Zuo W, Tauer S, Prokopchuk DE, Morris RH (2014) Organometallics 33:5791
150. Zuo W, Morris RH (2015) Nat Protoc 10:241
151. Brands KMJ, Payack JF, Rosen JD, Nelson TD, Candelario A, Huffman MA, Zhao MM, Li J, Craig B, Song ZJ, Tschaen DM, Hansen K, Devine PN, Pye PJ, Rossen K, Dormer PG, Reamer RA, Welch CJ, Mathre DJ, Tsou NN, McNamara JM, Reider PJ (2003) J Am Chem Soc 125:2129
152. Rautenstrauch V, Hoang-Cong X, Churlaud K, Abdur-Rashid K, Morris RH (2003) Chem Eur J 9:4954
153. Smith SA, Morris RH (2015) Synthesis 47:1775
154. Chen JS, Chen LL, Xing Y, Chen G, Shen WY, Dong ZR (2004) Acta Chimi Sin 62:1745
155. Yu S, Shen W, Li Y, Dong Z, Xu Y, Li Q, Zhang J, Gao J (2012) Adv Synth Catal 354:818
156. Li Y, Yu S, Wu X, Xiao J, Shen W, Dong Z, Gao J (2014) J Am Chem Soc 136:4031
157. Bigler R, Huber R, Mezzetti A (2015) Angew Chem Int Ed 54:5171
158. Tanaka K, Katsurada M, Ohno F, Shiga Y, Oda M, Miyagi M, Takehara J, Okano K (2000) J Org Chem 65:432
159. Miyagi M, Takehara J, Collet S, Okano K (2000) Org Process Res Dev 4:346
160. Naik A, Maji T, Reiser O (2010) Chem Commun 46:4475
161. Hopewell JP, Martins JED, Johnson TC, Godfrey J, Wills M (2012) Org Biomol Chem 10:134

162. Mohan Kandepi VVK, Cardoso JMS, Peris E, Royo B (2010) Organometallics 29:2777
163. Bata P, Notheisz F, Kluson P, Zsigmond A (2014) Appl Organomet Chem 29:45
164. Sánchez-Delgado RA, Rosales M, Esteruelas MA, Oro LO (1995) J Mol Catal A 96:231
165. Schlünken C, Esteruelas MA, Lahoz FJ, Oro LA, Werner H (2004) Eur J Inorg Chem 2477
166. Carmona Dlamata MP, Viguri F, Dobrinovich I, Lahoz FJ, Oro LA (2002) Adv Synth Catal 344:499
167. Faller JW, Lavoie AR (2001) Org Lett 3:3703
168. Baratta W, Ballico M, Del Zotto A, Siega K, Magnolia S, Rigo P (2008) Chem Eur J 14:2557
169. Slade AT, Lensink C, Falshaw A, Clark GR, Wright LJ (2014) Dalton Trans 43:17163
170. Coverdale JPC, Sanchez-Cano C, Clarkson GJ, Soni R, Wills M, Sadler P (2015) Chem Eur J 21:8043
171. Carmona D, Lahoz FJ, García-Orduña P, Oro LA (2012) Organometallics 31:3333
172. Vega E, Lastra E, Gamasa MP (2013) Inorg Chem 52:6193
173. Cuervo D, Gamasa MP, Gimeno J (2004) Chem Eur J 10:425
174. Le Page MD, James BR (2000) Chem Commun 1647
175. Phukan P, Sudalai A (2000) Synth Commun 30:2401
176. Upadhya TT, Katdare SP, Sabde DP, Ramaswamy V, Sudalai A (1997) Chem Commun 1119
177. Mohapatra SK, Sonavane SU, Jayaram RV, Selvam P (2002) Org Lett 4:4297
178. Alonso F, Riente P, Yus M (2011) Acc Chem Res 44:379
179. Shimura K, Shimizu K (2012) Green Chem 14:2983
180. Dong ZR, Li YY, Yu SL, Sun GS, Gao JX (2012) Chin Chem Lett 23:533
181. Zhang G, Hanson SK (2013) Chem Commun 49:10151
182. Neary MC, Parkin G (2015) Chem Sci 6:1859
183. Bényei A, Joó F (1990) J Mol Catal 58:151
184. Wu X, Wang C, Xiao J (2010) Platin Met Rev 54:3
185. Wei Y, Wu X, Wang C, Xiao J (2015) Catal Today 247:104
186. Li X, Chen W, Hems W, King F, Xiao J (2004) Tetrahedron Lett 45:951
187. Wu X, Li X, Hems W, King F, Xiao J (2004) Org Biomol Chem 2:1818
188. Wu X, Li X, King F, Xiao J (2005) Angew Chem Int Ed 44:3407
189. Wu X, Vinci D, Ikariya T, Xiao J (2005) Chem Commun 41:4447
190. Wu X, Liu J, Di Tommaso D, Iggo JA, Catlow CRA, Bacsa J, Xiao J (2008) Chem Eur J 14:7699
191. Wills M, Hannedouche J (2002) Curr Opin Drug Discov Dev 5:881
192. Wu X, Li X, McConvill M, Saidi O, Xiao J (2006) J Mol Catal A 247:153
193. Pavlova A, Meijer EJ (2012) ChemPhysChem 13:3496
194. Soltani O, Ariger MA, Vázquez-Villa H, Carreira EM (2010) Org Lett 12:2893
195. Vázquez-Villa H, Reber S, Ariger MA, Carreira EM (2011) Angew Chem Int Ed 50:8979
196. Ariger MA, Carreira EM (2012) Org Lett 14:4522
197. Wei Y, Xue D, Lei Q, Wang C, Xiao J (2013) Green Chem 15:629
198. Talwar D, Wu X, Saidi O, Poyatos Salguero N, Xiao J (2014) Chem Eur J 20:12835
199. Li L, Wu J, Wong F, Liao J, Zhang H, Lian C, Zhu J, Deng J (2007) Green Chem 9:23
200. Tang Y, Li X, Lian C, Zhu J, Deng J (2011) Tetrahedron Asymmetry 22:1530
201. Ma Y, Liu H, Chen L, Cui X, Zhu J, Deng J (2003) Org Lett 5:2103
202. Li J, Li X, Ma Y, Wu J, Wang F, Xiang J, Zhu J, Wang Q, Deng J (2013) RCS Adv 3:1825
203. Kang G, Lin S, Shiwakoti A, Ni B (2014) Catal Commun 57:111
204. Zhou Z, Sun Y (2009) Catal Commun 10:1685
205. Ahlford K, Lind J, Mäler L, Adolfsson H (2008) Green Chem 10:832
206. Zimbron JM, Dauphinais M, Charette AB (2015) Green Chem 17:3255
207. Li J, Zhang Y, Han D, Jia G, Gao J, Zhong L, Li C (2008) Green Chem 10:608
208. Li J, Tang Y, Wang Q, Li X, Cun L, Zhang X, Zhu J, Li L, Deng J (2012) J Am Chem Soc 134:18522
209. Zhou Z, Ma Q, Zhang A, Wu L (2011) Appl Organomet Chem 25:856
210. Huo H, Zhou Z, Zhang A, Wu L (2012) Res Chem Intermed 38:261
211. Kalsin AM, Peganova TA, Novikov VV, Zhamoytina AI, Gonsalvi L, Peruzzini M (2014) Chem Eur J 20:846
212. Romain C, Gaillard S, Elmkaddem MK, Toupet L, Fischmeister C, Thomas CM, Renaud J-L (2010) Organometallics 29:1992
213. Azua A, Mata JA, Peris E (2011) Organometallics 30:5532
214. Prakash O, Joshi H, Sharma KN, Lal Gupta P, Singh AK (2014) Organometallics 33:3804
215. Olivier-Bourbigou H, Magna L, Morvan D (2010) Appl Catal A 373:1

216. Berthold H, Schotten T, Hönig H (2002) Synthesis 11:1607
217. Baán Z, Finta Z, Keglevich G, Hermecz I (2009) Green Chem 11:1937
218. Zhou Z, Sun Y, Zhang A (2011) Cent Eur J Chem 9:175
219. Strádi A, Molnár M, Szakál P, Dibó G, Gáspár D, Mika LT (2015) RCS Adv 5:72529
220. Aydemir M, Rafikova K, Kystaubayeva N, Pasa S, Meric N, Ocak YS, Zazybin A, Temel H, Gürbüz N, Özdemir I (2014) Polyhedron 81:245
221. Liu X, Chen C, Xiu Y, Chen A, Guo L, Zhang R, Chen J, Hou Z (2015) Catal Commun 67:90
222. Vasiloiu M, Gaertner P, Zirbs R, Bica K (2015) Eur J Org Chem 2374
223. Uchimoto H, Tsuji T, Kawasaki I, Arimitsu K, Yasui H, Yamashita M, Ohta S, Nishide K (2015) Chem Pharm Bull 63:200
224. Hems WP, Jackson WP, Nightingale P, Bryant R (2012) Org Process Res Dev 16:461
225. Zhou G, Liu X, Liu X, Nie H, Zhang S, Chen W (2013) Adv Synth Catal 355:3575
226. Müller M, Orben CM, Schützenmeister N, Schmidt M, Leonov A, Reinscheid UM, Dittrich B, Griesinger C (2013) Angew Chem Int Ed 52:6047
227. Hansen KB, Chilenski JR, Desmond R, Devine PN, Grabowski EJJ, Heid R, Kubryk M, Mathre DJ, Varsolona R (2003) Tetrahedron Asymmetry 14:3581
228. Blacker AJ, Thompson P (2010) In: Blaser H-U, Federsel H-J (eds) Asymmetric Catalysis on Industrial Scale. Wiley-VHC, Weinheim, p 265
229. Luo Z, Qin F, Yan S, Li X (2012) Tetrahedron Asymmetry 23:333
230. Volpicelli R, Andretto M, Cotarca L, Nardi A, Verzini M (2012) WO2012120086 A1 to ZaCh System SpA
231. Zhang Q, Ma B-W, Wang Q-Q, Wang X-X, Hu X, Xie M-S, Qu G-R, Guo H-M (2014) Org Lett 16:2014
232. Buitrago E, Lundberg H, Andersson H, Ryberg P, Adolfsson H (2012) ChemCatChem 4:2082
233. Komiyama M, Itoh T, Takeyasu T (2015) Org Process Res Dev 19:315
234. Cortez NA, Aguirre G, Parra-Hake M, Somanathan R (2013) Tetrahedron Asymmetry 24:1297
235. Lu C, Luo Z, Huang L, Li X (2011) Tetrahedron Asymmetry 22:722
236. Zhang J, Blazecka PG, Bruendl MM, Huang Y (2009) J Org Chem 74:1411
237. Bligh CM, Anzalone L, Jung YC, Zhang Y, Nuget WA (2014) J Org Chem 79:3238
238. Kumaraswamy G, Ramakrishna G, Naresh P, Jagadeesh B, Balasubramanian S (2009) J Org Chem 74:8468
239. Fang Z, Wills M (2014) Org Lett 16:374

CrossMark

REVIEW

Imino Transfer Hydrogenation Reductions

Martin Wills[1]

Abstract   This review contains a summary of recent developments in the transfer hydrogenation of C=N bonds, with a particularly focus on reports from within the last 10 years and asymmetric transformations. However, earlier work in the area is also discussed in order to provide context for the more recent results described. I focus strongly on the Ru/TsDPEN class of asymmetric transfer hydrogenation reactions originally reported by Noyori et al., together with examples of their applications, particularly to medically valuable target molecules. The recent developments in the area of highly active imine-reduction catalysts, notably those based on iridium, are also described in some detail. I discuss diastereoselective reduction methods as a route to the synthesis of chiral amines using transfer hydrogenation. The recent development of a methodology for positioning reduction complexes within chiral proteins, permitting the generation of asymmetric reduction products through a directed modification of the protein environment in a controlled manner, is also discussed.

Keywords   Transfer · Hydrogenation · Imine · Amine · Reduction · Asymmetric

1 Introduction

In recent years, a significant amount of research has been carried out on the transfer hydrogenation of C=N bonds using complexes based on a range of metals, but most frequently on the use of ruthenium, iridium and rhodium. Many of the advances have

✉ Martin Wills
    m.wills@warwick.ac.uk

1   The Department of Chemistry, Warwick University, Coventry CV4 7AL, UK

∂ Springer

been in the use of asymmetric catalysts for this process, and several of these are closely related to similar catalysts for asymmetric hydrogenation using hydrogen gas as a reagent. In addition, the combination of organometallic reagents with organocatalysts has been developed, as has the use of purely organocatalytic processes. A large number of synthetic applications, notably to pharmaceutical targets, have been reported.
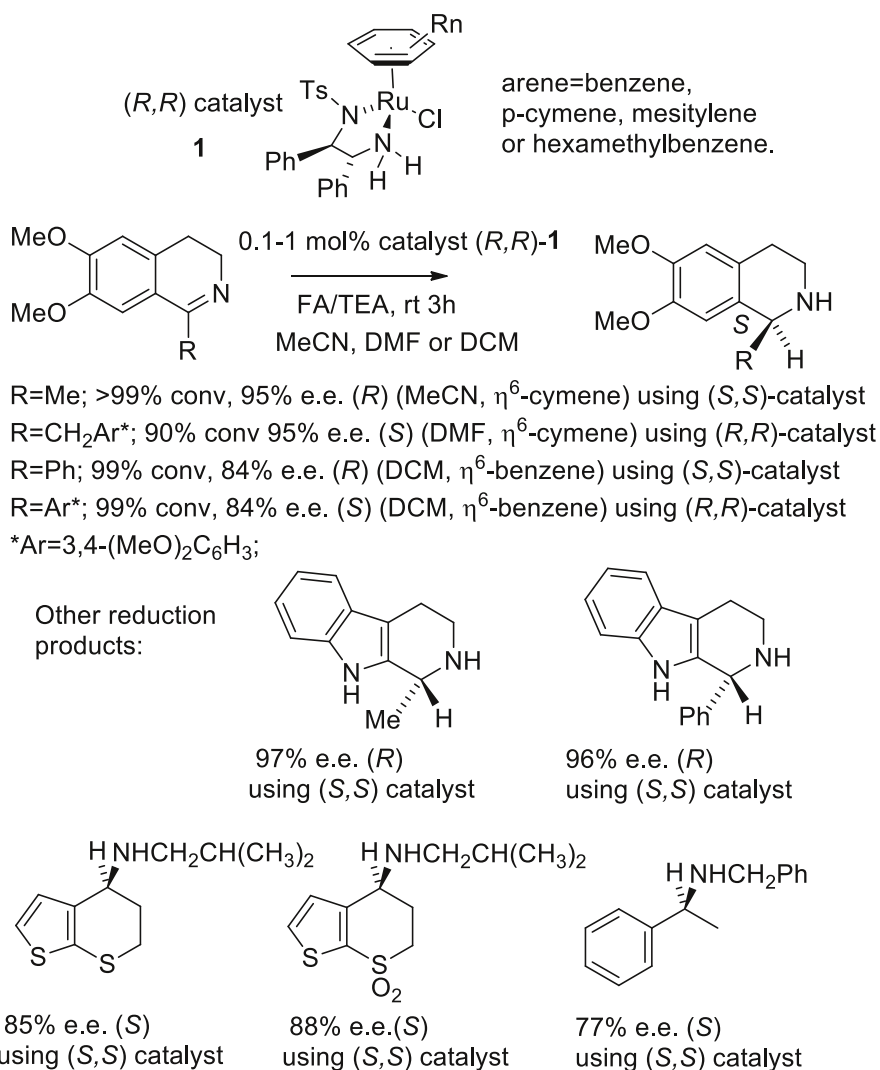
The objective of this review is not to recount the early history of the transfer hydrogenation of C=N bonds, including asymmetric versions, because this has been reported adequately in a range of other reviews [1–14]. In addition, the mechanisms of the reactions have been discussed in detail. Hence, whilst some recap is valuable in order to set the newer results into appropriate context, this review will focus primarily, although not exclusively, on newer developments in this area, reported in the last 10 years, i.e. since and including 2005. I will also focus on the *applications* of C=N reduction which have been reported and the development of *asymmetric* methods and catalysts for this process. These will be distinguished by abbreviations for transfer hydrogenation (TH) and asymmetric transfer hydrogenation (ATH). The reducing agents (hydrogen sources) in the great majority of cases are either an alcohol (normally isopropanol—IPA—which is also used as the solvent), a combination of formic acid and trimethylamine (FA/TEA—usually used as a 5:2 azeotrope) or an aqueous solution of sodium formate (SF). The review will not cover hydrosilylation reactions, although some excellent reports have appeared in this area [15–17]. Organocatalysis, not involving a metal catalyst, is covered elsewhere in the volume and therefore not featured here, although some reviews that have been published on this are highlighted for context [18, 19].

2 Organometallic Catalysts for the Transfer Hydrogenation of Imines

2.1 TsDPEN/Ru and Related Organometallic Catalysts

Chemical methods for the TH of C=N bonds, and notably the reduction of imines to amines, have been known for many decades, early examples being the use of ruthenium complex $Ru_3(CO)_{12}$ [20] and $[RuCl_2(PPh_3)]$ [21]. In both cases, IPA was used as the reducing agent and a base was used to activate the catalyst. Relevant to the latter example, it was later demonstrated that $[RuH_2(PPh_3)]$ was an active TH catalyst which did not require added base [22, 23].

One of the most significant developments in imine ATH was reported in the mid-1990s, when Noyori et al. reported their results on the use of the now very well-established ruthenium complexes **1** of monotosylated 1,2-diamines in the asymmetric reduction of imines (Fig. 1) [24]. This important paper contained the first report of the application of this highly practical asymmetric catalyst for imine ATH. Of the series of catalysts tested, *trans*-1,2-diphenylethane-1,2-diamine (DPEN) formed the basis of the ligands, which could be created by converting just one of the amine groups to a sulfonamide, with a range of sulfonamides proving to be compatible. Of these, the monotosylated derivative (TsDPEN) is now probably the most widely used in the field. There is also some scope for variation of the η^6-arene ring, and its selection can significantly influence the activity and selectivity of the reductions.

(R,R) catalyst

1

arene=benzene,
p-cymene, mesitylene
or hexamethylbenzene.

0.1–1 mol% catalyst (R,R)-**1**

FA/TEA, rt 3h
MeCN, DMF or DCM

R=Me; >99% conv, 95% e.e. (R) (MeCN, η^6-cymene) using (S,S)-catalyst
R=CH$_2$Ar*; 90% conv 95% e.e. (S) (DMF, η^6-cymene) using (R,R)-catalyst
R=Ph; 99% conv, 84% e.e. (R) (DCM, η^6-benzene) using (S,S)-catalyst
R=Ar*; 99% conv, 84% e.e. (S) (DCM, η^6-benzene) using (R,R)-catalyst
*Ar=3,4-(MeO)$_2$C$_6$H$_3$;

Other reduction products:

97% e.e. (R)
using (S,S) catalyst

96% e.e. (R)
using (S,S) catalyst

85% e.e. (S)
using (S,S) catalyst

88% e.e.(S)
using (S,S) catalyst

77% e.e. (S)
using (S,S) catalyst

Fig. 1 Asymmetric transfer hydrogenation of imines using Ru/TsDPEN complexes

Although a range of C=N bond-containing substrates were described, Noyori et al.'s study revealed cyclic imines such as dihydroisoquinolines (DHIQs) and dihydro-β-carbolines (DHBs) to be excellent substrates. The reducing agent in this case was FA/TEA, and an organic co-solvent was required. Their paper contained an account of the application of the methodology to the synthesis of precursors of the Merck drug MK-0417. The reduction of acyclic substrates reported at this time, however, proceeded in lower enantioselectivity (Fig. 1; note that the general reaction outcome using the (R,R)-configuration catalyst is illustrated; examples were given of the use of both catalyst enantiomers).

This initial result generated a great deal of future work in this area; many examples of applications of related reductions of substrates containing C=N bonds have since been reported and will be described later.

Closely related catalysts containing TsDPEN and related ligands with alternative metals—most significantly rhodium (III) and iridium (III)—have also been developed. In these examples, an η^5-pentamethylcyclopentadienyl(Cp′) replaces the η^6-arene in order to maintain an isoelectronic structure. Although Rh(III) complexes of TsDPEN were first used in the ATH of ketones, Baker reported in 1999 the use of complex **2** in imine reduction. In the majority of cases, the selectivities were high, although some differences to the Ru(II) catalysts were also observed; for example, the reduction of aromatic-substituted (as opposed to alkyl-substituted) and acyclic imines gave products of very low e.e. (Fig. 2) [25]. The commercialization of the Rh(III) derivatives was undertaken by a team at Avecia, who developed optimized approaches to a range of reductions of phosphinoyl-substituted imines, described in a later section [26].

Progress has been made towards an understanding of the mechanism of reduction of imines using Ru(II) complexes of TsDPEN, and a number of kinetic studies have been carried out [27, 28]. Bäckwall et al. [29] demonstrated that the protonated imine was required for reduction by using the stoichiometric hydride reagent for the reduction; whilst the iminium salt of a cyclic imine was reduced by this hydride, the unprotonated imine was not.

N-Alkylated derivatives of the catalysts, i.e. **3a–3f**, also work well in the reductions of imines, provided that benzene is used as the η^6-ring on the Ru(II) [30]. In these studies, the imine substrates were reduced within hours, whilst the ketones required one or more days. Interestingly, the N-methylated complex **3a** was slightly more active than the 'parent' complex **1** (Fig. 3) [31], whereas the more hindered complexes were less active. In all cases, the same product enantiomer was formed
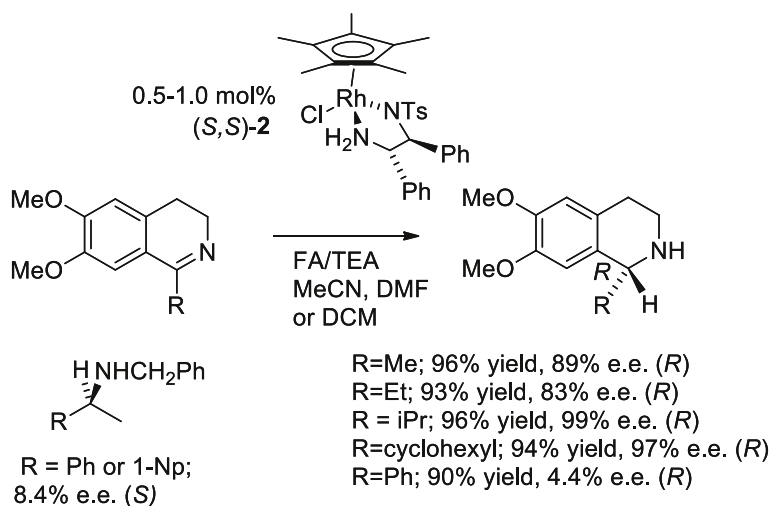
Fig. 2 Asymmetric transfer hydrogenation of imines using Rh/TsDPEN complexes
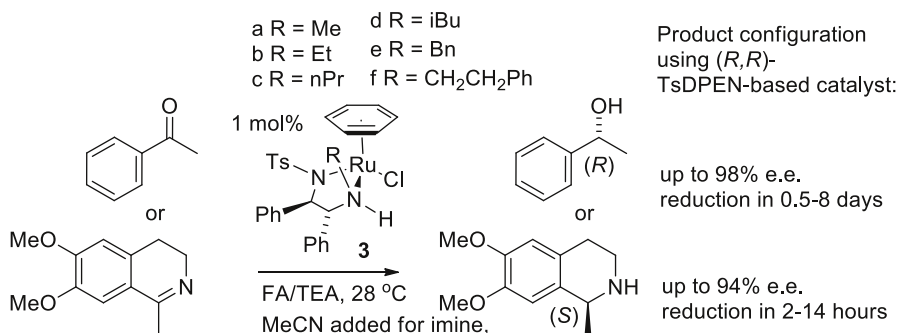
Fig. 3 Ketone and imine reduction using N-Alkyl Ru/TsDPEN complexes
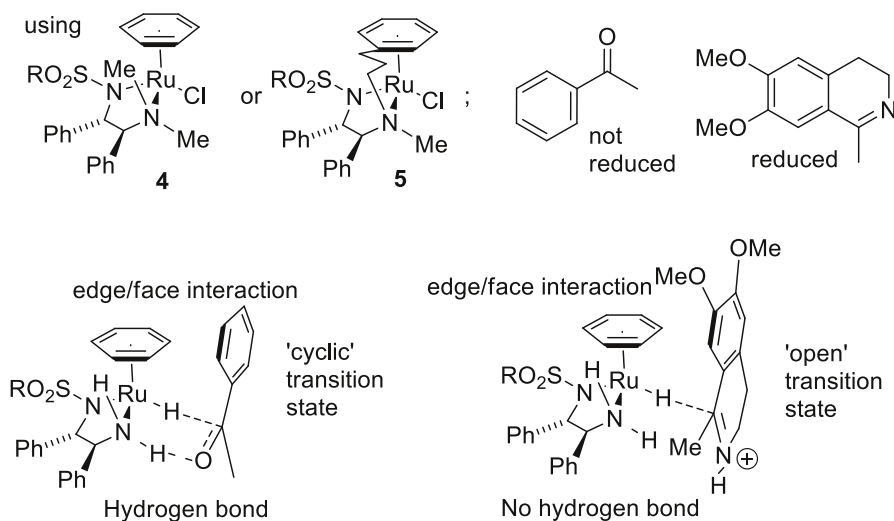
Fig. 4 Contrasting transition states for ketone Vs imine reduction

from each ketone and imine substrate, irrespective of the catalyst used, suggesting a common mechanism among all the complexes. However, it is worth noting that the hydride is delivered to a different relative substrate face for the ketone ((R,R)-catalysts give R-configuration alcohol) compared to the imine ((R,R)-catalysts give (S)-configuration alcohol). The requirement for a stabilizing H-bond between the NH of the ligand and the O atom of the ketone C=O group during the reduction of ketones is now well-established (Fig. 4). It would appear that a single alkyl group on the N atom of the ligand within the catalyst does not hinder this interaction [32].

Wills et al. subsequently demonstrated that catalyst **4**, derived from a modified TsDPEN containing a dimethylated amine, was effective in the reduction of imines but not of ketones. The same was the case with the N-methylated 'tethered' complex **5** [33]. This result provided evidence that the frequently cited cyclic N–H hydrogen

bond to the ketone, which is essential for its reduction [34], is *not essential* in the case of imine reduction (Fig. 4). On the basis of these results, it was proposed that imine reduction by Ru(II)/TsDPEN complexes proceeds through an 'open' (i.e. non-cyclic) transition state (Fig. 4), which would account for the major product enantiomer observed whilst permitting the established edge/face stabilizing interaction to operate between the H atoms on the η^6-arene ring of the catalyst and the aromatic ring of the substrate [3, 4]. This would be analogous to observations previously reported on certain hydrogenation reactions of imines, where an ionic hydrogen transfer is proposed [35–37].

A series of reductions of imines to tetrahydroisoquinoline and tetrahydro-β-carboline alkaloids in aqueous media was reported by Pihko et al. [38]. In this work, the addition of lanthanide salts resulted in improved selectivity and activity in the reductions, and the authors also proposed an 'open' transition state for the hydrogen transfer—in this case aided by the lanthanide as a co-catalyst (Fig. 5).

Subsequent molecular modelling studies by Václavík, Šot, Kuzma et al. also provided support for an ionic pathway for the reduction of protonated imines, but with an additional stabilizing interaction in the form of a hydrogen bond from the N–H bond from the substrate to the SO_2 group—serving to improve the direction and control of the reaction (Fig. 6) [39, 40].

A detailed study by the same group, using nuclear magnetic resonance (NMR), Fourier transform ion cyclotron resonance (FTICR) and vibrational circular dichroism spectroscopic techniques, demonstrated that the use of different bases in place of the commonly used triethylamine significantly influenced the activity and selectivity of imine reductions. A key finding was that the protonated base appeared to interact with the hydride form of the catalyst during the reduction,

Fig. 5 La-Promoted reduction of imines

La = lanthanide salt

Fig. 6 Intramolecular stabilization of the transition states for imine reduction
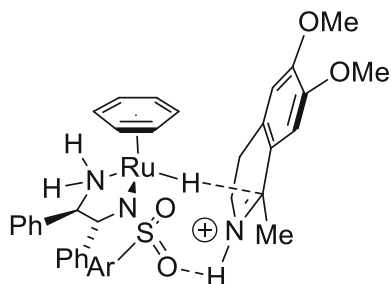
probably via a hydrogen bond to the SO$_2$ unit—in addition to the other predicted interactions of the protonated substrate [12, 41]. Hence, the selection of base can have a significant moderating effect. Further computational studies on a related catalyst for ketone and imine reduction demonstrated that the iminium cation reacted more quickly than the imine. A good catalyst for transfer hydrogenation was thus described as one which 'combines an electrophilic metal centre and a nucleophilic NH group' [42, 43].

2.2 Synthetic Applications of Ru/TsDPEN and Related Catalysts

ATH of dihydroisoquinolines was reported initially by Noyori, and an early observation was that the reaction was less enantioselective for substrates containing a 1-aryl group. Vedejs et al. reported several improvements to the reduction of these substrates (Fig. 7) [44]. Significantly, among a series of substrates tested in this application, the authors found that the *ortho*-bromophenyl substrate gave the best result (up to 98.7 % e.e.). A valuable example of an application was the asymmetric synthesis of (S)-(−)-cryptosyline **6**, which was formed in 83 % e.e. upon ATH. The e.e. was able to be raised to >99 %, however, through subsequent recrystallization [45]. This was a key step of the total synthesis of the neuromuscular blocking agent GW0430.

In a more recent example of Ru(II)/TsDPEN-catalysed ATH of 1-aryl-substituted dihydroisoquinolines, a wide range of substrates were reduced using FA/TEA and iPrOH as solvent, with 1 % catalyst. This series included challenging substrates with *ortho*-substituted aromatic rings [46]. In another report, 1-aryl substituted dihydrosoquinolines were demonstrated to be reduced in improved selectivity using a catalyst based on a borneolsulfonyl derivative of DPEN, compared to the more widely used TsDPEN [47].

A much larger number of reports have been published on the use of dihydroisoquinoline reduction where the 1-substituent is either an alkyl or a benzyl group, for which the enantioselectivity is generally high (Fig. 8). Reductions of this class of substrate have led to many valuable breakthroughs. In many cases, the reducing agent is FA/TEA (5:2 azeotrope); one of the earliest was the report by Sheldon et al., yielding products (intermediates in the synthesis of a series of
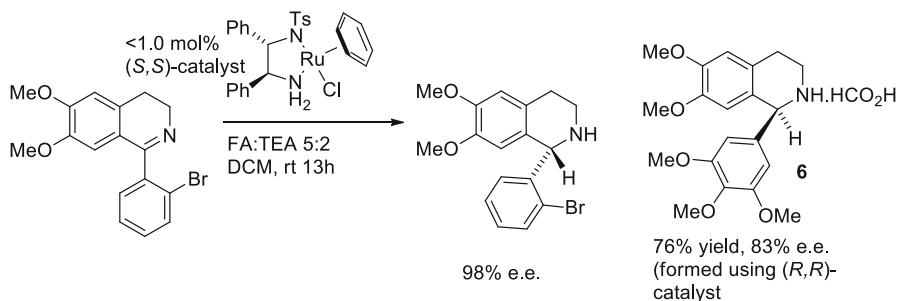
**Fig. 7** Asymmetric transfer hydrogenation of 1-aryl dihydroisoquinolines
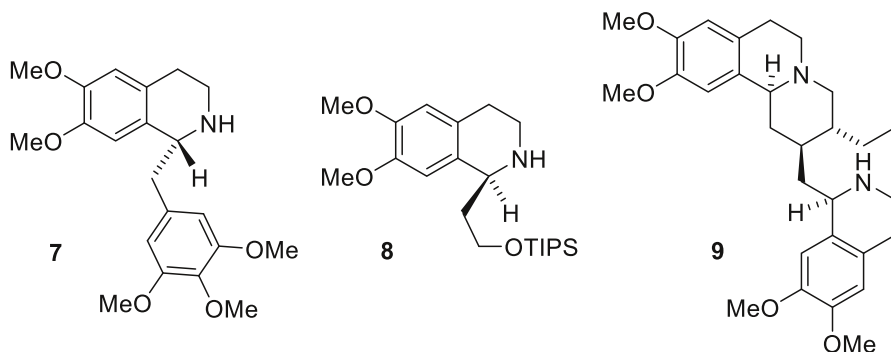
Fig. 8 Synthetic targets prepared by asymmetric transfer hydrogenation of cyclic imines

alkaloids) in up to 99 % e.e. [48]. Likewise, Boros et al. used an ATH with FA/TEA as reductant catalysed by a Ru(II)/TsDPEN catalyst for the synthesis of intermediate **7**, which is itself a component of a more complex product containing two tetrahydroisoquinoline rings [49]. Another example is the synthesis of emetines by Tietze et al. (intermediate **8**) [50] and by Itoh et al. of the synthesis of **9** [51]. Many functional groups can tolerate the use of FA/TEA in the ATH reactions, including esters [52] and phthalimides [53].

In an excellent example of the industrial application of this methodology, a useful comparison was made between asymmetric hydrogenation (i.e. with hydrogen gas; AH) and ATH approaches to almorexant (ACT-078573A), a dual orexin receptor antagonist variant using a Ru/TsDPEN catalyst scaled up to 100 s of kilograms of substrate. This specific targeted application worked very well under carefully optimized conditions, particularly when the methanesulfonate salt of the substrate was used. The use of a 1:1 ratio of FA:TEA gave a more rapid reaction compared to the more widely used 5:2 ratio, and the formation of a small amount of the formylated side product was observed, but this was minimized during the process optimization (Fig. 9) [54]. Following a recrystallization, 87 % of product was isolated in 99.7 % e.e. on an 18-kg scale, which required 17 g of catalyst.

In another excellent example of an application, the enantioselective total synthesis of (−)-(S)-stepholidine, a candidate drug for treatment of schizophrenia, was achieved through a C=N reduction, in >99 % e.e. and 42 % yield (Fig. 10) [55].

Reductions of imines can also be carried out under aqueous conditions. The aqueous process appears to be readily applicable to dihydroisoquinoline reduction and also for dihydro-β-carbolines (discussed in more detail later), but can be significantly enhanced by the addition of a silver salt and $Ln(OTf)_3$ or a closely related salt (Sc, Y, Ce, Yb, Bi salts were tested), and thus applied to more challenging substrates than would otherwise be possible (Fig. 11) [38]. The use of a combined methanol/water solvent also provides some advantages in the most difficult cases. The acceleration of the reduction through an 'open-TS' hydride
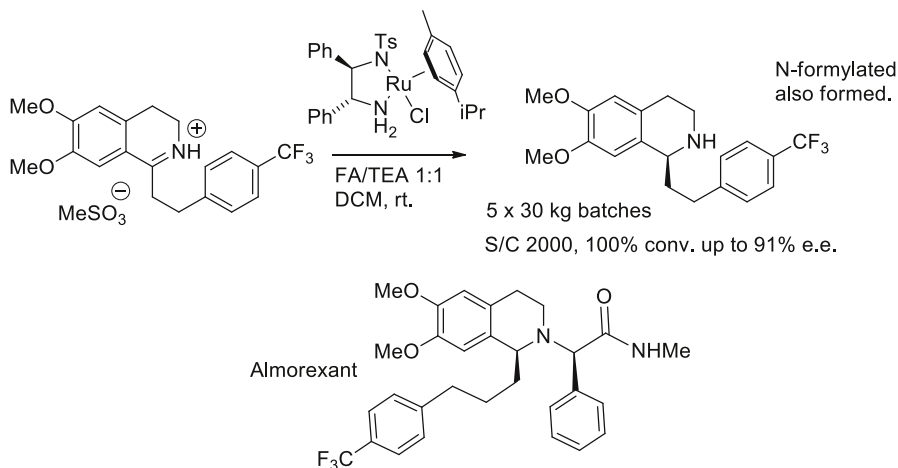
Fig. 9 A synthetic approach to almorexant
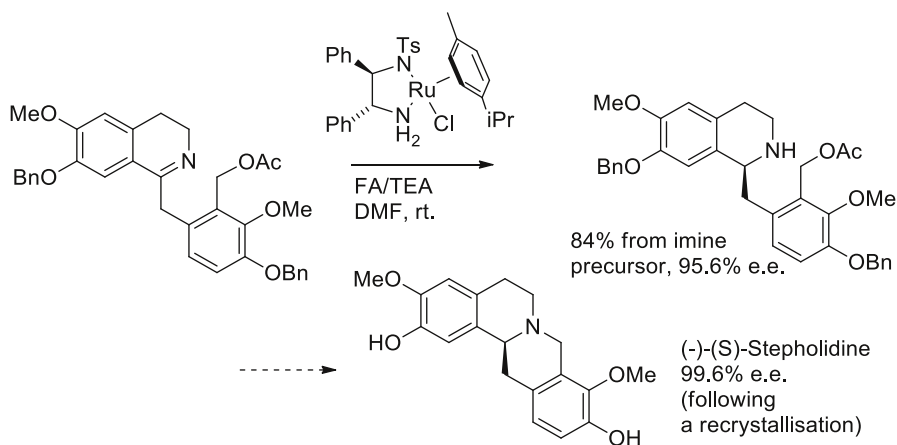
**Fig. 10** A synthetic approach to stepholidine

transfer mechanism using a lanthanide cation as a Lewis acid was described above (Fig. 5).

In a comparative study, two optimized approaches to mivacurium chloride (and other skeletal muscle relaxants) were reported. (R)-5′-Methoxylaudanosine was prepared by ATH of a dihydroisoquinoline, and the process was compared to a resolution strategy [56].

Several studies on the various parameters influencing the ATH of DHIQs have been reported [57, 58], and reductions have been monitored by NMR spectroscopy, generating valuable kinetic data [59, 60]. A study of five substrates revealed that rate and e.e. were substrate-dependent [61], whilst the effect of the η^6-aromatic ring
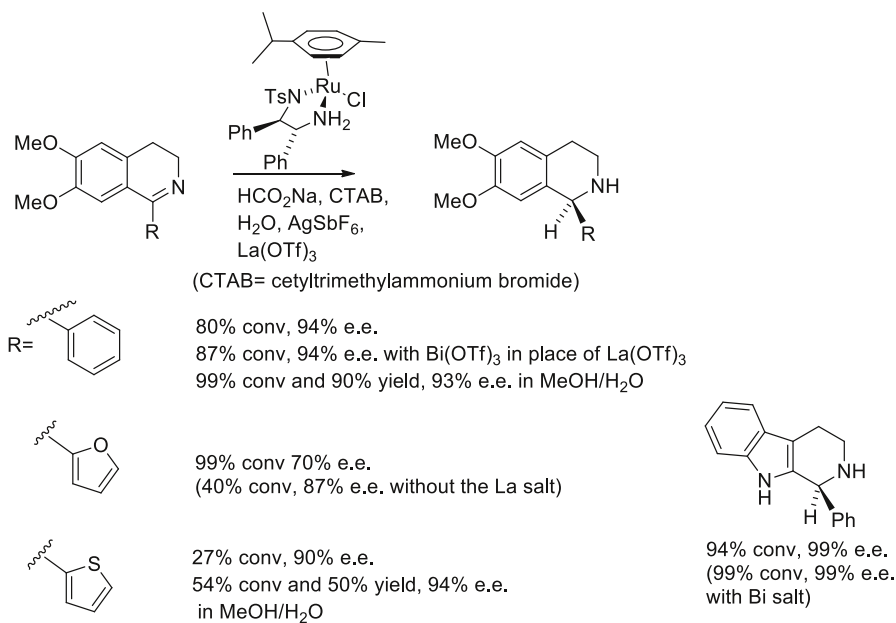
Fig. 11 Asymmetric transfer hydrogenation of imines in aqueous solution
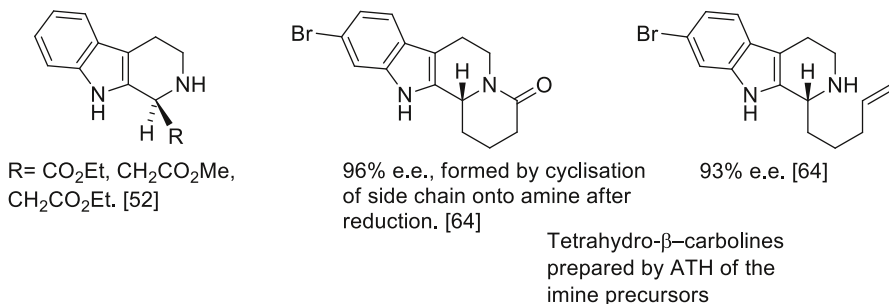
Fig. 12 Asymmetric transfer hydrogenation products from β-carbolines

revealed that the hexamethylbenzene series was very slow; two DHIQ substrates were investigated [62]. The ATH of imines (and ketones) using tethered Rh(III) catalysts has also been reported [63].

Cyclic dihydro-β-carbolines, originally exemplified by Noyori [24], are another class of substrate popular for ATH reactions, since their reduction products are represented in biologically active targets. Examples of targets which can be prepared through reduction in the popular FA/TEA system (often together with a co-solvent) are illustrated in Fig. 12 [52, 64].

Iminium salts are likewise an excellent substrate for ATH reactions. Czarnocki et al. completed a short synthesis of (R)-(+)-crispine A **10** through the reduction of
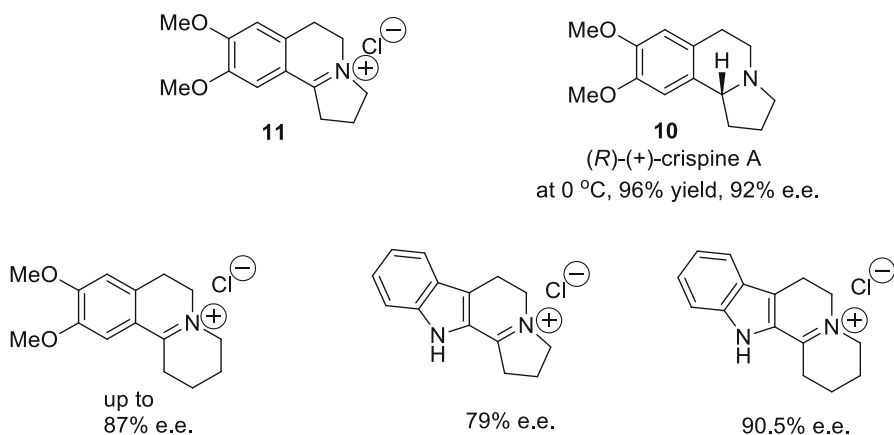
Fig. 13 Asymmetric transfer hydrogenation of iminium salts: reagents and products

the iminium salt **11** [65, 66], and this was extended to further iminium substrates (Fig. 13), which have been successfully reduced [67]. The compounds were purified to enantiomeric purity using a recrystalization after the reduction.

The use of a Ru(II) catalyst containing a proline-derived tetrazole ligand has been reported in a synthetic application: the reduction of an iminium cation en route to (S)-(−)-lennoxamine (Fig. 14). The study provided an interesting contrast between the use of the ATH and AH reduction methods, with selection dependent on the metal used [68].

In addition, good results were reported for the synthesis of new mono-N-tosylated diamine ligands based on (R)-(+)-limonene and their application to ATH of cyclic imines and iminium salts, with up to 98 % e.e. in some cases [69]. Reductions of iminium salts have been described with the use of 1.2 mol% of a Ru(II) catalyst, using sodium formate with cetyltrimethylammonium bromide (CTAB) in aqueous solution, with the addition of silver hexamethylantimonate [38].

ATH can be used to form sultams (Fig. 15) in a very efficient and selective reduction using Ru complexes [70]; indeed, this was one of the first reported applications of the Ru(II)/arene/TsDPEN complexes. Analogous Rh(III) complexes can also be used [25].

Dendrimer- and polymer-supported catalysts can be employed in the ATH of sultam precursors [71, 72], including examples where the supporting material has sulfonyl groups and therefore assists reactions in water [73]. The synthesis of an amphiphilic polystyrene-type immobilized TsDPEN ligand and its application in ATH of cyclic sulfonimines has been reported (Fig. 16) [74].

Acyclic N-sulfonylated imines can also be reduced by ATH, although selectivities are lower [72].

Other polymer-supported systems for C=N ATH feature polymer microspheres functionalized with a chiral ligand by precipitation polymerization [75] and the use of recyclable organoruthenium-functionalized mesoporous silica; reduction of quinolines in up to 99 % e.e. has been reported [76]. The efficient ATH of N-
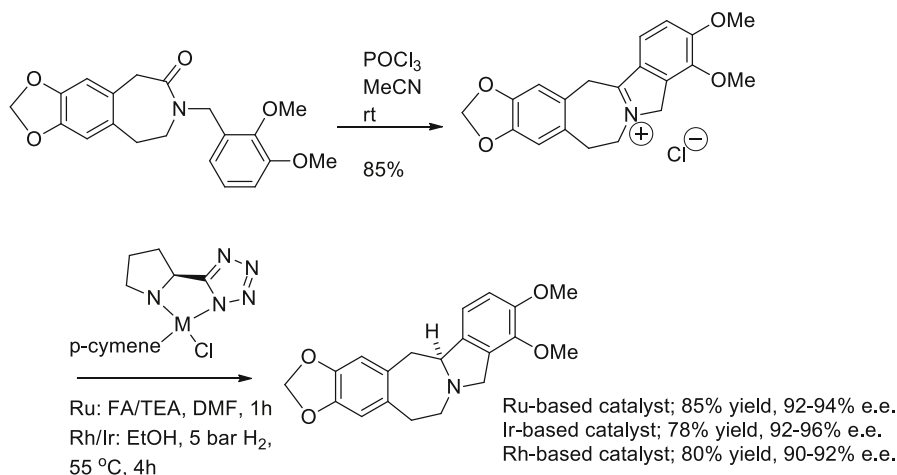
Fig. 14 A tetrazole-containing catalyst for asymmetric transfer hydrogenation of imines
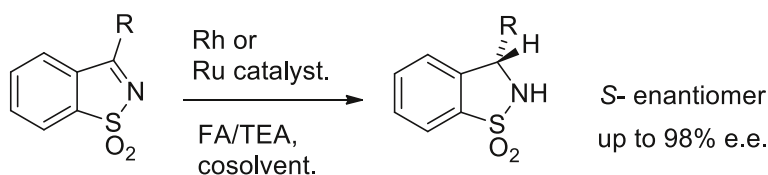
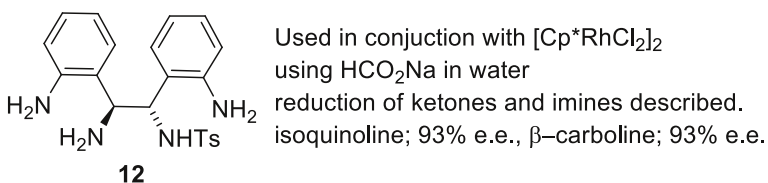Fig. 15 Asymmetric transfer hydrogenation to prepare sultams
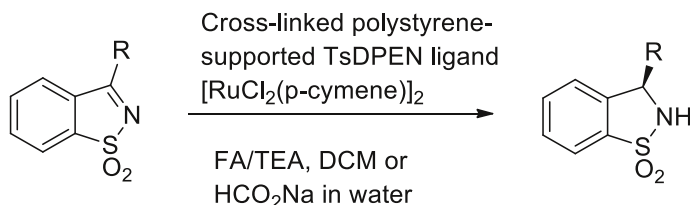
Fig. 16 Asymmetric transfer hydrogenation using a supported catalyst

sulfonyl imines on water using a Rh-imido complex proceeded with higher reactivity and enantioselectivity than the homogeneous reaction. Interestingly, the reactivity appears to depend on the stirring speed of the reaction as well as other experimental factors [77]. The ATH of imines and ketones under aqueous conditions has been reviewed in detail [78, 79].

In addition to the more established TsDPEN ligand derivatives, proline-derived water-soluble arene Ru(II) catalysts containing sulfonylated ligands have been used for ATH of α-aryl ketones and imines in aqueous solution [80]. The ligands in Fig. 17 were prepared and incorporated into Ru(II) aqua complexes (i.e. cationic;
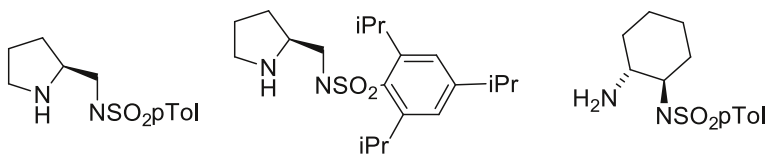
Fig. 17 Asymmetric ligands used in aqueous asymmetric transfer hydrogenation catalysts

Used in conjuction with [Cp*RhCl$_2$]$_2$
using HCO$_2$Na in water
reduction of ketones and imines described.
isoquinoline; 93% e.e., β–carboline; 93% e.e.

12

Fig. 18 An amine-functionalised diamine ligand

the effect of the pH in aqueous reductions was also studied and was optimal at about 8–9 with these catalysts.

Another example was reported of the reduction of ketones and imines with a novel water-soluble chiral diamine **12** as the ligand in neat water (Fig. 18) [81]. Cyclic imines were reduced in high e.e.

The combination of methanol and water gives improved results in some cases [38]. The use of Rh/TsDPEN catalysts on cyclic imine in a mixture of MeOH and water gives the highest rates, e.g. reduction in 20 min for 98 % conversion, whereas water or MeOH alone takes at least 300 min for a similar conversion [82]. A detailed paper on the use of cross-linked polystyrene demonstrated that the polymer-supported reagents could reduce benzyl amines in FA/TEA/DCM in up to 93 % yield; Ru(II) catalysts gave the best e.e. An amphiphilic version containing some sulfonic acid groups in water with sodium formate also reduced cyclic imine with good efficiency [83].

Further examples of supported catalysts used for ATH of imines include those based on recyclable silica [84], functionalized MCM-41 [85], siliceous mesocellular foam [86] and magnetic mesoporous silica. In the latter case, the reusable immobilized catalyst exhibited high activity and enantioselectivities in the ATH of imines in FA/TEA. It was able to be separated mechanically using an external magnet to facilitate ready recycling [87].

The enantioselective synthesis of α-trifluoromethyl arylmethylamines by Ru(II)/ aminoindanol ATH is very efficient, giving products in high yield and e.e. (Fig. 19). Several ligands have been used and tested, and a good number of examples have been reported, including an application for the synthesis of an analogue of a plant disease control agent [88].

Ru(II)-catalysed ATH of α-trifluoromethylimines was also achieved using TsDPEN-based catalysts under aqueous conditions (Fig. 20) [89].
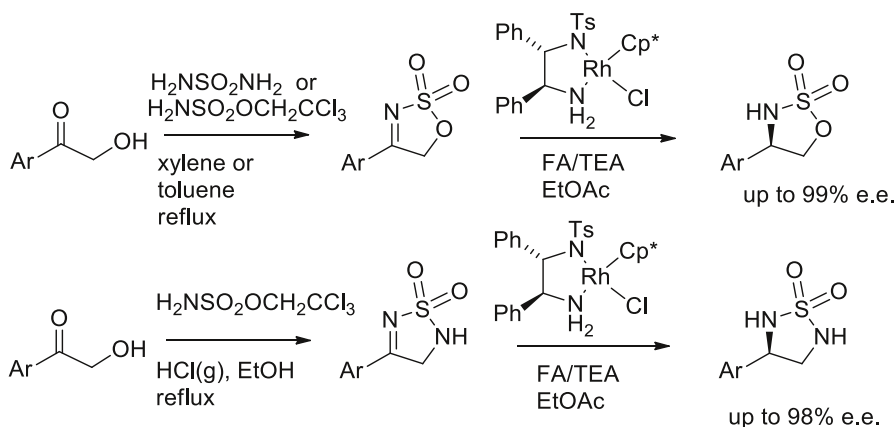
Several reports have recently appeared describing the ATH reduction of cyclic sulfamidates and sulfamides, following the report of this in 2010 [90]. The synthetic
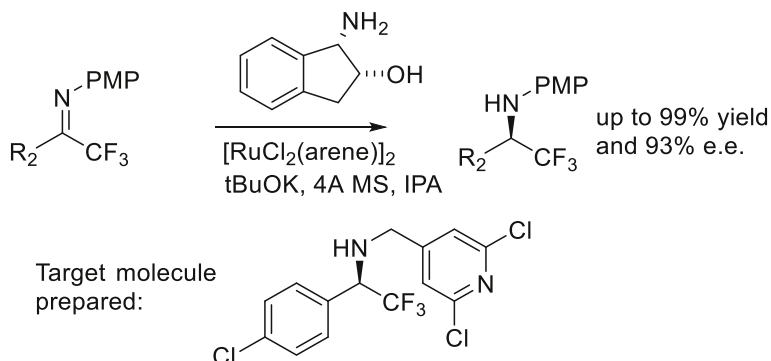
Fig. 19 Asymmetric transfer hydrogenation of trifluoromethyl imines
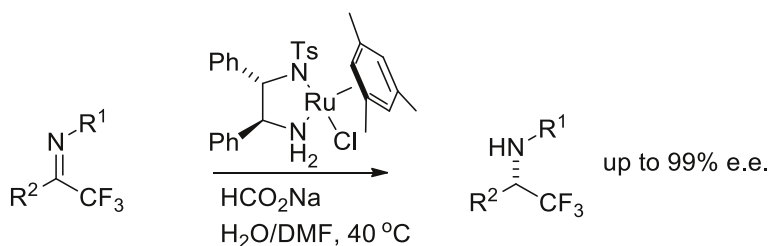

Fig. 20 Asymmetric transfer hydrogenation of trifluoromethyl imines in an aqueous system

Fig. 21 Asymmetric transfer hydrogenation of cyclic substrates

routes to key substrates and their reductions by Rh(III) catalysts are shown in Fig. 21. The e.e. of the reductions in all cases was excellent, and the reduction forms the basis of an efficient synthesis of enantiomerically enriched 1,2-aminoalcohols and diamines [91].

Fig. 22 Diastereoselective asymmetric transfer hydrogenation of cyclic substrates with dynamic kinetic resolution
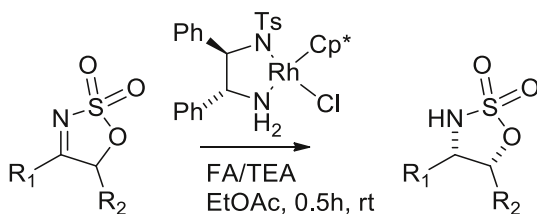
The reduction of this class of substrate can be extended to a dynamic kinetic resolution (DKR) process with C=N reduction coupled to racemization of the adjacent stereocentre. Of the Ru, Rh and Ir catalysts tested, the Rh catalyst gave the best results (Fig. 22). The resulting compounds were able to be converted into other products through the S_N2 ring-opening using phosphorus and nitrogen nucleophiles. The reductions typically exhibited a selectivity of >20:1 in favour of the *cis*-product, and e.e. was typically 94–97 %, but up to 99 % e.e. in a number of cases. An exception was for more hindered *ortho*-substituted substrates, e.g. $R^1=R^2=ortho$-ClC_6H_4, in which the e.e. was only 22 % [92].

The stereoselective synthesis of 4-substituted cyclic sulfamidate-5-carboxylases can be achieved using this process of coupled ATH/DKR (Fig. 23), and this method has been applied to the synthesis of (−)-epi-cytoxazone and the taxotere side chain. The *cis*-isomer was formed in high selectivity, typically >25:1. A wide range of examples were reported with 3- and 4-substituted aromatic groups, with e.e. up to 99 % in many cases and generally >95 % e.e. An example with cyclohexyl was less selective (Fig. 23) [93].

The application was efficiently extended to 5-phosphonate-containing substrates. In some cases, both the de and e.e. were >99 % (Fig. 24) [94].

Related work on the sequential reduction of two C=N bonds has been reported. In this case, the Ru(II) catalyst was used first and gave good results. Preferential reduction of one C=N was observed, but the other was stereoselectively reduced using lithium borohydride; the products were transformed into chiral diamines (Fig. 25) [95].

Asymmetric aziridines can be prepared by ATH of an azirine; this was one of the earliest reported applications using Ru(II) complexes, achieved using a bicyclic amino alcohol ligand (Scheme 26) [96].

The application of Rh(III) systems to the reduction of *N*-phosphinoyl imines was described in depth by researchers from Avecia, who were able to obtain some very valuable insights into the mechanism of the reaction and requirement for removal of carbon dioxide during the reaction [26]. In recent related work, Guijarro et al. described the use of chiral beta-amino alcohols as ligands for the Ru(II)-catalyzed ATH of phosphinyl ketamines. The study demonstrated that the reaction was possible using *cis*-amino indanol (CAI) as ligand for the catalyst (Fig. 26). A number of amino alcohols were tested, but CAI was the best of the series (Fig. 27). Most of the studies were conducted on acetophenone-derived imine, but in examples where Ar=Ph, R=Et gave a product of 82 % e.e. and Ar=pClC$_6$H$_4$, R=Me gave one of 80 % e.e. [97].
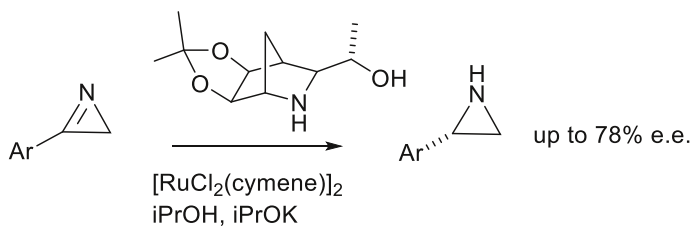
Fig. 23 Diastereoselective asymmetric transfer hydrogenation of cyclic substrates containing ester substituents
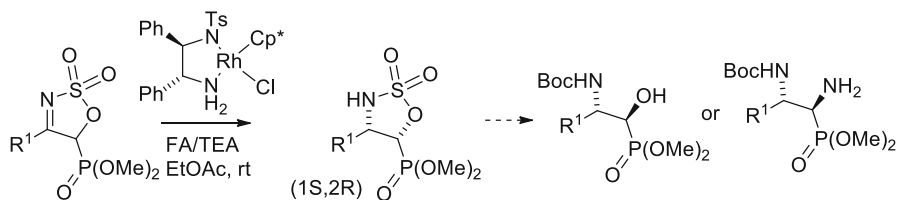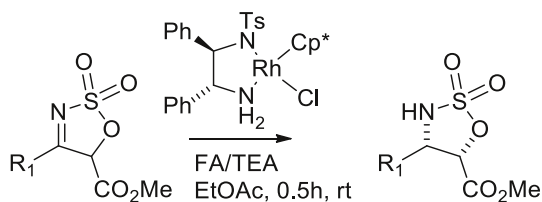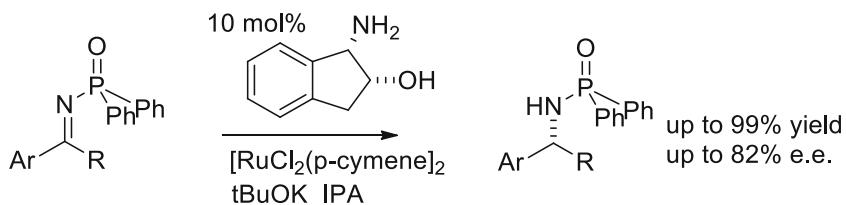

Fig. 24 Diastereoselective asymmetric transfer hydrogenation of cyclic substrates containing phosphonate substituents
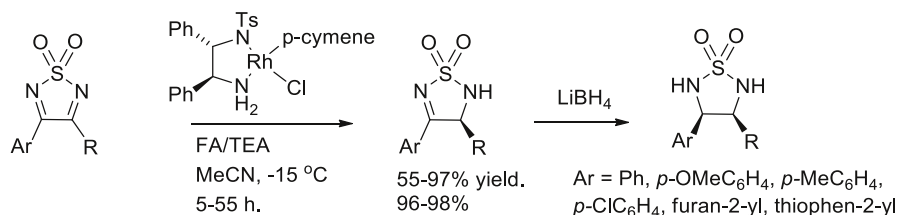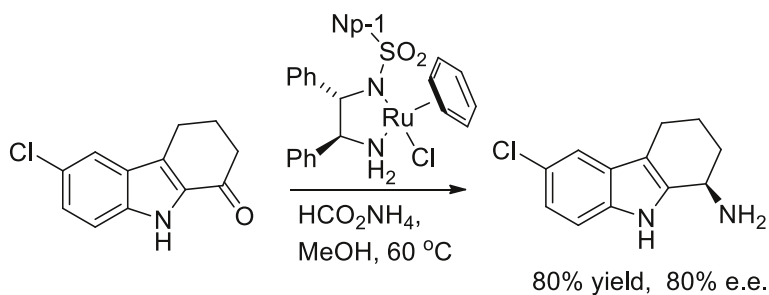

Fig. 25 Asymmetric transfer hydrogenation of a cyclic imine followed by diastereoselective reduction

Fig. 26 Asymmetric transfer hydrogenation of azirines

Fig. 27 Asymmetric transfer hydrogenation of N-Phosphinoyl imines

Fig. 28 Asymmetric transfer hydrogenation to form an exocyclic primary amine

In early work, Lassaletta et al. described a DKR reaction coupled to the formation of primary amines [98]. In a related process, an efficient ATH reaction was reported for the synthesis of an advanced intermediate to a drug for the treatment of human papillomavirus infections (Fig. 28). This involves an interesting *exo*—C=N reduction in an in situ process. The formation of an imine followed by a reduction using a Ru(II)/BINAP complex was also investigated, as was a diastereoselective method using alpha-methylbenzylamine as a directing group [99].

A similar reduction towards a primary amine intermediate was reported by scientists at Merck (Fig. 29). The target in this case was the HCV NS5a inhibitor MK-8742, and a key step was a highly enantioselective ATH of a C=N bond. Among the catalysts investigated, the best one proved to be the tethered catalyst reported by Wills et al. The synthesis of the complex target requires simple starting materials and just nine linear steps for completion [100].

Also in earlier work, Wills et al. described the formation of C–N bonds in a one-pot ATH starting from Boc-protected amines [101, 102]. This type of process was applied in an impressive intramolecular ATH reaction in a key step to the dual orexin inhibitor molecule suvorexant (MK-4305; Fig. 30) [103]. This excellent detailed paper on reductive amination employed Ru(II)/TsDPEN catalyst in the reductions, and the best results were obtained using a derivative containing a very hindered aromatic group on the sulfonamide unit. The operation of the 'open' transition state for hydride transfer to the imine is described. The paper contains details of extensive investigations into the effect of excess carbon dioxide on the reaction; purging this from the reaction gives better rates. The significance of the formation of two diastereoisomers of the hydride form of the catalyst, which has been previously observed for this type of catalyst, was also discussed in some depth.

Heteroaromatic substrates have been productive targets for both TH and ATH reactions. Quinoline and isoquinolium salts can be reduced by Ru(II) and Rh(III) catalysts by ATH [104, 105]. Chemoselective reductions of quinolines were achieved by TH using IPA with an iridium catalyst (Fig. 31) [106].

The importance of Ph-regulation for the TH of quinoxalines with a Cp*Ir/TsEN catalyst in water was demonstrated, with the reduction using HCO_2Na at ca pH 5.5 (regulated with a buffer) yielding the highest rates [107]. In another report, a dramatic effect of added iodide was shown to influence TH of a number of
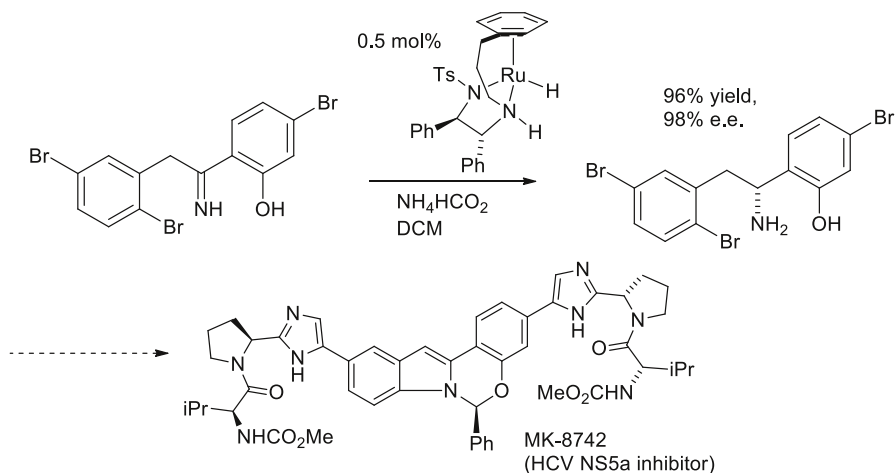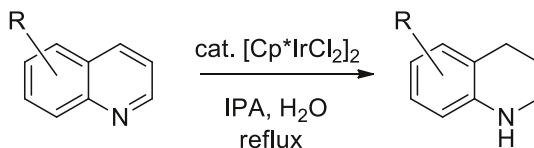
Fig. 29 Asymmetric synthesis of MK-8742
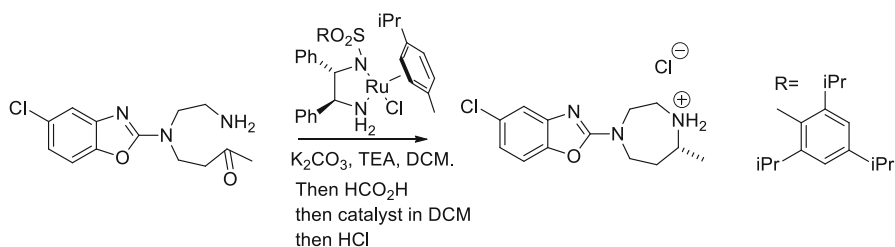
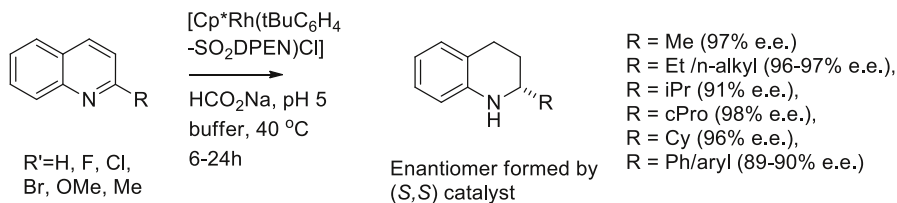**Fig. 30** An intramolecular reductive amination approach to a cyclic amine

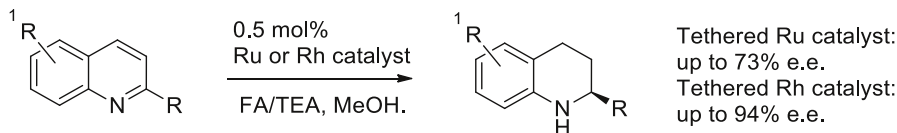**Fig. 31** Transfer hydrogenation of quinolines

N-heterocycles (quinolines, isoquinolines and quinoxalines) when a Cp*Ir catalysts was employed for their reduction in FA/TEA [108].

However, some important asymmetric examples have also been reported. Again, pH regulation was crucial to the successful ATH of quinolines in water with sodium formate as the reducing agent; the rate peaks at around pH 5.0, and formic acid with a formate buffer is used to regulate this. The best of a series of catalysts was a Cp*Rh complex of a *p*-(*t*-butyl)benzenesulfonyl DPEN, although other ligands were also viable. Reductions were complete typically within 6–24 h at 40 °C using 1 mol% of catalyst (Fig. 32) [109].

A similar process was reported using tethered Ru(II) catalysts (Fig. 33) [110].

R = Me (97% e.e.)
R = Et /n-alkyl (96-97% e.e.),
R = iPr (91% e.e.),
R = cPro (98% e.e.),
R = Cy (96% e.e.),
R = Ph/aryl (89-90% e.e.)

Fig. 32 Asymmetric transfer hydrogenation of quinolines

Tethered Ru catalyst:
up to 73% e.e.
Tethered Rh catalyst:
up to 94% e.e.

Fig. 33 Asymmetric transfer hydrogenation of quinolines using a tethered catalyst

A mesoporous silica-supported TsDPEN/Ru(II) catalyst was also productively applied to this transformation [76].

2.3 Shvo-type catalysts and other classes of organometallic catalysts

The Shvo diruthenium catalyst **13** (Fig. 34) has been used in non-asymmetric ketone and imine reduction, and the mechanism has been studied and reported in some detail [5, 111–115]. Catalyst **13** is also able to racemize amines [116], which allows it to be combined in a DKR process with an enzyme to create enantiomerically enriched amides.

Iron cyclopentadienone complexes have recently emerged as alternatives to Ru(II) catalysts, although their main focus is on ketone reduction rather than imine reduction [117].
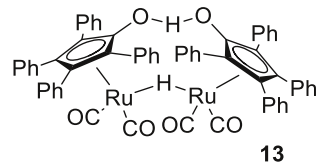
Bifunctional rhenium complexes related to the Shvo catalyst have been used in TH reactions, including tests on three non-prochiral imines, with TOFs up to 79 h^{-1} obtained for imines. In common with the Shvo catalysts, DFT calculations have indicated the operation of an outer-sphere mechanism for the reaction [118].

Cyclometallated complexes of Ru, Rh and Ir have been used as ATH catalysts; some examples of this catalyst class were prepared and reported previously; however, their application has now been extended to a broader range of target imines, both cyclic and acyclic (Fig. 35) [119].
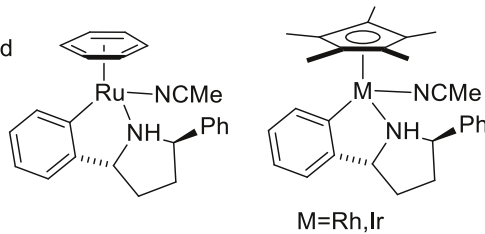
Ru–Pybox complexes have been used to achieve imine ATH in IPA; these complexes gave excellent results for imine derivatives of acetophenone, with products of up to 99 % e.e. in some cases, using 1 mol% of catalyst (Fig. 36). There was some mechanistic discussion and a number of examples were reported. In general, these complexes have been used much more widely for ketone ATH [120].

A very interesting report of a nickel-catalyzed ATH of hydrazones and related substrates has been published. Using a complex formed from a combination of (S)-

Fig. 34 The shvo complex

13

Cyclometallated cataysts

M=Rh,Ir

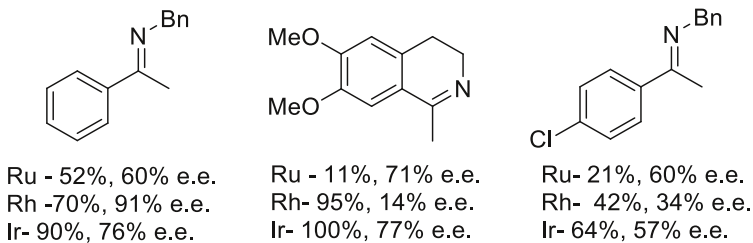Substrates reduced: (FA/TEA, DCM, [S]=0.016M, 1 mol% catalyst.

Ru - 52%, 60% e.e.
Rh -70%, 91% e.e.
Ir- 90%, 76% e.e.

Ru - 11%, 71% e.e.
Rh- 95%, 14% e.e.
Ir- 100%, 77% e.e.

Ru- 21%, 60% e.e.
Rh- 42%, 34% e.e.
Ir- 64%, 57% e.e.

Fig. 35 Cyclometallated catalysts for asymmetric transfer hydrogenation

L= ethene, PPh₃,
PMePh₂, P(OMe)₃
Gives up to 99% ee

1 mol% catalyst

IPA, 60 °C, tBuOK

98-99% e.e.
up to 99% e.e.

Can also be used in hydrogenation

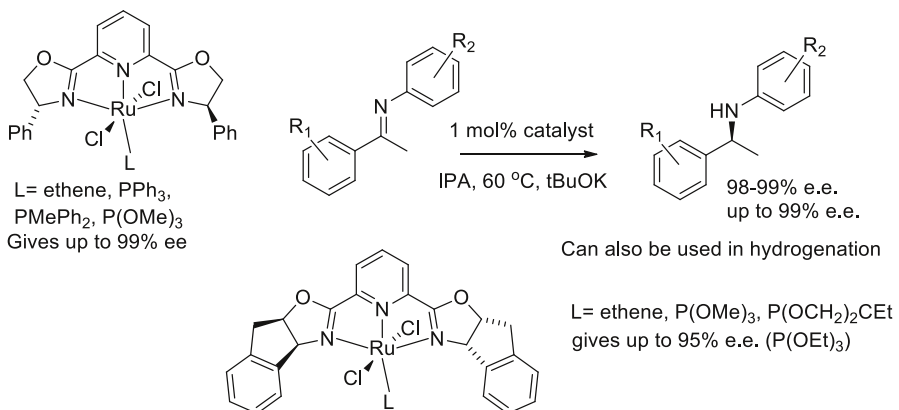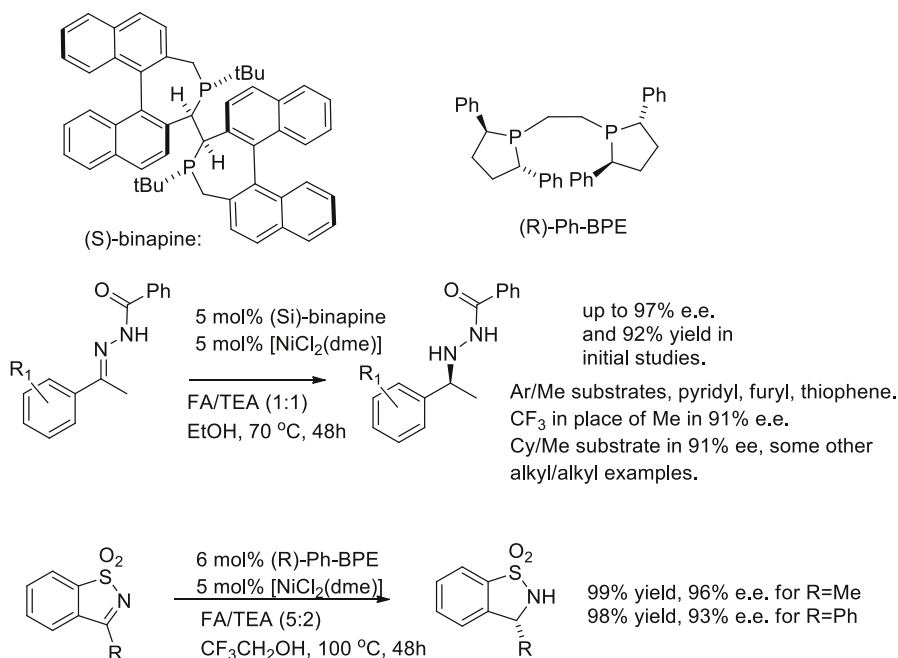L= ethene, P(OMe)₃, P(OCH₂)₂CEt
gives up to 95% e.e. (P(OEt)₃)

Fig. 36 PyBox-Type complexes for asymmetric transfer hydrogenation
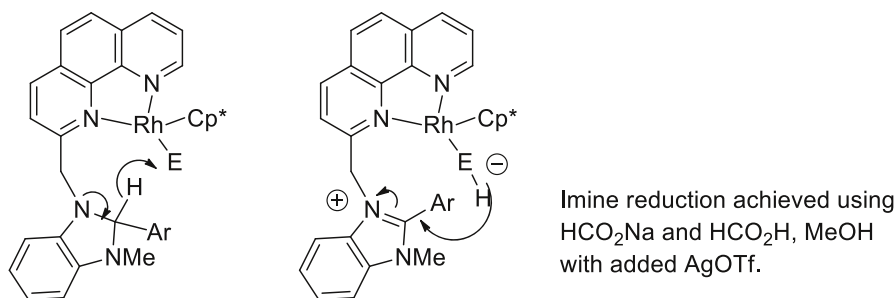
Fig. 37 A nickel-based catalyst for asymmetric transfer hydrogenation of C=N bonds

binapine and a Ni(II) source, with FA/TEA as the reducing agent, products of up to 97 % e.e. were formed in the reduction (Fig. 37). The reaction also works with sultams, giving products in 98–99 % e.e. Deuterium labelling studies were also carried out in D–FA and during the reduction, resulting in deuteration of the Me group, and indicating that exchange could be taking place through an enamine [121].
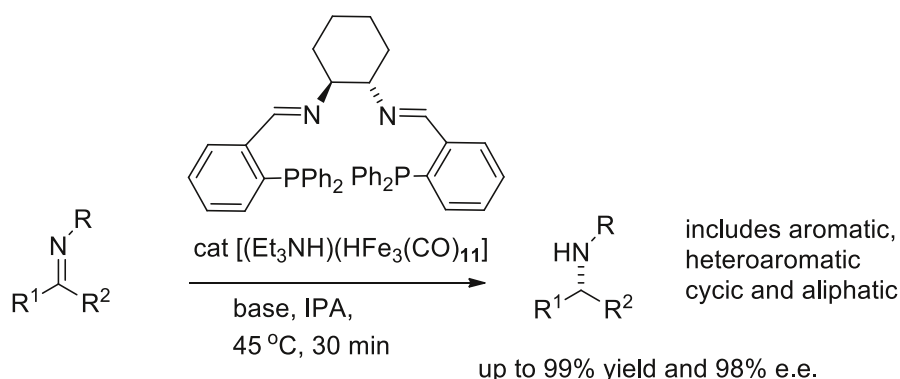
A bio-inspired catalyst comprising a combined organic hydride donor with metal centre has been reported for TH of imines. A previously used catalyst relied on a Hantzsch ester, but the newer derivative benefits from easier preparation and greater accessibility. Yields are high for the Rh complex containing all the components, and more than for the Ir complex or the complex containing the phenanthroline ligand alone (Fig. 38) [122, 123].

Several iron complexes for imine ATH have been developed by Morris et al., with IPA used in the reduction. Early examples of the PNNP-complexes (containing imine ligands) of iron gave 100 % reduction of PhCH=NPh but only 5 % of PhCMe=NPh [124]. Beller reported the use of an in situ-generated catalyst for ATH of imines with high yield and enantioselectivity (Fig. 39) [125].

However, Morris et al. later discovered that iron complexes containing a combination of one amine donor and one imine donor (e.g. **14**) were superior catalysts for ketone and imine ATH (Fig. 40). The researchers followed on from results indicating that the proposed reduction of one C=N bond of the original ligands was important to the mechanism. They prepared an amine/imine 'P–NH–N–

Fig. 38 Intramolecular hydride delivery in a rhodium complex

Imine reduction achieved using HCO_2Na and HCO_2H, MeOH with added AgOTf.

cat [(Et$_3$NH)(HFe$_3$(CO)$_{11}$]

base, IPA,
45 °C, 30 min

includes aromatic, heteroaromatic cycic and aliphatic

up to 99% yield and 98% e.e.

Fig. 39 An asymmetric iron-based complex for imine reduction

P' ligand first by adding one C–NH bond in a reductive amination process, and then forming the second C=N bond and finally the 'third-generation' complex **14** (Fig. 40). This new class of catalyst was effective in the rapid reduction of N-diphenylphosphinoyl-activated imines containing phosphinoyl groups in >99 % e.e. (Fig. 41) [126, 127].
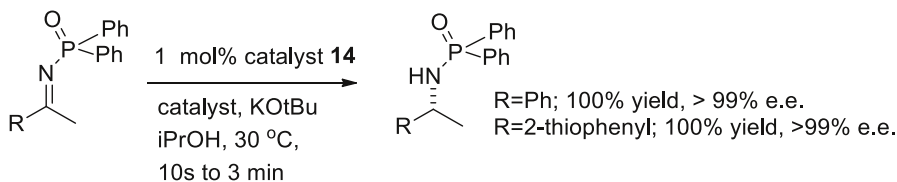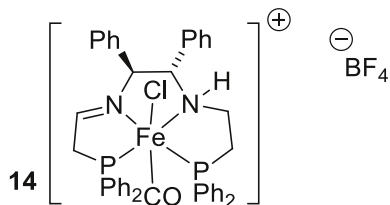
Fully documented details of synthesis and use, including pictures of the reaction setup, have been published [128].

Very few examples of osmium-catalysed ATH reactions of imines have been reported [129]. However, one example is provided by arene iminopyridine halido complexes which additionally exhibit properties as antitumor agents. Four complexes were prepared and tested, giving reductions in FA/TEA of ca. 22–23 % e.e. in each case (Fig. 42) [130].
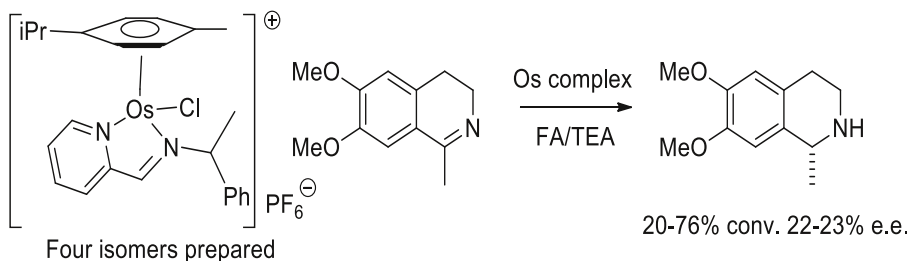
2.4 Incorporation of TH catalysts into proteins

A significant development within the decade leading up to this review has been the contributions made to the development of organometallic reagents contained within protein structures, relying on the asymmetric environment of the protein to generate

**Fig. 40** An iron complex containing a combined imine/amine-ligand

Fig. 41 Asymmetric transfer hydrogenation of a phosphinoyl imine using iron complex **14**

R=Ph; 100% yield, > 99% e.e.
R=2-thiophenyl; 100% yield, >99% e.e.

Four isomers prepared

20-76% conv. 22-23% e.e.

Fig. 42 Asymmetric transfer hydrogenation using an osmium complex

Fig. 43 Mode of hydride transfer within a streptavidin complex

Complex is embedded in a streptavidin variant
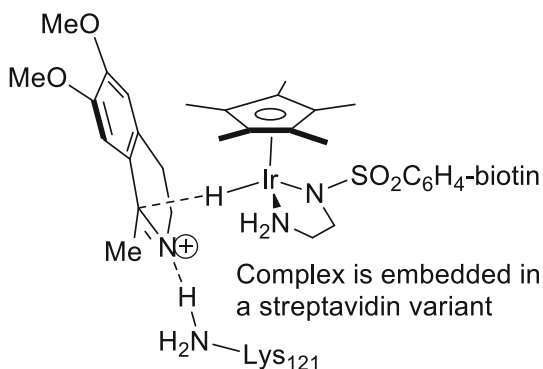
asymmetry in the reductions when a simple (i.e. non-chiral) complex is added to it. Many contributions have been made by Prof T. Ward et al., and principally through the attachment of an organometallic complex of a non-chiral Ts-diamine ligand to biotin, thus allowing it to be coordinated within the chiral environment of a

streptavidin molecule, and hence an asymmetric induction generated. Important to this process is the ability to modify the streptavidin structure in a selective manner in order to optimize the reactions towards these substrates. This section shall examine the principal developments in this area, which is a part of a larger programme on many applications of metal/protein complexes.

Following extensive work on optimizing the catalysts towards the reduction of ketones, studies were extended to imine reductions. Figure 43 illustrates how a component of the protein (i.e. a lysine side chain) can stabilize the iminium substrate during the reduction by an iridium catalyst which is chiral at the metal and within the chiral environment created by the protein. In common with other models previously described for imine ATH, the 'open' transition state for the reduction is proposed. This is based on observed results and X-ray crystallographic evidence; the S112A variant containing the Ir/TsEN (EN = ethane-1,2-diamine) complex attached to biotin was isolated, and the X-ray crystallographic structure was obtained [131, 132].

The streptavidin variant is generated as a part of a screen of modifications. In this work, no asymmetric induction was obtained without protein, and the wild-type streptavidin (Sav) gave a reduction product of up to 57 % e.e. (R). However, the S112A mutant of Sav gave an amine in up to 96 % e.e. (R), and in other cases (e.g. S112K mutant) the enantioselectivity could even be reversed. In addition, up to 4000 turnovers of the synthetic enzyme were able to be achieved [133–137]. Computational and molecular modelling has been applied to this process to aid optimization [138].

In parallel work, the synthetic enzyme has been gradually refined through further optimization. In a later paper [139], human carbonic anhydrase II was combined with a sulfonamide derived from pyridine/IrCp* to create a catalyst for the ATH of imines. The X-ray structure of a derivative was used to improve the catalytic performance, ultimately achieving 68 % e.e. A ribonuclease has also been used as the basis of an artificial amine reductase. In this case, the incorporation of a Cp*Ir complex gave an efficient and selective artificial enzyme for imine reduction [140].

With the most advanced streptavidin variants, the strategy in which a racemic catalyst is converted to a chiral-at-metal complex and then further assisted by residues in the chiral protein has led to the development of both R- and S-selective synthetic enzymes for imine reduction. Extensive kinetic data has been obtained for these new synthetic enzymes, and computer modelling of the complex structures (which contain four interacting subunits) serves to support and understand the results. An 'induced lock and key' where the host protein structure determines the catalyst structure and the reduction selectivity is proposed (Fig. 44) [141].

Optimization of a synthetic enzyme derived from human carbonic anhydrase II has been achieved in a similar manner, resulting in conversion of a wild-type selectivity of 70 % e.e. with a TON of 9 to a modified variant with several residue changes, giving a product in 96 % e.e. and a TON of 59. Again, X-ray crystallographic evidence demonstrated that the piano stool complex was embedded within the protein, which served to influence its configuration and assist in the asymmetric control of hydrogen transfer [142]. An ingenious method for amine deracemization can be achieved within a cascade of reactions which combines a
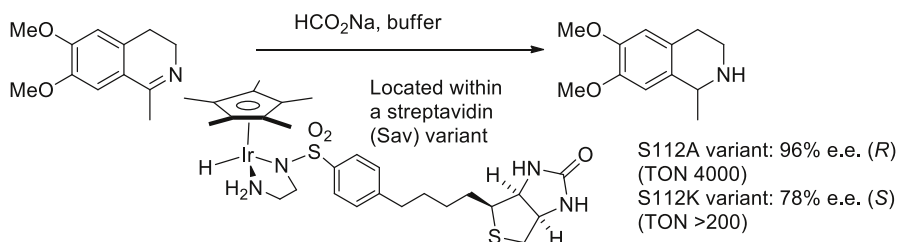
Fig. 44 Asymmetric reduction to either product enantiomer using an iridium complex within a protein

biocatalyst with the synthetic enzymes created in this work [143]. Related work has been reported on ketones rather than imine, and several informative reviews of Ward et al.'s work have been published [144–148]. A related example describing the influence of an external-directing group—in this case a homochiral phosphonic acid—on the transfer of hydride from a Cp*/Ir/TsEN complex to an imine has been reported [149]. Although hydrogen gas is used as the reducing agent, a similar process of chirality induction takes place at the Ir complex.

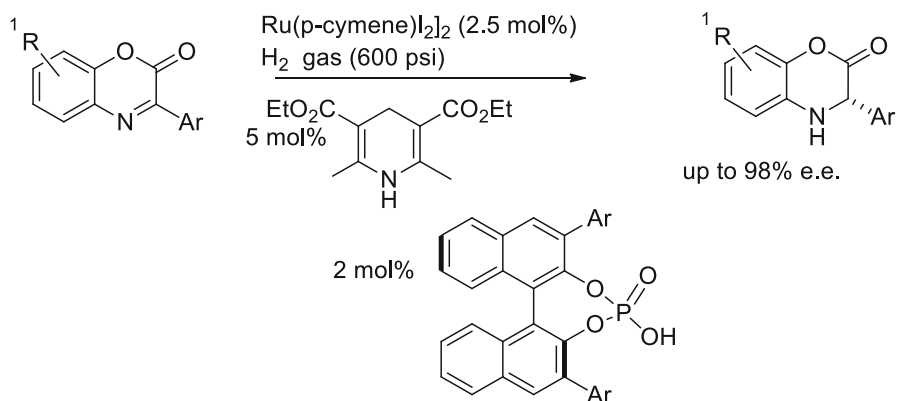## 2.5 Hydrogen Borrowing and Organocatalysis

Although technically a 'hydrogen borrowing' reaction rather than a reduction, a C=N reduction has been involved at a key stage to good effect in some specific applications where an alcohol is converted to a chiral amine. Cooperative catalysis by iridium complex and a chiral phosphonic acid can lead to asymmetric amines starting from racemic alcohols [150]. Likewise, the use of a chiral phosphonic acid with an Ir/TsDPEN complex gave a very interesting DKR and amination of alcohols in one process; from a mixture of four isomers, one product enantiomer is predominantly formed [151].

In recent years, several papers have been published on the combination of an organometallic catalyst with a chiral phosphonic acid in order to achieve enantioselective reduction of an imine. This obviates the requirement for a Hantzsch base by replacing it with the combination of an organometallic complex and hydrogen gas. However, since these involve the use of hydrogen gas, they are technically outside the scope of this review, although a recent overview is highlighted [152] and one example is illustrated (Fig. 45) [153].

The direct reductive amination of aromatic aldehydes has been achieved with excellent yields using a gold(I) catalyst along with a Hantzsch ester as the hydrogen source under mild reaction conditions [154]. In another example, $B(C_6F_5)_3$– is shown to act as a catalyst for the transfer of hydrogen from a Hantzsch ester to an imine [155].

3 Meerwein–Ponndorf–Verley (MPV) Reductions

The development of asymmetric MPV reactions has also been described [156]; notably, a very selective system based on Al(III)/BINOL complexes was reported (Fig. 46) [157]. In this example, the e.e. was determined for all products, although

Fig. 45 Asymmetric imine reduction promoted by a chiral phosphoric acid

Reduction products of phosphinoyl imines formed using iPrOH, AlMe₃, and (S)-BINOL (toluene, 60 °C)
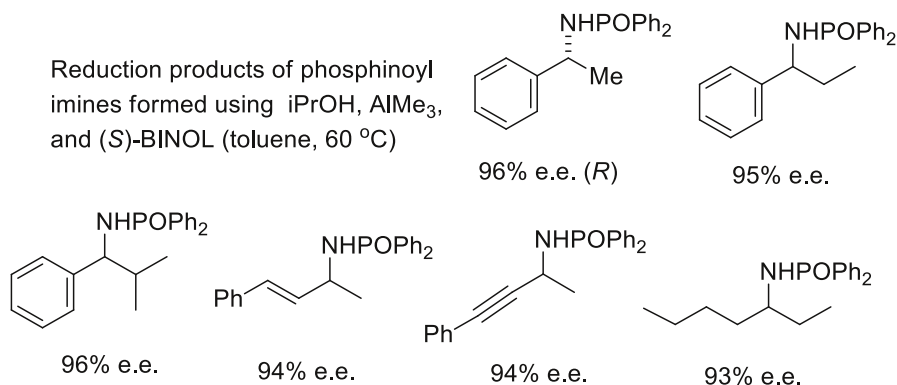
Fig. 46 Asymmetric transfer hydrogenation using an aluminium-based catalyst

only the configuration of the 1-phenylethylamine derivative was established. However, the absolute configurations of the other products can inferred (but are not shown) based on the steric size difference between the substituents flanking the imine in the substrate.

In a recent example, α-silylamines were prepared by MPV-type reduction of α-silylimines This does produce the amines in up to 99:1 er, although it is a stoichiometric rather than catalytic process, using a chiral amine as the donor of hydride (Fig. 47) [158].

4 Reductive Amination Reactions

Studies have reported that the Leuckart–Wallach reaction is effective for the synthesis of chiral amines, with some very important contributions by Kadyrov and Riermeier, who employed a Ru(II)/BINAP derivative to excellent effect, yielding
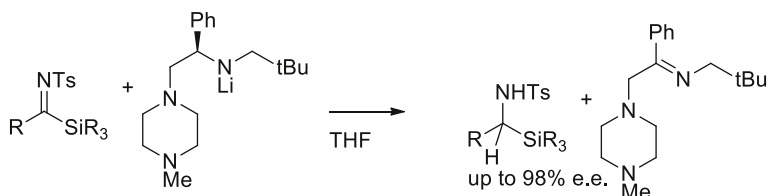
Fig. 47 Stoichiometric hydride transfer from a chiral amine
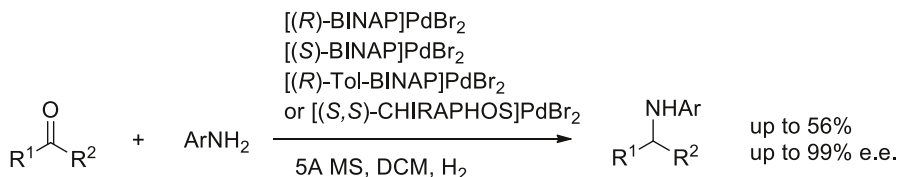
Fig. 48 A reductive amination catalysed by a palladium complex

products from acetophenone derivatives in up to 95 % e.e. [159]. The simple complex [Cp*Rh(III)Cl₂]₂ can be used to give racemic products [160]. In a recent related example, albeit a hydrogenation rather than a transfer hydrogenation, a BINAP/Pd complex was used to form products of up to 99 % e.e. in reductive amination of acetophenones using anilines (Fig. 48) [161].

5 Diastereoselective Asymmetric Reductions

A series of highly selective reactions have been reported by Guijarro et al., where a chiral sulfinyl group directs the ATH of an imine, using either an asymmetric catalyst or a racemic one (Fig. 49). Using *cis*-aminoindanol, very selective syntheses of amines are possible [162–164], and imine formation can be accelerated with microwave irradiation.

However, in later work it was found that a non-chiral ligand could also be used—the enantioselectivity being created by the sulfinyl group (Fig. 50) [165–167]. Microwave radiation can be used to accelerate the reaction [168].

The work has been applied to the synthesis of a series of heterocycles using halide-substituted substrates, and then completing the ring synthesis using a base-promoted process, followed by removal of the sulfinyl group (Fig. 51) [169].

6 Carbene Ligand-Based Catalysts

A wide range of complexes containing *N*-heterocyclic carbenes have been used in the TH of imines, and some examples are given in Fig. 52, along with an indication of the typical TONs for some of the reductions. In many cases, the turnover numbers
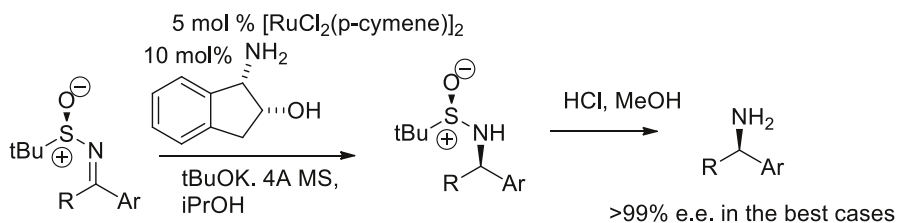
Fig. 49 Diastereoselective C=N bond reduction using a ruthenium catalyst containing a homochiral ligand
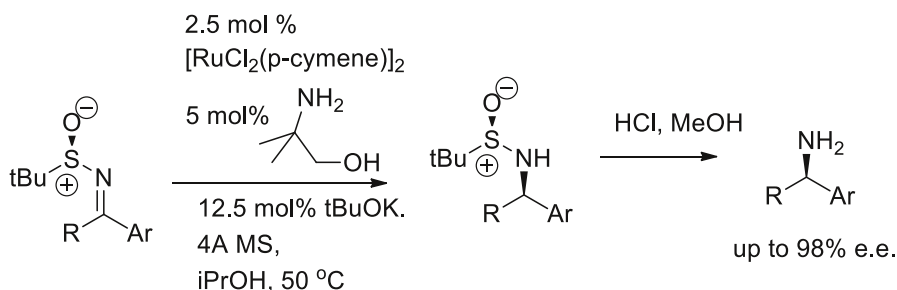

Fig. 50 Diastereoselective C=N bond reduction using a ruthenium catalyst combined with a non chiral ligand
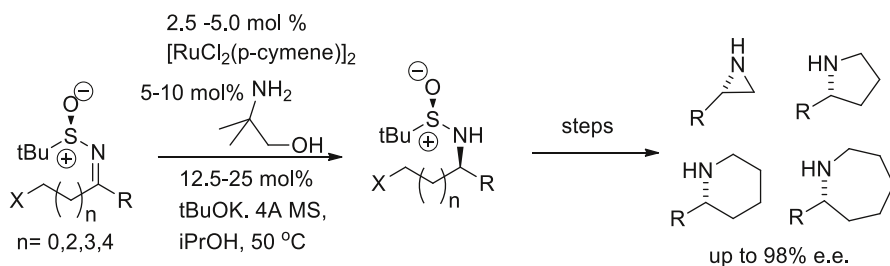
Fig. 51 Diastereoselective C=N bond reduction followed by an intramolecular cyclisation

are impressive [170–174], and this area has been reviewed in some depth [175–178].

A carbene derived from triazole was used in IPA with K_2CO_3 as base, for direct reductive amination of aldehydes with primary amines to form secondary amine products [179]. Other recent examples include (1) a base-free catalyzed reduction of a series of C=O bonds and of the C=N bond of benzylideneaniline (>99 % conversion was achieved in 48 h, with 0.1 mol% catalyst) [180]; (2) heteroditopic dicarbene Rh(I) and Ir(I) complexes containing 1,2,3-triazolylidene–imidazolylidene ligands, mostly tested on acetophenone but with one imine example [181]; (3) Ir complexes of *N*-benzyl-substituted *N*-heterocyclic carbenes where 0.5 mol% catalyst is used with 5 % KOH in IPA in reductions to give products in >99 %
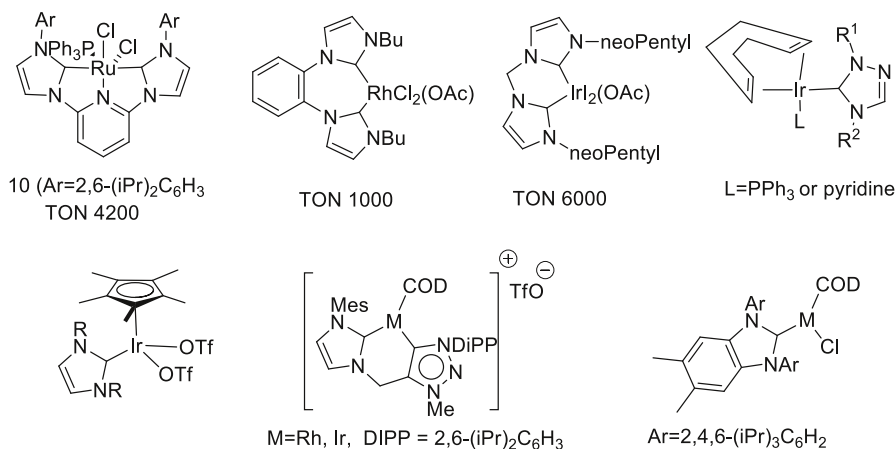
Fig. 52 Carbene complexes for the transfer hydrogenation of imines

yields [182]; and (4) Ir(III) and Ru(II) complexes with 4-acetylbenzyl-*N*-hetero-cyclic carbenes which are active in the reduction of C=O, C=N and hydrogen borrowing [183]. Half-sandwich Ru(II) picolyl-NHC complexes used to reduce C=O and C=N with just 0.1 mol% catalyst have also been reported; the catalyst has a bidentate donor containing an NHC and a pyridine donor, and works well in reductions [184]. Similar complexes with hemilabile OMe or pyridine ligands [185] and Ru(II) picolyl–NHC complexes have also been reported [186].

7 Other Non-Chiral Catalysts

Several examples of TH of imines have been reported using a range of complexes, most commonly based on precious metals including Ru, Ir and Rh [187, 188] Reduction aminations of ketones using ammonium formate with certain Cp*/Ir complexes have also been reported; these are pH-dependent with respect to rate [189]. A Ru phenylindenyl complex has been used in catalysis, primarily as applied to C=O reduction, although examples of imine reduction have also been reported [190]. A novel iminophosphorane-based [P2N2] rhodium complex representing a very innovative catalyst system was prepared and was used to reduce C=O and C=N bonds [191].

Some cobalt examples have recently been published; cobalt on a heterogeneous support was used in TH of C=O, C=N and C=C bonds using IPA as the reducing agent [192]. A cobalt catalyst containing a 'PNP' donor structure was used in ATH of a number of imines, although the focus was on ketones and aldehydes [193]. Nickel nanoparticles have also been used in imino TH [194]. Studies have been carried out on the activation and deactivation processes of a wide range of Cp*/Rh catalysts which have been developed as valuable supported reagents for C=N reductions in flow systems [195, 196]. Efficient and selective TH of pyridines to

tetrahydropyridines and piperidines has been achieved using Cp*Rh diiodide complexes, the method being general and wide in scope [197]. In some cases, an amine/borane complex has been used as the hydrogen source for the reduction [198], although there are also examples where a catalyst is not required [199].

Imine reductions with Ir catalysts have produced some very important breakthroughs in recent years. Xiao et al. reported a new class of cyclometallated Ir-based catalyst—e.g. **15**—or imine TH which is active at very low loadings, and which has been used extensively in reductive amination of ketones including carbohydrates FA/TEA [200]. Studies found that the control of the pH (best ca. 4.8) is critical for high chemoselectivity and activity, allowing the S/C to be as high as 10,000, and higher than in organic solvents, representing an environmentally friendly catalyst system with broad application (Fig. 53) [201]. One specific application of the catalyst has been in the transformation of levulinic acid into pyrrolidinones, which was achieved in high efficiency [202].
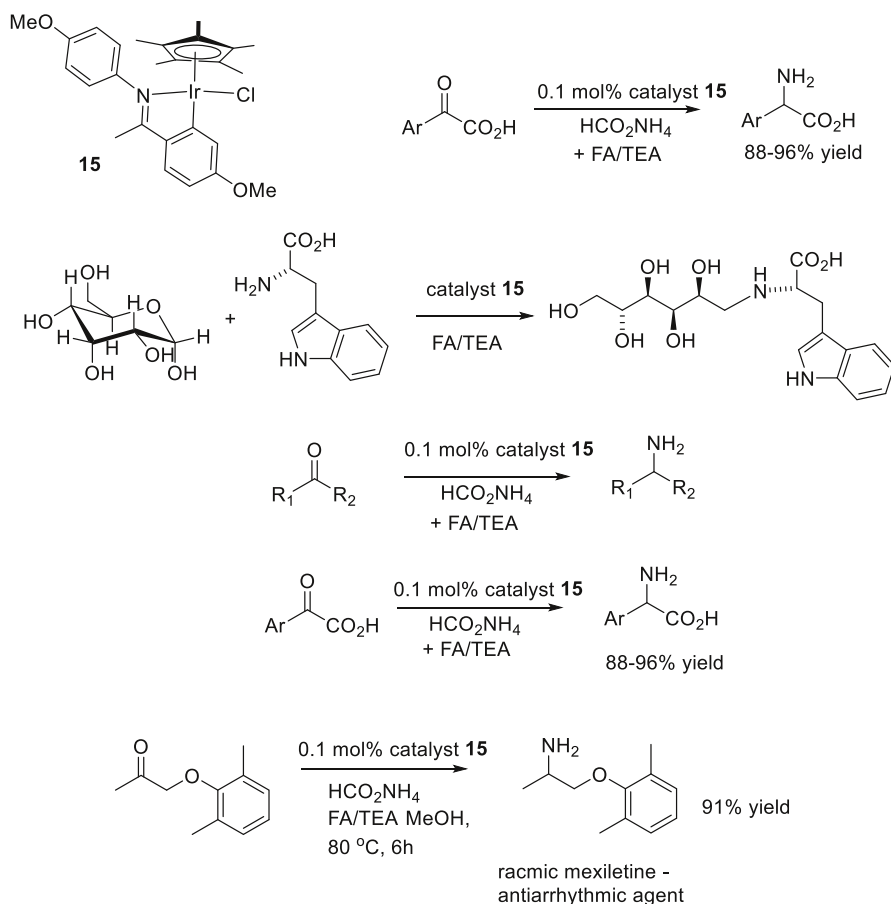
Fig. 53 Iridium-based catalysts for the transfer hydrogenation of imines
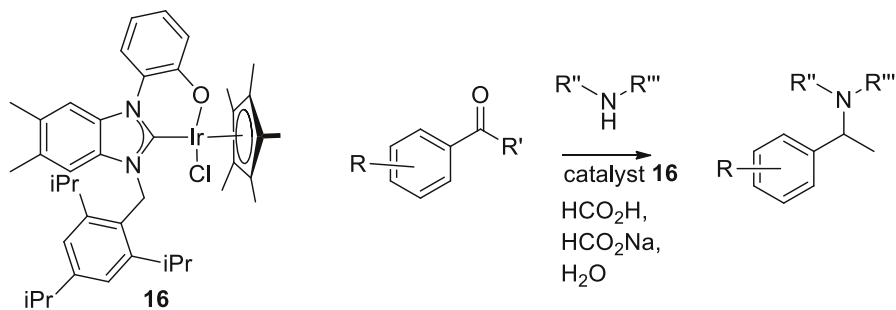
Fig. 54 Iridium-based catalysts for the transfer hydrogenation of imines in aqueous solution

The new catalyst **15** and its derivatives are applicable to the synthesis of primary amines by TH of ketones using sodium formate as well as FA/TEA in the reductions (Fig. 53). FA/TEA improves the results by increasing the acidity relative to ammonium formate alone, which gives products in lower conversions. A large number of examples are given, including substituted aryl and alkyl. Amino acids can be prepared directly from the α-keto acids. Chalcone is reduced to the saturated amine. α-keto ethers work well, and this has been used in the synthesis of an antiarrhythmic agent, as illustrated in Fig. 53 [203]. There are few other examples of the synthesis of amino acids through a reductive amination of this type [204]. A phenoxide-chelated Ir complex—**16** in Fig. 54—has also been prepared and demonstrated to be capable of C=N bond reduction by both hydrogenation and transfer hydrogenation via reductive amination [205].

The iridicycle catalysts also catalyse the TH of *N*-heterocycles (including quinolines, isoquinolines, indoles and pyridinium salts) in water under mild conditions; a solution of formic acid and sodium formate is employed in the reaction. TONs of up to 7500 and catalyst loadings as low as 0.01 mol% were used [206].

Another potentially very important development in TH reactions is the reduction of NAD+ to NADH by half-sandwich complexes of precious metals, which has also been shown to take place within living cells [207–211]. The activity of Ru/TsEN complexes against human ovarian cancer cells has been demonstrated to increase as much as 50-fold when non-toxic doses of formate are added [211].

8 Conclusion

In conclusion, a very wide range of new chemistry has been developed for the transfer hydrogenation of C=N bonds. Several new classes of catalyst have been reported, including several asymmetric catalysts, and applications to a large number of target molecules, notably including pharmaceutical intermediates, have been reported. This area looks set for significant continued growth in future years.

26612421784478373751185487# References

1. Wills M (2008) Modern reduction methods. In: Andersson PG, Munslow IJ (eds). Wiley-VCH, Weinheim, Chapter 11,271
2. Clapham SE, Hadzovic A, Morris RH (2004) Coord Chem Rev 248:2201
3. Gladiali S, Alberico E (2006) Chem Soc Rev 35:226
4. Ikariya T, Murata K, Noyori R (2006) Org Biomol Chem 4:393
5. Samec JSM, Bäckvall J-E, Andersson PG, Brandt P (2006) Chem Soc Rev 35:237
6. Ito JI, Nishiyama H (2014) Tetrahedron Lett 55:3153
7. Wang C, Villa-Marcos B, Xiao J (2011) Chem Commun 47:9773
8. Nugent TC, El-Shazly M (2010) Adv Synth Catal 352:753
9. Wang C, Wu X, Xiao J (2008) Chem Asian J 3:1750
10. Václavik J, Kačer P, Kuzma M, Červený L (2011) Molecules 16:5460
11. Václavik J, Šot P, Vilhanová B, Pecháček J, Kuzma M, Kačer P (2013) Molecules 18:6804
12. Václavik J, Šot P, Pecháček J, Vilhanová B, Matuška O, Kuzma M, Kačer P (2014) Molecules 19:6987
13. Bartoszewicz A, Ahlsten N, Martín-Matute B (2013) Chem Eur J 19:7274
14. Wang D, Astruc D (2015) Chem Rev 115:6621
15. Guizzetti S, Benaglia M, Cozzi F, Annunziata R (2009) Tetrahedron 65:6354
16. Guizzetti S, Benaglia M, Rossi S (2009) Org Lett 11:2931
17. Nolin KA, Ahn RW, Toste FD (2005) J Am Chem Soc 127:12462
18. de Vries JG, Mršić N (2011) Catal Sci Technol 1:727
19. Zheng C, You S-L (2012) Chem Soc Rev 41:2498
20. Basu A, Bhaduri S, Sharma K, Jones PG (1987) J Chem Soc Chem Commun 1126
21. Wang GZ, Bäckvall JE (1992) J Chem Soc Chem Commun 980
22. Mizushima E, Yamaguchi M, Yamagishi T (1999) J Mol Catal A Chem 148:69
23. Aranyos A, Csjernyik G, Kalman KJ, Bäckvall JE (1999) Chem Commun 351
24. Uematsu N, Fujii A, Hashiguchi S, Ikariya T, Noyori R (1996) J Am Chem Soc 118:4916
25. Mao J, Baker DC (1999) Org Lett 1:841
26. Blacker J, Martin J (2004) Scale up studies in asymmetric transfer hydrogenation. In: Blaser HU, Schmidt E (eds) Asymmetric catalysis on an industrial scale: challenges. Approaches and solutions. Wiley, New York, p 201
27. Blackmond D, Ropic M, Stefinovic M (2006) Org Proc Res Dev 10:457
28. Richards S, Ropic M, Blackmond D, Walmsley A (2004) Anal Chim Acta 519:1
29. Aberg JB, Samec JSM, Bäckvall J-E (2006) Chem Commun 2771
30. Martins JED, Clarkson GJ, Wills M (2009) Org Lett 11:847
31. Koike T, Ikariya T (2004) Adv Synth Catal 135:37
32. Martins JED, Contreras Redondo MA, Wills M (2010) Tetrahedron Asymm 21:2258
33. Soni R, Cheung FK, Clarkson GC, Martins JED, Graham MA, Wills M (2011) Org Biomol Chem 9:3290
34. Zhao B, Han Z, Ding K (2013) Angew Chem Int Ed 52:4744
35. Bullock RM (2004) Chem Eur J 10:2366
36. Magee MP, Norton JR (2001) J Am Chem Soc 123:1778
37. Guan H, Iimura M, Magee MP, Norton JR, Zhu G (2005) J Am Chem Soc 127:7805
38. Evanno L, Ormala J, Pihko PM (2009) Chem Eur J 15:12963
39. Václavik J, Kuzma M, Přech J, Kačer P (2011) Organometallics 30:4822
40. Šot P, Kuzma M, Václavik J, Pecháček J, Přech J, Januščák J, Kačer P (2012) Organometallics 31:6496
41. Kuzma M, Václavik J, Novák P, Přech J, Januščák J, Červený J, Pecháček J, Šot P, Vilhanová B, Matoušek V, Goncharova II, Urbanová M, Kačer P (2013) Dalton Trans 42:5174
42. Nova A, Taylor DJ, Blacker AJ, Duckett SB, Perutz RN, Eisenstein O (2014) Organometallics 33:3433
43. Blacker AJ, Clot E, Duckett, SB, Eisensttein O, Gace J, Nova A, Perutz RN, Taylor DJ, Whitwood AC (2009) Chem Commun 6801
44. Vedejs E, Trapencieris P, Suna E (1999) J Org Chem 64:6724
45. Samano V, Ray AJ, Thomson JB, Mook RA Jr, Jung DK, Koble CS, Martin MT, Bigham EC, Regitz CS, Feldman PL, Boros EE (1999) Org Lett 1:1993

46. Wu Z, Perez M, Scalone M, Ayad T, Ratovelomanana-Vidal V (2013) Angew Chem Int Ed 52:4925
47. Přech J, Václavik J, Šot P, Pecháček J, Vilhanová B, Januščák J, Syslová K, Pažout R, Maixner J, Zápal J, Kuzma M, Kačer P (2013) Catalysis Commun 36:67
48. Meuzelaar GJ, van Vliet MCA, Maat L, Sheldon RA (1999) Eur J Org Chem 2315
49. Kaldor I, Feldman PL, Mook RA Jr, Ray JA, Samano V, Sefler AM, Thompson JB, Travis BR, Boros ER (2001) J Org Chem 66:3495
50. Tietze LF, Rackelmann N, Muller I (2004) Chem Eur J 10:2722
51. Itoh T, Miyazaki M, Fukuoka H, Nagata K, Ohsawa A (2006) Org Lett 8:1295
52. Tietze LF, Zhou Y, Topken E (2000) Eur J Org Chem 2247
53. Roszkowski P, Maurin JK, Czarnocki Z (2006) Tetrahedron Asymm 17:1415
54. Verzijl GKM, de Vries AHM, de Vries JG, Kapitan P, Dax T, Helms M, Nazir Z, Skranc W, Imboden C, Stichler J, Ward RA, Abele S, Lefort L (2013) Org Process Res Dev 17:153
55. Cheng J-J, Yang Y-S (2009) J Org Chem 74:9225
56. Vilhanová B, Matoušek V, Václavík J, Syslová K, Přech J, Pecháček J, Šot P, Januščák J, Toman J, Zápal J, Kuzma M, Kačer P (2013) Tetrahedron Asymm 24:50
57. Gulamhussen AM, Kačer P, Prech J, Kuzma M, Červený L (1009) React Kinet Catal Lett 97:335
58. Pecháček J, Václavik J, Přech J, Šot P, Januščák B, Vilhanová B, Vavřík J, Kuzma M, Kačer P (2013) Tetrahedron Asymm 24:233
59. Václavik J, Kuzma M, Kačer P (2011) Chem Listy 105:S80
60. Václavik J, Pecháček J, Prech J, Kuzma M, Kačer P, Červený L (2012) Chem Listy 106:206
61. Václavik J, Pecháček J, Vilhanová B, Šot P, Januščák B, Matoušek V, Přech J, Bártová S, Kuzma M, Kačer P (2013) Catal Lett 143:555
62. Šot P, Vilhanová B, Pecháček J, Václavik J, Zápal J, Kuzma M, Kačer P (2014) Tetrahedron Asymm 25:1346
63. Wills M, Matharu DS, Martins JED (2008) Chem Asian J 3:1374
64. Santos LS, Pilli RA, Rawal VH (2004) J Org Chem 69:1283
65. Szawkalo J, Zawadzka A, Wojtasiewicz K, Leniewski A, Drabowicz J, Czarnocki Z (2005) Tetrahedron Asymm 16:3619
66. Szawkalo J, Czarnocki Z (2005) Monatsh Chem 1136:1619
67. Szawkalo J, Czarnocki SJ, Zawadzka A, Wojtasiewicz K, Leniewski A, Maurin JK, Csarnocki Z, Drabowicz J (2007) Tetrahedron Asymm 18:406
68. Mirabal-Gallardo Y, Piérola J, Shankaraiah N, Santos LS (2012) Tetrahedron Lett 53:3672
69. Roszkowski P, Maurin JK, Czarnockia Z (2013) Tetrahedron Asymmetry 24:643
70. Ahn KH, Ham C, Kim S-K, Cho CW (1997) J Org Chem 62:7047
71. Chen Y-C, Wu T-W, Jiang L, Deng J-G, Liu H, Zhu J, Jiang Y-Z (2005) J Org Chem 70:1006
72. Chen YC, Fei TW, Deng JG, Liu H, Cui X, Zhu J, Jiang YZ, Choi MCK, Chan ASC (2002) J Org Chem 67:5301
73. Wu J, Wang,F, Ma Y, Cui X, Cun L, Deng J, Yu B (2006) Chem Commun 1766
74. Sugie H, Hashimoto Y, Haraguchi N, Itsuno S (2014) J Organomet Chem 751:711
75. Haraguchi N, Nishiyama A, Itsuno S (2010) J Polym Sci A Polymer Chem 48:3340
76. Liu R, Cheng T, Kong L, Chen C, Liu G, Li H (2013) J Catal 307:55
77. Wang L, Zhou Q, Qu CH, Wang QW, Cun LF, Zhu J, Deng JG (2013) Tetrahedron 69:6500
78. Wei Y, Wu X, Wang C, Xiao J (2015) Catal Today 247:104
79. Robertson A, Matsumoto T, Ogo S (2011) Dalton Trans 40:10304
80. Canivet J, Suss-Fink G (2007) Green Chem 9:391
81. Li L, Wu J, Wang F, Liao J, Zhang H, Lian C, Zhu J, Deng J (2007) Green Chem 9:23
82. Shende VS, Shingote SK, Deshpande SH, Kuriakose N, Vanka K, Kelkar AA (2014) RSC Adv 4:46351
83. Haraguchi N, Tsuru K, Arakawa Y, Itsuno S (2009) Org Biomol Chem 7:69
84. Liu PN, Gu PM, Deng JG, Tu YQ, Ma YP (2005) Eur J Org Chem 3221
85. Šillová H, Leitmannová E, Ğervený L (2007) React Kinet Catal Lett 92:129
86. Huang X, Ying JY (2007) Chem Commun 1825
87. Li J, Zhang Y, Han D, Gao Q, Li C (2009) J Mol Catal A Chem 298:31
88. Dai X, Cahard D (2014) Adv Synth Catal 356:1317
89. Wu M, Cheng T, Ji M, Liu G (2015) J Org Chem 80:3708
90. Kang S, Han J, Lee ES, Choi EB, Lee H-K (2010) Org Lett 12:4184
91. Lee SA, Kwak SH, Lee K-I (2011) Chem Commun 47:2372
92. Han J, Kang S, Lee H-K (2011) Chem Commun 47:4004

93. Kim J-A, Seo YJ, Kang S, Han J, Lee HK (2014) Chem Commun 50:13706
94. Seo YJ, Kim J-A, Lee H-K (2015) J Org Chem 80:8887
95. Schüttler C, Li-Böhmer Z, Harms K, von Zezschwitz P (2013) Org Lett 15:800
96. Roth P, Andersson PG, Somfai P (2002) Chem Commun 1752
97. Pablo O, Guijarro D, Yus M (2011) Appl Sci 2:1
98. Ros A, Magriz A, Dietrich H, Ford M, Fernández R, Lassaletta JM (2005) Adv Synth Catal 347:1917
99. Boggs SD, Cobb JD, Gudmundsson KS, Jones LA, Matsuoka RT, Millar A, Patterson DE, Samano V, Trone MD, Xie S, Zhou X-M (2007) Org Process Res Dev 11:539
100. Mangion IK, Chen C-Y, Li H, Maligres P, Chen Y, Christensen M, Cohen R, Jeon I, Klapars A, Krska S, Nguyen H, Reamer RA, Sherry BD, Zavialov I (2014) Org Lett 16:2310
101. Williams GD, Pike RA, Wade CE, Wills M (2003) Org Lett 5:4227
102. Williams GD, Wade CE, Wills M (2005) Chem Commun 4735
103. Strotman NA, Baxter CA, Brands KMJ, Cleator E, Krska SW, Reamer RA, Wallace DJ, Wright TJ (2011) J Am Chem Soc 133:8362
104. Wu, J, Liao, J, Zhu, J, Deng J (2006) Synlett 2059
105. Watanabe Y, Ohta T, Tsuji Y, Hiyoshi T, Tsuji Y (1984) Bull Chem Soc Jpn 57:2440
106. Fujita K-I, Kitatsuji C, Furukawa S, Yamaguchi R (2004) Tetrahedron Lett 45:3215
107. Tan J, Tang W, Sun Y, Jiang Z, Chen F, Xu L, Fan Q, Xiao J (2011) Tetrahedron 67:6206
108. Wu J, Wang C, Tang W, Pettman A, Xiao J (2012) Chem Eur J18:9525
109. Wang C, Li C, Wu X, Pettman A, Xiao J (2009) Angew Chem Int Ed 48:6524
110. Parekh V, Ramsden JA, Wills M (2010) Tetrahedron Asymm 21:1549
111. Samec JSM, Bäckvall JE (2002) Chem Eur J 8:2955
112. Ell AH, Johnson JB, Bäckvall JE (2003) Chem Commun 1652
113. Samec JSM, Ell AH, Bäckvall J-E (2004) Chem Commun 2748
114. Casey CP, Johnson JB (2005) J Am Chem Soc 127:1883
115. Samec JSM, Ell AH, Aberg JB, Privalov T, Eriksson L, Bäckvall J-E (2006) J Am Chem Soc 128:14293
116. Pamies O, Ell AH, Samec JSM, Hermanns N, Bäckvall JE (2002) Tetrahedron Lett 43:4699
117. Quintard A, Rodriguex J (2014) Angew Chem Int Ed 53:4044
118. Landwehr A, Dudle B, Fox T, Blacque O, Berke H (2012) Chem Eur J 18:5701
119. Pannetier N, Sortais J-B, Issenhuth J-T, Barloy L, Sirlin C, Holuigue A, Lefort L, Panella L, de Vries JG, Pfeffer M (2011)Adv Synth Catal 353:2844
120. Menéndez-Pedregal E, Vaquero M, Lastra E, Gamasa P, Pizzano A (2015) Chem Eur J 21:549
121. Xu H, Yang P, Chuanprasit P, Hirao H, Zhou JS (2015) Angew Chem Int Ed 54:5112
122. McSkimming A, Chan B, Bhadbhade MM, Ball GE, Colbran SB (2014) Chem Eur J 21:2821
123. McSkimming A, Bhadbhade MM, Colbran SB (2013) Angew Chem Int Ed 52:3411
124. Sui-Seng C, Freutel F, Lough AJ, Morris RH (2008) Angew Chem Int Ed 47:940
125. Zhou S, Fleischer S, Junge K, Das S, Addis D, Beller M (2010) Angew Chem Int Ed 49:8121
126. Zuo W, Lough AJ, Li YF, Morris RH (2013) Science 342:1080
127. Sues PE, Demmans KZ, Morris RH (2014) Dalton Trans 43:7650
128. Zuo W, Morris RH (2015) Nat Protocol 10:241
129. Chelucci G, Baldino S, Baratta W (2015) Acc Chem Res 48:363
130. Fu Y, Soni R, Romero MJ, Pizarro AM, Salassa L, Clarkson GJ, Hearn JM, Habtemariam A, Wills M, Sadler PJ (2013) Chem Eur J 19:15199
131. Ringenberg M, Ward TR (2011) Chem Commun 47:8470
132. Dürrenberger M, Heinisch T, Wilson YM, Rossel T, Nogueira E, Knörr L, Mutschler A, Kersten K, Zimbron MJ, Pierron J, Schirmer T, Ward TR (2011) Angew Chem Int Ed 50:3026
133. Zimbron JM, Heinisch T, Schmid M, Hamels D, Nogueira ES, Schirmer T, Ward TR (2013) J Am Chem Soc 135:5384
134. Schwizer F, Köhler V, Dürrenberger M, Knörr L, Ward TR (2013) ACS Catal 3:1752
135. Nogueira ES, Schleier T, Dürrenberger M, Ballmer-Hofer K, Ward TR, Jaussi R (2014) Protein Express Purif 93:54
136. Quinto T, Schwizer F, Zimbron JM, Morina A, Köhler V, Ward TR (2014) Chem Cat Chem 6:1010
137. Wilson YM, Duerrenberger M, Nogueira ES, Ward TR (2014) J Am Chem Soc 136:8928
138. Muñoz Robles V, Vidossich P, Lledós A, Ward TR, Maréchal JD (2014) ACS Catal 4:833
139. Monnard FW, Nogueira ES, Heinisch T, Schirmer T, Ward TR (2013) Chem Sci 4:3269

140. Genz M, Köhler V, Krauss M, Singer D, Hoffmann R, Ward TR, Sträter N (2014) ChemCatChem 6:736
141. Muñoz Robles V, Dürrenberger M, Heinisch T, Lledós A, Schirmer T, Ward TR, Maréchal JD (2014) J Am Chem Soc 136:15676
142. Heinisch T, Pellizzoni M, Dürrenbergerm M, Tinberg CE, Köhler V, Klehr J, Häussinger D, Baker D, Ward TR (2015) J Am Chem Soc 137:10414
143. Köhler V, Wilson YM, Dürrenberger M, Ghislieri D, Churakova E, Quinto T, Knörr L, Häussinger D, Hollmann F, Turner NJ, Ward TR (2013) Nature Chem 5:93
144. Heinisch T, Ward TR (2010) Curr Opin Chem Biol 14:184
145. Köhler V, Wilson YM, Lo C, Sardo A, Ward TR (2010) Curr Opin Chem Biol 21:744
146. Ringenberg MR, Ward TR (2011) Chem Commun 47:8470
147. Ward TR (2011) Acc Chem Res 44:47
148. Duerrenberger M, Ward TR (2014) Curr Opin Chem Biol 19:99
149. Tang W, Johnson S, Iggo JA, Berry NG, Phelan M, Lian L, Basca J, Xiao J (2013) Angew Chem Int Ed 52:1668
150. Zhang Y, Lim C-S, Sim DSB, Pan HJ, Zhao Y (2014) Angew Chem Int Ed 53:1399
151. Rong Z-Q, Zhang Y, Chua RHB, Pan H-J, Zhao Y (2015) J Am Chem Soc 137:4944
152. Tang W, Xiao J (2014) Synthesis 46:1297
153. Chen QA, Chen MW, Yu CR, Shi L, Wang DS, Yang Y, Zhou YG (2015) J Am Chem Soc 133:16432
154. Zhang M, Yang H, Zhang Y, Zhu C, Li W, Cheng Y, Hu H (2011) Chem Commun 47:6605
155. Chatterjee I, Oestreich M (2015) Angew Chem Int Ed 54:1965
156. Nishide K, Node M (2002) Chirality 14:759
157. Graves CR, Scheidt KA, Nguyen ST (2006) Org Lett 8:1229
158. Kondo Y, Sasak M, Kawahata M, Yamaguchi K, Takeda K (2014) J Org Chem 79:3601
159. Kadyrov R, Riermeier TH (2003) Angew Chem Int Ed 42:5472
160. Kitamura M, Lee D, Hayashi S, Tanaka S, Yoshimura M (2002) J Org Chem 7:8685
161. Rubio-Pérez L, Pérez-Flores FJ, Sharma P, Velasco L, Cabrera A (2009) Org Lett 11:265
162. Guijarro D, Pablo O, Yus M (2009) Tetrahedron Lett 50:5386
163. GuijarroD, Pablo O, Yus M (2010) J Org Chem 75:5265
164. Collados JF, Toledano E, Guijarro D, Yus M (2012) J Org Chem 77:5744
165. Guijarro D, Pablo O, Yus M (2011) Tetrahedron Lett 52:789
166. Pablo O, Guijarro D, Kovacs G, Lledós A, Ujaque G, Yus M (2012) Chem Eur J 18:1969
167. Guijarro D, Pablo O, Yus M (2013) J Org Chem 78:3647
168. Pablo O, Guijarro D. Yus M (2014) Eur J Org Chem 7034
169. Pablo O, Guijarro D, Yus M (2013) J Org Chem 78:9181
170. Kuhl S, Schneider R, Fort Y (2003) Organometallics 22:4184
171. Danopoulos AA, Winston S, Motherwell WB (2002) Chem Commun 1376
172. Albrecht M, Crabtree RH, Mata J, Peris E (2002) Chem Commun 32
173. Miecznikowski JR, Crabtree RH (2004) Polyhedron 23:2857
174. Burling S, Whittlesey MK, Williams JMJ (2005) Adv Synth Catal 347:591
175. Diez-Gonzalez S, Marion N, Nolan SP (2009) Chem Rev 109:2527
176. Peris E, Crabtree RH (2004) Coord Chem Rev 248:2239
177. Saidi O, Williams JMJ (2011) Top Organomet Chem 34:77
178. Dragutan V, Dragutan I, Delaude L, Demonceau A (2007) Coord Chem Rev 251:765
179. Gnanamgari D, Moores A, Rajaseelan E, Crabtree RH (2007) Organometallics 26:1226
180. Corberán R, Peris E (2008) Organometallics 27:1954
181. Sluijter SN, Elsevier CJ (2014) Organometallics 33:6389
182. Gülcemal S, Gökçe AG, Çetinkaya B (2013) Inorg Chem 52:10601
183. Zhu X-H, Cai L-H, Wang C-X, Wang Y-N, Guo X-Q, Hou X-F (2014) J Mol Catal A Chem 393:134
184. Fernández FE, Puerta MC, Valerga P (2011) Organometallics 30:5793
185. Jiménez MV, Fernández-Tornos J, Pérez-Torrente JJ, Modrego FJ, Winterle S, Cunchillos C, Lahoz FJ, Oro LA (2011) Organometallics 30:5493
186. Fernández FE, Puerta MC, Valerga P (2012) Organometallics 31:6868
187. Cami-Kobeci G, Williams JMJ (2004) Chem Commun 1072
188. Galmari V, Rengan R (2006) Inorg Chem Commun 9:703
189. Ogo S, Makihara N, Kaneko Y, Watanabe Y (2001) Organometallics 20:4903

190. Manzini S, Urbina Blanco CA, Nolan SP (2012) Adv Synth Catal 354:3036
191. Buchard A, Payet E, Auffrant A, Le Goff X, Le Floch P (2010) New J Chem 34:2943
192. Long J, Zhou Y, Li Y (2015) Chem Commun 51:2331
193. Zhang G, Hanson SK (2013) Chem Commun 49:10151
194. Alonso F, Riente PA, M Yus M (2008) Synlett 1289
195. Sherborne GJ, Chapman MR, Blacker AJ, Bourne RA, Chamberlain TW, Crossley BD, Lucas SJ, McGowan PC, Newton MA, Screen TEO, Thompson P, Willans CE, Nguyen BN (2015) J Am Chem Soc 137:4151
196. Lucas SJ, Crossley BD, Pettman AJ, Vassileiou AD, Screen TEO, Blacker AJ, McGowan PC (2013) Chem Commun 49:5562
197. Wu J, Tang W, Pettman A, Xiao J (2013) Adv Synth Catal 355:40
198. Nixon TD, Whittlesey MK, Williams JMJ (2011) Tetrahedron Lett 52:6652
199. Yang X, Zhao L, Fox T, Wang Z-X, Berke H (2010) Angew Chem Int Ed 48:2058
200. Wang C, Pettman A, Bacsa J, Xiao J (2010) Angew Chem Int Ed 49:7548
201. Lei Q, Wei Y, Talwar D, Wang C, Xue D, Xiao J (2013) Chem Eur J 19:4021
202. Wei Y, Wang C, Jiang X, Xue D, Li J, Xiao J (2013) Chem Commun 49:5408
203. Talwar D, Salguero NP, Robertson CM, Xiao J (2014) Chem Eur J 20:245
204. Ogo S, Uehara K, Abura T, Fukuzumi S (2004) J Am Chem Soc 126:3020
205. Gülcemal D, Gülcemal S, Robertson CM, Xiao J (2015) Organometallics 34:4394
206. Talwar D, Li HY, Durham E, Xiao J (2015) Chem Eur J21:5370
207. Streckham E, Herrmann S, Ruppert R, Thömmes J (1990) Wandrey. C Angew Chem Int Ed 29:388
208. Liu Z, Sadler PJ (2014) Acc Chem Rev 47:1174
209. Betanzos-Lara S, Liu Z, Habtemariam A, Pizarro AM, Qamar B, Sadler PJ (2012) Angew Chem Int Ed 51:3897
210. Soldevila-Barreda JJ, Romero-Canelon I, Habtemariam A, Sadler PJ (2015) Nat Commun 6:6582
211. Quinto T, Häussinger D, Köhler V, Ward T (2015) Org Biomol Chem 13:357

CrossMark

REVIEW

Organocatalytic Transfer Hydrogenation and Hydrosilylation Reactions

Raquel P. Herrera[1]

Abstract The reduction of different carbon–carbon or carbon–heteroatom double bonds is a powerful tool that generates in many cases new stereogenic centers. In the last decade, the organocatalytic version of these transformations has attracted more attention, and remarkable progress has been made in this way. Organocatalysts such as chiral Brønsted acids, thioureas, chiral secondary amines or Lewis bases have been successfully used for this purpose. In this context, this chapter will cover pioneering and seminal examples using Hantzsch dihydropyridines **1** and trichlorosilane **2** as reducing agents. More recent examples will be also cited in order to cover as much as possible the complete research in this field.

1 Introduction

The reduction of different carbon–carbon or carbon–heteroatom double bonds is an important transformation that generates in many cases new stereogenic centers. Particularly, the asymmetric reduction of prochiral ketimines represents one of the most important methods and straightforward procedures for preparing chiral amines. This approach is one of the key reactions and powerful tools in synthetic organic

✉ Raquel P. Herrera
raquelph@unizar.es

1 Laboratorio de Organocatálisis Asimétrica. Instituto de Sintesis Química y Catálisis Homogénea (ISQCH-CSIC), Saragossa, Spain

Springer
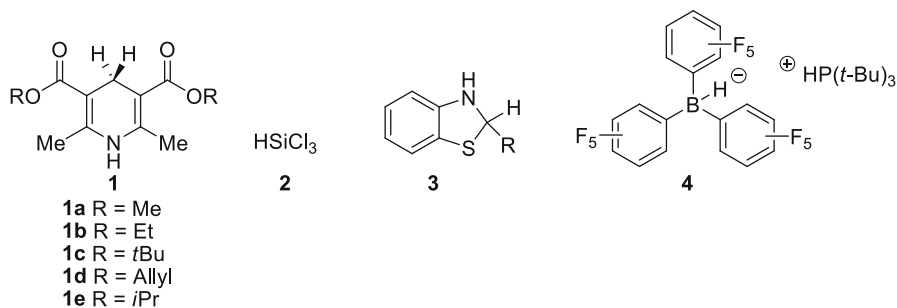
Fig. 1 Model reducing agents

chemistry, which provides precious building blocks for natural products, pharmaceutical, and other fine chemical industries [1]. Until the last decade, available chemical catalysts for the enantioselective reduction of these substrates were mostly limited to chiral transition metal complexes, which often required elevated pressures and/or the use of additional additives to afford high yields and ee values (for reviews, see [2–10]). However, with the increasing interest during the last years in the development of the organocatalysis field [11–13], the organocatalytic version of these transformations has attracted more attention, and remarkable progress has been made in this way (For selected reviews on organocatalytic transfer hydrogenations, see [14–20]). The organocatalytic transfer hydrogenation is carried out by four fundamentally different approaches (Fig. 1): (1) reduction with Hantzsch dihydropyridines **1**, mainly catalyzed by chiral Brønsted acids, which activate the electrophilic substrates (for reviews, see: [21–26]); (2) hydrosilylation with trichlorosilane **2**, catalyzed through chiral Lewis-bases, which, in contrast, activate the nucleophilic hydride source [27–30]; and more recently, (3) transfer hydrogenation using benzothiazolines **3** as the reducing agent (Benzothiazoline **3** was firstly introduced by Akiyama's group for asymmetric transfer hydrogenation reactions: [31, 32]; [33]) and (4) hydrogen activation by frustrated Lewis pair **4** [34].

Interestingly, **1a–c** and **2** are commercially available, while **1d–e** must be synthesized. Trichlorosilane **2** is cheaper than the other reagents and **1a** is the most expensive one. Trichlorosilane **2** has shown a great spectrum of reactivity, as the reader will find in the second part of this chapter.

Although this field has been extensively reported, only pioneering and seminal examples using Hantzsch dihydropyridines **1** and trichlorosilane **2**, as reducing agents, will be disclosed in this chapter. More recent examples will be also cited in order to cover as much as possible the complete research in this field.

2 Hantzsch Esters as Hydride Source

Inspired by Nature, and trying to reproduce the enzymatic reductions using NAD(P)H as cofactor in living organisms, many research groups have focused part of their investigation on the development of new environmentally friendly and successful reducing agents trying to simulate its reactivity. That is the case of

Hantzsch esters **1** as a hydride source [35, 36], which were initially synthesized following a multicomponent approach as an interesting synthetic example of 1,4-dihydropyridines. Although, it was only in the last decade when Hantzsch esters **1** became a key piece in the reduction processes using organocatalysts, the first reported example of transfer hydrogenation using this hydride source without metals is dated from 1989 ([37], for earlier examples on the transfer hydrogenation of imines with Hantzsch esters **1**: [38–40]). In the next pages, the pioneering enantioselective examples using Hantzsch dihydropyridines **1** in organocatalysis, and the most recent advances in this subarea of research will be briefly covered.

2.1 Chiral Phosphoric Acid Catalyzed Transfer Hydrogenation

The reduction of imines is potentially useful for the synthesis of enantiomerically pure amines, since chiral amines appear in numerous interesting compounds in nature, and they have also a remarkable use as ligands in metal catalysis or as chiral organocatalysts. However, until 2001, this approach had been mainly explored using metal catalysts [2–10].

The first enantioselective Brønsted acid-catalyzed transfer hydrogenation of ketimines using Hantzsch ester **1b** was reported by Rueping's [41] (Scheme 1) and, independently, by List's groups (Scheme 2) [42] affording excellent results in terms of enantioselectivity and reactivity and, in both cases, using chiral phosphoric acid derivatives **6** and **9**. Interestingly, in the latter case, the authors significantly improved the results employing 20-fold reduction in the catalyst loading.

Based on previous studies where the imines were reduced with Hantzsch dihydropyridines in the presence of achiral Lewis [43] or Brønsted acid catalysts, [44] joined to the capacity of phosphoric acids to activate imines (for reviews about chiral phosphoric acid catalysis, see: [45–58]), the authors proposed a reasonable catalytic cycle to explain the course of the reaction (Scheme 3) [41]. A first protonation of the ketimine with the chiral Brønsted acid catalyst would initiate the cycle. The resulting chiral iminium ion pair **A** would react with the Hantzsch ester **1b** giving an enantiomerically enriched amine product and the protonated pyridine salt **B** (Scheme 3). The catalyst is finally recovered and the byproduct **11** is obtained in the last step. Later, other research groups also supported this mechanism (for mechanistic studies of this reaction, see: [59–61]).
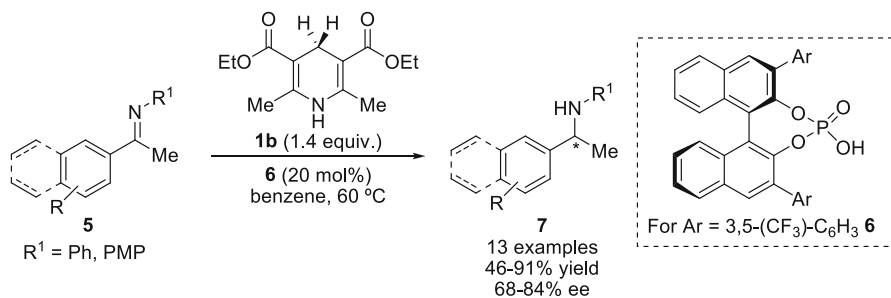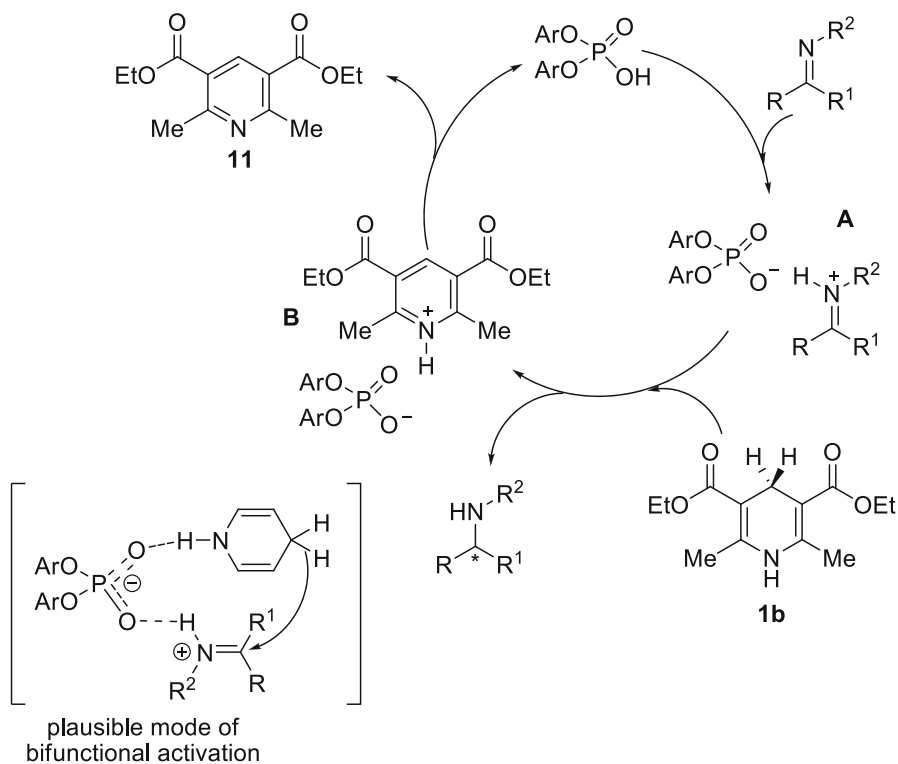

Scheme 1 Reduction of imines using phosphoric acid **6** as catalyst
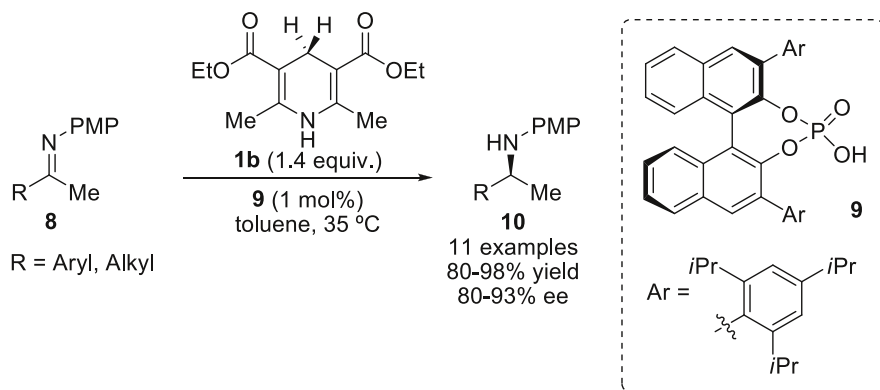
Scheme 2 Reduction of imines using Brønsted acid **9** as catalyst

Scheme 3 Proposed catalytic cycle for the reduction of ketimines

Since these seminal organocatalytic reports, other groups have used the same strategy for the reduction of different interesting imine derivatives such as MacMillan [62] [It is important to remark that as declared by the authors, the complete details of MacMillan's group concerning reductive amination were first

published via oral presentation in August 2005 in presentations in Germany, Wales, Japan, and the USA prior to submission of their manuscript on this field (October 23rd, 2005) (see Ref. [21], You [63, 64], and Antilla [65]).

Because of the importance of chiral nitrogen on heterocycles constituting the structural core of many natural alkaloids and synthetic drugs, a great extension of this protocol has been performed during the last decade mainly by Rueping's group, affording different and valuable chiral heterocyclic products. In the next pages some pivotal examples reported by this research group will be disclosed and commented on.

Thus, Rueping and co-workers used their abovementioned methodology for the interesting activation of quinolines **12** by catalytic protonation and subsequent transfer hydrogenation, which involved a 1,4-hydride addition, isomerization, and final 1,2-hydride addition to generate the desired 1,2,3,4-tetrahydroquinolines **14** in a cascade process (Scheme 4) [66]. These compounds have proven to be interesting synthetic scaffolds in the preparation of pharmaceuticals and agrochemicals [67]. In this context, and having developed a general and enantioselective protocol, the authors demonstrated the applicability of this new methodology to the synthesis of biologically active tetrahydroquinoline alkaloids: galipinine **15a** [68, 69], cuspareine **15b**, [69, 70], and angustureine **15c** [69] (Scheme 4) (for a report on the achiral transfer hydrogenation of differently substituted quinolines, see also [71]) (for similar methodologies as an extension of this approach, see: [72–78]; for transfer hydrogenation of 1,2-dihydroquinolines, see: [79]).

Biologically active tetrahydroquinoline alkaloids **15** were prepared by simple *N*-methylation of intermediates **14** to lead the desired natural products in good overall yields and high enantioselectivities (for examples of dual catalysis, see: [80, 81], for more recent examples, see: [82–84]).

To explain the obtained products, the authors hypothesized that the first step should be the protonation of the quinoline **12** through the phosphoric acid catalyst **13** to generate the iminium ion **A** (Scheme 5). Transfer of a first hydride from the
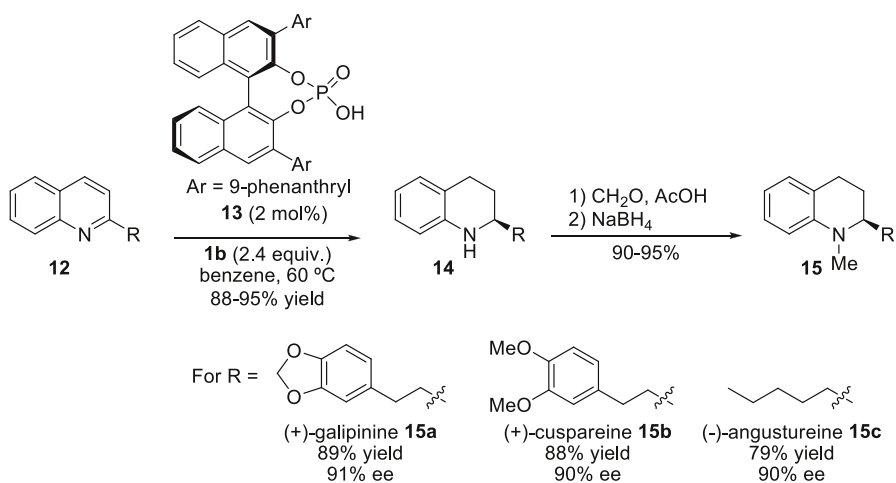
Scheme 4 Syntheses of biologically active tetrahydroquinoline alkaloids **15**

dihydropyridine **1b** would generate the enamine intermediate **16** and pyridinium salt **B**, which would regenerate the acid catalyst **13** and release pyridine **11**. The enamine **16** would interact with another molecule of Brønsted acid **13** to produce iminium **C**, which would receive the attack of a second molecule of hydride giving rise to the desired tetrahydroquinoline **14**. Subsequent proton transfer would recycle again the Brønsted catalyst **13** and would generate a second equivalent of pyridine **11** (Scheme 5).

The reduction of quinolines was applied to the asymmetric preparation of the anti-bacterial agent (*R*)-flumequine **18** [85, 86], starting from quinoline **12a** and generating the key tetrahydroquinoline intermediate **14a** for the total synthesis and using **17** as catalyst (Scheme 6) [87].
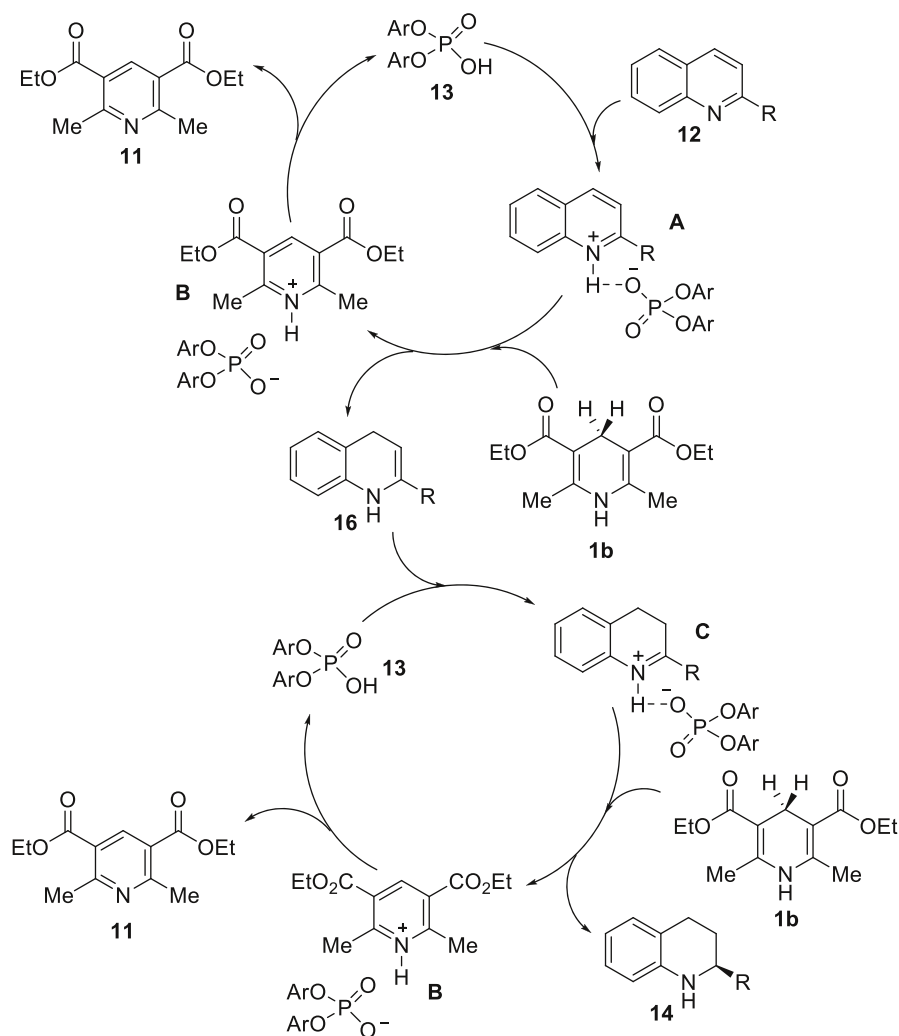
Scheme 5 Mechanism for the cascade transfer hydrogenation of quinolines **12**

Gong and co-workers developed the first step-economical synthesis of the previously described process. The approach involves a Friedländer condensation [88, 89] followed by a transfer hydrogenation catalyzed by a combination of an achiral Lewis acid and a chiral Brønsted acid. This affords the direct conversion of 2-aminobenzaldehyde derivatives **19** and ketones **23** into highly optically active 1,2,3,4-tetrahydroquinoline derivatives **22** and **24**, with enolizable dicarbonyl compounds **20** (Scheme 7) [90].

The Lewis acid (LA) is believed to only participate in the catalyzed Friedländer condensation, while the chiral phosphoric acid (B*-H) could participate in the first condensation to give **25** and in the asymmetric transfer hydrogenation of **A** (Scheme 8). The success of this approach relies in the compatibility and synergic effect of both catalysts, the Lewis acid, and the chiral Brønsted acid.

Rueping's group pioneered the first example of a catalyzed enantioselective reduction of pyridines giving rise to direct access to enantiomerically pure piperidines **26** (Fig. 2) [91].

The applicability of this new method was demonstrated in the formal synthesis of *diepi*-pumiliotoxin C **31** from the pumiliotoxin family (Scheme 9) [91]. Hence, the reduction of pyridine **29a**, which can be readily prepared according to Bohlmann and Rahtz's procedure starting from **27** and **28** [92, 93], gives the corresponding (*S*)-2-propylhexahydroquinolinone **30a** as a key intermediate for the subsequent transformation (Scheme 9) [94].

A plausible mechanism of the reduction was also proposed to explain the final products. Thus, in the first step, the pyridines **29** would be activated through catalytic protonation by the phosphoric acid catalyst **21**, resulting in the formation of a chiral ion pair **A** (Scheme 10). A subsequent hydride transfer from the Hantzsch
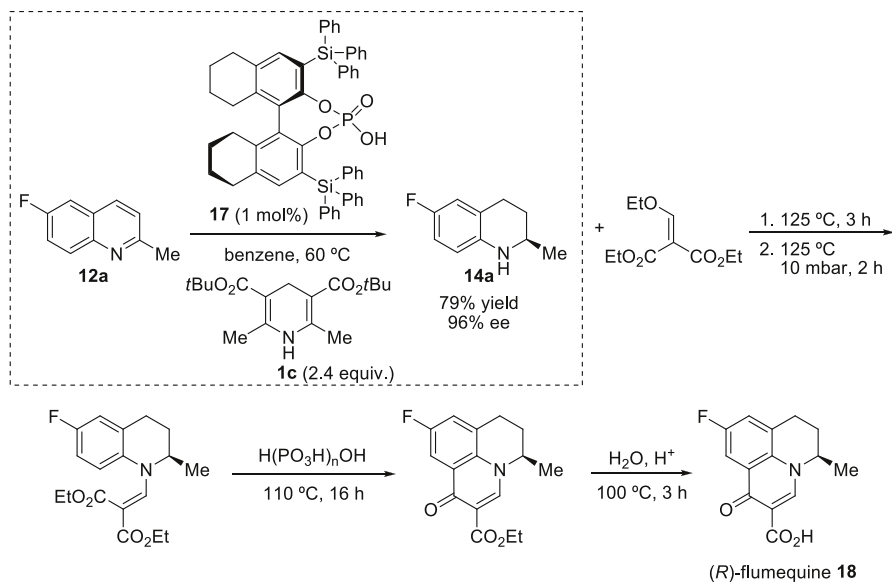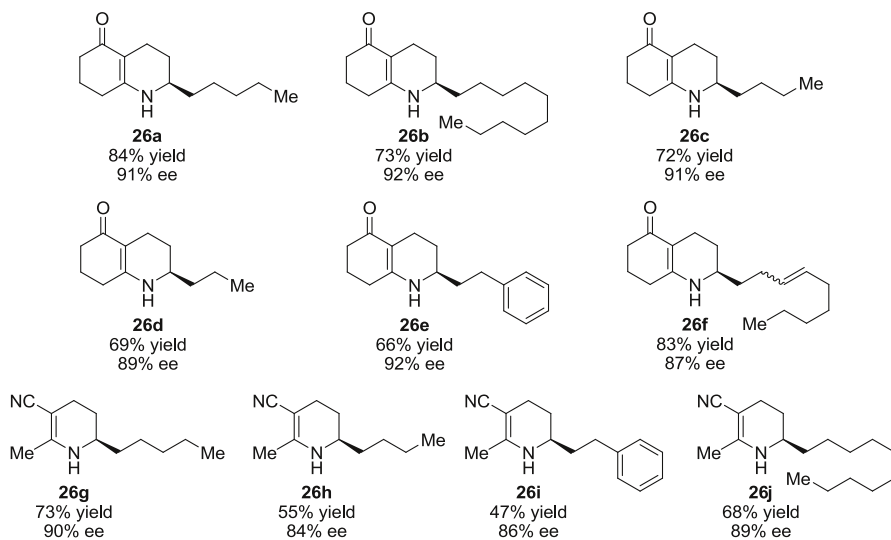


Scheme 6 Synthesis of (*R*)-flumequine **18**
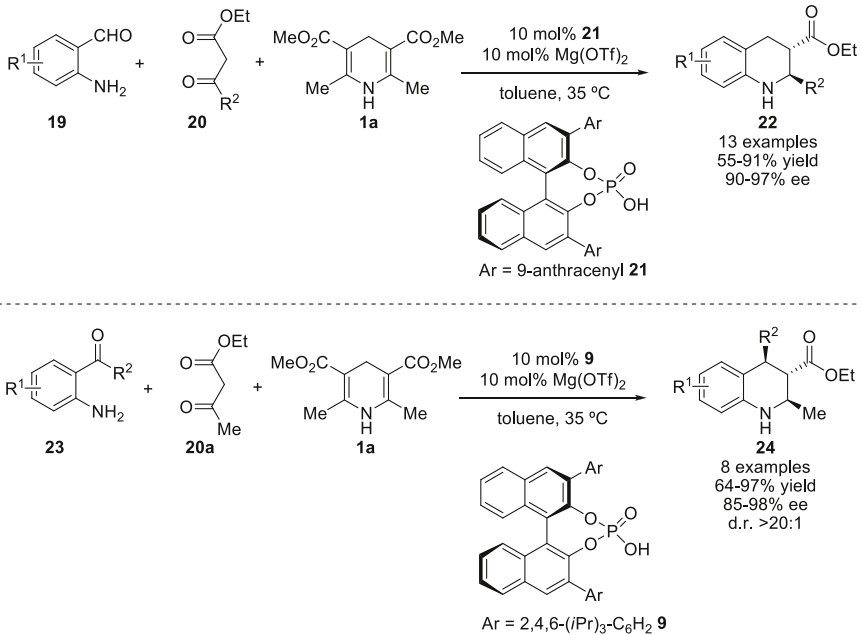
Scheme 7 Step-economical syntheses of tetrahydroquinolines **22** and **24**
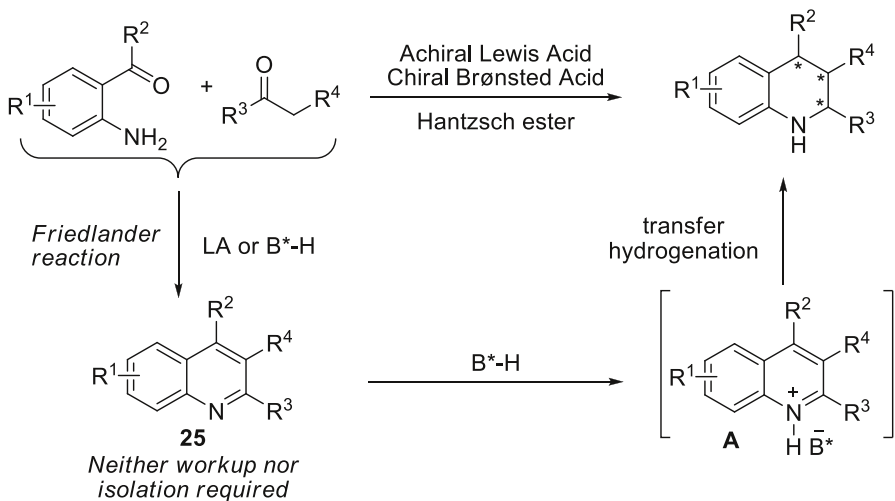
Scheme 8 Proposed mechanism

ester **1b** would afford adduct **B**, which would be transformed into the iminium ion **C** through an isomerization. A second hydride transfer would render the desired product **26** or **30**, and **21** would be regenerated (Scheme 10).

**Fig. 2** Scope of reduction of pyridines
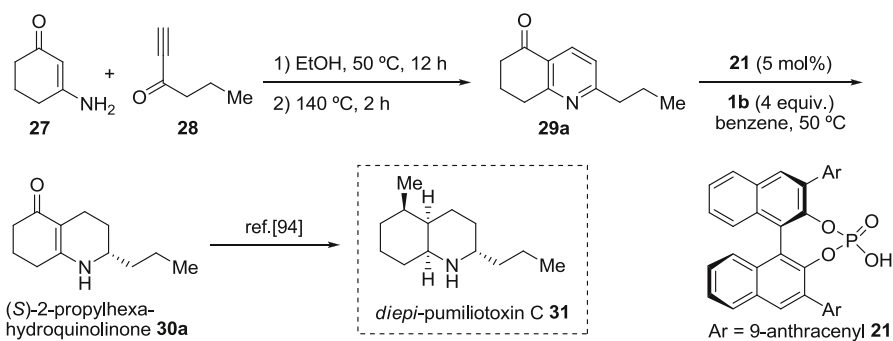
**Scheme 9** Formal synthesis of *diepi*-pumiliotoxin C **31**

The same research group developed a similar protocol for the reduction of benzoxazines **32**, benzothiazines **33,** and benzoxazinones **34** as key examples of heterocyclic compounds (Fig. 3) [95].

With the increasing interest experienced by enantioselective domino reactions as powerful tools for the direct construction of enantioenriched complex targets starting from simple and readily available precursors, many investigations have been developed in this area of research, where the organocatalysis has gained an important position [96–98].

In this context, Rueping's group envisioned the asymmetric organocatalytic multiple-reaction cascade version of the abovementioned process in which a six-step sequence was catalyzed by the chiral Brønsted acid catalyst **21** providing direct access to a broad scope of valuable tetrahydropyridines **26** and azadecalinones **35** with high enantioselectivities (Scheme 11) [99].
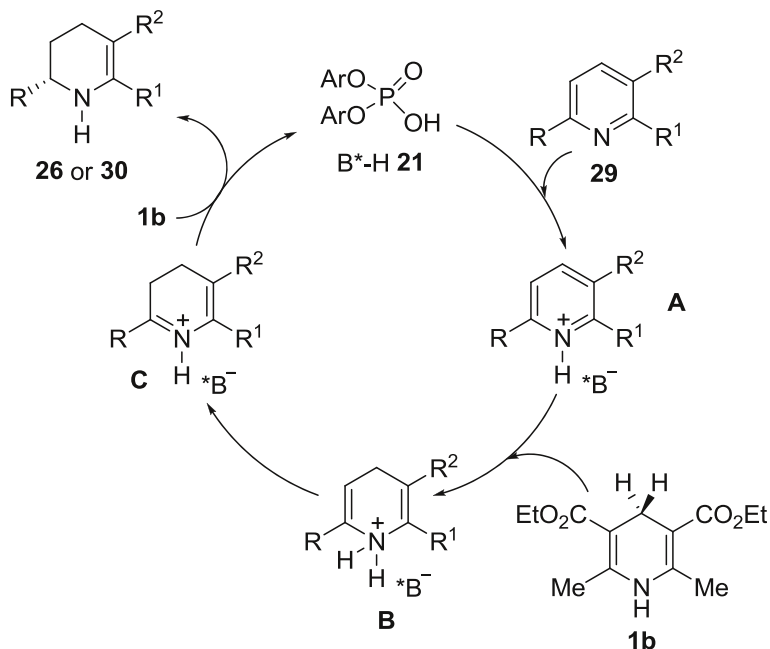
Scheme 10 Proposed mechanism giving rise to piperidines **26** and **30**

| 32 | 33 | 34 |
| benzoxazines | benzothiazines | benzoxazinones |
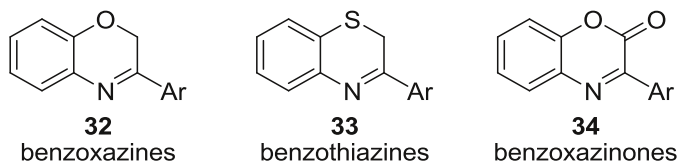
Fig. 3 Model heteroaromatic compounds reduced

An interesting mechanism was suggested by the authors to explain the final products obtained through this methodology, where the chiral Brønsted acid catalyst **21** would participate in the six reaction steps proposed (Scheme 12).

Other interesting examples of catalytic transfer hydrogenation have been also described for the transformation of quinoxaline and quinoxalinones into the corresponding 2-tetrahydroquinoxalines **36** (Fig. 4) and 3-dihydroquinoxalinones **37** (Fig. 5) [100], with a structural core which exhibits remarkable biological properties [101–104].

Interestingly, Shi, Tu, and co-workers developed the tandem version of the abovementioned protocol comprising a cyclization/transfer hydrogenation strategy leading to enantioenriched tetrahydroquinoxalines **36** and dihydroquinoxalinones **37** from readily accessible materials with excellent results in terms of reactivity and enantioselectivity (Scheme 13) [105].

In order to explain the stereochemical outcome observed in this process, the authors proposed a plausible reaction pathway and transition state on the basis of
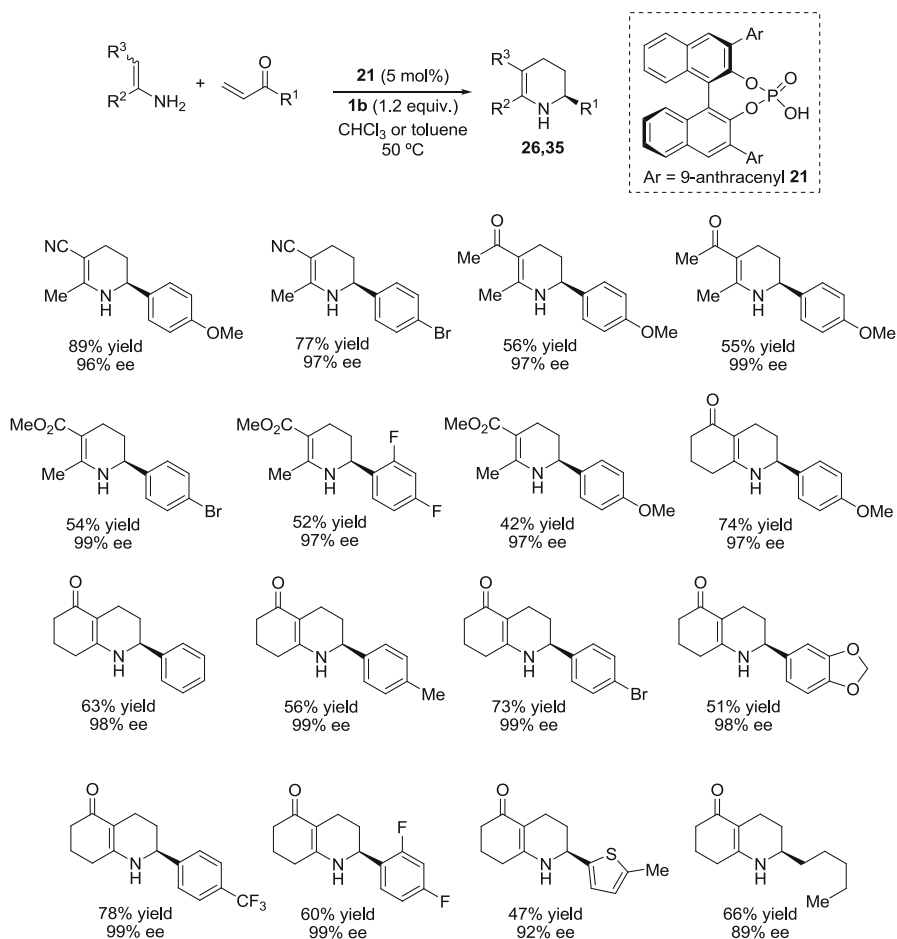
Scheme 11 Synthesis of tetrahydropyridines **26** and azadecalinones **35**

their experimental results and previously reported calculations on transfer hydro-genation of imines [59–61] (Scheme 14). In this mechanism, the phosphoric acid catalyst **21** would act in a bifunctional mode, and the attack of the hydride in the TS justifies the absolute (R)-configuration observed in final products **36** and **37**.

Rueping and co-workers have recently developed a highly enantioselective synthesis of differently substituted tetrahydroquinolines **40** via a first photocyclization of substituted 2-aminochalcones **38** and subsequent Brønsted acid catalyzed asymmetric reduction of the in situ generated quinoline **39**, to give final products in moderate to high yields and with excellent enantioselectivities (Scheme 15) [106, 107].

The same research group applied the above methodology for the synthesis of valuable 4H-chromenes **43** in good yields and with excellent enantioselectivities. The approach consists of a dual light and Brønsted acid mediated isomerization–cyclization reaction starting from enones **41** to yield 2H-chromen-2-ol intermediates **A**. The subsequent Brønsted acid catalyzed elimination of water leads to an
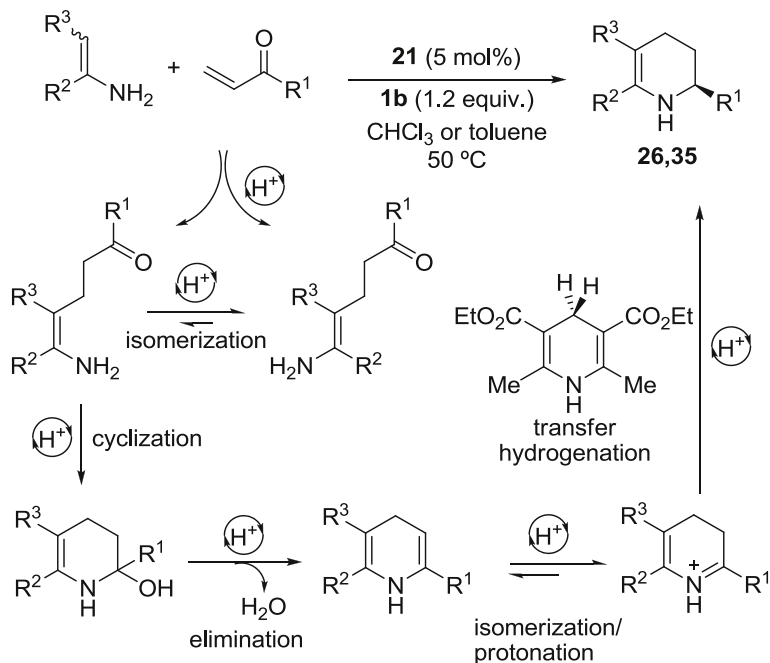
Scheme 12 Proposed mechanism for the cascade reaction

unprecedented intermediary chiral ion pair between a benzopyrylium ion and a chiral phosphate anion **B**. The following transfer hydrogenation exclusively occurs in the 4-position, providing the desired enantioenriched 4*H*-chromenes **43** (Scheme 16) [108].
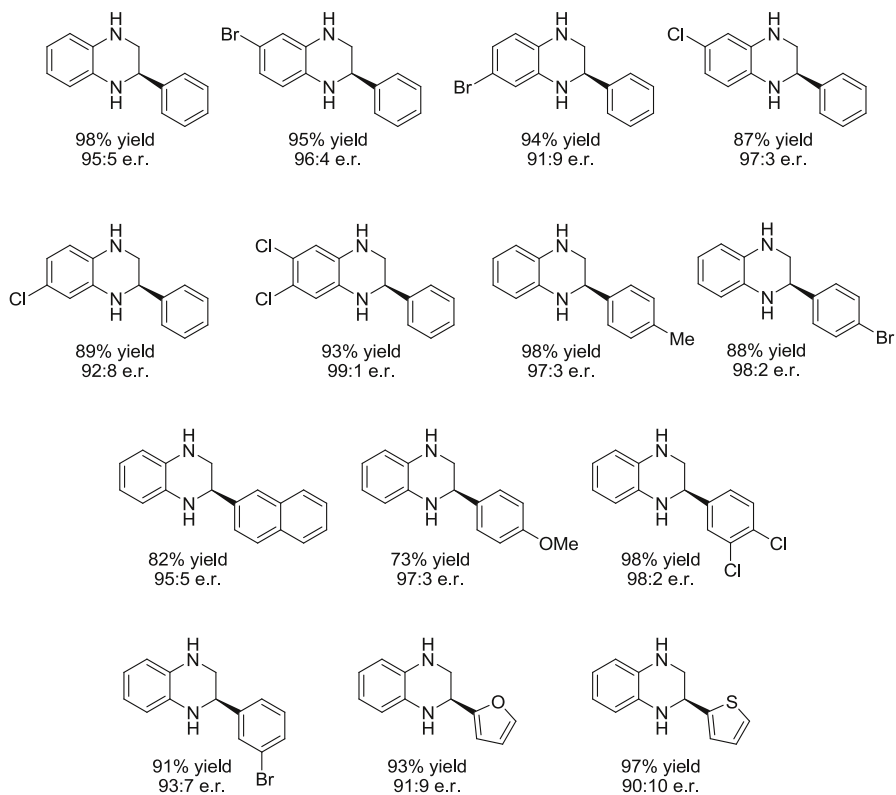
Recently, a pioneering organocatalytic asymmetric reduction strategy for the synthesis of chiral 1,1-diarylethanes **46** with high efficiency and enantioselectivity was reported by Zhu, Lin, Sun, and co-workers (Scheme 17) [109].

A plausible reaction mechanism is hypothesized by the authors. The electron-rich styrene substrate **44** would be protonated by phosphoric acid catalysts **45** to generate the tertiary carbocation intermediate **A**. The neutral resonance structure **B**, activated by B*-H would receive the subsequent hydride addition giving the observed products **46** and regenerating the chiral acid catalyst **45** (Scheme 18).
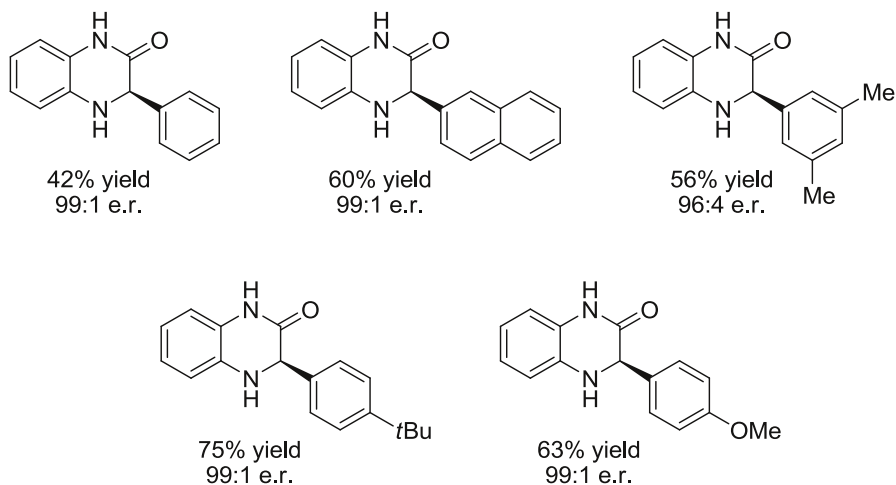
To support the reaction mechanism and to better understand the role of each species, the authors performed B3LYP-D3 density functional theory (DFT) calculations. Interestingly, the method was applied to a broad spectrum of substrates, and a lead compound with impressive inhibitory activity against a number of cancer cell lines was also identified.

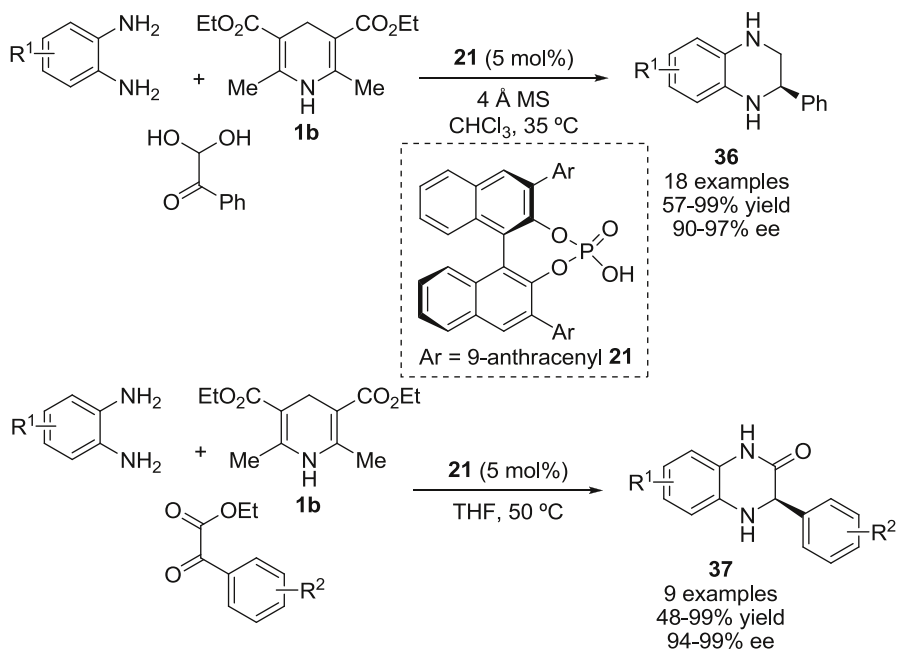## 2.2 Aminocatalysis Promoted Transfer Hydrogenation

Another great area of research in organocatalysis that has experienced an incredible growth has been aminocatalysis. Proof of this progress is the huge number of works

98% yield
95:5 e.r.

95% yield
96:4 e.r.

94% yield
91:9 e.r.

87% yield
97:3 e.r.

89% yield
92:8 e.r.

93% yield
99:1 e.r.

98% yield
97:3 e.r.

88% yield
98:2 e.r.

82% yield
95:5 e.r.

73% yield
97:3 e.r.

98% yield
98:2 e.r.

91% yield
93:7 e.r.

93% yield
91:9 e.r.

97% yield
90:10 e.r.

Fig. 4 Scope of the reaction for the generation of 2-tetrahydroquinoxalines **36**

42% yield
99:1 e.r.

60% yield
99:1 e.r.

56% yield
96:4 e.r.

75% yield
99:1 e.r.

63% yield
99:1 e.r.

Fig. 5 Scope of the reaction for the generation of 3-dihydroquinoxalinones **37**

ⓩ Springer

**Scheme 13** Tandem approach for the preparation of **36** and **37**
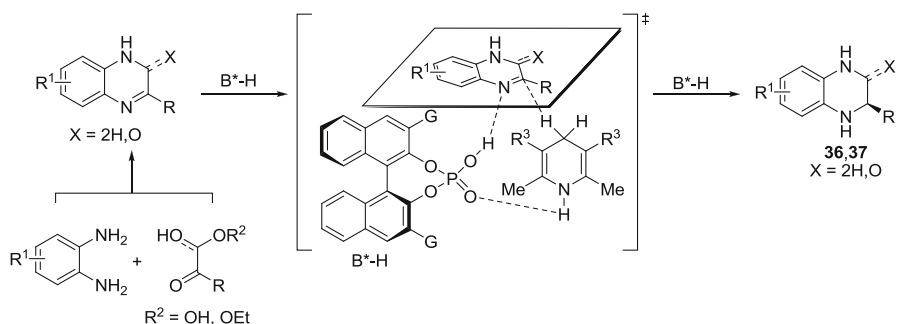
Scheme 14 Plausible reaction pathway and transition state

focused on this field (for selected reviews concerning the aminocatalysis field, see: [110–129]). Among all of them, pivotal contributions related to transfer hydrogenations have been also developed in this area. Although less explored than the phosphoric acid catalyzed examples, these pivotal works will be recovered in the next examples.

In 2004, List and co-workers [130] pioneered only one chiral example of a novel iminium catalytic conjugate reduction of α,β-unsaturated aldehyde **47a** (Scheme 19a). In 2005, and independently, List's (Scheme 19b) [131] and MacMillan's groups (Scheme 19c) (as reported by the authors in Ref. [21], the complete details of their studies into transfer hydrogenation were first published via oral presentation on
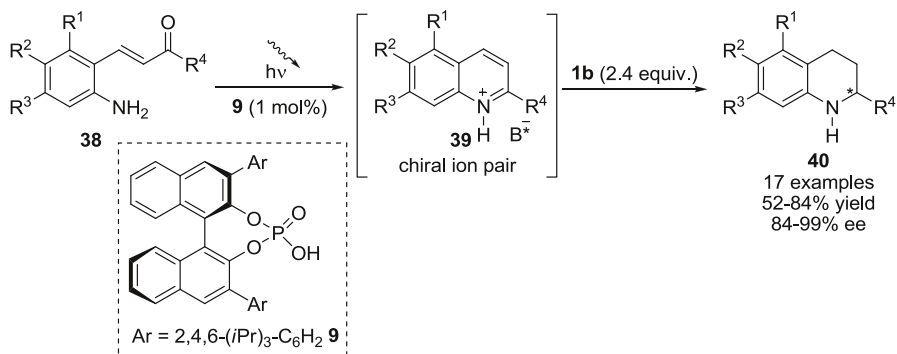
**Scheme 15** Photocyclization-asymmetric reduction of **38**
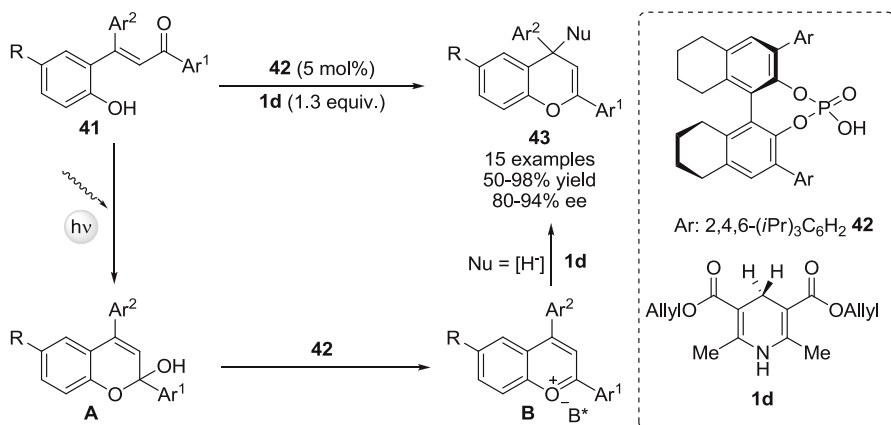
Scheme 16 First asymmetric Brønsted acid catalyzed hydrogenation of benzopyrylium ion **B**

March 1st, 2003, at the Eli Lilly Young Award symposium, Indianapolis. Their work was further communicated in >15 presentations in Europe, USA, Australia, and Asia prior to submission of their manuscript (October 10th, 2004) [132]) reported two more extensive protocols for the enantioselective conjugate reduction of α,β-unsaturated aldehydes **47** and **51** using chiral imidazolinone catalysts **50** and **52**.

List's group proposed a reasonable mechanism to explain the observed absolute configuration in their final products **49**. The process would firstly proceed by formation of iminium ion **54**, which could isomerize quickly via dienamine **55** (Scheme 20). The authors assume that the rate determining step would be the hydride transfer from **1a** to iminium (*E*)-**54** via the transition state **A**, which would occur faster than (*Z*)-**54** [$k(E) > k(Z)$] and, as a result, the enantiomer *R* would be predominantly formed (Scheme 20) [131].

Later, the first enantioselective organocatalytic transfer hydrogenation involving cyclic enones was reported by MacMillan and co-workers following an operationally simple and rapid protocol that allowed access to chiral β-substituted
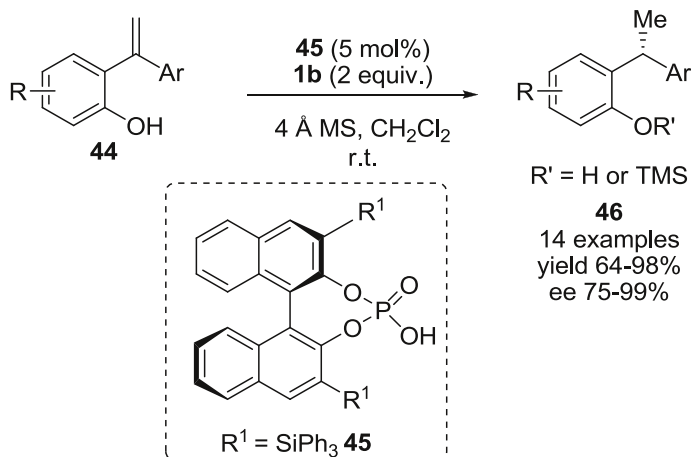
**Scheme 17** Enantioselective synthesis of 1,1-diarylethanes **46**
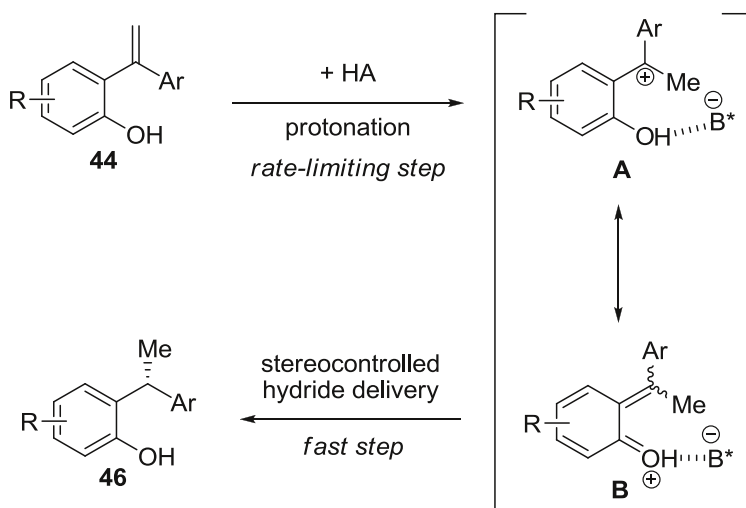
Scheme 18 Plausible reaction mechanism

cycloalkenones **58** with very good yields and high enantioselectivities (Scheme 21) [133] (for an application of this methodology by the same research group, see: [134]).

In order to explain the sense of the asymmetric induction observed in final products **58**, the authors proposed a plausible attack of the hydride based on the selective engagement of the Hantzsch ester reductant **1c** over the *Si* face of the *cis*-iminium isomer **A** (Scheme 22).

Interestingly, in this work the authors compared the efficiency of esters **1b**, **1c** and **1d**, in order to observe a possible structural effect of them over the
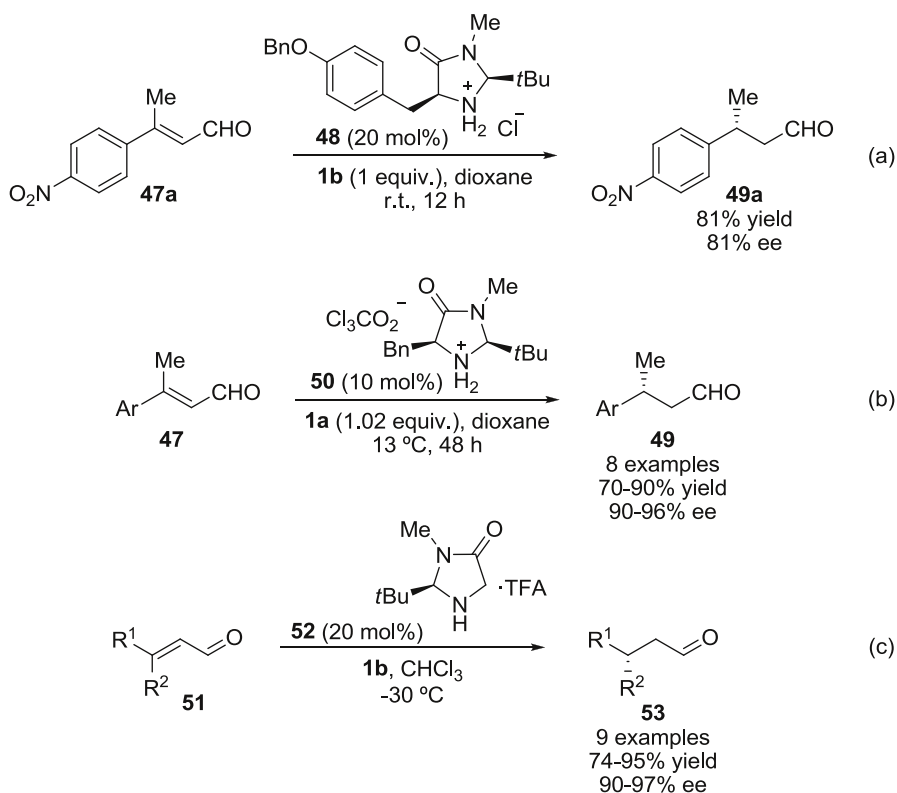
Scheme 19 Pioneering examples of conjugated reduction of α,β-unsaturated aldehydes

enantioselectivity and the reactivity of this process. In fact, a significant impact on both aspects was found with a plausible correlation on the size of the ester functionality at the 3,5-dihydropyridine site (**1b**: Et, 96 % conversion, 74 % ee; **1d**: *i*-Pr, 78 % conversion, 78 % ee and **1c**: *t*-Bu, 86 % conversion, 91 % ee). The enantiocontrol results were explained in terms of electronic factors between the hydrogen substituents at the 4-position and the nitrogen lone-pair. The boat conformation found for **1c** would facilitate the overlap between one H (4-position) in an axial orientation with the nitrogen lone-pair in the ground state. In contrast, the **1b** ring is found in a planarized form wherein poor π-orbital overlap between the analogous C–H bond and nitrogen renders a less reactive hydride reagent. This hypothesis is consistent with not only an increase in enantiocontrol when using the more bulky *tert*-butyl Hantzsch ester **1c** but also improved reaction rate and efficiency [21, 133].

Bringing together the concept of aminocatalysis and the activation mode of chiral phosphoric acids, List and co-workers introduced the concept of *asymmetric counter anion directed catalysis* (ACDC) and they applied this idea to the asymmetric reduction of enals **47** (Scheme 23) [135]. The catalytic species is formed by an achiral ammonium ion **60** and a chiral phosphate anion **59** derived from 3,3′-bis(2,4,6-triisopropylphenyl)-1,1′-binaphthyl-2,2′-diyl hydrogen phosphate **9** (TRIP).
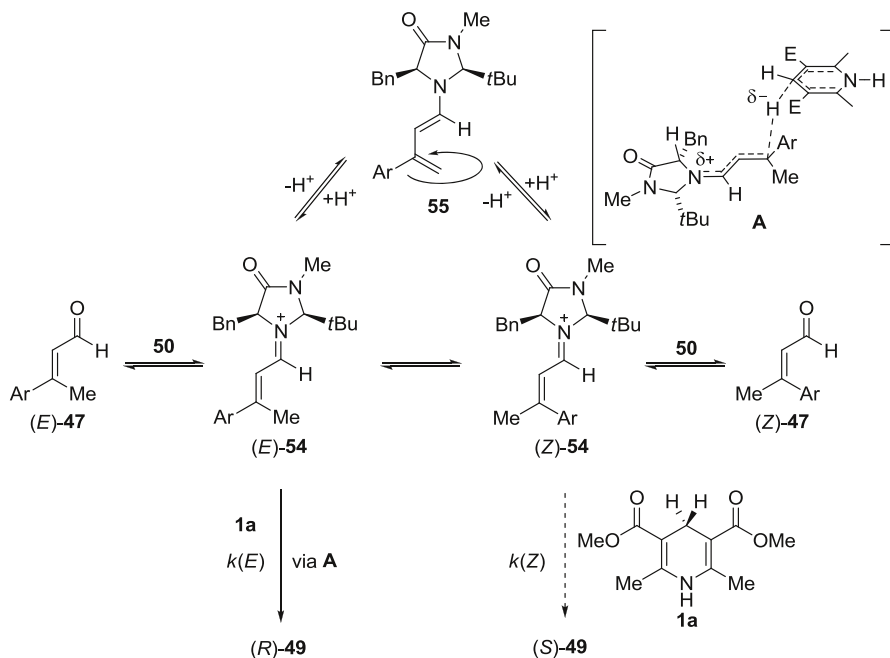
Scheme 20 Mechanistic hypothesis of the organocatalytic asymmetric transfer hydrogenation

All reduced β,β-disubstituted enals **49** were obtained in good yields (up to 90 %) and excellent enantioselectivities (up to 99 % ee). Moreover, the methodology was applied to the interesting reduction of citral **61** into the (*R*)-citronellal **62** and to the asymmetric reduction of farnesal **63**, in all cases with excellent enantioselectivies and high yields (Scheme 24).

Remarkably, the same final enantiomer was obtained in the products even starting from *Z* enals, which is in agreement with a stereoconvergent catalytic system and a rapid *E*–*Z* equilibration, as detected by NMR spectroscopic studies. The mechanism is believed to occur via an iminium ion intermediate since salts of tertiary amines seem to be ineffective.

An extension of this work was reported by the same research group for the asymmetric conjugate reduction of α,β-unsaturated ketones **65**, affording final reduced products **67** with high yields and good to excellent enantioselectivities (Scheme 25) [136].

More recently, Lear and co-workers applied this new concept as a key synthetic step in the high yielding route leading to the (−)-platensimycin core ([137], for further studies in this field, see also: [138–140]).

2.3 Thiourea-Catalyzed Transfer Hydrogenation

Another big family of organocatalysts that has been successfully used in hydrogen transfer, although less explored, is the chiral thiourea organocatalysts (for pivotal reviews concerning chiral thioureas, see: [141–154] and for the pioneering use of
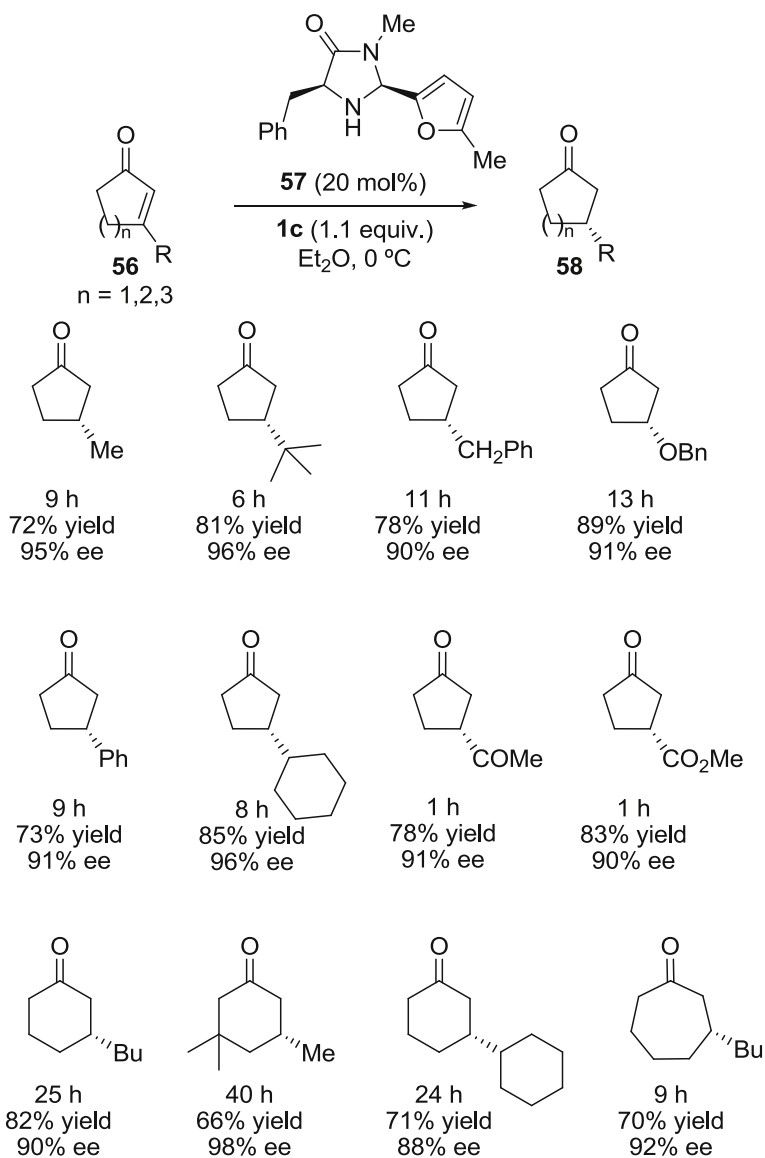
**Scheme 21** Scope of the organocatalytic enone hydrogenation

non-chiral thioureas in a transfer-hydrogenation reaction, see: [155]). In this context, List and co-workers reported the first example of conjugate reduction of nitroolefins **68** mediated by thiourea organocatalyst **69** (Scheme 26) ([156], for the non-enantioselective version of this reaction, see: [157]).

As disclosed, the process was suitable for a broad substrate scope, leading to final products **70** with high yields and enantioselectivities for diverse β-alkylsubstituted nitrostyrenes **68**.
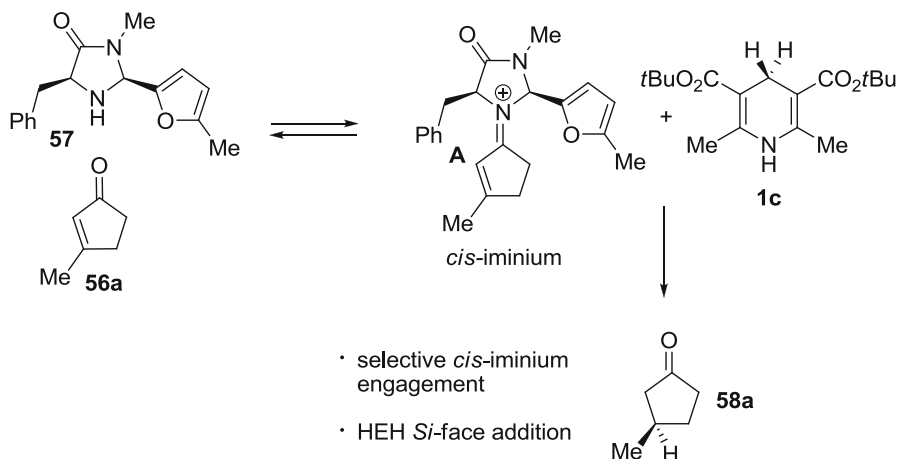
Scheme 22 Enantioselective hydride addition mechanism
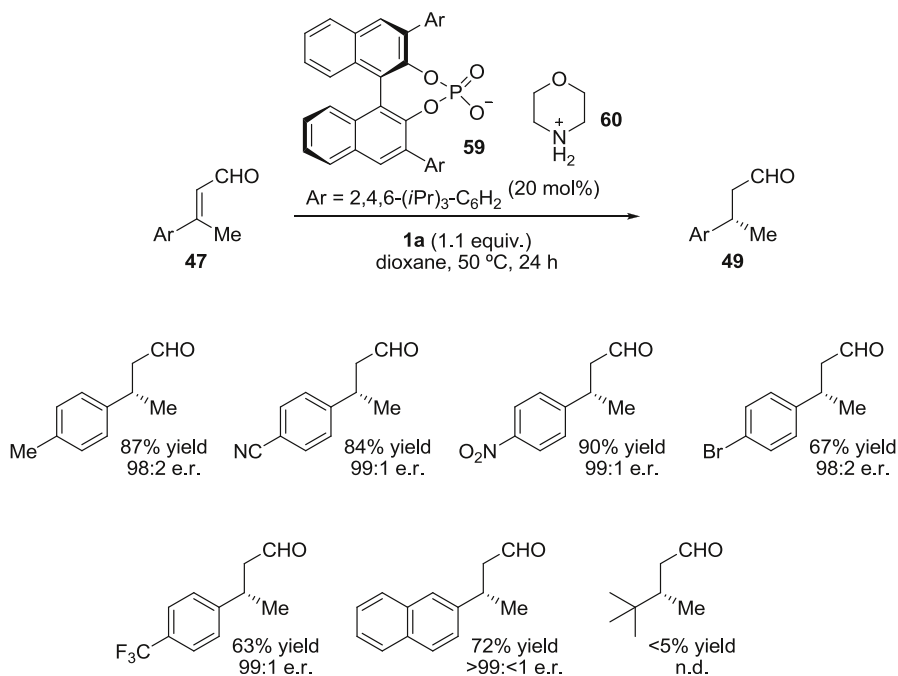
Scheme 23 ACDC approach applied to the reduction of enals **47**

The reaction could proceed via a hydrogen-bonding interaction between the NH of the thiourea moiety and the nitro group and further enantioselective attack of the hydride from the Hantzsch ester **1c**.

An extension of this work was reported by the same research group using β-nitroacrylates **71** and the same thiourea organocatalyst **69** with the main aim of
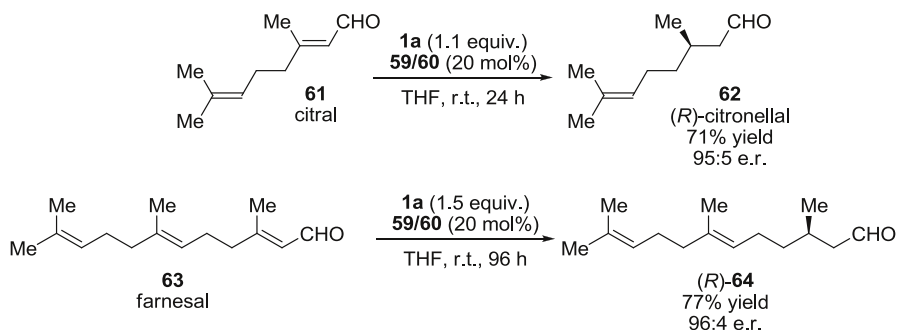
Scheme 24 Catalytic asymmetric transfer hydrogenation of citral **61** and farnesal **63**

preparing the corresponding saturated β-nitroesters **72** in high yields and enantioselectivities, which can be easily converted into β²-amino acids via hydrogenation (Scheme 27) ([158], for other developed methods of asymmetric transfer hydrogenation of nitroolefins using thioureas, see: [159, 160]).

The same approach was used by Benaglia's group for the enantioselective organocatalytic reduction of β-trifluoromethyl nitroalkenes **73**, with the aim of achieving chiral β-trifluoromethyl amines **75** (Scheme 28) [161]. The authors also performed the organocatalyzed reduction of α-substituted-β-trifluoromethyl nitroalkenes, although with poorer results. The stereochemical result of the reaction and the behavior of thiourea catalyst **74** were discussed based on computational studies and DFT transition-state analysis.

Simultaneously, although independently, Bernardi, Fochi and co-workers developed an extraordinary additional example of highly enantioselective transfer hydrogenation using β-trifluoromethyl nitroalkenes to give easy access to optically active β-trifluoromethyl amines with excellent results [162].
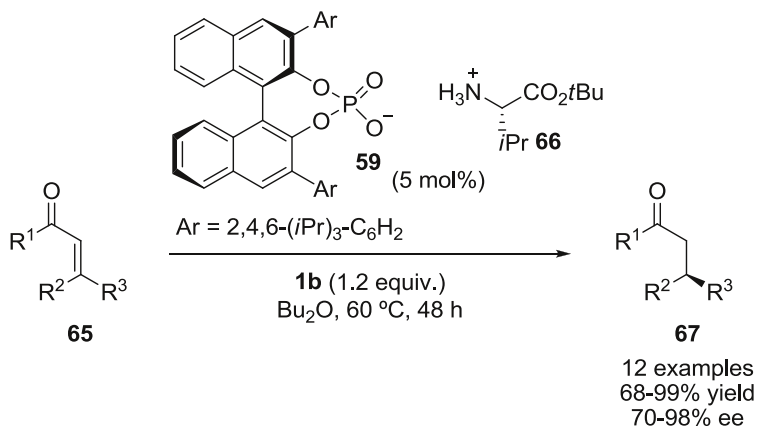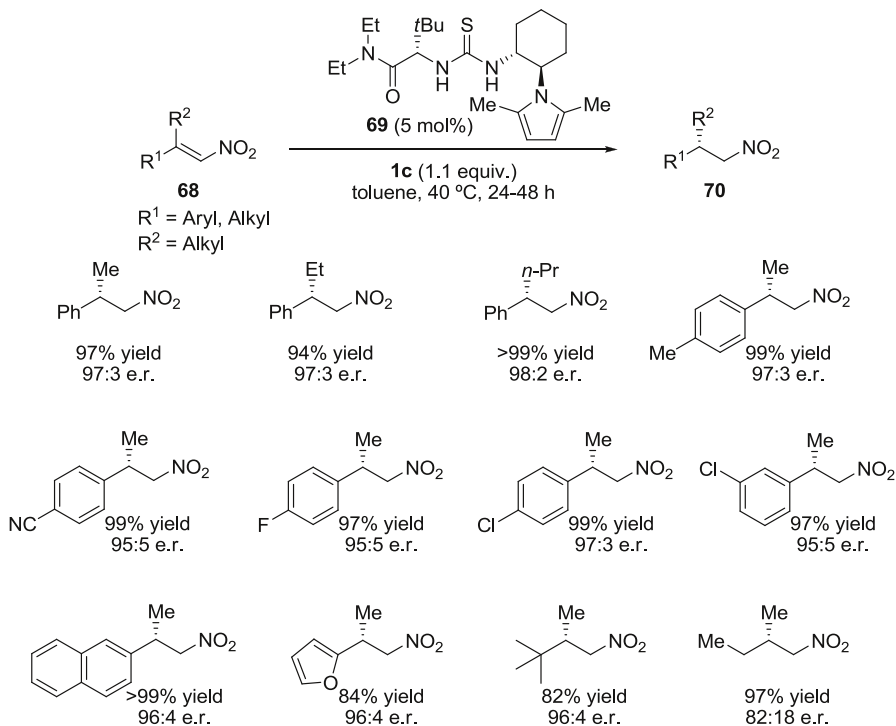

Scheme 25 Asymmetric reduction of ketones **65**

3 Trichlorosilane-Mediated Stereoselective Reduction of C=X Bonds

In the last decade, great progress has been made in the development of highly enantioselective Lewis basic organocatalysts for the reactions of trichlorosilyl derivatives as the reducing agents. The **2** is activated by the base moiety of the catalyst to generate an hexacoordinate hydridosilicate (for the activation of trichlorosilyl reagents by Lewis bases, see also: [163, 164]). Here is reported the successful application on the enantioselective reduction of prochiral ketimines, ketones and C=C bond using trichlorosilane **2** as an effective hydride source.
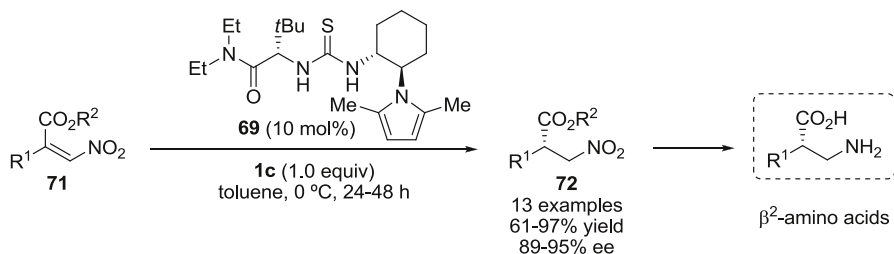
3.1 Reduction of Ketimines

#### 3.1.1 N-Formylpyrrolidine Derivatives

In a pioneering work, Matsumura and co-workers presented a new finding where trichlorosilane **2** activated with *N*-formylpyrrolidine derivatives **77** was an effective catalyst for the reduction of imines **76**. Reducing agent **2** showed much higher selectivity towards the imino group rather than the carbonyl group, because the carbonyl moiety in the catalysts was not reactive against the reduction (Scheme 29) [165]. Later, Tsogoeva's group demonstrated the use of pyrrolidine **78** as a

Scheme 26 Thiourea promoted asymmetric transfer hydrogenation

Scheme 27 Asymmetric reduction of β-nitroacrylates
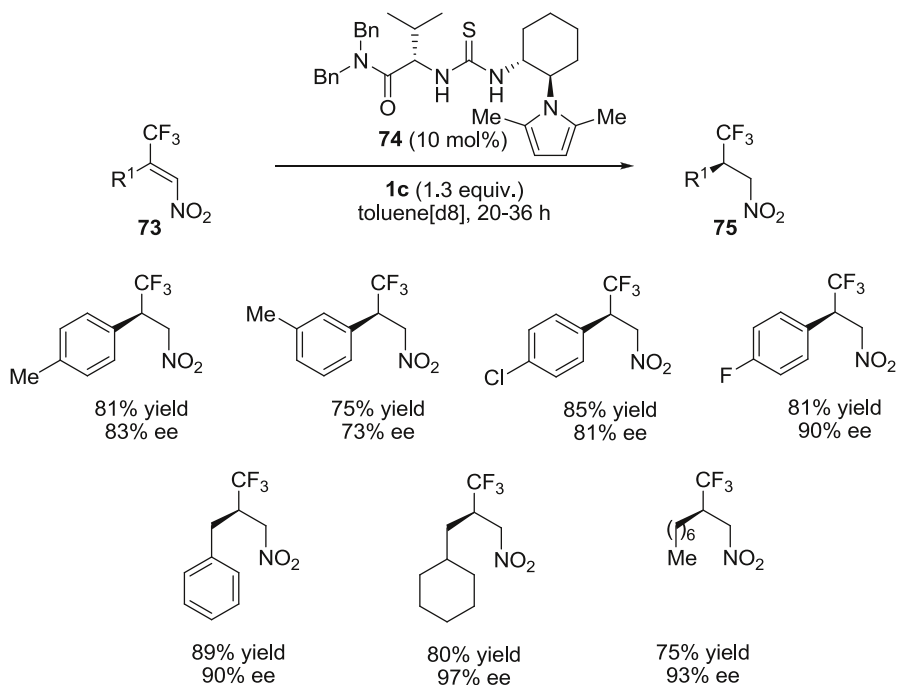
Scheme 28 Organocatalyzed reduction of fluorinated nitroolefins **73**

suitable catalyst for ketimines reduction, although only for one example and using HMPA as additive [166]. More recently, Lewis base **79** was successfully employed for the hydrosilylation of α-imino esters as direct precursors of α-amino acids ([167], for the use of additional picolinoyl catalyst derivatives, see also: [168–172]).

The role of the carbonyl groups in the catalysts seemed to be responsible for the silicium activation (for other pyrrolidine derivatives, see: [173–175]). In order to explain the sense of the stereoselectivity in final products, Matsumura's group suggested that the reduction predominantly proceeded through a transition state **A** rather than the most hindered transition state **B**, justifying the major enantiomer observed (Fig. 6). This mechanistic proposal was an early hypothesis, which was later modified by other authors on the basis of more experimental results (see below).

3.1.2 L-Valine-Derived N-methyl Formamides

Malkov, Kočovský, and co-workers have developed different L-valine-based Lewis basic catalysts such as **81** [176, 177], for the efficient asymmetric reduction of ketimines **76** with trichlorosilane **2**, or catalyst **82** [178] with a fluorous tag, which allows an easy isolation of the product and can be used in the next cycles, while preserving high enantioselectivity in the process. Sigamide catalyst **83** [179, 180] and Lewis base **84** [181] were employed in a low amount (5 mol%) affording final chiral amines **80** with high enantioselectivity (Scheme 30) [182]. Interestingly, **83** was used for the enantioselective preparation of vicinal α-chloroamines and the subsequent synthesis of chiral 1,2-diaryl aziridines. In these developed approaches the same absolute enantiomer was observed in the processes.

From these studies, the authors suggested different important conclusions: (1) the structure–reactivity studies showed that the product configuration seems to be controlled by the nature of the side chain of the catalyst scaffold, and the electronic properties of the substituents in the phenyl ring on the Lewis base. Interestingly, catalysts of the same absolute configuration may induce the formation of the opposite enantiomers of the product; (2) hydrogen bonding and arene–arene interactions between the catalyst and the imine appear to be crucial for the success of determining the enantiofacial selectivity; (3) the activation of trichlorosilane seems to be in agreement with a bidentate coordination with both carbonyl groups of the amide moiety in the catalyst, as previously invoked (Fig. 7) [176]. It is remarkable that the mode of activation in this case differs from that proposed previously by Matsumura's group in Fig. 6 [165].

3.1.3 L-Pipecolinic Acid Derived N-Formamides

Sun and co-workers developed a novel Lewis basic organocatalyst **86** (Scheme 31), easily synthesized from commercially available L-pipecolinic acid. The catalyst **86** promoted the reduction of N-aryl ketimines **85** with HSiCl₃ **2** in high yield and
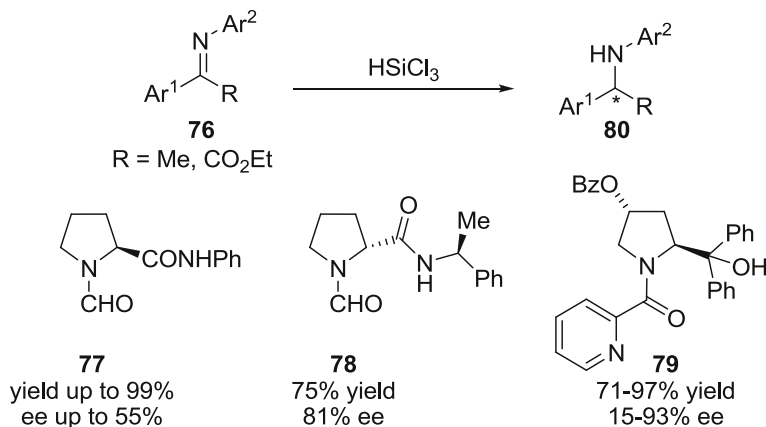
**Scheme 29** Reduction of imines with N-formylpyrrolidine-based catalysts
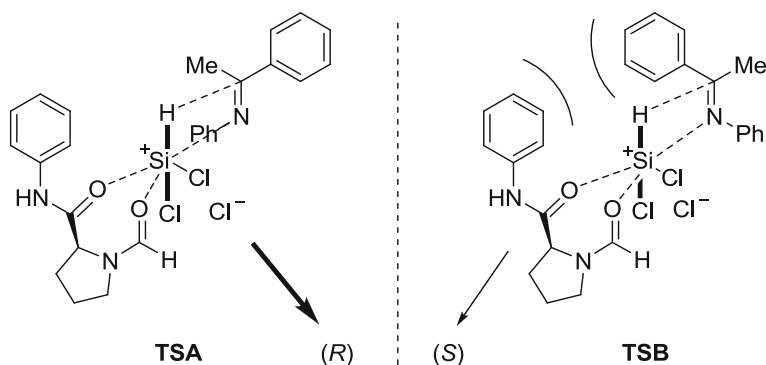
Fig. 6 Mechanism of hydrosilylation of imines

excellent ee values under mild conditions with an unprecedented spectrum of substrates [183]. The same group also found that the L-pipecolinic acid derived *N*-formamide **87** was a highly effective Lewis basic organocatalyst for the same reaction [184].

On the basis of the experimental results, the methoxy group on C2′ has proven to be critical for the high efficiency of catalyst **87** in the reduction of the imines. A hexacoordinate silicon transition structure was proposed to justify the experimental observations. In a more extended mechanistic study *N*-funtionalized pipecoli-namides **88** were proposed as an example of efficient catalyst after several variations in the C2 and the *N*-protected group ([185], for more recent L-pipecolinic basic organocatalysts for hydrosilylation of imines, see: [186, 187]).
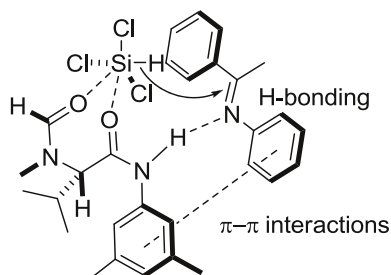
3.1.4 Piperazine Lewis base Organocatalyst

Sun and co-workers envisioned that the piperidinyl ring on the abovementioned catalysts could be replaced by a piperazinyl backbone, considering that the
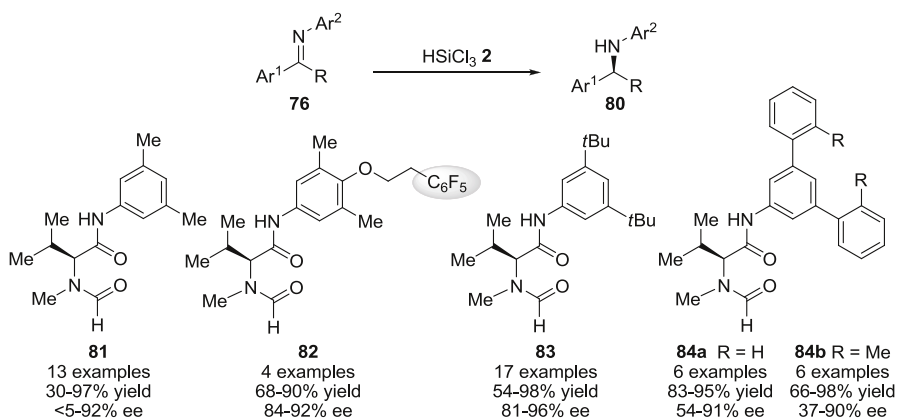
Scheme 30 Pioneering examples of L-valine-based Lewis basic catalysts

Fig. 7 Mechanism of hydrosilylation of imines



H-bonding

π–π interactions

additional secondary amino group on the 4-position (N4) should provide a suitable site to introduce structural variations and thus accurately to modify the catalytic properties. In this context, a new catalyst **91** was designed (Scheme 32) [188, 189], which promoted the unprecedented reduction of the relatively bulky ketimines **90**, becoming a complementary structure to the existing catalytic systems. The reductions of both *N*-aryl acyclic methyl ketimines and non-methyl ketimines **90** were catalyzed for a broad spectrum of substrates affording the desired chiral amines **92** in high yields and with high ee values.

Unfortunately, other *N*-substituted phenyl ketimines **93a–e** afforded lower ee values compared with **90**. The *N*-benzyl ketimine **93e** was also proven to be an unsuitable substrate using **91** as catalyst. The authors found that the arene sulfonyl group on N4 and the 2-carboxamide groups were crucial for the high enantiose-lectivity of the process and the efficiency of the catalytic system.

3.1.5 S-Chiral Sulfinamide Derivatives

Although stereogenic sulfur centers had been used as the source of chiral auxiliaries and ligands [190–195], organocatalysts incorporating chirality solely through the sulfur atom had been almost overlooked in the literature before the development of
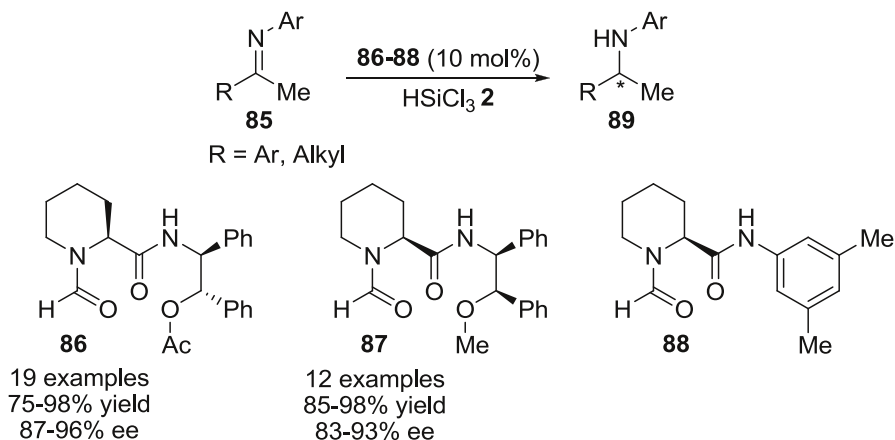

Scheme 31 Model L-pipecolinic acid derived *N*-formamide catalysts **86–88**

this subarea of research. In this context, Sun's group developed the first highly effective example of sulfinamide organocatalyst **95** to promote the asymmetric hydrosilylation of ketimines with **2** in high yield and enantioselectivity (Scheme 33) [196]. Having in mind the idea that two molecules of monosulfinamide catalyst could participate in the mechanism of the reaction (Fig. 8), the same authors designed bissulfinamide **96** [197] incorporating two sulfinamide units, which efficiently promoted the asymmetric reduction of *N*-aryl ketimines in high yields and improved enantioselectivities (Scheme 33). Compound **96** resulted to be a better catalyst than the former monosulfinamide **95**.

The same group developed a new Lewis base organocatalyst **97,** which included stereogenic atoms represented by a sulfinamide group and a α-amino acid framework bearing Lewis basic carboxamide functionality, both for the activation of HSiCl$_3$ **2**. Excellent enantioselectivities and high yields for a wide range of aromatic *N*-alkyl ketimines were achieved (Scheme 33) ([198], for more recent examples belonging to the same research group, see also: [199, 200]).

3.1.6 Supported Lewis Base Organocatalysts

With the increasing interest in developing catalysts able to be easily separated from the final product, many efforts have been devoted to the preparation of immobilized structures (for reviews on polymer-supported organocatalysts, see: [201–204], for a more recent example, see also: [205]). In this field, Kočovský's group has also reported interesting Lewis base supported catalysts for the efficient asymmetric hydrosilylation of ketimines with silane **2**. The first reported example was an *N*-methylvaline-derived Lewis basic formamide anchored to a polymeric support with
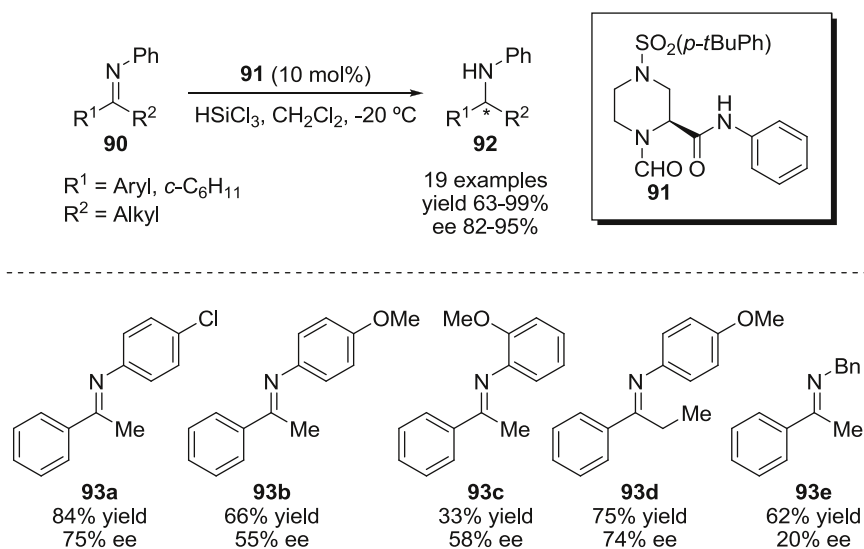
Scheme 32 Reduction of imines using piperazine Lewis base derivative **91**

a varying spacer **100**. This protocol represented a considerable simplified procedure to isolate the catalyst from the crude of the reaction, which is not a trivial task, for instance on a large scale protocol (Scheme 34). The polymer-supported catalyst was reused at least five times without any loss of activity [206].

The same research group designed a soluble catalyst **102** with the main aim of avoiding the problems associated with the heterogeneous systems, and related to the common supported catalysts [207]. The main advantage of this system is the inverted solubility pattern that this catalyst exhibits, since it is soluble in non-polar solvents and insoluble in polar media (Fig. 9). This feature simplified the recovery (up to 99 %) and re-use of the catalyst at least five times without loss of activity, improving the results obtained with catalyst **100** (for the preparation of other immobilized catalysts easily recoverable, see: [208]).

In order to enable the isolation procedure of the organocatalysts, Kočovský's group also reported an alternative approach using a dendron-anchored organocatalyst **103** to efficiently reduce the imines with trichlorosilane **2** [209]. The isolation procedure of the catalyst from the crude was substantially simplified, since most of the catalyst (≥90 %) could be recovered by precipitation and centrifugation (Fig. 10).

3.2 Reduction of Ketones

Although the reduction of imines has been widely explored, as described above, the reduction of carbonyl groups has been less studied until now. Specifically, the reduction of ketones is more limited due to the low reactivity shown by these compounds. In this field, the pioneering works using trichlorosilane as reducing agent and a chiral Lewis base were reported by Matsumura and co-workers in 1999,
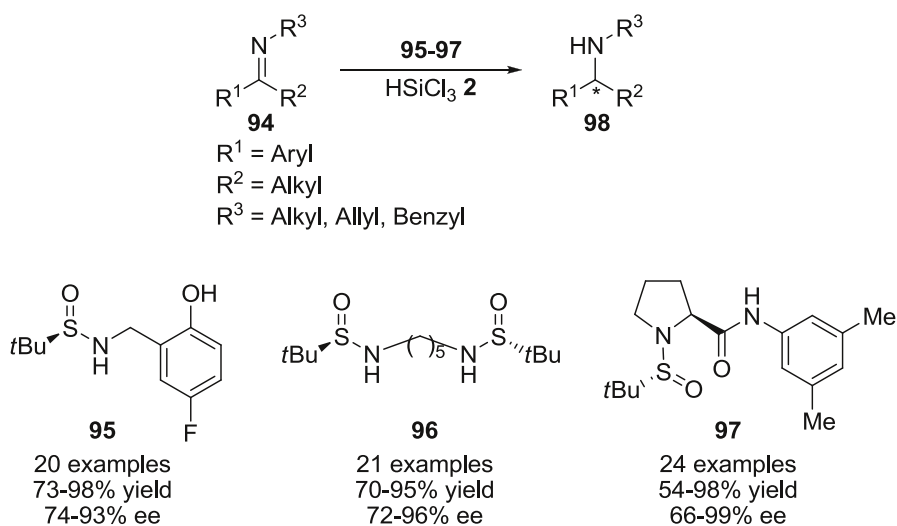
Scheme 33 Example of efficient sulfinamide organocatalysts **95–97**

Fig. 8 Mode of action of monosulfinamide organocatalysts

R = Ph   82% yield, 81% ee
R = 2-naphthyl   72% yield, 79% ee
R = 4-CF$_3$C$_6$H$_4$ 67% yield, 81% ee
R = 4-MeOC$_6$H$_4$ 62% yield, 77% ee
R = 2,5-Me$_2$-3-furyl 67% yield, 78% ee
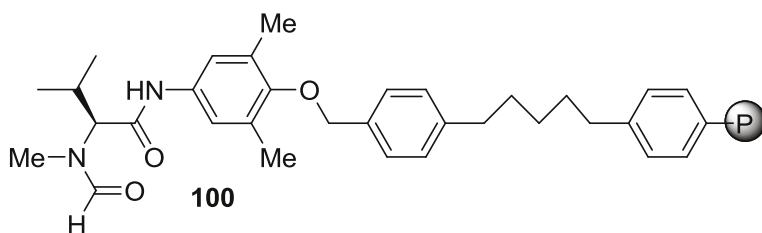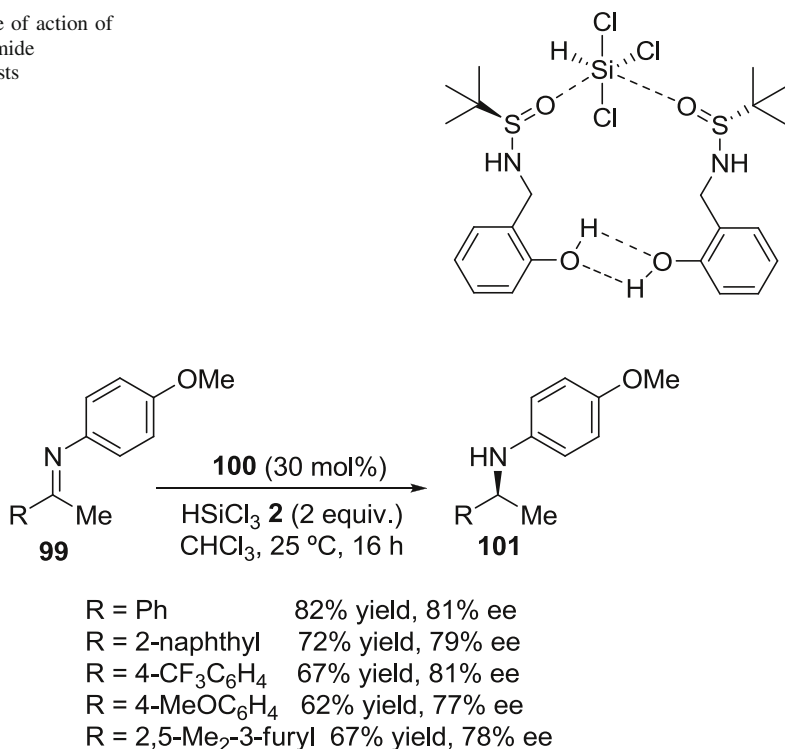

Scheme 34 Application of polymer-supported organocatalyst **100**

affording low to moderate enantioselectivities (for the seminal enantioselective work using Lewis base to reduce carbonyl groups, see: [210], for pioneering works using chiral lithium salts, see: [211–213]). More recently and independently, Malkov, Kočovský, and co-workers [214] and Matsumura's group [215], reported isoquinolinyloxazoline **105** and *N*-formylpyrrolidine **106**, respectively, as new catalysts to significantly improve the enantioselectivity of the process in comparison with the pioneering work (Scheme 35).

In these examples the carbonyl compounds were limited to aromatic ketones. Based on the experimental results, the authors proposed the following TS to explain the enantioinduction observed in their work (Fig. 11) [214].
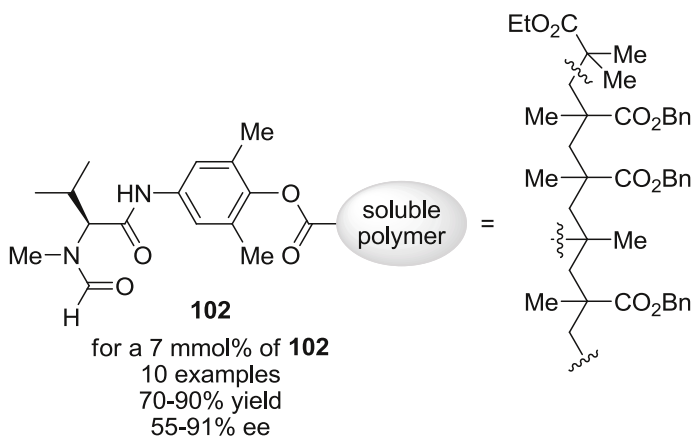
Fig. 9 Soluble supported catalyst **102**

The **2** would be chelated by the catalyst forming an activated hydrosilylating species, while a second molecule of HSiCl$_3$ would likely activate the ketone by coordination to the oxygen atom. The attack of the hydride would take place from the less hindered *Si* face. Additionally, the π–π interaction between the heteroaromatic ring of the catalyst and the aromatic ring in the ketone would stabilize the system.

Later, Sun's group also used their pipecolinic acid derivative **87** for the first efficient reduction of aliphatic and aromatic ketones with silane **2** in moderate to high enantioselectivity [184]. A plausible transition state was proposed in order to explain the results observed, where the catalyst **87** would act as a tridentate activator and would promote the hydrosilylation of ketones through the heptacoordinate silicon structure depicted in Fig. 12.

It is remarkable that the hydrosilylation procedure has been successfully used for the synthesis of important targets. Matsumara and co-workers demonstrated the applicability of their developed method in the preparation of optically active lactone **109** from keto ester **108** in 93 % yield with 97 % ee (Scheme 36) [215]. Lactone **109** is an important building block for the synthesis of a variety of biologically active substances [216–218].

3.3 Reduction of β-Enamino Esters

In the last decade, increasing efforts have been devoted to the asymmetric preparation of structurally diverse β-amino acids (for selected reviews, see: [219–222]), due to their involvement in the synthesis of peptidomimetics and as valuable building blocks.

In this field of research, enantiomerically enriched β-amino acids could be also obtained through transfer hydrogenation using β-enamino esters ([223], for pioneering works using metals, see: [224, 225]). This approach was initiated by Matsumara and co-workers [173] reporting a single example using catalyst **111**
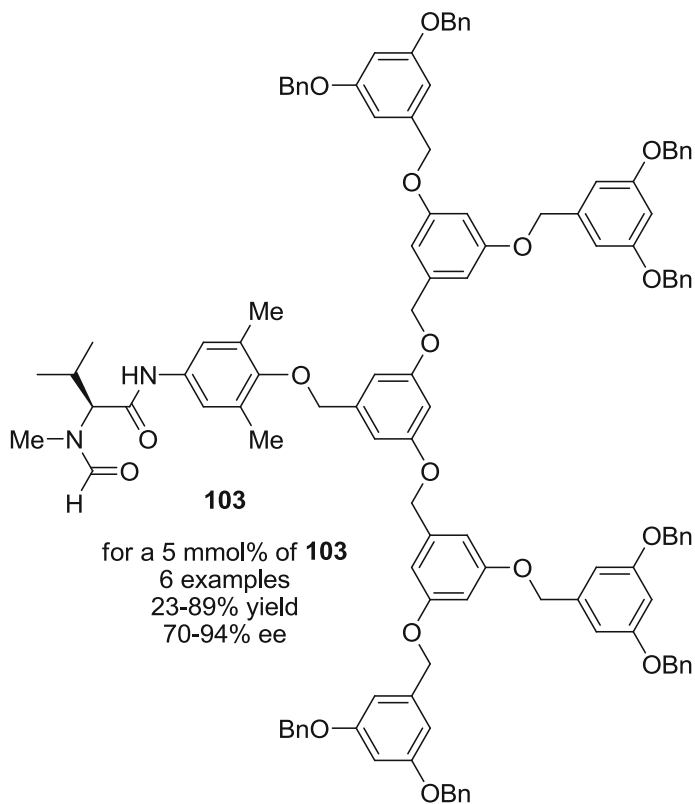
Fig. 10 Dendron-anchored organocatalyst **103**
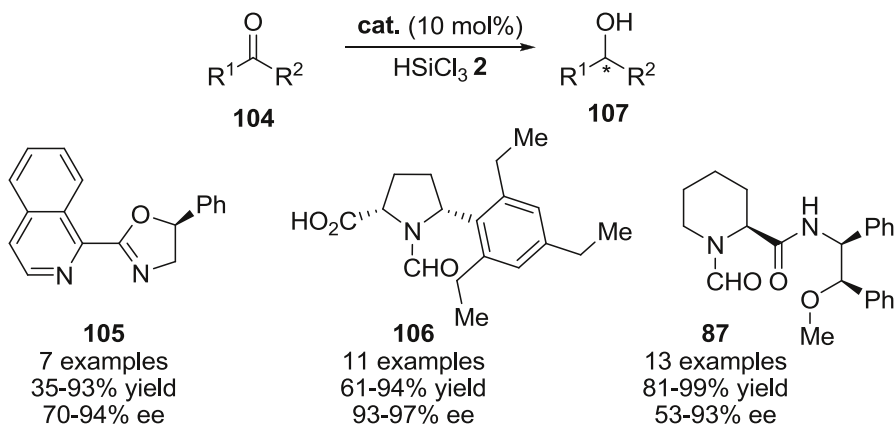
Scheme 35 Enantioselective reduction of ketones **104**

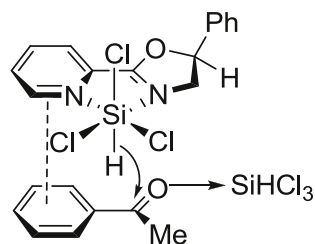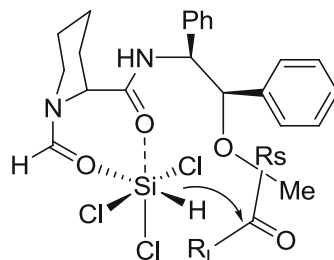**Fig. 11** Activation proposal

Fig. 12 Role of pipecolinic
acid derivative **87**

(Scheme 37). Later, the methodology was improved by Zhang's group with Lewis base catalyst **112** [226] and **113** [227], and also Benaglia and co-workers with catalysts **114** (Scheme 37) [228]. Remarkably, Sun's group reported an interesting methodology using water as additive and the Lewis base catalyst **115** [229]. The addition of 1 equiv. of water resulted to be crucial for the success of both reactivity and enantioselectivity of the process (Scheme 37). All these approaches were potentially useful for the preparation of enantiomerically enriched β-amino acid derivatives, which in all cases was achieved with good yield and good enantios-electivies [230].

Interestingly, in order to extend the applicability of the reduction of β-enamino esters, the protocol developed by Zhang and co-workers using catalyst **113** was
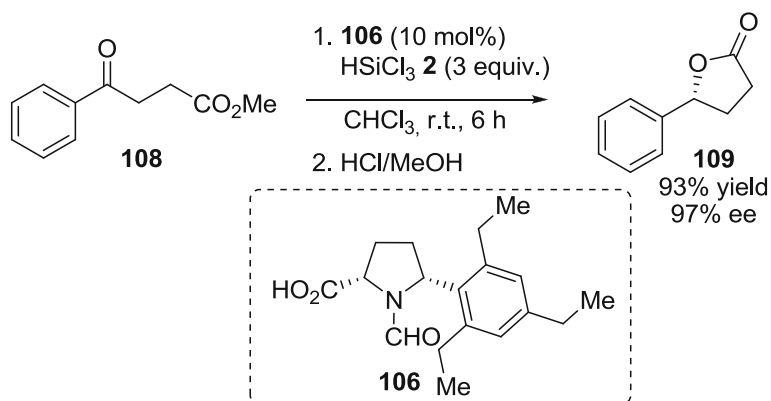
Scheme 36 Synthesis of optically active lactone **109**
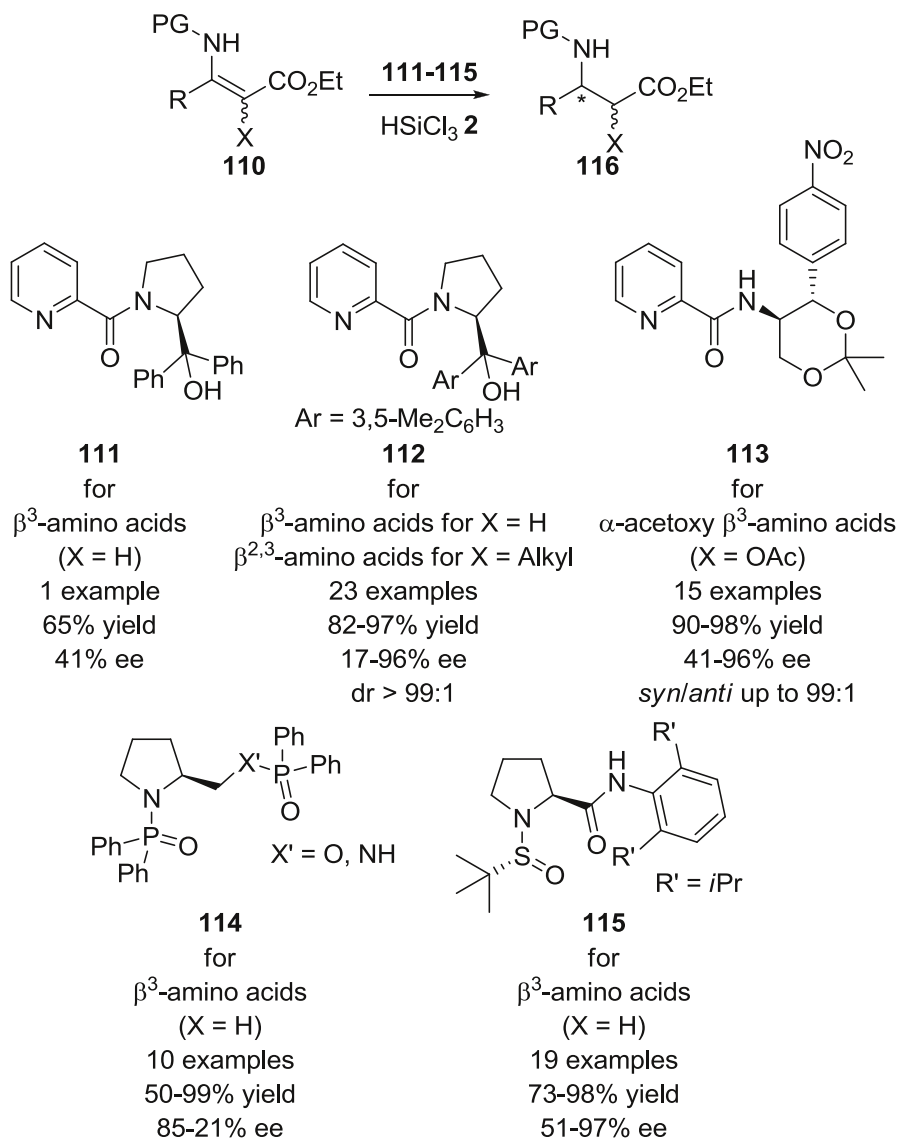
Scheme 37 Reduction of β-enamino esters **110** (for other examples of reduction of enamines, see: [231–233])

successfully applied in the synthesis of the taxol C13 side chain **117** and oxazolidinone **118**, which is a potent hypocholesterolemic agent (Schemes 38, 39) [227].

Malkov, Kočovský, and coworkers also reported the interesting synthesis of $\beta^{2,3}$-amino acids, in which synthesis is still a challenge, using organocatalyst **83** (Scheme 40) [236]. This approach is based on the fast equilibration between the
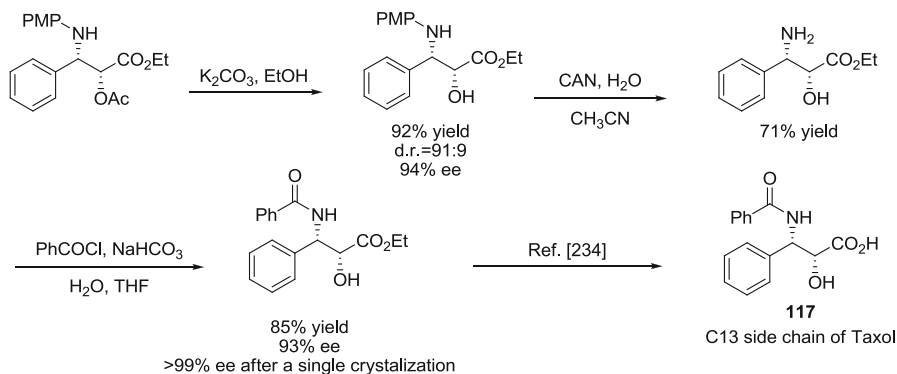
Scheme 38 Enantioselective synthesis of the taxol C13 side chain **117** [234]
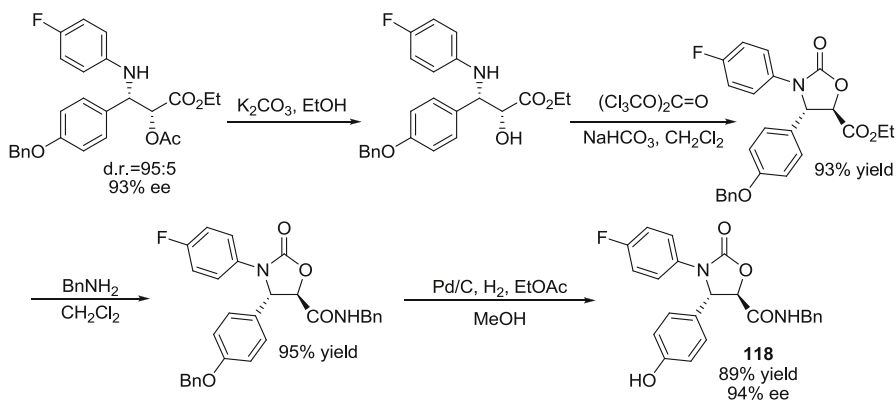
Scheme 39 Enantioselective synthesis of oxazolidinone **118** [235]

enamine and imine forms. A subsequent reduction of the equilibrated mixture with $HSiCl_3$, afforded the corresponding amino esters and amino nitriles with good results.

AcOH was used in order to maintain the concentration of H^+ constant. Although the presence of H^+ also catalyzed the competing nonselective reduction, under the optimized reaction conditions, the use of one equivalent of AcOH provided a good compromise between reactivity and selectivity.

4 Conclusions

A great number of organocatalytic examples of reduction of different C=N, C=O and C=C double bonds affording new stereogenic centers has been illustrated. The organocatalytic transfer hydrogenation has been mainly focused on the pioneering examples using Hantzsch dihydropyridines **1** and trichlorosilane **2** as hydride
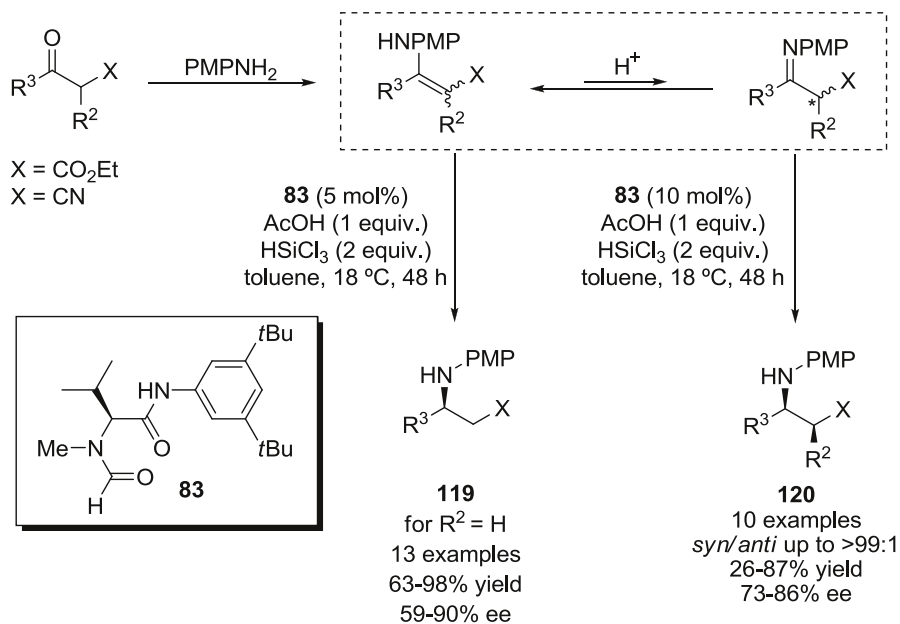
Scheme 40 Enantioselective synthesis of β³- and β²,³-amino acid derivatives **119** and **120**

sources, although other reducing agents have being explored in the last few years. Organocatalysts such as chiral Brønsted acids, thioureas, and chiral secondary amines or Lewis bases have been successfully used in all the reported examples. As reflected in the numerous examples, this field is the focus of great interest. This is proof of the importance that the asymmetric transfer hydrogenation arouses, and the power of this approach to achieve the final target. Certainly, in the near future new hydride sources and novel organocatalysts will be designed to achieve this goal in a greener and more environmentally friendly manner.

References

1. Nugent TC (ed) (2010) Chiral amine synthesis. Wiley-VCH, Weinheim
2. Kobayashi S, Ishitani H (1999) Chem Rev 99:1069–1094
3. Palmer MJ, Wills M (1999) Tetrahedron Asymmetry 10:2045–2061
4. Carpentier J-F, Bette V (2002) Curr Org Chem 6:913–936
5. Tang W, Zhang X (2003) Chem Rev 103:3029–3069
6. Blaser H-U, Malan C, Pugin B, Spindler F, Steiner H, Studer M (2003) Adv Synth Catal 345:103–151
7. Riant O, Mostefaï N, Courmarcel J (2004) Synthesis 2943–2958
8. Tararov VI, Börner A (2005) Synlett 203–211
9. Samec JSM, Bäckvall J-E, Andersson PG, Brandt P (2006) Chem Soc Rev 35:237–248
10. Cho BT (2006) Tetrahedron 62:7621–7643
11. Berkessel A, Gröger H (2005) Asymmetric organocatalysis. Wiley-VCH, Weinheim
12. Dalko PI (ed) (2007) Enantioselective organocatalysis. Wiley, New York

13. Dalko PI (ed) (2013) Comprehensive enantioselective organocatalysis. Wiley-VCH, Weinheim
14. Adolfsson H (2005) Angew Chem Int Ed 44:3340–3342
15. Tripathi RP, Verma SS, Pandey J, Tiwari VK (2008) Curr Org Chem 12:1093–1115
16. Rueping M, Dufour J, Schoepke FR (2011) Green Chem 13:1084–1105
17. Zheng C, You S-L (2012) Chem Soc Rev 41:2498–2518
18. Benaglia M, Bonsignore M, Genoni A (2013) In: Rios R (ed) Stereoselective organocatalysis: bond formation methodologies and activation modes. Wiley, Hoboken, pp 529–558
19. Li G, Antilla JC (2013) In: Dalko PI (ed) Comprehensive enantioselective organocatalysis. Wiley-VCH, Weinheim, pp 941–974
20. Kortmann F, Minnaard A (2013) In: Andrushko V, Andrushko N (eds) Stereoselective synthesis of drugs and natural products. Wiley, Hoboken, pp 993–1014
21. Ouellet SG, Walji AM, MacMillan DWC (2007) Acc Chem Res 40:1327–1339
22. You S-L (2007) Chem Asian J 2:820–827
23. Connon SJ (2007) Org Biomol Chem 5:3407–3417
24. Wang C, Wu X, Xiao J (2008) Chem Asian J 3:1750–1770
25. Rueping M, Sugiono E, Schoepke FR (2010) Synlett 852–865
26. Bernardi L, Fochi M, Franchini MC, Ricci A (2012) Org Biomol Chem 10:2911–2922
27. Kočovský P, Malkov AV (2007) In: Dalko PI (ed) Enantioselective organocatalysis. Reactions and experimental procedures. Wiley-VCH, Weinheim, pp 275–278
28. Kočovský P, Stončius S (2010) In: Nugent TC (ed) Chiral amine synthesis. Wiley-VCH, Weinheim, pp 131–156
29. Guizzetti S, Benaglia M (2010) Eur J Org Chem, 5529–5554
30. Jones S, Warner CJA (2012) Org Biomol Chem 10:2189–2200
31. Zhu C, Akiyama T (2009) Org Lett 11:4180–4183
32. Sakamoto T, Mori K, Akiyama T (2012) Org Lett 14:3312–3315
33. Zhu C, Saito K, Yamanaka M, Akiyama T (2015) Acc Chem Res 48:388–398
34. Rossi S, Benaglia M, Massolo E, Raimondi L (2014) Catal Sci Technol 4:2708–2723
35. Hantzsch A (1881) Ber. 14:1637–1638
36. Hantzsch A (1882) Justus Liebigs Ann Chem 215:1–82
37. Singh S, Batra UK (1989) Ind J Chem Sect B 28:1–2
38. Steevens JB, Pandit UK (1983) Tetrahedron 39:1395–1400
39. Fujii M, Aida T, Yoshihara M, Ohno A (1989) Bull Chem Soc Jpn 62:3845–3847
40. Itoh T, Nagata K, Kurihara A, Miyazaki M, Ohsawa A (2002) Tetrahedron Lett 43:3105–3108
41. Rueping M, Sugiono E, Azap C, Theissmann T, Bolte M (2005) Org Lett 7:3781–3783
42. Hoffmann S, Seayad AM, List B (2005) Angew Chem Int Ed 44:7424–7427
43. Itoh T, Nagata K, Miyazaki M, Ishikawa H, Kurihara A, Ohsawa A (2004) Tetrahedron 60:6649–6655
44. Rueping M, Azap C, Sugiono E, Theissmann T (2005) Synlett, 2367–2369
45. Akiyama T (2007) Chem Rev 107:5744–5758
46. Terada M (2008) Chem Commun, 4097–4112
47. Adair G, Mukherjee S, List B (2008) Aldrichim Acta 41:31–39
48. You S-L, Cai Q, Zeng M (2009) Chem Soc Rev 38:2190–2201
49. Kampen D, Reisinger CM, List B (2010) Top Curr Chem 291:395–456
50. Terada M (2010) Synthesis, 1929–1982
51. Terada M (2010) Bull Chem Soc Jpn 83:101–119
52. Yu J, Shi F, Gong L-Z (2011) Acc Chem Res 44:1156–1171
53. Terada M (2011) Curr Org Chem 15:2227–2256
54. Rueping M, Kuenkel A, Atodiresei I (2011) Chem Soc Rev 40:4539–4549
55. Schenker S, Zamfir A, Freund M, Tsogoeva SB (2011) Eur J Org Chem 2209–2222
56. Čorić I, Vellalath S, Müller S, Cheng X, List B (2013) Top Organomet Chem 44:165–194
57. Parmar D, Sugiono E, Raja S, Rueping M (2014) Chem Rev 114:9047–9153
58. Held FE, Grau D, Tsogoeva SB (2015) Molecules 20:16103–16126
59. Marcelli T, Hammar P, Himo F (2008) Chem Eur J 14:8562–8571
60. Simón L, Goodman JM (2008) J Am Chem Soc 130:8741–8747
61. Marcelli T, Hammar P, Himo F (2009) Adv Synth Catal 351:525–529
62. Storer RI, Carrera DE, Ni Y, MacMillan DWC (2006) J Am Chem Soc 128:84–86
63. Kang Q, Zhao Z-A, You S-L (2007) Adv Synth Catal 349:1657–1660
64. Kang Q, Zhao Z-A, You S-L (2008) Org Lett 10:2031–2034

65. Li G, Liang Y, Antilla JC (2007) J Am Chem Soc 129:5830–5831
66. Rueping M, Antonchick AP, Theissmann T (2006) Angew Chem Int Ed 45:3683–3686
67. Katritzky AR, Rachwal S, Rachwal B (1996) Tetrahedron 52:15031–15070
68. Rakotoson JH, Fabre N, Jacquemond-Collet I, Hannedouche S, Fouraste I, Moulis C (1998) Planta Med 64:762–763
69. Jacquemond-Collet I, Hannedouche S, Fabre N, Fouraste I, Moulis C (1999) Phytochem 51:1167–1169
70. Houghton PJ, Woldemariam TZ, Watanabe Y, Yates M (1999) Planta Med 65:250–254
71. Rueping M, Theissmann T, Antonchick AP (2006) Synlett, 1071–1074
72. Rueping M, Theissmann T, Raja S, Bats JW (2008) Adv Synth Catal 350:1001–1006
73. Guo Q-S, Du D-M, Xu J (2008) Angew Chem Int Ed 47:759–762
74. Metallinos C, Barrett FB, Xu S (2008) Synlett, 720–724
75. Han Z-Y, Xiao H, Chen X-H, Gong L-Z (2009) J Am Chem Soc 131:9182–9183
76. Rueping M, Sugiono E, Steck A, Theissmann T (2010) Adv Synth Catal 352:281–287
77. Rueping M, Theissmann T (2010) Chem Sci 1:473–476
78. Rueping M, Theissmann T, Stoeckel M, Antonchick AP (2011) Org Biomol Chem 9:6844–6850
79. Li G, Liu H, Lv G, Wang Y, Fu Q, Tang Z (2015) Org Lett 17:4125–4127
80. Tu X-F, Gong L-Z (2012) Angew Chem Int Ed 51:11346–11349
81. Shi F, Gong L-Z (2012) Angew Chem Int Ed 51:11423–11425
82. Chen M-W, Cai X-F, Chen Z-P, Shi L, Zhou Y-G (2014) Chem Commun 50:12526–12529
83. Guo R-N, Chen Z-P, Cai X-F, Zhou Y-G (2014) Synthesis 46:2751–2756
84. Aillerie A, de Talancé VL, Moncomble A, Bousquet T, Pélinski L (2014) Org Lett 16:2982–2985
85. Hayakawa I, Atarashi S, Yokohama S, Imamura M, Sakano K-I, Furukawa M (1986) Antimicrob Agents Chemother 29:163–164
86. Seiyaku D (1992) Drugs Future 17:559–563
87. Rueping M, Stoeckel M, Sugiono E, Theissmann T (2010) Tetrahedron 66:6565–6568
88. Friedländer P (1882) Ber Dtsch Chem Ges 15:2572–2575
89. Marco-Contelles J, Pérez-Mayoral E, Samadi A, Carreiras MC, Soriano E (2009) Chem Rev 109:2652–2671
90. Ren L, Lei T, Ye J-X, Gong L-Z (2012) Angew Chem Int Ed 51:771–774
91. Rueping M, Antonchick AP (2007) Angew Chem Int Ed 46:4562–4565
92. Bohlmann F, Rahtz D (1957) Chem Ber 90:2265–2272
93. Bagley MC, Brace C, Dale JW, Ohnesorge M, Phillips NG, Xiong X, Bower J (2002) J Chem Soc Perkin Trans 1:1663–1671
94. Sklenicka HM, Hsung RP, McLaughlin MJ, Wie L-L, Gerasyuto AI, Brennessel WB (2002) J Am Chem Soc 124:10435–10442
95. Rueping M, Antonchick AP, Theissmann T (2006) Angew Chem Int Ed 45:6751–6755
96. Tietze LF, Brasche G, Gericke KM (eds) (2006) Domino reactions in organic synthesis. Wiley-VCH, Weinheim
97. Enders D, Grondal C, Hüttl MRM (2007) Angew Chem Int Ed 46:1570–1581
98. Walji AM, MacMillan DWC (2007) Synlett, 1477–1489
99. Rueping M, Antonchick AP (2008) Angew Chem Int Ed 45:5836–5838
100. Rueping M, Tato F, Schoepke FR (2010) Chem Eur J 16:2688–2691
101. Fantin M, Marti M, Auberson YP, Morari M (2007) J Neurochem 103:2200–2211
102. TenBrink RE, Im WB, Sethy VH, Tang AH, Carter DB (1994) J Med Chem 37:758–768
103. Li S, Tian X, Hartley DM, Feig LA (2006) J Neurosci 26:1721–1729
104. Patel M, McHush RJ Jr, Cordova BC, Klabe RM, Erickson-Viitanen S, Trainor GL, Rodgers JD (2000) Bioorg Med Chem Lett 10:1729–1731
105. Shi F, Tan W, Zhang H-H, Li M, Ye Q, Ma G-H, Tu S-J, Li G (2013) Adv Synth Catal 355:3715–3726
106. Liao H-H, Hsiao C-C, Sugiono E, Rueping M (2013) Chem Commun 49:7953–7955
107. Sugiono E, Rueping M (2013) Beilstein J Org Chem 9:2457–2462
108. Hsiao C-C, Liao H-H, Sugiono E, Atodiresei I, Rueping M (2013) Chem Eur J 19:9775–9779
109. Wang Z, Ai F, Wang Z, Zhao W, Zhu G, Lin Z, Sun J (2015) J Am Chem Soc 137:383–389
110. Dalko PI, Moisan L (2004) Angew Chem Int Ed 43:5138–5175
111. Seayed J, List B (2005) Org Biomol Chem 3:719–724
112. List B (2006) Chem Commun, 819–824
113. Marigo M, Jørgensen KA (2006) Chem Commun, 2001–2011

114. Guillena G, Ramón DJ (2006) Tetrahedron Asymmetry 17:1465–1492
115. Sulzer-Mossé S, Alexakis A (2007) Chem Commun, 3123–3135
116. Tsogoeva SB (2007) Eur J Org Chem, 1701–1716
117. Vicario JL, Badía D, Carrillo L (2007) Synthesis, 2065–2092
118. Almaşi D, Alonso DA, Najera C (2007) Tetrahedron Asymmetry 18:299–365
119. Pellissier H (2007) Tetrahedron 63:9267–9331
120. Dondoni A, Massi A (2008) Angew Chem Int Ed 47:4638–4660
121. Melchiorre P, Marigo M, Carlone A, Bartoli G (2008) Angew Chem Int Ed 47:6138–6171
122. Gruttadauria M, Giacalone F, Noto R (2009) Adv Synth Catal 351:33–57
123. Bertelsen S, Jørgensen KA (2009) Chem Soc Rev 38:2178–2189
124. Ueda M, Kano T, Maruoka K (2009) Org Biomol Chem 7:2005–2012
125. Nielsen M, Jacobsen CB, Holub N, Paixão MW, Jørgensen KA (2010) Angew Chem Int Ed 49:2668–2679
126. Nielsen M, Worgull D, Zweifel T, Gschwend B, Bertelsen S, Jørgensen KA (2011) Chem Commun 47:632–649
127. Marqués-López E, Herrera RP (2011) Curr Org Chem 15:2311–2327
128. Jurberg ID, Chatterjee I, Tannert R, Melchiorre P (2013) Chem Commun 49:4869–4883
129. Paz BM, Jiang H, Jørgensen KA (2015) Chem Eur J 21:1846–1853
130. Yang JW, Fonseca MTH, List B (2004) Angew Chem Int Ed 43:6660–6662
131. Yang JW, Fonseca MTH, Vignola N, List B (2005) Angew Chem Int Ed 44:108–110
132. Ouellet SG, Tuttle JB, MacMillan DWC (2005) J Am Chem Soc 127:32–33
133. Tuttle JB, Ouellet SG, MacMillan DWC (2006) J Am Chem Soc 128:12662–12663
134. Huang Y, Walji AM, Larsen CH, MacMillan DWC (2005) J Am Chem Soc 127:15051–15053
135. Mayer S, List B (2006) Angew Chem Int Ed 45:4193–4195
136. Martin NJA, List B (2006) J Am Chem Soc 128:13368–13369
137. Eey ST-C, Lear MJ (2010) Org Lett 12:5510–5513
138. Akagawa K, Akabane H, Sakamoto S, Kudo K (2008) Org Lett 10:2035–2037
139. Akagawa K, Akabane H, Sakamoto S, Kudo K (2009) Tetrahedron Asymmetry 20:461–466
140. Hoffman TJ, Dash J, Rigby JH, Arseniyadis S, Cossy J (2009) Org Lett 11:2756–2759
141. Schreiner PR (2003) Chem Soc Rev 32:289–296
142. Takemoto Y (2005) Org Biomol Chem 3:4299–4306
143. Breuzard JAJ, Christ-Tommasino ML, Lemaire M (2005) Top Organomet Chem 15:231–270
144. Connon SJ (2006) Chem Eur J 12:5418–5427
145. Taylor MS, Jacobsen EN (2006) Angew Chem Int Ed 45:1520–1543
146. Doyle AG, Jacobsen EN (2007) Chem Rev 107:5713–5743
147. Zhang Z, Schreiner PR (2009) Chem Soc Rev 38:1187–1198
148. Marqués-López E, Herrera RP (2009) An Quim 105:5–12
149. Kotke M, Schreiner PR (2009) In: Pihko PM (ed) Hydrogen bonding in organic synthesis. Wiley-VCH, Weinheim, pp 141–351
150. Connon SJ (2009) Synlett, 354–376
151. Marqués-López E, Herrera RP (2012) In: Pignataro B (ed) New strategies in chemical synthesis and catalysis. Wiley-VCH, Weinheim, pp 175–199
152. Narayanaperumal S, Rivera DG, Silva RC, Paixão MW (2013) ChemCatChem 5:2756–2773
153. Jakab G, Schreiner PR (2013) In: Dalko P (ed) Comprehensive enantioselective organocatalysis. Wiley-VCH, Weinheim, pp 315–341
154. Serdyuk OV, Heckel CM, Tsogoeva SB (2013) Org Biomol Chem 11:7051–7071
155. Menche D, Arikan F (2006) Synlett, 841–844
156. Martin NJA, Ozores L, List B (2007) J Am Chem Soc 129:8976–8977
157. Zhang Z, Schreiner PR (2007) Synthesis, 2559–2564
158. Martin NJA, Cheng X, List B (2008) J Am Chem Soc 130:13862–13863
159. Schneider JF, Falk FC, Fröhlich R, Paradies J (2010) Eur J Org Chem, 2265–2269
160. Schneider JF, Lauber MB, Muhr V, Kratzer D, Paradies J (2011) Org Biomol Chem 9:4323–4327
161. Massolo E, Benaglia M, Orlandi M, Rossi S, Celentano G (2015) Chem Eur J 21:3589–3595
162. Martinelli E, Vicini AC, Mancinelli M, Mazzanti A, Zani P, Bernardi L, Fochi M (2015) Chem Commun 51:658–660
163. Denmark SE, Fu J (2003) Chem Rev 103:2763–2793
164. Denmark SE, Beutner GL (2008) Angew Chem Int Ed 47:1560–1638

165. Iwasaki F, Onomura O, Mishima K, Kanematsu T, Maki T, Matsumura Y (2001) Tetrahedron Lett 42:2525–2527
166. Baudequin C, Chaturvedi D, Tsogoeva SB (2007) Eur J Org Chem, 2623–2629
167. Xue Z-Y, Jiang Y, Yuan W-C, Zhang X-M (2010) Eur J Org Chem, 616–619
168. Zheng H, Deng J, Lin W, Zhang X (2007) Tetrahedron Lett 48:7934–7937
169. Xue Z-Y, Jiang Y, Peng X-Z, Yuan W-C, Zhang X-M (2010) Adv Synth Catal 352:2132–2136
170. Chen X, Zheng Y, Shu C, Yuan W, Liu B, Zhang X (2011) J Org Chem 76:9109–9115
171. Genoni A, Benaglia M, Massolo E, Rossi S (2013) Chem Commun 49:8365–8367
172. Barrulas PC, Genoni A, Benaglia M, Burke AJ (2014) Eur J Org Chem, 7339–7342
173. Onomura O, Kouchi Y, Iwasaki F, Matsumura Y (2006) Tetrahedron Lett 47:3751–3754
174. Wang Z, Wei S, Wang C, Sun J (2007) Tetrahedron Asymmetry 18:705–709
175. Kanemitsu T, Umehara A, Haneji R, Nagata K, Itoh T (2012) Tetrahedron 68:3893–3898
176. Malkov AV, Mariani A, MacDougall KN, Kočovský P (2004) Org Lett 6:2253–2256
177. Malkov AV, Stončius S, MacDougall KN, Mariani A, McGeoch GD, Kočovský P (2006) Tetrahedron 62:264–284
178. Malkov AV, Figlus M, Stončius S, Kočovský P (2007) J Org Chem 72:1315–1325
179. Malkov AV, Stončius S, Kočovský P (2007) Angew Chem Int Ed 46:3722–3724
180. Malkov AV, Vranková K, Stončius S, Kočovský P (2009) J Org Chem 74:5839–5849
181. Malkov AV, Vranková K, Sigerson RC, Stončius S, Kočovský P (2009) Tetrahedron 65:9481–9486
182. Ge X, Qian C, Chen X (2014) Tetrahedron Asymmetry 25:1450–1455
183. Wang Z, Ye X, Wei S, Wu P, Zhang A, Sun J (2006) Org Lett 8:999–1001
184. Zhou L, Wang Z, Wei S, Sun J (2007) Chem Commun, 2977–2979
185. Collados JF, Quiroga-Feijóo ML, Alvarez-Ibarra C (2009) Eur J Org Chem, 3357–3367
186. Xiao Y-C, Wang C, Yao Y, Sun J, Chen Y-C (2011) Angew Chem Int Ed 50:10661–10664
187. Wang ZY, Wang C, Zhou L, Sun J (2013) Org Biomol Chem 11:787–797
188. Wang Z, Cheng M, Wu P, Wei S, Sun J (2006) Org Lett 8:3045–3048
189. Wu P, Wang Z, Cheng M, Zhou L, Sun J (2008) Tetrahedron 64:11304–11312
190. Ellman JA, Owens TD, Tang TP (2002) Acc Chem Res 35:984–995
191. Fernandez I, Khiar N (2003) Chem Rev 103:3651–3705
192. Ellman JA (2003) Pure Appl Chem 75:39–46
193. Zhou P, Chen B-C, Davis FA (2004) Tetrahedron 60:8003–8030
194. Senanayake CH, Krishnamurthy D, Lu Z-H, Han Z, Gallou I (2005) Aldrichim Acta 38:93–104
195. Morton D, Stockman RA (2006) Tetrahedron 62:8869–8905
196. Pei D, Wang Z, Wei S, Zhang Y, Sun J (2006) Org Lett 8:5913–5915
197. Pei D, Zhang Y, Wei S, Wang M, Sun J (2008) Adv Synth Catal 350:619–623
198. Wang C, Wu X, Zhou L, Sun J (2008) Chem Eur J 14:8789–8792
199. Liu X-W, Wang C, Yan Y, Wang Y-Q, Sun J (2013) J Org Chem 78:6276–6280
200. Wang C, Wu X, Zhou L, Sun J (2015) Org Biomol Chem 13:577–582
201. Benaglia M, Puglisi A, Cozzi F (2003) Chem Rev 103:3401–3429
202. Cozzi F (2006) Adv Synth Catal 348:1367–1390
203. Kristensen TE, Hansen T (2010) Eur J Org Chem, 3179–3204
204. Kristensen TE, Hansen T (2013) In: Dalko PI (ed) Comprehensive enantioselective organocatalysis. Wiley-VCH, Weinheim, pp 651–672
205. Ge X, Qian C, Yea X, Chen X (2015) RSC Adv 5:65402–65407
206. Malkov AV, Figlus M, Kočovský P (2008) J Org Chem 73:3985–3996
207. Malkov AV, Figlus M, Prestly MR, Rabani G, Cooke G, Kočovský P (2009) Chem Eur J 15:9651–9654
208. Malkov AV, Figlus M, Cooke G, Caldwell ST, Rabani G, Prestly MR, Kočovský P (2009) Org Biomol Chem 7:1878–1883
209. Figlus M, Caldwell ST, Walas D, Yesilbag G, Cooke G, Kočovský P, Malkov AV, Sanyal A (2010) Org Biomol Chem 8:137–141
210. Iwasaki F, Onomura O, Mishima K, Maki T, Matsumura Y (1999) Tetrahedron Lett 40:7507–7511
211. Pini D, Iuliano A, Salvadori P (1992) Tetrahedron Asymmetry 3:693–694
212. Schiffers R, Kagan HB (1997) Synlett, 1175–1178
213. LaRonde FJ, Brook MA (1999) Tetrahedron Lett 40:3507–3510
214. Malkov AV, Liddon AJPS, Ramírez-López P, Bendová L, Haigh D, Kočovský P (2006) Angew Chem Int Ed 45:1432–1435
215. Matsumura Y, Ogura K, Kouchi Y, Iwasaki F, Onomura O (2006) Org Lett 8:3789–3792

216. Brown HC, Kulkarni SV, Racherla US (1994) J Org Chem 59:365–369
217. Hilborn JW, Lu Z-H, Jurgens AR, Fang QK, Byers P, Wald SA, Senanayake CH (2001) Tetrahedron Lett 42:8919–8921
218. Kamal A, Sandbhor M, Shaik AA (2003) Tetrahedron Asymmetry 14:1575–1580
219. Steer DL, Lew RA, Perlmutter P, Smith AI, Aguilar M-I (2002) Curr Med Chem 9:811–822
220. Juaristi E, Soloshonok VA (2005) Enantioselective synthesis of β-amino acids. Wiley-VCH, Hoboken
221. Sleebs BE, Van Nguyen TT, Hughes AB (2009) Org Prep Proced Int 41:429–478
222. Weiner B, Szymański W, Janssen DB, Minnaard AJ, Feringa BL (2010) Chem Soc Rev 39:1656–1691
223. Weickgenannt A, Oestreich M (2011) ChemCatChem 3:1527–1529
224. Hsiao Y, Rivera NR, Rosner T, Krska SW, Njolito E, Wang F, Sun Y, Armstrong JD III, Grabowski EJJ, Tillyer RD, Spindler F, Malan C (2004) J Am Chem Soc 126:9918–9919
225. Dai Q, Yang W, Zhang X (2005) Org Lett 7:5343–5345
226. Zheng H-J, Chen W-B, Wu Z-J, Deng J-G, Lin W-Q, Yuan W-C, Zhang X-M (2008) Chem Eur J 14:9864–9867
227. Jiang Y, Chen X, Zheng Y, Xue Z, Shu C, Yuan W, Zhang X (2011) Angew Chem Int Ed 50:7304–7307
228. Bonsignore M, Benaglia M, Annunziata R, Celentano G (2011) Synlett, 1085–1088
229. Wu X, Li Y, Wang C, Zhou L, Lu X, Sun J (2011) Chem Eur J 17:2846–2848
230. Sugiura M, Kumahara M, Nakajima M (2009) Chem Commun, 3585–3587
231. Guizzetti S, Benaglia M, Bonsignore M, Raimondi L (2011) Org Biomol Chem 9:739–743
232. Xiao Y-C, Wang C, Yao Y, Sun J, Chen Y-C (2011) Angew Chem Int Ed 50:10661–10664
233. Liu X-W, Yan Y, Wang Y-Q, Wang C, Sun J (2012) Chem Eur J 18:9204–9207
234. Torssell S, Kienle M, Somfai P (2005) Angew Chem Int Ed 44:3096–3099
235. Chrzanowska M, Dreas A (2006) Heterocycles 69:303–310
236. Malkov AV, Stončius S, Vranková K, Arndt M, Kočovský P (2008) Chem Eur J 14:8082–8085

CrossMark

REVIEW

Proton-Coupled Electron Transfer in Organic Synthesis: Fundamentals, Applications, and Opportunities

David C. Miller[1] · Kyle T. Tarantino[1] ·
Robert R. Knowles[1]

Abstract Proton-coupled electron transfers (PCETs) are unconventional redox processes in which both protons and electrons are exchanged, often in a concerted elementary step. While PCET is now recognized to play a central a role in biological redox catalysis and inorganic energy conversion technologies, its applications in organic synthesis are only beginning to be explored. In this chapter, we aim to highlight the origins, development, and evolution of the PCET processes most relevant to applications in organic synthesis. Particular emphasis is given to the ability of PCET to serve as a non-classical mechanism for homolytic bond activation that is complimentary to more traditional hydrogen atom transfer processes, enabling the direct generation of valuable organic radical intermediates directly from their native functional group precursors under comparatively mild catalytic conditions. The synthetically advantageous features of PCET reactivity are described in detail, along with examples from the literature describing the PCET activation of common organic functional groups.

1 Introduction

'Proton-coupled electron transfer' (PCET) describes any elementary step (or series of elementary steps) in which both a proton and an electron are exchanged [1–9]. Within this broad definition, further distinctions may be drawn: if the proton and

✉ Robert R. Knowles
rknowles@princeton.edu

[1] Department of Chemistry, Princeton University, Princeton, NJ 08544, USA
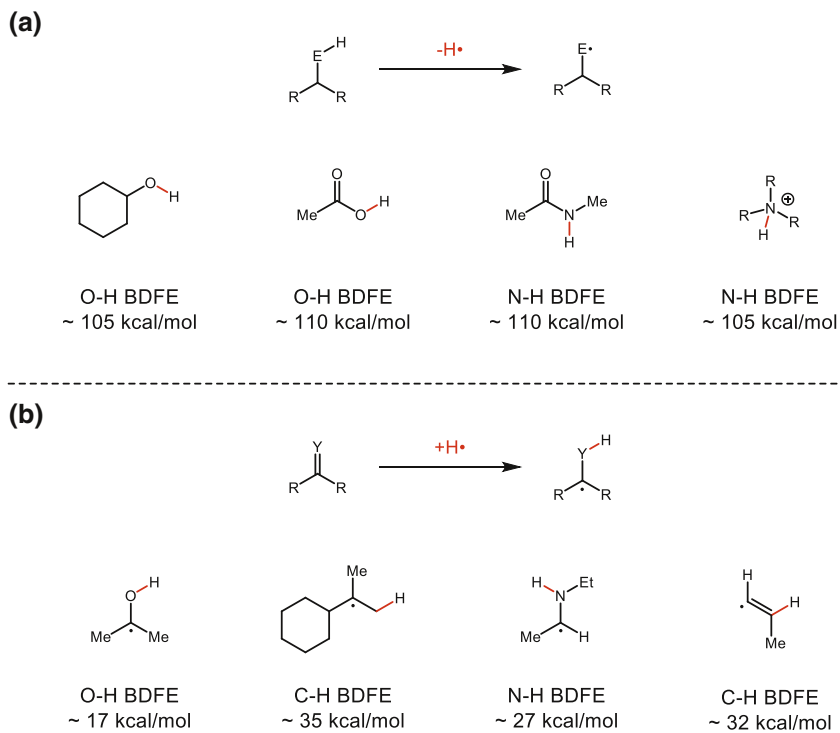
electron move simultaneously, the elementary step is referred to as a concerted PCET. Alternatively, if electron transfer precedes a rapid proton-transfer event (or vice versa), the series of elementary steps is said to be stepwise. The proton and electron in a PCET process need not originate from the same bond, or even the same molecule: when the proton and electron are delivered to two separate acceptors or arrive from two distinct donors, the PCET event is said to be multisite.

In recent years, PCET has been shown to play a central role in important biological redox processes, such as photosynthetic water oxidation [10], ribonucleotide reduction in DNA biosynthesis [11, 12], oxygen reduction by cytochrome C oxidase [13], enzymatic C–H bond oxidation [14, 15], natural product biosynthesis [16], DNA photolyase activity [17], and numerous synthetic inorganic technologies for small molecule activation [18, 19]. Concurrently, extensive physical and theoretical studies have provided a number of important insights into PCET reaction mechanisms [20, 21]. However, the applications of PCET as a mechanism of substrate activation in organic synthesis have only recently begun to be explored. The focus of this review is to highlight both the basic reactivity trends and beneficial attributes of concerted PCET reactions for synthetic applications, and to discuss the chemistry of common organic functional groups known to engage in concerted PCET reactivity. This review is not meant to serve as a comprehensive overview of documented PCET processes in biology or an exhaustive overview of their physical origins. Rather, it is meant as a primer for organic chemists who may wish to design or utilize PCET reactions in their own work, or to become acquainted with the synthetically relevant literature in this large and diverse area of research. The structure of this review starts with an introductory discussion of the energetics of PCET reactions, followed by mechanistic discussion as organized by functional groups. Where applicable, synthetic examples are included to demonstrate the capacity of PCET to furnish desirable radical synthons and explore their often-unique selectivities.

2 Energetic Characteristics of PCET Activation

From a synthetic perspective, multisite PCET is similar to traditional hydrogen atom transfer (HAT) reactions in that both involve the addition or removal of the elements of H• to furnish a neutral free radical product. However, PCET has the potential to enable the direct homolytic activation of many common organic functional groups that are energetically inaccessible using conventional H-atom transfer platforms. In HAT reactions, the thermodynamic driving force is taken to be proportional to the difference in bond strengths of the bonds being broken and formed in the exchange. As such, cleaving a strong bond to hydrogen in the donor requires formation of a similarly strong or even stronger bond to hydrogen in the acceptor. Similar constraints apply in the reactions of H-atom donors, wherein the new bond to hydrogen formed upon HAT to an acceptor must be of similar strength (or stronger than) the bond to hydrogen in the donor. These energetic constraints present a significant challenge to developing effective catalysts for the homolytic activation of many common organic functional groups (Fig. 1). With respect to oxidative HAT activation, the bonds to hydrogen in many of the most common protic organic functional groups (including alcohols,

(a)

| O–H BDFE ~ 105 kcal/mol | O–H BDFE ~ 110 kcal/mol | N–H BDFE ~ 110 kcal/mol | N–H BDFE ~ 105 kcal/mol |

(b)

| O–H BDFE ~ 17 kcal/mol | C–H BDFE ~ 35 kcal/mol | N–H BDFE ~ 27 kcal/mol | C–H BDFE ~ 32 kcal/mol |

Fig. 1 **a** Examples of strong bonds of common organic functional groups. **b** Examples of weak bonds vicinal to radical centers derived from common organic functional groups

amides, ammonium ions, and carboxylic acids) feature bonds strengths well in excess of 100 kcal mol^{-1} (Fig. 1a). As such, even the most powerful molecular HAT reagents, such as the ferryl groups in metalloproteins such as cytochrome P450, do not possess a sufficient driving force to activate many polar N–H and O–H bonds [22]. Moreover, these polar functional groups are often embedded in hydrocarbon frameworks containing much weaker aliphatic C–H bonds that are often preferentially activated by strong H-atom acceptors.

Similarly, for the reductive HAT activation of π-systems, the new bond to hydrogen is dramatically destabilized by virtue of being vicinal to an unpaired electron (Fig. 1b). As such, few if any HAT donors have been shown to be competent to activate ketones, imines, arenes, or certain classes of olefins [23–26] via HAT. In fact, the weakest, well-characterized metal hydride is Norton's H-V(CO)$_4$(dppb), which features a V–H BDFE of 50 kcal mol^{-1} [27]. While exceptionally weak, this bond it is still far too strong to serve as an effective H-atom donor to many common organic π-systems such as those depicted in Fig. 1b.

In light of these limitations, it is interesting to consider how one might rationally design new HAT catalysts to target specific organic functional groups. Classically, the homolytic strengths of covalent bonds are analyzed using a simple thermodynamic cycle popularized by Bordwell [28]. In this scheme, the bond dissociation free energy (BDFE) is defined as the energy required to heterolytically break the

bond (represented as a pK_a value) summed together with the energies required to oxidize the resulting anion to a neutral radical and reduce the remaining proton to H•. As such, this formalism would suggest that to create a molecular H-atom donor with a weaker R–H bond, one must either increase the Brønsted acidity of the donor, make its conjugate base more reducing, or some combination thereof. Unfortunately, within any single molecule these two key physical properties—the pK_a and the oxidation potential of the conjugate base—are interdependent and inversely correlated. The energetic benefits of making a donor more acidic will be largely compensated for by a concomitant loss in the reducing ability. Analogous difficulties arise in the design of new oxidative HAT reagents, wherein any increase in basicity of an H-atom acceptor will be compensated in part by a correlated decrease in oxidizing power. This leveling effect suggests that rational design of more powerful molecular H-atom donors and acceptors through variation of these parameters is likely to be challenging (Fig. 2).

However, Mayer has pointed out that this method for conceptualizing covalent bond strengths suggests a thermodynamic equivalency between direct HAT, in which the transferring proton and electron originate in the same chemical bond, and a multisite PCET mechanism wherein the proton and electron traveling to the acceptor originate from site-separated and independent donors—a Brønsted acid and a one-electron reductant (Fig. 3) [29]. While no bond is formally homolyzed in such a process, summing the pK_a and redox potential values in a similar fashion provides an 'effective' bond strength, which quantitatively reflects the capacity of any given acid/reductant combination to function jointly as a hydrogen atom donor. Significantly, in this PCET manifold the pK_a of the proton donor and the potential of the reductant may be varied independently. This in turn allows the effective BDFE of any given acid/reductant (or oxidant/base) pair to be varied over an arbitrarily wide range of energies. While not all bases are compatible with all oxidants [30], the use of excited-state redox partners as PCET components tends to allow for

$$BDFE \text{ (kcal/mol)} = 1.37 \text{ p}K_a(\text{R-H}) + 23.06 \ E°(\text{R}^-/\text{R}^•) + 23.06 \ E°(\text{H}^+/\text{H}^•)$$
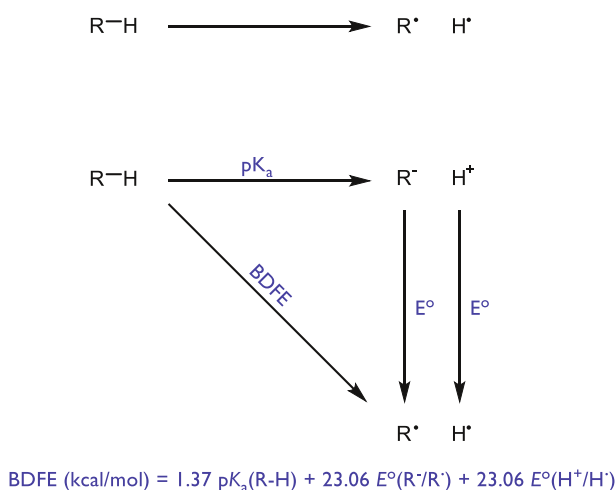
Fig. 2 A square scheme for the determination of BDFEs as popularized by Bordwell [28]
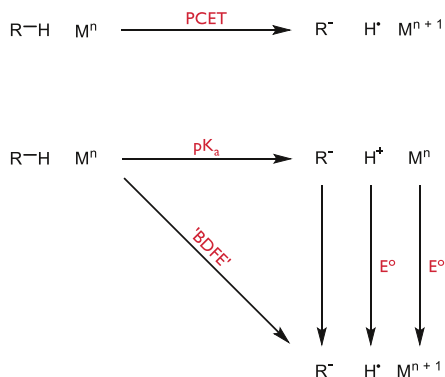
$$BDFE(kcal/mol) = 1.37\ pK_a + 23.06\ E^{\circ}\ (M^n/M^{n+1}) + 23.06\ E^{\circ}\ (H^+/H^{\bullet})$$

Hydrogen Atom Acceptor Pairs					Hydrogen Atom Donor Pairs				
Oxidant	Base	E^0 (V)	pKa	'BDFE'	Reductant	Acid	E^0 (V)	pKa	'BDFE'
$Fe^{III}(bpy)_3$	pyridine	0.70	12.5	87	Cp_2Co	$PhCO_2H$	−1.34	21.5	54
$^*Ru^{II}(bpy)_3$	acetate	0.39	23.5	96	$(CpMe_5)_2Co$	lutidinium	−1.47	14.1	40
$^*Ru^{II}(bpz)_3$	lutidine	1.07	14.1	100	$Ru^I(bpy)_3$	pyridinium	−1.71	12.5	33
$^*Ir^{III}(dF(CF_3)ppy)_2(bpy)$	DMAP	1.0	18	103	$Ru^I(bpy)_3$	PTSA	−1.71	8.6	27

Fig. 3 A square scheme for 'effective' BDFEs as popularized by Mayer [29] along with example bond strengths available by the joint action of select bases/oxidants and acids/reductants, respectively. *Asterisks* denote ET from an excited state except for Cp*, which refers to pentamethylcyclopentadiene. *bpy* 2,2′-bipyridine, *bpz* 2,2′-bipyrazine, *ppy* 2-phenylpyridinato-C^2, *dF(CF$_3$)ppy* 2-(2,4-difluorophenyl)-5-(trifluoromethyl)pyridinato-C^2, *DMAP* 4-dimethylamino pyridine, *PTSA* p-toluenesulfonic acid

greater flexibility with respect to which bases may be used [31]. The same principle applies for combinations of acids and reductants. This formalism provides a straightforward means to identify acid/reductant combinations with effective bond strengths far weaker (<20 kcal/mol) than those found for any known molecular H• donor catalysts. Similarly, thermochemical arguments can be constructed for combinations of bases and oxidants that act in unison as thermodynamically potent hydrogen atom abstractors, with effective BDFEs in excess of 110 kcal/mol. In principle, this remarkable energetic range can enable the rational identification of catalyst systems that are thermodynamically competent to effect homolytic activation of many common organic functional groups that are currently inaccessible using traditional HAT technologies. Even if PCET to a substrate is endergonic, several synthetic examples highlight that even highly endergonic PCET events can be coupled with secondary chemical reactions in catalysis [31, 32].

In addition to enabling access to more powerful HAT reagents, the preferences for site selectivity in multisite PCET reactions are expected to be orthogonal to those of many traditional HAT catalysts. Selectivity in HAT processes is generally a function of bond strength differential, with the weakest bonds in the substrate being oxidized most rapidly [33]. In fact, such relationships are often presented as

evidence for radical-based mechanisms of bond cleavage. In contrast, the site-selectivity of multisite PCET mechanisms is dictated by specific hydrogen bonding interactions [6]. In physical descriptions of PCET reactivity, significant emphasis is placed on the length scales of the transfer reactions. While electrons tunnel readily over large distances (>10 Å), heavier protons can only travel over relatively small distances (1–2 Å). Consequently, pre-association by hydrogen bonding is a characteristic feature of concerted multisite PCET activation as it defines the proton transfer reaction coordinate and confines it to an appropriate length scale. As typical C–H bonds are poor hydrogen bond donors, separated base/oxidant catalyst systems should, in principle, be able to activate stronger O–H and N–H bonds of polar H-bond donors selectively. Similarly, concerted PCET activation of ketones and other polar π bonds should be possible in preference to the activation of olefins, despite a large thermodynamic bias for the latter pathway.

Lastly, in addition to the these thermodynamic advantages, concerted PCET processes often exhibit rates that are significantly faster than the constituent electron transfer (ET) or proton transfer (PT) steps in isolation (Fig. 4). This observation follows from the fact that PCET kinetics, like those of ET and HAT, are functions of the reaction's thermodynamic driving force [34–36]. The products formed directly in the concerted pathway are necessarily lower in energy than the intermediates formed in the competing stepwise pathways. This thermodynamic bias is manifested kinetically, enabling facile charge transfer to occur with catalyst potentials that are far less energetic than the thermodynamic potentials of their substrates. These kinetic advantages are well precedented in a large number of molecular systems and are thought to underlie the pervasive use of concerted PCET mechanisms in biological redox catalysis.

In light of these advantages, PCET has significant potential to expand the scope of homolytic bond activation catalysis in organic synthesis, and enable the direct generation of valuable radical intermediates directly from their native functional group precursors [37]. In support of this hypothesis, the remaining sections of this
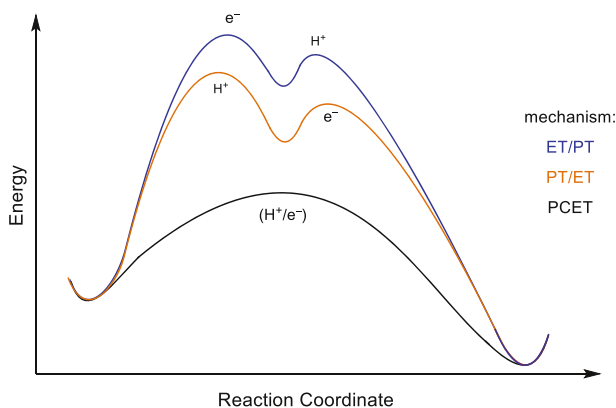

Fig. 4 A sample reaction coordinate demonstrating the diminished barriers for concerted PCET relative to stepwise ET/PT or PT/ET

chapter are devoted to mechanistic studies and relevant synthetic examples of PCET segmented by functional groups.

3 Metal-Oxo Complexes for C–H Bond Oxidation

Among the most synthetically important PCET reactions are the oxidations of C–H bonds by metal-oxo complexes. However, prior to a full discussion of metal-oxo PCET reactions, it is important to comment in more detail on the distinctions between HAT and PCET. Meyer has proposed a definition for HAT that is limited to reactions in which "the transferring electron and proton come from the same bond" [5, 38, 39]. Mayer has noted a number of problems associated with this definition that are especially pertinent in the reactions of metal-oxo complexes [29]. Specifically, Mayer cites compound I in cytochrome P450 enzymes where the metal oxo (Fe = O) group accepts a proton at oxygen while the electron is transferred into a ligand-centered orbital of the porphyrin radical cation [40]. He further elaborates that a forward abstraction step could be accurately defined as a HAT step, as the proton and electron come from the C–H bond, but not its microscopic reverse, where the proton comes from the O–H bond and the electron comes from a ligand-centered orbital. Accordingly, he suggests HAT to be more broadly defined as "concerted transfer of [a proton] and [an electron] from a single donor to a single acceptor." While this definition suggests that classical HAT is a specific subset of concerted PCET reactions, subtleties between the two elementary steps preclude these terms from being truly interchangeable (or, in many cases, from being readily distinguished) [39, 41, 42]. In light of these problems in both terminology and identification, we present examples pertinent to PCET-type

Fig. 5 A sample Pourbaix diagram of magnesium in water; the *dashed blue lines* represent the potentials at which water is oxidized (*top line*) and reduced (*bottom line*). Reprinted with permission from [43]. Copyright 2012 American Chemical Society
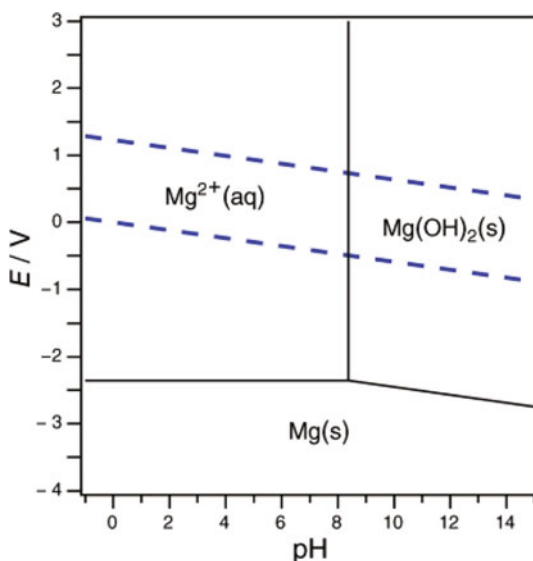
mechanisms and have adopted the nomenclature presented by the original authors. We defer judgment regarding the aptness and accuracy of these classifications to the reader.

In his doctoral thesis in 1945, Pourbaix established the use of "potential-pH diagrams"—now referred to as Pourbaix diagrams—to predict the equilibrium state of a given element and its ions in aqueous solution (Fig. 5) [43, 44]. Since that time, Pourbaix diagrams for many elements have been developed for their utility in assessing the thermodynamic viability of certain processes, especially corrosion [45]. Crossing a line on the diagram represents changes in the dominant species in situ; such boundaries are dependent on both the pH and the potential and (if the potential is reversible) can be outlined using the following form of the Nernst equation [29]:

$$E = E^0 - \frac{RT}{nF} ln \frac{[\text{H}_m\text{A}^{(n-m)-}]}{[\text{A}]} - \frac{RT}{F} \frac{m}{n} \text{pH}$$

In the above equations, m represents the number of protons transferred, n refers to the number of electrons transferred, R is the ideal gas constant, F is Faraday's constant, and T is the temperature. At a constant, standard temperature of 298 K, the value (RT/F) is 59 mV and is constant. As the pH changes, the slope $\Delta E/\Delta \text{pH}$ reflects the ratio of protons to electrons (m/n) transferred in a single step: a horizontal line ($m = 0$) indicates no proton transfer occurs, vertical lines ($n \sim 0$) imply no involvement of electron transfer, and diagonal lines indicate both protons and electrons transfer for a net loss of protons and electrons in some ratio m/n. For example, the net loss of a hydrogen atom (i.e., one proton and one electron) proceeds with $m/n = 1$. An important note, however, is that a Pourbaix diagram only provides *thermochemical* information for a PCET event and does not distinguish between stepwise or concerted processes: further mechanistic analysis is required to distinguish the operative mechanisms. In addition, for aqueous solutions such diagrams are limited to potential/pH regimes in which water is stable. Nevertheless, boundaries of thermochemical viability are valuable to the synthetic chemist seeking to choose reagents to affect a particular PCET process.

The idea that both the pH and applied voltage affects the stability of metal oxo, hydroxo, and aquo species has proven influential over time. Based on these diagrams, the community has come to understand the influence of both the substrate $\text{p}K_a$ and the potential associated with its (de)protonated form on the overall bond strength of a species and how these may be leveraged to tune said bond strengths. For a metal oxo, the O–H bond strength inherent to a metal oxo is determined by both its basicity and its oxidizing power. As further examples will demonstrate, the basicity is oftentimes the dominant contributor to the bond strength of this species. The importance of oxo basicity was highlighted by Green and Gray in their seminal studies of chloroperoxidase, which identified that chloroperoxidase compound II (CPO-II) must have a minimum aqueous $\text{p}K_a$ of ~ 8.2 [22]. The basicity implies this species is protonated at physiological pH; these authors credit remarkable unusually high basicity to the binding of an axial thiolate ligand. In a later study, Green concluded that the ferryl forms of P540$_{\text{BM3}}$ and P450$_{\text{cam}}$ were protonated at

physiological pH using a combination of Mössbauer spectroscopy and density functional calculations [46]. Where iron-heme complexes such as Horseradish peroxidase C (and its associated Compounds I and II) are poorly oxidizing (approximately 1.08 V at pH = 6.5) [47], these enzymes are among a small set of enzymes capable of cleaving strong C–H bonds [48]. The bond strengths of these species are thought to be a direct function of the oxo basicity; where the thiolate decreases the oxidation potential of the iron center, it concomitantly increases the basicity of the oxo such that the O–H bond strength is strong despite a lack of oxidative driving force. Moreover, the axial ligation of the metal oxo in iron heme proteins has been demonstrated to have a profound effect on the pK_a of the Fe^{IV} oxo form of the enzyme [49] as well as the Fe–O bond strength observed in model systems [50].

More broadly, discrete metal-oxo complexes have garnered intense interest because of their stability, tunability, and utility as model systems for the study of metalloproteins. In 1978, Meyer disclosed the ruthenium-oxo species **1**, and demonstrated its acid-dependent redox transformations to form **2** and **3** (Fig. 6) [51]. Where **3** has a pK_a of 10.8 in aqueous 0.33 M $NaSO_4$, a sharp decrease in pK_a to 0.85 in 1 M $HClO_4/LiClO_4$ solution is observed upon one-electron oxidation to $[Ru^{III}OH_2]^{3+}$. Above pH = 2, the corresponding potentials between Ru^{IV}/Ru^{III} and Ru^{III}/Ru^{II} are observed to change by 59 mV per pH unit, indicative of a one-proton one-electron process. Based on thermochemical values furnished by Meyer, Mayer estimated that the bond strengths for the O–H bonds in **3** and **2** are approximately 82 and 85 kcal mol^{-1} respectively [29, 52, 53]. Accordingly, concerted PCET between **1** and **3** to form two equivalents of **2** has been documented [54]. Comproportion-ation of these species is demonstrated to be first order in both **1** and **3**, and the associated barriers associated with initial proton or electron transfer are demonstrated to be too high to correspond to the experimentally measured activation barrier, consistent with a concerted process. In addition, the redox step is demonstrated to have a solvent KIE of 16.1, a clear indicator that O–H bond cleavage of water is involved in the rate-determining step. While also documented to participate in stoichiometric oxygen-atom transfer to triphenyl phosphine [55] and dimethyl sulfide [56], **1** and **2** have been demonstrated to oxidize hydroquinone through both concerted and stepwise PCET mechanisms depending on the nature of the aqueous environment [39]. Evidence for proton movement concomitant to the redox step is supported by H_2O/D_2O KIEs for these reactions, which are 28.7 and
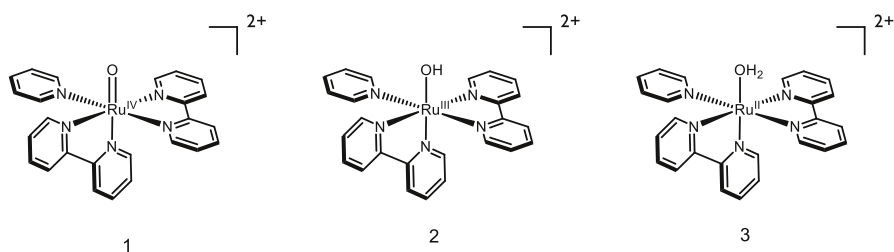
Fig. 6 Ruthenium species reported by Meyer [51]

9.3 for abstraction by **1** and **2**, respectively, with the difference in magnitude attributed to differences in both the hybridization of oxygen and the hydrogen bond distances [5]. These complexes may also cleave the O–H bonds of hydrogen peroxide by PCET [57, 58] (reclassified from HAT [5]) with similarly large solvent KIEs. In one example, in which aniline is proposed to be oxidized to phenyl nitrene or its associated nitrenium ion, complex **1** is demonstrated to accept one proton and two electrons in a single elementary step [59]. Under the disclosed conditions this intermediate is captured either by water to form the corresponding hydroxylamine or by another equivalent of aniline to form the corresponding hydrazine, both of which undergo further (non-PCET) oxidations. Evidence for nitrene (or nitrenium) involvement is provided by a significant $ArNH_2/ArND_2$ KIE of 15.5 for aniline and 10.2 for p-toluidine, no direct oxo transfer of the metal oxo as determined by ^{18}O isotopic labeling, sensitivity of the product distribution between hydroxylamine and hydrazine products (but not the rate law) on the concentration of water, initial formation of **3** rather than **2** in these oxidations, and a negative correlation on the rate of aniline oxidation against the Hammett parameter σ^+.

Manganese-oxo complexes have also been designed for PCET and HAT reactions, and have been studied extensively in the context of the special role of manganese oxo clusters in the oxygen-evolving complex of photosystem II [60–63]. Borovik has disclosed a compound with the backbone structure **4**, which features an unusual non-bridging terminal hydroxo ligand, and has measured its pK_a and redox properties (Fig. 7) [64–66]. In a preliminary study of **4** and its isomers, the Mn^{IV} oxo was observed to abstract the hydrogen atom from TEMPO–H, cyclohexadiene, dihydroanthracene, 1,2-diphenyl hydrazine, and 2,4,6-tri-*tert*-butyl phenol. However, the oxo was incapable of abstracting a hydrogen atom from triphenylmethane, diphenyl methane, ethyl benzene, or 2,3-dimethyl-2-butene. Further study indicated the BDFE to be 89 kcal mol^{-1} [67], which is in agreement to the O–H BDFE of non-heme manganese terminal oxo complex prepared by Stack [68, 69]. The bond strength in the Mn^{IV} oxo form is driven by the high basicity of the oxygen, which is akin to that of methoxide (methanol $pK_a \sim 29.0$ in DMSO [70]). Investigation of C–H abstraction from dihydroanthracene (DHA) using the Mn^{III} and Mn^{IV} oxo forms of the complex revealed two competing mechanisms based on the oxidation state of the metal [67]. Citing a large entropic barrier ($\Delta S^{\ddagger} = -49$ kcal mol^{-1}) and
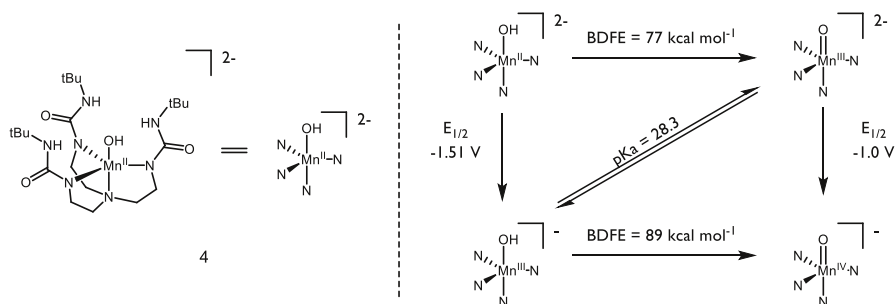
Fig. 7 Borovik's manganese complexes for HAT reactions. All potentials are measured in DMSO and referenced to the Fc/Fc$^+$ couple [64–66]

a primary KIE of 6.8, the Mn^{IV} oxo is suspected to abstract the C–H bond by a PCET event. Initial proton or electron transfer is indicated to be highly unfavorable. On the other hand, the Mn^{III} oxo boasts a much smaller entropic barrier ($\Delta S^{\ddagger} = -15$ kcal mol^{-1}) and primary KIE (2.6). The cited pK_a of 28 matches well with that of DHA (30 in DMSO [71]), suggesting a stepwise PT-ET mechanism for HAT. Together, these divergent mechanisms demonstrate the sensitivity of PCET on the thermodynamics of the oxo species in question. Recent work by Borovik on analogous complexes has demonstrated that oxidation of the [Mn^{III} hydroxo]$^-$ species to the neutral Mn^{IV} hydroxo further increases the BDFE to 95 kcal mol^{-1} [72]. In the presence of an external reductant such as diphenyl hydrazine or hydrazine, Borovik has reported the catalytic reduction of oxygen to water using a slightly modified version of **4** [73]. Study of **4** highlights key thermodynamic contributors to overall bond strength and the sensitivity of the mechanism of net HAT on such parameters and is exemplary of metal oxos of this class.

Binuclear manganese complexes featuring bridging oxo ligands are also capable of engaging in PCET/HAT reactivity (Fig. 8). Complex **5** has been extensively studied by Pecoraro, who has reported a pK_a of 13.4 (MeCN), the protonated redox potential of 0.42 V v. NHE, and a BDFE of 77 kcal mol^{-1} for the D(O–H) bond of the corresponding hydroxo-bridged species [74, 75]. PCET in this case is accompanied by conversion of one bridging oxo to a hydroxo and reduction of one of the Mn centers to Mn^{III}. The value provided is consistent with the observation that 2,4,6-tri-*tert*-butyl phenol (OH BDFE = 82 kcal mol^{-1}) undergoes PCET with this complex, but not phenol (O–H BDFE = 88 kcal mol^{-1}). The pK_a of the oxo bridges in **5** are sensitive to the oxidation state of the manganese sites and have been predicted to drop approximately 10.5 pK_a units upon oxidation of a Mn center [76]. When a modified salpn ligand, which creates a bridging oxo species by virtue of a tethered alkoxide, is used to form binuclear manganese complex **6**, the

$[Mn^{IV}(salpn)(\mu-O)]_2$

5
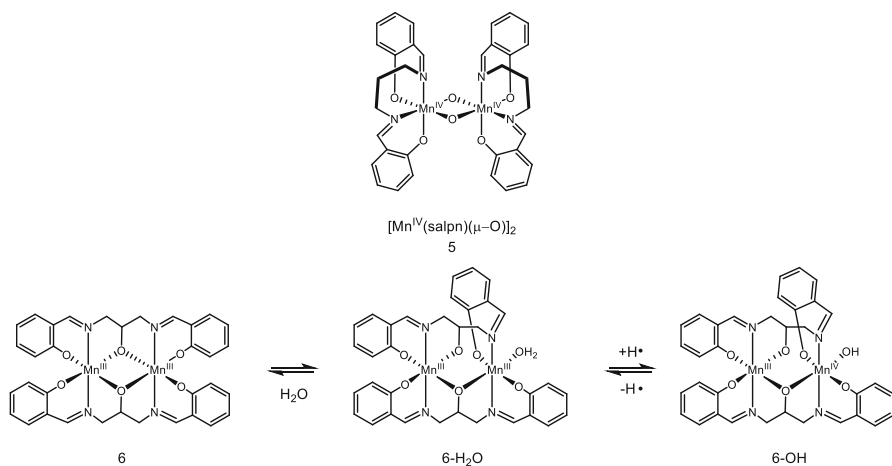
**Fig. 8** Complexes with bridging oxo ligands known to engage in HAT reactivity [74, 75]

molecule is known to reversibly bind water and engage in HAT reactivity [77]. The strength of the O–H bond in **6-H$_2$O** is measured to be 85 kcal mol^{-1}; upon initial oxidation (0.54 V in 16 M H$_2$O/MeCN vs. NHE), the bond strength is increased to 89 kcal mol^{-1}. These bond strengths are noticeably stronger than those of bridging hydroxo ligands, demonstrating the sensitivity of the O–H bond strength on both the binding mode of water (i.e., bridging or terminal) as well as the ligand framework on the metal center.

Mayer identified that species **7** was capable of oxidizing toluene by an initial hydride abstraction, with concomitant proton transfer to the oxo and *two* electron transfers to the manganese centers (Fig. 9) [78]. Based on the thermochemistry of interconversion between isomers, it is evident that **7** lacks the oxidizing power (0.95 V in MeCN v. Fc/Fc$^+$) to oxidize toluene (2.08 V in MeCN v. Fc/Fc$^+$) and initial electron transfer is too endergonic to proceed, eliminating mechanisms, which rely on an initial ET event. Upon two-electron reduction of **7** to the Mn^{III} dimer, the pK_a of the bridging oxo is $\sim$15 in MeCN, which also suggests **7** is not nearly basic enough to deprotonate toluene. The authors observe that nitrotoluene is unreactive with **7** under their conditions and notice that diphenymethane reacts 100 times faster than toluene; taken together, they cite these data as strong evidence for a highly electron deficient transition state and accordingly argue against an initial HAT event. The measured hydride affinity of the complex is provided to be 122 kcal mol^{-1} by the authors. The mechanism of activation by these complexes is highly substrate-dependent and may proceed by initial HAT, electron transfer, or hydride transfer [79]. On the other hand, prior reduction of this species to the Mn^{IV}-Mn^{III} allows for HAT reactivity: (phen)$_2$Mn(μ-O)$_2$Mn(phen)$_2$]$^{3+}$ may undergo two HAT events to form the bridged hydroxo species (phen)$_2$Mn(μ-OH)$_2$Mn(phen)$_2$]$^{3+}$. Based on thermochemical data, addition of the first hydrogen atom to the bis-oxo species has an O–H BDFE of 79 kcal mol^{-1}, where addition of the second hydrogen atom to form the bis-hydroxo species has an O–H BDFE of 75 kcal mol^{-1} [80]. While these complexes are thought to engage substrates such as dihydroanthracene by HAT, a Pourbaix diagram of the (bpy) variant **8** demonstrates a pH-dependent potential corresponding to a one-proton, one-electron transfer event [81]. Under the proper circumstances, it is possible **8** may be able to react by a PCET mechanism.

Moving to further-bridged species, Dismukes has reported the synthesis and kinetics of PCET for "cubane" type species **9** and **10** (Fig. 10) [82]. **9** is thought to feature two Mn^{III} and two Mn^{IV} sites, and **10** to have one Mn^{III} and three Mn^{IV} sites. Movement between these oxidation states comes with reactive consequence: **9** is thought to undergo PCET with pzH **11** to form the pz radical, where **10** is observed to undergo hydride transfer with **11** (net one proton two electron PCET) to form the pz cation [83]. The original assessment of the hydroxo species was based on the capacity for **9** to engage *para*-cyanophenol in PCET, giving a lower limit of the O–H BDFE as $\sim$94 kcal mol^{-1}; inclusion of the potential necessary to move from **9** to **10** furnishes an approximate hydride affinity of $\sim$127 kcal mol^{-1} [84]. Important to note is that **9** does not engage the anion pz$^-$ in redox activity, strongly implying that electron transfer between these complexes must be accompanied by proton transfer. In addition, the pKa of protonated **9** (pK_a < 3) is not basic enough to

deprotonate pzH (pK_a = 22) [85]. The bond strength of **9** is among the strongest reported for a bridging oxo species.

Iron-oxo species are also documented to undergo HAT and PCET reactions (Fig. 11). In particular, complex **12**, reported by Que, Nam, and Münck in 2004, has garnered a great deal of attention for its reactivity, as it is capable of abstracting the C–H bond from cyclohexane (BDE = 99 kcal mol^{-1}) at room temperature [86]. While no mechanism is posed in the initial disclosure, the authors note a large KIE for abstraction from ethyl benzene (k_H/k_D = 30) at ambient temperature that parallels those observed for other systems known to engage in hydrogen atom abstraction [87, 88]. Moreover, a correlation between the hydrocarbon BDE and the rate of the reaction strongly indicates an initial C–H abstraction event [89, 90]. Fukuzumi and Nam further studied this complex for its capacity to undergo both HAT as well as acid-assisted PCET [91]. The rate constant for oxidation of hexamethylbenzene was found to be three orders of magnitude higher in the presence of HClO$_4$ (57 M^{-1} s^{-1}) than without (5.1 × 10^{-2} M^{-1} s^{-1}); the authors posit a change in mechanism from HAT to a stepwise PCET event in which the protonated iron-oxo first oxidizes hexamethylbenzene followed by deprotonation. Protonation of the oxo is found to shift the potential of **12** by 0.92 V [92]. Complex **13**, prepared from a two-electron oxidation of the Fe(III) analogue and reported in

[(phen)$_2$Mn^{IV}(μ–O)$_2$Mn^{IV}(phen)$_2$]
7

[(bpy)$_2$Mn^{IV}(μ–O)$_2$Mn^{IV}(bpy)$_2$]
8
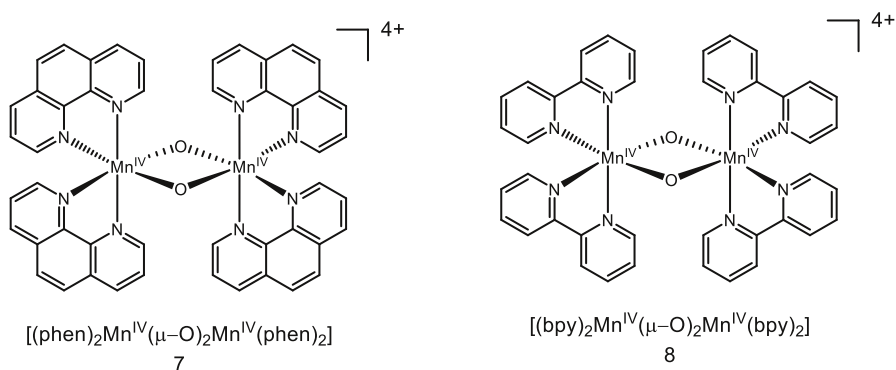
Fig. 9 Bridging manganese oxo species with phen and bpy ligands

9

10

11
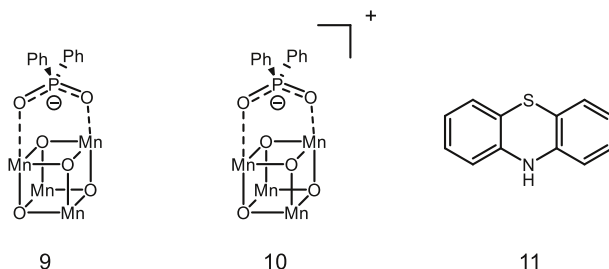
Fig. 10 Cubane complexes **9** and **10** introduced by Dismukes, as well as phenothiazine (pzH) **11**. Note that each face is thought to bind one molecule of phosphate: these are omitted for structural clarity
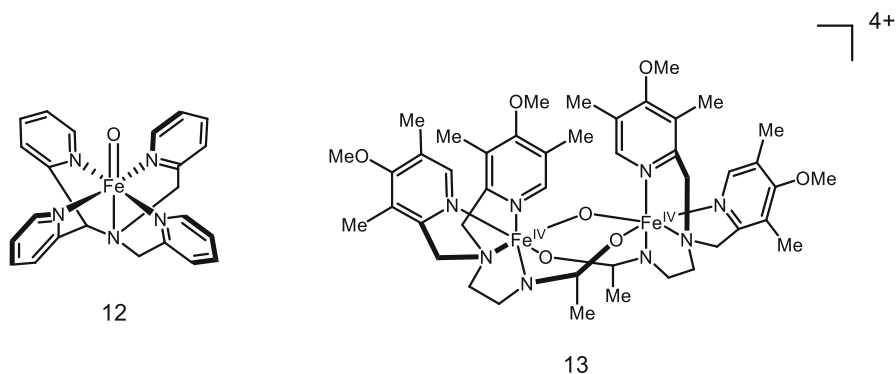
**Fig. 11** Various non-heme iron oxo complexes for C–H abstraction

2009 by Que and Münck, has also demonstrated a remarkable affinity for hydrogen atoms [93]. The first oxidation potential of this complex is provided as 1.50 V v. Fc/Fc$^+$ in MeCN and is thereby strongly oxidizing. In comparison to **12**, which has a potential of 0.9 v. Fc/Fc$^+$ in MeCN [94], **13** abstracts the hydrogen atom from cyclohexane 10^2–10^3 times more rapidly.

The authors noticed no C–H/C–D isotope effect for the reaction of **13** with methanol and *tert*-butanol, but saw a KIE ($k_H/k_D = 1.4$) for the O–H/O–D bond, suggesting that the stronger O–H bond is activated preferentially over the weaker C–H bonds (Fig. 12). In addition, the authors observed the formation of acetone upon the oxidation of *tert*-butanol. Upon comparison of rate constants (which have been normalized to account for the amount of hydrogens available for abstraction), *tert*-butanol reacts 50 times faster than cyclohexane. The authors propose a proton-coupled electron transfer event is responsible for the observed selectivity; this complex represents a rare case in which O–H bonds may be homolyzed preferentially to C–H bonds. In further study, **13** was shown to oxidize water to the hydroxyl radical by PCET [95]. Under pseudo-first-order conditions, conversion of **13** to its one-electron reduced state was found to have a second-order dependence on the concentration of water, in stark contrast to the first-order dependence observed for aliphatic hydrocarbons and alcohols. Based on the thermoneutral oxidation of water (2.13 V v. NHE in MeCN under neutral conditions [96]) by **13** (2.14 V v. NHE in MeCN under neutral conditions) and the rate dependence, the authors propose a proton-coupled electron transfer event in which water serves as a base. While the mechanism for O–H bond cleavage of alcohols and water is not well understood in these instances, the capacity to cleave a stronger O–H bond in the presence of much weaker C–H bonds is a tremendous advance in metal-oxo chemistry and represents an exciting avenue for chemoselective substrate activation.

Heme mimics have also been a fruitful area of research for metal-oxo reactivity (Fig. 13). Goldberg has reported the synthesis of metal complexes featuring the corrolazine framework, which serves as a porphyrin-like donor ligand for the study of high valent transition metals [97, 98]. The manganese (**14**) and chromium (**15**) variants of these complexes can be synthesized and even isolated by benchtop
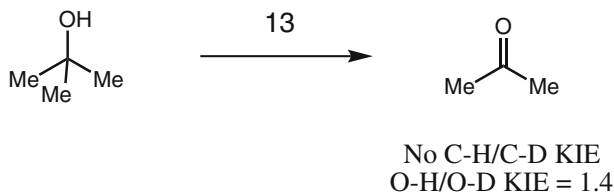
Fig. 12 Products and C–H/D and O–H/D KIEs for oxidation of *tert*-butanol by 13 [93]
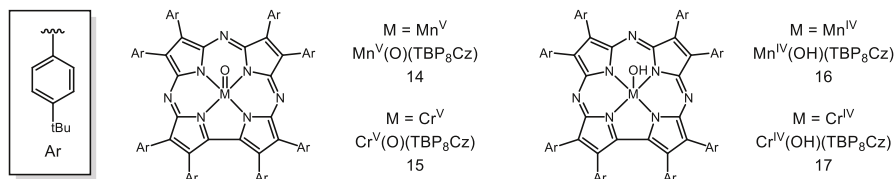
Fig. 13 Porphyrinoids **14** and **15** and their reduced counterparts **16** and **17** [97, 98]

chromatography [99]. Based on the capacity of **14** to abstract the oxygen-bound H atom from 2,4,6-tri–*tert*-butyl phenol but not the methyl-bound H atom from hexamethylbenzene, the $Mn^{IV}O$–H bond in **16** is estimated to be between 80 and 83 kcal mol^{-1}; likewise, the capacity of **15** to abstract from TEMPO–H but not from xanthene places the O–H bond in **17** between 67 and 73 kcal mol^{-1}. In the presence of dimethyl ferrocene ($E_{1/2}$ = –0.24 V v. Fc/Fc$^+$ in MeCN) and acetic acid (pK_a = 23.5 in MeCN), which together have an effective BDFE of 82 (cf. Fig. 3, [29]), **14** may be converted to **16** in a multisite PCET process. In the absence of either reductant or acid, no **16** is observed, demonstrating the necessity of both components to forge the O–H bond and the accuracy of the bracketed BDFE. The pK_a of **16** is estimated to be approximately 22, which is thought to contribute most of the energy to the effective O–H BDFE of **16** given the low potential of the Mn^{IV}/Mn^V couple (–0.05 V v. SCE) [100, 101]. Moreover, the basicity of **14** is largely credited for the discrepancy between the O–H bond strengths of **16** and **17** given the small difference in M^V/M^{IV} potential of Mn and Cr (ΔE = –100 mV, where chromium features a more positive potential; ca. 2.3 kcal mol^{-1} difference).

The HAT and PCET capabilities of **14** have been extensively studied. Work by Fukuzumi and Goldberg has demonstrated that **14** will engage acridinium species in hydride transfer and two-electron reduction by ferrocene derivatives in the presence of proton donors [102]. The strength of the added proton donor correlated to the rate of reduction, suggesting a proton-coupled mechanism for the formal reduction of **14**. Hydride transfer is not thought to be concerted, instead proceeding first by an initial PCET event to transfer an H-atom followed by electron transfer. The addition of anionic ligands to bind the unoccupied axial site of **14** was found to have a profound impact on the rate of HAT [103]. Compared to the rate of HAT from 9,10-dihydroanthracene to **14** in the absence of external anion donors, addition of F$^-$ and CN$^-$ were found to increase the reaction rate by factors of 2100 and 16,000 respectively. DFT calculations of the bond strengths of these complexes suggest that
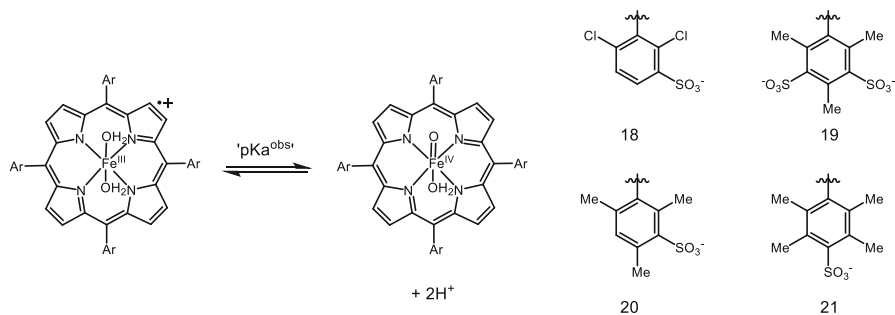
Fig. 14 Iron-porphyrin complexes synthesized by Groves [105]

the basicity of the oxo species is principally responsible for the large increase in the O–H BDFE. In the presence of light, oxygen, and acid, hexamethylbenzene may be oxidized to the corresponding alcohol (18 turnovers) and aldehyde (9 turnovers) respectively, demonstrating the potential for catalytic HAT using these scaffolds [104].

Non-heme porphyrin complexes such as **18–21** have also been synthesized by Groves (Fig. 14) [105]. Unique about these systems is the existence of a proton-coupled hydrogen atom transfer equilibrium, which may be thought of as a formal two-proton, one-electron transfer step. Because HAT in this instance is proton-coupled, the authors define a metric for the bond dissociation energy, $D(OH_2)$ which accounts for both hydrogen-atom abstraction as well as protonation of the oxo-species that can be described using the following, modified Bordwell equation [106]:

$$D(OH_2) = 23.06E'_{por} + 1.37\left[2\left(pK_A^{obs}\right)\right] - 1.37pH + 57$$

For **19**, the pK_a^{obs} is found to be 5.5, and the potential $E' = 1.06$ v. NHE, furnishing a final $D(OH_2)$ of 90–93 kcal mol^{-1}. When HAT is not coupled with proton transfer, the conventional O–H BDFE is calculated to be 87 kcal mol^{-1} using the canonical Bordwell equation; this species accordingly has a $pK_a \sim 7$. Where prior examples cite the basicity of the oxo as a direct contributor to the O–H BDFE, complexes **18–21** present a unique situation in which a second, concomitant protonation increases the driving force for hydrogen atom abstraction from a given substrate. Accordingly, C–H abstraction from xanthene demonstrates KIEs not only for the C–H/D bonds in xanthene ($k_{H/D} = 1.80$), but also for the solvent D_2O/H_2O ($k_{H/D} = 2.2$), demonstrating the reliance on HAT and proton-transfer in the rate-determining step. While unconventional (or underappreciated) for metal-oxo species, two-proton one-electron transfer events have been previously documented in optical excitation of hydrogen bonded dyes by Meyer [107] and are predicted to play a role in proton transport by Chen and Liu [108]. In addition, many analogous manganese oxo porphyrins have recently been documented by Groves to catalyze aliphatic C–H fluorination [109], azidation [110], and chlorination [111], as well as pH-dependent conversion of chlorite to chlorine dioxide [112, 113].

Metal oxos are among the most dynamic, well-studied examples of PCET and continue to attract the attention of the community at large. The oxo basicity and oxidative power of the metal contribute significantly to the BDFEs involved in PCET processes, which is further influenced by the coordination geometry of the oxo as well as the ancillary ligation on the metal center. The development of catalytic protocols utilizing such species bears much promise for synthetic chemists for mild substrate modification.

4 Phenols

Phenols are perhaps the organic functional group whose PCET reactivity has been explored most extensively. The redox activity of the phenolic amino acid tyrosine is known to play an important role in many biological redox processes. As noted by Svistunenko [114], some of the earliest examples of tyrosyl radicals documented in proteins include the bacteriophage T4-induced ribonucleotide reductase by Sjöberg in 1982 [115], Photosystem II by Babcock and Barry in 1988 [116], and prostaglandin endoperoxide synthase-2 by Hoganson and Babcock in 1994 [117]. Since these seminal discoveries, the role of tyrosyl radicals in proteins has been subject to intense study, both in clarifying their role in catalysis as well as documenting further examples.

The first evidence for concerted PCET activation of phenols in non-enzymatic systems was provided by Linschitz, studying the quenching kinetics of C_{60} and tetracene fluorescence by hydroquinone in the presence of variously substituted pyridines [118]. The authors identified strong correlations between the rate of quenching and the pK_a of the corresponding pyridinium species, with higher pK_a's trending with an increased rate of reaction. In addition, voltammetric studies of solutions containing both phenol and pyridine exhibited a new and irreversible anodic wave occurring at more positive potentials than for the phenol alone, consistent with a PCET process. In further studies, the relevant intermediates (i.e., the C_{60} radical anion, the phenoxyl radical, and the pyridinium salt) of the PCET step in benzonitrile (PhCN) were observed by flash photolysis with 4-hydroxyanisole in the presence of 7,8-benzoquinoline [119] and 1-naphthol in the presence of collidine [120].

These observations have sparked significant mechanistic interest in the underpinnings of PCET in phenol O–H homolysis, with particular emphasis placed on the role of hydrogen-bonding. Several model systems containing intramolecular hydrogen bonds have been developed (Fig. 15). Matsumura and colleagues synthesized compounds 22–25, of which 22 demonstrates a reversible oxidation potential ($E_{1/2} = 757$ mV v. Ag/AgCl reference) and a UV–Vis spectra characteristic of phenoxyl radicals [121]. Compounds 23 and 24 show partially reversible CV traces and have similar potentials, whereas 25 demonstrates an irreversible redox couple. The persistence of the phenoxyl derived from 22 is attributed to stabilization of the radical by an intramolecular hydrogen bond. Savéant has attributed partial reversibility of the CV traces of closely related compounds to instability at low scan rates, as the current response for voltammograms with scan rates of 5 V/s were
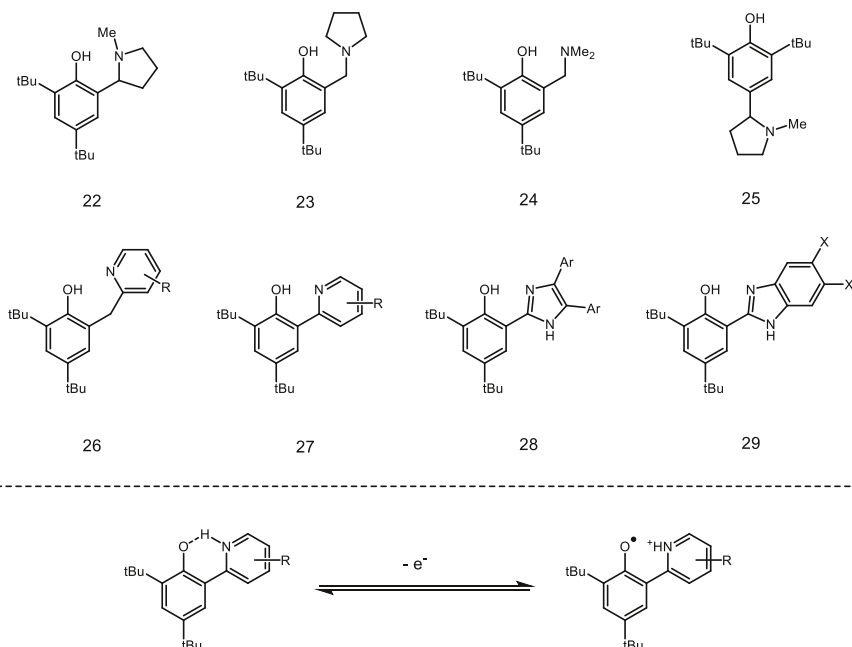
Fig. 15 Phenol model systems capable of intramolecular hydrogen boding synthesized by Matsumura (**22–25**) and Mayer (**26–29**) as model systems for the study of PCET in biological contexts. Variation of the amine donor allows for deep interrogation of hydrogen bonding on PCET processes

found to be completely reversible [122]. In certain circumstances, phenoxyl radicals are *preferentially* stabilized by hydrogen bonding relative to the parent phenol, resulting in decreased O–H BDFEs and longer radical lifetimes [123]. In these instances, the phenoxyl radical may serve to increase the acidity of additional O–H or N–H bonds present in the molecule or serve as direct hydrogen-bond acceptors.

Along with measures of stability, Mayer has examined correlations between the rates of phenol PCET and various intramolecular hydrogen bonding parameters with pyridyl and imidazoyl bases of type **26–29** [124, 125]. In pyridyl-substituted compounds such as **26** and **27**, the rate constant for PCET is found to vary linearly with the thermodynamic driving force (ΔG_{PCET}). Important to note, however, is that the rate of oxidation of various analogues of **26** can be impacted by changing the driving force as a function of pyridyl substitution *or* the identity of the oxidant, which implies a constant intrinsic reaction barrier λ. In addition, variation of the pyridyl substitution has a minimal impact on the rate of PCET. However, when the pyridine base is conjugated with the phenol (as in **27**) both ΔG_{PCET} and λ vary as a function of pyridyl substitution, with electron-withdrawing R-groups demonstrating slower rates relative to electron-donating groups. It is worth noting the pK_a's of the corresponding pyridinums associated with scaffolds **26** and **27** show a positive correlation with the –OH ^{1}H NMR resonance and a negative correlation with the both the O–N bond distance and the potential of the substrate. For the oxidations of imidazole-type systems **28** and **29**, a similar rate dependence on ΔG_{PCET} was also
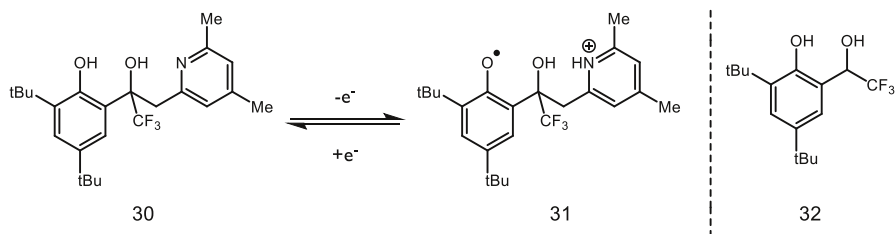
Fig. 16 A mechanistic example of a hydrogen-bond relay, capable of transferring a proton to the pyridyl nitrogen while simultaneously removing a proton from the phenoxyl oxygen

observed. Moving from electron-rich to electron-poor substituents on the aryl or –X groups was found to have a monotonic effect on the driving force and consequentially little impact on the overall rate of PCET. As the identity of the base is changed—from imidazoles, pyridines, aliphatic amine bases, or other motifs—the rate of PCET is dependent on not only the driving force, but also λ as well as the associated probabilities for tunneling [126, 127].

Hydrogen bonding to phenols may also serve as template for long-range proton transfer (Fig. 16), providing a mechanism for proton transport across relatively large distances. Savéant has prepared polyol **30**, which upon electrochemical oxidation converts to **31** in a single elementary step with a reversible potential [128]. The stability of **31** is such, in fact, that upon bulk electrolysis the authors can observe it by UV–Vis spectroscopy and cite a change in the pyridine bands of the IR spectra of **30** as evidence for proton transfer from the phenol to the pyridyl species. Alternatively, for the substrate lacking the pyridine terminus (**32**) voltammetric experiments demonstrated that the oxidation is irreversible. These experiments elucidate not only the role for hydrogen bonding in proton transfer, but also corroborate work by Thomas demonstrating increased stability of hydrogen-bound phenoxyl radicals [129]. Proton movement in PCET processes is limited to short (i.e., hydrogen-bonding contact) distances [130]; however, hydrogen-bonding networks are frequently used as "proton wires" [131] to accomplish long-range proton transfer and are well documented in GFP [132], ferredoxin I of *Azotobacter vinelandii* [133], cytochrome *c* oxidase [134], and numerous other proteins [135]. In a notable example, a hydrogen-bonding network between Tyr122 and Cys439 in ribonucleotide reductase (RNR) allows for a net proton transfer over >30 Å [136]. Over longer distances this process may be stepwise, but in carbonic anhydrase PT is calculated to be concerted over a distance as long as 8 Å [137]. Hammarström demonstrated that the presence of an internal hydrogen accelerates concerted PCET relative to reactions with the same driving force without an internal hydrogen bond [138]; it has also been suggested that hydrogen bonding intrinsically lowers the reorganization energy by virtue of weakening the O–H force constant [139, 140].

Along with the distances associated with proton transfer, the distance-dependence of electron transfer on PCET reactions of phenols has also been of considerable interest. To study the effect of distance on the rates of phenol oxidation, Wenger and coworkers synthesized a series of heteroleptic ruthenium polypyridine complexes where the distance from the metal to the distal phenol was varied as a function of the

| n	R_{DA} (Å)	k_{CPET} [s^{-1}]
1	12.2	1.07×10^9
2	16.5	3.35×10^8
3	20.8	3.41×10^6
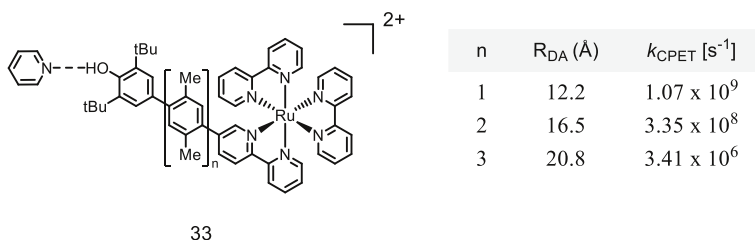
33

Fig. 17 Wenger's model polypyridyl system with spacers, Ru–O distances, and corresponding rates of concerted PCET [141]

number of xylene spacers incorporated into the bpy ligand (Fig. 17) [141]. While the electron transfer rates decrease with increasing distance, long range electron transfer with an exogenous pyridine base still proceeds with rate constants greater than 10^6 s^{-1} when the donor–acceptor difference is ~ 20 Å. Long-range electron transfers from phenols involved in enzymatic PCET processes have been documented for photosystem II (ca. ~ 10 Å) [10], the R1 subunit of RNR (~ 7 Å) [11], and prostaglandin-H synthase-2 (~ 7 Å) [142] among others [143].

In biological settings, spatial separation between redox-active sites may be a consequence of mitigating back electron transfer when excited states are involved. In a particularly dramatic example from Photosystem II, electron transfer between a Tyr$_Z$/His190 pair (Y_z) and P680$^+$ proceeds with a forward rate constant $\sim 10^7$ s^{-1}, with back-electron transfer between P680$^+$ and Q$_A^{\bullet-}$ proceeding at $\sim 10^3$ s^{-1} [144]. In the forward reaction, Meyer has noted that the necessity of His190 in water oxidation [145–147] provides strong evidence for the necessity of proton movement in oxidation of Yz [144]. Sluggish back electron transfer can be attributed to the both long distance involved (17–18 Å) as well as the high driving force (-1.4 eV); the thermodynamic favorability causes back electron transfer to occur in the Marcus-inverted region and the distance of electron transfer further slows this charge recombination process.

Similar ruthenium complexes have also been modified in numerous ways to study phenol oxidation via PCET with respect to factors other than distance (Fig. 18) [148]. Upon irradiation with visible light, these complexes become stronger oxidants and reductants, concomitant with a MLCT event, wherein a metal-centered electron is transferred into a ligand-based antibonding orbital [149], further increasing the driving force (and thereby the rate) of PCET. Reductive quenching of the excited states of [Ru(bpy)$_2$(bpz)]$^{2+}$ **34** [150] and [Ru(bpz)$_3$]$^{2+}$ **35** [151] by phenols has been identified by Meyer and Wenger, with the unbound nitrogen on the bpz ligand serving as the basic site for the reaction. Using **35** as the oxidant, the effect of electron rich and electron poor substituents on the phenol component was thoroughly examined: Wenger calculated the ligand-phenol association constant (K_A) for a number of *para*-substituted phenols ranging from 1478 M^{-1} (R = OMe) to 5 M^{-1} (R = CN). While the rate constants for PCET of the protiated phenols do not appreciably differ (R = OMe 1.87×10^6 s^{-1} and R = CN $1.73 * 10^6$ s^{-1}) as a function of substituent, virtually no KIE was observed for R = OMe ($k_H/k_D = 1.03$) while a significant KIE was observed for R = CN ($k_H/k_D = 10.18$). In addition, the
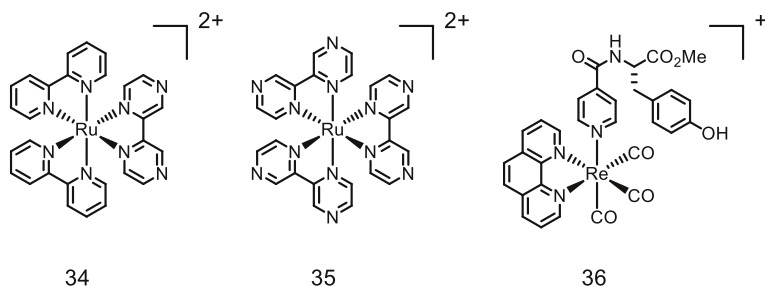
Fig. 18 Various Ruthenium complexes used to induce oxidative PCET, as well as a Rhenium complex featuring an unconjugated phenol ligand, which readily forms the phenoxyl in the presence of base [148]

driving force of each PCET event differs by merely 0.07 eV. On the basis of KIEs the authors suggest an ET-PT event for R = OMe and a concerted PCET event for R = CN, demonstrating how subtle differences in substrate-complex association may have a dramatic effect on the mechanism of charge transfer. In another related example, the rhenium-complex **36** synthesized by Nocera, featuring a tyrosine-like ligand directly appended to the metal center, is documented to form the phenoxyl radical in the presence of exogenous pyridine or imidazole with rate constants of 4.1 $\times$ 10^5 s^{-1} and 4.8 $\times$ 10^6 s^{-1} for pyridine and imidazole, respectively [152]. The equilibrium constant for hydrogen bonding was measured as 16 and 157 M^{-1} for pyridine and imidazole respectively, suggesting that hydrogen bonding is still crucial for the proton-transfer event in these systems. The role of hydrogen bonding on the rate of PCET, as exemplified by these two case studies, is complicated and highly variable pending choice of hydrogen bond partner.
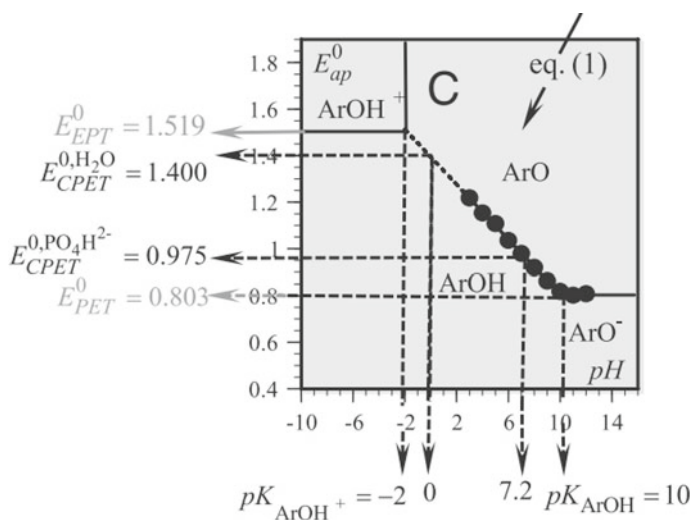
Fig. 19 A Pourbaix diagram for phenol oxidation in water with concentration regimes for favored concerted proton-coupled electron transfer (CPET), proton-first stepwise PCET (PET), or electron-first stepwise PCET (EPT). Figure reprinted with permission from Proc Nat Acad Sci [153]

Springer

In addition to kinetic and spectroscopic methods, electrochemical methods have also proven useful in examination of phenol PCET given the precise control over pH and applied potential. Such techniques can provide not only kinetic data, but also useful thermodynamic data as demonstrated by the Pourbaix diagram for phenol generated by Savéant (Fig. 19) [153]. The slope of the Pourbaix diagram demonstrates the PCET event to form the phenoxyl radical in the concerted PCET regime is a one-proton one-electron event; where Pourbaix diagrams alone do not shed light on the concerted nature of the oxidation process, the authors were able to fit the experimental data to detailed kinetic models and demonstrate the concerted PCET is the most rapid and thereby predominant mechanism of phenol oxidation. The authors also needed to employ low concentrations of phenols and high scan rates to mitigate deleterious phenoxyl dimerization. Unbuffered water proved necessary to observe dominant concerted PCET: in the presence of phosphate buffer, i.e., HPO_4^{2-}, the reaction is driven to a predominant stepwise, proton-first PCET event. Otherwise, water serves as a proton acceptor in a concerted PCET process. Direct rate constants (uncorrected from double layer effects) for concerted PCET were derived as 25 ± 5 and 10 ± 2 cm s^{-1} for protiated and deuterated phenol respectively, demonstrating a significant KIE of ~ 2.5.

Electrochemical techniques can provide exquisite information with relatively simple experiments, even for more complex systems. A recent report by Tommos has demonstrated the applicability of such electrochemical analyses to assess the role of PCET (concerted or otherwise) in the model protein $\alpha_3 Y$ using a Pourbaix diagram (Fig. 20) [154, 155]. In this system, the tyrosine residue is positioned inside a protein matrix in a desolvated and well-structured environment. Voltammetric study of its oxidation displays a reversible square-wave and differential pulse voltammogram under basic conditions. The tyrosine residue in question exhibits a potential of 0.910 and 1.070 against NHE at pH 8.5 and 5.5, respectively [156]. Based on expected rate constants for side reactions associated with square-wave voltammetry [157, 158], the authors initially suspected the radical species in question must have a lifetime of at least 30 ms: in collaboration with Hammarström, transient absorption spectroscopy has placed the half-life somewhere between 2 and

Fig. 20 A Pourbaix diagram for reversible oxidation of a tyrosine residue in the $\alpha_3 Y$ protein; the *gray line* is a nonlinear regression featuring a slope of 59 ± 5 mV. Reprinted with permission from figure reprinted with permission from Proc Nat Acad Sci [154]
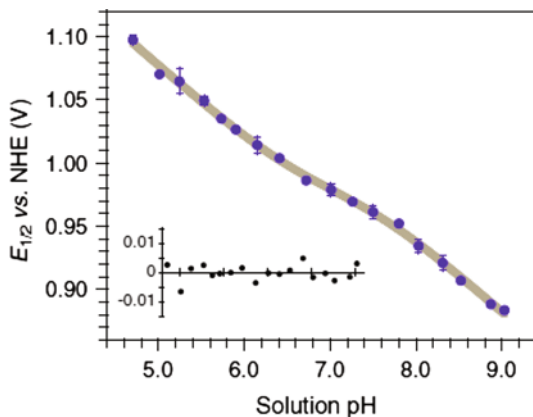
10 s [159]. Decay of this signal was observed to follow second-order kinetics by intramolecular coupling, suggesting dimerization of the protein. Observation of an emission spectrum consistent with dityrosine and the long lifetime are cited as further evidence of this process. Such a model system provides a thermochemical estimate for the properties of tyrosine residues otherwise buried in hydrophobic pockets, with a model system that allows for excellent characterization of this species.

Phenol PCET, more than any other substrate class for these reactions, provides insight into the role of hydrogen bonding. The judicious design of model systems affords examination of thermodynamic, kinetics, and exploration of Marcus-related reorganization energies. The lessons learned from studies of phenols serve an excellent primer on important design motifs for the future design of PCET reactions; in addition, the work provided has provided some evidence to the machinery of life required during enzymatic redox catalysis.

5 Indoles

Indoles, ubiquitous in redox-active proteins, also serve as important biological charge carriers. In many instances, PCET is necessary to facilitate otherwise endergonic ET steps for charge transfer in biological contexts. Of note, however, are the thermodynamics of such processes: indole is 0.25 V easier to oxidize than phenol and features an N–H bond that is ~ 3 kcal mol^{-1} stronger than the phenol O–H bond. Accordingly, Mayer has noted that phenols are far more likely to undergo concerted PCET, whereas indole activation typically proceeds through the radical cation in a stepwise fashion [29]. Documented evidence of concerted PCET activations of the indole N–H bond is relatively scarce. In 2011, Hammarström studied the viability PCET of tryptophan with water as a proton acceptor, tethered to a ruthenium photocatalyst (Fig. 21) [160]. Both **37** and **39** undergo stepwise ETPT below pH = 10; only above pH = 10 do these reactions occur by concerted PCET. Compounds **38** and **40**, however, show a constant pH dependence. These studies have been repeated in bimolecular fashion with free indole and an unbound Ru(bpy)$_3^{2+}$ or Ru(dmb)$_3^{2+}$ oxidant [161]. Even without a molecular tether, which causes the oxidant and indole to travel as a single molecular entity, these reactions are kinetically competent to engage in concerted PCET as well as ET/PT mechanisms. With the weaker oxidant Ru(dmb)$_3^{2+}$, the ethyl ester of tryptophan is demonstrated to undergo concerted PCET regardless of pH: use of the stronger oxidant Ru(bpy)$_3^{2+}$ only results in concerted PCET at pH values greater than 6. Concurrently, Meyer reported that N-acetyl-tryptophan could undergo concerted PCET with hydroxide as a base with Os(bpy)$_3^{3+}$ as the oxidant in water [162]. Hydroxide is uniquely effective in this respect, as the use of other bases (2-amino-2-(hydroxymethyl)propane-1,3-diol, monobasic phosphate, or dibasic phosphate) did not result in concerted PCET. The sensitivity of concerted PCET and ET/PT mechanisms in aqueous conditions—to the oxidant employed, the role of hydroxide, and other contributors—demonstrates the subtle interplay between facile oxidation of the indole moiety and the importance of N–H activation by proton acceptors.
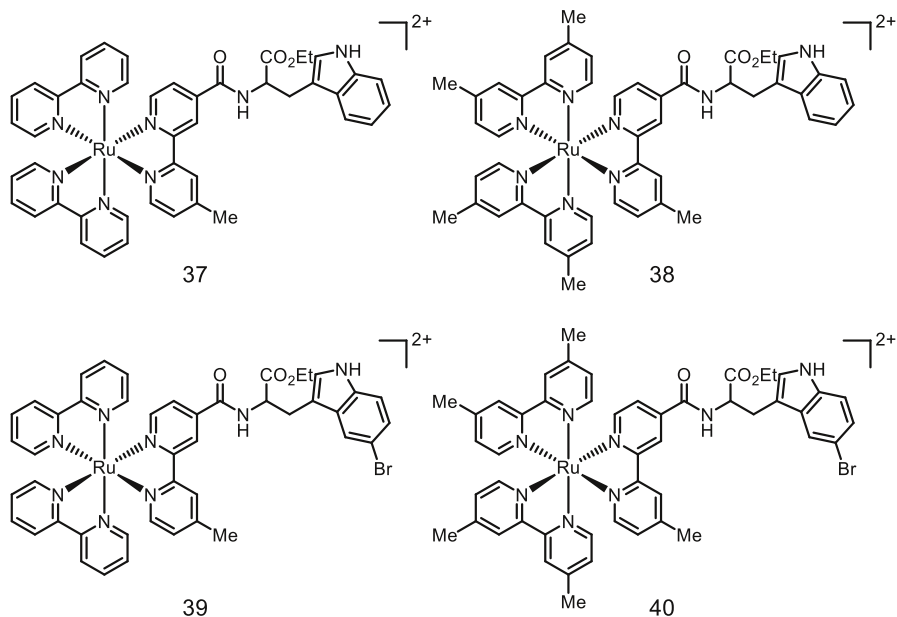
Fig. 21 Ruthenium complexes synthesized by Hammarström for studies of indole PCET [160]

One recently proposed example of concerted PCET in a biological context is the unusual intramolecular aryl–aryl coupling of chromopyrrolic acid **41** (CPA) in route to staurosporine catalyzed by cytochrome P450 StaP (Fig. 22). In an extensive computational study, Shaik and colleagues predicted that an initial PCET event through a hydrogen-bonding triad involving two water molecules and a histidine residue could serve as a proton shuttle from the substrate to the iron-oxo moiety [16]. The necessity of the water-histidine-water triad was analyzed using two changes: using a modified version of **41** where the hydrogen at the 7-position is chlorinated as well as modifying the protein such that the His$_{250}$ residue was mutated into phenylalanine or alanine. In the prior case, substitution of chlorine was
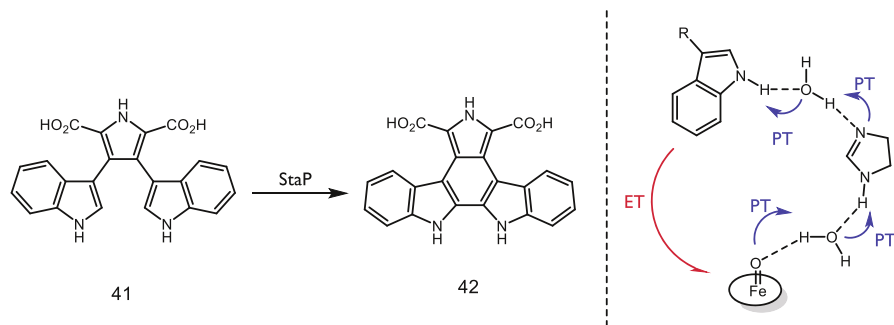
Fig. 22 Oxidation of CPA (**41**) by StaP P450 Cpd1 into a precursor (**42**) to staurosporine with a schematic for the PCET activation step proposed by Shaik [16]

found to expel water from the active site for steric considerations and resulted in significantly decreased activity for the aryl–aryl coupling. In the absence of histidine, enzyme function decreases to 25 % for alanine and 72 % for phenylalanine. A computational analysis attributed this reactivity to a water diad serving as a hydrogen-bonding chain from the indole to the iron-oxo. The substrate is thought to react as the dianion, which is anchored into the active site by a number of short hydrogen bonds to the carboxylate moieties [163]. His250 is conserved across P450 StaP as well as relatives RebP and AtmP, suggesting the importance of PCET in the construction of indolocarbazole cores by these enzymes [164, 165].

The majority of PCET reactions to indoles in biology proceed in a stepwise fashion through the indole radical cation. However, even if a proton cannot transfer (i.e., move from one atom to another) in the same step, movement in the relative position of a proton within a hydrogen-bonding interface is documented to influence the rate of electron transfer in PCET [167–171]. Provided an appropriate hydrogen-bond acceptor is present, the potentials of indoles can be attenuated. Nordlund and Eklund have identified a triad of residues in ribonucleotide reductase (RNR), Trp48, Asp237, and His118 which are highly conserved across various species (Fig. 23) [143, 172, 173]. It is thought this network modulates the potential of the indole moiety, presumably by stabilizing the radical cation through hydrogen bonding [174]. Moreover, His118 in this triad is directly coordinated to the Fe1 center. When a water molecule binds to Fe1, it enables Tyr122 to engage in HAT and abstract a hydrogen atom from said water; Siegbahn has presented computational evidence that suggests this process proceeds in a single step to ultimately form the Trp48 radical cation [136, 175]. The Trp48, Asp237, and His118 catalytic triad may also enable this reactivity. While Trp48 in this instance serves as a hydrogen-bond donor, study of tryptophan-centered radicals in RNR by EPR and ENDOR spectroscopies by Lendzian and Lassmann indicates two neutral tryptophan moieties, one of which (Trp111 [176]) is a hydrogen bond acceptor and posit hydrogen bond donation by nearby E204 [177]. Given the prominence of tryptophan residues thought to engage in electron transfer in RNR and the documentation of

Fig. 23 A highly conserved hydrogen bonding triad Trp48, Asp237, and His118 [166] in Ribonucleotide Reductase (RNR). Adapted with permission from [136]. Copyright 1998 American Chemical Society
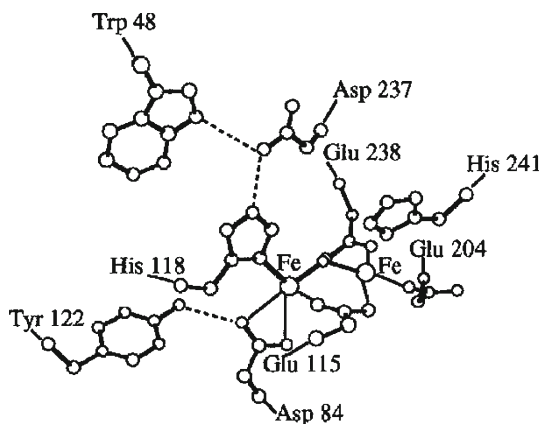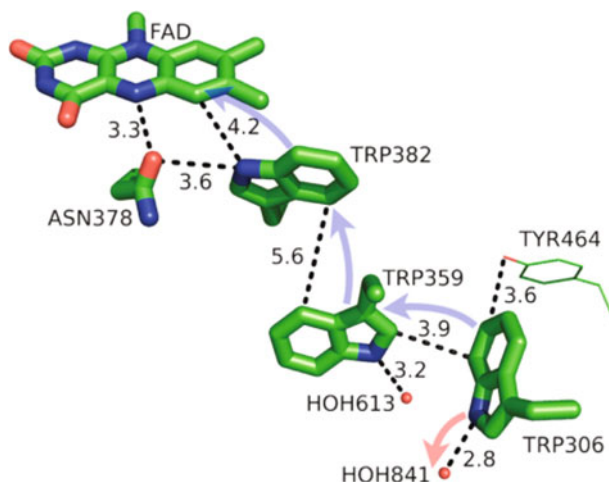
Fig. 24 A model of the PCET pathway from DNA photolyase. Reproduced with permission from [1]. Copyright 2014 American Chemical Society. This article may be accessed online at the following URL: http://pubs.acs.org/doi/pdf/10.1021/cr4006654

long-range PCET in these complexes [11], redox-modulation through the agency of hydrogen bonds provides a plausible mechanism for charge transfer.

Further examples of tryptophan residues involved in charge transfer in proteins come from DNA photolyase and azurin (Fig. 24). In the former, Brettel has demonstrated that FAD initiates oxidation of Trp382, which engages in a hole-hopping oxidation of Trp359 and finally Trp306, which deprotonates to yield the neutral tryptophan radical [1, 178, 179]. For the oxidation of the terminal Trp306 found in *E. coli* photolyase, Schelvis and coworkers have demonstrated the electron transfer proceeds by concerted PCET below pH = 6.5, but otherwise undergoes stepwise PCET via an initial electron transfer [180]. Moreover, charge recombination between FADH• and Trp306 is pH-dependent, slowing down at increased pH [181, 182], presumably in accord with this mechanistic switch. In azurin, tryptophan residues have been demonstrated by Gray and coworkers to greatly accelerate electron transfer by enabling electron "hopping" between amino acid residues [183]. Where tunneling over 19 Å is slow, tryptophan-mediated transfer is more rapid by approximately two orders of magnitude. In tyrosine-depleted mutants of azurin (AzC), two tryptophan-centered radicals have been observed by ultrahigh field EPR [184] attributed to neutral tryptophan radicals Trp108 and Trp48. Based on ^{2}H ENDOR experiments, Stoll and Britt determine that Trp108 is hydrogen bound and Trp48 exists as an unbound radical species. Trp48 is nestled in a hydrophobic pocket of the protein and thought to be important in long-range charge transfer in azurin [185]. In further studies, Trp48 has proven necessary for redox activity in azurin mutants [186] and shows significant fluorescence quenching in the presence of copper [187], further demonstrating the profound effect of protonation state on tryptophan-mediated charge transfer. The properties of indoles and their capacity to engage in both concerted and stepwise PCET afford these species great

flexibility as electron-shuttle residues in redox-active proteins; model systems allow for close examination of the subtleties pertinent to both concerted and stepwise PCET pathways and their consequences.

6 Thiols

Thiols are classical HAT agents in free radical chemistry, and recently their ability to participate in multisite PCET chemistry has also been explored. Meyer has studied the potential for PCET to the cysteine (or *N*-acetyl cysteine) S–H bond using $[Os(bpy)_3]^{3+}$ as a stoichiometric oxidant and various buffer conditions (Fig. 25) [188]. Through kinetic modeling, the authors conclude that (along with other pathways) cysteine can be activated by multisite, concerted PCET in the presence of the appropriate buffers, which include AcO^- and $H_2PO_4^-$. When tested with buffer conditions relevant to biological reactions, the authors conclude this pathway is likely dominant given the relative acidity of the S–H proton as well as the high concentration of buffer. The influence of buffer effects on the oxidation of glutathione by $[IrCl_6]^{2-}$ had been previously documented by Alvarez, who found that the observed rate constant for oxidation trended with an increase in the pK_a of various buffers (including citrate and phosphate) when $pH = pK_a$ [189]. Moreover, the rate of the reaction is also accelerated as a function of the concentration of phosphate buffer at constant pH's of 5.0 or 7.0, suggesting some dependence on the buffer ion itself.

In analogy to phenol oxidations (see discussion above), Wenger has demonstrated that thiophenol may also undergo oxidative PCET upon treatment with photoexcited $[Ru(bpz)_3]^{2+}$ (Fig. 26) [190]. In this case, the substituents on the thiophenol were found to have a profound effect on the mechanism of S–H bond activation. For thiol **43**, no KIE is observed upon luminescence decay of the photocatalyst excited state, suggesting the quenching event is not accompanied by a

Fig. 25 MS-EPT of cysteine by base and $[Os(bpy)_3]^{3+}$ [188]

Ar	Species
2,4,6-Me	43
2,4,6-Cl	44
C_6F_5	45
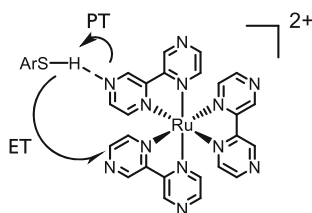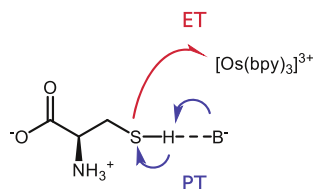
Fig. 26 PCET of thiophenol by $[Ru(bpz)_3]^{2+}$ [190]

significant degree of proton motion. In contrast, **44** and **45** show KIEs of 1.6 and 1.5 respectively, indicating that proton motion is likely involved in excited-state quenching. This trend is consistent with the PhSH/PhSH$^{\bullet+}$ potentials for **43**–**45**: compared to the Ru^{II}/Ru^{I} potential (0.92 V against Fc/Fc$^+$ [151]), **43** has a potential close enough to undergo straight electron transfer (0.95 V against Fc/Fc$^+$), whereas **44** (1.7 V against Fc/Fc$^+$) and **45** (>2.0 V against Fc/Fc$^+$) would require a much stronger oxidant to proceed by stepwise ET/PT. Based on the aqueous pK_a data, the pK_a of protonated [Ru(bpz)$_3$]$^{2+}$ (2.3) is much lower than that of **44** (4.8) and marginally lower than that of **45**; the authors acknowledge these trends may not hold for acetonitrile solution (where the relevant acidities have not been determined) and ultimately conclude the marginal pK_a difference between the catalyst and thiols is not enough to clearly distinguish between PT/ET and concerted PCET.

In synthetic contexts, thiyl radicals are known to engage in a number of useful reactions [191–198], including C–H bond abstraction [197, 199–203]. Recently, MacMillan has demonstrated the capacity of catalytically generated thiyl radicals to cleave the C–H bond of benzylic ethers for radical coupling reactions (Fig. 27) to form diaryl methanols (a) [204] or β-amino ethers (b) [205]. The light source is either a Blue LED or a Compact fluorescent lamp (CFL), as designated above. In both reactions, a wide variety of arene components and ether substitutions are tolerated to furnish a diverse set of products and only a catalytic amount of methyl thioglycolate is necessary to affect the desired C–H HAT event. In the formation of diaryl ethers (Fig. 27a), phosphate serves as the base, whereas the β-amino ether
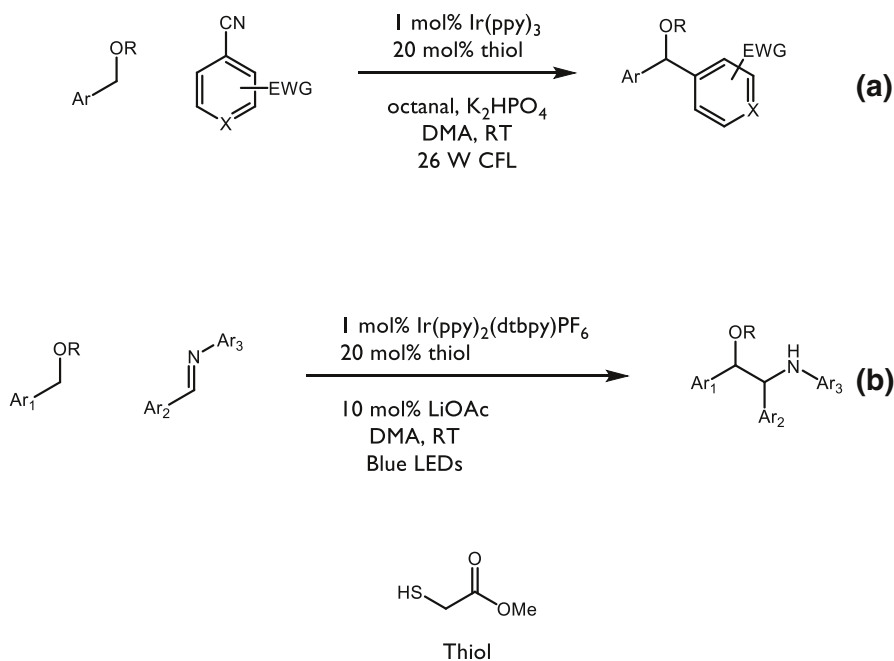
Fig. 27 Recent benzylic C–H activations reported by MacMillan [204, 205]

protocol (Fig. 27b) employs acetate. In the latter case, Stern–Volmer quenching studies were employed to elucidate the nature of thiyl generation. The excited state of the photocatalyst was found to be incapable of oxidizing the catalyst thiol in the absence of base, but inclusion of acetate resulted in quenching of the excited state. While sequential ET/PT may be ruled out based on these results, the similarity in pK_a's between methyl thioglycolate (13 in DMSO [206]) and acetate (acetic acid p$K_a \sim$ 12.6 in DMSO [207]) do not permit further classification of this activation into concerted PCET or stepwise PT/ET activation. Nevertheless, the use of PCET to generate a synthetically versatile radical under mild catalytic conditions presents an exciting new avenue for C–H bond functionalization chemistry.

7 Amides

Recently our group has developed concerted PCET-based methods for the activation of amide N–H bonds to form neutral amidyl radicals. Long recognized as valuable synthons for C–N bond formation [203, 208–213], these intermediates have not enjoyed widespread application in synthesis because of the inability to access these intermediates directly from native amide N–H bond precursors. The most common methods of amidyl generation typically require N-functionalized amides or the use of strong stoichiometric oxidants to effectively furnish the radical species. Few methods for catalytic amidyl generation have been reported [214]. We suspected that PCET could provide an amenable solution to producing neutral amidyls under mild catalytic conditions directly by activation of the amide N–H bond.

Our initial efforts focused on developing a PCET-based protocol for olefin carboamidation (Fig. 28) [31]. In this process, PCET activation of N-aryl amide N–H bonds using an Ir-based visible-light photoredox catalyst as the oxidant and a weak Brønsted base would furnish reactive amidyls that could undergo intramolecular addition to a proximal olefin. Following C–N bond formation, the nascent carbon-centered radical could react with an acrylate species to form an α-carbonyl radical. Turnover of the catalysts could be achieved by one-electron reduction of this electrophilic radical to its corresponding enolate by the reduced form of the photocatalyst, followed by subsequent protonation by the conjugate acid of the catalytic base. Using Mayer's effective BDFE formalism [29], we identified a number of combinations of photocatalysts and bases which could furnish the desired carboamidation product. However, the highest-yielding combination was found to be the tetrabutylammonium salt of dibutyl phosphate Bu_4N^+ $(BuO)_2PO_2^-$ and [Ir{dF(CF$_3$)ppy}$_2$(bpy)]PF$_6$. The reaction is demonstrated to have a broad substrate scope, tolerating electron-rich and electron-deficient arenes, as well as a number of arene substitution patterns. Various olefin substitutions are tolerated, including tetrasubstituted olefins and, as are substrates which lead to fused rings and spirocyclic products. Lastly, various electron-deficient olefins other than acrylates may be employed as trapping reagents, including vinyl pyridine, acrylonitrile, acrolein, and α,β-unsaturated ketones.

In an effort to address the role of PCET in the initial N–H activation step, we turned to luminescence quenching experiments using acetanilide as a model
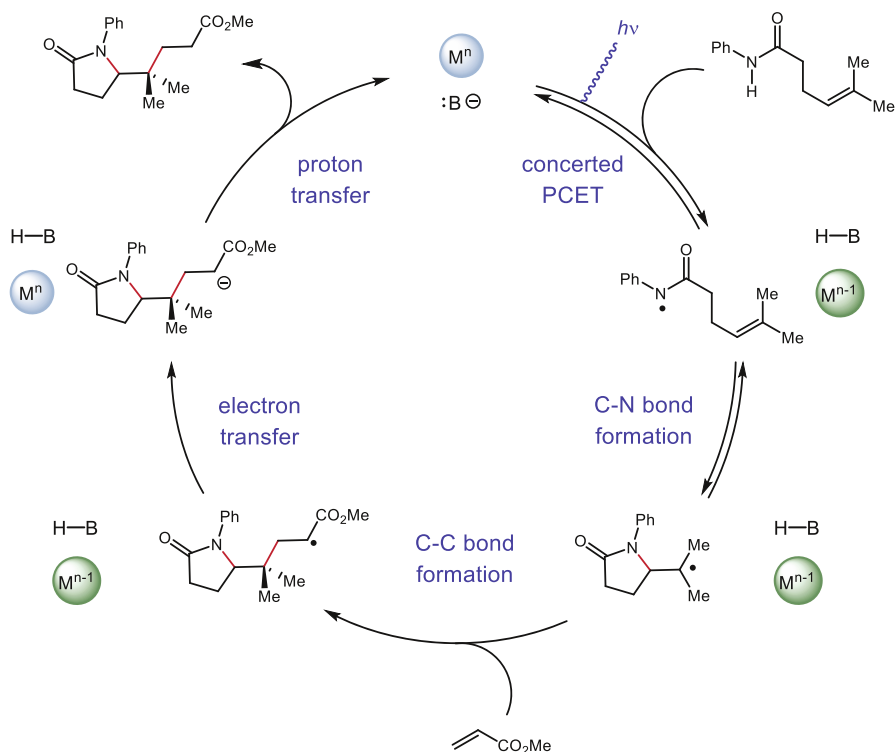
Fig. 28 The proposed catalytic cycle [215] for our disclosed carboamidation protocol. Reprinted with permission from [31]. Copyright 2015 American Chemical Society

substrate in acetonitrile solvent (Fig. 29). In the absence of base, the photocatalyst luminescence is not affected by the presence of the amide: this is consistent with the observation that the excited-state potential of the catalyst ($*E_{1/2} = 1.0$ V vs. Fc/Fc$^+$ in MeCN) is not competent to oxidize acetanilide ($*E_{1/2} = 1.2$ V vs. Fc/Fc$^+$ in MeCN). With the inclusion of a constant quantity of phosphate base, however, variation of the amide concentration leads to efficient and linear quenching of the Ir excited state. An analogous experiment with a constant concentration of acetanilide and varied phosphate demonstrates first-order concentration dependence on the phosphate as well. Given the difference in pK_a between the phosphate and the substrate ($\Delta pK_a \sim 20$) and the short excited-state lifetime of the catalyst (2.3 μs in MeCN at RT [216]), it is unlikely activation proceeds through stepwise PT/ET. Lastly, independent quenching experiments with *N*-protiated and *N*-deuterated acetanilide demonstrated a KIE of 1.15; such small KIEs have been demonstrated to be consistent with proton-involvement in multisite PCET processes [46, 217–221]. Taken together, our mechanistic data are most consistent with amide activation proceeding through concerted PCET.

Looking to expand on these results and develop further olefin amidofunctionalization reactions, we questioned if we could identify a suitable hydrogen-atom

(a)

(b)
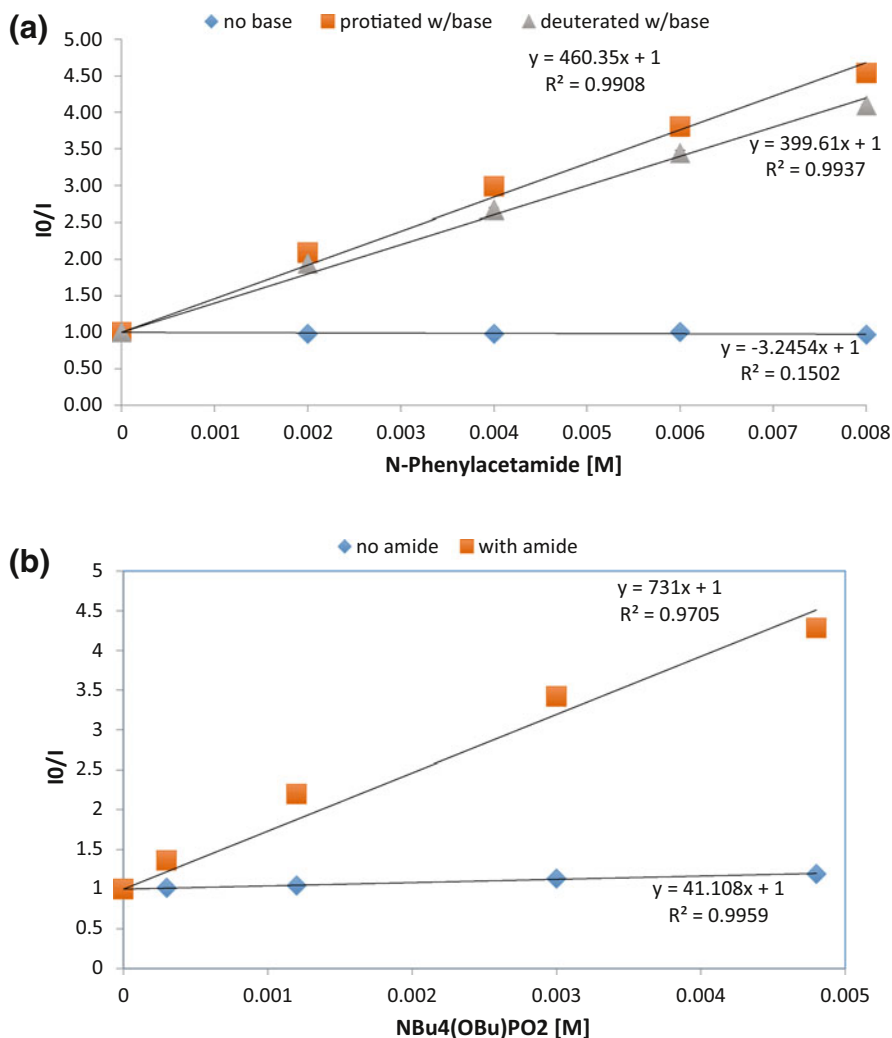
Fig. 29 Luminescence quenching data evidence for amide N–H activation by PCET. **a** Analysis of photocatalyst excited-state quenching as a function of the concentration of protiated acetanilide in the presence and absence of base, as well as quenching as a function of concentration of deuterated acetanilide in the presence of base. **b** Quenching as a function of base concentration in the presence and absence of acetanilide. Reprinted with permission from [31]. Copyright 2015 American Chemical Society

donor reagent capable of furnishing a hydroamidation product, as illustrated in Fig. 30 [222]. Based on this catalytic cycle, we anticipated such a donor would ideally enable facile HAT to the cyclized radical alkyl species, as well as a R•/R⁻ redox couple suitable to oxidize the reduced state of the photocatalyst, resulting in the formation of an anion basic enough to deprotonate the phosphoric acid generated during the initial PCET event. Electing to retain our successful combination of photocatalyst and oxidant, we screened a number of potential hydrogen-atom donors
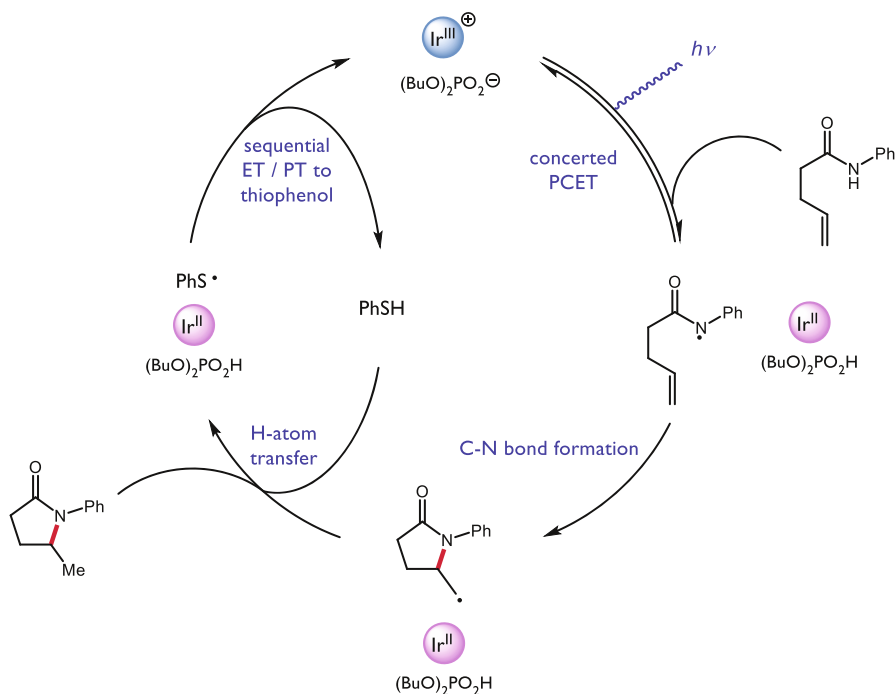
Fig. 30 Proposed catalytic cycle for PCET-enabled hydroamidation [222]

and ultimately identified thiophenol as a competent HAT catalyst capable of furnishing the desired hydroamidation product in high yield. Compared to our carboamidation conditions, the hydroamidation protocol demonstrated an even broader substrate scope, capable of addition to terminal olefins and competent to form more exotic ring-fused species.

With respect to the proposed mechanism, the success of thiophenol as a catalytic hydrogen atom donor was surprising; not only are thiophenols observed to undergo multisite PCET reactivity as outlined in the previous section, but the large difference in bond strengths between thiophenol and the *N*-aryl amide (ΔBDFE $\sim$ 20 kcal mol^{-1}) would suggest preferential activation of the weaker S–H bond. To elucidate the underlying kinetic selection between N–H and S–H activation, we undertook another set of luminescence quenching studies with acetanilide and thiophenol as our model substrates using DCM as solvent (Fig. 31). Consistent with the observations in our carboamidation protocol, photocatalyst emission in DCM was unaffected by amide alone and demonstrated first-order dependence in the presence of a catalytically relevant concentration of the phosphate base with $K_{SV} = 2860$ M^{-1} (Fig. 31a, b). Analogously, concentration-dependent quenching with thiophenol was only observed in the presence of base (Fig. 31c, d), albeit with a smaller K_{SV} (480 M^{-1}). In a final set of experiments, increasing the concentration of acetanilide in the presence of constant concentrations of base *and* thiophenol was found to quench the excited state of the
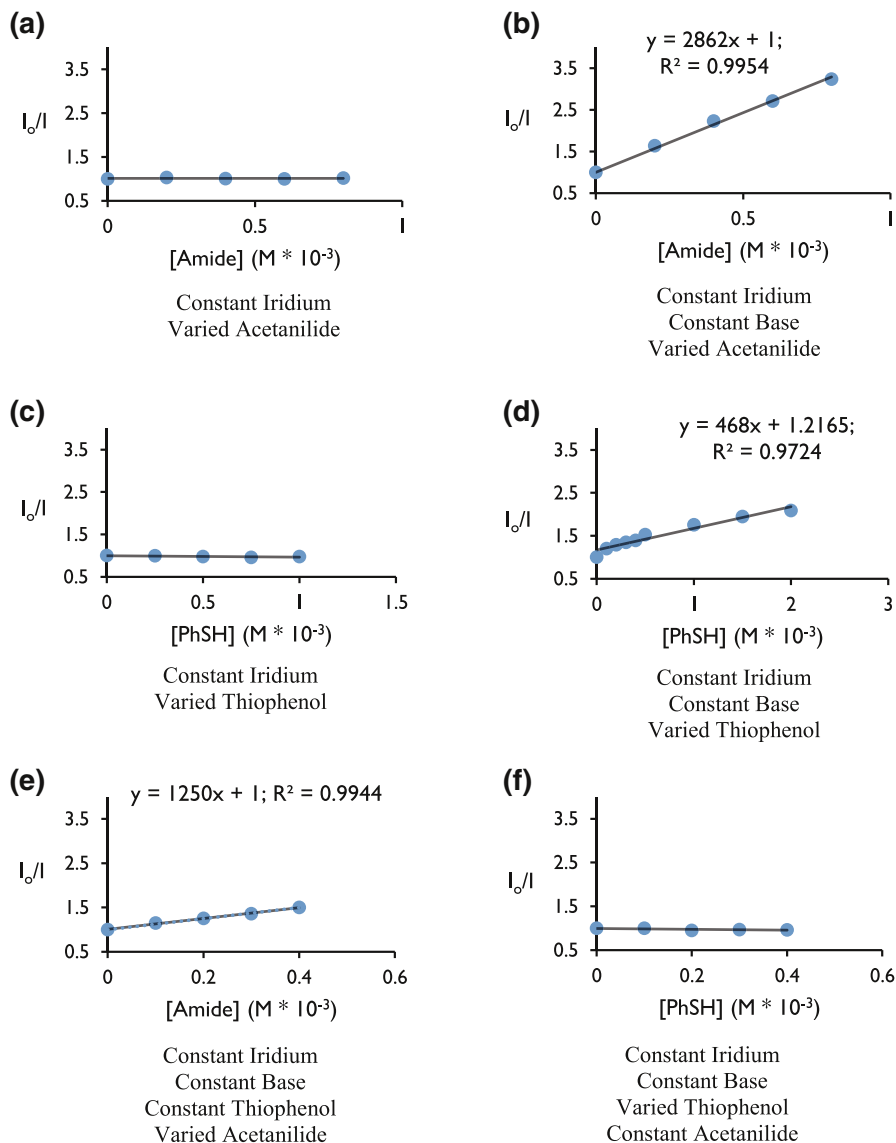
Fig. 31 Luminescence quenching data for mechanistic studies to elucidate the selectivity for amide activation in the presence of thiophenol (vide infra). Figures reprinted with permission from [222]. Copyright 2015 American Chemical Society. This article may be accessed online at the following URL: http://pubs.acs.org/doi/pdf/10.1021/jacs.5b09671

photocatalyst in a concentration-dependent manner (Fig. 31e), albeit with a diminished K_{SV} (1250 M^{-1}) relative to quenching in the absence of thiophenol. When this experiment is inverted such that the concentration of thiophenol is varied in the presence of constant concentrations of base *and* amide (Fig. 31f), the

luminescence intensity was found not to vary as a function of increasing thiophenol concentration.

The rate constants from Stern–Volmer analysis of excited-state quenching in the presence of base for acetamide ($2860 \ M^{-1}$) and thiophenol ($480 \ M^{-1}$) lie within an order of magnitude, suggesting that the observed kinetic bias for amide N–H activation does not correspond simply to difference in the quenching rate constant as demonstrated by Fig. 31f. In PCET reactivity, pre-equilibrium hydrogen bonding is required to associate the proton donor and acceptor in solution prior to the electron transfer step. Accordingly, we hypothesized that the observed selectivity might be the result of a stronger affinity for phosphate hydrogen bonding to the N–H bond relative to the S–H bond. This hypothesis is consistent with all of the data presented in Fig. 31 and corroborated by DFT calculations, which suggest the phosphate-amide hydrogen bond is stronger than the phosphate-thiophenol hydrogen bond by $5.2 \ kcal \ mol^{-1}$. Such selectivity further highlights the importance of hydrogen bonding in concerted PCET and may serve as a design principle for future synthetic reactions invoking PCET activation of stronger bonds in the presence of weaker bonds.

The concept of coupled proton and electron movement can be used not only to cleave strong amide N–H bonds by the joint action of a base and oxidant, but can also serve to *weaken* the amide N–H bond such that it can be activated by a weak H-atom abstractor. Exploiting the concept of bond-weakening upon coordination to redox-active metals [223–232], our lab demonstrated that a redox-active titanium catalyst $Cp*_2Ti^{III}Cl$ and a weak hydrogen atom acceptor TEMPO enable intramolecular additions of amides to Michael acceptors (Fig. 32) [223]. The substrate scope allows for N–H activation of amides, carbamates, thiolcarbamates, and ureas bearing phenyl or electron-rich arenes in uniformly high yield. Upon coordination to the titanium catalyst, the strength of the amide N–H bond is predicted to decrease from ~ 99 to $\sim 66 \ kcal \ mol^{-1}$ based on DFT calculations. Related N-aryl carbamates were predicted to experience enhanced bond-weakening

(a)

(b)
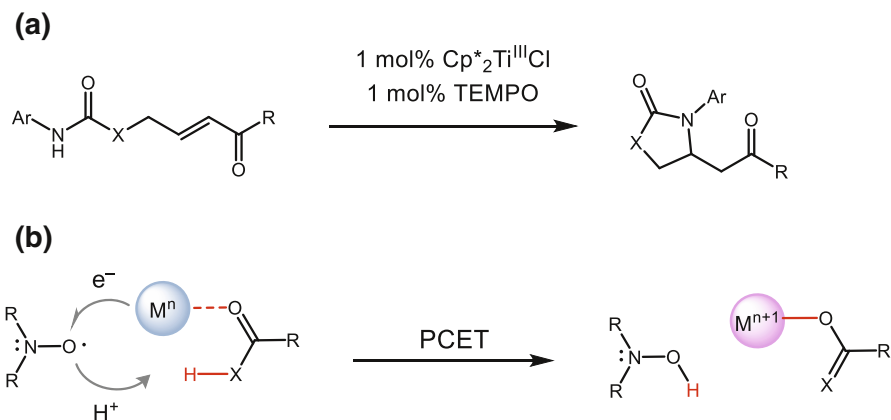
Fig. 32 Amide activation via bond-weakening PCET to nitroxyl species. Adapted with permission from [233]. Copyright 2015 American Chemical Society

of up to 39 kcal mol^{-1}. Formal HAT to TEMPO is thought to proceed as a concerted PCET event, where the proton originates from the N–H bond and the titanium(III) species provides the necessary electron, resulting in the formation of a closed-shell aza-enolate species in the absence of an identifiable base. As a testament to the mildness of these base-free conditions, an acrylate featuring a base-labile FMOC group was maintained in this reaction; repeating this reaction under standard basic conditions resulted in quantitative deprotection of the ester.

It is known that $Cp_2Ti^{III}Cl$ and TEMPO form a bond of approximately 25 kcal mol^{-1}; in light of this, we were unable to observe any conjugate amination at elevated temperatures using these two catalysts or the known complex $Cp_2Ti^{IV}Cl$-OTEMP [234–236]. Our DFT calculations estimate the strength of the $Cp^*_2Ti^{IV}Cl$-OTEMP bond to be 23 kcal mol^{-1} weaker than that of the $Cp_2Ti^{IV}Cl$-OTEMP complex, putting an approximate value of this BDFE at 2 kcal mol^{-1}. This finding is consistent with the observed room temperature EPR spectra of a 1:1 mixture of $Cp^*_2Ti^{III}Cl$ and TEMPO (Fig. 33), which demonstrates a signal consistent with both titanium- and oxyl-centered radical species present together in solution. Simulations of the individual EPR spectra for each component overlay with the experimentally observed mixed spectra, indicating weak (if any) bonding between these species in solution. Destabilization of the Ti–O bond is credited to the increased steric bulk of the cyclopentadienyl ligand, which would encounter significant steric repulsion with TEMPO upon binding. In this way, this system can be thought of as an intriguing
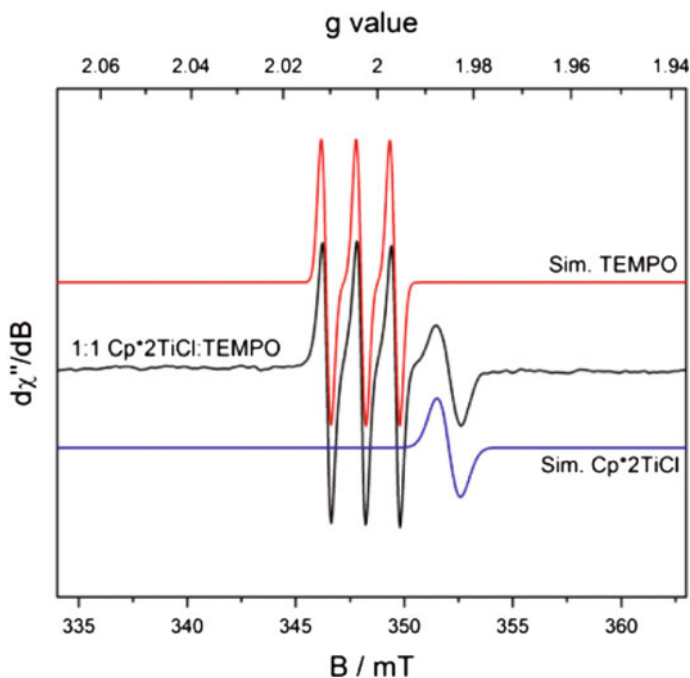
Fig. 33 EPR spectra and simulations for $Cp^*_2Ti^{III}Cl$, TEMPO, and a 1:1 mixture in MeCN. Adapted with permission from [233]. Copyright 2015 American Chemical Society

one-electron parallel to traditional frustrated Lewis pair chemistry in which the steric bulk of both the Lewis acid and the Lewis base prevent undesired association between the two, yet allow for joint substrate activation. Together, these three synthetic examples demonstrate the power of PCET in two different synthetic contexts to activate strong amide N–H bonds and generate synthetically useful amidyl and aza-enolate intermediates.

8 Quinones

The ability of Brønsted acids to modulate the redox properties of quinones has long been recognized and has been the subject of extensive study [237–241]. Selected examples relevant to synthetic applications are discussed below. A seminal report in 1989 from Fukuzumi and coworkers demonstrated the ability of Brønsted acids to catalyze electron–transfer between various ferrocene derivatives and simple quinones [242]. Ferrocene is known to undergo oxidation by strong organic oxidants such as 2,3–dicholoro–5,6–dicyano–p–benzoquione, and 7,7,8,8–tetracyano–p–quinodimethane; no reaction occurs with weaker oxidants such as p–benzoquinone. However, the addition of $HClO_4$ was shown to catalyze efficient electron transfer between 1,1′–dimethylferrocene and p–benzoquinone to afford dihydroquinone and 1,1′–dimethylferrocenium. By plotting the concentration of 1,1′–dimethylferrocenium ion vs. the ratio of benzoquinone to 1,1′–dimethylferrocene, the stoichiometry for the reduction was experimentally determined to be 2:1 with respect to ferrocene to benzoquinone (Fig. 34). Moreover, kinetic experiments showed the rate of reduction increases as $HClO_4$ concentration increases. Analogous experiments employing cis–$[Et_2Co(bpy)_2]^+$ as the one–electron reductant exhibited the same rate dependence on $[HClO_4]$, consistent with a PCET process.

Later Fukuzumi studied the mechanism of p–benzoquinone reductions by NADH analogues [243, 244]. Kinetic experiments again revealed an increase in the rate of reduction of p–benzoquinone (Q) and analogues as a function of increasing $HClO_4$ concentration. Additionally, independent kinetic runs using protiated and deuterated 10–methylacridine ($AcrH_2$ or $ArcD_2$) revealed primary KIEs for a variety of p–benzoquinone derivatives (Fig. 35). These kinetic observations are consistent with three possible mechanisms: rate-limiting, acid-catalyzed hydride transfer from $AcrH_2$, proton transfer from $AcrH_2^{\bullet+}$ to semiquinone radical, or hydrogen atom transfer from $AcrH_2^{*+}$ to semiquinone radical. An observed correlation between $E_o(QH^\bullet/QH_2)$ vs. k_H/k_D led the authors to conclude that reversible electron transfer followed by rate limiting hydrogen–atom transfer between $AcrH_2^{\bullet+}$ and the neutral semiquinone radical ($QH^\bullet$) is the most likely reaction pathway (Fig. 36).

Fukuzumi reported a detailed mechanistic study of quinone reduction catalyzed by protonated amino acids [245]. Kinetic experiments, EPR spectroscopy and cyclic voltammetry were employed to illustrate the role protonated histidine plays in mediating electron transfer between NADH analog 9,10–dihydro–10–methyl-lacridine ($AcrH_2$) and 1–(p–tolylsulfinyl)–2,5– benzoquinone (TolSQ). Cyclic voltammetry experiments demonstrate a 0.55-V positive shift in the one–electron reduction potential of TolSQ in the presence of 5.0×10^{-2} M of protonated
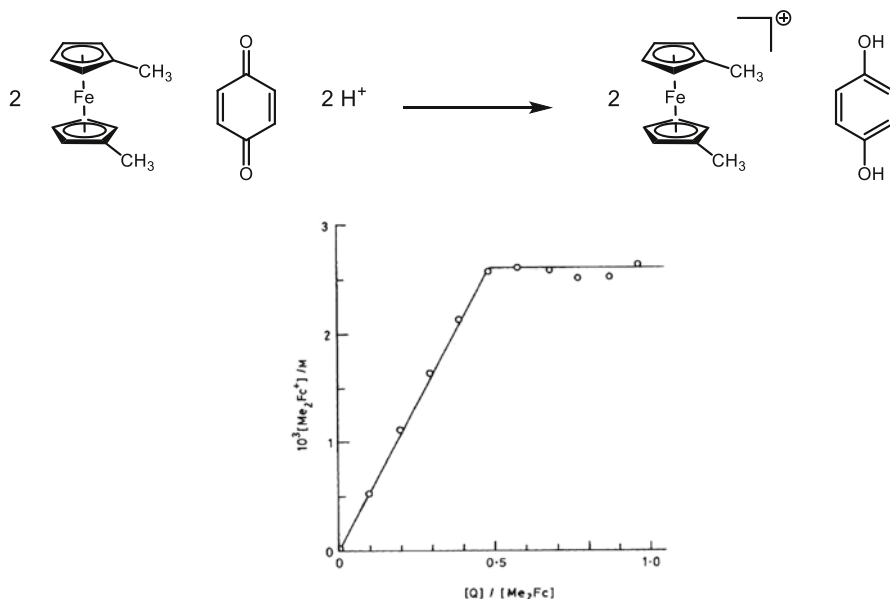
Figure 1. Plot of the concentration of 1,1'-dimethylferricenium ion, [Me₂Fc⁺], formed by the electron-transfer reaction from 1,1'-dimethylferrocene to *p*-benzoquinone in the presence of HClO₄ (0.10M) in MeCN *versus* the ratio of *p*-benzoquinone to 1,1'-dimethylferrocene, [Q]/[Me₂Fc]

Fig. 34 Perchloric acid-promoted quinone reduction by ferrocene derivatives. Reproduced from [242] with permission of the Royal Society of Chemistry

p–benzoquinone derivative	k_H / k_D
p–chloranil	2.7
2,6–dichloro–*p*–benzoquinone	2.5
p–benzoquinone	2.5
methyl–*p*–benzoquinone	4.0
2,6–dimethyl–*p*–benzoquinone	4.1
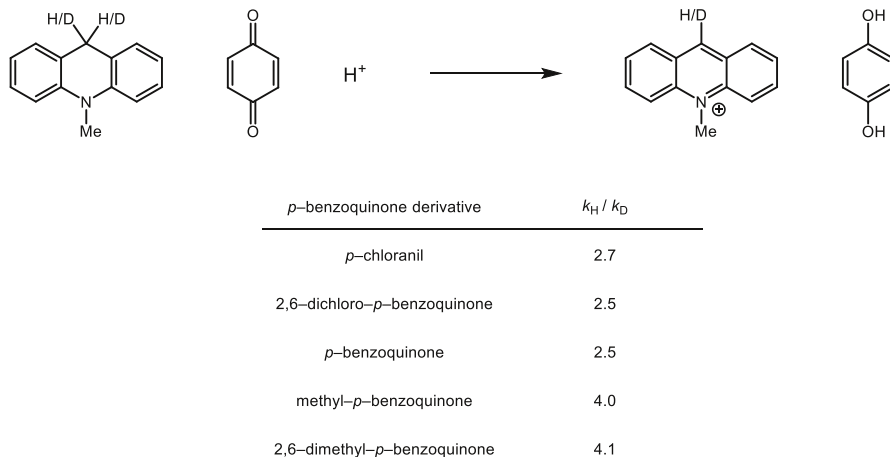
Fig. 35 KIEs for various benzoquinone reductions by 10-methylacridine [243]

histidine. This change in the reduction potential was attributed to the stabilizing effect of hydrogen bonding interactions between protonated histidine and TolSQ radical anion, which was observed by EPR spectroscopy (Fig. 37).
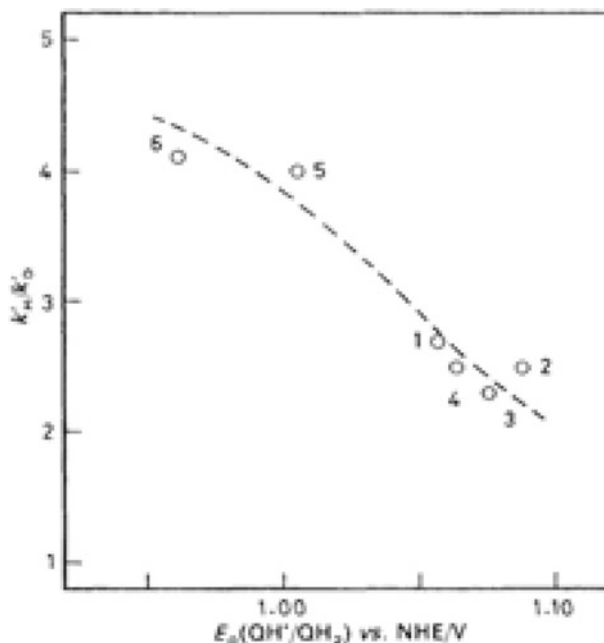
Fig. 36 Plot of the primary kinetic isotope effects for the acid-catalyzed rate constant k'_H/k'_D vs. E_o ($QH\bullet/QH_2$) in the reduction of *p*-benzoquinone derivatives by AcrH$_2$ and AcrD$_2$ in H$_2$O-EtOH (5:1 v/v) at 298 K. Reproduced from [244] with permission of the Royal Society of Chemistry

The ability of Brønsted acids to increase the oxidizing power of benzoquinone derivatives was further investigated by Rathore in the context of the Scholl reaction [246]. Arene substrates with oxidation potentials as high as +1.7 V vs. SCE were readily oxidized by dichlorodicyano–*p*–benzoquinone (E_{red} = +0.60 V vs. SCE) in the presence of methane sulfonic acid (Fig. 38). However, no reaction was observed in the absence of acid.

Recently, Jacobsen and Nocera investigated the ability of various hydrogen–bond donors to affect the rates and thermodynamics of quinone reductions [247]. Energetically favorable associations between hydrogen bond donors and quinone radical anions provide the additional thermodynamic driving force necessary to enable otherwise endergonic electron transfers, as quantified by the following expression:

$$\Delta G_{net} = \Delta G_{ET} + \Delta G_{association}$$

This study is particularly notable in being the first to study these effects in electron-deficient quinones. Prior work has focused on comparatively electron-rich quinones, which are more Lewis basic and thereby provide a higher association energy, resulting in a larger $\Delta E_{1/2}$. In this work, the authors sought to quantify the activation of more electron deficient quinones that have oxidation potentials closer to those of synthetically relevant functional groups. In particular, a variety of hydrogen bond donors were prepared to evaluate their ability to promote the reduction of *ortho*–
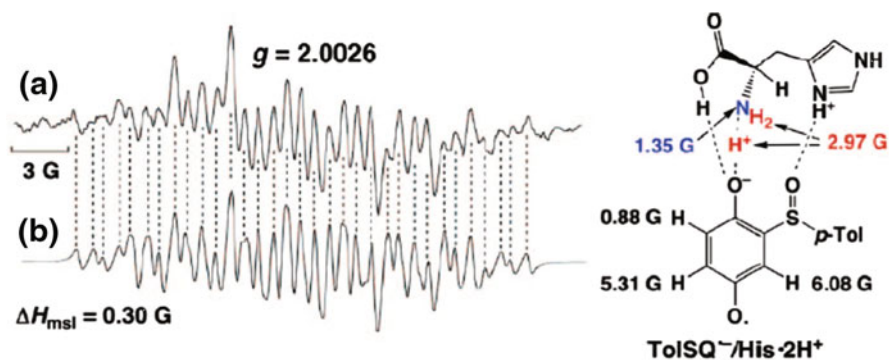
Fig. 37 EPR spectra of semiquinone radical—protonated histidine interactions. Adapted with permission from [245]. Copyright 2008 American Chemical Society

Fig. 38 MsOH-promoted arene oxidation [246]

chloranil (Fig. 39). To evaluate the ability of the H-bond donors to promote quinone reduction, the authors experimentally determined the association constants for binding between the hydrogen bond donors and both the oxidized and reduced forms of *ortho*–chloranil, K_Q and $K_{Q^{\cdot-}}$ respectively, using cyclic voltammetry experiments and the following equation derived from the Nernst relation:

$$\Delta E_{1/2} = 0.059V \log \frac{1 + K_{Q^{\cdot-}}[HBD]}{1 + K_Q[HBD]}$$

Fitting the current response for each individual H-bond donor revealed the stoichiometry of binding to be 2:1 for the monocationic and neutral catalysts, and 1:1 for the bisamidinium catalyst. To further support this proposed mechanism, additional kinetic studies revealed a second-order dependence on the rate of quinone reduction with monocationic catalysts, and a first-order dependence on the rate of reduction using the biscationic amidinium salt.

After studying the mechanism by which hydrogen bond donors catalyze electron transfer, the authors developed a novel oxidative lactonization reaction to demonstrate the synthetic utility of hydrogen–bond coupled electron transfer (Fig. 40). Importantly, this work extends the current understanding of how hydrogen bonding can promote electron transfer events in synthetic contexts, even in the absence of a formal proton transfer event.
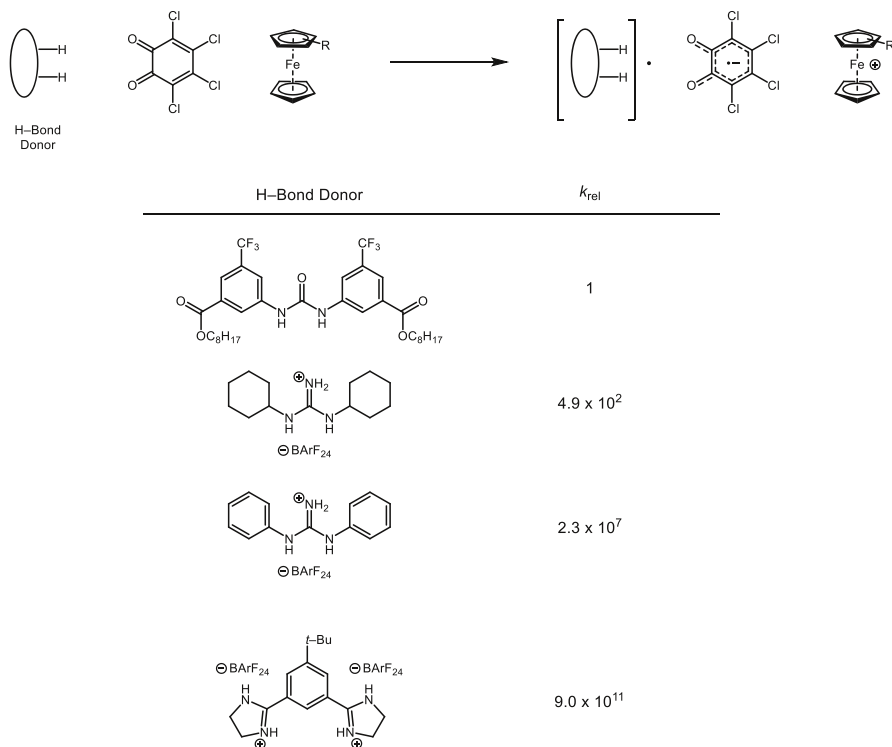
Fig. 39 Quinone reduction promoted by hydrogen-bond donors [247]
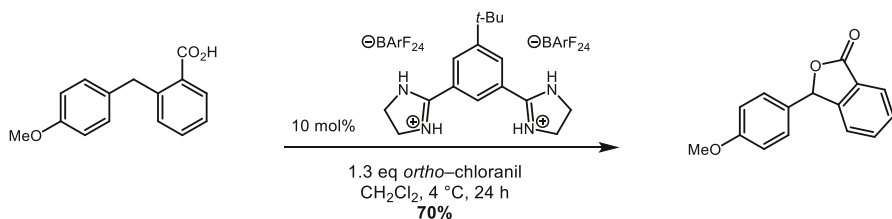
Fig. 40 Hydrogen bond-coupled electron transfer promoted oxidative lactonization [247]

9 Ketones and Carbonyl Derivatives

In pioneering work in the mid-1980's, Fukuzumi and coworkers identified that strong Brønsted acids can catalyze electron transfer reactions between outer-sphere reductants and acetophenone derivatives [242]. Specifically, they demonstrated that while the excited state of $[Ru(bpy)_3]^{2+}$ cannot donate an electron to acetophenone derivatives directly in acetonitrile [248], addition of 0.1 M $HClO_4$ led to efficient charge transfer. Through the use of luminescence quenching assays, the authors were able to quantify a positive shift in the one-electron reduction potential of ketones in the presence of $HClO_4$ and the corresponding rates of acid-catalyzed ET.

		$k_{et}/1\ mol^{-1}$ in the presence of		
R	E°_{red} V	$Bu^n_4ClO_4$ (0.10 M)	$HClO_4$ (0.10 M)	ΔE_{red} / V
p–NO$_2$	−0.93	5.8 x 10^8	6.7 x 10^8	0
m–NO$_2$	−1.02	4.9 x 10^7	4.9 x 10^7	0
H	−2.10	–	5.1 x 10^6	1.01
p–Me	−2.20	–	1.3 x 10^7	1.14
p–OMe	−2.22	–	4.3 x 10^7	1.19
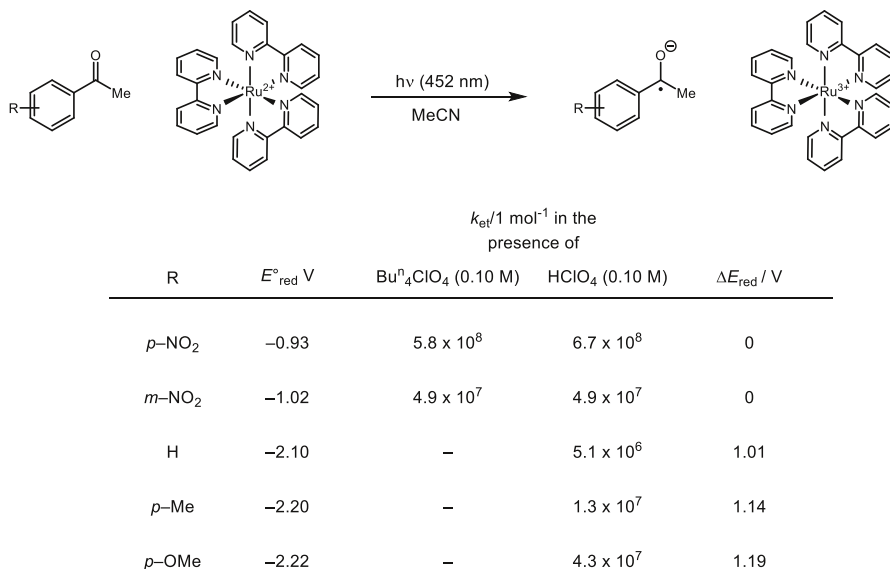
Fig. 41 Perchloric acid catalyzed ET from photoexcited Ru(bpy)$_3^{2+}$ to acetophenone derivatives. ΔE_{red} corresponds to the positive shift in the one-electron reduction potential observed in the presence of perchloric acid relative to the one-electron reduction potential observed in the absence of perchloric acid [242]

Acetophenone derivatives containing electron-donating groups possess $E^{red}_{1/2}$ values significantly more negative than the excited state of $[Ru(bpy)_2]^{+3}$. As a consequence, electron transfer does not occur in the absence of HClO$_4$. However, upon inclusion of 0.1 M HClO$_4$ electron transfer proceeds rapidly (Fig. 41). The authors speculate that protonation of the ketyl radical anion is stabilizing, thereby providing additional thermodynamic driving force which is observed as an increase in k_{ET}. For acetophenone derivatives bearing electron-withdrawing substituents (*meta* or *para* nitro) no increase in k_{ET} was observed upon inclusion of HClO$_4$. The authors postulate that electron-withdrawing groups decrease the basicity of the ketyl radical anion to such a degree that protonation by HClO$_4$ is not favorable.

To study the mechanism by which HClO$_4$ catalyzes electron transfer, the kinetic order in acid was measured by performing a series of Stern–Volmer luminescence quenching experiments at various concentrations of HClO$_4$. These experiments revealed a linear relationship between k_{et} and [HClO$_4$] (Fig. 42) showing electron transfer from $[Ru^*(bpy)_3]^{2+}$ is first order in acid. In this work, the authors proposed a stepwise ET/PT mechanism in which protonation of the ketyl radical anion provides additional thermodynamic driving force which causes an increase in k_{ET}. This work predated the wide-spread acceptance of concerted proton–coupled electron transfer as an elementary step, however these seminal observations provided the conceptual framework for PCET to be applied further in contemporary synthetic chemistry.

The Fukuzumi group later investigated the mechanism of reduction of α–haloketones using NADH model compounds [249, 250]. This non–enzymatic model system was developed to investigate the role of Brønsted acids in enzymatic ketone
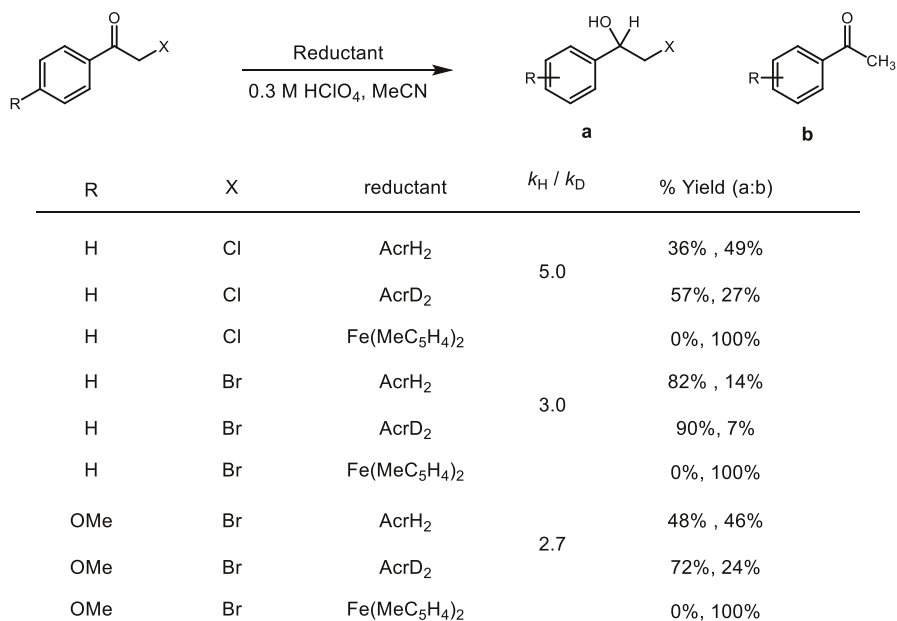
Fig. 42 k_{ET} v. [HClO$_4$] for electron transfer between Ru(bpy)$_3^{2+}$ and acetophenone. Reproduced from [242] with permission of the Royal Society of Chemistry
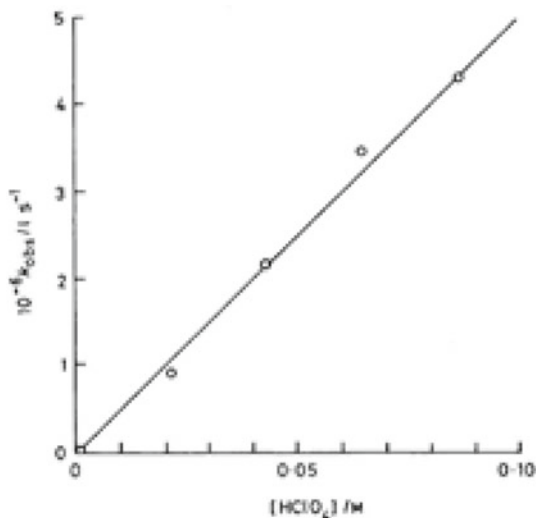
reductions. The use of an acid-stable NADH analogue enabled the authors to study the reaction both in the presence and absence of HClO$_4$. By comparing these results to kinetic experiments employing classical outer–sphere reductants, the authors were able to demonstrate that ketone reduction by NADH model compounds proceeds through an initial Brønsted acid-promoted electron transfer step. To investigate the mechanism of ketone reduction, kinetic data was obtained for a series of α–haloketone reductions by an acid-stable NADH analog 10–methylacridan (AcrH$_2$) with HClO$_4$ in acetonitrile (Fig. 43). Additionally, the rate of electron transfer from classical one–electron reductants such as Fe(MeC$_5$H$_4$)$_2$ and [Ru*(bpy)$_3$]$^{2+}$ was measured for the same series of ketones. Comparing the two sets of rate data allowed the authors to draw conclusions about the mechanism of acid catalyzed ketone reduction by NADH analogues. While no reduction was observed in the absence of acid with any reductant, a linear correlation between the rate of electron transfer k_{et} was observed with increasing HClO$_4$ concentration with Fe(MeC$_5$H$_4$)$_2$ as well as [Ru*(bpy)$_3$]$^{2+}$. Additionally, a linear correlation was observed between the rate constant (log k_{obs}) for the reduction of α–haloketone by AcrH$_2$, and the rate constants (log k_{et}) for electron transfers from Fe(MeC$_5$H$_4$)$_2$ and [Ru*(bpy)$_3$]$^{2+}$. On the basis of these findings, the authors suggest that the first step in acid-catalyzed ketone reductions by NADH model compounds involves initial electron transfer to an activated ketone substrate.

Despite this correlation, different product distributions were observed when the reduction is run with AcrH$_2$ vs. Fe(MeC$_5$H$_4$)$_2$ (Fig. 43). This observation can be rationalized by considering the subsequent steps of the reduction mechanism (Fig. 44). The 1,2 reduction product forms as a result of hydrogen–atom transfer from the AcrH$_2$ radical cation to yield the α–halohydrin product. Since this pathway is unavailable for the outersphere one–electron reductants, only the dehalogenated acetophenones are observed.

Unactivated aldehydes and ketones do not undergo reduction by NADH analogues readily, however in the presence of HClO$_4$ and acetonitrile compounds

| R	X	reductant	k_H / k_D	% Yield (a:b)
H	Cl	AcrH$_2$		36% , 49%
H	Cl	AcrD$_2$	5.0	57%, 27%
H	Cl	Fe(MeC$_5$H$_4$)$_2$		0%, 100%
H	Br	AcrH$_2$		82% , 14%
H	Br	AcrD$_2$	3.0	90%, 7%
H	Br	Fe(MeC$_5$H$_4$)$_2$		0%, 100%
OMe	Br	AcrH$_2$		48% , 46%
OMe	Br	AcrD$_2$	2.7	72%, 24%
OMe	Br	Fe(MeC$_5$H$_4$)$_2$		0%, 100%

Fig. 43 α-haloketone reduction with NADH model compound vs. dimethyl ferrocene [249, 250]

are rapidly reduced to the corresponding alcohols (Fig. 45) [251]. First the authors measured the rate of reduction (k_{obs}) of acetaldehyde and related compounds by AcrH$_2$ in the presence of HClO$_4$. Next, the rate of electron transfer (k_{et}) from [Ru*(bpy)$_3$]$^{2+}$ to the same series of carbonyl compounds was measured by Stern–Volmer luminescence quenching experiments. A plot of log k_{obs} vs. log k_{et} again revealed a linear relationship, suggesting that acid catalyzed electron transfer may play an important role in the reductions of aldehydes and ketones by NADH analogs
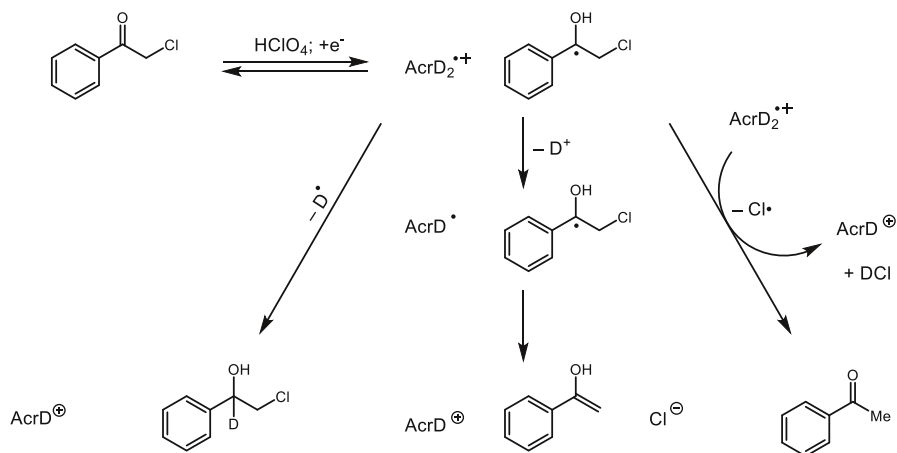
Fig. 44 Mechanistic rationale for product distribution employing different reductants
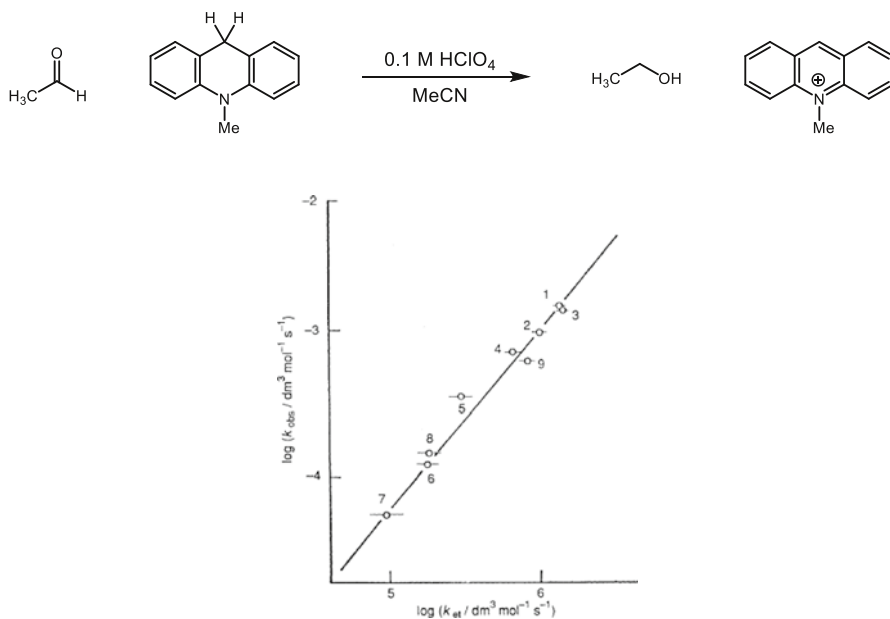
Fig. 45 Non-enzymatic acetaldehyde reduction. Adapted from [251] with permission of The Royal Society of Chemistry

such AcrH$_2$ as well (Fig. 45). In these papers, the authors propose a stepwise mechanism in which electron transfer first occurs to generate a radical anion, which is rapidly protonated by acid. However, in light of more recent advances, mechanisms involving stepwise PT–ET, or concerted proton–coupled electron transfer should also be considered. In particular. given the pK_a of HClO$_4$ (-0.7 in MeCN) relative to a typical ketone (p$K_a = -0.1$ for acetophenone in MeCN) the possibility of electron transfer to a protio–oxocarbenium ion cannot be easily discounted.

In an analogous set of experiments, this model system was again used by the Fukuzumi group to investigate the mechanism of flavin reduction [252]. NADH and flavins are coenzymes which play an essential role in many biological redox processes, including the reduction of dioxygen in respiration. In this work, the authors investigate the acid catalyzed reduction of flavin analogues by both NADH model 10–methyl–9,10–dihydroacridine (AcrH$_2$), and *cis*–dialkylcobalt(III) complexes. Kinetics experiments were performed to study the mechanism by which flavin reduction occurs. These experiments revealed an increase in k_{obs} associated with an increase in [HClO$_4$] for both AcrH$_2$ as well as the outer sphere reductants *cis*–[Me$_2$Co(bpy)$_2$]$^+$ and *cis*–[Et$_2$Co(bpy)$_2$]$^+$. From the obtained rate data, the authors calculated a positive shift in the one–electron reduction potential as a function of increasing [HClO$_4$], further demonstrating the ability of acid to catalyze electron transfers.

Building upon these early observations that Brønsted acids can play a significant role in catalyzing electron transfers, Yoon and coworkers reported an acid-catalyzed
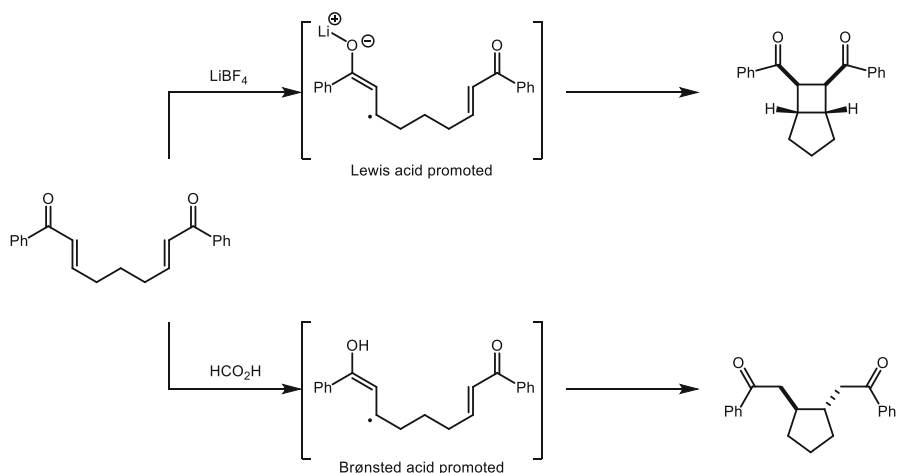
Fig. 46 Brønsted acid-promoted reductive cyclization

reductive cyclization of enones in the context of visible light photoredox catalysis (Fig. 46) [253]. The Yoon lab had previously demonstrated the ability of Lewis acid salts to activate similar systems [254, 255], however different products were formed based on the method of enone activation. Specifically, it was proposed that Lewis acid activation affords a radical anion intermediate, whereas Brønsted acid activation results in a neutral radical. These distinct radical intermediates are known to have different reaction chemistries, and this difference was proposed to be the origin of the differing product distributions.

The authors propose the Brønsted acid-catalyzed mechanism (Fig. 47), which begins by reductive quenching of $[Ru*(bpy)_3]^{2+}$ by a sacrificial reductant, such as iPr$_2$NEt to afford the more reducing $[Ru(bpy)_3]^+$. Next, electron transfer occurs from $[Ru(bpy)_3]^+$ to a proto–oxocarbenium ion to afford a neutral radical intermediate. Carbon–carbon bond formation occurs through a 5–*exo*–trig cyclization to afford an α–carbonyl radical. It was proposed the cyclized radical could be reduced either through HAT from the radical cation of iPr$_2$NEt or sequential electron transfer from the photoredox catalyst, followed by protonation of the enolate. However, considering the large difference in pK_a between formic acid (p$K_a \sim 23$ in MeCN) and typical ketones (–0.1 acetophenone in MeCN) protio–oxocarbenium formation may be less favorable than activation through hydrogen bonding. The authors demonstrated the utility of this protocol in 24 examples with yields ranging from 60–95 % and including both aryl and alkyl enones, and demonstrated the use of stoichiometric Brønsted acids to facilitate electron transfer to substrates with reduction potentials previously inaccessible using common photoredox catalysts.

In 2013, our lab demonstrated the feasibility of concerted proton–coupled electron transfer as a mechanism of substrate activation in the development of a catalytic ketyl–olefin coupling protocol [32]. The thermodynamics associated with ketone reduction make them particularly well suited for activation by concerted
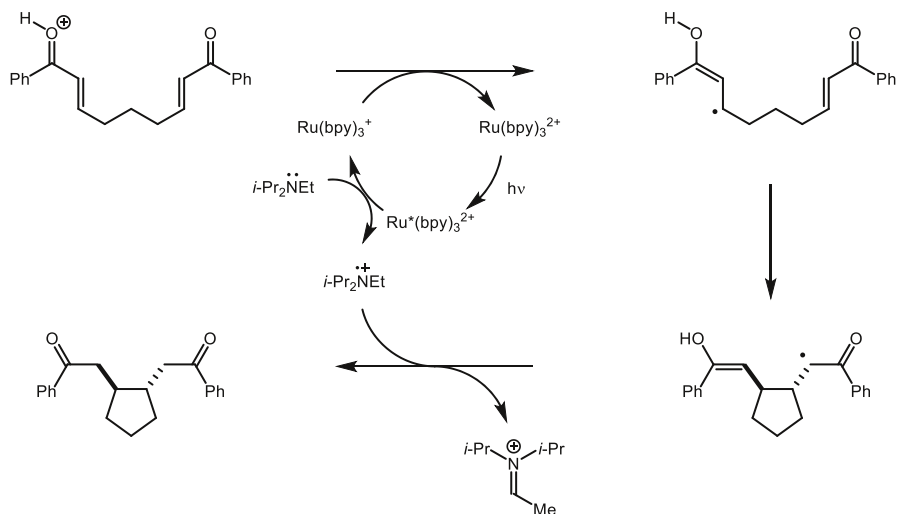
Fig. 47 Plausible mechanism for reductive enone coupling. Adapted from [253] with permission of The Royal Society of Chemistry

PCET. The strongly negative reduction potentials ($E_{1/2}^{red}$ = −2.48 V vs. Fc for acetophenone) and poor basicity (pK_a in MeCN = −0.1 for acetophenone) of typical ketones require extremely reducing or acidic conditions for activation by either sequential transfer pathway. However, we anticipated that through a concerted PCET mechanism, ketyl formation could be viable using suitable combinations of Brønsted acids and one-electron reductants with values far removed from those required for either sequential transfer pathway. Furthermore, we postulated a concerted PCET mechanism would benefit from decreased kinetic barriers relative to mechanisms involving stepwise transfer associated with the generation of high-energy charged species along the reaction coordinate.

Notably, the ability for a given pair of Brønsted acid and one–electron reductant to jointly activate ketones through concerted PCET could be predicted using the effective BDFE formalism outlined by Mayer [29]. As outlined in the introduction, the equation in Fig. 48 enables an energy value thermodynamically equivalent to a BDFE to be calculated for a given acid–reductant combination. This effective BDFE value formally represents the strength of the X–H bond that may be formed from a given acid–reductant combination in a thermoneutral process. We expected combinations of acids and reductants with effective BDFEs significantly higher than the ketyl radical O–H bond (BDFE = 26 kcal/mol) would not possess sufficient thermodynamic driving force to enable ketyl formation via PCET (Fig. 48, entries 1–4). However, when the combination of acid and reductant furnish an effective BDFE at or below the threshold required for ketyl formation, PCET activation will be favorable and substrate **41** will rapidly cyclize to give products **42** and **43** (Fig. 48, entries 5–10).

After establishing conditions required for ketyl formation, we proposed the following mechanism for the catalytic ketyl–olefin coupling (Fig. 49). The intermediate ketyl radicals would undergo 5–*exo*–trig cyclization with pendant

acid catalyst	redox catalyst	'BDFE'	% yield	2:3
–	Ru(bpy)$_3$(BAr^F)$_2$	–	0	–
BzOH	Ru(bpy)$_3$(BAr^F)$_2$	45	0	–
NEt$_3$·HBF$_4$	Ru(bpy)$_3$(BAr^F)$_2$	41	0	–
lutidine·HBF$_4$	Ru(bpy)$_3$(BAr^F)$_2$	35	0	–
(PhO)$_2$PO$_2$H	Ru(bpy)$_3$(BAr^F)$_2$	33	78	4.6:1
pTSA	Ru(bpy)$_3$(BAr^F)$_2$	27	74	4.3:1
(PhO)$_2$PO$_2$H	Ir(ppy)$_2$(dtbpy)PF$_6$	29	93	4.8:1
(PhO)$_2$PO$_2$H	fac-Ir(ppy)$_3$	24	92	4.8:1
lutidine·HBF$_4$	Ir(ppy)$_2$(dtbpy)PF$_6$	31	74	4.9:1
(PhO)$_2$PO$_2$H	Ru(bpy)$_3$(BAr^F)$_2$	33	89	10:1[a]

$$\text{BDFE(kcal/mol)} = 1.37\ pK_a + 23.06\ E^\circ + 54.9\ \text{kcal/mol (RT in MeCN)}$$

Fig. 48 Evaluation of acid/reductant pairs for PCET. Reprinted with permission from [32]. Copyright 2013 American Chemical Society

olefins to form a new carbon–carbon bond and afford an α-carbonyl radical. These radicals can be subsequently reduced by hydrogen–atom transfer from Hantzsch ester to afford the cyclized products. Electron transfer from the oxidized HEH to the excited state of [Ru(bpy)$_3$]$^{2+}$, followed by proton transfer to phosphate will regenerate both Brønsted acid and photoredox catalyst and close the catalytic cycle.

To determine whether substrate activation occurs through concerted PCET or a sequential transfer pathway, luminescence quenching studies were conducted using acetophenone as a model substrate together with diphenyl phosphoric acid and an excited-state reductant, Ir*(ppy)$_3$. Notably, no quenching of the Ir excited state was observed in solutions of acetophenone or diphenyl phosphoric acid individually. However admixtures of these two reagents led to efficient quenching that exhibited a first-order kinetic dependence on the concentration of each component. Additionally a deuterium kinetic isotope effect (k_H/k_D) of 1.22 ± 0.02 was observed when these luminescence quenching experiments were run using either the protiated or deuterated form of diphenyl phosphoric acid. Taken together, these experiments are inconsistent with rate-limiting ET activation. Similarly, rate-limiting proton transfer was ruled out on energetic grounds, as the difference in pK_a between diphenyl phosphoric acid (pK_a = 13, MeCN) and acetophenone (pK_a = –0.1, MeCN) corresponds to a free energy difference of 18 kcal/mol. Taking this unfavorable free energy change as the minimum kinetic barrier for proton transfer, rate of proton transfer cannot exceed 2.6 x 10^{-3} M^{-1} s^{-1}. This process is thus much too slow to be competitive with luminescent decay of the catalyst excited state, which has a lifetime of 1.9 μs. As both
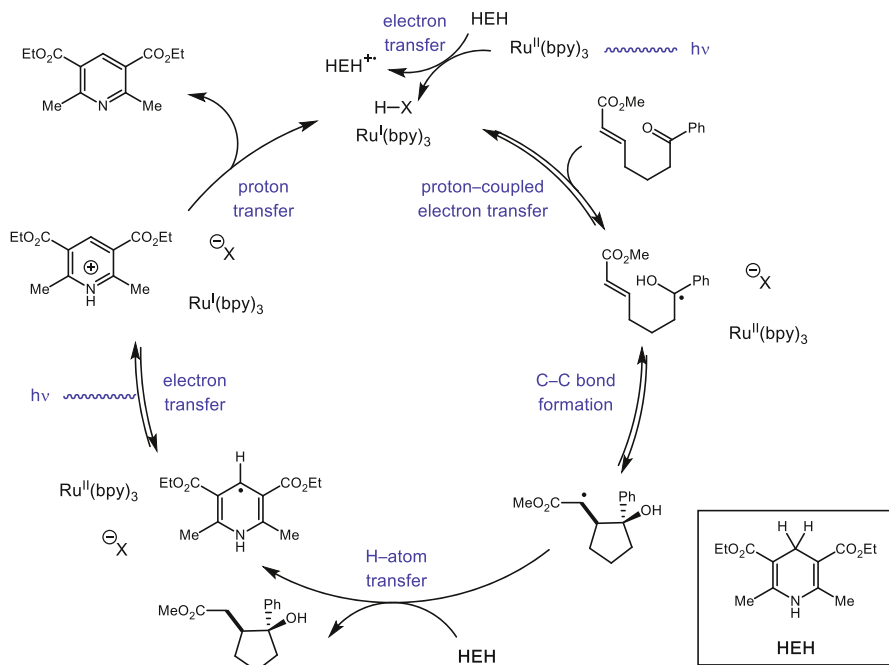
Fig. 49 Plausible mechanism for ketyl-olefin cyclization. Reprinted with permission from [32]. Copyright 2013 American Chemical Society

stepwise pathways can be ruled out, these results are most consistent with a concerted PCET mechanism of ketone activation (Fig. 50).

Building on these results, we next questioned whether a chiral Brønsted acid could be used to serve as a handle for asymmetric induction in photoredox catalysis [256]. A key challenge would be to identify conditions in which a hydrogen–bonding interaction between a neutral ketyl intermediate and the conjugate base of achiral Brønsted acid catalyst are maintained throughout subsequent bond forming events. We demonstrated the feasibility of this proposal in the successful development of a catalytic asymmetric aza–pinacol coupling promoted by reductive proton–coupled electron transfer. Chiral phosphoric acid catalysts were employed with Ir-based visible light photoredox catalysts to jointly activate ketones to form neutral ketyl radicals. These free radical intermediates remain associated with the chiral phosphate through a stabilizing hydrogen–bonding interaction throughout carbon–carbon bond formation to afford vicinal amino–alcohols in high yield and enantioselectivities.

We propose the reaction may proceed by the following mechanism (Fig. 51). First, reductive quenching of the Ir^{III}(ppy)$_2$(dtbpy) excited state by Hantzsch ester will afford the more reducing Ir^{II}(ppy)$_2$(dtbpy). PCET would then occur to a hydrogen bond complex between substrate and chiral phosphoric acid to afford the neutral ketyl radical. This neutral ketyl radical would remain associated with the chiral phosphate throughout the subsequent carbon–carbon bond formation to afford
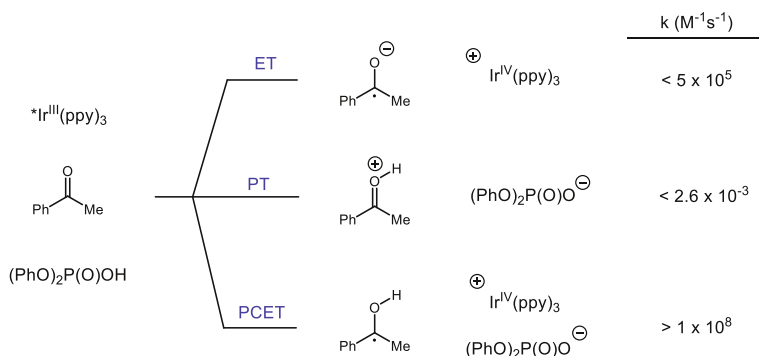
Fig. 50 Summary of mechanistic data supporting PCET reactivity

a cyclized hydrazyl radical. HAT from Hantzsch ester would afford the closed–shell product. Electron transfer followed by proton transfer will again regenerate both catalysts and close the catalytic cycle.

Catalyst and reaction parameter optimization led to the identification of 2 mol % [Ir(ppy)$_2$(dtbpy)](PF6), 10 mol % (R–R)–2,2′–TPS–binol phosphoric acid and Hantzsch ester as the stoichiometric reductant in dioxane solvent as the optimal conditions. The reaction afforded a variety of cyclized vicinal amino–alcohols in high yields and enantioselectivities. Density functional calculations demonstrate neutral ketyl radicals are excellent hydrogen bond donors and can engage in highly stabilizing hydrogen bonding interactions with phosphate anions (Fig. 52). Consistent with this view, we observed that high enantioselectivity was maintained even in polar solvents with relatively high dielectric constants (81 % ee in MeCN, 88 % ee in DME). This reaction first demonstrated the ability of hydrogen bonding in a PCET event to serve as a platform for asymmetric induction in photoredox-catalyzed free radical transformations.

In 2015 Rueping and coworkers described the reductive homodimerization of carbonyls catalyzed by Brønsted acids [257]. The authors employ iridium and ruthenium-based visible light photoredox catalysts and NBu$_3$ as a stoichiometric reductant to form ketyl radical intermediates which rapidly dimerize to form symmetrical pinacol products. The authors note that electron transfer between the excited state of [Ir(dF(CF$_3$)(ppy)]$_2$(dtbpy)PF$_6$ ($E_{1/2}^{red} = -1.69$ V vs. Fc) and acetophenone ($E_{1/2}^{red} = -2.48$ V vs. Fc) is significantly endergonic. As such, they propose the reduction is catalyzed by trace Brønsted acid formed from the oxidation of NBu$_3$. To probe this hypothesis the authors investigated the effect of acidic and basic additives on the homodimerization of acetophenone (Fig. 53). The observation that basic additives inhibit the reaction and additional acids promote the reaction is consistent with PCET as the mechanism of substrate activation in these reductive homodimerizations. The reaction was shown to be efficient for the reductive homocoupling of a variety of diverse benzaldehyde and acetophenone derivatives providing pinacol products in high yield. Additionally the methodology
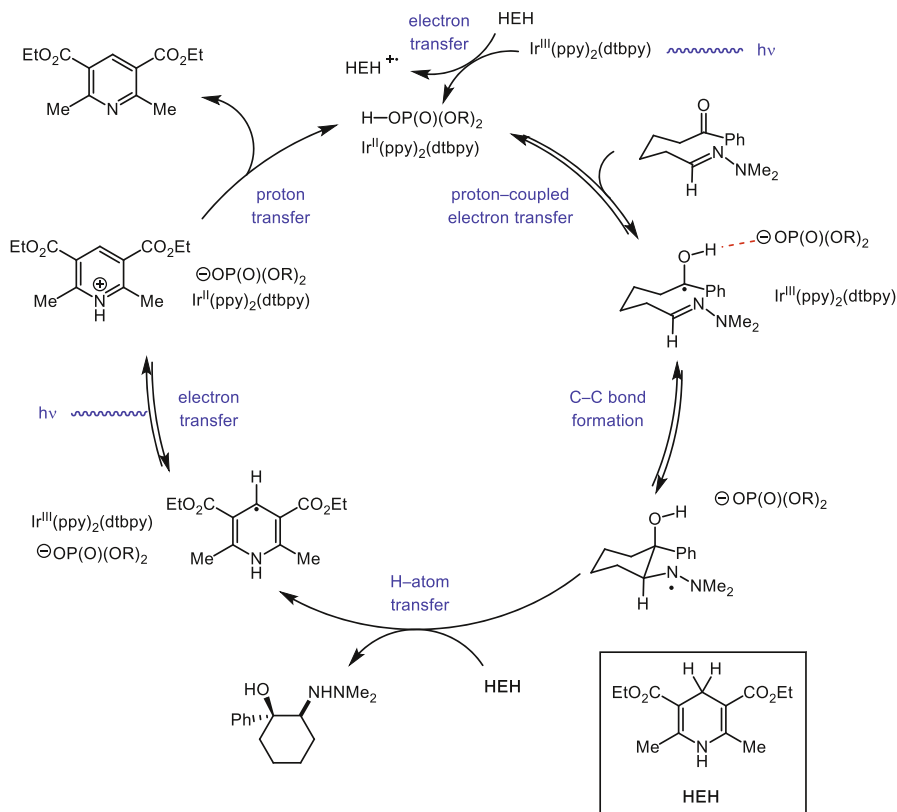
Fig. 51 Proposed mechanism for asymmetric aza-pinacol coupling. Reprinted with permission from [256]. Copyright 2013 American Chemical Society

Fig. 52 Computational estimate of ketyl-phosphate hydrogen bond strength. Reprinted with permission from [256]. Copyright 2013 American Chemical Society
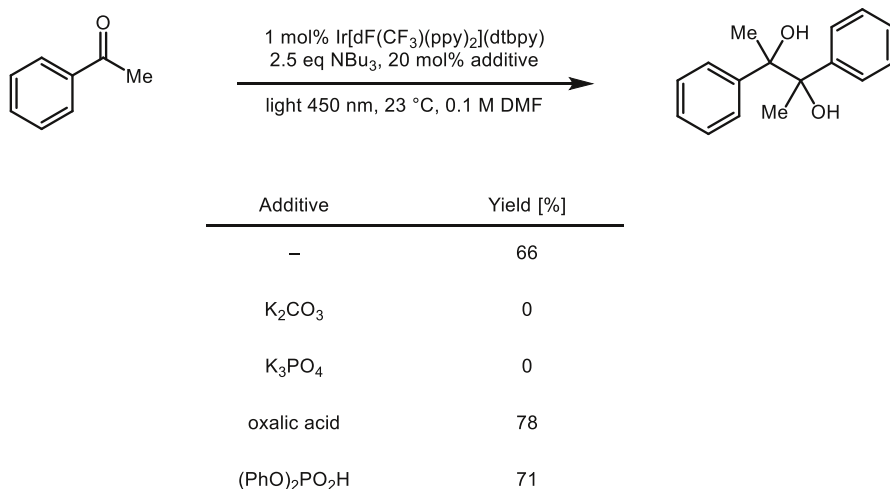
Fig. 53 Reductive homocoupling of ketones promoted by Brønsted acids [257]

Additive	Yield [%]
–	66
K_2CO_3	0
K_3PO_4	0
oxalic acid	78
$(PhO)_2PO_2H$	71

was successfully applied to imines to afford vicinal diamines in good to excellent yields.

With respect to PCET coupling of imine derivatives, Sigman has reported the synthesis of piperazines by the reductive coupling of bisimines with a combination of Brønsted acids and elemental manganese as a one–electron reductant (Fig. 54) [258]. The authors found that the success of the reaction correlated with the acidity of the Brønsted acid additive, consistent with a PCET process. The high diastereoselectivity of this transformation was a noteworthy compared to other previously reported imine dimerizations. A radical–radical coupling mechanism was proposed to account for the observed diastereocontrol. While it is possible that the reaction proceeds through radical addition to a second equivalent of imine followed by subsequent reduction, we defer to the mechanism put forward by the authors.

Related to the ketones examples shown above, in 2014 DiRocco and coworkers reported the late stage functionalization of biologically active small molecules using Brønsted acids and photoredox catalysts to activate peresters (Fig. 55) [259]. The presence of trifluoroacetic acid enables one–electron reduction of *tert*–butyl peracetate and biscyclopropanecarbonyl peroxide by visible light photoredox catalysts. This proton-coupled reduction event initiates a series of bond fragmentations, which afford methyl or cyclopropyl radicals. These radical species then undergo efficient Minisci-type additions to heteroaromatic compounds to enable late stage diversification of drugs and drug candidates (Fig. 56). As peresters have reduction potentials ~ 1 V endergonic relative to the redox catalyst employed, the authors suggest that Brønsted acid additives catalyze the reduction via concerted PCET.
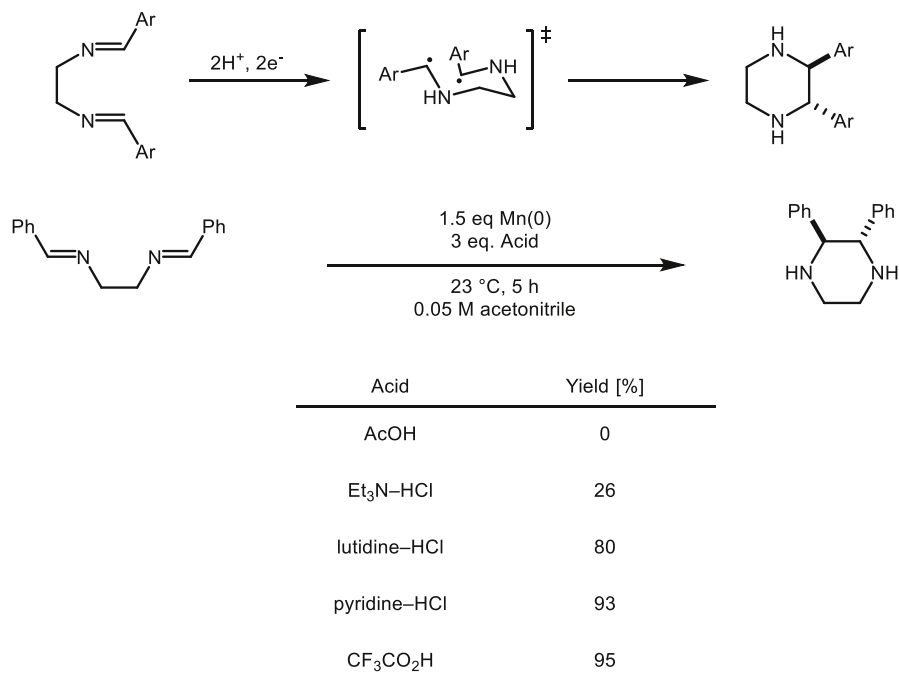
Fig. 54 Reductive coupling of bisimines [258]

Acid	Yield [%]
AcOH	0
Et$_3$N–HCl	26
lutidine–HCl	80
pyridine–HCl	93
CF$_3$CO$_2$H	95
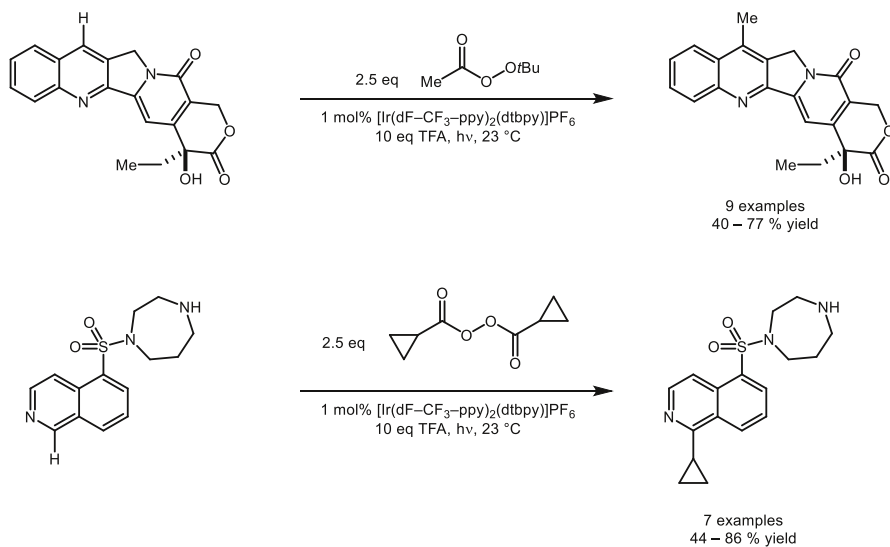
Fig. 55 Late-stage diversification enabled by PCET
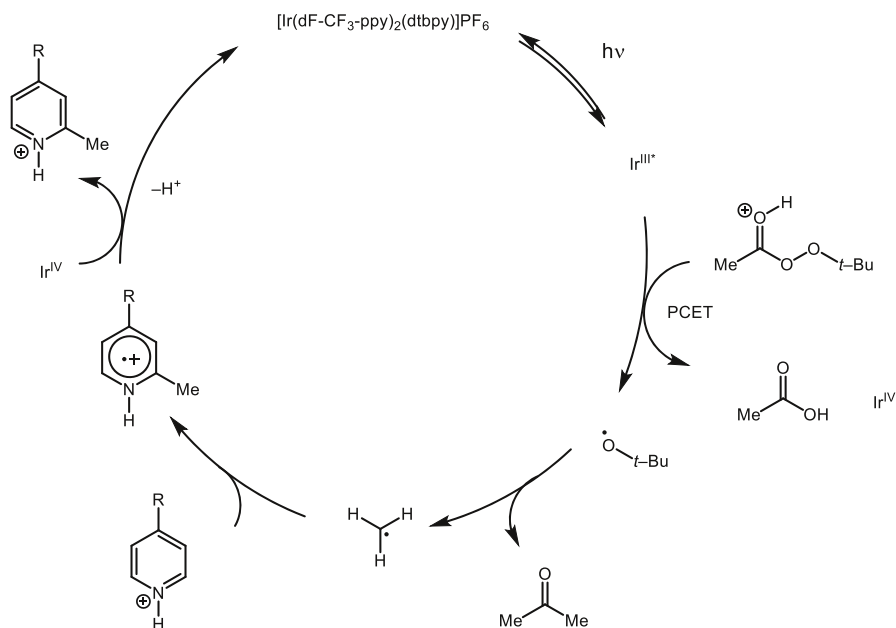
Fig. 56 Proposed mechanism of perester reduction

10 Concluding Remarks

We believe that the examples and discussion above highlight the potential of PCET processes for applications for organic synthesis. Together with the large body of biological, organic, and inorganic mechanistic studies and limited synthetic examples, we are optimistic that PCET will continue to develop as a general mode of organic substrate activation and provide solutions to longstanding challenges in homolytic bond activation catalysis and the associated reaction chemistry of the resulting radicals.

References

1. Migliore A, Polizzi NF, Therien MJ, Beratan DN (2014) Chem Rev 114:3381–3465
2. Reece SY, Hodgkis JM, Stubbe J, Nocera DG (2006) Philos Trans R Soc B 361:1351–1364
3. Cukier RI, Nocera DG (1998) Annu Rev Phys Chem 49:337–369
4. Mayer JM (2004) Annu Rev Phys Chem 55:363–390
5. Huynh MHV, Meyer TJ (2007) Chem Rev 107:5004–5064
6. Weinberg DR, Gagliardi CJ, Hull JF, Murphy CF, Kent CA, Westlake BC, Paul A, Ess DH, McCafferty DG, Meyer TJ (2012) Chem Rev 112:4016–4093
7. Wenger OS (2013) Acc Chem Res 46:1517–1526
8. Warren JJ, Mayer JM (2015) Biochemistry 54:1863–1878
9. Saveant J-M (2014) Annu Rev Anal Chem 7:537–560
10. Meyer TJ, Huynh MHV, Thorp HH (2007) Angew Chem Int Ed 46:5284–5304

11. Stubbe J, Nocera DG, Yee CS, Chang MCY (2003) Chem Rev 103:2167–2201
12. Minnihan EC, Nocera DG, Stubbe J (2013) Acc Chem Res 46:2524–2535
13. Kaila VRI, Verkhovsky MI, Wikström M (2010) Chem Rev 110:7062–7081
14. Lehnert N, Solomon EI (2003) J Biol Inorg Chem 8:294–305
15. Hatcher E, Soudackov A, Hammes-Schiffer S (2004) J Am Chem Soc 126:5763–5775
16. Wang Y, Chen H, Makino M, Shiro Y, Nagano S, Asamizu S, Onaka H, Shaik S (2009) J Am Chem Soc 131:6748–6762
17. Sancar A (2003) Chem Rev 103:2203–2237
18. Costentin C, Drouet S, Robert M, Saveant JM (2012) Science 338:90–94
19. Symes MD, Surendranath Y, Lutterman DA, Nocera DG (2011) J Am Chem Soc 133:5174–5177
20. Hammes-Schiffer S, Iordanova N (2004) Biochim Biophys Acta 1655:29–36
21. Hammes-Schiffer S (2012) Energy Environ Sci 5:7696
22. Green MT, Dawson JH, Gray HB (2004) Science 304:1653–1656
23. Li C, Danovich D, Shaik S (2012) Chem Sci 3:1903–1918
24. Lo JC, Yabe Y, Baran PS (2014) J Am Chem Soc 136:1304–1307
25. Iwasaki K, Wan KK, Oppedisano A, Crossley SWM, Shenvi RA (2014) J Am Chem Soc 136:1300–1303
26. King SM, Ma X, Herzon SB (2014) J Am Chem Soc 136:6884–6887
27. Choi J, Pulling ME, Smith DM, Norton JR (2008) J Am Chem Soc 130:4250–4252
28. Bordwell FG, Cheng JP, Harrelson JA (1988) J Am Chem Soc 110:1229–1231
29. Warren JJ, Tronic TA, Mayer JM (2010) Chem Rev 110:6961–7001
30. Waidmann CR, Miller AJM (2012) Ng C-WA, Scheuermann ML, Porter TR, Tronic TA, Mayer JM. Energy Environ Sci 5:7771–7780
31. Choi GC, Knowles RR (2015) J Am Chem Soc 137:9226–9229
32. Tarantino KT, Liu P, Knowles RR (2013) J Am Chem Soc 135:1002–10025
33. Salamone M, Bietti M (2015) Acc Chem Res 48:2895–2903
34. Mayer JM (2011) Acc Chem Res 44:36–46
35. Mayer JM (2011) J Phys Chem Lett 2:1481–1489
36. Both HAT and PCET have been observed to obey Marcus-type kinetics. The rate constant predicted by the Marcus cross relation is dependent on the driving force of the reaction: more favorable reactions typically result in more rapid kinetics. Consult [34] and [35] for details
37. Yayla HY, Knowles RR (2014) Synlett 20:2819–2826
38. Meyer TJ, Huynh MHV (2003) Inorg Chem 42:8140–8160
39. Binstead RA, McGuire ME, Dovletoglou A, Seok WK, Roecker LE, Meyer TJ (1992) J Am Chem Soc 114:173–186
40. Meunier B, de Visser SP, Shaik S (2004) Chem Rev 104:3947–3980
41. Hammes-Schiffer S, Soudacov AV (2008) J Phys Chem B 112:14108–14123
42. Lingwood M, Hammond JR, Hrovat DA, Mayer JM, Borden WT (2006) J Chem Theory Comput 2:740–745
43. Pesterfield LL, Maddox JB, Crocker MS, Schweitzer GK (2012) J Chem Educ 89:891–899
44. Pourbaix M (1945) Thermodynamique des solutions aqueuses diluées: représentation graphique du rôle du pH et du potentiel. Delft University of Technology, Dissertation
45. Pourbaix M (1974) Atlas of Electrochemical Equilibria in Aqueous Solution. Houston, Texas
46. Behan RK, Hoffart LM, Stone KL, Krebs C, Green MT (2006) J Am Chem Soc 128:11471–11474
47. Hayashi Y, Yamazaki I (1979) J Biol Chem 254:9101–9106
48. Green MT (2009) Curr Opin Chem Biol 13:84–88
49. Yosca TH, Behan RK, Krest CM, Onderko EL, Langston MC, Green MT (2014) J Am Chem Soc 136:9124–9131
50. Namuswe F, Kasper GD (2010) Narducci Sarjeant AA, Hayashi T, Krest CM, Green MT, Moënne-Loccoz P, Goldberg DP. J Am Chem Soc 132:157–167
51. Moyer BA, Meyer TJ (1978) J Am Chem Soc 100:3601–3603
52. Moyer BA, Meyer TJ (1981) Inorg Chem 20:436–444
53. Lebeau EL, Binstead RA, Meyer TJ (2001) J Am Chem Soc 123:10535–10544
54. Binstead RA, Moyer BA, Samuels GJ, Meyer TJ (1981) J Am Chem Soc 103:2897–2899
55. Moyer BA, Sipe BK, Meyer TJ (1981) Inorg Chem 20:1475–1480
56. Roecker L, Dobson JC, Vining WJ, Meyer TJ (1987) Inorg Chem 26:779–781
57. Gilbert JA, Gersten SW, Meyer TJ (1982) J Am Chem Soc 104:6872–6873
58. Gilbert J, Roecker L, Meyer TJ (1987) Inorg Chem 26:1126–1132

59. Seok WK, Meyer TJ (2004) Inorg Chem 43:5205–5215113
60. Gupta R, Taguchi T, Lassalle-Kaiser B, Bominaar EL, Yano J, Hendrich MP, Borovik AS (2015) Proc Nat Acad Sci. USA 112:5319–5324
61. Yano J, Kern J, Sauer K, Latimer MJ, Pushkar Y, Biesiadka J, Loll B, Saenger W, Messinger J, Zouni A, Yachandra VK (2006) Science 314:821–825
62. Britt RD, Campbell KA, Peloquin JM, Gilchrist ML, Aznar CP, Dicus MM, Robblee J, Messinger J (2004) Biochim Biophys Acta 1655:158–171
63. Yachandra VK, Sauer K, Klein MP (1996) Chem Rev 96:2927–2950
64. Gupta R, MacBeth CE, Young VG Jr, Borovik AS (2002) J Am Chem Soc 124:1136–1137
65. Gupta R, Borovik AS (2003) J Am Chem Soc 125:13234–13242
66. Borovik AS (2011) Chem Soc Rev 40:1870–1874
67. Parsell TH, Yang MY, Borovik AS (2009) J Am Chem Soc 131:2762–2763
68. Goldsmith CR, Cole AP, Stack TDP (2005) J Am Chem Soc 127:9904–9912
69. Goldsmith CR, Stack TDP (2006) Inorg Chem 45:6048–6055
70. Olmstead WN, Margolin Z, Bordwell FG (1980) J Org Chem 45:3295–3299
71. Bordwell FG, Cheng J, Ji GZ, Satish AV, Zhang X (1991) J Am Chem Soc 113:9790–9795
72. Taguchi T, Stone KL, Gupta R, Kaiser-Lassalle B, Yano J, Hendrich MP, Borovik AS (2014) Chem Sci 5:3064–3071
73. Shook RL, Peterson SM, Greaves J, Moore C, Rheingold AL, Borovik AS (2011) J Am Chem Soc 133:5810–5817
74. Baldwin MJ, Pecoraro VL (1996) J Am Chem Soc 118:11325–11326
75. Pecoraro VL, Baldwin MJ, Gelasco A (1994) Chem Rev 94:807–826
76. Amin M, Vogt L, Vassiliev S, Rivalta I, Sultan MM, Bruce D, Brudvig GW, Batista VS, Gunner MR (2013) J Phys Chem B 117:6217–6226
77. Caudle MT, Pecoraro VL (1997) J Am Chem Soc 119:3415–3416
78. Lockwood MA, Wang K, Mayer JM (1999) J Am Chem Soc 121:11894–11895
79. Larsen AS, Wang K, Lockwood MA, Rice GL, Won TJ, Lovell S, Sadilek M, Tureček F, Mayer JM (2002) J Am Chem Soc 124:10112–10123
80. Wang K, Mayer JM (1997) J Am Chem Soc 119:1470–1471
81. Thorp HH, Sarneski JE, Brudvig GW, Crabtree RH (1989) J Am Chem Soc 111:9249–9250
82. Ruettinger WF, Ho DM, Dismukes GC (1999) Inorg Chem 38:1036–1037
83. Maneiro M, Ruettinger WF, Bourles E, McLendon GL, Dismukes GC (2003) Proc Nat Acad Sci USA 100:3707–3712
84. Carrel TG, Bourles E, Lin M, Dismukes GC (2003) Inorg Chem 42:2849–2858
85. Bordwell FG, Zhang XM, Cheng JP (1993) J Org Chem 58:6410–6416
86. Kaizer J, Klinker EJ, Oh NY, Rohde JU, Song WJ, Stubna A, Kim J, Münch E, Nam W, Que L (2004) J Am Chem Soc 126:472–473
87. Price JC, Barr EW, Tirupati B, Krebs C, Bollinger JM (2003) J Am Chem Soc 125:13008–13009
88. Nesheim JC, Lipscomb JD (1996) Biochemistry 35:10240–10247
89. Kumar D, Hirao H, Que L, Shaik S (2005) J Am Chem Soc 127:8026–8027
90. Mayer JM (1998) Acc Chem Res 31:441
91. Park J, Lee YM, Nam W, Fukuzumi S (2013) J Am Chem Soc 135:5052–5061
92. Park J, Morimoto Y, Lee YM, Nam W, Fukuzumi S (2012) J Am Chem Soc 134:3903–3911
93. Wang D, Farquhar ER, Stubna A, Münch E, Que L (2009) Nature Chem 1:145–150
94. Collins MJ, Ray K, Que L (2006) Inorg Chem 45:8009–8011
95. Wang D, Que L (2013) Chem Commun 49:10682–10684
96. Sawyer DT, Sobkowiak A, Robers JL (1995) Electrochemistry for Chemists. John Wiley and Sons, New York
97. Ramdhaine B, Stern CL, Goldberg DP (2001) J Am Chem Soc 123:9447–9448
98. Goldberg DP (2007) Acc Chem Res 40:626–634
99. Baglia RA, Prokop-Prigge KA, Neu HM, Siegler MA, Goldberg DP (2015) J Am Chem Soc 137:10874–10877
100. Lansky DE, Goldberg DP (2006) Inorg Chem 45:5119–5125
101. Lansky DE, Mandimutsira B, Ramdhanie B, Clausén M, Penner-Hahn J, Zvyagin SA, Telser J, Krzystek J, Zhan R, Ou Z, Kadish KM, Zakharov L, Rheingold AL, Goldberg DP (2005) Inorg Chem 44:4485–4498
102. Fukuzumi S, Kotani H, Prokop KA, Goldberg DP (2011) J Am Chem Soc 133:1859–1869
103. Prokop KA, de Visser SP, Goldberg DP (2010) Angew Chem Int Ed 49:5091–5095

104. Neu HM, Jung J, Baglia RA, Siegler MA, Ohkubo K, Fukuzumi S, Goldberg DP (2015) J Am Chem Soc 137:4614–4617
105. Boaz NC, Bell SR, Groves JT (2015) J Am Chem Soc 137:2875–2885
106. Bordwell FG (1988) Acc Chem Res 21:456–463
107. Westlake BC, Brennaman MK, Concepcion JJ, Paul JJ, Bettis SE, Hampton SD, Miller SA, Lebedeva NV, Forbes MDE, Moran M, Meyer TJ, Papanikolas JM (2011) Proc Nat Acad Sci. USA 108:8554–8558
108. Chen X, Ma G, Sun W, Dai H, Xiao D, Zhang Y, Qin X, Liu Y, Bu Y (2014) J Am Chem Soc 136:4515–4524
109. Liu W, Huang X, Cheng MJ, Nielsen RJ, Goddard WA III, Groves JT (2012) Science 337:1322–1325
110. Huang X, Bergsten TM, Groves JT (2015) J Am Chem Soc 137:5300–5303
111. Liu W, Groves JT (2010) J Am Chem Soc 132:12847–12849
112. Umile TP, Groves JT (2011) Angew Chem Int Ed 50:695–698
113. Umile TP, Wang D, Groves JT (2011) Inorg Chem 50:10353–10362
114. Svistunenko DA, Cooper CE (2004) Biophys J 87:582–595
115. Sahlin M, Graslund A, Ehrenberg A, Sjöberg BM (1982) J Biol Chem 257:366–369
116. Debus RJ, Barry BA, Babcock GT, McIntosh L (1988) Proc Nat Acad Sci. USA 85:427–430
117. Hsi LC, Hoganson CW, Babcock GT, Smith WL (199) Biochem Biophys Res Commun 202:1592–1598
118. Biczók L, Linschitz H (1995) J Phys Chem 99:1843–1844
119. Biczók L, Gupta N, Linschitz H (1997) J Am Chem Soc 119:12601–12609
120. Gupta N, Linschitz H, Biczók L (1997) Fullerene Sci Tech 5:343–353
121. Maki T, Araki Y, Ishida Y, Onomura O, Matsumura Y (2001) J Am Chem Soc 123:3371–3372
122. Costentin C, Robert M, Savéant JM (2007) J Am Chem Soc 129:9953–9963
123. Lucarini M, Mugnaini V, Pedulli GF, Guerra M (2003) J Am Chem Soc 125:8318–8329
124. Markle TF, Rhile IJ, DiPasquale AG, Mayer JM (2008) Proc Nat Acad Sci. USA 105:8185–8190
125. Markle TF, Tronic TA, DiPasquale AG, Kaminsky W, Mayer JM (2012) J Phys Chem A 116:12249–12259
126. Markle TF, Mayer JM (2008) Angew Chem Int Ed 47:738–740
127. Rhile IJ, Markle TF, Nagao H, DiPasquale AG, Lam OP, Lockwood MA, Rotter K, Mayer JM (2006) J Am Chem Soc 128:6075–6076
128. Costentin C, Robert M, Savéant JM (2010) Angew Chem Int Ed 49:3803–3806
129. Thomas F, Jarjayes O, Jamet H, Hamman S, Saint-Aman E, Duboc C, Pierre JL (2004) Angew Chem Int Ed 43:594–597
130. Reece SY, Nocera DG (2009) Annu Rev Biochem 78:673–699
131. Nagle JF, Morowitz HJ (1978) Proc Natl Acad Sci USA 75:298–302
132. Shinobu A, Agmon N (2009) J Phys Chem A 113:7253–7266
133. Chen K, Hirst J, Camba R, Bonagura CA, Stout CD, Burgess BK, Armstrong FA (2000) Nature 405:814–817
134. Rottenberg H (1998) Biochim Biophys Acta 1364:1–16
135. Wraight CA (2006) Biochim Biophys Acta 1757:886–912
136. Siegbahn PEM, Eriksson L, Himo F, Pavlov M (1998) J Phys Chem B 102:10622–10629
137. Cui Q, Karplus M (2003) J Phys Chem B 107:1071–1078
138. Sjödin M, Irebo T, Utas J, Lind J, Merényi G, Åkermark B, Hammarström L (2006) J Am Chem Soc 128:13076–13083
139. Rhile IJ, Mayer JM (2004) J Am Chem Soc 126:12718–12719
140. Sjödin M, Styring S, Åkermark B, Sun L, Hammarström L (2000) J Am Chem Soc 122:3932–3936
141. Chen J, Kuss-Peterman M, Wenger OS (2014) Chem Eur J 20:4098–4104
142. Rogge CE, Liu W, Wu G, Wang L-H, Kulmacz RJ, Tsai AL (2004) Biochemistry 43:1560–1568
143. Dempsey JL, Winkler JR, Gray HB (2010) Chem Rev 110:7024–7039
144. Gagliardi CJ, Westlake BC, Kent CA, Paul JJ, Papanikolas JM, Meyer TJ (2010) Coord Chem Rev 254:2459–2471
145. Roffey RA, Kramer DM (1994) Govindjee, Sayre RT. Biochim Biophys Acta 1185:257–270
146. Mamedov F, Sayre RT, Styring S (1998) Biochemistry 37:14245–14256
147. Svensson B, Etchebest C, Tuffery P, van Kan P, Smith J, Styring S (1996) Biochemistry 35:14486–14502
148. Wenger OS (2015) Coord Chem Rev 282–283:150–158

149. Prier CK, Rankic DA, MacMillan DWC (2013) Chem Rev 113:5322–5363
150. Concepcion JJ, Brennaman MK, Deyton JR, Lebedeva NV, Forbes MDE, Papnikolas JM, Meyer TJ (2007) J Am Chem Soc 129:6968–6969
151. Bronner C, Wenger OS (2012) J Phys Chem Lett 3:70
152. Pizano AA, Yang JL, Nocera DG (2012) Chem Sci 3:2457–2461
153. Costentin C, Louault C, Robert M, Savéant JM (2009) Proc Nat Acad Sci USA 106:18143–18148
154. Berry BW, Martinez-Rivera MC, Tommos C (2012) Proc Nat Acad Sci USA 109:9739–9743
155. Tommos C, Skalicky JJ, Pilloud DL, Wand J, Dutton DP (1999) Biochemistry 38:9495–9507
156. Martinez-Rivera MC, Berry BW, Valentine KG, Westerlund K, Hay S, Tommos C (2011) J Am Chem Soc 133:17786–17795
157. O'Dea JJ, Osteryoung J, Osteryoung RA (1981) Anal Chem 53:695–701
158. Miles AB, Compton RG (2000) J Phys Chem B 104:5331–5342
159. Glover SD, Jorge C, Liang L, Valentine KG, Hammarström L, Tommos C (2014) J Am Chem Soc 136:14039–14051
160. Zhang MT, Hammarström L (2011) J Am Chem Soc 133:8806–8809
161. Zhang MT, Nilsson J, Hammarström L (2012) Energy Environ Sci 5:7732–7736
162. Gagliardi CJ, Binstead RA, Thorp HH, Meyer TJ (2011) J Am Chem Soc 133:19594–19597
163. Wang Y, Hirao H, Chen H, Onaka H, Nagano S, Shaik S (2008) J Am Chem Soc 130:7170–7171
164. Makino M, Sugimoto H, Shiro Y, Asamizu S, Onaka H, Nagano S (2007) Proc Nat Acad Sci. USA 104:11591–11596
165. De Montellano O (ed) (2015) Cytochrome P450: Structure, Mechanism, and Biochemistry. Springer, Cham
166. Ekberg M, Pötsch S, Sandin E, Thunnissen M, Nordlund P, Sahlin M, Sjöberg BM (1998) J Biol Chem 273:21003–21008
167. Young ER, Rosenthal J, Hodgkiss JM, Nocera DG (2009) J Am Chem Soc 131:7678–7684
168. Hodgkiss JM, Damrauer NH, Pressé S, Rosenthal J, Nocera DG (2006) J Phys Chem B 110:18853–18858
169. Pressé S, Silbey R (2006) J Chem Phys 124:164504
170. Clare LA, Pham AT, Magdaleno F, Acosta J, Woods JE, Cooksy AL, Smith DK (2013) J Am Chem Soc 135:18930
171. Alligrant TM, Alvarez JC (2011) J Phys Chem C 115:10797–10805
172. Nordlund P, Eklund H (1993) J Mol Bio 232:123–164
173. Nordlund P, Sjöberg BM, Eklund H (1990) Nature 345:593–598
174. Hogböm M, Galander M, Andersson M, Kolberg M, Hofbauer W, Lassman G, Nordlund P, Lendzian F (2003) Proc Nat Acad Sci USA 100:3209–3214
175. Himo F, Seigbahn PEM (2003) Chem Rev 103:2421–2456
176. Lendzian F (2005) Biochim Biophys Acta 1707:67–90
177. Lendzian F, Sahlin M, MacMillan F, Bittl R, Fiege R, Pötsch S, Sjöberg BM, Gräslund A, Lubitz W, Lassmann G (1996) J Am Chem Soc 118:8111–8120
178. Byrdin M, Eker APM, Vos MH, Brettel K (2003) Proc Nat Acad Sci USA 100:8676–8681
179. Aubert C, Vos MH, Mathis P, Eker APM, Brettel K (2000) Nature 405:586–590
180. Zieba AA, Richardson C, Lucero C, Dieng SD, Gindt YM, Schelvis JPM (2011) J Am Chem Soc 133:7824–7836
181. Kapetanaki SM, Ramsey M, Gindt YM, Schelvis JPM (2004) J Am Chem Soc 126:6214
182. Byrdin M, Sartor V, Eker APM, Vos MH, Aubert C, Brettel K, Mathis P (2004) Biochim Biophys Acta 1655:64–70
183. Shih C, Museth AK, Abrahamsson M, Blanco-Rodriguez AM, Di Bilio AJ, Sudhamsu J, Crane BR, Ronayne KL, Towrie M, Vlcek A Jr, Richards JH, Winkler JR, Gray HB (2008) Science 320:1760–1762
184. Stoll S, Shafaat HS, Krzystek J, Ozarowski A, Tauber MJ, Kim JE, Britt RD (2011) J Am Chem Soc 133:18098
185. Farver O, Skov LK, Young S, Bonander N, Karlsson BG, Vännguard T, Pecht I (1997) J Am Chem Soc 119:5453–5454
186. Fujita K, Nakamura N, Ohno H, Leigh BS, Niki K, Gray HB, Richards JH (2004) J Am Chem Soc 126:13954–13961
187. Gilardi G, Mei G, Rosato N, Canters GW, Finazzi-Agrò A (1994) Biochemistry 33:1425
188. Gagliardi CJ, Murphy CF, Binstead RA, Thorp HH, Meyer TJ (2015) J Phys Chem C 119:7028–7038

189. Medina-Ramos J, Oyesanya O, Alvarez JC (2013) J Phys Chem C 117:902–912
190. Kuss-Peterman M, Wenger OS (2013) J Phys Chem Lett 4:2535–2539
191. Griesbaum K (1970) Angew Chem Int Ed 9:273–287
192. Heiba EAI, Dessau RM (1967) J Org Chem 32:3837–3840
193. Hoyle CE, Bowman CN (2010) Angew Chem Int Ed 49:1540–1573
194. Tyson EL (2014) Niemeyer Zl, Yoon TP. J Org Chem 79:1427–1436
195. LeBel NA, DeBoer A (1967) J Am Chem Soc 89:2784–2785
196. Benati L, Leardini R, Minozzi M, Nanni D, Scialpi R, Spagnolo P, Strazzari S, Zanardi G (2004) Angew Chem Int Ed 43:3598–3601
197. Denes F, Pichowicz M, Povie G, Renaud P (2014) Chem Rev 114:2587–2693
198. Dang HS, Kim KM, Roberts BP (1998) Chem Commun 1413–1414
199. Zhao R, Lind J, Merenyi G, Eriksen TE (1994) J Am Chem Soc 116:12010–12015
200. Fujisawa H, Hayakawa Y, Sasaki Y, Mukaiyama T (2001) Chem Lett 30:632–633
201. Huyser ES, Kellogg RM (1966) J Org Chem 31:3366–3369
202. Dang HS, Roberts BP (1999) Tet Lett 40:8929–8933
203. Kemper J, Studer A (2005) Angew Chem Int Ed 44:4914
204. Qvortrup K, Rankic DA, MacMillan DWC (2014) J Am Chem Soc 136:626–629
205. Hager D, MacMillan DWC (2014) J Am Chem Soc 136:16986–16989
206. Li JN, Liu L, Fu Y, Guo QX (2006) Tetrahedron 62:4453–4462
207. Kolthoff IM, Chantooni MK, Bhowmik S (1968) J Am Chem Soc 90:23–28
208. Newcomb M, Esker JL (1991) Tetrahedron Lett 32:1035–1038
209. Boivin J, Callier-Dublanchet AC, Quiclet-Sire B, Schiano AM, Zard SZ (1995) Tetrahedron 51:6517–6528
210. Guin J, Frolich R, Studer A (2008) Angew Chem Int Ed 47:779–782
211. Choi CM, Guin J, Mück-Lichtenfeld C, Grimme S, Studer A (2011) Chem-Asian J 6:1197–1209
212. Nicolaou KC, Baran PS, Zhong YL, Barluenga S, Hunt KW, Kranich R, Vega JA (2002) J Am Chem Soc 124:2233–2244
213. Tang Y, Li C (2004) Org Lett 6:3229–3231
214. Li Z, Song L, Li C (2013) J Am Chem Soc 135:4640–4643
215. While many reactions presented throughout the review are done so as closed catalytic cycles, the community has become increasingly aware of potential chain mechanisms. In all instances, we defer to the mechanism presented by the author. For more information, consult: Cismesia MA, Yoon TP (2015) Chem Sci 6:5426–5434
216. Hanss D, Freys JC, Bernardinelli GR, Wenger OS (2009) Eur J Inorg Chem 2009:4850–4859
217. Warren JJ, Menzeleev AR, Kretchmer JS, Miller TF III, Gray HB, Mayer JM (2013) J Phys Chem Lett 4:519–523
218. Warren JJ, Mayer JM (2011) J Am Chem Soc 133:8544–8551
219. Schrauben JN, Cattaneo M, Day TC, Tenderholt AL, Mayer JM (2012) J Am Chem Soc 134:16635–16645
220. Megiatto JD Jr, Méndez-Hernández DD, Tejeda-Ferrari ME, Teillout AL, Llansola-Portolés MJ, Kodis G, Moore TA, Moore AL (2014) Nat Chem 6:423–428
221. Edwards SJ, Soudackov AV, Hammes-Schiffer S (2009) J Phys Chem A 113:2117–2126
222. Miller DC, Choi GC, Orbe HS, Knowles RR (2015) J Am Chem Soc 137:13492–13495
223. Estes DP, Grills DC, Norton JR (2014) J Am Chem Soc 136:17362–17365
224. Roth JP, Mayer JM (1999) Inorg Chem 38:2760–2761
225. Manner VW, Mayer JM (2009) J Am Chem Soc 131:9874–9875
226. Jonas RT, Stack TDP (1997) J Am Chem Soc 119:8566–8567
227. Semproni SP, Milsmann C, Chirik PJ (2014) J Am Chem Soc 136:9211–9224
228. Fang H, Ling Z, Lang K, Brothers PJ, Bruin B, Fu X (2014) Chem Sci 5:916–921
229. Miyazaki S, Kojima T, Mayer JM, Fukuzumi S (2009) J Am Chem Soc 131:11615–11624
230. Wu A, Mayer JM (2008) J Am Chem Soc 130:14745–14754
231. Wu A, Masland J, Swartz RD, Kaminsky W, Mayer JM (2007) Inorg Chem 46:11190–11201
232. Mislmann C, Semproni SP, Chirik PJ (2014) J Am Chem Soc 136:12099–12107
233. Tarantino KT, Miller DC, Callon TA, Knowles RR (2015) J Am Chem Soc 137:6440–6443
234. Huang K, Han JH, Cole AP, Musgrave CB, Waymouth RM (2005) J Am Chem Soc 127:3807–3816
235. Huang K, Han JH, Musgrave CB, Waymouth RM (2006) Organometallics 25:3317–3323
236. Gansauer A, von Laugenberg D, Kube C, Dahmen T, Michelmann A, Behlendorf M, Sure R, Seddiqzai M, Grimme S, Sadasivam DV, Fianu GD, Flowers RA (2015) Chem Eur J 21:280–289

237. Jeftic L, Manning G (1970) J Electroanal Chem 26:195–200
238. Quan M, Sanchez D, Wasylkiw MF, Smith DK (2007) J Am Chem Soc 129:12847–12856
239. Gupta N, Linschitz H (1997) J Am Chem Soc 119:6384–6391
240. Okamoto K, Ohkubo K, Kadish KM, Fukuzumi S (2004) J Phys Chem A 108:10405–10413
241. Gomez M, Gomez-Castro CZ, Padilla-Martinez II, Martinez-Martinez FJ, Gonzalez FJ (2004) J Electroanal Chem 567:269–276
242. Fukuzumi S, Ishikawa K, Hironaka K, Tanaka T (1987) J Chem Soc Perkin Trans II:751–760
243. Fukuzumi S, Ishikawa M, Tanaka T (1989) J Chem Soc Perkin Trans II:1811–1816
244. Ishikawa M, Fukuzumi S (1990) J Chem Soc, Faraday Trans 86:3531–3536
245. Yuasa J, Yamada S, Fukuzumi S (2008) J Am Chem Soc 130:5808–5820
246. Zhai L, Shukla R, Wadumethrige SH, Rathore R (2010) J Org Chem 75:4748–4760
247. Turek AK, Hardee DJ, Ullman AM, Nocera DG, Jacobsen EN (2015) Angew Chem Int Ed 54: doi:10.1002/ange.201508060
248. Bock CR, Connor JA, Gutierrez AR, Meyer TJ, Whitten DG, Sullivan BP, Nagle JK (1997) J Am Chem Soc 101:4815–4824
249. Fukuzumi S, Mochizuki S, Tanaka T (1989) J Am Chem Soc 111:1497–1499
250. Fukuzumi S, Mochizuki S, Tanaka T (1990) J Phys Chem 94:722–726
251. Ishikawa M, Fukuzumi S (1990) J Chem Soc Chem Commun 1353–1355
252. Fukuzumi S, Kuroda S, Goto T, Ishikawa K, Tanaka T (1989) J Chem Soc Perkin Trans II:1047–1053
253. Du J, Espelt LR, Guzei IA, Yoon TP (2011) Chem Sci 2:2115–2119
254. Ischay MA, Anzovino ME, Du J, Yoon TP (2008) J Am Chem Soc 130:12886–12887
255. Du J, Yoon TP (2009) J Am Chem Soc 131:14604–14605
256. Rono LJ, Yayla HY, Wang DY, Armstrong MF, Knowles RR (2013) J Am Chem Soc 135:17735–17738
257. Nakajima M, Fava E, Loescher S, Jiang Z, Rueping M (2015) Angew Chem Int Ed 54:8828–8832
258. Mercer GJ, Sigman MS (2003) Org Lett 5:1591–1594
259. DiRocco DA, Dykstra K, Krska S, Vachal P, Conway DV, Tudge M (2014) Angew Chem Int Ed 53:4802–4806

CrossMark

R E V I E W

Hydrogen-Atom Transfer Reactions

Liang Wang[1] · **Jian Xiao**[1] (ORCID)

Abstract   The cascade [1,n]-hydrogen transfer/cyclization, recognized as the *tert*-amino effect one century ago, has received considerable interest in recent decades, and great achievements have been made. With the aid of this strategy, the inert $C(sp^3)$–H bonds can be directly functionalized into C–C, C–N, C–O bonds under catalysis of Lewis acids, Brønsted acids, as well as organocatalysts, and even merely under thermal conditions. Hydrogen can be transferred intramolecularly from hydrogen donor to acceptor in the form of hydride, or proton, followed by cyclization to furnish the cyclic products in processes featuring high atom economy. Methylene/methine adjacent to heteroatoms, e.g., nitrogen, oxygen, sulfur, can be exploited as hydride donor as well as methylene/methine without heteroatom assistance. Miscellaneous electrophilic subunits or intermediates, e.g., alkylidene malonate, carbophilic metal activated alkyne or allene, α,β-unsaturated aldehydes/ketone, saturated aldehydes/iminium, ketenimine/carbodiimide, metal carbenoid, electron-withdrawing groups activated allene/alkyne, in situ generated carbocation, can serve as hydride acceptors. This methodology has shown preeminent power to construct 5-, 6-, or 7-membered heterocyclic as well as carbon rings. In this chapter, various hydrogen donors and acceptors are adequately discussed.

Keywords   Hydrogen transfer · Hydrogen donors · Hydrogen acceptors · $C(sp^3)$–H functionalization · Heterocycles

---

✉   Jian Xiao
     chemjianxiao@163.com

[1]   College of Chemistry and Pharmaceutical Sciences, Qingdao Agricultural University, Qingdao 266109, China

⁂ Springer

Abbreviations

Cbz	Benzyloxycarbonyl
Cod	1,5-Cyclooctadiene
CSA	Camphorsulfonic acid
DCE	1,1-Dichloroethane
DFT	Density functional theory
DMF	*N,N*-dimethylformamide
DNBS	2,4-Dinitrobenzensulfonic acid
DPP	Diphenyl phosphate
ERC	Electrocyclic ring closure
Fmoc	9-Fluorenylmethoxycarbonyl
HT	Hydrogen transfer
IBX	*O*-iodoxybenzoic acid
m-CPBA	*meta*-Chloroperbenzoic acid
MW	Microwave
MS	Molecular sieves
Pg	Protecting group
*P*TSA	*p*-Toluenesulfonic acid
RT	Room temperature
TCE	1,1,2-Trichloroethane
TFA	Trifluoroacetic acid
TMS	Trimethylsilyl

1 Introduction

When talking about hydride donors, undoubtedly miscellaneous metal hydrides serving as reducing agents should be mentioned first, e.g., $NaBH_4$, $LiAlH_4$, Red-Al, selectride, etc. In addition, organic molecules can also play the role of hydride donors, which could be retrospected to 1853 when Cannizzaro reported base-mediated disproportionation of benzaldehyde into benzyl alcohol and benzoic acid via intermolecular hydride transfer from a deprotonated hemiacetal intermediate onto an aldehyde [1–3]. The Tishchenko reaction may be considered as the seminal example of a reaction proceeding by an intramolecular hydride shift. Evans et al. further developed this reaction to diastereoselectively construct β-hydroxy ketones, which is known as the Evans–Tishchenko reaction [4]. Similarly, by changing the redox state of the reactants in the Tishchenko reaction, the alcohol can be readily oxidized to aldehyde via the Meerwein–Pondorf–Verley (MPV) reduction [5–7], and aldehyde can be reduced to alcohol via the reverse Oppenauer oxidation, which operate by means of an identical Al^{3+}-preorganized intramolecular 1,5-hydride shift [8–10].

Over the past decades, tremendous progress has been made in functionalization of inert C–H with the demand of green and sustainable chemistry [11–14]. The fast development of this vigorous research field arises from the recognition by the chemical community that such methodologies are able to streamline synthetic routes

and facilitate the direct formation of C–C bonds and C–Z bonds (Z=O, N, B, Si, etc.) without prefunctionalization of inert C–H bonds to C–X bonds (X = halogens, OTf, etc.). In this context, a large number of innovative and efficient synthetic methodologies have been developed, thus offering chemists powerful tools for the rapid buildup of molecules with complex architectures. Among these methodologies, the transition metal-catalyzed $C(sp^2)$–H bond activation has dominated this area and the direct functionalization of inert $C(sp^3)$–H bonds still remains a great challenge owing to the high bond dissociation energy of $C(sp^3)$–H bonds. Only recently, some promising catalytic processes for the selective functionalization of $C(sp^3)$–H have been reported with noble metal salts, e.g., Pd, Rh as catalysts. Despite numerous challenges posed by direct $C(sp^3)$–H bond activation, the cascade [1,n]-hydrogen transfer/cyclization process opens new avenues, which provides organic chemists unusual solutions to address their synthetic challenges [15–20]. This fascinating chemistry was discovered in 1895, which was initially termed as 'tert-amino effect' by Meth-Cohn and Suschitzky in 1972 [21]. This name refers to the tendency of substituted N,N-dialkylanilines to undergo unusually facile ring-closing reactions involving various groups at the ortho position. However, the tertiary amine group is neither necessary nor sufficient to guarantee a successful reaction for a particular substrate.

The substrate requires a hydride acceptor proximal to a C–H bond serving as hydride donor, and the reaction is initiated by a hydride shift (or related H-atom-transfer step), which formally oxidizes the carbon donor and reduces the hydride acceptor. The new C–X bond will be formed at the hydride-donor atom, after the hydride shift takes place. The defining characteristic for these reactions is the functionalization of a C–H bond concurrent with a hydride shift. The names proposed by Sames ("HT-cyclization") and Akiyama ("Internal Redox Cascade") would seem more appropriate if focusing more on the unique hydride-shift mechanism that draws together a diverse group of substrates, at least for intramolecular examples.

This cascade process has been recognized as an efficient and powerful method for selective activation and direct functionalization of inactive $C(sp^3)$–H bonds. It represents an intriguing sequential $C(sp^3)$–H activation/C–C, C–N or C–O bonds formation process and proves to be a versatile protocol to construct 5-, 6-, or 7–membered hetero/carbon spiro or fused cycles, such as tetrahydroquinolines [22], chromans [23–25], spiroethers [26–30], and tetrahydropyrans [31–36], which are common moieties in biologically important natural products and pharmaceuticals.

A series of significant review papers have been published on this chemistry [15–18] and we aim to cover the progress in this field since 2006. Some reputable groups such as Sames, Seidel, Akiyama, Vidal, Liu, and Gagosz showed preeminent applications of this methodology to build various hetero/carbon spirocycles and fused rings. In the following, these elegant findings will be categorized according to the types of hydride donors (i.e., tert-amino effect, $C(sp^3)$–H bonds α to ethereal oxygen and sulfur, benzylic $C(sp^3)$–H bond, non-benzylic $C(sp^3)$–H bond) and the types of hydrogen acceptors (benzylidene malonate, transition metal activated alkyne or allene, enal or enone, aldehyde or

imine, ketenimine/carbodiimide). This review will provide elementary insight into these cascade reactions concerning the mechanism, the reactivity of hydrogen donor and acceptor, migration modes of hydrogen, etc.

2 Mechanistic Insight into [1,5]-Hydrogen Transfer

[1,5]-Hydrogen transfer is selected as a model reaction for discussing the mechanism as it is the most common mode of hydrogen migration.

2.1 Possible Reaction Pathways

The exact nature of the hydrogen transfer is still a matter of debate in the scientific community. Some argue that hydrogen is transferred via a sigmatropic shift, whereas others believe that the migration of hydrogen to the acceptor occurs in the form of a hydride anion [37–42]. A plausible mechanism of this transformation is depicted in Scheme 1. Initially, **1** and zwitterion **B** form a resonance hybrid. Subsequently **B** undergoes [1,5]-hydrogen transfer in the form of a sigmatropic hydrogen, resulting in zwitterion **A**. A consecutive intramolecular nucleophilic attack affords the final cyclic product **2** [43–45].

This cascade process can also be rationalized in an alternative way (Scheme 2). The zwitterion **A** is generated from **1** via [1,5]-hydrogen transfer from the carbon α to heteroatom **X** to the electrophilic acceptor in the form of hydride anion, followed by an intramolecular 6-*endo-trig* cyclization (or intramolecular nucleophilic attack), giving rise to the heterocycle **2** [46–48]. DFT calculations show that [1,5]-hydride (or hydrogen) transfer is the rate-determining step and the energy barrier of the subsequent cyclization step is very low [49–52]. Generally speaking, the second theoretical explanation is more reasonable because the aromatic ring is dispensable and the cascade HT-cyclization can proceed smoothly within many aliphatic substrates.

The final cyclization can also proceed in the manner of a 6π-electrocyclic ring closure (6π-ERC) (Scheme 3). After a [1,5]-hydride transfer, the conjugated 1,3,5-hexatriene intermediate **I** can be produced, which undergoes subsequent 6π-ERC to give the cyclized product **4**. Thus, the formation of unstable zwitterionic intermediate **A** (Schemes 1, 2) with charge separation is avoided [52–56].
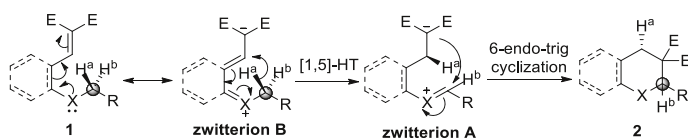
Scheme 1 The sigmatropic transfer of hydrogen

Scheme 2 The transfer of hydride anion through space

X = NR, O, CH₂, CHR; E= electron-withdrawing groups, e.g. CO₂R
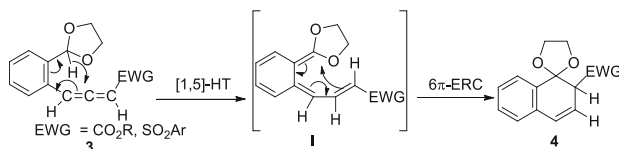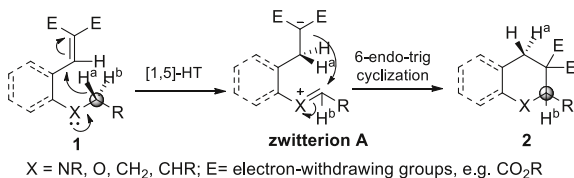
Scheme 3 Cascade [1,5]-hydride transfer/6π-electrocyclic ring closure

2.2 Reactivity of Different Hydrogen Donors

Heteroatoms, e.g., nitrogen, oxygen, and sulfur, adjacent to hydrogen donors (methylene or methine) can facilitate the hydride migration, so do aryl groups and alkyl groups. Theoretically, the heteroatoms play three roles. Firstly, heteroatoms with high electronegativities will polarize the C–X bond, causing the weakening of the C–H bond. Secondly, the hyperconjugation effect of σ^*C–H orbital with a neighboring atom lone pair or π-orbital promotes the hydride shift (Fig. 1) [57–59]. This effect not only weakens the $C(sp^3)$–H bond but also increases the negative charge density of the hydrogen atom.

Thirdly, the carbocationic intermediate generated upon hydride migration, with which iminium, oxocarbenium, and thiocarbenium can form resonance hybrids, would be stabilized by adjacent heteroatoms via p–p conjugation. Consequently, the rate of $C(sp^3)$–H bond cleavage is closely associated with the stability of cationic intermediate, thus any factor that can stabilize this intermediate will dramatically promote this process, while the groups destabilizing it will retard the proximal $C(sp^3)$–H bond cleavage. In contrast to iminium cation, which has considerable stability, oxocarbenium- and thiocarbenium ions are less stable and more difficult to generate, not to mention benzylic and *tert*-alkyl carbocation (Fig. 2). DFT calculations and experimental results show that the thiocarbenium ion exhibits a little bit higher stability than the oxocarbenium species [60]. The cationic

Fig. 1 The electronic assistance from heteroatom and aryl group
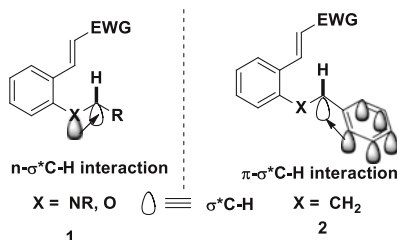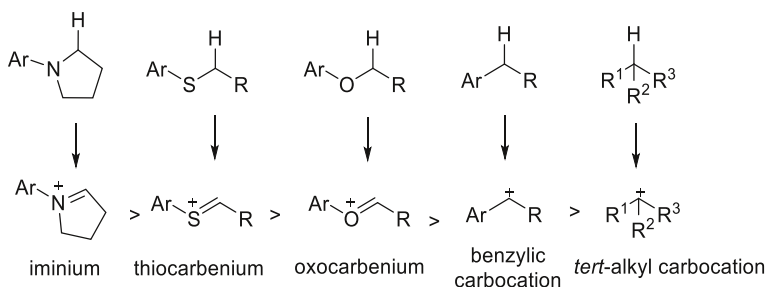
Fig. 2 Stability comparison of different cations

intermediate can also be stabilized by the aromatic or alkyl substituents on the hydrogen donors via π–p conjugation or σ–p hyperconjugation, respectively. Primary C–H bond is rarely exploited as hydrogen donor except in Zhang's and Chatani's reports [40, 61, 62]. In addition to the above-mentioned hydride donors, acetalic and dithioacetalic C–H bonds can also work as the hydride donors [52, 57–59].

2.3 Activation Mode of Hydride Acceptors

Almost all the electrophilic groups or electrophilic intermediates can be employed as the hydride acceptors, e.g., alkylidene malonates, carbophilic transition metals activated alkynes or allenes, enal/enones, aldehyde/ketones, imines, ketenimine/carbodiimides, metal carbenoids, alkynes carrying electron-withdrawing groups, as well as in situ-generated carbocations (Fig. 3).

The feasibility of hydrogen transfer strongly depends on the natures of hydrogen acceptors and donors. It can be imagined that there is competition between the transient cationic subunits and the electrophilic hydride acceptors for the hydride after cleavage of the inert $C(sp^3)$–H bond (Fig. 3). If the hydride acceptor is
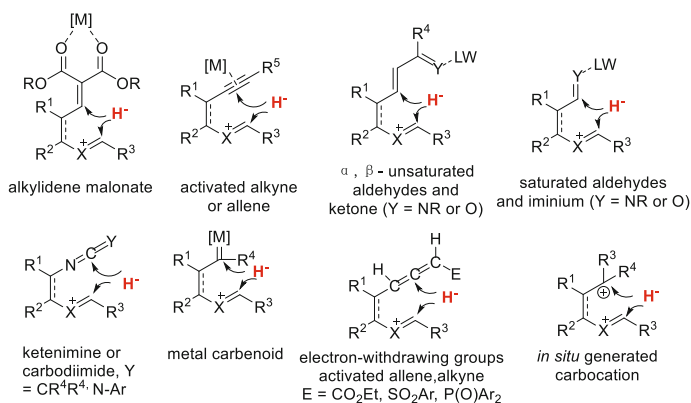
Fig. 3 Different types of hydride acceptors and activation modes

electrophilic enough, it can "snatch" hydride to give the zwitterion **A**, followed by an intramolecular nucleophilic attack to give the cyclized product **2** (Scheme 2); whereas if not, the cationic subunit will "retrieve" hydride and no reaction will occur. Therefore, two strategies are applicable to facilitate the cascade process, i.e., increasing the electrophilicity of the hydride acceptor or increasing the stability of the cationic subunit generated in situ upon hydride migration. Remarkably, hydrogen can be transferred not only in the form of hydride anion but also in the form of protons and hydrogen atoms [63]. If the hydrogen acceptor is a relatively strong nucleophile, hydrogen will be abstracted by the acceptor in the form of a proton [53, 62, 64–68], and if the hydrogen acceptor is a free radical, the C–H of hydrogen donator will be homolyzed to give the hydrogen atom, which is then transferred to the hydrogen acceptor [63]. The hydrogen can be transferred not only in [1,5]-manner but also in the manners of [1,4]-[69, 70] [1,6]-[39, 66, 71–77], and [1,9]-manner [78]. If the hydride donor and acceptor are active enough, the hydride migration may occur through space, giving rise to a zwitterionic intermediate. Only if the nucleophile and electrophile in the zwitterionic intermediate are located in proper geometric positions, the subsequent intramolecular nucleophilic attack will occur, resulting in the formation of 5- [72, 73], 6-, or 7- [41, 79, 80] membered products. If no nucleophile is available or cyclization was blocked by steric hindrance, hydride will merely serve as reductant [81–84] or unwanted side products will be produced [74].

3 C(sp^3)–H Bond Adjacent to *Tert*-Amino Moieties as Hydride Donor (*tert*-Amino Effect)

The term "*tert*-amino effect" is used to describe ring-closure of *N*, *N*-dialkyl-substituted anilines with an unsaturated electrophilic *ortho* substituent to afford fused tetrahydroquinolines [22] or other *N*-heterocycles [15, 19, 20, 46, 85–87]. The *tert*-amino effect has been widely utilized in the synthesis of pyridine, pyrimidine, and pyridazine derivatives, which has been well reviewed by Mátyus et al. [15].

3.1 Electrophilic Benzylidene Malonates as the Hydride Acceptors

Hurd et al. elegantly elaborated this methodology in the key step of total synthesis of PNU-286607 (Scheme 4) [88]. The benzylidene intermediate **5** was prepared in situ and [1,5]-hydride migration readily proceeded under thermal conditions to give zwitterionic intermediate **6**. Via *trans–cis* isomerization of methyl group, the zwitterion **6** was converted to thermodynamically more favorable zwitterion **7**, and a subsequent intramolecular equatorial attack of the enolate on the iminium subunit furnished *cis* (−)-PNU-286607 in 74 % yield and >99:1 er.

For a long time, harsh thermal conditions were always needed to overcome the high energy barrier of [1,5]-hydride transfer, which severely limited the application of this strategy. Seidel et al. employed Ga(OTf)$_3$ to catalyze the cascade process of **8**, via which tetrahydroquinolines **9** could be furnished in 90 % yield within 15 min at room temperature (Scheme 5) [89]. Meanwhile, the chiral bisoxazoline

magnesium complex **10** was employed to catalyze the asymmetric version of this reaction, furnishing the enantio-enriched product **9** in 74 % yield and 30 % ee, which presented the first report of enantioselective cascade [1,5]-HT/cyclization.

Akiyama et al. disclosed a chiral phosphoric acid **13**-catalyzed asymmetric cascade [1,5]-HT/cyclization of **11**, which afforded tetrahydroquinolines **12** with good to excellent enantioselectivity (Scheme 6) [90]. The benzylidene malonate subunit forms hydrogen bonds with the proton of phosphoric acid **13**, which not only increased the electrophilicity of hydride acceptor but also governed the asymmetric step. Presumably, the stereoselectivity is mostly controlled at the hydride shift step and the enantiotopic hydrogen is selectively activated by chiral phosphoric acid **13**.

One more asymmetric version of cascade [1,5]-hydride transfer/cyclization was reported by Feng et al. using his well-known chiral *N, N′*-dioxide-Co(II) complex **14** as catalyst. The optically active tetrahydroquinolines **15** were obtained in excellent yields and high enantioselectivities (Scheme 7) [91]. Theoretically, the oxygen atoms of *N, N′*-dioxide, amide, and the benzylidene malonate are coordinated to cobalt(II) in a hexadentate manner, hence the carbanion prefers to attack the *Re* face rather than the *Si* face of the iminium because the latter is strongly shielded by the nearby anthracenyl ring, furnishing the (*S*)-configured products.
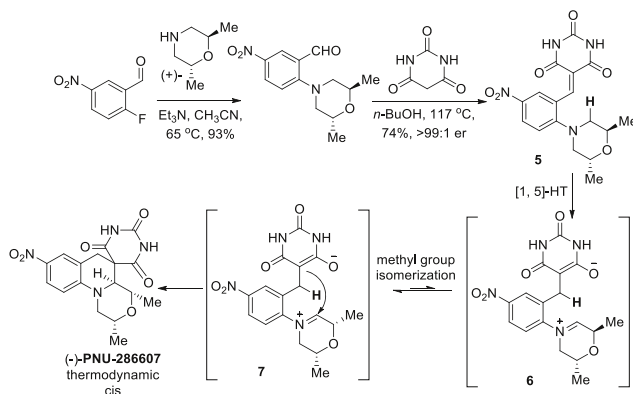
Scheme 4 Elegant elaboration of the cascade 1,5-HT/cyclization in the total synthesis of (−)-PNU-286607
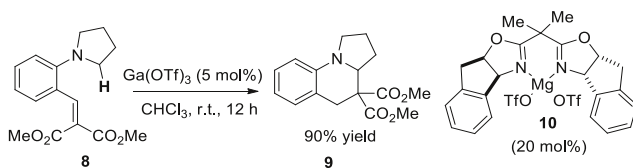
Scheme 5 Lewis acid-catalyzed formation of tetrahydroquinolines
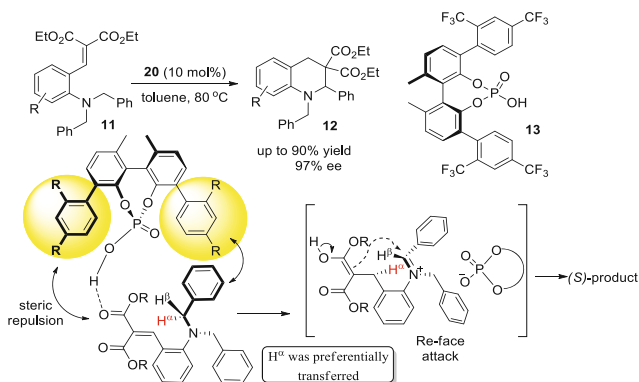
Scheme 6 Chiral phosphoric acid-catalyzed asymmetric synthesis of tetrahydroquinoline

Scheme 7 Chiral complex of *N,N′*-dioxide and cobalt(II)-catalyzed synthesis of tetrahydroquinolines
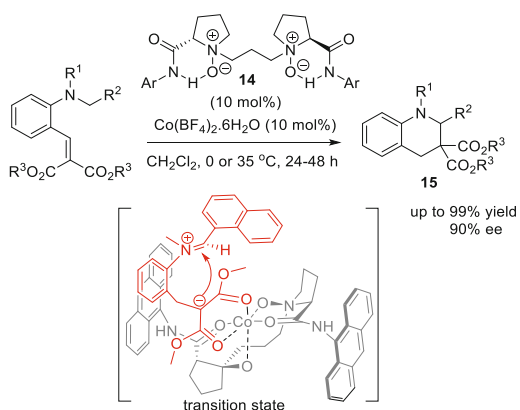
Luo et al. exploited a binary catalytic system, which involved Mg(BF$_4$)$_2$ and chiral phosphoric acid **18** to facilitate the cascade reaction of **16**, furnishing the enantio-enriched products **17** in high yields and enantioselectivities (Scheme 8) [49, 50]. Both H^a and H^b on the isoquinoline methylene carbon atom may participate in [1,5]-hydride transfer, requiring two different helical conformations **I** and **II**. Due to the suprafacial constraint, however, **I** is more favorable than **II** owing to its space tolerance. Therefore, the selective activation in complex **I** initiates enantiotopic [1,5]-H^b transfer, leading to the chiral helical zwitterionic intermediate. Finally, the C–C bond can be formed spontaneously with preserved stereochemistry after a small conformational change.

Matyus et al. described a cascade Knovenagel/1,5-hydride transfer/cyclization reactions of 4-aryl-2-phenyl-1,4-benzoxazepine derivatives **19**, which furnished fused *O,N*-heterocycles **20** containing tetrahydro-1,4-benzoxazepine and tetrahydroquinoline moieties with high yields and diastereoselectivity (Scheme 9) [92]. Basically, under thermal conditions, the benzylidene intermediate **I** generated in situ

Scheme 8 Catalytic enantioselective *tert*-amino cyclization by asymmetric binary acid catalysis
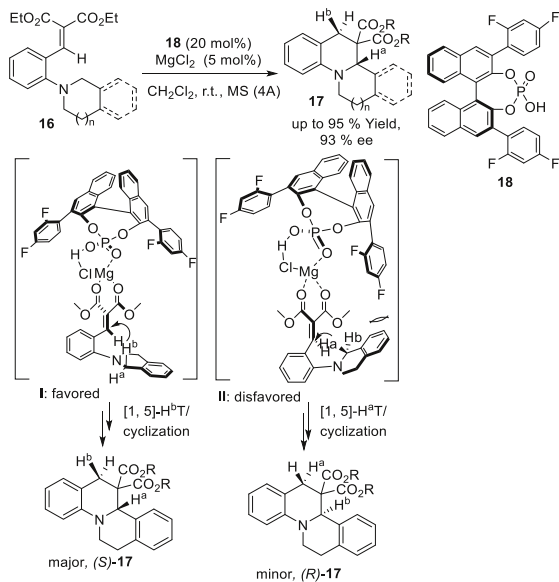
Scheme 9 Synthesis of 1,4-benzoxazepines by domino Knoevenagel–[1,5]-hydride shift cyclization reaction
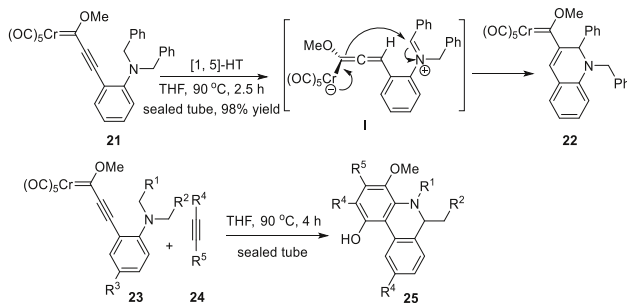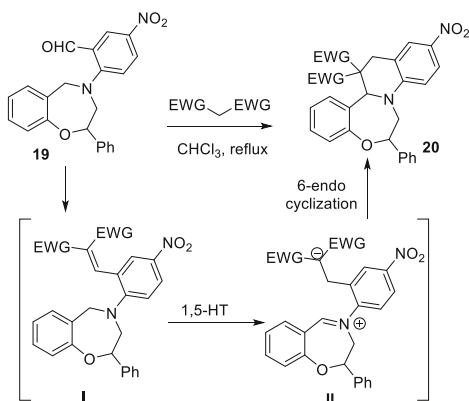
Scheme 10 Synthesis of 1,2-dihydroquinolinyl carbene complexes via [1,5]-HT/cyclizations

underwent sequential 1,5-hydride shift and intramolecular 6-endo cyclization readily to furnished **20**.

3.2 Electrophilic Activated Alkyne as the Hydride Acceptor

Electron-deficient alkyne can also serve as an ideal hydride acceptor. Barluenga et al. described a [1,5]-hydride transfer/cyclization process of alkynyl Fischer carbene complexes **21**, which afforded 1,2-dihydroquinolynyl carbene complexes **22** (Scheme 10) [51]. The alkyne moiety in **21** activated by electrophilic Fischer carbene was a good hydride acceptor. Theoretically, migration of hydride from the benzylic methylene to the highly electrophilic β carbon of the triple bond generates zwitterionic intermediate **I** and a subsequent cyclization leads to the new carbene complex **22**, which can be further elaborated [51, 93]. The presence of strong electron-withdrawing chromium pentacarbonyl moiety is crucial to trigger the energy-demanding [1,5]-hydride transfer. When alkynyl carbene complex **23** was heated with four equivalents of 1-hexyne **24**, 5,6-dihydrophenantridine derivative **25** could be afforded.

The alkynes activated by alkynophilic metals, e.g., platinum and ruthenium, are considerably electrophilic, which can be employed as good hydride acceptors for the cascade [1,5]-HT/cyclization process. Chatani et al. reported a cycloisomerization of 9-carbazolyl substituted 1-alkyl-2-ethynylbenzene **26** catalyzed by alkynophilic metal salts PtCl$_2$ and [RuCl$_2$(CO)$_3$]$_2$ under mild conditions, which produced substituted indene **27** (Scheme 11) [40]. Basically, the metal-vinylidene complex **I** is formed initially via π-activation of alkyne moiety, then benzylic hydride is delivered in [1,5]-manner to the most electrophilic α-carbon of metal vinylidene, resulting in zwitterionic intermediate **II**. Afterwards, the metal carbenoid intermediate **III** generated via resonance of intermediate **II** undergoes 6π-electrocyclization to give intermediate **IV** and a final reductive elimination gives rise to the cyclized product **27**.

A methylene group adjacent to a protected secondary amine, e.g., carbamate, could also be exploited as hydride donor. Remarkably, as the lone pair of nitrogen was partially transferred to carbonyl group via p–π conjugation, the electron-donating ability of nitrogen was significantly decreased and the negative charge

Scheme 11 Platinum and ruthenium-catalyzed cyclo-isomerization of 1-alkyl-2-ethynylbenzenes
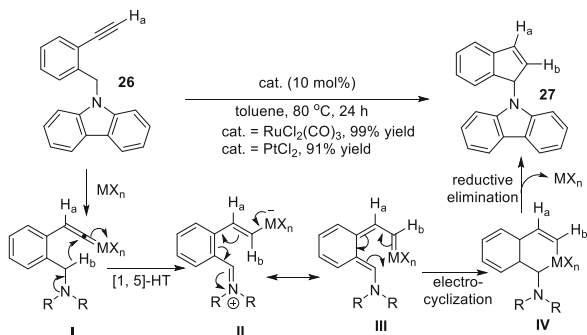
density of the hydrogen atom could only be partially increased by nitrogen via hyper-conjugative interaction compared with *tert*-amine. Therefore, high valent metal salts owning stronger activation ability should be employed to facilitate the cascade process. Additionally, because of the electron-withdrawing nature of carbamates, electron density on the nitrogen atom was decreased, resulting in comparative difficulty in forming alkoxycarbonyl-iminium intermediate, which is less stable than that generated from *tert*-amine. Sames et al. reported a PtI₄-catalyzed α-alkenylation of protected cyclic secondary amines **28**, which afforded annulation products **29** (Scheme 12) [39]. Spirocyclization products **29** could also be furnished in good yield via the cascade protocol if the terminal alkyne was substituted at C(2) of cyclic amine **30**. Theoretically, the platinum vinylidene **I** is formed via π-activation of the alkyne moiety, followed by [1,6]-hydride transfer through space to afford intermediate **II**, in which the nucleophilic vinyl-platinum attacks the electrophilic alkoxycarbonyl-iminium fragment to give the intermediate **III**. A final platinum salt elimination gives rise to the fused products **29** or **31**.

Liang et al. described a palladium-catalyzed cascade [1,5]-HT/cyclization of propargylic esters **32** to construct substituted naphthylamines **33** (Scheme 13) [53]. Notably, propargylic esters substituted with electron-rich aryl groups, which led to electron-rich allenyl-palladium complex at the propargylic position, always gave better yields than the ones with electron-withdrawing substituents, and the electron-withdrawing acyl or sulfonyl group on the nitrogen was crucial to the reaction. These clues indicated the hydrogen was abstracted by nucleophilic allenyl-palladium in the form of proton. Mechanistically, the nucleophilic allenyl-palladium intermediate **II** is generated from the propargylic compound **32** under the catalysis of Pd(0), then [1,5]-proton transfer follows to afford the intermediate **III**, the direct 6π-electrocyclic ring closure (ERC) of which leads to the intermediate **IV**. Afterwards, **IV** undergoes [1,3]-hydrogen shift and elimination to afford the final product **33** (path A). Alternatively, the intermediate **VI** may also be formed via a [1,3]-palladium shift of the intermediate **III**. The following insertion of the C-Pd bond and hydrogen elimination afford the product **33** (path B).

Scheme 12 Platinum-catalyzed *N*-alkenylation via [1,6]-HT/cyclization
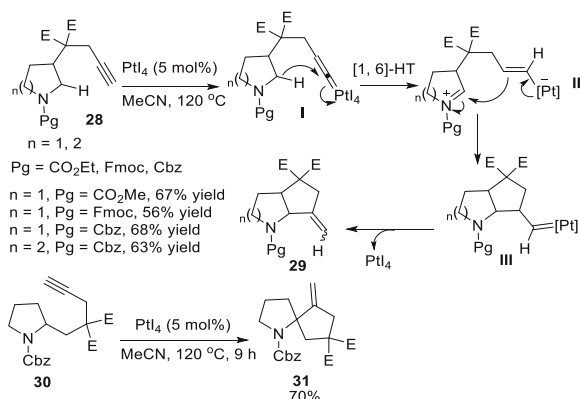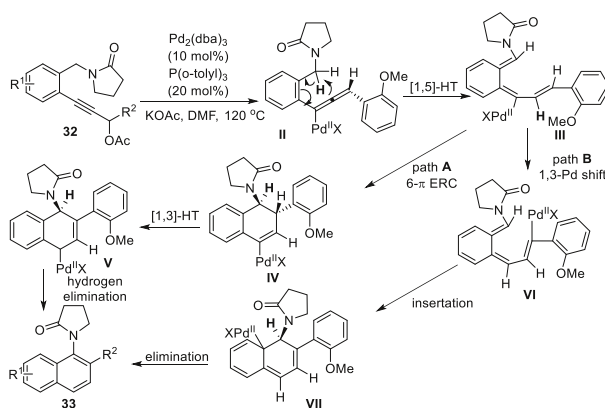
Scheme 13 Palladium-catalyzed [1,5]-proton migration of propargylic esters toward substituted naphthylamines
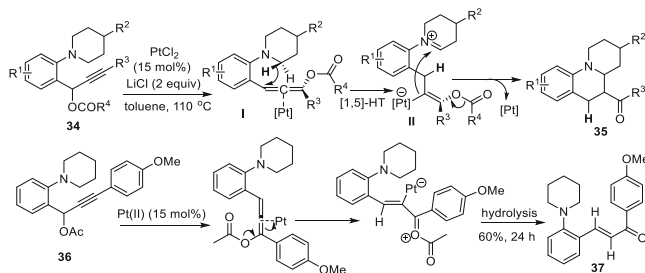
Scheme 14 Platinum-catalyzed synthesis of ring-fused tetrahydroquinolines

The same group also reported a PtCl$_2$-catalyzed hydro-functionalization reaction of allenes formed in situ from propargylic esters **34**, which furnished multi-functionalized tetrahydroquinolines **35** (Scheme 14) [42]. If R^3 is an electron-withdrawing group, the formation of products **35** is favored. Mechanistically, hydride is delivered initially to C(1)-carbon of platinum activated allene intermediate **I** formed via platinum-catalyzed [1,3]-OAc migration. The resulting vinyl-platinum species **II** then attacks the iminium to furnish the fused tetrahydroquinoline **35**. A completely different transformation occurred in the case of propargylic ester **36** bearing a strong electron-donating 4–MeOC$_6$H$_5$ group in R^3, furnishing an α, β-unsaturated ketone **37**, which suggested that electron-donating 4–OMeC$_6$H$_5$ group in R^3 decreased the electrophilicity of C(1), and the hydration of allene would be more favored than [1,5]-hydride shift.

Zhang et al. reported an efficient synthesis of piperidin-4-ones based on gold-catalyzed cascade process (Scheme 15) [61, 68]. One-pot sequential *m*-CPBA oxidation and gold-catalysis with Ph$_3$PAuNTf$_2$ led to an excellent yield of piperidin-4-one **39**. This chemistry allowed facile preparation of 5-, 6-, and 7-membered ring-fused or spiro-piperidin-4-ones. Initially, Zhang et al. speculated that tertiary
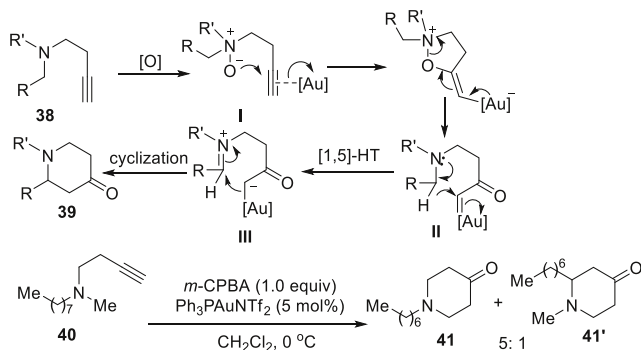
Scheme 15 Formal [4 + 2] approach toward piperidin-4-ones via Au catalysis

aliphatic amine *N*-oxide **I** generated via *m*-CPBA oxidation of tertiary amine **38** might undergo gold-catalyzed intramolecular alkyne oxidation [94] to furnish α-oxo gold carbene **II**, in which α-hydride would migrate to the electrophilic gold carbene, leading to the formation of zwitterion **III** containing an electrophilic iminium and a nucleophilic gold-enolate. A subsequent intramolecular cyclization furnished piperidin-4-one **39**. Notably, the less-substituted methyl in amine **40** was preferentially involved in the ring formation with serviceable regioselectivities (5:1). In all the substrates whose *tert*-amine moieties are unsymmetrical, the chemistry behavior of hydrogen donors was rather unusual, i.e., the poor hydride donors were more active than good hydride donors, e.g., methyl > methylene and benzylic methylene, methylene > methine, electron-rich benzylic methylene ≈ electron-deficient benzylic methylene. Although the proposed mechanism could account for the formation of product **41** and **41'**, it failed to explain the regioselectivity. Thus, the initially proposed mechanism of [1,5]-hydride transfer/cyclization is quite questionable.

Based on DFT calculation and a variety of control experiments, Zhang and Houk et al. argued that the mechanism involving the sequential ring opening and [1,5]-proton **s**hift was energetically more favorable (Scheme 16) [62]. Presumably, the first step is a *syn* addition of gold-coordinated *N*-oxide **42** to alkyne, resulting in the formation of intermediate **43**, which undergoes a hetero-retro-ene ([1,5]-proton **s**hift) to furnish intermediate **44**, thus the formation of gold-carbenoid intermediate **III** is avoided. The final step is a cyclization of **44** to yield piperidin-4-one derivatives **45** and regenerate the catalyst, which was calculated to be the rate-determining step. In **43**, phosphine ligand makes the adjacent carbon more
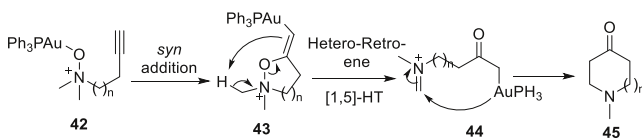
Scheme 16 Mechanism of Au(I)-catalyzed rearrangements of acetylenic amine-*N*-oxides

nucleophilic, thus the proton is abstracted from the least sterically hindered amine-substituent.

3.3 Electrophilic α,β-Unsaturated Aldehyde and Acyl Oxazolidinone as the Hydride Acceptors

Sames et al. reported a PtCl$_4$-catalyzed α-alkylation of protected pyrrolidine **46**, via which the fused cycles **47** was furnished in good yield and high diastereoselectivity (dr > 15:1) (Scheme 17) [95]. Notably, the conformational rigidity of the substrate **46** could be increased significantly by the malonate moiety, which led to a more reactive hydride acceptor [96]. Because the iminium subunit in intermediate **II** could be significantly destabilized by carbamate, which rendered secondary C–H bond in intermediate **I** serving as hydride donor less reactive, high catalyst loading (30 mol%) of highly active PtCl$_4$ was indispensable to get decent yield (77 %).

Seidel et al. exploited the complex of Mg(OTf)$_2$ and chiral bisoxazoline **50** to catalyze the cascade reaction of substrates **48** carrying α, β-unsaturated acyl oxazolidinone, which produced chiral tetrahydroquinolines **49** in good yields and high enantioselectivities (Scheme 18) [97]. The employment of nickel perchlorate in combination with ligand **50** also furnished **49** in good diastereo- and enantioselectivity.

Chiral secondary amine could be employed to catalyze this cascade process. Kim et al. utilized Jørgensen catalyst **53** successfully to catalyze the cascade [1,5]-HT/ring closure sequences of o-N-pyrrolidinyl-substituted cinnamaldehydes **51** via sequential iminium and enamine activation, affording chiral tetrahydroquinolines **52** in high enantioselectivities (Scheme 19, a) [98]. Products incorporated with 7- to

Scheme 17 PtCl$_4$-catalyzed hydroalkylation of α, β-unsaturated aldehydes
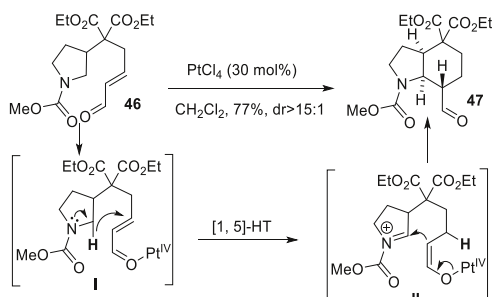
Scheme 18 Chiral Mg-bisoxazolidine complex-catalyzed intramolecular redox reactions via [1,5]-HT/cyclization
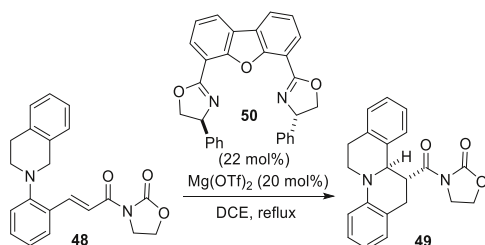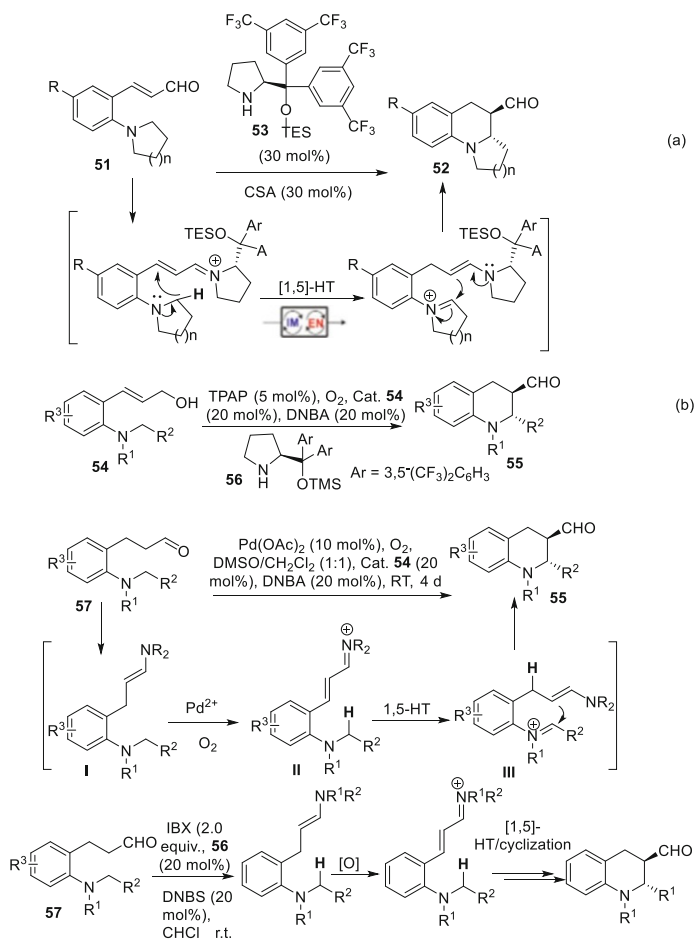
Scheme 19 Organocatalyzed enantioselective C–H bond functionalization via cascade [1,5]-HT/ring closure

9-membered azacycles could also be formed with excellent enantioselectivities. The enal could also be furnished in situ via aerobic oxidation of allylic alcohol. The same group described a one-pot transformation of 3-arylprop-2-en-1-ol derivatives **54** into tetrahydroquinolines **55** via a sequence of Ru(VII)-catalyzed aerobic oxidation/1,5-hydride transfer/cyclization (Scheme 19, b) [99], in which an in situ generated enal served as hydride acceptor. TMS substituted prolinol ether **56** was exploited as chiral catalyst, achieving high levels of enantioselectivity. Additionally, the saturated aldehyde **57** could be employed as the precursor of hydride acceptor, which was transformed in situ to α,β-unsaturated iminium **II** via Pd(II)-catalyzed aerobic oxidation (Scheme 19, c). Via a cascade Saegusa-type oxidative enamine catalysis/1,5-HT/cyclization sequences, which was catalyzed by Pd(II) and prolinol ether **56** in a relay style [100], tetrahydroquinolines **55** was prepared in
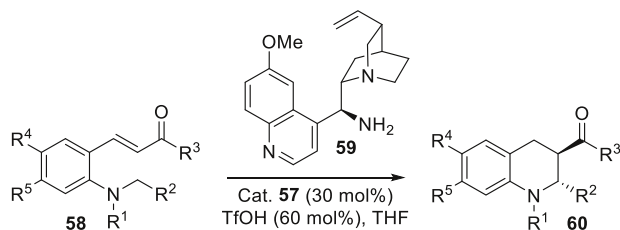
Scheme 20 Chiral primary amine-catalyzed asymmetric synthesis of tetrahydroquinolines via 1,5-HT/cyclization
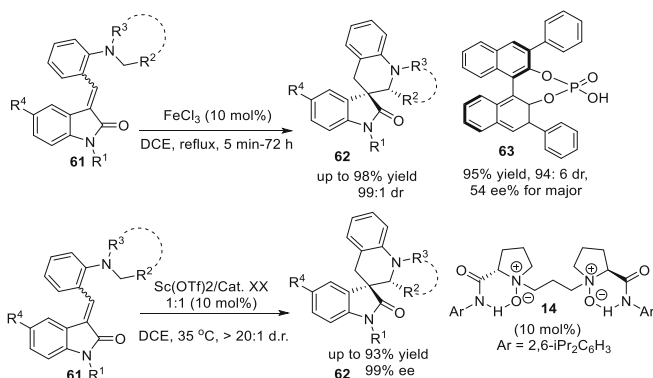
Scheme 21 FeCl$_3$-catalyzed synthesis of spirooxindole tetrahydroquinolines

moderate yields and high levels of enantioselectivity. Furthermore, the electrophilic α,β-unsaturated iminium **II** could also be generated under metal-free oxidation condition (Scheme 19, d) [101]. The same group reported a Jørgensen catalyst **56**-catalyzed enantioselective three-step cascade reaction of substrate **57** involving oxidation/[1,5]-hydride transfer/ring closure, [102] in which IBX was exploited as oxidative agent to transform enamine to hydride acceptor **II**, furnishing tetrahydroquinolines **58** in moderate yields, moderate-to-high diastereoselectivities and excellent enantioselectivities.

A similar reaction could also be implemented with enone **58** as hydride acceptor. This time, Kim et al. employed chiral primary amine **59** as chiral catalyst to prompt the cascade process [103], affording tetrahydroquinine derivatives **60** in moderate yields and with high enantioselectivities (up to 97 % ee) (Scheme 20).

Yuan et al. reported a FeCl$_3$-catalyzed stereoselective cascade [1,5]-HT/ring closure of **61**, furnishing structurally diverse spirocyclic oxindolyl tetrahydroquinolines **62** bearing contiguous quaternary or tertiary stereogenic carbon centers in high yields and with good diastereoselectivities (Scheme 21) [104]. The asymmetric reaction could be catalyzed by chiral phosphoric acid **63** (20 mol%), affording the enantio-enriched tetrahydroquinoline in 95 % yield, 94:6 dr and 54 % ee (R^1 = CO$_2$Et, R^2, R^3 = butylene, R^4 = H). The same reaction was further

investigated by Feng et al. with his well-known chiral *N, N'*-dioxide-scandium complex **14** [105], resulting in the optically active spirooxindolyl tetrahydroquino-lines **62** in good yields (up to 97 %) with excellent diastereoselectivities (>20:1) and enantioselectivities (up to 94 % ee). Strong chiral memory effect was found using a chiral substrate.

If two or more hydride donators and acceptors are available in the substrate, multiple cascade processes will occur to furnish complex cyclic products. Akiyama et al. reported a fascinating Yb(OTf)$_3$-catalyzed double C(sp^3)–H bond function-alizations of benzylamine derivative **64** through a sequential dual hydride shift/cyclization process, which carries two potential hydrogen donors, i.e., methylene **a** and methylene **b** (Scheme 22) [106]. The key feature was the initial hydride shift ([1,4]- or [1,6]-hydride shift), which was completely controlled by the bulkiness of α substituent of trifluoromethyl ketone. Through variation of the R group of ketone, the sequence of functionalization of two potential hydrogen donors could be totally reversed. A bicyclo[3.2.2]nonane skeleton **65** afforded from the substrate **64a** with *trans*-α,β-unsaturated trifluoroacetyl group (R^1=H) by a sequential [1,6]-and [1,5]-hydride shift process (equation A). On the other hand, a [1,4]- and [1,5]-hydride shift occurred successively in the substrate **64b** with a benzyl group α to a trifluoroacetyl group, resulting in the formation of bicyclic product **66** (equation B). The regioselectivity of initial C(sp^3)–H activation was elegantly rationalized by Akiyama via DFT calculation and theoretical studies revealed that the resonance stabilization in the benzylidene carbonyl moiety and the steric repulsion of the α-substituent (R) were the key to change the reaction course.

The enone could be prepared in situ via Knoevenagel condensation. Wang et al. reported a ZnCl$_2$-catalyzed tandem Knoevenagel condensation/1,5-hydride shift/cy-clization of *o*-aminiobenzaldehyde **67** with substrate **68** carrying reactive methylene
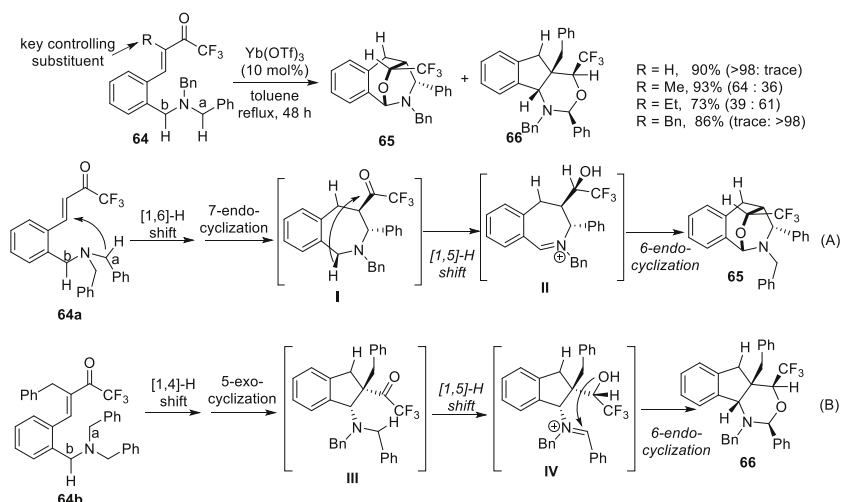
Scheme 22 Double C(sp^3)–H bond functionalization mediated by sequential hydride shift/cyclization process for construction of polyheterocycles

Scheme 23 ZnCl$_2$-catalyzed construction of spiropyrazolo-tetrahydroquinolines via cascade [1,5]-HT cyclization sequence
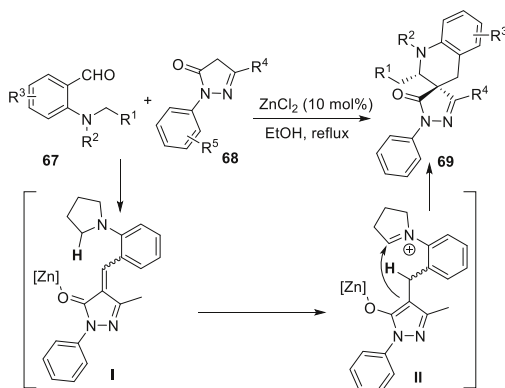
(Scheme 23) [107], which produced spiropyrazolo-terahydroquinoline derivatives **69** in good to high yields with good to excellent diastereoselectivities (up to 95 % yield, >95:5 dr). The strong Lewis acid, i.e., ZnCl$_2$, could not only facilitate the formation of enone **I** and enolate **II** but also increase the electrophilicity of enone by chelation of the carbonyl of enone to promote 1,5-hydride shift.

3.4 Saturated Aldehydes and Imines as the Hydride Acceptors

The C–H bond can be functionalized not only into C–C bond but also into C–O bond and C–N bond via similar cascade processes. Mátyus et al. reported a microwave-assisted synthesis of tricyclic angularly annulated aminal **71** from *ortho*-dialkylaminobenzaldehdyde **70** with H$_2$O as solvent (Scheme 24) [108, 109]. Even though the reaction was conducted under harsh conditions, i.e., at 210 °C for 50 min and employment of stoichiometric K$_2$CO$_3$, aminal **71** could only be obtained in low yield. According to the report by Maulide et al., Lewis acidic condition should be beneficial to the transformation [110], which was not investigated in Mátyus' report

The annulated aminal can be employed as unstable intermediate for further C–H functionalization of tertiary amines. Maulide et al. described a Sc(OTf)$_3$-catalyzed one-pot C–H functionalization of cyclic tertiary amines **72**, in which the sacrificial reduction of a neighboring carboxaldehyde group directed addition of Grignard reagents and lithium alkynyl trifluoroborates to the α-position of amine moiety, resulting in the corresponding α-functionalized products **74** and **74′** bearing a wide range of appendages in good to excellent yields. (Scheme 25) [110]. Basically, the formation of **73/73′** from **72** is under thermodynamic control and **73** is the
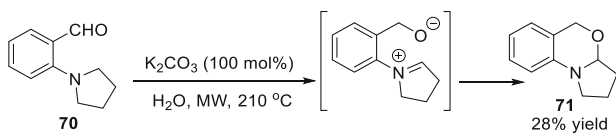
Scheme 24 Microwave-assisted synthesis of tetrahydroquinoline applying the *tert*-amino effect
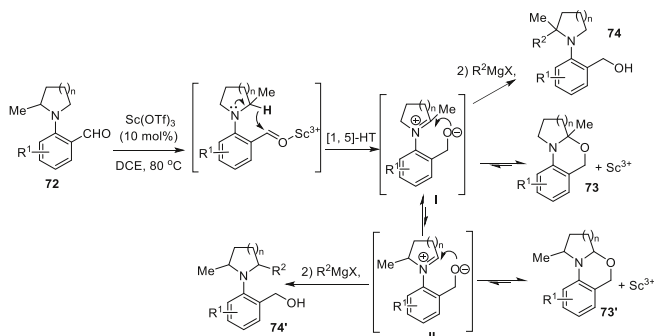
Scheme 25 Sc(OTf)$_3$-catalyzed intramolecular redox-triggered C–H functionalization

Scheme 26 TiF$_4$-catalyzed hydro-*O*-alkylation of aldehydes via cascade [1,5]-HT/cyclization
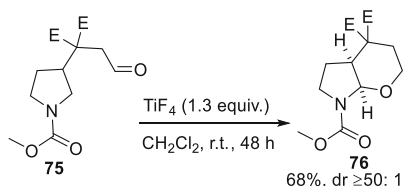
thermodynamically favored product. The aminals **73** and **73′** can be reversed to intermediate **I** and **II**, thus an equilibrium for interconversion exists between **73** and **73′**. The more favorable iminium intermediate **I** (stabilized by more substituents) and less favorable iminium intermediate **II** can be trapped by more nucleophilic reagents, leading to the final stable products **74** and **74′**, respectively.

Sames et al. reported a highly active TiF$_4$-catalyzed intramolecular hydro-*O*-alkylation of aldehyde substrate **75** (Scheme 26), via which the *N*-protected pyrrolidine substrate **75** was transformed into a *cis*-fused bicyclic aminal **76** as a single diastereomer [37]. Because of the electron-withdrawing nature of carbamate and less activity of secondary C–H bond, the employment of highly active and oxophilic TiF$_4$ with high catalyst loading (1.3 eq) was crucial for successful transformation, which resulted in the fused aminal in 68 % yield and good diastereoselectivity (≥50:1).

The in situ-generated iminium could also be exploited as hydride acceptor, via which inert C(sp^3)–H bond could be functionalized to C–N bond efficiently. Seidel et al. reported a trifluoroacetic acid-catalyzed cascade [1,6]-hydride transfer/cyclization of **77** to synthesize 7,8,9-trisubstituted dihydropurine derivatives **78** (Scheme 27) [73]. TFA plays two roles in this process: (1) promotion of imine formation and (2) protonation of imine for acceleration of the hydride shift process. Meth-Cohn and Volochnyuk et al. reported similar reactions in 1967 [71] and 2007, respectively [72].

The same group also described a TfOH-catalyzed one-pot synthesis of aminals **81** from *o*-aminobenzaldehydes **79** and primary aromatic or aliphatic amines **80** (Scheme 28) [111]. The protonated imine **I** worked as hydride acceptor. Almost at

Scheme 27 Synthesis of 7,8,9-trisubstituted dihydropurine derivatives via *tert*-amino effect cyclization
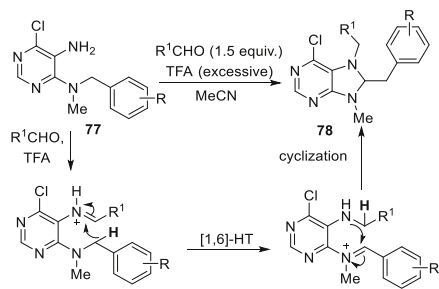
Scheme 28 Synthesis of cyclic aminals via cascade 1,5-hydride transfer/cyclization
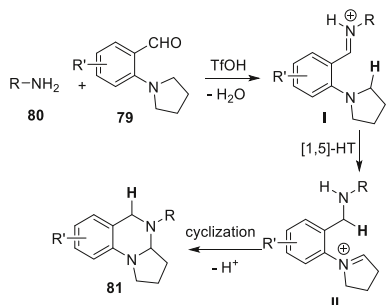
Scheme 29 Asymmetric sp³ C–H functionalization via a chiral Brønsted acid-catalyzed redox reaction
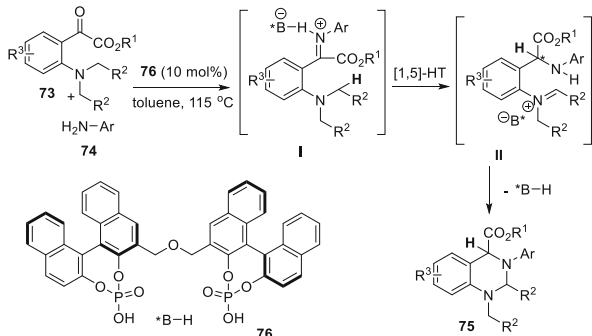
the same time, Akiyama et al. reported a similar catalytic approach to synthesize quinazolines and TsOH·H$_2$O was identified as the optimal catalyst [112].

Ketoesters could be exploited to generate iminium intermediate employed as hydride acceptor. Gong et al. reported a chiral Brønsted acid **85**-catalyzed asymmetric cascade [1,5]-hydride transfer/cyclization of 2-pyrrolidinyl phenyl ketoesters **82** with anilines **83**, which produced the enantio-enriched cyclic aminals **84** (Scheme 29) [113]. The iminium subunit in intermediate **I** served as hydride acceptor, which was generated in situ through the condensation of *o*-aminobenzoketone **82** with aniline **83** in the presence of **85**.

Seidel et al. also reported a metal-free one-pot α-amination of cyclic secondary amines **78** with 2-aminobenzaldehyde **77**, which efficiently furnished ring-fused

aminals **79** in good yields (Scheme 30) [64–66]. Both the electronic structure and the geometry of the amines have profound effects on reactivities and yields. Via an extensive exploration of possible pathways using DFT calculations based on the original experimental results, Seidel and Houk proposed an unusual mechanism involving cascade [1,5]-proton transfer/cyclization [66]. Initially amino-benzalde-hyde **77** reacts with secondary amine **78** to furnish hemi-aminal **I**, which undergoes subsequent dehydration to give quinoidal intermediates **II**. The nucleophilic imine subunit then abstracts a proton from the methylene adjacent to *tert*-amine moiety ([1,6]-proton shift), resulting in azomethine ylide **III**, which is rapidly protonated by ethanol. Subsequently, **IV** is furnished via internal proton transfer and finally ring-fused aminal **79** is formed by intramolecular nucleophilic attack. Dang and Bai et al. also reported a similar cascade process for preparation of tetrahydro-pyrimido[4,5-*d*]pyrimidine [114].

The electrophilic iminium could also be prepared in situ from alkyne via gold catalysis. Gong et al. disclosed a catalytic domino hydroamination/redox reaction, which could directly assemble the tertiary amine substituted 3-en-1-yne derivatives **80** and various amines **81** into cyclic aminals **82** in excellent yields and moderate to high diastereoselectivities by using the combination of gold(I) complex and TfOH (Scheme 31) [115]. Theoretically, terminal alkyne **80** undergoes gold(I)-catalyzed intermolecular hydroamination with aniline **81** to give imine intermediate **II**, which is protonated by Brønsted acid to give electrophilic iminium species **III**; this intermediate then undergoes a subsequent [1,5]-hydride transfer to generate a transient intermediate **IV**, which ultimately suffers an intramolecular nucleophilic attack to afford **82**. The asymmetric version could be facilitated by over-stoichiometric chiral phosphoric acid and 5 mol% $Ph_3PAuNTf_2$, giving rise to enantio-enriched **82** in high yield and excellent enantioselectivity.

3.5 Electrophilic Metal Carbenoids as the Hydride Acceptors

As an electrophilic species, metal carbenoid can also serve as an ideal hydride acceptor. Saa et al. elegantly demonstrated a [Cp*Ru(cod)Cl]-catalyzed cyclization of protected alkynyl pyrrolidine **83**, which furnished 1-Azaspiro[4,4]-nonane **84** carrying versatile TMS moiety as a single diastereomer in good yield (Scheme 32) [76]. Mechanistically, the ruthenium carbenoid **I** is afforded from N_2CHTMS and [Cp*Ru(cod)Cl], which undergoes cycloaddition with **83** to give
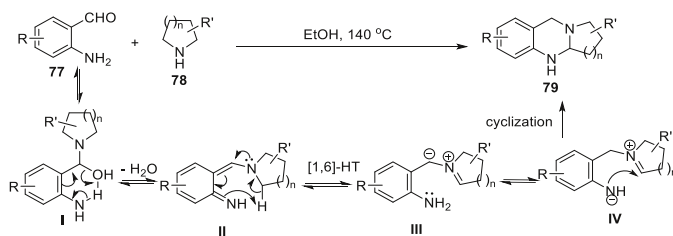
Scheme 30 Synthesis of ring-fused aminals via cascade [1,6]-proton transfer/cyclization
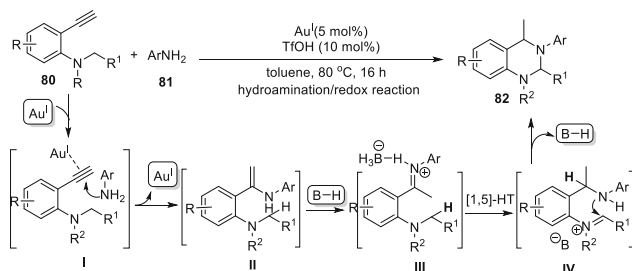
Scheme 31 Catalytic enantioselective *tert*-aminocyclization by asymmetric binary acid catalysis
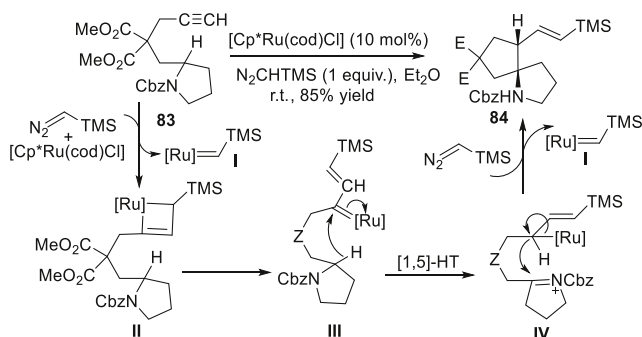
Scheme 32 Intramolecular α-alkylation of C(2)-linked pyrrolidine by catalytic ruthenium carbene insertion
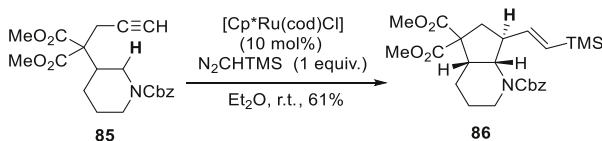
Scheme 33 Intramolecular α-alkylation of C(3)-linked pyrrolidine by catalytic ruthenium carbene insertion

metallacyclobutene **II**. A subsequent ring opening of **II** leads to the electrophilic Ru-vinyl carbenoid **III**, which suffers [1,5]-hydride shift to furnish intermediate **IV**. Ultimately, an intramolecular nucleophilic attack gives rise to the spiro product **84**.

C3-linked piperidine **85** was also readily cyclized under the optimal condition with less reactive secondary C–H bonds α to protected secondary amine as the hydride donor, furnishing the fused bicyclic piperidine **86** in good yields (Scheme 33).

3.6 Other Electrophiles as the Hydride Acceptors

The in situ-generated carbocation can be exploited as a good hydride acceptor. Zhang et al. reported an enantioselective catalytic intramolecular redox reaction of yne-enones **87** in the presence of Au(I) catalyst and chiral ligand **89**, affording 7-membered tetrahydroazepines **88** in high yield and with high to excellent enantioselectivity (Scheme 34) [41, 79]. Compared with relatively inactive C–H bond α to *tert*-amine, oxygen of carbonyl is more nucleophilic and ready to attack the electrophilic alkyne activated by Au(I) catalyst. Basically, alkynophilic Au(I) catalyst triggers a heterocyclization (first cyclization) by activation of the alkyne to generate the furanyl carbocationic subunit in intermediate **II**, which is exploited as the hydride acceptor.

Nitroalkene is a versatile electron-deficient olefin, which might be exploited as the hydride acceptor as well. The cascade process was investigated by Jordis et al. with (*E*)-1-(2-(2-nitrovinyl)phenyl)pyrrolidine **90** as the substrate (Scheme 35) [116]. This transformation could be accomplished under thermal conditions (118 °C) in 80 h, leading to the cyclized product **91** and **91′** in 39 % yield (*syn/ anti* = 12: 1).

Nitroalkene could also be activated by Lewis acids, e.g., Sc(OTf)$_3$, Yb(OTf)$_3$, and Zn(OTf)$_2$ to increase its electrophilicity. According to the unpublished result in Pfaltz group, the cascade process could be facilitated by Yb(OTf)$_3$, which furnished the cyclized product **91** in 60 % yield at 80 °C within 12 h (Scheme 36). The transformation was diastereospecific and only *anti* diastereomer was observed. The diastereoselectivity can be explained through Zimmer–Traxler transition state **II** in which the orientation of substituents would be pseudoequatorial, leading to the *anti*-product via intramolecular nucleophilic attack.

The electrophilic vinylogous iminium could also be exploited as hydride acceptor. Seidel et al. reported a diphenyl phosphate (DPP)-catalyzed cascade [1,5]-hydride shift/cyclization with doubly nucleophilic indole **93** and *o*-aminobenzaldehydes **92** as substrates, which gave rise to 7-membered rings **94** in good to excellent yields (Scheme 37) [80]. Mechanistically, the acid-catalyzed reaction of aldehyde **92** with indole **93** initially furnishes the electrophilic vinylogous iminium **I** via

Scheme 34 Enantioselective Au-catalyzed selective formation of ring-fused tetrahydroazepines
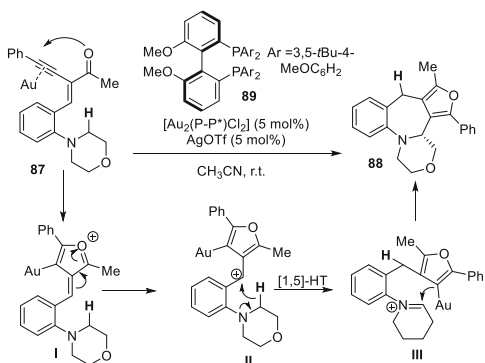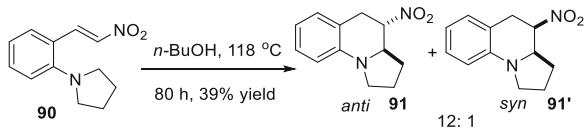
Scheme 35 Synthesis of nitro-substituted tetrahydroquinoline via [1,5]-HT/cyclization under thermal conditions
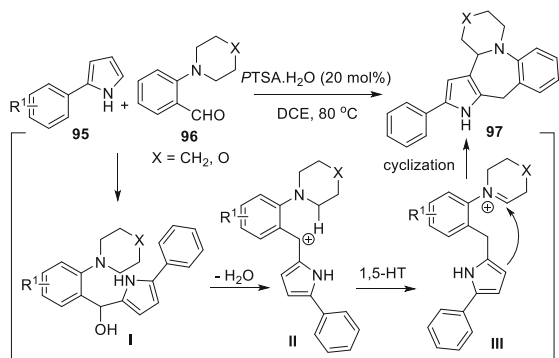
Scheme 36 Lewis acid-catalyzed synthesis of nitro-substituted tetrahydroquinoline via [1,5]-HT/cyclization
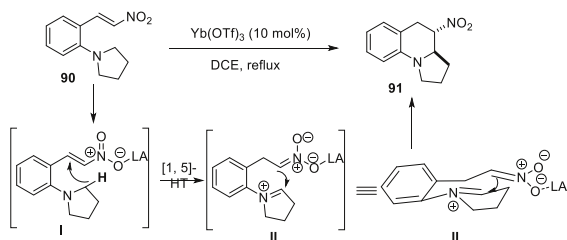
Scheme 37 Brønsted acid-catalyzed redox-neutral indole annulation cascades
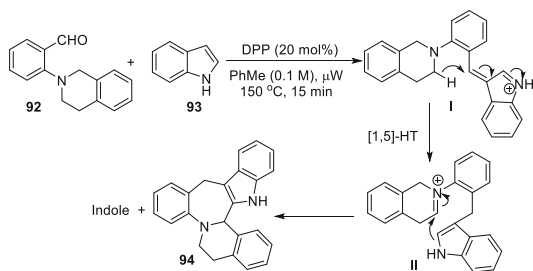
Scheme 38 Brønsted acid-catalyzed synthesis of 1,2-pyrrole-annulated benzazepines through a redox-neutral domino reaction


sequential Friedel–Crafts reaction and dehydration. A subsequent intramolecular [1,5]-hydride transfer leads to electrophilic iminium **II**, which traps nucleophilic C2 of indole to afford 7-membered product **94**.

Sun and Xu et al. reported a Brønsted acid-catalyzed cascade dehydration/1,5-hydride shift/cyclization of 2-arylpyrroles **95** and 2-(pyrrolidin-1-yl)-, 2-(piperidin-

1-yl), or 2-morpholinobenzaldehydes **96** (Scheme 38) [117], which produced structurally diverse 7-membered 1,2-pyrrole-annulated benzazepines **97** in yields of 25–65 %. Both the initial Friedel–Crafts reaction and subsequent dehydration were promoted by *P*TSA, resulting in the carbocationic intermediate **II**, which served as hydride acceptor.

The same group also reported a *P*TSA-catalyzed synthesis of spiroindolenines **100** from 2-substituted (Me, Et) indoles **98** and 2-(pyrrolidin-1-yl)benzaldehydes **99** via a [1,5]-hydride shift/cyclization sequence with good to excellent yields and moderate diastereoselectivity (dr 3.5:1)(Scheme 39) [118]. The major diastereoisomer product could be readily obtained with up to >20/1 d.r. by simple washing with isopropyl ether after flash chromatography. Similar to Seidel's report, the in situ-generated vinylogous iminium intermediate **I** served as the hydride acceptor, which underwent subsequent [1,5]-hydride transfer and cyclization to furnish spiroindolenines **100**. As C2 of indole moiety was substituted by an alkyl group, the more nucleophilic C3 will attack the iminium moiety instead, resulting in the dearomatization of indole subunit.

Gong et al. discovered a MsOH-catalyzed cascade oxidation/C(sp^3)–H functionalization of unactivated terminal alkynes **101** with **102** as the oxidant, which yielded 2,3-dihydroquinolin-4(1H)-ones **103** (Scheme 40) [119]. Mechanistically, the nucleophilic nitrogen atom initially captures a proton that is delivered to alkynes subsequently. Intermediate **I** is formed by dearomatization of styrene cation. Afterwards, two possible pathways might operate to afford the final products. In path **A**, the nucleophilic attack of pyridine-*N*-oxide onto intermediate **I** generates enolate **II**, which undergoes sequential delocalization and [1,5]-hydride transfer/ring-closure to furnish a final intermediate **III**. The interaction between methanesulfonic anion and pyridine cation in **III** facilitates C–H and N–O bonds cleavage to afford **103**. In path **B**, the hydride of intermediate **I** migrates preferentially, which is followed by cyclization and nucleophilic attack of pyridine-*N*-oxide onto benzylic cation **IV**, resulting in the intermediate **III**.
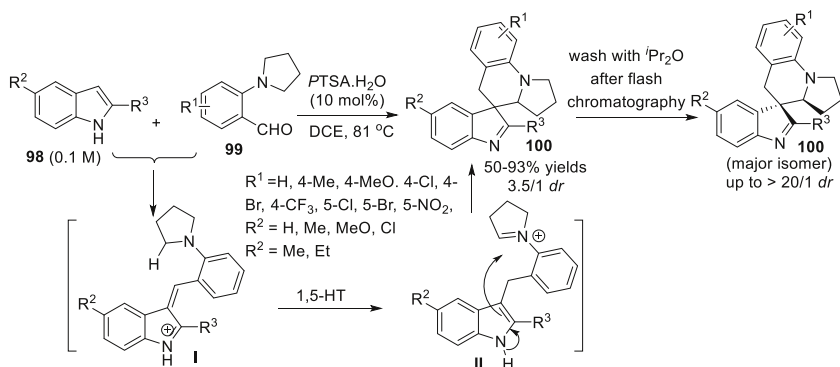
Scheme 39 Brønsted acid-catalyzed synthesis of spiroindolenines via [1,5]-hydride shift/cyclization sequence

Scheme 40 Metal-free
oxidation/C(sp³)–H
functionalization of unactivated
alkynes
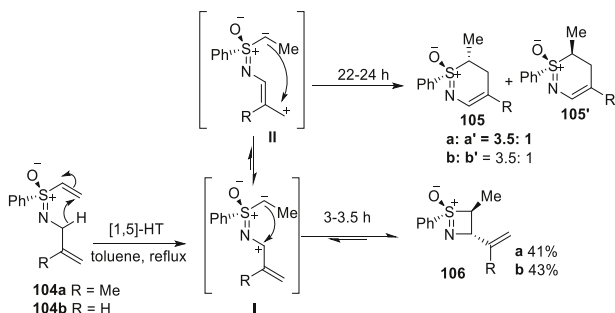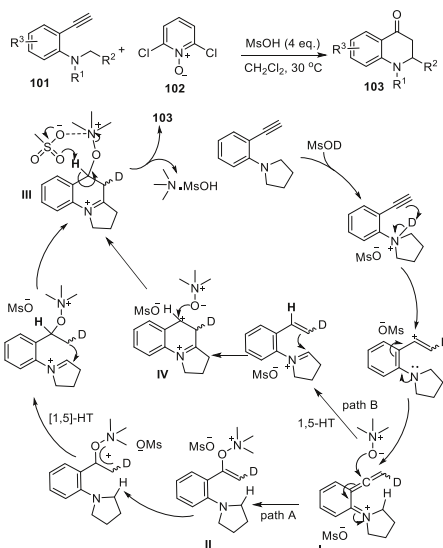
Scheme 41 C–H activation in *S*-alkenyl sulfoximines

Harmata et al. developed an intramolecular redox C–H activation process of
alkenyl sulfoximines to synthesize 4- and 6-membered heterocycles **106** and **105**
(Scheme 41) [120]. Terminal alkene activated by sulfoximines worked as hydride
acceptor and allylic C–H bond served as hydride donor. Notably, the reaction time
strongly influenced the formation of final products. When **104** was refluxed in
toluene for 3.5 h, the 4-membered cyclic species **106** could be obtained in 41 %
yield as the major product; whereas if the reaction was refluxed for around 24 h,
6-membered thiazines **105** were isolated as a mixture of diastereomers in 40 %
yield. Mechanistically, an intramolecular [1,5]-hydride migration operates initially,
leading to zwitterionic intermediate **I**. Subsequent ring closure can be formulated as
the intramolecular collapse of the zwitterionic intermediate **I** or **II**. The formation of
4-membered product **106** might be kinetically favorable and reversible. Although
intermediate **II** might be less stable than intermediate **I** for the reason that the allylic

Scheme 42 Construction of oxadiazepines via Lewis acid-catalyzed tandem 1,5-HT/cyclization
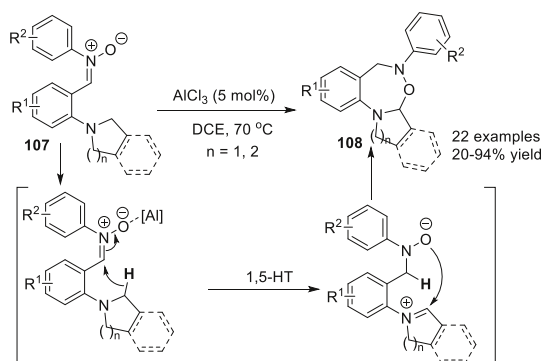
positive charge in intermediate **I** can be dispersed by more substituents, the conversion of 4-membered **106** to **105** is thermodynamically favorable and the driving force might be the release of cyclic strain of **106**.

Nitrones have been widely exploited in various cycloaddition reactions. Intriguingly, these electrophilic species can also serve as the hydride acceptors. Sun and Xu et al. reported an expeditious access to structurally diverse oxadiazepines **108** via 1,5-hydride shift/cyclization of pyrrolidine- or tetrahydroiso-quinoline-containing nitrones **107** with nitrones as hydride acceptors and AlCl$_3$ was exploited as Lewis to promote the cascade process (Scheme 42) [121]. Furthermore, the nitrone **107** could be furnished in situ, which underwent subsequent 1,5-hydride shift, and ring cyclization through a one-pot process to afford **108** in good yields.

4 C(sp^3)–H Bond Adjacent to Ethereal Oxygen as The Hydride Donors

In addition to the C–H bond adjacent to *tert*-amino moieties, methylene (or methine) adjacent to ethereal oxygen could also be employed as hydride donor. As discussed in the section of mechanistic insight, the C–H bond adjacent to ethereal oxygen is less reactive than that adjacent to *tert*-amine, thus more reactive hydride acceptors are required.

4.1 Electrophilic Benzylidene Malonates and Their Derivatives as the Hydride Acceptors

Sames et al. reported a Sc(OTf)$_3$-catalyzed intramolecular hydroalkylation of isolated electron-deficient olefins (Scheme 43) [95]. Tetrahydropyrans or tetrahy-drofurans carrying C(2)-linked α, β-unsaturated malonate side chain **109** and **111** were employed as substrate to furnish the spiroether product **110** and **112** in excellent yields. Notably, germinal substitution along the olefin tether was not required for efficient annulation for the reason that benzylidene malonate activated by Sc(OTf)$_3$ were reactive enough, thus higher conformational rigidity to increase the reactivity of hydride acceptor was not indispensable [96].

Scheme 43 Sc(OTf)$_3$-catalyzed C–H functionalization of cyclic ether via [1,5]-HT/cyclization
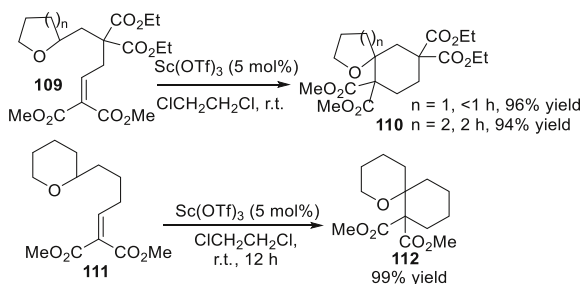
Scheme 44 Sc(OTf)$_3$-catalyzed hyrdoalkylation via [1,5]-HT/cyclization
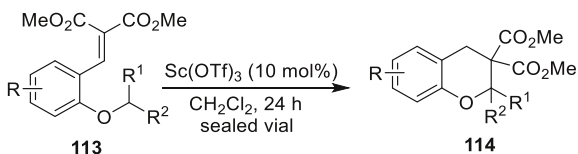
The same group also reported a Sc(OTf)$_3$-catalyzed [1,5]-hydride transfer/cyclization of *ortho*-vinylaryl alkyl ethers **113**, via which highly substituted dihydrobenzopyran **114** could be prepared in excellent yields (Scheme 44) [122].

SnCl$_4$ could also be employed as Lewis acid to efficiently catalyze the cascade process for synthesis of a benzopyran skeleton **116** from benzyloxy benzylidene malonate **115** (Scheme 45) [123]. Notably, the methyl *ortho* to the alkoxy group or the benzylidene moiety could enhance the reactivity drastically compared with non-substituted substrate. This remarkable enhancement of the reactivity could be well rationalized by following two factors: (1) the conformational behavior of the benzyloxy group and (2) the "*buttressing effect*". In the case of **115** having an *o*-methyl group, the conformational equilibrium largely shifted to the left conformer **115a** because of the severe steric repulsion. As a consequence, the "*buttressing effect*" between the methyl group and the benzyloxy group made the hydrogens on the benzyl group much closer to benzylidene electrophilic carbon. As a result of the synergetic effect of these two factors, hydride can be delivered more readily to the acceptor, thus both catalyst loading and reaction time could be dramatically reduced.

4.2 Electrophilic Activated Alkyne and Allene as the Hydride Acceptors

Yamamoto et al. reported a PtBr$_2$-catalyzed cyclization of 1-ethynyl-2-(1-alkoxy-but-3-enyl)-benzenes **117**, which furnished functionalized indenes **118** in good to allowable yields (Scheme 46) [124]. Notably, the allyl group substituted at benzylic position was indispensable for the success of this cyclization, without which the reaction did not work at all. This observation suggests that the coordination of olefin to platinum at a right position/geometry might be essential for the indene formation.

Chatani et al. employed other alkynophilic metals such as PtCl$_2$, PtCl$_4$, and [RuCl$_2$(CO)$_3$]$_2$ to catalyze the cyclization of non-allyl substituted 1-ethynyl-2-(1-

Scheme 45 Remarkable enhancement of reactivity by an *ortho* substituent

(1) conformational behavior of benzyloxy group

(2) buttressing effect
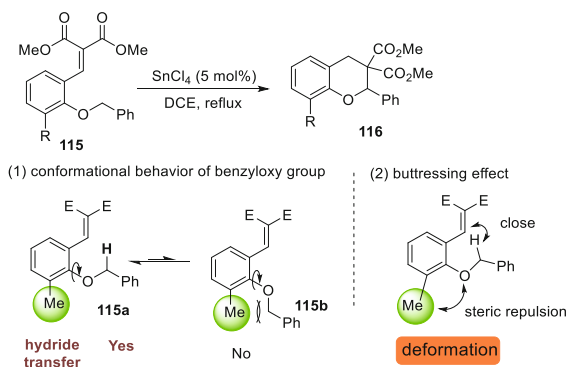
Scheme 46 PtBr$_2$-catalyzed cyclization of allyl(o-ethynylaryl) carbinol derivatives

R: alphatic substituent
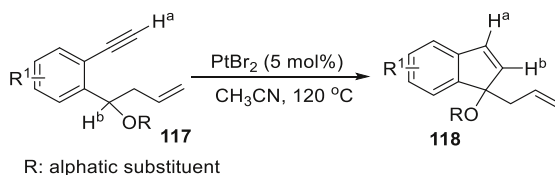
**Scheme 47** Alkynophilic metal-catalyzed cyclization of non-allyl substituted 1-ethynyl-2-(1-alkoxyalkyl)-benzenes
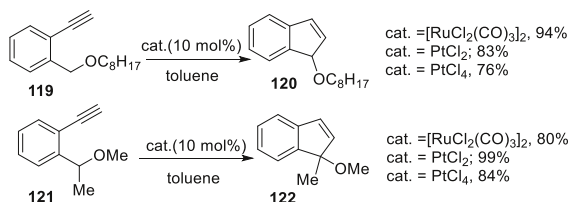
alkoxyalkyl) benzenes **119** and **121** under mild condition, via which the desired indenes **120** and **122** were furnished in high yields (Scheme 47) [40]. In contrast to Yamamoto's results [124], the substrates without allyl group still worked well.

The same group also investigated catalytic cyclization of 2-alkyl-1-ethynylbenzene derivatives carrying silyl ether groups as in **123** and **125** (Scheme 48) [40]. In contrast to Liu's result [44], when silyl ether-substituted 2-methy-1-ethynylbenzene was subjected to the reaction, only silyl ether-substituted indenes **124** and **126** were afforded in good to excellent yields.

Liu et al. also reported a TpRuPPh$_3$(CH$_3$CN)$_2$·SbF$_6$-catalyzed cyclization of 2-alkyl-1-ethynylbenzenes **127** bearing a siloxy group, which produced synthetically valuable 1-indanones **128** or 1*H*-1-indenols **129** in reasonable yields and in short periods (Scheme 49) [44]. Basically, terminal alkyne subunit is transformed to ruthenium-vinylidene **I** initially, which undergoes a [1,5]-hydride shift to give ruthenium-containing 1,3,5-hexatriene **II**. A subsequent 6π-electrocyclization of intermediate **II** furnishes ruthenium-containing cyclohexadiene **III**, which suffers reductive elimination to produce 1-substituted-1*H*-indene **128**. Afterwards, the cationic ruthenium catalyst attacks C(2) carbon of indene to form benzyl cation **IV**,

Scheme 48 Catalytic cyclization of 2-alkyl-1-ethynylbenzene derivatives carrying silyl ether groups to indenes
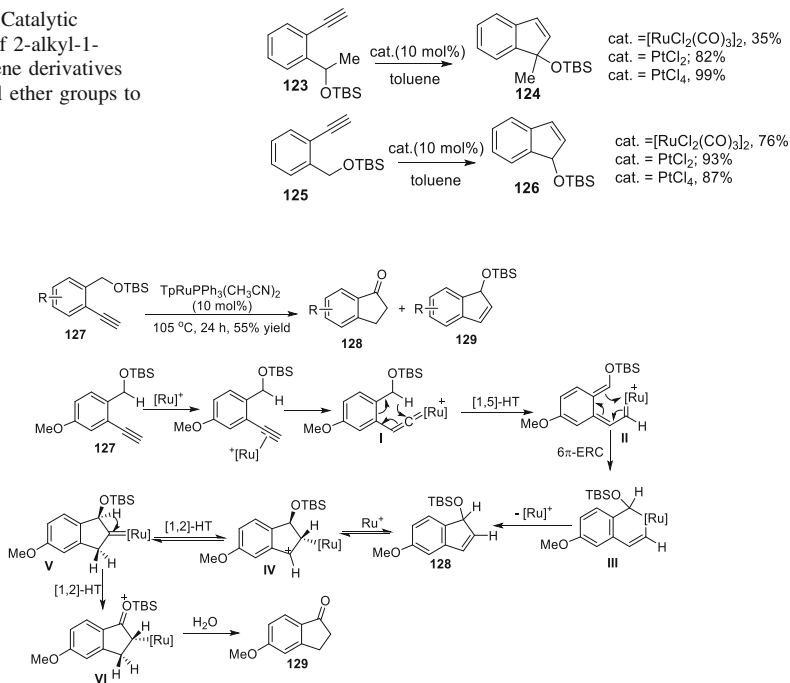
Scheme 49 Ruthenium-catalyzed cyclization of 2-alkyl-1-ethynylbenzene carrying a silyl ether group
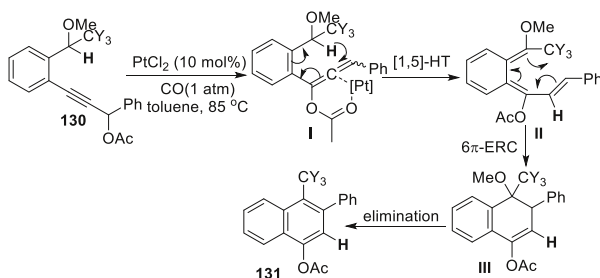
Scheme 50 Synthesis of naphthalenyl acetate from propargylic esters via Pt-catalyzed [1,5]-HT/cyclization

followed by [1,2]-hydride shift to afford ruthenium cyclopentylidene **V**. Ultimately, 1-indanone **129** is produced via a second hydride shift and hydrolysis.

Liang et al. reported a PtCl₂-catalyzed transformation of 3-(2-alkyl)phenyl-propynyl acetate **130** to prepare naphthalenyl acetate **131** (Scheme 50) [45]. The electrophilic Pt–allene complexes formed in situ worked as hydride acceptors. Mechanistically, the Pt(II)-promoted [1,3]-OAc shift leads to the formation of platinum-activated allenyl ester **I**, which undergoes a [1,5]-hydride shift to form 1,3,5-hexatriene **II**. A subsequent 6π-electrocyclic ring closure affords intermediate

III, which further eliminates the methoxy group, resulting in rearomatization to afford **131**.

Liu et al. reported a PPh$_3$AuCl/AgSbF$_6$-catalyzed cycloisomerization of allenene acetal functionality **132**, via which bicyclo[3.2.1]oct-6-en-2-ones **133** were prepared in high yields, high chemoselectivities, and high stereoselectivities (Scheme 51) [125]. In most cases, only one single stereoisomer of the resulting cyclic products was formed despite their molecular complexities. Mechanistically, substrate **132** initially undergoes Au(I)-catalyzed allene cyclization to give electrophilic Au(I)-alkenyl carbenoid **I**, which abstracts acetalic hydride through [1,5]-hydride transfer, leading to the formation of Au(I)-η^1-allyl species **II** containing a dimethoxymethyl cation. A subsequent S$_E$2′ addition of Au(I)-η^1-allyl functionality at this oxocarbeniums opposite the neighboring methyl group affords tricyclic species **III** with its methyl group on the same side as the adjacent hydrogen and ethyl group. A final acid-catalyzed deprotection leads to **133**.

Urabe et al. described a Rh$_2$(TFA)$_4$-catalyzed cyclization of alkynyl ethers **134**, which afforded dihydropyrans **135** in good yield (Scheme 52) [126]. Ring closure proceeded in a highly regioselective manner, and no isomeric five-membered product **136** was detected. Notably, the sulfonyl moiety was critical for the success of this reaction. Mechanistically, initial coordination of Rh(II) to alkyne subunit generates a cationic carbon β to sulfonyl group, which abstracts a hydride from methylene α to ethereal oxygen, generating a zwitterionic intermediate **III**. A final intramolecular nucleophilic attack furnishes the product **135**.

Sames et al. developed an α-alkenylation of cyclic ethers to synthesize both annulation and spirocyclization products (Scheme 53) [39]. Four types of electronically diverse hydride donors were investigated and remarkably the selection of suitable catalysts was crucial to the success of cascade processes. As to substrate **137**, in which relatively unreactive secondary C–H bond was exploited as hydride donor, no aromatic group was available to stabilize the oxocarbenium generated via [1,5]-HT. Hypervalent platinum catalyst PtI$_4$ was the optimal catalyst, which affected complete conversion of **137** to furnish the product **138** in 86 % yield, whereas PtI$_4$ only led to complete decomposition of **141** despite higher reactivity of
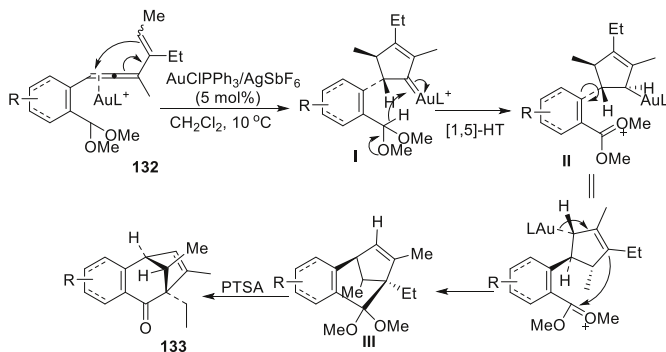
Scheme 51 Gold-catalyzed stereoselective synthesis of bicyclo[3.2.1]oct-6-en-2-ones

Scheme 52 Rhodium-catalyzed intramolecular redox reaction of alkynyl ethers
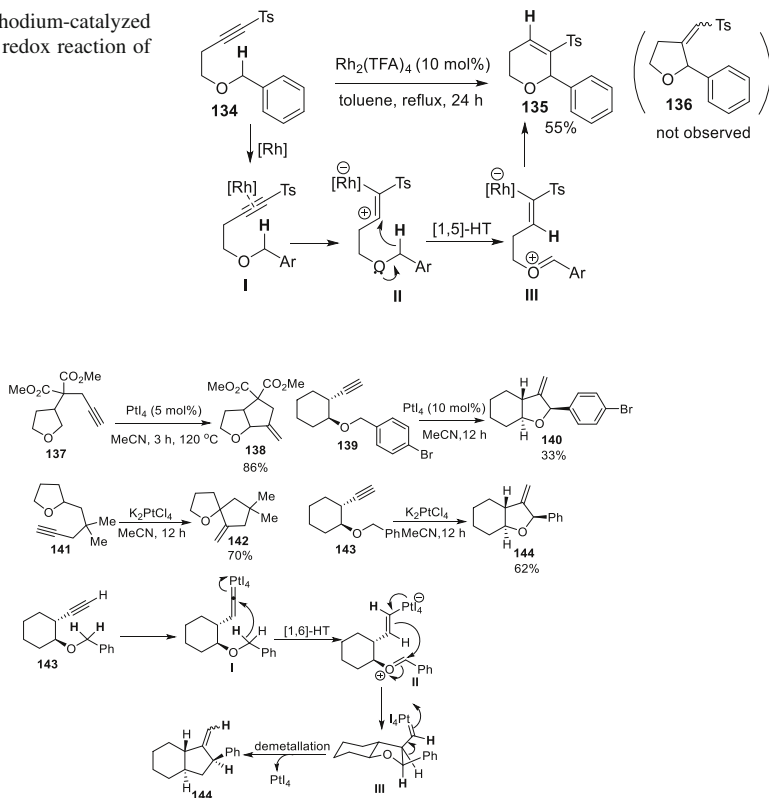
Scheme 53 Platinum-catalyzed α-alkenylation of cyclic ethers based on cascade [1,5]-HT/cyclization
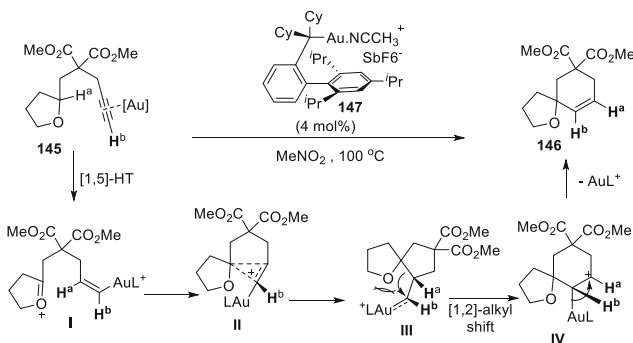
Scheme 54 Gold(I)-catalyzed *a*-alkylation of C(2)-linked terminal alkynyl ethers

its tertiary C–H bond. Less active platinum catalyst K_2PtCl_4 was the optimal catalyst to produce spirocycles **142** in 70 % isolated yield. With K_2PtCl_4 as catalyst, substrate **143** could also be transformed into fused product **144** in 62 % yield. Although hydride donor in **143** was a less active secondary C–H bond, the

oxocarbenium generated upon [1,5]-HT could be stabilized by adjacent phenyl group, thus less active K_2PtCl_4 could facilitate the conversion. The brominated derivative **139** gave a lower yield of compound **140** (33 %) even though highly active PtI_4 was employed, showing a considerable sensitivity of this reaction to electron-withdrawing substituents, particularly in *para-* and *ortho*-position due to their destabilization of oxocarbenium intermediates. Theoretically, the platinum vinylidene **I** is formed initially, followed by through-space [1,6]-hydride transfer to produce zwitterionic intermediate **II**, which affords the final product via a sequential C–C bond formation and platinum salt elimination.

Gagosz et al. reported Au(I) catalyst **147**-catalyzed alkylation of alkynyl ethers which produced cyclohexane **146** as major product (Scheme 54) [127]. Theoretically, the electrophilic activation of the alkyne **145** by Au(I) initiates a [1,5]-hydride shift to furnish oxocarbenium ion **I**, interaction of which with the pendant nucleophilic vinyl-gold moiety affords cyclopropenium intermediate **II**. Carbocation **IV**, which would finally collapse into cyclohexene **146** after elimination of the gold(I) catalyst might be generated via a [1,2]-alkyl shift on Au-carbene intermediate **III**.

In contrast to C(2)-linked terminal alkynes **145**, gold-catalyzed alkylation of C(3)-linked tetrahydrofurans bearing terminal alkyne functions **148** mainly led to the formation of major product *exo*-methylene cyclopentanes **149** and minor products **150** (Scheme 55). This reversed selectivity might be explained by the relative stability of intermediates **III** and **V**. Steric constrains should be weaker for the fused bicyclic intermediate **V** (in Scheme 55) than intermediate **III** (in Scheme 54), thus allowing a rapid [1,2]-hydride shift, which leads to **VI** rather than a [1,2]-alkyl shift, which leads to **III**.

Gold-activated allene can also be employed as hydride acceptor. Gagosz et al. demonstrated that a phosphite gold complex **154**-catalyzed intramolecular hydroalkylation of allenes **151**, which afforded the spiro compound **152** and undesired fused bicyclic compound **153** in 30 and 61 % yields, respectively (Scheme 56) [128]. The selectivity could be reversed if $HNTf_2$ was exploited.
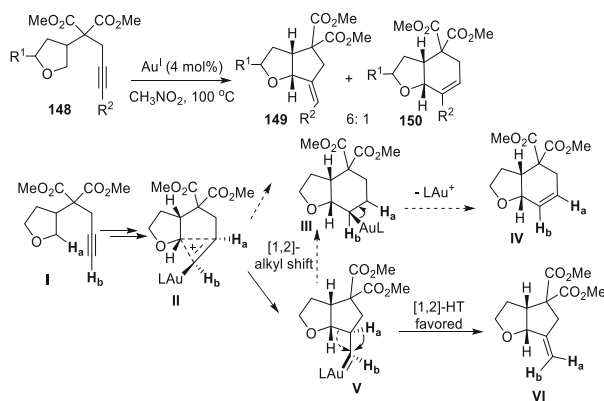
Scheme 55 Gold(I)-catalyzed α-alkylation of C(3)-linked terminal alkynyl ethers
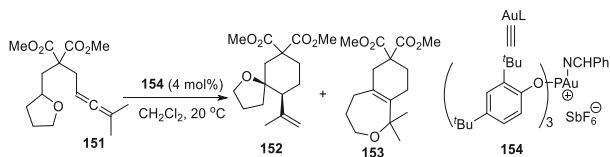
Scheme 56 Gold and Brønsted acid-catalyzed hydride shift onto allenes
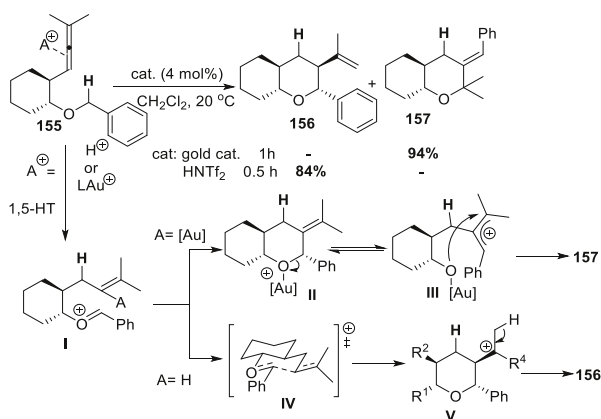
**Scheme 57** Gold and Brønsted acid-catalyzed α-alkylation of benzyl ether

Under Brønsted acidic condition, the transformation was slower but furnished exclusively the desired spiro compound **152** in an excellent yield. The two reactions under Au(I) or Brønsted acid catalysis proceeded under very mild conditions in a stereoselective manner and two new contiguous asymmetric centers were formed.

A similar complete divergence in product selectivity was observed when the substrates **155** possessing a benzyl ether moiety were treated with either gold complex **154** or HNTf$_2$ (Scheme 57) [128]. Under gold catalysis, tetrahydropyran **157** was obtained in 94 % yield, while tetrahydropyran **156** was produced in 84 % yield with HNTf$_2$ as the catalyst. The stereoselective formation of compound **156** can be explained by the highly ordered chair-like transition state **IV**, which leads to carbocation **V** from oxocarbenium **I**. The relative *trans* relationship between the phenyl and isopropenyl substituents in product **156** results from the pseudoequatorial orientation of the phenyl and isopropylidene group in transition state **IV**. An analogous disposition explained the *cis* relationship between the phenyl group and the alkyl substituent at C(6).

4.3 Electrophilic α, β-Unsaturated Aldehydes and Ketones as the Hydride Acceptors

The electrophilicity of alkene subunit of α, β-unsaturated aldehydes can be dramatically increased if activated by BF$_3$·Et$_2$O, which serves as an ideal hydride

Scheme 58 BF$_3$·Et$_2$O-catalyzed intramolecular hydroalkylation of isolated α,β-enals
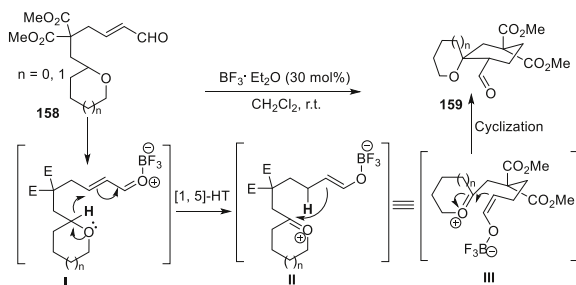
acceptor. Sames et al. described a BF$_3$·Et$_2$O-catalyzed intramolecular hydroalkylation reaction of α, β- unsaturated aldehydes **158**, via which spirocycles **159** could be furnished in good yields at ambient temperature as a mixture of diastereomers (Scheme 58) [95].

In addition to tertiary C–H bonds, secondary C–H bonds could also be directly functionalized (Scheme 59) [95]. Compared with tertiary C–H bond, secondary C–H bond was less reactive, therefore more active Lewis acid, i.e., PtCl$_4$ (10 mol%) was employed to facilitate hydroalkylation of enal **160**, giving rising to the fused annulation product **161** in 40 % yield and good diastereoselectivity (dr >15: 1).

In addition to the more active α, β-enal, hydroalkylation of less active enones **162** also proceeded smoothly (Scheme 60) [95]. Under the catalysis of 30 mol% of BF$_3$·Et$_2$O and with comparatively active tertiary C–H as hydride donor, the substrate **162a** or **162b** carrying α, β-unsaturated methyl and phenyl ketone units were efficiently transformed into spirocycles **163a** and **163b**, respectively, in excellent yields and moderate diastereoselectivities.

The 2,3-disubstituted tetrahydropyran **165** could be obtained in high diastereoselectivity via treatment of acyclic ether **164** with a substoichiometric amount of BF$_3$·Et$_2$O at elevated temperature (Scheme 61) [95]. The less active secondary C–H bond acted as hydride donor and less active methyl ketone was employed as hydride acceptor. Because the oxocarbenium could be stabilized by adjacent phenyl group, relatively mild Lewis acid BF$_3$·Et$_2$O (75 mol%) was active enough to promote the cascade process efficiently, resulting in the formation of desired product **165** in high yield (90 %) and good diastereoselectivity (dr >15: 1).

A simple and economical intramolecular hydroalkylation of olefins was elegantly demonstrated by Sames et al. based on the generation of highly reactive alkenyl-oxocarbenium intermediates **I** in situ from acetals (Scheme 62) [38]. Under the catalysis of BF$_3$·Et$_2$O, the cyclic product **167** could be obtained in good yield and diastereoselectivity from acetal **166** within 1 h. Direct comparison of **166** to the corresponding unprotected aldehyde showed a drastic increase in both reactivity and chemical yield, as well as an improvement in diastereoselectivity. Theoretically, BF$_3$·Et$_2$O opens cyclic acetal **166** to generate oxocarbenium intermediate **I**, which activates conjugated alkene moiety for subsequent hydride abstraction. After hydride transfer, the resulting oxocarbenium-enol ether intermediate **II** undergoes rapid C–C bond formation and the acetal can be reformed from the new oxocarbenium species **III**, producing **167**. The observed high stereoselectivity can

Scheme 59 PtCl₄-catalyzed intramolecular hydroalkylation of isolated α, β-enals
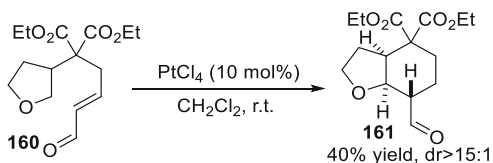
Scheme 59 PtCl$_4$-catalyzed intramolecular hydroalkylation of isolated α, β-enals

Scheme 60 BF₃·Et₂O-catalyzed intramolecular hydroalkylation of isolated α,β-unsaturated ketones

Scheme 60 BF$_3$·Et$_2$O-catalyzed intramolecular hydroalkylation of isolated α,β-unsaturated ketones

Scheme 61 BF₃·Et₂O-catalyzed intramolecular hydroalkylation of α,β-unsaturated ketones
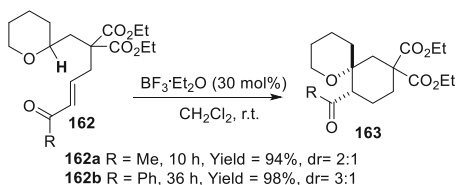
Scheme 61 BF$_3$·Et$_2$O-catalyzed intramolecular hydroalkylation of α,β-unsaturated ketones

Scheme 62 BF₃·Et₂O-catalyzed alkylation through highly activated alkenyl-oxocarbenium intermediates
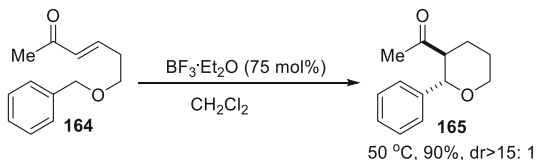
Scheme 62 BF$_3$·Et$_2$O-catalyzed alkylation through highly activated alkenyl-oxocarbenium intermediates

Scheme 63 BF₃·Et₂O-catalyzed C–H bond functionalization with enone as hydride acceptors
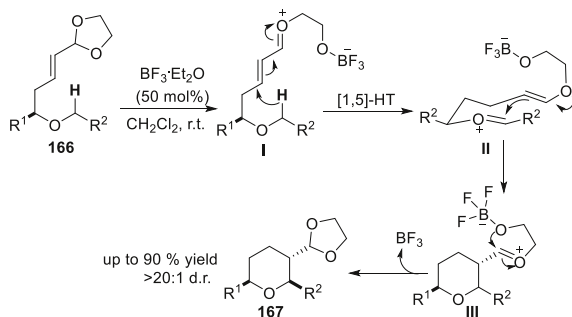
Scheme 63 BF$_3$·Et$_2$O-catalyzed C–H bond functionalization with enone as hydride acceptors
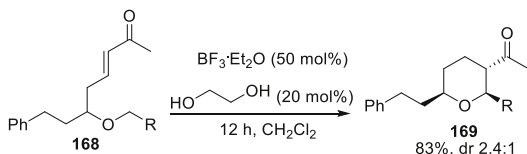
be explained by the favorable transition state **II** in which all the substituents are in equatorial positions.

The intramolecular hydroalkylation of enones could be readily implemented as well via this strategy (Scheme 63) [38]. The addition of ethylene glycol had a dramatic effect on the reaction rate as demonstrated in the cyclization of enones **168**; the reaction could be completed within 12 h, furnishing the cyclized products

169 in good yields but with low diastereoselectivities. This strategy could not only drastically increase the reaction rate but also improve the isolated yields and stereoselectivities.

Tu et al. reported a Macmillan's catalyst **172**-catalyzed asymmetric α-alkylation of tetrahydrofuran **170** containing an α,β-unsaturated aldehyde, via which chiral spiroether **171** could be prepared (Scheme 64) [129]. The sequential [1,5]-hydride transfer/cyclization was facilitated via cascade iminium/enamine activation. The presence of strong acid was indispensable to ensure sufficient electrophilicity of the iminium intermediate. Theoretically, substrate **170** reacts with **172** to give iminium intermediate **I**. Owing to the steric interaction of the bulky *tert*-butyl group, the *E* enamine **II** is formed preferentially upon [1,5]-HT, which exists in two possible conformers **III** and **IV**. Because of dipole repulsion between the cyclic-oxocarbenium and enamine moieties in conformer **III**, **IV** is the more favored conformer, which undergoes intramolecular C–C bond formation to afford the final product **171**.

4.4 Saturated Aldehyde and Ketone as the Hydride Acceptors

Sames et al. described a BF$_3$·Et$_2$O-catalyzed intramolecular hydro-*O*-alkylation of aldehyde substrates **173**, which led to spiroketal products **174** (Scheme 65) [37]. Because oxocarbenium generated upon hydride migration is also a highly electron-deficient species, which would compete for hydride with aldehyde, thus how to deliver hydride to acceptor is challenging. Sames' protocol to address this problem was to employ BF$_3$·Et$_2$O (30 mol%) for activation of carbonyl of **161**, rendering hydride acceptor more electrophilic to "snatch" hydride. Tetrahydropyran substrate **173** could be converted to spiroketal **174** in high isolated yield at ambient temperature. Remarkably, the final cyclization step was a reversible process, which was under thermodynamic control, thus the cascade process was highly
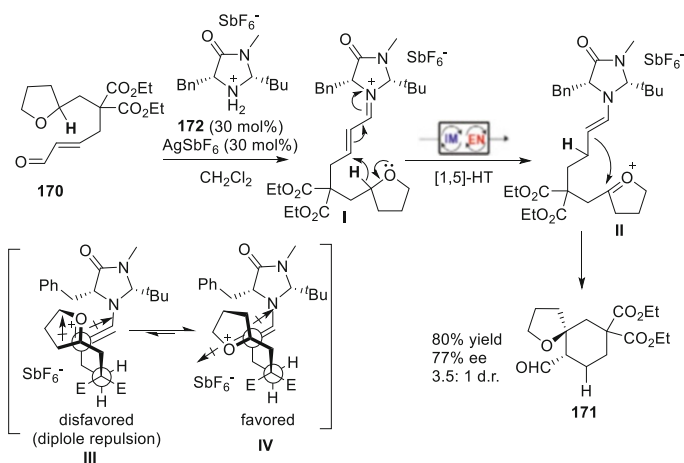
Scheme 64 Organocatalyzed asymmetric direct C(sp^3)–H functionalization of cyclic ethers

Scheme 65 BF$_3$·Et$_2$O-catalyzed intramolecular hydro-*O*-alkylation of C(2)-linked aldehydes
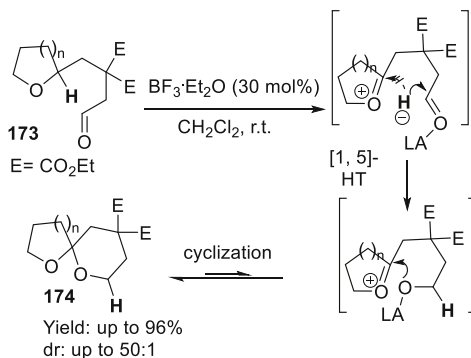
diastereoselective. Both 6, 6-scaffolds and 5, 6 spiroketals could be obtained in excellent yields.

The *cis*-fused bicyclic acetal **176** could also be afforded as a single diastereomer via this strategy with **175** as the substrate (Scheme 66) [37]. Mild Lewis acid, e.g., BF$_3$·Et$_2$O, was inactive and only the stronger oxophilic Lewis acid TiF$_4$ (20 mol%) could facilitate the transformation for the reason that secondary C–H was less reactive than the tertiary C–H bond in **173**.

In addition to aldehyde substrates, less electrophilic ketone **177** could also be converted into spiroketal **178** in 30 % yield and excellent diastereoselectivity under the mediation of stoichiometric TiF$_4$ (Scheme 67) [37]. BF$_3$·Et$_2$O was not active enough to promote this hydro-*O*-alkylation, which might be ascribed to the poor reactivity of methyl ketone.

## 4.5 Electrophilic Metal Carbenoid as the Hydride Acceptors

Saa et al. discovered a ruthenium-catalyzed diastereoselective cyclization of linear alkynyl ether **179** involving cyclic and acyclic ethers, which produced spirocycles **180** in fairly good yields (Scheme 68) [76]. The ring size of the cyclic ether had a dramatic effect on the reaction time and yields.

Similarly, acetalic C–H bond could be exploited as hydride donor as well, and via ruthenium-catalyzed cyclization of linear alkynyl acetals **181**, spirobicycles **182** could be furnished in fairly good yield (Scheme 69) [76], along with the formation of linear hydroxyester **183**, which was generated by hydrolysis of intermediate **I**. Notably, rigid cyclic acetal afforded a higher yield of spiro compound in comparison to the linear acetals [96].
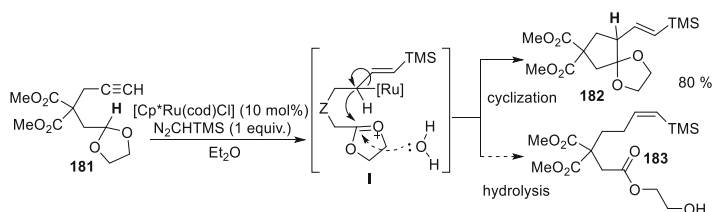
**Scheme 66** TiF$_4$-catalyzed intramolecular hydro-*O*-alkylation of C(3)-linked aldehydes
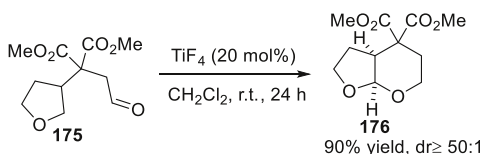
Scheme 67 TiF$_4$-catalyzed intramolecular hydro-*O*-alkylation of C(2)-linked methyl ketone

30%, dr ≥50: 1

n = 1, 79%
n = 2, 48%

179   **180**
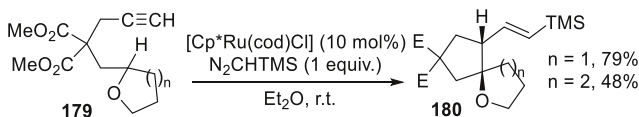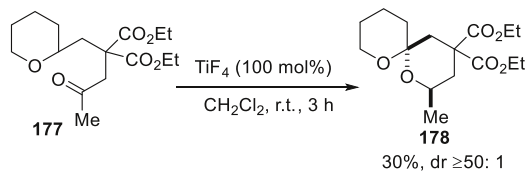
Scheme 68 Intramolecular α-alkylation of C(2)-cyclic ether

80 %

182

cyclization

hydrolysis

183

Scheme 69 Intramolecular alkylation of dioxolane by catalytic ruthenium carbene insertion

185
81%
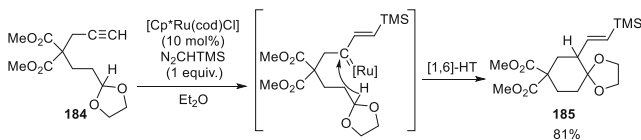
Scheme 70 Intramolecular alkylation of dioxolane via cascade [1,6]-HT/cyclization

[1,6]-hydride shift/cyclization process could occur when specially designed dioxolane substrate **184** was subjected to the reaction, affording 5,6-spirocyclic product **185** in excellent yield (Scheme 70) [76]. The examples showed again the hydride could be delivered through space and the distance between hydride donor and acceptor was not an issue. A comparison of the cyclizations of dioxolanes **181** and **184** shows the more rapid formation of the 1,4-dioxaspiro[4,5]decane **185** versus 1,4-dioxaspiro[4,4] nonane **182**, which clearly indicated that the conformation of metallic intermediate played a definitive role during the course of the reaction.

Fukuyama et al. exploited highly reactive rhodium carbenoids as hydride acceptors to construct tetrahydrofuran moieties in his total syntheses for many times. The mechanism should be the cascade [1,5]-Hydride migration/cyclization, whereas Fukuyama et al. argued that their reactions proceed via metal carbene C–H insertion reactions [130–135].
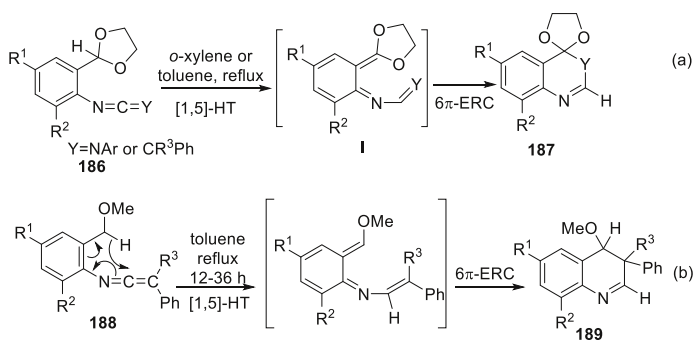
4.6 Ketenimines and Carbodiimides as Hydride Acceptors

Alajarin and Vidal et al. discovered dihydroquinolines and spirocyclic dioxolano-quinazolines **187** could be readily accessed via cascade [1,5]-hydride transfer/6π-ERC under thermal conditions (Scheme 71, a) [58]. Basically, with active ketenimine or carbodiimide as hydride acceptor whose central carbon atom is highly electrophilic, the cascade process is facilitated by the hydricity of the acetalic C–H bonds in **186**. After hydride migration, the 1,3,5-conjugated hexatriene **I** can be generated, which had a long conjugate system and can be stabilized to a large extent. The ketenimines **188** bearing ether moiety could also be transformed exclusively into dihydroquinolines **189** (Scheme 71, b) [56].

The same group described a Sc(OTf)$_3$-catalyzed three-step cascade reaction of **190** involving hydride shift/cyclization/hydrolysis as well, which produced indanones **191** (Scheme 72) [70]. Hydride was delivered to acceptor in an uncommon [1,4]-manner and Lewis acid activation was indispensable. Sc(OTf)$_3$ was the preferable Lewis acid that could catalyze the cascade process. Because of the oxophilicity of Sc(OTf)$_3$, it not only catalyzed the cascade process but also promoted the hydrolysis of acetalic function.

4.7 Electron-Withdrawing Group Activated Allene as Hydride Acceptor

Allene could be activated not only by carbophilic transition metals but also by electron-withdrawing groups at the terminal carbon atom. Alajarin, Sanchez-Andrada, and Vidal et al. disclosed that 2-(1,3-dioxolan-2-yl)phenylallenes **192** containing a range of electron-withdrawing substituents such as phosphinyl, alkoxycarbonyl, sulfonyl at the cumulenic C3 position could be converted into 1-(2-hydroxy)-ethoxy-2-substituted naphthalenes **193** under thermal conditions (Scheme 73) [52]. Mechanistically, an initial [1,5]-hydride shift of the acetalic H atom onto the central cumulene carbon atom affords the conjugated 1,3,5-hexatriene **I**, which undergoes a subsequent 6π-electrocyclic ring-closure of **I** to furnish spirocycle intermediate **II**. A final aromatization step with concomitant ring opening of 1,3-dioxolane fragment produces the substituted naphthalenes **193**.
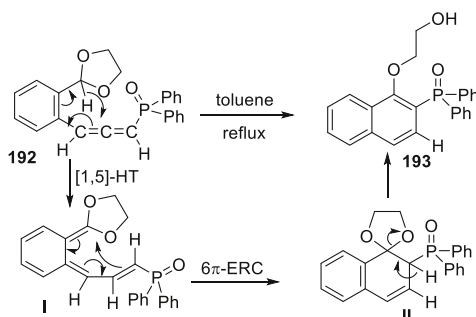

Scheme 71 Hydricity-promoted [1,5]-HT/cyclization in acetalic/ethereal ketenimines and carbodiimides

Scheme 72 Sc(OTf)$_3$-catalyzed cascade [1,4]-HT/cyclization/ hydrolysis
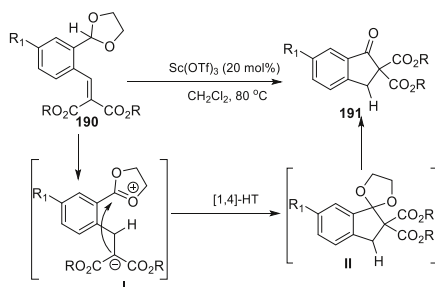
Scheme 73 Hydricity-promoted intramolecular hydroalkylation of electron-deficient allene


5 C(sp^3)–H Bond Adjacent to Sulfur as the Hydride Donor

The methylene (or methine) adjacent to sulfur atom can also work as hydride donor. With reactive electrophilic moieties as hydride acceptors, the cascade [1,5]-hydride transfer/cyclization can occur to give thio-heterocycles. Alajarin and Vidal et al. contributed much to this chemistry.

5.1 1,3-Dithiolane as the Hydride Donor and Benzylidene Malonate as the Hydride Acceptors

Alajarin and Vidal et al. described a Sc(OTf)$_3$-catalyzed cascade [1,4]-hydride shift/cyclization of substrate **194** carrying 1,3-dithiolane, which produced spiro-cyclic products **195** in moderate to good yields (Scheme 74) [70]. Tertiary C–H bond in 1,3-dithiolane worked as hydride donor. Because Sc(OTf)$_3$ is not thiophilic but oxophilic, the dithiolane moiety could remain intact after the cascade [1,4]-
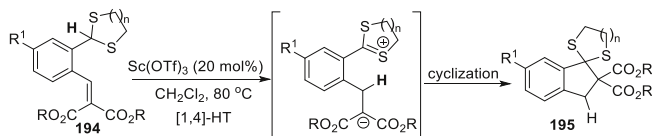
Scheme 74 Cascade [1,4]-HT/cyclization with dithioacetalic C–H as hydride donor

hydride shift/cyclization. Compared with substrate **190** carrying 1,3-dioxolane, the disturbing hydrolysis of the acetalic function was thoroughly suppressed.

5.2 Ketenimine and Carbodiimide as the Hydride Acceptors

Alajarin and Vidal et al. discovered that under thermal conditions (refluxed in toluene), the single thioether **196** carrying ketenimine moiety could be transformed into 4-ethylthio-3,4-dihydroquinoline **197** in good yield via cascade [1,5]-hydride transfer/6π-ERC (Scheme 75) [56].

6 Benzylic C(sp^3)–H Bond as the Hydride Donors

Although a range of cascade reactions of heteroatom-containing substrates (X = NR, O, or S) have been described, their corresponding carbon analogues (X = CH$_2$ or CHR) have been rarely investigated, which might be ascribed to difficulties posed by the rate-determining step of [1,5]-hydride transfer without the assistance of adjacent heteroatom. Sames et al. disclosed that the secondary and tertiary benzylic C–H bond without an adjacent heteroatom could also be exploited as hydride donor. After [1,5]-hydride transfer, the carbocation that develops on benzylic carbon can be stabilized by adjacent electron-rich aromatic groups and alkyl groups via π–p conjugation and hyperconjugation, respectively.

6.1 Electrophilic Benzylidene Malonates and Their Derivatives as the Hydride Acceptors

Sames et al. elegantly demonstrated a PtCl$_4$-catalyzed cascade process involving benzylic methines that lacked the stabilization of α-heteroatom (Scheme 76) [95]. The aryl substrate **198** and thiophene substrate **200** were consumed up within 24 h at 50 °C. Although the electrophilic alkene was activated by two electron-withdrawing carboxylate groups and the cation generated upon [1,5]-hydride transfer could be stabilized by adjacent aromatic group, high-valent PtCl$_4$ was still indispensable for successful transformation, under the catalysis of which hexa-substituted cyclohexanes **199** and **201** could be obtained in moderate to good yield.

Fillion et al. reported a one-pot construction of tetrahydrobenzo-[b]fluoren-11-ones **204** under the catalysis of Sc(OTf)$_3$ (Scheme 77) [136]. The substrates **202** carrying highly electrophilic benzylidene Meldrum's acids and benzylic methylene or methine functions could undergo a cascade [1,5]-hydride shift/cyclization to
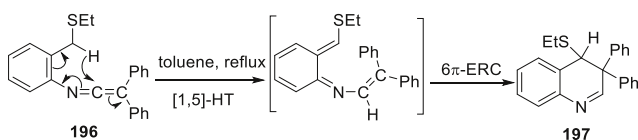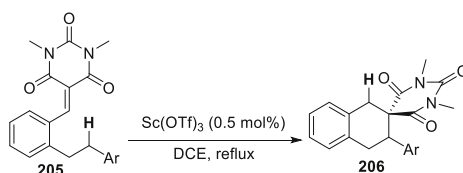

Scheme 75 Cascade [1,5]-HT/6p-ERC to synthesize 3,4-dihydroquinoline

Scheme 76 PtCl$_4$-catalyzed direct C(sp^3)–H functionalization of benzylic methines
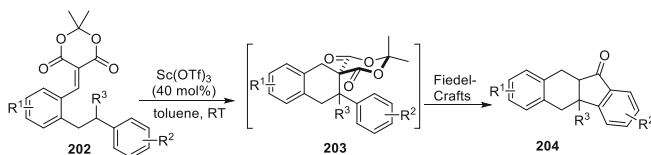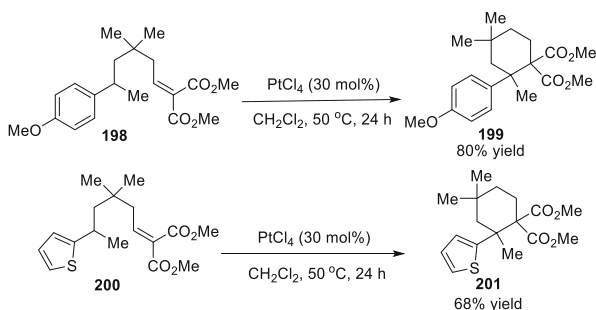
Scheme 77 Sc(OTf)$_3$-catalyzed synthesis of tetrahydro-benzo[*b*]fluoren-11-ones

Scheme 78 Synthesis of 3-aryltetralin skeleton via cascade [1,5]-HT/cyclization


afford spirocycles **203**, which suffered subsequent intramolecular Friedel–Crafts acylation to generate tetracycles **204**.

Akiyama et al. reported a Sc(OTf)$_3$-catalyzed construction of 3-aryltetralin skeleton **206** from simple phenethyl derivatives **205** (Scheme 78) [59]. The electronic and steric properties of the aromatic ring adjacent to C–H bond serving as hydride donor significantly influenced the reactivity of this transformation.

Yu and Luo et al. reported a catalytic enantioselective benzylic C(sp^3)–H functionalization of **207** via a [1,5]-hydride transfer/cyclization sequence with the chiral complex of copper(II) and side-armed bisoxazoline **209** as catalyst, which provided tetrahydronaphthalene derivatives **208** in moderate to high yield with up to 69 % ee (Scheme 79).

6.2 Activated Alkynes as the Hydride Acceptors

Liu et al. reported a TpRuPPh$_3$ (CH$_3$CN)$_2$·PF$_6$-catalyzed cycloisomerization of *cis*-3-en-1-ynes **I** or their precursor alcohols **210**, which afforded cyclopentadiene **211** (Scheme 80) [43]. Mechanistically, **210** undergoes ruthenium-catalyzed dehydration to afford the real substrates *cis*-3-en-1-ynes **I**, which is converted into ruthenium-vinylidene intermediate **II** via [1,2]-shift of alkynyl hydrogen. A [1,5]-
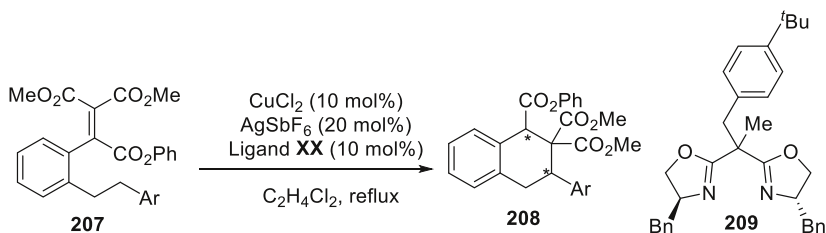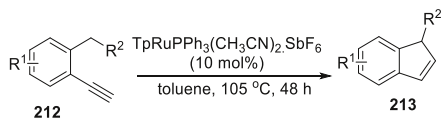
Scheme 79 Catalytic enantioselective C(sp3)–H functionalization via [1,5]-HT/cyclization

Scheme 80 Ruthenium-catalyzed cycloisomerization of *cis*-3-en-1-ynes to cyclopentadienes
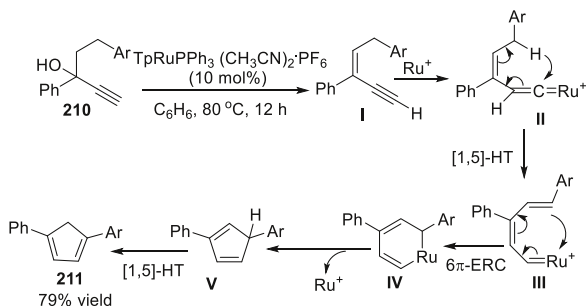
Scheme 81 Ruthenium-catalyzed cyclization of 2-alkyl-1-ethynyl-benzenes


Hydride shift ensues to generate ruthenium haxa-1,3,5-triene **III**, which undergoes 6π-electrocyclic ring closure and reductive elimination to furnish cyclopentadiene **IV**. Ultimately, the most stable regioisomer **211** is yielded via a [1,5]-hydrogen shift.

Liu et al. reported a TpRuPPh₃(CH₃CN)₂SbF₆ (10 mol%)-catalyzed cyclization of 2-alkyl-1-ethynylbenzene derivatives **212**, which yielded 1-substituted-1*H*-indene products **213** in moderate to good yields (Scheme 81) [44]. The counterions were critical to the success of the reaction.

He et al. described a PtCl₂-catalyzed intramolecular cyclization of *o*-isopropyl or *o*-benzyl arylalkynes **214**, which yielded functionalized indenes **215** (Scheme 82) [69]. In contrast to a previous report [44], the terminal carbon of alkyne in this reaction was substituted with aryl substituent. Notably, CuBr (2.0 equiv.) was indispensable to achieve high yield. Theoretically, platinum(II)-activated electrophilic alkyne initially abstracts a hydride from benzylic C–H in [1,4]-manner to generate a benzylic carbocation **I**, which subsequently intercepts nucleophilic alkenyl-platinum(II) to afford the 5-membered ring.

Chatani et al. reported a cycloisomerization of 1-alkyl-2-ethynylbenzenes catalyzed by PtCl₂, PtCl₄, and [RuCl₂(CO)₃]₂ for preparing substituted indenes
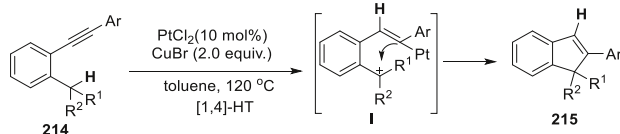
Scheme 82 PtCl$_2$-catalyzed intramolecular cyclization of *ortho*-substituted aryl alkynes via [1,4]-HT/cyclization

**Scheme 83** Gold-catalyzed oxidative cyclizations of *cis*-3-en-1-ynes
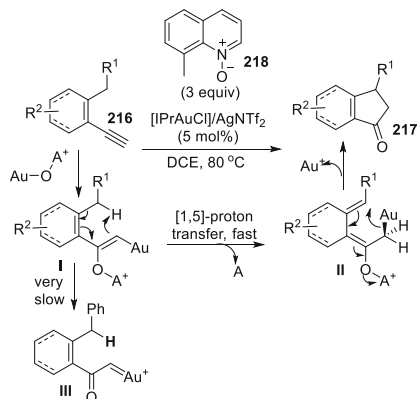
[40]. Remarkably, the benzylic primary C–H bond could participate in this cascade process to afford indene in 44 % yield. In contrast to Zhang's report [61], it is the hydride that transfers in [1,5]-manner this time.

Liu et al. described a [IPrAuCl]/AgNTf$_2$-catalyzed oxidative cyclizations of *cis*-3-en-1-ynes **216** with 8-methylisoquinoline oxide **218** as oxidant, which gave rise to cyclopentenone skeletons **217** (Scheme 83) [67]. Basically, the initially formed gold-containing enol ether **I** has a high energy barrier to overcome to form hypothetical carbenoid **III**. Instead, **I** undergoes a rapid [1,5]-hydrogen shift to generate intermediate **II**. Remarkably, hydrogen is transferred in the form of proton because hydrogen is captured by electron-rich gold-alkenyl subunit and the electron-withdrawing substituent in the benzylic position is beneficial to the cascade process. Afterwards, a subsequent cyclization of **II** leads to **217**. This proposed mechanism explains the observation that an acidic C–H bond can accelerate this oxidative cyclization. Similar mechanisms of transferring proton in [1,5]-manner have also been described by Zhang et al. [62, 64–66].

6.3 Electrophilic Imine, Hydrazone, Oxime Ester as the Hydride Acceptors

In the total synthesis of D-Homosteroid, Tietze et al. reported a BF$_3$·OEt$_2$-catalyzed cascade [1,5]-hydride transfer/cyclization of **219**, which produced an unusually bridged steroid alkaloid **220** in 85 % yield at room temperature (Scheme 84) [137–139]. Although benzylic methine and imine in **219** are comparatively inactive hydride donor and acceptor, with the assistance of electron-donating methoxy group
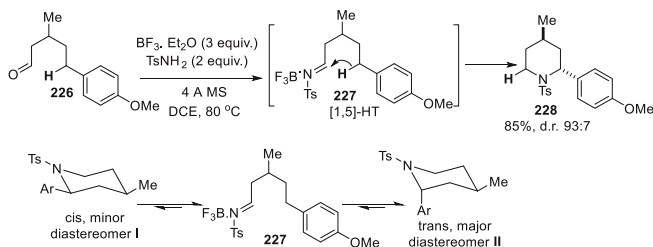
Scheme 84 BF$_3$·Et$_2$O-
catalyzed intramolecular hydro-
N-alkylation of phenyl imine
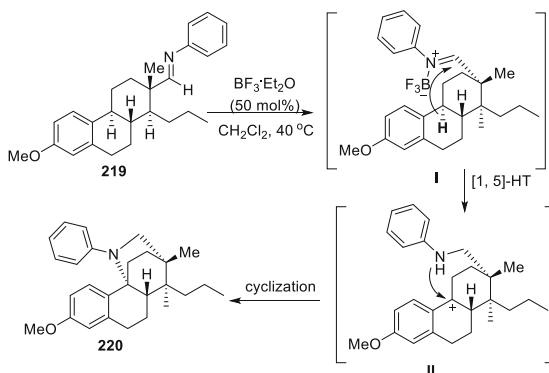
at *para*-position and activation by BF$_3$·OEt$_2$, hydride could migrate to imine moiety readily. A subsequent nucleophilic attack of amino group on carbocation on **II** led to the formation of bridged steroidal azacycles **220**. In addition to phenyl substituted imine, hydrazones and oxime ethers could also work as hydride acceptor in the presence of Lewis acid. Frank et al. described a similar BF$_3$·Et$_2$O-catalyzed intramolecular hydro-N-alkylation of hydrazones and oxime ethers [140].

Akiyama et al. described a Sc(OTf)$_3$-catalyzed reaction to access isoquinoline skeleton **222** (Scheme 85) [141]. The tosyl imine formed in situ and benzylic methylene worked as hydride acceptor and donor, respectively. Sc(OTf)$_3$ played dual roles, one of which was to promote the condensation of benzaldehyde **221** and tosylamide. Because the hydride donor in the reaction was inactive benzylic methylene, electron-withdrawing tosyl group was indispensable to increase the electrophilicity of C=N bond, additionally Sc(OTf)$_3$ could further activate the imine. The methodology was elegantly elaborated in the formal synthesis of (±)-tetrahydropalmatine **225**.

Sames et al. reported a highly stereoselective intramolecular amination of benzylic C(sp^3)–H bonds via cascade [1,5]-HT/cyclization of N-tosylimine **227** generated in situ from aliphatic aldehyde **226**, which constructed 2-arylpiperidines **228** and 3-aryl-1,2,3,4-tetrahydroisoquinolines (Scheme 86) [96]. Remarkably, the conformational freedom of substrates had a profound influence on the chemical behaviors of hydride acceptors: the substrates with high conformational rigidity had
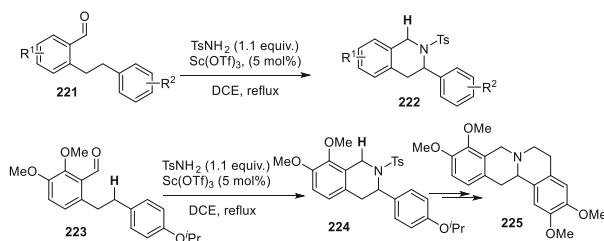
Scheme 85 Sc(OTf)$_3$-catalyzed hydro-N-alkylation of tosyl imines to form 3-arylisoquinolines

Scheme 86 BF$_3$·Et$_2$O-catalyzed stereoselective intramolecular amination of benzylic C(sp^3)–H bonds
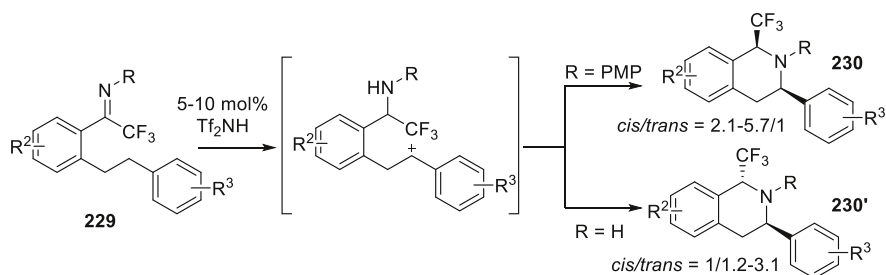
Scheme 87 Brønsted acid-catalyzed C(sp^3)–H bond functionalization for synthesis of 3-aryl-1-trifluoromethyltetrahydroisoquinolines

higher reactivities than those with high conformational freedom. The cascade [1,5]-HT/cyclization was highly stereoselective, which could be rationalized by the reversible cyclization step. The high stereoselectivity resulted from thermodynamic control and the aryl ring preferred to adopt an axial orientation in diastereomer **II** to avoid the steric interaction (pseudo-allylic strain) with the sulfonamide group in diastereomer **I**.

Akiyama et al. reported a Brønsted acid-catalyzed synthesis of 3-aryl-1-trifluoromethyltetrahydroisoquinolines **230** and **230′** by a benzylic [1,5]-hydride shift-mediated C–H bond functionalization (Scheme 87) [142], which features the diastereo-divergent synthesis of 3-aryl-1-trifluoromethyltetrahydroisoquinolines **230** and **230′** by tuning the substituents on nitrogen atom. The trifluoromethylketimine derived from *para*-anisidine and activated by Tf$_2$NH served as hydride acceptor and the substituents on ketimines had dramatic impacts on the diastereoselectivities: *cis*-product **230** could be furnished as major product when R was PMP group, whereas the diastereoselectivity was reversed with R as hydrogen.

6.4 Ketenimine and Carbodiimide as Hydride Acceptors

Alajarin et al. described a concise protocol for synthesis of 3,4-dihydroquinolines **232** and 3,4-dihydroquinazolines **234** (Scheme 88) [55]. Triphenyl substituted methines and electrophilic ketenimine/carbodiimide worked as hydride donors and acceptors, respectively. Because of the high electrophilicity of ketenimine and

Scheme 88 Direct C(sp^3)–H functionalization of tri(di)arylmethane
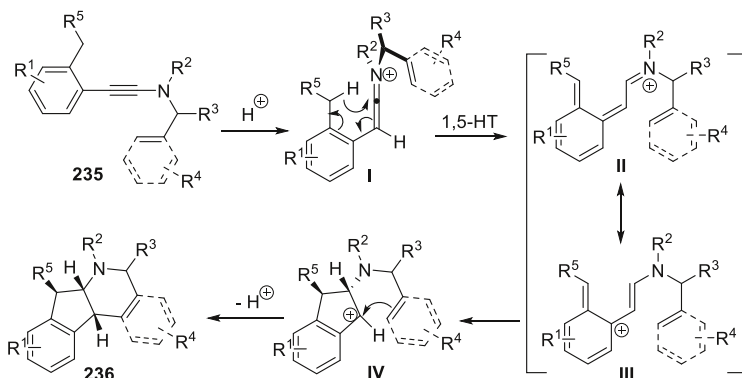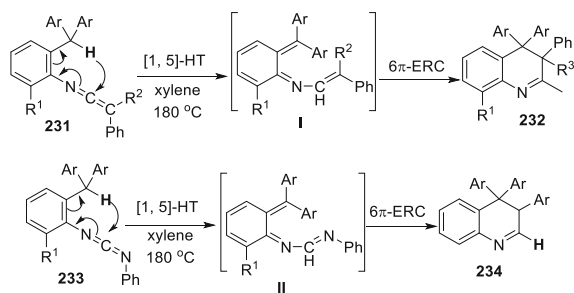
Scheme 89 Keteniminium ion-initiated cascade cationic polycyclization

carbodiimide, and highly stabilizing effect of adjacent three aromatic groups, thermal conditions alone could efficiently facilitate the cascade process, under which **231** and **233** could be transformed into **232** and **234**, respectively, in moderate to good yield. Mechanistically, the C–H bond of the triarylmethane fragment is cleaved via a [1,5]-hydride shift to give conjugated 1,3,5-hexatriene **I** or **II**, which suffers subsequent 6π-electrocyclic ring closure to produce the sterically congested **232** and **234**.

Thibaudeau and Evano et al. reported a TfOH or Tf$_2$NH-catalyzed keteniminium-initiated cationic polycyclization of ynamides **235** (Scheme 89) [143], which provided a straightforward access to polycyclic nitrogen heterocycles **236** possessing up to three contiguous stereocenters and seven fused cycles. Basically, the reaction is initiated by protonation of electron-rich alkyne of ynamide **XX**, yielding a highly reactive N-tosyl- or N-acyl-keteniminium ion **I**, which served as hydrogen acceptor. A [1,5]-sigmatropic hydrogen shift would then ensue to generate conjugated iminium **II** (in resonance with the bis-allylic carbocationic form **III**). The first cycle would be formed by a 4π conrotatory electrocyclization, producing **IV** in the manner of Nazarov reaction. Finally, a second cyclization between the benzylic carbocation **IV** and the arene/alkene subunit leads to the formation of polycycle **236**.

7 Non-benzylic C(sp^3)–H Bonds as the Hydride Donors

The cascade [1,5]-hydride transfer/cyclization summarized above have entailed the electronic assistance of adjacent heteroatoms or aromatic groups for stabilizing the carbocation formed upon hydride shift. However, hydride abstraction from an aliphatic, non-benzylic position is still a challenging task, and its realization would improve the usefulness of the cascade strategy in synthetic organic chemistry. Because of the lack of electronic assistance from adjacent heteroatom or aromatic group, the dissociation energy of C–H bond in aliphatic non-benzylic position is quite high. It was not until 2011 that Akiyama et al. managed to employ non-benzylic methylene as the hydride donor.

7.1 Electrophilic Benzylidene Malonates and Their Derivatives as the Hydride Acceptors

Akiyama et al. first reported an unprecedented cascade [1,5]-hydride transfer/cyclization with non-benzylic methine as hydride donor (Scheme 90) [74]. Treatment of benzylidene barbituric acid **237** with 3 mol% Sc(OTf)$_3$ in refluxing ClCH$_2$CH$_2$Cl for 24 h could furnish the desired tetraline **238** in excellent yield. Notably, the substrate with a linear side chain **239** did not give the desired product **240**, even with a catalyst loading of 30 mol%. This result suggested that the substitution degree at the hydride-releasing carbon atom was crucial for the success of the cascade process.

7.2 Gold-Activated Alkynes as the Hydride Acceptors

Barluenga et al. elegantly demonstrated an intriguing manifold reactivity of alkynylcyclopropanes **241** bearing a spirane core (Scheme 91) [144]. Remarkably, comparatively inactive non-benzylic secondary C–H bond could work as hydride donor. The cyclopropane moiety was crucial for the success of the cascade process, which rendered inactive methylene group closer to electrophilic alkyne moiety. Thus, the proximate hydride could be readily abstracted by electrophilic alkyne activated by gold catalyst. The diverse fate of the resulting cationic gold species could be efficiently controlled by simple option of appropriate catalyst (either

Scheme 90 Sc(OTf)$_3$-catalyzed direct functionalization of aliphatic tertiary C(sp^3)–H bond
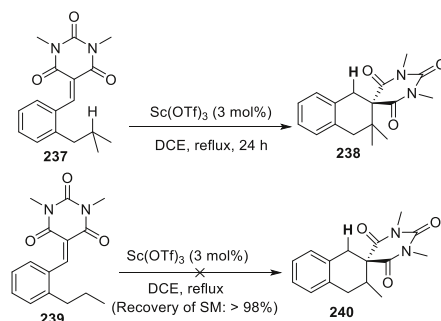
Scheme 91 Gold-catalyzed direct functionalization of secondary non-benzylic C(sp^3)–H bonds
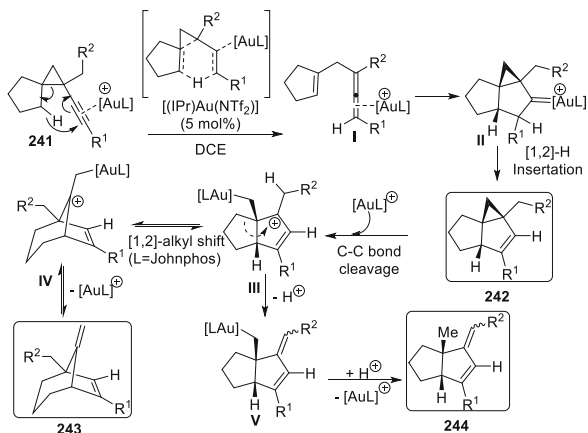
[(JohnPhos)Au(MeCN)]-[SbF$_6$] or [(IPr)Au-(NTf$_2$)]) and reaction temperature. A range of cyclic structures, e.g., pentalene derivatives **242** and **244**, and bicycles **243** could be accessed with complete selectivity. Mechanistically, the gold-alkyne coordination triggers a [1,5]-hydride transfer with concomitant ring opening of cyclopropane. The generated 1,4-enallenyl gold intermediate **I** might then undergo a cyclization via intermediate **II** to afford tricycle **242**. The subjection of **242** to harsher reaction conditions leads to the formation of **243** and **244**, and **III** might be their common intermediate, which is formed by regioselective gold-catalyzed C–C bond cleavage. The formation of **243** can be rationalized by a [1,2]-alkyl migration of **III** and metal elimination of **IV**. Alternatively, deprotonation of **III** and a subsequent protodemetallation of **V** would provide pentalene **244**.

7.3 Electrophilic Imine as the Hydride Acceptor

One more example of using aliphatic non-benzylic methine as hydride donor was also reported by Akiyama et al. in which the tosyl imine **I** generated in situ from **245** was employed as hydride acceptor (Scheme 92) [141]. Three-step cascade transformations involving imine formation/[1,5]-hydride shift/cyclization occurred to afford isoquinoline with Sc(OTf)$_3$ as catalyst. In order to get decent yield, 30 mol% catalyst loading was employed, whereas the tetraline **246** was obtained only in 32 % yield even with a prolonged reaction time (72 h).
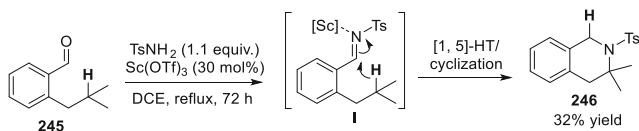
Scheme 92 Sc(OTf)$_3$-catalyzed hydro-N-alkylation with aliphatic tertiary C(sp^3)–H bond as hydride donor

8 Conclusions and Perspectives

In this review, we have introduced the recent advances of cascade $[1,n]$-hydrogen transfer/cyclization as a versatile protocol to directly functionalize inactive $C(sp^3)$–H bond into C–C, C–N, and C–O bonds in an atom-economic manner. A variety of hydrogen donors and acceptors as well as different activation modes of hydrogen acceptors have been well organized and discussed. This methodology has proven to be powerful in delivering molecular complexity, especially in the synthesis of a variety of useful and pharmaceutically important heterocycles, e.g., 5-, 6-, 7-membered fused or spiro-hetero, or full carbon cycles. The facile construction of C–C, C–N, and C–O bonds and ring skeletons renders this strategy attractive to access value-added molecules from readily available starting materials. In addition to the benefit of atom-economy, the reaction conditions are mild, and expensive transition metal catalysts are not required in many cases.

Despite the significant developments in recent years, there is still much left to do in this chemistry, for instance, the types of hydride donors and acceptors are still rather limited. More $C(sp^3)$–H α to heteroatoms, which have lone pairs, e.g., phosphorus, bromine, chlorine, etc., are likely to be exploited as hydrogen donors and more diverse electron-deficient species can be employed as hydrogen acceptors.

Another hot research topic in this area is the asymmetric catalytic version of this reaction, and more efficient and selective catalytic systems needs to be developed. Although this methodology has shown an appealing application to construct complex moieties, it has been rarely exploited in total syntheses and the synthetic potential of this methodology in natural product synthesis has to be further exploited.

Finally, the mechanistic pathway behind this reaction should be studied in depth and some problems need to be addressed such as the influencing factors of the hydride transfer and the essence of the hydrogen transferred. On the basis of the above clarifications and deeper understanding of these transformations, discovery of new highly active and selective catalysts for this methodology and development of novel reactions are expected in the future.

References

1. Deno NC, Peterson HJ, Saines GS (1960) Chem Rev 60:7
2. Russell AE, Miller SP, Morken JP (2000) J Org Chem 65:8381
3. Yoshizawa K, Toyota S, Toda F (2001) Tetrahedron Lett 42:7983
4. Evans DA, Hoveyda AH (1990) J Am Chem Soc 112:6447
5. Evans DA, Nelson SG, Gagne MR, Muci AR (1993) J Am Chem Soc 115:9800
6. Node M, Nishide K, Shigeta Y, Shiraki H, Obata K (2000) J Am Chem Soc 122:1927
7. Ooi T, Ichikawa H, Maruoka K (2001) Angew Chem Int Ed 40:3610
8. Ishihara K, Kurihara H, Yamamoto H (1997) J Org Chem 62:5664
9. Ooi T, Otsuka H, Miura T, Ichikawa H, Maruoka K (2002) Org Lett 4:2669
10. Suzuki T, Morita K, Tsuchida M, Hiroi K (2003) J Org Chem 68:1601
11. Godula K, Sames D (2006) Science 312:67
12. Chen X, Engle KM, Wang DH, Yu JQ (2009) Angew Chem Int Ed 48(28):5094

13. Giri R, Shi BF, Engle KM, Maugel N, Yu JQ (2009) Chem Soc Rev 38(11):3242
14. Gunay A, Theopold KH (2010) Chem Rev 110:1060
15. Mátyus P, Éliás O, Tapolcsányi P, Polonka-Bálint Á, Halász-Dajka B (2006) Synthesis (16):2625–2639. doi:10.1055/s-2006-942490
16. Peng B, Maulide N (2013) Chem Eur J 19:13274
17. Haibach MC, Seidel D (2014) Angew Chem Int Ed 53:5010
18. Wang L, Xiao J (2014) Adv Synth Catal 356:1137
19. Pan SC (2012) Beil J Org Chem 8:1374
20. Wang M (2013) ChemCatChem 5:1291
21. Pinnow J (1895) Ber Dtsch Chem Ges 28:3039
22. Katritzky AR, Rachwal S, Rachwal B (1996) Tetrahedron 52:15031
23. Koufaki M, Theodorou E, Galaris D, Nousis L, Katsanou ES, Alexis MN (2006) J Med Chem 49:300
24. Lee SB, Lin CY, Gill PMW, Webster RD (2005) J Org Chem 70:10466
25. Toyota M, Omatsu I, Asakawa Y (2001) Chem Pharm Bull 924
26. Nozoe S, Morisaki M, Iitaka Y, Takahashi N, Tamura S, Ki K, Shirasaka M (1965) J Am Chem Soc 87:4968
27. Entzeroth M, Blackman AJ, Mynderse JS, Moore RE (1985) J Org Chem 50:1255
28. Aoki S, Watanabe Y, Sanagawa M, Setiawan A, Kotoku N, Kobayashi M (2006) J Am Chem Soc 128:3148
29. Macias FA, Galindo JLG, Varela RM, Torres A, Molinillo JMG, Fronczek FR (2006) Org Lett 8:4513
30. Katsoulis IA, Kythreoti G, Papakyriakou A, Koltsida K, Anastasopoulou P, Stathakis CI, Mavridis I, Cottin T, Saridakis E, Vourloumis D (2011) ChemBioChem 12(8):1188
31. Boivin TLB (1987) Tetrahedron 43:3309
32. Elliott MC, Williams E (2001) J Chem Soc Perkin Trans 1(19):2303
33. Marmsater FP, West FG (2002) Chem Eur J 8:4347
34. Hale KJ, Hummersone MG, Manaviazar S, Frigerio M (2002) Nat Prod Rep 19(4):413
35. Haustedt LO, Hartung IV, Hoffmann HM (2003) Angew Chem Int Ed 42(24):2711
36. Wang L, Li P, Menche D (2010) Angew Chem Int Ed 49(48):9270
37. Pastine SJ, Sames D (2005) Org Lett 7:5429
38. McQuaid KM, Sames D (2009) J Am Chem Soc 131:402
39. Vadola PA, Sames D (2009) J Am Chem Soc 131:16525
40. Tobisu M, Nakai H, Chatani N (2009) J Org Chem 74:5471
41. Zhou G, Liu F, Zhang J (2011) Chem Eur J 17:3101
42. Xia X, Song X, Wang N, Wei H, Liua X, Liang Y (2012) RSC Adv 2:560
43. Datta S, Odedra A, Liu R (2005) J Am Chem Soc 127:11606
44. Odedra A, Datta S, Liu R (2007) J Org Chem 72:3289
45. Shu X, Ji K, Zhao S, Zheng Z, Chen J, Lu L, Liu X, Liang Y (2008) Chem Eur J 14:10556
46. Meth-Cohn O (1996) Adv Heterocycl Chem 65:1
47. Nijhuis WHN, Verboom W, Reinhoudt DN (1987) J Am Chem Soc 109:3136
48. Nijhuis WHN, Verboom W, El-Fadl AA, Hummel GJV, Reinhoudt DN (1987) J Org Chem 54:209
49. Chen L, Zhang L, Lv J, Cheng J, Luo S (2012) Chem Eur J 18:8891
50. Zhang L, Chen L, Lv J, Cheng J-P, Luo S (2012) Chem Asian J 7:2569
51. Barluenga J, Fananas-Mastral M, Aznar F, Valdes C (2008) Angew Chem Int Ed 47:6594
52. Alajarin M, Bonillo B, Marin-Luna M, Sanchez-Andrada P, Vidal A (2013) Chem Eur J 47:16093
53. Zhao S, Shu X, Ji K, Zhou A, He T, Liu X, Liang Y (2011) J Org Chem 76:1941
54. Alajarin M, Bonillo B, Ortin M-M, Sanchez-Andrada P, Vidal A (2011) Eur J Org Chem 1896–1913. doi:10.1002/ejoc.201001372
55. Alajarin M, Bonillo B, Ortin M, Sanchez-Andrada P, Vidal A, Orenes R (2010) Org Biomol Chem 8:4690
56. Alajarin M, Bonillo B, Orenes RA, Ortin MM, Vidal A (2012) Org Biomol Chem 10(48):9523
57. Brunet P, Wuest JD (1996) J Org Chem 61:2020
58. Alajarin M, Bonillo B, Ortin M, Sanchez-Andrada P, Vidal A (2006) Org Lett 8:5645
59. Mori K, Sueoka S, Akiyama T (2011) Chem Lett 40(12):1386
60. Apeloig Y, Karni M (1988) J Chem Soc Perkin Trans II:625
61. Cui L, Peng Y, Zhang L (2009) J Am Chem Soc 131:8394
62. Noey EL, Luo Y, Zhang L, Houk KN (2012) J Am Chem Soc 134:1078

63. Yu P, Lin JS, Li L, Zheng SC, Xiong YP, Zhao LJ, Tan B, Liu XY (2014) Angew Chem Int Ed 53(44):11890
64. Zhang C, De CK, Mal R, Seidel D (2008) J Am Chem Soc 130:416
65. Richers MT, Deb I, Platonova AY, Zhang C, Seidel D (2013) Synthesis 45:1730
66. Dieckmann A, Richers MT, Platonova AY, Zhang C, Seidel D, Houk KN (2013) J Org Chem 78:4132
67. Bhunia S, Ghorpade S, Huple DB, Liu R (2012) Angew Chem Int Ed 51:2939
68. Cui L, Ye L, Zhang L (2010) Chem Commun 46(19):3351
69. Yang S, Li Z, Jian X, He C (2009) Angew Chem Int Ed 48:3999
70. Alajarin M, Marin-Luna M, Vidal A (2011) Adv Synth Catal 353(4):557
71. Meth-Cohn O, Naqui MA (1967) Chem Commun 1157
72. Volochnyuk DM, Shivanyuk AN, Tolmachev AA, Ryabukhin SV, Plaskon AS (2007) J Org Chem 72:7417
73. Che X, Zheng L, Dang Q, Bai X (2008) Synlett (15):2373–2375. doi:10.1055/s-2008-1078212
74. Mori K, Sueoka S, Akiyama T (2011) J Am Chem Soc 133:2424
75. Reinhoudt DN, Visser GW, Verboom W, Benders PH, Pennings MLM (1983) J Am Chem Soc 105:4775
76. Cambeiro F, Lopez S, Varela JA, Saa C (2012) Angew Chem Int Ed 51(3):723
77. Orlemans EM, Lammerink BHM, Veggel FCJMV, Verboom W, Harkema S, Reinhoudt DN (1988) J Org Chem 53:2278
78. Dunkel P, Turos G, Bényeib A, Ludanyic K, Matyus P (2010) Tetrahedron 66:2331
79. Zhou G, Zhang J (2010) Chem Commun 46:6593
80. Haibach MC, Deb I, De CK, Seidel D (2011) J Am Chem Soc 133:2100
81. Cao T, Fan W, Zhu C (2013) Org Lett 15:2254
82. Lo VK-Y, Wong M-K, Che C-M (2008) Org Lett 10:517
83. Kuang J, Ma S (2010) J Am Chem Soc 132:1786
84. Sugiishi T, Nakamura H (2012) J Am Chem Soc 134:2504
85. Meth-Cohn O, Suschitzky H (1972) Adv Heterocycl Chem 14:211
86. Verboom W, Reinhoudt DN (1990) Recl Trav Chim Pays-Bas 109:311
87. Quintela JM (2003) Recent Res Dev Org Chem 7:259
88. Ruble JC, Hurd AR, Johnson TA, Sherry DA, Barbachyn MR, Toogood PL, Bundy GL, Graber DR, Kamilar GM (2009) J Am Chem Soc 131:3991
89. Murarka S, Zhang C, Konieczynska MD, Seidel D (2009) Org Lett 11:129
90. Mori K, Ehara K, Kurihara K, Akiyama T (2011) J Am Chem Soc 133:6166
91. Cao W, Liu X, Wang W, Lin L, Feng X (2011) Org Lett 13:600
92. Toth L, Fu Y, Zhang HY, Mandi A, Kover KE, Illyes TZ, Kiss-Szikszai A, Balogh B, Kurtan T, Antus S, Matyus P (2014) Beilstein J Org Chem 10:2594
93. Barluenga J, Fañanás-Mastral M, Fernández A, Aznar F (2011) Eur J Org Chem 1961–1967. doi:10.1002/ejoc.201001717
94. Xiao J, Li X (2011) Angew Chem Int Ed 50(32):7226
95. Pastine SJ, McQuaid KM, Sames D (2005) J Am Chem Soc 127:12180
96. Vadola PA, Carrera I, Sames D (2012) J Org Chem 77:6689
97. Murarka S, Deb I, Zhang C, Seidel D (2009) J Am Chem Soc 131:13226
98. Kang YK, Kim SM, Kim DY (2010) J Am Chem Soc 132:11847
99. Suh CW, Kim DY (2014) Org Lett 16(20):5374
100. Suh CW, Woo SB, Kim DY (2014) Asian J Org Chem 3(4):399
101. Zhang S-L, Xie H-X, Zhu J, Li H, Zhang X-S, Li J, Wang W (2011) Nat Commun 2:211
102. Kang YK, Kim DY (2014) Chem Commun 50(2):222
103. Kang YK, Kim DY (2013) Adv Synth Catal 355:3131
104. Han Y, Han W, Hou X, Zhang X, Yuan W (2012) Org Lett 14:4054
105. Cao W, Liu X, Guo J, Lin L, Feng X (2015) Chem Eur J 21(4):1632
106. Mori K, Kurihara K, Yabe S, Yamanaka M, Akiyama T (2014) J Am Chem Soc 136(10):3744
107. Zhao T, Zhang H, Cui L, Qu J, Wang B (2015) RSC Adv 5(105):86056
108. Kaval N, Dehaen W, Mátyus P, Eycken EV (2004) Green Chem 6:125
109. Kaval N, Halasz-Dajka B, Vo-Thanh G, Dehaen W, Eycken JV, Matyus P, Loupy A, Eyckena EV (2005) Tetrahedron 61:9052
110. Jurberg ID, Peng B, Woestefeld E, Wasserloos M, Maulide N (2012) Angew Chem Int Ed 51:1950
111. Zhang C, Murarka S, Seidel D (2009) J Org Chem 74:419

112. Mori K, Ohshima Y, Ehara K, Akiyama T (2009) Chem Lett 38:524
113. Du Y, Luo S, Gong L (2011) Tetrahedron Lett 52:7064
114. Zheng L, Yang F, Dang Q, Bai X (2008) Org Lett 10:889
115. He YP, Wu H, Chen DF, Yu J, Gong LZ (2013) Chem Eur J 19(17):5232
116. Rabong C, Hametner C, Mereiter K, Kartsev VG, Jordisa U (2008) Heterocycles 75:799
117. Wang P-F, Huang Y-P, Wen X, Sun H, Xu Q-L (2015) Eur J Org Chem 2015(30):6727
118. Wang PF, Jiang CH, Wen X, Xu QL, Sun H (2015) J Org Chem 80:1155
119. Chen D, Han Z, He Y, Yu J, Gong L (2012) Angew Chem Int Ed 51:12307
120. Gao X, Gaddam V, Altenhofer E, Tata RR, Cai Z, Yongpruksa N, Garimallaprabhakaran AK, Harmata M (2012) Angew Chem Int Ed 51(28):7016
121. Chang YZ, Li ML, Zhao WF, Wen X, Sun H, Xu QL (2015) J Org Chem 80(19):9620
122. McQuaid KM, Long JZ, Sames D (2009) Org Lett 11:2972
123. Mori K, Kawasaki T, Sueoka S, Akiyama T (2010) Org Lett 12:1732
124. Bajracharya GB, Pahadi NK, Gridnev ID, Yamamoto Y (2006) J Org Chem 71:6204
125. Bhunia S, Liu R (2008) J Am Chem Soc 130:16488
126. Shikanai D, Murase H, Hata T, Urabe H (2009) J Am Chem Soc 131:3166
127. Jurberg ID, Odabachian Y, Gagosz F (2010) J Am Chem Soc 132:3543
128. Bolte B, Gagosz F (2011) J Am Chem Soc 133:7696
129. Jiao Z, Zhang S, He C, Tu Y, Wang S, Zhang F, Zhang Y, Li H (2012) Angew Chem Int Ed 51:8811
130. Koizumi Y, Kobayashi H, Wakimoto T, Furuta T, Fukuyama T, Kan T (2008) J Am Chem Soc 130:16854
131. Kurosawa W, Kan T, Fukuyama T (2003) J Am Chem Soc 125:8112
132. Kurosawa W, Kan T, Fukuyama T (2003) Synlett 1028–1030
133. Kurosawa W, Kobayashi H, Kan T, Fukuyama T (2004) Tetrahedron 60:9615
134. Reddy RP, Lee GH, Davies HML (2006) Org Lett 8:3437
135. Wakimoto T, Miyata K, Ohuchi H, Asakawa T, Nukaya H, Suwa Y, Kan T (2011) Org Lett 13:2789
136. Mahoney SJ, Moon DT, Hollinger J, Fillion E (2009) Tetrahedron Lett 50:4706
137. Woelfling J, Frank É, Schneider G, Tietze L (1999) Angew Chem Int Ed 38:200
138. Wölfling J, Frank E, Schneider G, Tietze LF (1999) Eur J Org Chem 3013–3020
139. Wölfling J, Frank E, Schneider G, Tietze LF (2004) Eur J Org Chem 90–100. doi:10.1002/ejoc. 200300500
140. Frank É, Schneider G, Kádár Z, Wölfling J (2009) Eur J Org Chem 3544–3553. doi:10.1002/ejoc. 200900301
141. Mori K, Kawasaki T, Akiyama T (2012) Org Lett 14:1436
142. Mori K, Umehara N, Akiyama T (2015) Adv Synth Catal 357(5):901
143. Theunissen C, Metayer B, Henry N, Compain G, Marrot J, Martin-Mingot A, Thibaudeau S, Evano G (2014) J Am Chem Soc 136(36):12528
144. Barluenga J, Sigueiro R, Vicente R, Ballesteros A, Tomas M, Rodriguez MA (2012) Angew Chem Int Ed 51(41):10377

CrossMark

REVIEW

C-Alkylation by Hydrogen Autotransfer Reactions

Yasushi Obora[1]

Abstract The development of practical, efficient, and atom-economical methods for the formation of carbon–carbon bonds remains a topic of considerable interest in current synthetic organic chemistry. In this review, we have summarized selected topics from the recent literature with particular emphasis on *C*-alkylation processes involving hydrogen transfer using alcohols as alkylation reagents. This review includes selected highlights concerning recent progress towards the modification of catalytic systems for the α-alkylation of ketones, nitriles, and esters. Furthermore, we have devoted a significant portion of this review to the methylation of ketones, alcohols, and indoles using methanol. Lastly, we have also documented recent advances in β-alkylation methods involving the dimerization of alcohols (Guerbet reaction), as well as new developments in *C*-alkylation methods based on sp^3 C–H activation.

1 Introduction

The construction of carbon–carbon bonds is one of the most important transformations in organic synthesis, and considerable research efforts have been directed towards the development of new methods in this area. Importantly, transformations of this type provide access to a wide variety of organic compounds that can be used as synthetic building blocks in the fine chemical and pharmaceutical industries, as well as key intermediates in the preparation of drugs and functional materials.

✉ Yasushi Obora
obora@kansai-u.ac.jp

1 Department of Chemistry and Materials Engineering, Faculty of Chemistry, Materials and Bioengineering, Kansai University, Suita, Osaka 564-8680, Japan

The classical methodology for the formation of carbon–carbon bonds involves cation–anion-based nucleophilic substitution reactions between organometallic reagents and organohalides. However, there are several disadvantages associated with methods of this type, including the handling of reactive reagents (such as air- and moisture-sensitive organometallic agents) and the production of stoichiometric amounts of salt-based waste products during the course of the reaction [1–7].

Recent progress in this area has culminated in the development of transition-metal-catalyzed cross-coupling reactions, which have provided several useful *C*-alkylation methods for introducing various aryl, vinyl, and alkyl groups [8]. Furthermore, significant research efforts have recently been focused on the development of "direct coupling" methods involving the oxidative activation of C–H bonds. Notably, these reactions do not require organometallic and/or organohalide substrates, and are therefore much more atom-economical and environmentally friendly than their predecessors [9–19].

As a promising alternative to the *C*-alkylation methods described above, hydrogen transfer using alcohols represents a useful and environmentally benign process, which uses alcohols as alkylation agents with water being generated as the only major by-product. Considerable research interest has recently been focused on the development of highly atom-efficient processes capable of minimizing the amount of waste generated in the form of by-products during organic transformations. In this regard, *C*-alkylation reactions involving a transfer hydrogenation step (or hydrogen borrowing/hydrogen autotransfer methodologies) represent one of the ultimate goals of modern synthetic chemistry for the formation of C–C bonds [20–22].

This field presents many opportunities; therefore, there has been a significant increase in the number of research groups working towards the development of new *C*-alkylation processes involving transfer hydrogenation. Consequently, many interesting review articles have been reported to date regarding all aspects of this emerging methodology [23–45].

Some of the most commonly reported *C*-alkylation methods involving the transition-metal-catalyzed transfer hydrogenation of alcohols can be described as follows: (1) the α-alkylation of ketones and carbonyl compounds; (2) alcohol–alcohol coupling reactions to afford ketones; and (3) β-alkylation by alcohol dimerization, which is also referred to as a Guerbet reaction.

The first of these reactions, the α-alkylation of ketones and carbonyl compounds, involves the following process (as shown in Schemes 1, 2) [46–57]: (1) the initial oxidation of the alcohol substrate, through a hydrogen transfer process to give the corresponding aldehyde and metal-hydride intermediate; (2) the aldol condensation of the enol (generated by the tautomerization of the ketone substrate) with the
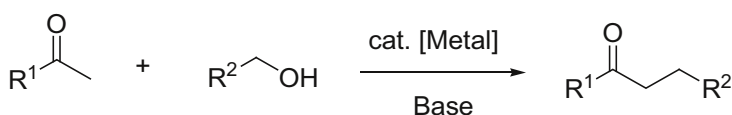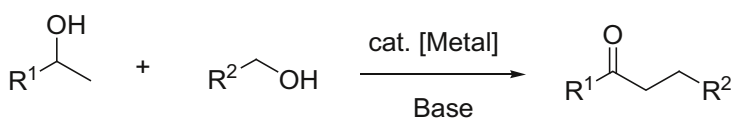

Scheme 1 Metal-catalyzed α-alkylation of ketones
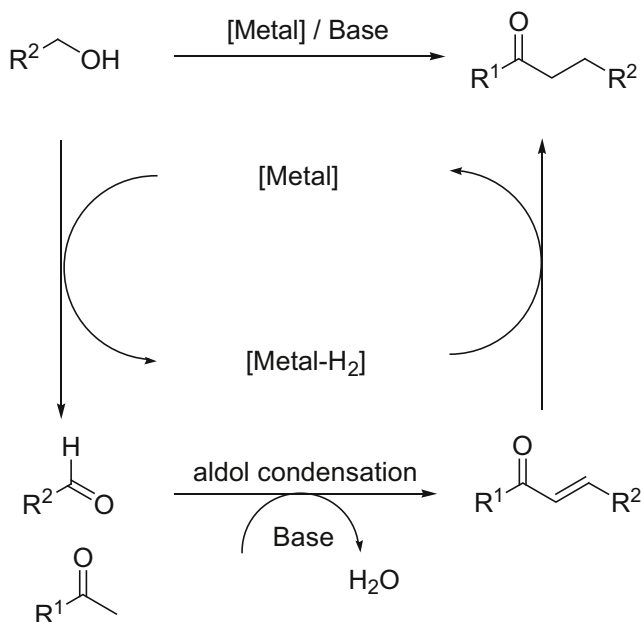
Scheme 2 Representative reaction pathway for the α-alkylation of ketones

aldehyde generated in the previous step to give the corresponding α,β-unsaturated ketone; and (3) the hydrogenation of the α,β-unsaturated ketone with the metal hydride generated in step (1) of this process to give the α-alkylated ketone product.

The second of the three reactions described above (i.e., alcohol–alcohol coupling reactions to afford ketones) provides another route for the construction of *C*-alkylated ketones via the formation of two distinct aldehydes from the different alcohols [58–68].

The alcohol–alcohol coupling reaction involves the following steps (Schemes 3, 4): (1) the initial simultaneous transition-metal-catalyzed dehydrogenation of the two different alcohols to afford the corresponding carbonyl compounds and metal halide; and (2) the aldol condensation of the carbonyl compounds and the subsequent hydrogenation of the resulting unsaturated carbonyl compounds in a similar manner to that described above for the ketone α-alkylation reaction (Schemes 3, 4) to give the *C*-alkylated ketone product.

The third of the reactions described above (i.e., the Guerbet reaction of primary alcohols) allows for the self-condensation/dimerization of alcohols to give the
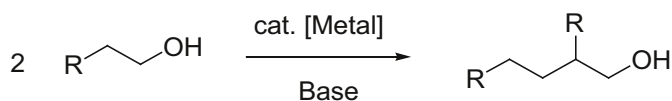

**Scheme 3** Metal-catalyzed *C*-alkylation of ketones from primary and secondary alcohols

 Springer
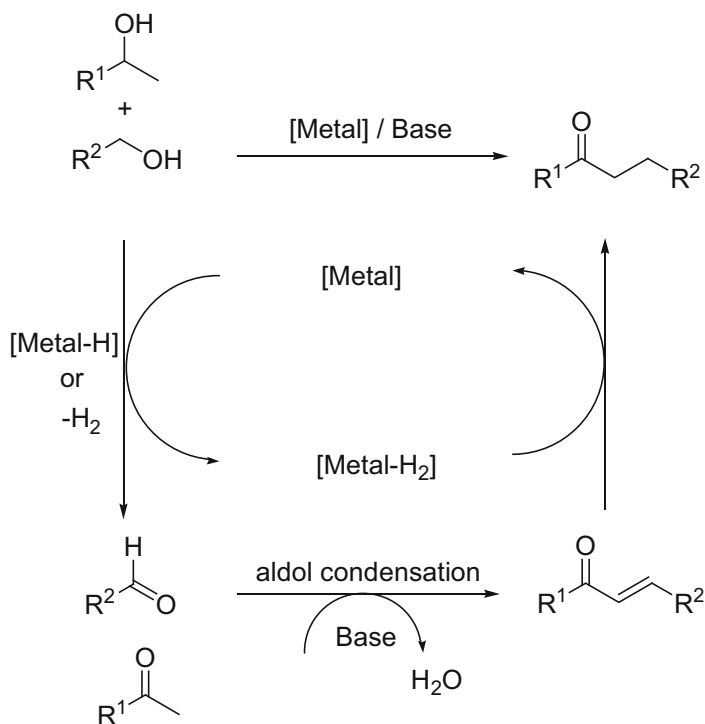
Scheme 4 Representative reaction pathway for the *C*-alkylation of primary and secondary alcohol to afford ketones

corresponding β-alkylation products (Schemes 5, 6) [69–90]. This process involves the following steps: (1) the initial metal-catalyzed dehydrogenation of the primary alcohol substrate to afford two molecules of the corresponding aldehyde and a metal-hydride intermediate; (2) the aldol condensation of these aldehydes to afford the corresponding α,β-unsaturated aldehyde; and (3) the hydrogenation of this system to afford the desired β-alkylated product (Scheme 6).

In this review, we have focused primarily on developments towards *C*-alkylation methods involving the use of alcohols as alkylating agents through hydrogen transfer during the last 3 years.

Scheme 5 Metal-catalyzed β-alkylation by alcohol dimerization (Guerbet reaction)
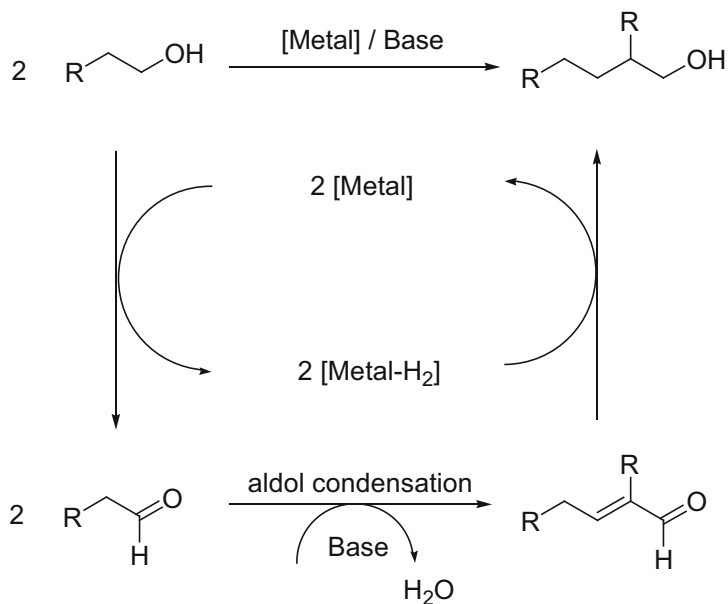
**Scheme 6** Representative reaction pathway for the β-alkylation of alcohols

2 *C*-Alkylation Based on Ligand Modifications to the Transition-Metal Catalyst

2.1 *C*-Alkylation Based on Ligand Modifications Involving an Ir Catalyst

Research towards increasing the catalytic activity of transition-metal catalysts (e.g., iridium and ruthenium) with the aim of transferring hydrogenation through the modification of the ligands involved in their metal–ligand complexes has been a topic of recent interest [91–106]. To date, several research groups have reported the development of effective *C*-alkylation catalysts by the ligand modification of the transition-metal complex.

With regard to most interesting examples reported during the last 3 years, Ding and co-workers reported an Ir complex bearing a benzoxazolyl ligand, which exhibited high catalytic activity towards the *C*-alkylation of numerous ketones and

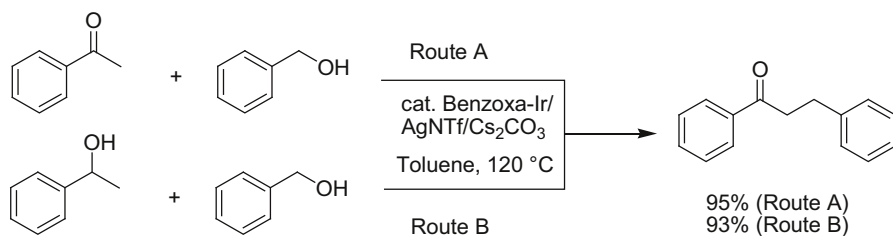**Scheme 7** Benzoxazolyl–iridium complex
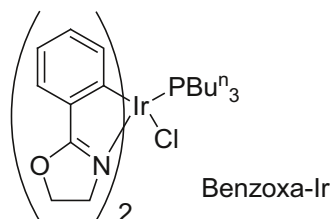
alcohols with alcohol through a transfer hydrogen reaction. For example, the reaction of acetophenone (1.0 mmol) with benzyl alcohol (1.1 mmol) in the presence of a benzoxazolyl iridium(III) complex (as shown in Scheme 7) (2 mol%, 0.02 mmol) combined with AgNTf (0.02 mmol) and cesium carbonate (1.0 mmol) in toluene at 120 °C gave the corresponding α-alkylation product 1,3-diphenyl-1-propanone in 95 % yield (Scheme 8, route A).

Furthermore, the same catalytic system was successfully applied to the alkylation reaction of secondary and primary alcohols. For example, the reaction of 1-phenylethanol (1.0 mmol) with benzyl alcohol (1.1 mmol) under the conditions described above gave 1,3-diphenyl-1-propanone in 93 % yield (Scheme 8, route B).

This catalytic system also performed effectively under solvent-free conditions, where it afforded the desired C-alkylated products in high yields. Moreover, the same authors reported that the analogous benzothienyl–iridium complexes afforded high levels of catalytic activity in the C-alkylation reactions of primary and secondary alcohols, as well as the reaction of ketones and primary alcohols through transfer hydrogen processes [107–109].

The ligand modification of Cp*Ir complexes has also been investigated as a strategy for the development of active C-alkylation catalysts. In a recent example of this approach, Li and co-workers reported the development of a Cp*Ir complex bearing a bipyridonate ligand (as shown in Scheme 9), which performed as an effective catalyst for the α-alkylation of ketones [110]. In a typical example, the reaction of acetophenone (1.0 mmol) with benzyl alcohol (1.1 mmol) was carried out in the presence of a catalytic amount of the Cp*Ir-bipyridonate complex (see Scheme 9; 1.0 mol%) and Cs_2CO_3 (0.1 mol) in t-amyl alcohol at 110 °C under air to give 1,3-diphenyl-1-propanone in 92 % yield. Notably, several other conventional Ir complexes such as $[Cp*IrCl_2]_2$ and $[Ir(cod)Cl]_2$ exhibited low catalytic activity towards this reaction under the same conditions.

It has been proposed that the carbonyl group of the bipyridonate ligand could activate the alcohol substrate (as a reactant) by accepting a proton from this species, which would serve as an important step in the transfer hydrogenation reaction. The Cp*Ir-bipyridonate complex described above also showed high catalytic activity towards the α-methylation of ketones with methanol. The details of this reaction will be described in greater detail later in this article.

Scheme 8 Benzoxazolyl–iridium complex-catalyzed C-alkylation reactions

Scheme 9 Bipyridonate
iridium Cp* complex

Bipyridonate-Ir
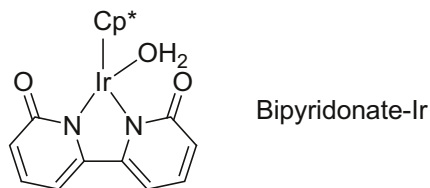
## 2.2 Ruthenium-Catalyzed *C*-Alkylation Reactions

Several ruthenium-based catalysts have also been developed as effective *C*-alkylation catalysts. In a recent example of work in this area, Taddei and co-workers reported that [Ru(cod)Cl$_2$]$_n$/PTA (PTA = 1,3,5-triaza-7-phosphaadamantane: shown in Scheme 10) showed high catalytic activity in the coupling of secondary and primary alcohols to afford the corresponding ketone products [111].

In a representative example of this work, the reaction of 1-phenylethanol (1.0 mmol) with benzyl alcohol (1.1 mmol) in the presence of [Ru(cod)Cl$_2$]$_n$ (2.5 mol%) combined with PTA (5 mol%) and *t*-BuOK (1.0 mmol) in toluene led to the formation of 1,3-diphenyl-1-propanone in 76 % yield, together with negligible amounts of the homo-coupled products. Using this [Ru(cod)Cl$_2$]$_n$/PTA catalyst system, the *C*-alkylation reactions of the secondary and primary alcohols proceeded smoothly at the relatively low temperature of 55 °C.

Zhang and co-workers reported the use of this Ru-catalyzed α-alkylation methodology to synthesize a series α-pyridyl methylated ketones using pyridyl methanol derivatives (Scheme 11) [112].

In a typical example of this process, acetophenone (1.2 mmol) was reacted with 3-(hydroxymethylpyridine) (1.0 mmol) in the presence of [RuCl$_2$(*p*-cymene)]$_2$ (1 mol%) combined with xantphos (1 mol%; the structure is shown in Scheme 12) and *t*-BuOK (0.4 mmol) in *t*-amyl alcohol at 120 °C to give 3-(3-pyridinyl)-1-phenylpropan-1-one in 92 % yield.

It was considered that the reaction initiated by dehydrogenation of pyridyl methanol through base-assisted deprotonation of the OH group/Ru-catalyzed β-hydride elimination led to the corresponding aldehyde. Aldol condensation of the
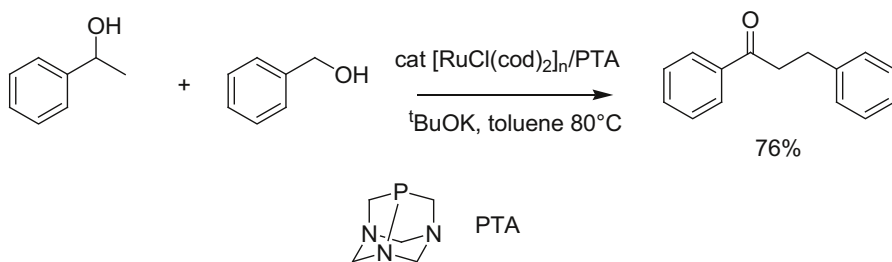
Scheme 10 Ru/PTA (PTA = 1,3,5-triaza-7-phosphaadamantane)-catalyzed α-alkylation reaction

cat [RuCl(*p*-cymene)]$_2$
Xantphos

^{t}BuOK, ^{t}Amyl alcohol

OH

92%
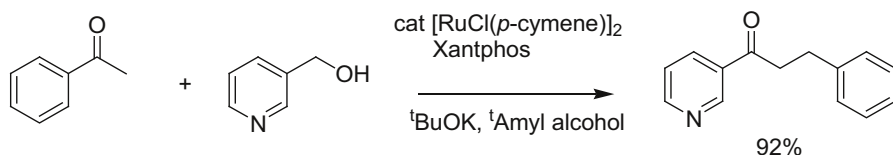
Scheme 11 Ru/xantphos-catalyzed α-alkylation of 3-pyridinyl alcohol

Scheme 12 Xantphos ligand

PPh$_2$ PPh$_2$
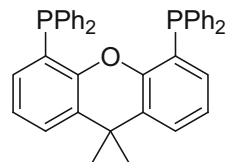
resulting aldehyde with ketone led the enone followed by hydrogenation to give the α-alkylation product.

2.3 Osmium-Catalyzed α-Alkylation Reactions

In addition to recent advances in iridium- and ruthenium-based catalysts for the *C*-alkylation reactions, osmium has also been identified as an efficient catalyst for this process.

In a recent example of the use of osmium in this regard, Esteruelas and co-workers reported the development of an osmium catalyst bearing an *N*-heterocyclic carbene complex (NHC) (Scheme 13), which exhibited efficient catalytic activity towards the α-alkylation of methyl ketones as well as arylacetonitriles [113].

In a representative example of the α-alkylation of methyl ketones using this system, acetophenone (3.0 mmol) was reacted with benzyl alcohol in the presence of an Os–NHC complex (as shown in Scheme 13) (1 mol%) combined with KOH (20 mol%) in toluene (0.3 M) at 110 °C for 1.5 h to give 1,3-diphenyl-1-propanone in 99 % yield. This reaction proceeded at a fast rate and the turnover frequency at 50 % conversion was calculated to be 194 h^{-1}.

This osmium catalyst system was also found to be effective for the α-alkylation of aryl acetonitrile, where it exhibited a high turnover frequency of up to 675 h^{-1}.

Me   iPr   OTf

Os

L   OH

L =

^{i}Pr ^{i}Pr

N   N

^{i}Pr ^{i}Pr
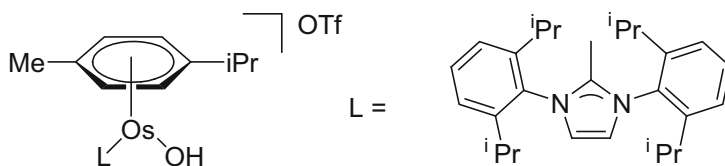
Scheme 13 Osmium–NHC complex used as a catalyst for α-alkylation reactions

3 C-Alkylation of Methanol in Hydrogen Transfer Reactions

3.1 Methylation Reactions Using Methanol Involving Hydrogen Transfer Reaction

Because methylation plays a vital role in the functionalization of biologically active compounds, the development of synthetic methods for the methylation of various substrates continues to attract considerable interest [114, 115].

The methylation of ketones is traditionally achieved using diazomethane or iodomethane, which are both highly toxic materials that pose significant handling issues. Furthermore, the former of these two agents is highly explosive. For this reason, the application of diazomethane and iodomethane on an industrial scale has been limited and there is an urgent need for safer alternatives [116, 117].

The use of a hydrogen transfer method involving methanol provides an efficient alternative to iodomethane or diazomethane that can be applied to the methylation of various substrates through the activation of methanol. Methanol is the simplest of all of the alcohols and represents an abundant bio-based resource and fundamental renewable C1 source [118, 119].

Methanol has been utilized as a practical C1 source in bulk-scale methanol-to-gasoline and methanol-to-olefin processes [120–123], as well as processes for the production of acetic acid, such as the Monsanto and Cativa processes [124–128].

However, the use of methanol in methylation processes is considered to be inefficient because of the high level of dehydrogenation energy required by these transformation compared with those of higher alcohols [129, 130].

Several methanol dehydrogenation processes have recently been developed using transition-metal catalysts to afford formaldehyde, hydrogen, and carbon dioxide [131–137].

As part of their pioneering work towards the development of novel methanol-based C–C coupling methodologies, Krische and co-workers reported the C–C coupling of methanol with allenes using an o-cyclometalated iridium complex, which provided access to the corresponding homoallylic alcohol products [138]. Li et al. [139, 140] subsequently reported an iridium-catalyzed method for the preparation of 3,3′-bisindolylmethanes using methanol and indoles. Several other interesting reactions have also been reported involving the use of methanol, including the N-formylation and methylation reactions of amines, as well as the formation of dialkyl ketones via the C–H bond activation of N-methylamine [141–143].
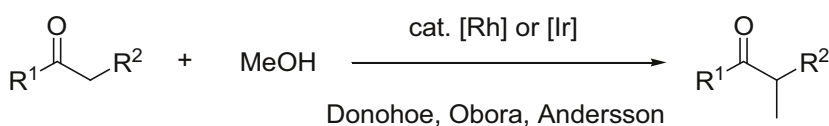
Scheme 14 Transition-metal-catalyzed α-methylation of ketones using methanol

With regard to the α-methylation of ketones using methanol as an alkylating agent through a hydrogen transfer process, several iridium and rhodium catalysts have recently been developed to achieve this transformation (Scheme 14).

Donohoe and co-workers reported the development of a rhodium-catalyzed reaction for the methylation of ketones (Scheme 15). In a typical example of this reaction, phenyl butyl ketone (0.3 mmol) was reacted with methanol (1.5 mL) in the presence of $[Cp^*RhCl_2]_2$ (5 mol%) combined with Cs_2CO_3 (5 equiv) to give the corresponding methylated product in 98 % yield (Scheme 15) [144].

Obora and co-workers reported the development of an iridium-catalyzed process for the methylation of ketones using methanol. In a representative example of this method, acetophenone (1.0 mmol) was reacted with methanol (1.5 mL) in the presence of a catalytic amount of $[Cp^*IrCl_2]_2$ (5 mol%) combined with KOH (50 mol%) at 120 °C to give the corresponding α,α-dimethylated product in 83 % yield with high selectivity (Scheme 16) [145].

In the methylation reaction, the choice of the base efficiently controlled the mono- and dimethylation selectivity. Thus, the $[Cp^*IrCl_2]_2$-catalyzed reaction of benzyl ethyl ketone (1.0 mmol) with methanol (1.5 mL) carried out under these conditions by using a strong base like KOH gave the dimethylated product, while the use of Na_2CO_3 gave monoalkylation product exclusively (Scheme 17).
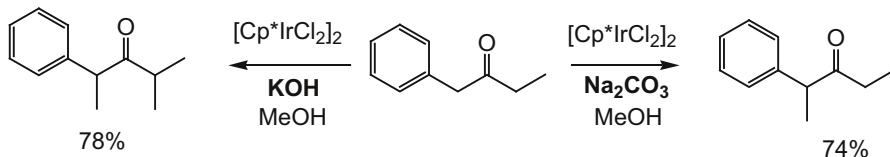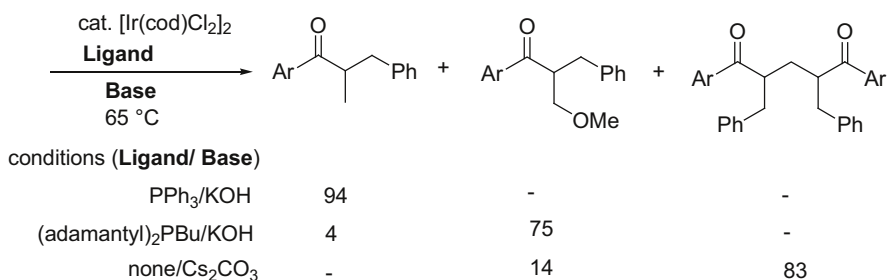
In another example of the Ir-catalyzed α-methylation of ketones, Donohoe and co-workers reported the α-methylation of an arylalkylketone with methanol using $[Ir(cod)Cl_2]_2$ (1 mol%) as a catalyst with PPh_3 (4 mol%) and KOH (2 equiv) under an oxygen atmosphere, which gave the α-methylated product in 94 % yield. Notably, the choice of ligand and base was discovered to be critical to controlling the selectivity of this reaction (Scheme 18) [146].

The reaction is considered to proceed by an Ir-catalyzed hydrogen transfer (or hydrogen borrowing) process by using ketone and methanol. Furthermore, the use of methanol in transfer hydrogenation is difficult. Here, the use of dioxygen (O_2) is effective to enhance the reactivity of methylation and methylenation. In addition, the choice of hindered phosphine in the presence of oxygen is also effective to interrupt the enone hydrogenation step.

With regard to the methylation of ketones using methanol as a methyl source, Andersson and co-workers reported the use of an Ir-NHC complex as an efficient catalyst for these reactions [147]. In a typical example of this process, phenylpropyl ketone (0.1 mmol) was reacted with methanol (0.5 mL) in the presence of a catalytic amount of the Ir-NHC catalyst (as shown in Scheme 19) (1.0 mol%)
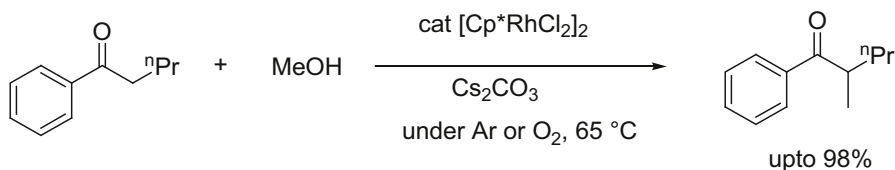
Scheme 15 Donohoe's Rh-catalyzed α-methylation of ketones using methanol

O

+ MeOH

cat. [Cp*IrCl$_2$]$_2$

KOH
120 °C

83%
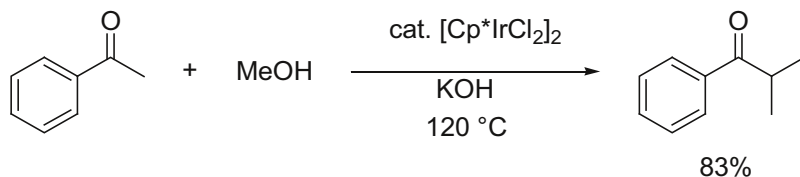
Scheme 16 Obora's Ir-catalyzed α-methylation of ketones using methanol

78%

[Cp*IrCl$_2$]$_2$
KOH
MeOH

[Cp*IrCl$_2$]$_2$
Na$_2$CO$_3$
MeOH

74%

Scheme 17 Mono- and dimethylation reactions of ketones

O
Ar ⟍⟍ Ph   +   MeOH

Ar = methoxyphenyl

cat. [Ir(cod)Cl$_2$]$_2$
Ligand
Base
65 °C

Ar—C(O)—CH(CH$_3$)—Ph + Ar—C(O)—CH(CH$_2$OMe)—Ph + Ar—C(O)—CH(CH$_2$Ph)—CH$_2$—CH(CH$_2$Ph)—C(O)—Ar

conditions (**Ligand/ Base**)

PPh$_3$/KOH	94	-	-
(adamantyl)$_2$PBu/KOH	4	75	-
none/Cs$_2$CO$_3$	-	14	83
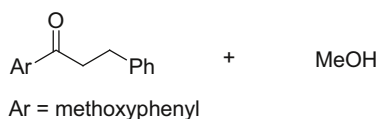
Scheme 18 Selectivity of the Ir-catalyzed α-methylation of ketones with methanol reported by Donohoe

combined with Cs$_2$CO$_3$ (5 equiv) at 65 °C to give the corresponding α-methylated product in 97 % yield (Scheme 19).

3.2 Methylation of Alcohols Using Methanol as an Alkylating Agent

With regard to using methanol as a methyl source in methylation reactions, Beller and co-workers reported a ruthenium-catalyzed reaction for the methylation of 2-arylethanols with methanol [148]. In a typical example of this transformation, 2-phenylethanol (2.5 mmol) was reacted with methanol (2 mL) in the presence of a mixture of Ru-MACHO (0.1 %), Shvo's Ru complex (0.05 %) and NaOMe (10 %) at 140 °C to give the methylated product in 87 % yield (Scheme 20). In this
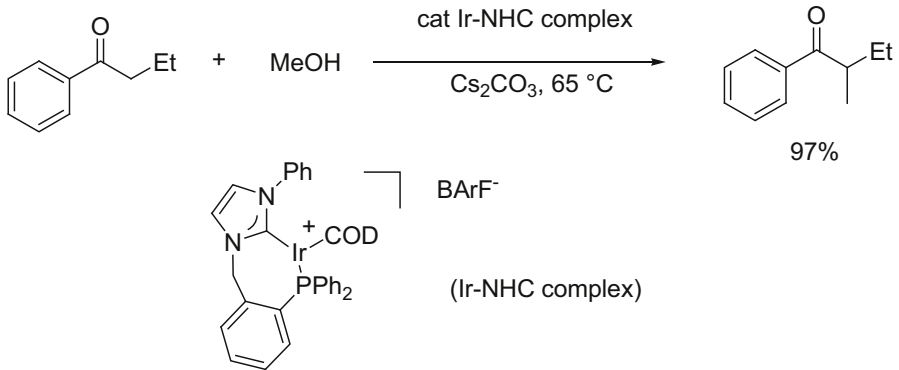
Scheme 19 Andersson's Ir-catalyzed α-methylation of ketones using methanol
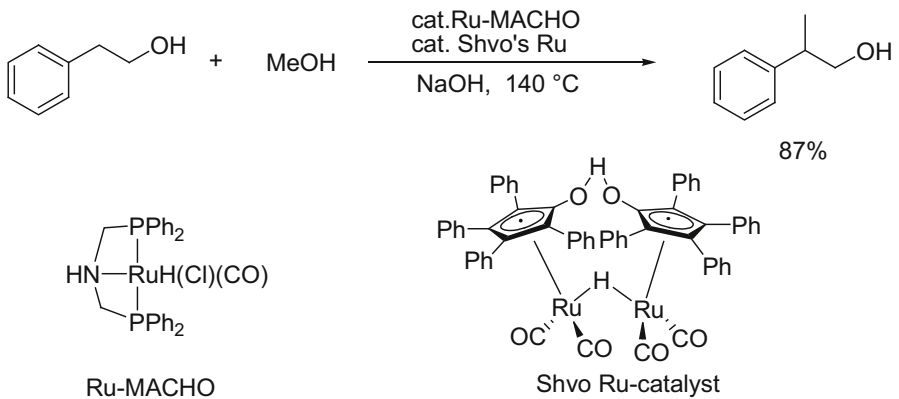
Scheme 20 Beller's Ir-catalyzed methylation of alcohols using methanol

reaction, the use of a combination of two different ruthenium complexes (i.e., Ru-MACHO and Shvo's Ru complex) and the release of any pressure formed in the reactor during the reaction were essential to achieve a high yield of the desired product.
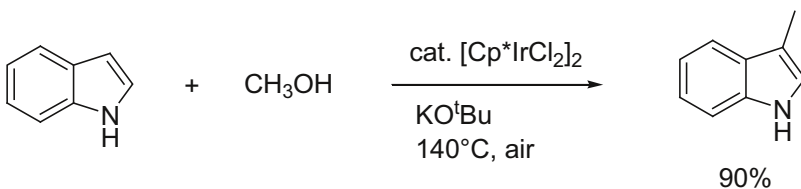
Scheme 21 Cai's Ir-catalyzed methylation of indole using methanol

3.3 Methylation of Indoles and Pyrroles Using Methanol as an Alkylating Agent

Cai and co-workers reported the Ir-catalyzed methylation of indoles using methanol. According to this report, the reaction of indole (0.3 mmol) with methanol in the presence of [Cp*IrCl$_2$]$_2$ (1 mol%) combined with *t*-BuOK (1 equiv) at 140 °C under an air atmosphere gave the corresponding methylated product in 90 % yield (Scheme 21) [149].

Notably, this reaction can also be applied to the methylation of pyrroles under the same conditions, with the use of 3,5-dimethylpyrrole as a substrate leading to the formation of a mixture of 2,3,5-tri- and 2,3,4,5-tetramethylpyrrole in high yield (Scheme 22).

4 α-Alkylation of Nitriles, Acetonitrile, Acetoamide, and Esters

4.1 α-Alkylation of Nitriles

Following on from the pioneering works of Grigg, Watanabe, and Tsuji, there has been an intense period of research focused on the α-methylation of arylnitriles using methanol with a transfer hydrogenation method [150–162].

In contrast to the previously reported α-alkylation reactions of arylnitriles using alcohols in the presence of a Ru, Pd, Ir, or Os complex catalyst (which gave the corresponding α-alkylated arylacetonitriles), Li and co-workers reported the reaction of arylacetonitriles with primary alcohols to give the corresponding α-alkylated arylacetamides using a Rh complex catalyst. In this reaction, the resulting α-alkylated arylacetonitriles were hydration by H$_2$O, which was generated as a by-product during the reaction, to achieve "complete atom economy". In a typical example of this reaction, phenylacetonitrile (1.0 mmol) was reacted with benzyl alcohol (1.1 mmol) in the presence of a catalytic amount of [Rh(cod)Cl$_2$]$_2$ (1 mol%) combined with PPh$_3$ (10 mol%) and KOH (0.4 mmol) in *t*-amyl alcohol at 130 °C to give 2,3-diphenylpropanamide in 95 % yield. The selectivity towards the α-alkylated arylacetonitrile and α-alkylated arylacetamide products could be controlled by varying the nature of the phosphine ligand and base used in the reaction; conducting the reaction in the presence of PCy$_3$/KOH (ligand/base) or PPh$_3$/K$_3$PO$_4$ mainly led to the selective formation of the α-alkylated arylacetonitrile products (Scheme 23).

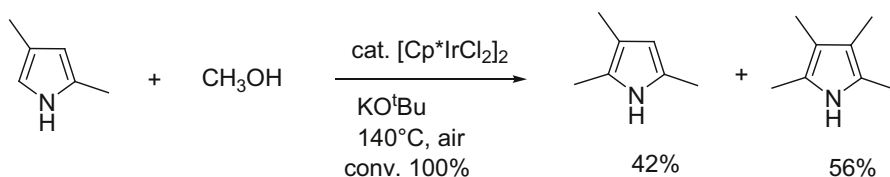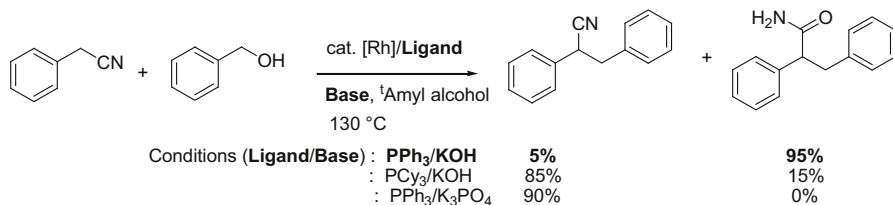**Scheme 22** Ir-catalyzed methylation of 3,5-dimethylpyrrole using methanol

Scheme 23 Rh-catalyzed formation of arylacetamide by the reaction of arylacetonitriles with primary alcohols
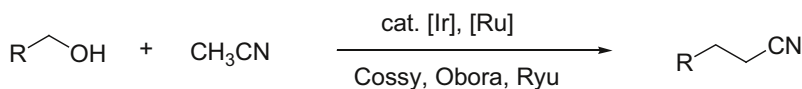
4.2 α-Alkylation Reactions of Acetonitrile and Acetamides

Acetonitrile is produced as a by-product of the industrial Sohio process during the synthesis of acrylonitrile [163]. The *C*-alkylation of acetonitrile by transfer hydrogenation using methanol as an alkylating agent therefore represents an efficient route for the synthesis of functionalized nitrile compounds.

Several recently reported examples of the α-alkylation of acetonitrile include (1) Cossy and co-workers' study, which reported that the reaction of acetonitrile with benzyl alcohol in the presence of [IrCl(cod)]$_2$ as a catalyst combined with Cs$_2$CO$_3$ at 180 °C afforded the corresponding α-alkylated nitriles; (2) Obora and co-worker's study, which reported that the reaction of acetonitrile with *n*-hexanol in the presence of [Ir(OH)(cod)]$_2$ as a catalyst combined with PPh$_3$ and *t*-BuOK at 130 °C gave the corresponding α-alkylation products; and (3) Ryu and co-workers' study, which reported that the use of a mixture of [RuHCl(CO)(PPh$_3$)$_3$] and K$_3$PO$_4$ as a catalyst for the reaction of acetonitrile with benzyl alcohol afforded the alkylated product in good yield (Scheme 24) [164–166].

α-Alkylation of poorly activated acetamides represents another challenging target for this area of research. In a recent example of research in this area, Huang and co-workers reported the use of an Ir-pincer complex as an effective catalyst for the α-alkylation of acetamides (Scheme 25). In a typical example of this process, benzyl alcohol was reacted with 2 equivalents of *N,N*-dimethylacetamide using 2 mol% of an Ir-pincer-type complex combined with 2 equivalents of *t*-BuOK at 120 °C to give the corresponding alkylated product in 81 % yield (Scheme 25) [167].

In another study pertaining to the α-alkylation of acetamide reported by Ryu and co-workers, the reaction of *N,N*-dimethylacetamide with benzyl alcohol was carried

Conditions: [Ir(cod)Cl]$_2$ (catalyst), Cs$_2$CO$_3$ (base), 180 °C (Cossy)
[Ir(OH)(cod)]$_2$ (catalyst), PPh$_3$ (Ligand), ^{t}BuOK (base), 130 °C (Obora)
[RuHCl(CO)(PPh$_3$)] (catalyst), K$_3$PO$_4$ (base), 110 °C (Ryu)

Scheme 24 α-Alkylation reactions of acetonitriles
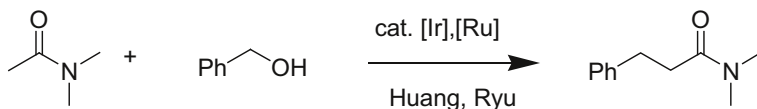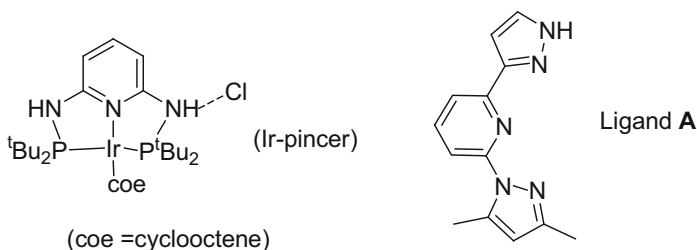
Scheme 25 α-Alkylation of acetamide

out in the presence of 3 mol% [RuHCl(CO)(PPh$_3$)$_3$] combined with *N,N,N*-tridentate ligand **A** (as shown in Scheme 25) and *t*-BuOK to give the desired alkylation product in 76 % yield (Scheme 25) [168].

4.3 α-Alkylation of Esters

The α-alkylation of esters is an important process in organic chemistry and the transition-metal-catalyzed α-alkylation of esters with alcohols using a transfer hydrogenation method represents an attractive alternative to conventional processes involving the reaction of metal-based enols with alkylhalides [169–171].

Ishii and co-workers reported the α-alkylation of *t*-butyl esters using an iridium catalyst [172]. In a typical example of this process, *t*-butyl acetate (10 mmol) was reacted with *n*-butanol (1.0 mmol) in the presence of a catalytic amount of [IrCl(cod)]$_2$ (5.0 mol) combined with PPh$_3$ (15 mol%) and *t*-BuOK (2 equiv) in *t*-BuOH at 100 °C to give the desired α-alkylated product in 74 % yield (Scheme 26).

Huang and co-workers subsequently reported the use of an Ir-pincer complex as an effective catalyst for the α-alkylation of esters (Scheme 27) [173]. For the reaction of *t*-butyl acetate, the optimized reaction conditions were reported to be as follows: mix 10 equivalents of *t*-butyl acetate with benzyl alcohol in the presence of
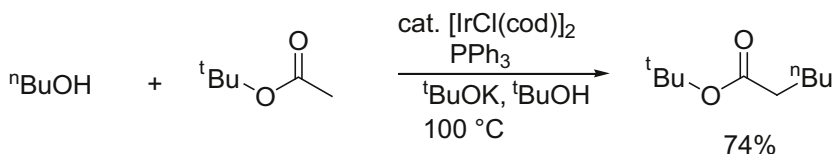
Scheme 26 α-Alkylation of *t*-butyl acetate
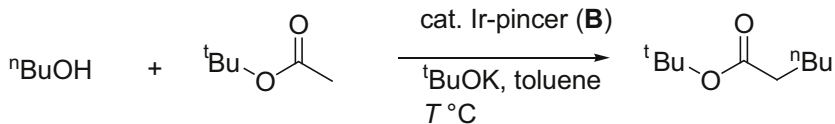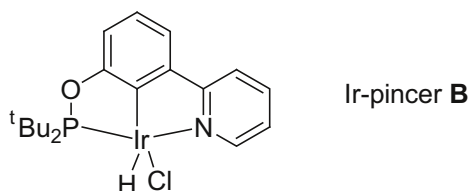
Scheme 27 Huang's α-alkylation of *t*-butyl acetate

2 mol% of Ir-pincer complex **B** (as shown in Scheme 27) combined with 2 equivalents of *t*-BuOK in toluene at 110 °C to give the corresponding α-alkylated ester in 99 % yield (Scheme 27). Notably, the reaction of *t*-butyl acetate with benzyl alcohol was successfully conducted with a molar ratio of 1.2:1 using a smaller amount of the Ir-pincer catalyst (0.5 mol%) and a lower reaction temperature (60 °C). Under these conditions, the desired alkylated product was formed in high yield (89 %) (Scheme 27).

This ester alkylation system was also successfully applied to the synthesis of valproic acid. According to the reported procedure, a mixture of methyl valerianate (10 mmol) was reacted with *n*-propanol (8 mL) under the Ir-catalyzed conditions described above to give the corresponding valproic ester, which was hydrolyzed to give valproic acid in 70 % overall yield (Scheme 28).

5 α-Alkylation of Methyl-*N*-Heteroaromatic Compounds

Transition-metal-catalyzed *C*-alkylation methods have been successfully applied to the alkylation of several methyl-*N*-heteroaromatic compounds, including methyl pyrimidines and methyl quinolones.
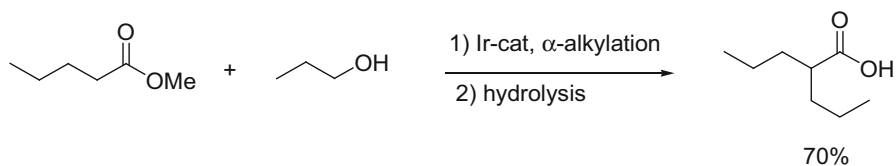
Scheme 28 Synthesis of valproic acid via the α-alkylation of an ester

The *C*-alkylation of methyl piperidine was achieved by Kempe and co-workers using an Ir complex containing a pyridyl-bearing phosphine ligand. In a typical example of this procedure, *N*-benzylated 4-methylpyrimidin-2-ylamine (1.0 mmol) was reacted with benzyl alcohol (1.1 mmol) in the presence of [IrCl(cod)]$_2$ (1 mol%) combined with (iPr)$_2$PNPy$_2$ (Pr = propyl, Py = pyridinyl) (2 mol%) (as a ligand) and *t*-BuOK (1.1 mmol) in diglyme at 110 °C to give the *C*-alkylated product in 98 % yield (Scheme 29) [174].

With regard to the alkylation of methyl quinolones, Obora and co-workers reported that the reaction of 2-methylquinoline (3.0 mmol) with benzyl alcohol (1.0 mmol) in the presence of [Ir(OH)(cod)]$_2$ (5 mol%) combined with PPh$_3$ (20 mol%) and *t*-BuOK (50 mol%) in 1,4-dioxane at 130 °C gave the desired *C*-alkylated product in 92 % isolated yield (Scheme 30) [175].

Furthermore, Shimizu and co-workers achieved the additive-free *C*-alkylation of methylquinoline using an alcohol as the alkylating agent with a heterogeneous Pt/γ-Al$_2$O$_3$ catalyst [176].

6 Ruthenium-Catalyzed Synthesis of 1,2,3,4-Tetrahydronaphthyridines via the Transfer Hydrogenation of a Pyridyl Ring with Alcohol

The hydrogen transfer method has been successfully applied to the synthesis of several heterocyclic compounds using a transition-metal-catalyzed annulation reaction [177].

Zhang and co-workers recently reported the ruthenium-catalyzed synthesis of 1,2,3,4-tetrahydronaphthyridines from (2-amino-pyridin-3-yl)methanol and a suitable alcohol. In a typical example of this reaction, (2-aminopyridin-3-yl)methanol (0.5 mmol) was reacted with 1-(*p*-tolyl)ethanol (0.5 mmol) in the presence of Ru$_3$(CO)$_{12}$ (1 mol%) combined with xantphos (3 mol%) and *t*-BuOK (50 mol%) in *t*-amyl alcohol at 130 °C to give 7-(*p*-tolyl)-1,2,3,4-tetrahydro-1,8-naphthyridine in 90 % yield with high selectivity (Schemes 31, 32) [178].
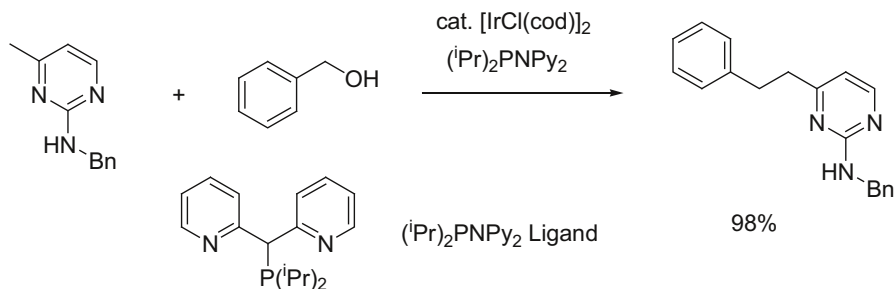
Scheme 29 *C*-Alkylation of methyl pyrimidine
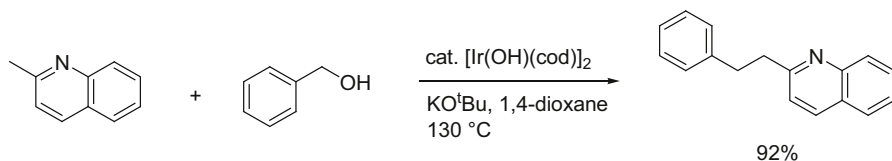
Scheme 30 *C*-Alkylation of methylquinoline
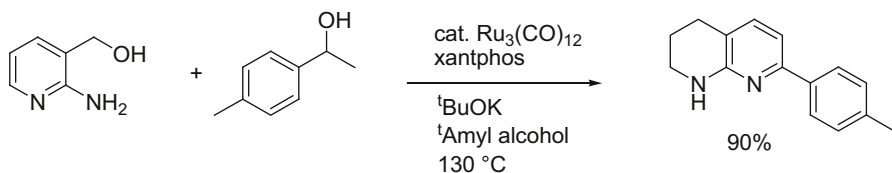
Scheme 31 Ru-catalyzed synthesis of tetrahydronaphthyridines
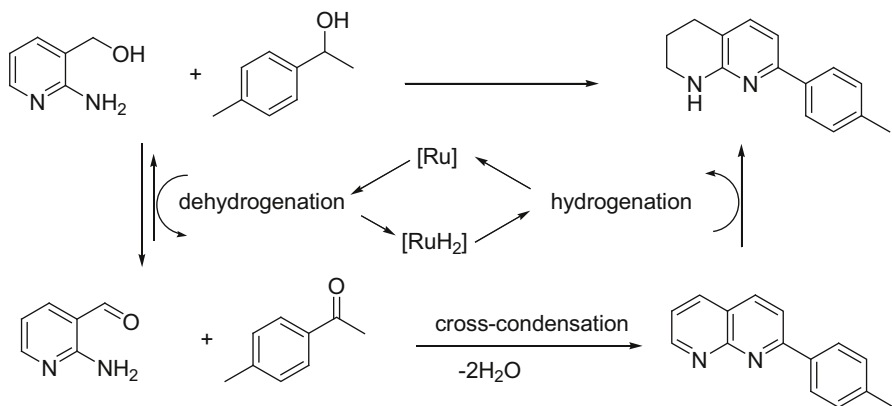
Scheme 32 A possible reaction pathway

7 β-Alkylation of Alcohols Using Hydrogen Autotransfer Reactions

Alcohol–alcohol coupling reactions leading to the formation of β-alkylated products are known as the Guerbet reaction, and numerous examples of this reaction have been reported in the literature [179–182]. The Guerbet reaction has been used extensively to afford long-chain higher alcohols from readily accessible short-chain alcohols.

In the recent literature, Ramón and co-workers reported the successful Guerbet cross-alkylation reaction of two different alcohols using an iridium/magnetite catalyst [183]. In a typical example of this reaction, a mixture of 2-phenylethanol (1.0 mmol) and benzyl alcohol (2.0 mmol) was reacted with a catalytic amount of iridium/magnetite nanoparticles of IrO_2–Fe_3O_4 (0.14 mol%) combined with KOH

in toluene at 110 °C to give the corresponding Guerbet reaction product in 96 % yield (Scheme 33). Notably, the iridium/magnetite (IrO$_2$–Fe$_3$O$_4$) catalyst used in this case was reused more than 10 times without any discernible decrease in its catalytic activity by simply washing the catalyst with toluene.

Furthermore, Jia and co-worker recently reported the Ru-catalyzed Guerbet-type β-alkylation of primary and secondary alcohols [184]. In a representative example of this reaction, 1-phenyl ethanol (1.0 mmol) was reacted with benzyl alcohol (2.0 mmol) in the presence of RuCl$_2$(PPh$_3$)$_2$(2-NH$_2$CH$_2$Py) (2-NH$_2$CH$_2$Py = 2-aminomethyl pyridine) (1 mol%) combined with t-BuOK in toluene at 105 °C to give the corresponding β-alkylated product in quantitative yield (Scheme 34).

Considerable research interest has recently been directed towards the use of ethanol as a bioresource substrate to provide access to n-butanol and higher alcohols using the Guerbet process.

For example, Wass and co-workers recently reported that trans-[RuCl$_2$(DPPM)$_2$] (DPPM = bis(diphenylphosphino)methane) showed good catalytic activity for the selective conversion of ethanol to n-butanol and that the selectivity towards butanol was 94.1 % at conversions greater than 20 % [185].

Tian and co-workers reported the hydrothermal synthesis of n-butanol from ethanol [186]. This process used commercially available cobalt powder as a catalyst combined with NaHCO$_3$ (0.01 mol) as a base under hydrothermal conditions using 0.15 mol of ethanol and water (11.24 mL) at 200 °C for 3 days to give n-butanol with 69 % selectivity.

8 Iridium-Catalyzed Guerbet/Decarbonylation Reaction of Arylalkanols

In an extension of the Guerbet reaction, Obora and co-workers reported the development of an Ir-catalyzed reaction for the conversion of arylalkanols to α,ω-diarylalkanes [187], which have been widely used as chromophores and functional fluorescent materials [188–191].

In a typical example of this transformation, 2-phenylethanol (2.0 mmol) was treated with t-BuOK (40 mol%) in p-xylene in the presence of [Cp*IrCl$_2$]$_2$ (1 mol%) at 120 °C to give 1,3-diphenylpropane in 81 % yield with a small amount of toluene (5 %) as a by-product (Scheme 35). This reaction proceeded via the formation of the dimerized β-alkylation alcohol (Guerbet reaction product) as an intermediate. The resulting alcohol was subsequently dehydrogenated by the iridium complex to afford an aldehyde, followed by sequential decarbonylation and
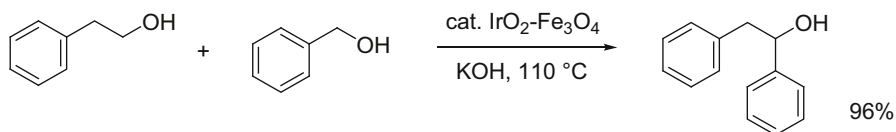
Scheme 33 Ir-catalyzed Guerbet reaction involving the cross-alkylation of two alcohols
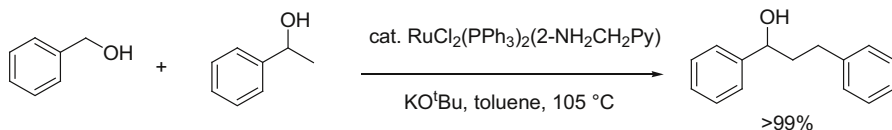
Scheme 34 Ru-catalyzed Guerbet reaction involving the cross-alkylation of two alcohols
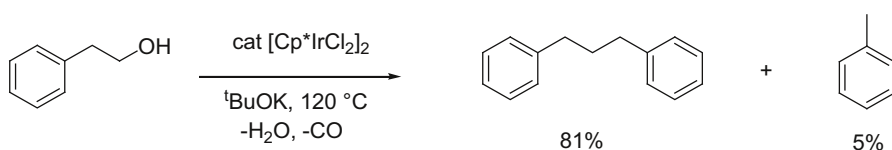
Scheme 35 Ir-catalyzed formation of 1,3-diphenylpropane from 2-phenylethanol

hydrogenation reactions to give the α,ω-diarylalkane product. Notably, the use of 2-arylethanol as a substrate in this reaction led to the "direct" formation of α,ω-diarylalkane, as shown in Scheme 35.

In contrast, the use of arylalkanols with longer alkyl chains as substrates, such as 3-phenylpropanol, required the use of a two-step reaction to attain the desired α,ω-diarylalkane products. This process is shown in Scheme 36. Briefly, the reaction of 3-phenylpropanol (2.0 mmol) with [Cp*IrCl$_2$]$_2$ (1 mol%) and t-BuOK (40 mol%) in 1,4-dioxane at 120 °C in a pressure tube led to the formation of β-(phenyl-methyl)benzenepentanol as the Guerbet reaction product in 89 % yield. The subsequent reaction of this product with [Cp*IrCl$_2$]$_2$ (2 mol%), [IrCl(cod)]2 (4 mol%), dppe (dppe = 1,2-bid(diphenylphosphino)ethane) (8 mol%), and K$_2$CO$_3$ (20 mol%) in mesitylene at 160 °C gave 1,5-diphenylpentane in 96 % yield (Scheme 36).
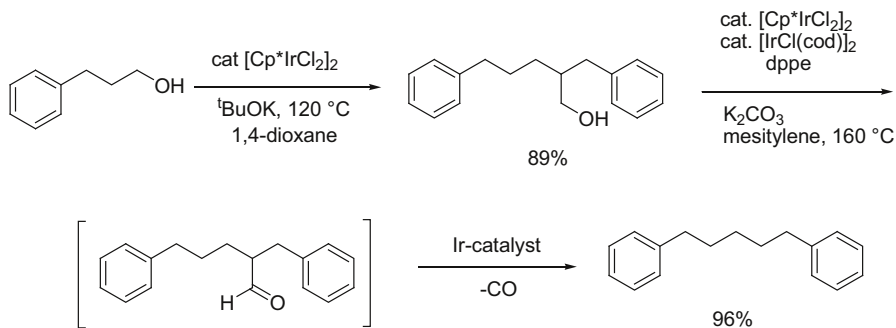
Scheme 36 Ir-catalyzed formation of 1,5-diphenylpentane by the two-step reaction of 3-phenylpropanol

9 Dehydrogenative Cross-Coupling by Transfer Hydrogenation

9.1 Dehydrogenative Cross-Coupling of Alcohols Involving Transfer Hydrogenation

Madsen and co-worker reported that a ruthenium–NHC complex (shown in Scheme 37) showed good catalytic activity towards the dehydrogenative Guerbet reaction of secondary alcohols to give the corresponding dimeric ketones with the concomitant release of hydrogen and water as by-products. In this reaction, the alcohol substrate underwent a β-alkylation/self-coupling reaction in a similar manner to the Guerbet reaction to afford the β-alkylated alcohol through an aldol reaction. The subsequent dehydrogenation took place under this catalyst system (Scheme 38) [192].

In a typical example of this process, 2-hydroxyhexane (5.0 mmol) was reacted with a catalytic amount of [RuCl$_2$(IiPr)(p-cymene)] (2 mol%) in the presence of PCy$_3$·HBF$_4$ (20 mol%) and KOH (5 mmol) in toluene at 110 °C to give the corresponding dehydrogenative self-coupling product in 95 % yield (Scheme 38).

9.2 Dehydrogenative Alcohol–Alcohol Cross-Coupling Reactions

The dehydrogenative cross-coupling of primary alcohols in the presence of an amine has been further extended to the synthesis of α,β-unsaturated aldehydes via the formation of imine intermediates.

For example, Porcheddu and co-workers recently reported the synthesis of a series of α,β-unsaturated aldehydes by the dehydrogenative cross-coupling of primary alcohols, which reacted with an amine to form the corresponding imine, followed by a Mannich-type condensation reaction (Scheme 39) [193].

In a typical example of this process, benzyl alcohol (3.0 mmol) was reacted with heptanol (1.0 mmol) in the presence of RuH$_2$(CO)(PPh$_3$)$_3$ (4 mol%) combined with xantphos (4 mol%), silica-immobilized amine (0.9 mmol), and crotononitrile (5.0 mmol) as a hydrogen acceptor at 120 °C under microwave irradiation for 3 h to give the corresponding cross-coupled α,β-unsaturated aldehydes in 75 % yield (Scheme 39). In this reaction, the silica-immobilized amine was recycled (by simple filtration) at least five times without considerable loss in its catalytic activity.

Scheme 37 Ruthenium–NHC complex
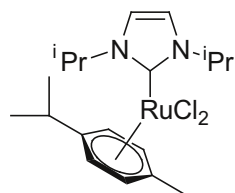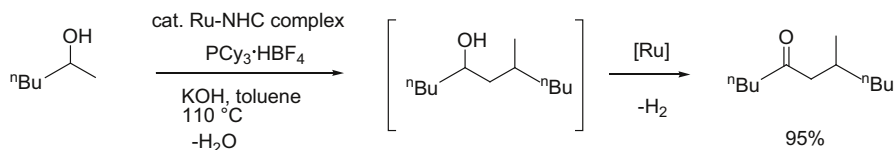
Scheme 38 Ruthenium–NHC complex-catalyzed dehydrogenative Guerbet reaction
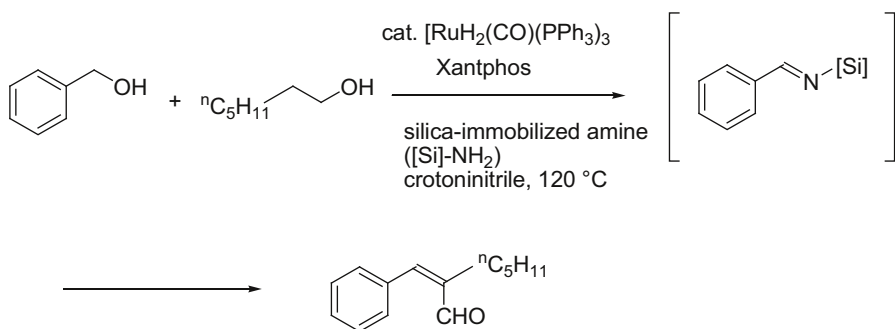
Scheme 39 Ruthenium–NHC complex-catalyzed dehydrogenative Guerbet reaction

10 Heterogeneous Catalysts for *C*-Alkylation Reactions

Heterogeneous catalysts can efficiently catalyze hydrogen transfer reactions and show good recyclability characteristics, as well as achieving high turnover numbers (TONs). To date, various heterogeneous metal/metal nanoparticle catalysts immobilized on metal oxide supports (e.g., TIO_2, MgO, mesoporous silica) have been used as catalysts for transfer hydrogenation reactions involving alcohols [194–223].

In a recent example of this type of reaction, Seayad and co-workers reported the use of an effective silica-supported palladium catalyst, which showed high catalytic activity towards the α-alkylation of ketones. In a representative example of this transformation, acetophenone (2.0 mmol) was reacted with benzyl alcohol (6.0 mmol) in the presence of the silica-supported heterogenized palladium catalyst (as shown in Scheme 40) combined with LiOH (20 mol%) at 140 °C to give the corresponding α-alkylated product, 1,3-diphenylpropan-1-one, in 83 % yield. Using this heterogenized Pd catalyst system, it is possible to recycle the catalyst by a

Scheme 40 Silica-supported heterogenized palladium catalyst for the α-alkylation of ketones
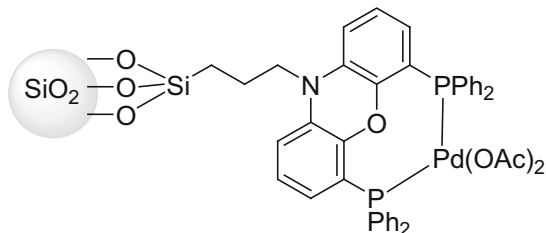
simple filtration step and still achieve a high turnover number (up to 4000) for the α-alkylation (Scheme 40) [224].

11 Activation of sp^3 C–H bonds Involving Hydrogen Transfer Reactions

The functionalization of sp^3 C–H bonds by the arylation of the α-carbon of a ketone through a direct oxidative coupling has recently been developed as a viable strategy for the formation of C–C bonds [225–233].

Alternatively, Dixneuf and co-workers reported the Ru-catalyzed alkylation of the sp^3 C–H bonds of alcohols using an alkene via the dehydrogenation of the alcohol substrate (Scheme 41) [234]. In a representative example of this transformation, benzyl 2-pyridyl alcohol (0.25 mmol) was reacted with methyl acrylate (1.0 mmol) in the presence of [RuCl$_2$(p-cymene)]$_2$ (5 mol%) combined with Cu(OAc)·H$_2$O (0.8 equiv) in dichloroethane to give the corresponding α-alkylated product in 80 % yield (Scheme 41).

Achard and co-workers reported the development of an Ir-catalyzed reaction for the formation of julolidines via a cyclization step involving a hydrogen transfer reaction with 1,3-propanediol and tetrahydroquinoline. In a representative example, 1,3-propanol (1 equiv) was reacted with 1,2,3,4-tetrahydroquinoline (2 equiv) in the presence of [Cp*IrCl$_2$]$_2$ (1 mol%) combined with diphenylphosphinobenzoic acid (DPPBA) (2 mol%) in toluene at 130 °C to give julolidine in 91 % yield (Scheme 42) [235]. This reaction proceeded via the formation of an enaminoiminium intermediate.

12 Transition-Metal-Free C-Alkylation

In 2010, Crabtree and co-workers reported β-alkylation reaction of 1-phenylethanol (2 mmol) with benzyl alcohol was achieved by using simple alkali base KOH (2 mmol) under transition-metal free aerobic conditions, giving the corresponding ketones and alcohols in 78 and 21 %, respectively (Scheme 43) [236]. The reaction proceeded by an Oppenauer oxidation of these alcohols to give the ketone and aldehyde. Subsequently, base-assisted aldol reaction followed by Meerwein–Ponndorf–Verley (MPV) reduction and isomerization gave the β-alkylated products.
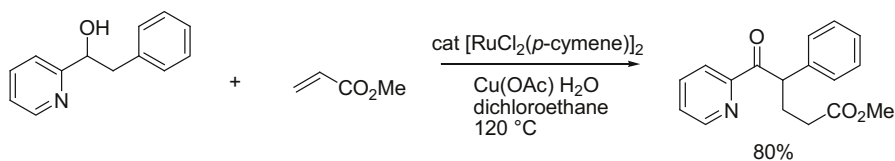
Scheme 41 Ru-catalyzed alkylation of the sp^3 C–H bond of an alcohol
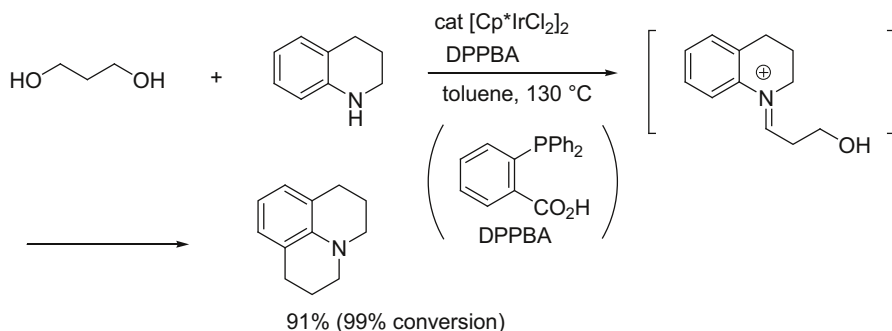
Scheme 42 Ir-catalyzed synthesis of julolidine by transfer hydrogenation
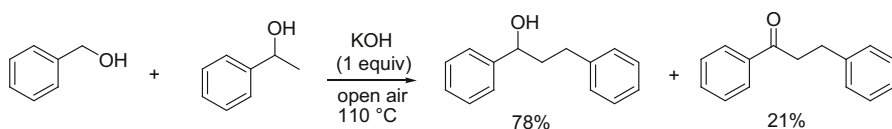
Scheme 43 Transition-metal-free β-alkylation with alcohols

In addition, transition-metal-free dehydrogenative α-alkylation of ketones with primary alcohols involving the Meerwein–Ponndorf–Verley–Oppenauer redox cycle has recently been developed by using LiO*t*Bu or NaOH as base [237, 238].

13 Conclusion and Future Outlook

This review has focused on recent advances in *C*-alkylation methods involving transfer hydrogenation with an alcohol as the alkylating agent. This area of research has continued to grow and provide environmentally benign and practical organic synthetic methodologies.

Although transition-metal-free *C*-alkylation reactions have only recently been developed [236–238], existing transition-metal-catalyzed *C*-alkylation methods involving the transfer hydrogenation of an alcohol have been enhanced considerably though ligand modification, reaction rate acceleration, and the development of reactions that run under base-free conditions. Furthermore, these methods may be used for the activation of unactivated compounds, such as methanol, acetonitrile, acetamide, and esters, which are all important chemical feedstock in organic synthesis.

C-Alkylation methods involving the transfer hydrogenation of alcohols represent atom-economical and green chemical transformations. With this in mind, we hope that this review will act as an informative reference and provide support to researchers interested in the utilization of hydrogen transfer as a *C*-alkylation method. We also hope that this review will inspire researchers to develop new innovative transformations in the field of *C*-alkylation involving transfer hydrogenation.

References

1. Cain D (2000) In: Fleming I, Trost BM (eds) Comprehensive organic synthesis. Pergamon, Oxford, pp 1–63
2. Reetz MT (1982) Angew Chem Int Ed 21:96–108
3. Casiraghi G, Battistini L, Curti C, Rassu G, Zanardi F (2011) Chem Rev 111:3076–3091
4. Palomo C, Oiarbide M, Garcia JM (2004) Chem Soc Rev 33:65–75
5. Arya P, Qin H (2000) Tetrahedron 56:917–928
6. Miynarski J, Gut B (2012) Chem Soc Rev 41:587–596
7. Cheong PHY, Legault CY, Um JM, Celebi-Olcum N, Houk KN (2011) Chem Rev 111:5042–5137
8. Shi Z, Yu D (2013) In: Keedij KJ, Poeppelmeier K (eds) Comprehensive inorganic chemistry II, 6th edn. Elsevier, Amsterdam, pp 47–77
9. Chen X, Engle KM, Wang DH, Yu JQ (2009) Angew Chem Int Ed 48:5094–5115
10. Guo X, Gu D, Wu Z, Zhang W (2015) Chem Rev 115:1622–1651
11. Wendel-Delord J, Glorius F (2013) Nat Chem 5:369–375
12. Kozhushkov SI, Ackermann L (2013) Chem Sci 4:886–896
13. Arockiam PB, Bruneau C, Dixneuf PH (2012) Chem Rev 112:5879–5918
14. Yamaguchi J, Yamaguchi AD, Itami K (2012) Angew Chem Int Ed 51:8960–9009
15. Neufeldt SR, Sanford MS (2012) Acc Chem Res 45:936–946
16. Song G, Wang F, Li X (2012) Chem Soc Rev 41:3651–3678
17. Campell AN, Stahl SS (2012) Acc Chem Res 45:851–863
18. Wencel-Deload J, Droege T, Liu F, Glorius F (2011) Chem Soc Rev 40:4740–4761
19. Lyons TW, Sanford MS (2010) Chem Rev 110:1147–1169
20. Trost BM (1991) Science 254:1471–1477
21. Trost BM (2002) Acc Chem Res 35:695–705
22. Li C, Trost BM (2008) Proc Natl Acad Sci USA 105:13197–13202
23. Guillena G, Ramon DJ, Yus M (2007) Angew Chem Int Ed 46:2358–2364
24. Hamid MHSA, Slatford PA, Williams JMJ (2007) Adv Synth Catal 349:1555–1575
25. Nixon TD, Whittlesey MK, Williams JMJ (2009) Dalton Trans 753–765
26. Dobereiner GE, Crabtree RH (2010) Chem Rev 110:681–703
27. Bahn S, Imm S, Neubert L, Zhang M, Neumann H, Beller M (2011) ChemCatChem 3:1853–1864
28. Marr AC (2012) Catal Sci Technol 2:279–287
29. Pan S, Shibata T (2013) ACS Catal 3:704–712
30. Mata JA, Hahn FE, Peris E (2014) Chem Sci 5:1723–1732
31. Hollman D (2014) ChemSusChem 7:2411–2413
32. Guillena G, Ramón D, Yus M (2010) Chem Rev 110:1611–1641
33. Watson AJA, Williams JMJ (2010) Science 329:635–636
34. Alonso F, Riente P, Yus M (2011) Acc Chem Res 44:379–391
35. Fujita K, Yamaguchi R (2005) Synlett 4:560–571
36. Yamaguchi R, Fujita K, Zhu M (2010) Heterocycles 81:1093–1140
37. Obora Y, Ishii Y (2011) Synlett 1:30–51
38. Gunanathan C, Milstein D (2013) Science 341:1229712
39. Gunanathan C, Milstein D (2011) Acc Chem Res 44:588–602
40. Pera-Titus M, Shi F (2014) ChemSusChem 7:2411–2413
41. Obora Y, Nakamura K, Hatanaka S (2012) Chem Commun 48:6720–6722
42. Obora Y, Hatanaka S, Ishii Y (2009) Org Lett 11:3510–3513
43. Hatanaka S, Obora Y, Ishii Y (2010) Chem Eur J 16:1883–1888
44. Obora Y, Sawaguchi T, Tsubakimoto K, Yoshida H, Ogawa S, Hatanaka S (2013) Synthesis 45:2115–2119
45. Muzart J (2015) Eur J Org Chem 2015:5693–5707
46. Díez-Gonzáles S, Marion N, Nolan SP (2009) Chem Rev 109:3612–3676
47. Suzuki T (2011) Chem Rev 111:1825–1845
48. Strakis M, Garcia H (2012) Chem Rev 112:4469–4506
49. Allen SE, Walvoord RR, Padilla-Salinas R, Kozlowski MC (2013) Chem Rev 113:6234–6458
50. Obora Y (2014) ACS Catal 4:3972–3981
51. Cho CS, Kim BT, Kim TJ, Shim SC (2002) Tetrahedron Lett 43:7987–7989
52. Cho CS, Shim SC (2006) J Organomet Chem 691:4329–4332

53. Martinez R, Brand GJ, Ramón DJ, Yus M (2005) Tetrahedron Lett 46:3683–3686
54. Martinez R, Ramón DJ, Yus M (2006) Tetrahedron 62:8988–9001
55. Kwon MS, Kim N, Seo SH, Park IS, Cheedrala RK, Park J (2005) Angew Chem Int Ed 44:6913–6915
56. Yamada YMA, Uozumi Y (2006) Org Lett 8:1375–1378
57. Taguchi K, Nakagawa H, Hirabayashi T, Sakaguchi S, Ishii Y (2004) J Am Chem Soc 126:72–73
58. Fujita K, Asai C, Yamaguchi T, Hanasaka F, Yamaguchi R (2005) Org Lett 7:4017–4019
59. Viciano M, Sanau M, Peris E (2007) Organometallics 26:6050–6054
60. Prades A, Viciano M, Sanau M, Peris E (2008) Organometallics 27:4254–4259
61. Da Costa AP, Viciano M, Sanau M, Merino S, Tejeda J, Peris E, Royo R (2008) Organometallics 27:1305–1309
62. Satyanarayana P, Reddy GM, Maheswaren H, Kantama ML (2013) Adv Synth Catal 355:1859–1867
63. Oded K, Musa S, Gelman D, Blum J (2012) Catal Commun 20:68–72
64. Musa S, Shaposhnikov I, Cohen S, Gelman D (2011) Angew Chem Int Ed 50:3533–3537
65. Musa S, Fronton S, Vaccaro L, Gelman D (2013) Organometallics 32:3069–3073
66. Xu Q, Chen J, Liu Q (2013) Adv Synth Catal 355:697–704
67. Musa S, Ackermann L, Gelman D (2013) Adv Synth Catal 355:3077–3080
68. Cho CS, Ren WX, Shim SC (2005) Bull Korean Chem Soc 26:1611–1613
69. Machemer H (1952) Angew Chem 64:213–220
70. Veibel S, Nielsen JI (1967) Tetrahedron 23:1723–1733
71. Gregorio G, Pregaglia GF, Ugo R (1972) J Organomet Chem 37:385–387
72. Burk PL, Pruett RL, Campo KS (1985) J Mol Catal 33:1–14
73. Carlini C, Macinai A, Galletti AMR, Sbrana G (2004) J Mol Catal A Chem 212:65–70
74. Pratt EF, Kubler DG (1954) J Am Chem Soc 76:52–56
75. Ueda W, Kawahara T, Ohshida T, Morikawa Y (1990) J Chem Soc Chem Commun 1558–1559
76. Carlini C, Marchionna M, Noviello M, Galetti AMR, Sbrana G, Basile F, Vaccari A (2005) J Mol Catal A 232:13–20
77. Cho CS, Kim BT, Kim HS, Kim TJ, Shim SC (2003) Organometallics 22:3608–3610
78. Adair GRA, Williams JMJ (2005) Tetrahedron Lett 46:8233–8235
79. Martinez R, Ramón DJ, Yus M (2006) Tetrahedron 62:8982–8987
80. Matsu-ura T, Sakaguchi S, Obora Y, Ishii Y (2006) J Org Chem 71:8306–8308
81. Koda K, Matsu-ura T, Obora Y, Ishii Y (2009) Chem Lett 38:838–839
82. Xu C, Goh L, Pullarkat SA (2011) Organometallics 30:6499–6502
83. Gong X, Zhang H, Li X (2011) Tetrahedron Lett 52:5596–5600
84. Gnanamgari D, Leung CH, Schley ND, Hilton ST, Crabtree RG (2008) Org Biomol Chem 6:4442–4445
85. Chang X, Chuan L, Yongxin L, Pullarkat SA (2012) Tetrahedron Lett 53:1450–1455
86. Cheung H, Lee T, Lui H, Yeung C, Lau C (2008) Adv Synth Catal 350:2975–2983
87. Kose O, Saito S (2010) Org Biomol Chem 8:896–900
88. Liao S, Yu K, Li Q, Tian H, Zhang Z, Yu X, Xu Q (2012) Org Biomol Chem 10:2973–2978
89. Miura T, Kose O, Li F, Kai S, Saito S (2011) Chem Eur J 17:11146–11151
90. Yang J, Liu X, Meng D, Chen H, Zong Z, Feng T, Sun K (2012) Adv Synth Catal 354:328–334
91. Kawahara R, Fujita K, Yamaguchi R (2010) J Am Chem Soc 132:15108–15111
92. Kawahara R, Fujita K, Yamaguchi R (2011) Adv Synth Catal 353:1161–1168
93. Fujita K, Yamamoto K, Yamaguchi R (2002) Org Lett 4:2691–2694
94. Fujita K, Fujii T, Yamaguchi R (2004) Org Lett 6:3525–3528
95. Bartoszewicz A, Marcos R, Sahoo S, Inge AK, Zou X, Martín-Matute B (2012) Chem Eur J 18:14510–14519
96. Yamaguchi R, Kawagoe S, Asai C, Fujita K (2008) Org Lett 10:181–184
97. Saidi O, Blacker AJ, Farah MM, Marsdenb SP, Williams JMJ (2010) Chem Commun 46:1541–1543
98. Black PJ, Edwards MG, Williams JMJ (2006) Eur J Org Chem 2006:4367–4378
99. Black PJ, Cami-Koberi G, Edwards MG, Slatford PA, Whittlesey MK, Williams JMJ (2006) Org Biomol Chem 4:116–125
100. Saidi O, Blacker AJ, Lamb GW, Marsden SP, Taylor JE, Williams JMJ (2010) Org Process Res Dev 14:1046–1049
101. Blank B, Madalska M, Kempe R (2008) Adv Synth Catal 350:749–758
102. Blank B, Michlok S, Kempe R (2009) Chem Eur J 15:3790–3799

103. Michlik S, Kempe R (2010) Chem Eur J 16:13193–13198
104. Hille T, Irrgang T, Kempe R (2014) Chem Eur J 20:5569–5572
105. Cumpstey I, Agrawal S, Borbasa KE, Martín-Matute B (2011) Chem Commun 47:7827–7829
106. Agrawal S, Lenormand M, Martín-Matute B (2012) Org Lett 14:1456–1459
107. Wang D, Zhao K, Xu C, Miao H, Ding Y (2014) ACS Catal 4:3910–3918
108. Wang D, Zhao K, Yu X, Miao H, Ding Y (2014) RSC Adv 4:42924–42929
109. Wang D, Zhao K, Ma P, Xu C, Ding Y (2014) Tetrahedron Lett 55:7233–7235
110. Li F, Ma J, Wang N (2014) J Org Chem 79:10447–10455
111. Jumde VR, Gonsalvi L, Guerriero A, Peruzzini M, Taddei M (2015) Eur J Org Chem 2015:1829–1833
112. Yan F, Zhang M, Wang X, Xie F, Chen M (2014) Tetrahedron 70:1193–1198
113. Bull ML, Esteruelas MA, Herrero J, Izquiedo S, Pastor IM, Yus M (2013) ACS Catal 3:2072–2075
114. Barreiro EJ, Kummerle AE, Fraga CAM (2011) Chem Rev 111:5215–5246
115. Schoenherr H, Cernak T (2013) Angew Chem Int Ed 52:12256–12267
116. Langhals E, Langhals H (1990) Tetraheron Lett 31:859–862
117. Maruoka K, Concepcion AB, Yamamoto H (1994) Synthesis 1994:1283–1290
118. The Methanol Institute. http://www.methanol.org. Accessed 22 Feb 2016
119. Cifre PG, Badr O (2007) Energy Convers Manag 48:519–527
120. Chang C, Silvestri A (1977) J Catal 47:249–259
121. Haw J, Song W, Marcus DM, Nicholas JB (2003) Acc Chem Res 36:317–326
122. Ahn JH, Temel B, Iglesia E (2009) Angew Chem Int Ed 48:3814–3816
123. Dutta P, Roy SC, Nandi LN, Samuel P, Pillai SM, Bhat BD, Ravindranathan M (2004) J Mol Catal A Chem 223:231–235
124. Maitlis PM, Haynes A, Sunley GJ, Howard MJ (1996) J Chem Soc Dalton Trans 11:2187–2196
125. Thomas CM, Suss-Fink G (2003) Coord Chem Rev 243:125–142
126. Haynes A, Maitlis PM, Morris GE, Sunley GJ, Adams H, Badger PW, Bowers CM, Cook DB, Eliott PIP, Ghaffar T, Green H, Griffin TR, Payne M, Pearson JM, Taylor MJ, Vickers PW, Watt RJ (2004) J Am Chem Soc 126:2847–2861
127. Qian M, Liauw M, Emig G (2003) Appl Catal A 238:211–222
128. Lin W, Chang H (2004) Catal Today 97:181–188
129. Yamagata T, Iseki A, Tani K (1997) Chem Lett 12:1215–1216
130. Tani K, Iseki A, Yamagata T (1999) Chem Commun 18:1821–1833
131. Rodriguez-Lugo RE, Trincado M, Vogt M, Tewes F, Santiso-uinones G, Grützmacher H (2013) Nat Chem 5:342–347
132. Langer R, Fuchs I, Vogt M, Balaraman E, Diskin-Posner Y, Shimon LJW, Ben-David Y, Milstein D (2013) Chem Eur J 19:3407–3414
133. Nielsen M, Alberico E, Baumann W, Drexler HJ, Junge H, Gladiali S, Beller M (2013) Nature 495:85–90
134. Alberico E, Sponholz P, Cordes C, Nielsen M, Drexler HJ, Baumann W, Junge H, Beller M (2013) Angew Chem Int Ed 52:14162–14166
135. Monney A, Barsch E, Sponholz P, Junge H, Ludwig R, Beller M (2014) Chem Commun 50:707–709
136. Hu P, Diskin-Posner Y, Ben-David Y, Milstein D (2014) ACS Catal 4:2649–2652
137. Dang T, Ramalingam B, Seayad AM (2015) ACS Catal 5:4082–4088
138. Moran J, Preetz A, Mesch RA, Krische MJ (2011) Nat Chem 3:287–290
139. Li Y, Xue D, Lu W, Wang C, Liu Z, Xiao J (2014) Org Lett 16:66–69
140. Sun C, Zou X, Li F (2013) Chem Eur J 19:14030–14033
141. Jo E, Lee J, Jun C (2008) Chem Commun 44:5779–5781
142. Ortega N, Richer C, Glorius F (2013) Org Lett 15:1776–1779
143. Li F, Xie J, Shan H, Sun C, Chen L (2012) RSC Adv 2:8645–8652
144. Chan LKM, Poole DL, Shen D, Healy MP, Donohoe TJ (2014) Angew Chem Int Ed 53:761–765
145. Ogawa S, Obora Y (2014) Chem Commun 50:2491–2493
146. Shen D, Poole DL, Shotton CC, Kornahrens AF, Healy MP, Donohoe TJ (2015) Angew Chem Int Ed 54:1642–1645
147. Quan X, Kerdphon S, Andersson PG (2015) Chem Eur J 21:3576–3579
148. Li Y, Li H, Junge H, Beller M (2014) Chem Commun 50:14991–14994
149. Chen S, Lu G, Cai C (2015) RSC Adv 5:70329–70332
150. Li F, Zou X, Wang N (2015) Adv Synth Catal 357:1405–1415

151. Grigg R, Mitchell TRB, Sutthivaiyakit S (1981) Tetrahedron Lett 22:4107–4110
152. Grigg R, Mitchell TRB, Sutthivaiyakit S, Tongpenyai N (1981) J Chem Soc Chem Commun 12:611–615
153. Watanabe Y, Tsuji Y, Ohsugi Y (1981) Tetrahedron Lett 22:2667–2670
154. Motokura K, Nishimura D, Mori K, Mizugaki T, Ebitani K, Kaneda K (2004) J Am Chem Soc 126:5662–5663
155. Löfberg C, Grigg R, Whittaker MA, Keep A, Derrick A (2006) J Org Chem 71:8023–8027
156. Motokura K, Fujita N, Mori K, Mizugaki T, Ebitani K, Jitsukawa K, Kaneda K (2006) Chem Eur J 12:8228–8239
157. Cheung H, Li J, Zheng W, Zhou Z, Chiu Y, Lin Z, Lau C (2010) Dalton Trans 39:265–274
158. Grigg R, Löfberg C, Whitney S, Sridharan V, Keep A, Derrick A (2009) Tetrahedron 65:849–854
159. Cho CS, Kim BT, Kim TJ, Shim SC (2001) J Org Chem 66:9020–9022
160. Onodera G, Nishibayashi Y, Uemura S (2006) Angew Chem Int Ed 45:3819–3822
161. Morita M, Obora Y, Ishii Y (2007) Chem Commun 27:2850–2852
162. Iuchi Y, Hyotanishi M, Miller BE, Maeda K, Obora Y, Ishii Y (2010) J Org Chem 75:1803–1806
163. Weissermel K, Arpe HJ (eds) (2010) Industrial organic chemistry, 5th edn. Wiley-VCH, Weinheim
164. Anxionnat B, Gomez Pardo D, Ricci G, Cossy J (2011) J Org Lett 13:4084–4087
165. Sawaguchi T, Obora Y (2011) Chem Lett 40:1055–1057
166. Kuwahara T, Fukuyama T, Ryu I (2013) Chem Lett 42:1163–1165
167. Guo L, Lin Y, Yao W, Leng X, Huang Z (2013) Org Lett 15:1144–1147
168. Kuwahara T, Fukuyama T, Ryu I (2013) RSC Adv 3:13702–13704
169. Zakarian A, Batch A, Holton RA (2003) J Am Chem Soc 125:7822–7824
170. Danishefsky S, Vaughan K, Gadwood R, Tsuzuki K (1981) J Am Chem Soc 103:4136–4141
171. Ling T, Chowdhury C, Kramer BA, Vong BG, Palladino MA, Theodorakis A (2001) J Org Chem 66:8843–8853
172. Iuchi Y, Obora Y, Ishii Y (2010) J Am Chem Soc 132:2536–2537
173. Guo L, Ma X, Fang H, Jia X, Huang Z (2015) Angew Chem Int Ed 54:4023–4027
174. Blank B, Kempe R (2010) J Am Chem Soc 132:924–925
175. Obora Y, Ogawa S, Yamamoto N (2012) J Org Chem 77:9429–9433
176. Chaudhari C, Siddiki SMAH, Shimizu K (2013) Tetrahedron Lett 54:6490–6493
177. Nandakumar A, Midya SP, Landge VG, Balaraman E (2015) Angew Chem Int Ed 54:11022–11034
178. Xiong B, Li Y, Lv W, Tan Z, Jiang H, Zhang M (2015) Org Lett 17:4054–4057
179. Waykole C, Bhowmick D, Pratap A (2014) J Am Oil Chem Soc 91:1407–1416
180. Xu G, Lammens T, Liu Q, Wang X, Dong L, Caiazzo A, Ashraf N, Guan J, Mu X (2014) Green Chem 16:3971–3977
181. Silvester L, Lamonier JF, Faye J, Capron M, Vanner RN, Lamoniew C, Dubois JL, Coururier JL, Calais C, Dumeignil F (2015) Cat Sci Technol 5:2994–3006
182. Kozlowski JT, Davis RJ (2013) ACS Catal 3:1588–1600
183. Cano R, Yus M, Ramón DJ (2012) Chem Commun 48:7628–7630
184. Bai W, Jia G (2015) Inorg Chim Acta 431:234–241
185. Dowson GRM, Haddow MF, Lee J, Wingad RL, Wass DF (2013) Angew Chem Int Ed 52:9005–9008
186. Zhang X, Lin Z, Xu X, Yue H, Tian G, Feng S (2013) ACS Sustain Chem Eng 1:1493–1497
187. Obora Y, Anno Y, Okamoto R, Matsu-ura T, Ishii Y (2011) Angew Chem Int Ed 50:8618–8622
188. Ikeda T, Lee B, Kurihara S, Tazuke S, Ito S, Yamamoto M (1988) J Am Chem Soc 110:8299–8304
189. Wang J, Doubleday C Jr, Turro NJ (1989) J Am Chem Soc 111:3962–3965
190. Yamaji M, Tsukada H, Nishimura J, Shizuka H, Tobita S (2002) Chem Phys Lett 357:137–142
191. Tani K, Tohda Y, Takemura H, Ohkita H, Ito S, Yamamoto M (2001) Chem Commun 19:1914–1915
192. Makarov IS, Madsen R (2013) J Org Chem 78:6593–6598
193. Mura MG, De Luca L, Taddei M, Williams JAM, Porcheddu A (2014) Org Lett 16:2586–2589
194. Shimizu K (2015) Cat Sci Technol 5:1412–1427
195. Shan SP, Tuan DT, Seayad AM, Ramalingam B (2014) ChemCatChem 6:808–814
196. Peeters A, Claes L, Geukens I, Stassen I, De Vos D (2014) Appl Catal A 469:191–197
197. Yamaguchi K, He J, Oishi T, Mizuno N (2010) Chem Eur J 16:7199–7207
198. Rasero-Almansa AM, Corma A, Iglesias M, Sanchez F (2014) ChemCatChem 6:1794–1800
199. Wang D, Guo X, Wang C, Wang Y, Zhong R, Zhu X, Cai L, Gao Z, Hou X (2013) Adv Synth Catal 355:1117–1125

200. Corma A, Navas J, Sabater MJ (2012) Chem Eur J 18:14150–14156
201. He L, Qian Y, Ding R, Liu Y, He H, Fan K, Cao Y (2012) ChemSusChem 5:621–624
202. Ishida T, Takamura R, Takei T, Akita T, Haruta M (2012) Appl Catal A 413–414:261–266
203. Tang C, He L, Liu Y, Cao Y, He H, Fan K (2011) Chem Eur J 17:7172–7177
204. He L, Lou X, Ni J, Liu Y, Cao Y, He H, Fan K (2010) Chem Eur J 16:13965–13969
205. Liu H, Chuah G, Jaenicke S (2012) J Catal 292:130–137
206. Shimizu K, Shimura K, Nishimura M, Satsuma A (2011) ChemCatChem 3:1755–1758
207. Shimizu K, Nishimura M, Satsuma A (2009) ChemCatChem 1:497–503
208. Cano R, Yus M, Ramon DJ (2011) Tetrahedron 67:8079–8085
209. Zhang Y, Qi X, Cui X, Shi F, Deng Y (2011) Tetrahedron Lett 52:1334–1338
210. Shirasaki Y, Fujiwara K, Sugano Y, Ichikawa S, Hirai T (2013) ACS Catal 3:312–320
211. Ousmane M, Perrussel G, Yan Z, Clacens JM, De Campo F, Pera-Titus M (2014) J Catal 309:439–452
212. Corma A, Rodenas T, Sabater MJ (2010) Chem Eur J 16:254–260
213. Mehta A, Thakev A, Londhe V, Nandan SR (2014) Appl Catal A 478:241–251
214. Shimizu K, Imaiida N, Kon K, Siddiki SMAH, Satsuma A (2013) ACS Catal 3:998–1005
215. Ueno S, Usui K, Kuwano K (2011) Synlett 2011:1303–1307
216. Santoro F, Psaro R, Ravasio N, Zaccheria F (2014) RSC Adv 4:2596–2600
217. Dixit M, Mishra M, Joshi PA, Shah DO (2013) Catal Commun 33:80–83
218. Santoro F, Psaro R, Ravasio N, Zaccheria F (2012) ChemCatChem 4:1249–1254
219. Perez JM, Cano R, Yus M, Ramon DJ (2012) Eur J Org Chem 2012:4548–4554
220. He J, Yamaguchi K, Mizuno N (2010) Chem Lett 39:1182–1183
221. Likhar PR, Arundhathi R et al (2009) Eur J Org Chem 2009:5383–5389
222. Gonzalez-Arellano C, Yoshida K, Luque R, Gai PL (2010) Green Chem 12:1281–1287
223. Yu X, Liu C, Jiang L, Xu Q (2011) Org Lett 13:6184–6187
224. Dang T, Shan S, Ramalingam B, Seayad AM (2015) RSC Adv 5:42399–42406
225. Culkin DA, Hartwig JF (2003) Acc Chem Res 36:234–245
226. Bellina F, Rossi R (2010) Chem Rev 110:1082–1146
227. Li C (2009) Acc Chem Res 42:335–344
228. Campos KR (2007) Chem Soc Rev 36:1069–1084
229. Li H, Li J, Shi Z (2011) Catal Sci Technol 1:191–206
230. Fox JM, Huang X, Chieffi A, Buchwald SL (2000) J Am Chem Soc 122:1360–1370
231. Doherty S, Knight JG, Smyth CH, Harrington RW, Clegg W (2008) Organometallics 27:1679–1682
232. Nguyen HN, Huang X, Buchwald SL (2003) J Am Chem Soc 125:11818–11819
233. Liao X, Weng Z, Hartwig JF (2008) J Am Chem Soc 130:195–200
234. Li B, Darcel C, Dixneuf PH (2014) Chem Commun 50:5970–5972
235. Labed A, Jiang F, Labed I, Lator A, Peters M, Achard M, Kabouche A, Kabouche Z, Sharma GVM, Bruneau C (2015) ChemCatChem 7:1090–1096
236. Allen LJ, Crabtree RH (2010) Green Chem 12:1362–1364
237. Xu Q, Chen J, Tian H, Yuan X, Li S, Zhou C, Liu J (2014) Angew Chem Int Ed 53:225–229
238. Liang Y, Zhou X, Tang S, Huang Y, Feng Y, Xu H (2013) RSC Adv 3:7739–7742

CrossMark

R E V I E W

N-Alkylation by Hydrogen Autotransfer Reactions

Xiantao Ma[1,2] · Chenliang Su[2] · Qing Xu[1]

Abstract Owing to the importance of amine/amide derivatives in all fields of chemistry, and also the green and environmentally benign features of using alcohols as alkylating reagents, the relatively high atom economic dehydrative *N*-alkylation reactions of amines/amides with alcohols through hydrogen autotransfer processes have received much attention and have developed rapidly in recent decades. Various efficient homogeneous and heterogeneous transition metal catalysts, nano materials, electrochemical methods, biomimetic methods, asymmetric *N*-alkylation reactions, aerobic oxidative methods, and even certain transition metal-free, catalyst-free, or autocatalyzed methods, have also been developed in recent years. With a brief introduction to the background and developments in this area of research, this chapter focuses mainly on recent progress and technical and conceptual advances contributing to the development of this research in the last decade. In addition to mainstream research on homogeneous and heterogeneous transition metal-catalyzed reactions, possible mechanistic routes for hydrogen transfer and alcohol activation, which are key processes in *N*-alkylation reactions but seldom discussed in the past, the recent reports on computational mechanistic studies of the *N*-alkylation reactions, and the newly emerged *N*-alkylation methods based on novel alcohol activation protocols such as air-promoted reactions and transition metal-free methods,

✉ Qing Xu
    qing-xu@wzu.edu.cn

1   College of Chemistry and Materials Engineering, Wenzhou University, Wenzhou, Zhejiang 325035, China

2   SZU-NUS Collaborative Innovation Center for Optoelectronic Science and Technology, Key Laboratory of Optoelectronic Devices and Systems of Ministry of Education and Guangdong Province, College of Optoelectronic Engineering, Shenzhen University, Shenzhen 518060, China

⦰ Springer

are also reviewed in this chapter. Problems and bottlenecks that remained to be solved in the field, and promising new research that deserves greater future attention and effort, are also reviewed and discussed.

1 Introduction and Background

Nitrogen is one of the most important essential elements for life. It has been chosen by nature to build essential molecules such as amino acids and nucleotides in the construction of life. Consequently nitrogen-containing compounds play important roles in all fields of chemistry, and in all aspects of life in living organisms. For example, nitrogen functionalities and organonitrogen blocks are abundant in numerous natural products, biologically active molecules, agrochemicals, synthetically and pharmaceutically significant compounds. Commonly used pharmaceuticals usually contain at least one nitrogen atom.

Amines and amine derivatives are the most fundamental and significant organonitrogen compounds because they can be used as starting materials for the preparation of other organonitrogen blocks. The reaction of ammonia/amines with organohalides to produce alkylated amines [1], namely the Hofmann *N*-alkylation reaction discovered by A. W. Hofmann in 1850 [2], is included in all text books as a basic method of amine derivative synthesis [3]. However, this method uses active and toxic organohalides as reactants, and is low in selectivity and atom efficiency, producing a mixture of different amines and inevitable ammonium salts as byproducts, which leads to serious problems with product separation and purification. Since then, various more selective, efficient, and atom economic methods have been developed for the synthesis of different amines and amine derivatives to meet specific synthetic needs, which include mainly the Gabriel method, reduction of nitro compounds, Ullmann/Buchwald–Hartwig type transition metal (TM)-mediated/catalyzed couplings of N–H compounds with aryl halides and pseudohalides, reductive alkylation of amines with carbonyl compounds, transition metal-catalyzed hydroamination/hydroaminomethylation of carbon–carbon unsaturated compounds, as well as dehydrative *N*-alkylation reactions of amines/amides with alcohols. The latter method, *N*-alkylation of amines/amides using alcohols as the alkylating reagents (Eq. 1), seemingly a direct dehydrative substitution of alcohol's hydroxyl group by the amines/amides, is a relatively environmentally benign alternative, not only because comparatively high atom efficiency can be achieved by generating water as the only byproduct, but also because alcohols are more available, more stable, lower in toxicity, more easily stored and handled, much lower in cost,

and are a class of greener chemicals than the corresponding organohalides or carbonyl compounds.

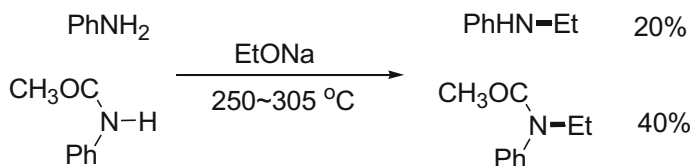$$\begin{array}{c} R^1 \\ R^2 \end{array}\!\!>\!\!OH \ + \ H\!-\!N\!\!<\!\!\begin{array}{c} R^3 \\ R^4 \end{array} \longrightarrow \begin{array}{c} R^1 \\ R^2 \end{array}\!\!>\!\!N\!\!<\!\!\begin{array}{c} R^3 \\ R^4 \end{array} \ + \ H_2O \qquad (1)$$
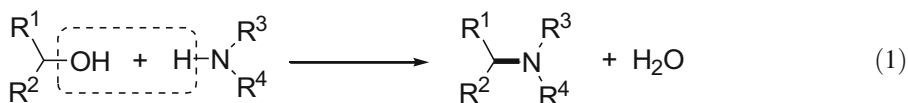
In fact, in the early twentieth century, just half a century after Hofmann's report, J. U. Nef [4] first discovered that *N*-alkylation of amines/amides could be achieved using alcohols at high temperatures under strong basic conditions, albeit the yields and selectivities were not high (Scheme 1). This is mostly due to the fact that alcohols are generally inactive in nature, and because hydroxyl is not a good leaving group and thus activation for further transformations is difficult.

Following Nef's report, other chemists also developed a number of methods for *N*-alkylation of amines with alcohols, by using main group metal (Na, K, Al, Mg, etc.) hydroxides or alkoxides [5–9], or heterogeneous transition metal (TM)-impregnated silica or alumina catalysts, or metal alloys, metal salts, mixed oxides of metals, or directly silica-alumina as the catalysts [10–12]. However, these methods still require forcing reaction conditions such as high temperatures (200–400 °C), high pressure, using large amounts of bases, and still suffer from the problems of long reaction time, low yields, and low selectivities.

As more and more TM complexes were developed and applied in organic synthesis, TM-catalyzed synthetic methods progressed quickly. In 1981 and 1982, the groups of Grigg [13], Watanabe [14], and Murahashi [15] independently reported the earliest homogeneous TM-catalyzed *N*-alkylation reactions of amines with alcohols using [Ru], [Ir] or [Rh] complexes. A main difference of these reactions compared to the previous methods is that, by using the noble transition metal complexes, *N*-alkylation reactions could be achieved under milder conditions (<200 °C) and tolerate a broader scope of substrates. Realizing TM catalysts' higher activity in alcohol activation, and their potential in the dehydrative alkylation reactions, more and more chemists became interested in this research and the field has progressed rapidly in the past three decades, especially after the 1990s due to chemists' growing awareness of environmental concerns regarding chemical reactions, and the need to develop greener and more sustainable reactions to replace traditional methods. In addition, in 2005, the ACS Green Chemistry Institute (GCI) and global pharmaceutical companies founded an ACS GCI Pharmaceutical Roundtable to promote the development of green chemistry and green engineering

$$\begin{array}{ccc} PhNH_2 & & PhHN\!-\!Et \quad 20\% \\ & \xrightarrow[\text{250~305 °C}]{\text{EtONa}} & \\ \begin{array}{c} CH_3OC \\ \quad\quad N\!-\!H \\ Ph \end{array} & & \begin{array}{c} CH_3OC \\ \quad\quad N\!-\!Et \quad 40\% \\ Ph \end{array} \end{array}$$

Scheme 1 Nef's initial findings on dehydrative *N*-alkylation [4]

in pharmaceutical industry. The inclusion of direct transformations of alcohols into pharmaceutically useful chemicals as one of its key research areas by the ACS GCI Pharmaceutical Roundtable also promoted the progress of alcohol-based research in organic and pharmaceutical synthesis. Therefore, numerous homogeneous and heterogeneous TM-, Lewis acids-, Brönsted acids-, or co-catalysts-catalyzed methods for dehydrative N-alkylation of amines and amides with alcohols have been developed in recent years.

In general, these alcohol-based dehydrative N-alkylation reactions can be classified into two categories. One is the direct nucleophilic substitution of the hydroxy group by amines/amides mediated/catalyzed by Brönsted acids, Lewis acids, or TM complexes via formation of carbocation or coordinated cationic metal complexes under acidic conditions (Scheme 2) [16–20]. The famous Ritter reaction of nitriles and alcohols giving alkylated amides may be classified as one of these reactions, in which the nitriles serve as the N-nuleophile (Eq. 2) [21, 22].

$$R-CN \ + \ HO-\overset{R^1}{\underset{R^3}{\diagup}}R^2 \ \xrightarrow{\text{BA, LA, or TM-cat.}} \ R\overset{O}{\diagup}\underset{H}{N}\overset{R^1}{\diagup}\overset{R^2}{\underset{R^3}{\diagup}} \quad (2)$$
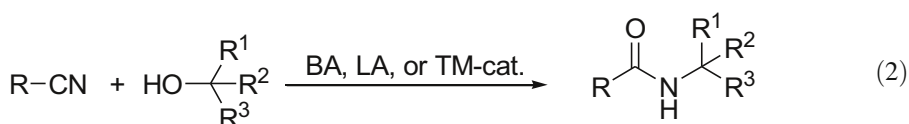
The other category, as termed by the leading chemists in the area, is the "borrowing hydrogen" [12, 23–32] or "hydrogen autotransfer" [9] methodology, or more simply "hydrogen transfer reactions" [33, 34] that involve characteristic hydrogen transfer processes in the reactions (Scheme 3). In these reactions, alcohols are generally believed to be dehydrogenatively activated under inert conditions by TM catalysts to form the more active aldehydes and the reducing hydridometal species [MH] or [MH$_2$], which then return the hydrogen atoms to the intermediate imines to give the final alkylated amine/amide products. The method is thus mainly suitable for primary amines and alcohols. According to this recapitulatory general
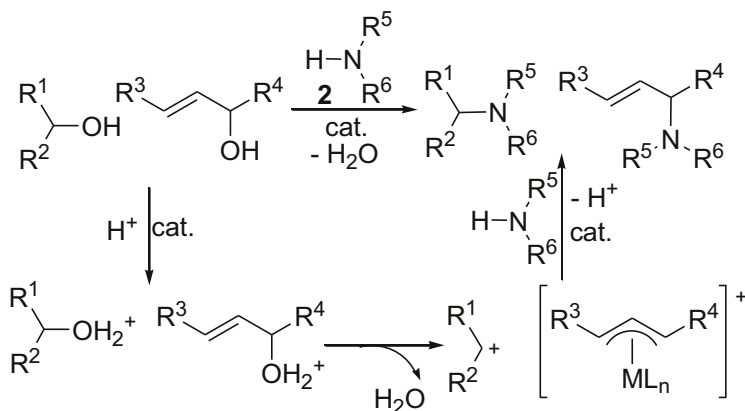
Scheme 2 General mechanism for direct nucleophilic substitution reactions of alcohols by amines/amides
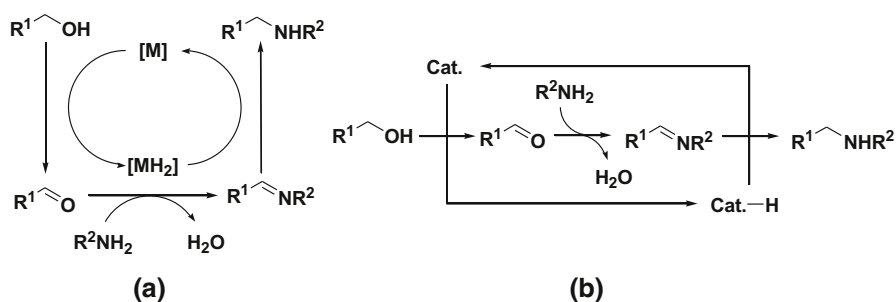
Scheme 3 General mechanism for alcohol-based borrowing hydrogen (**a**) or hydrogen autotransfer reactions (**b**)

mechanism (Scheme 3), hydrogen transfer from alcohols to TM catalysts and then from [MH]/[MH$_2$] to intermediate imines are the typical key processes of the methods. It should also be pointed out that inorganic bases were usually required in hydrogen autotransfer reactions for deprotonation of the alcohols to facilitate their coordination with TM catalysts. Since bases were usually used in large excess amounts in the early TM-free methods [4–10], they were used only as additives but not as catalysts in TM-catalyzed reactions [10–12, 23–34], even though in many cases they were also used in catalytic amounts.

The direct nucleophilic substitution reactions (Scheme 2) [16–22], restricted mainly to π-activated alcohols such as secondary arylmethanols, allylic and propargylic alcohols, and tertiary alcohols that can readily form stable carbocationic intermediates, are mechanistically different to hydrogen autotransfer reactions. Although these reactions are not the focus of this chapter, since they are also very relevant research areas, this brief introduction is anticipated to provide potentially helpful references to assist interested researchers in their studies, especially in boardline research where elucidation of reaction mechanisms is difficult.

In the case of *N*-alkylation reactions by hydrogen autotransfer processes, asymmetric reactions, nano materials, electrochemical methods, biomimetic methods, reactions using amines as the alkylating reagents, the more practical aerobic *N*-alkylation methods, and even some simple and efficient TM-free methods have also been reported in recent years. It was proposed that, in addition to anaerobic dehydrogenative for activation of the alcohols (Scheme 4, methods A–B), more alternative protocols should also be available, which may include the use of
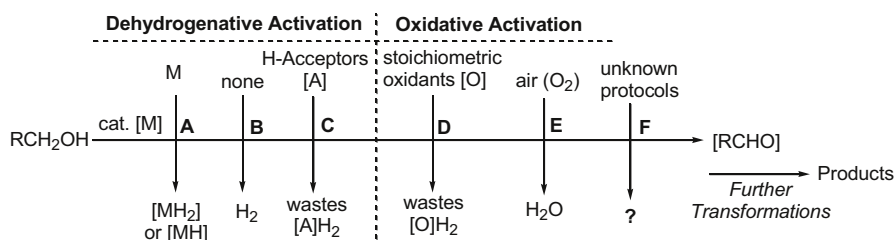
Scheme 4 Known and potential protocols for alcohol activation

hydrogen acceptors, oxidants or organocatalysts, aerobic oxidative methods, etc. (methods C–F) [36]. Since TM-catalyzed aerobic oxidation of alcohols has been the standard method for aldehyde synthesis [36–41], oxidative dehydrogenation methods using various oxidants have been intensively employed in cross-dehydrogenative coupling (CDC) reactions for substrate activation [42, 43], and stoichiometric oxidants have also been employed for synthesis of alkylated amines from alcohols and amines by one-pot multi-step oxidation–reduction reactions [44, 45], these new protocols for alcohol activation should be good complements to the anaerobic dehydrogenation protocol.

Since there have been several important and excellent reviews on N-alkylation reactions of the hydrogen transfer type in recent years [10–12, 23–35], this chapter highlights mainly some typical examples of the main progress, technical and conceptual advances, and recent mechanistic achievements contributing to development of this research in the last decade. In addition to mainstream research on homogeneous and heterogeneous transition metal-catalyzed reactions, possible mechanistic routes for hydrogen transfer and alcohol activation that are the key processes in N-alkylation reactions but seldom discussed in the past, recent achievements on computational mechanistic studies of the N-alkylation reactions, and some newly emerged N-alkylation methods based on novel alcohol activation protocols such as air-promoted aerobic N-alkylation reactions and transition metal-free methods are also reviewed in this chapter. Problems and bottlenecks remain in the field, and promising new research that deserves greater future attention and effort, such as potential protocols for alcohol and amine activation, meaningful and attractive new methods or catalysts, and experimental and computational mechanistic studies that can provide deeper insight into the alcohol activation and hydrogen transfer processes and contribute to the design and development of new N-alkylation methods, are also reviewed and discussed.

2 Hydrogen Autotransfer N-Alkylation Reactions Using Alcohols as the Alkylating Reagents

2.1 Mechanistic Aspects of TM-Catalyzed N-Alkylation Reactions

TM-catalyzed N-alkylation reactions of amines/amides with alcohols are usually held to proceed via the general borrowing hydrogen or hydrogen autotransfer mechanism (Scheme 3) [10–12, 23–34]. This is based mostly on the concept that TM catalysts can "borrow" and "return" hydrogen atoms from the alcohols and to the products with temporary hydrogen storage by formation of [MH]/[MH$_2$] species. Therefore, the key to judge whether an N-alkylation reaction is a true borrowing hydrogen or hydrogen autotransfer reaction would be the determination of the [MH]/[MH$_2$] species formed in situ in the reaction medium. However, this is not that easy. Alternatively, according to the proposed general mechanism (Scheme 3), whether the TM catalyst can directly produce aldehydes by alcohol dehydrogenation: (1) under anaerobic conditions, (2) without external oxidants or hydrogen acceptors, and (3) without aldehyde contamination in the substrate alcohols, which

could lead to misleading results and conclusions, are also acting standards to help making the judgement.

In fact, the borrowing hydrogen or hydrogen autotransfer concept, and generation of [MH]/[MH$_2$] species in alcohol-based *N*-alkylation reactions were, to a large extent, based on the well-documented transfer hydrogenation reactions of unsaturated compounds, especially the carbonyl compounds and imines with alcohols [46–51]. The last step of the borrowing hydrogen mechanism (Scheme 3), namely the reduction of imine intermediates by alcohols, is, in effect, a transfer hydrogenation reaction. The only difference is, in conventional transfer hydrogenation reactions, excess alcohols such as isopropanol are used only as a hydrogen source, and byproduct acetone is generated as a waste product [46–51]; while in *N*-alkylation reactions, the alcohols are both the hydrogen and alkyl source, and byproduct aldehydes are recovered in the catalytic cycle. Therefore, the mechanistic aspects of these two transformations have much in common.

2.1.1 Mechanistic Possibilities for Transfer of Hydrogens from Alcohols to Intermediate Imines

In spite of much work, the mechanism of a given *N*-alkylation reaction, especially the question of how hydrogens are transferred from alcohols to intermediate imines, remains to be elucidated specifically in each case. Several possibilities might exist, and the reaction mechanism may vary depending on the substrates, TMs and ligands used, and the specific reactions conditions employed [26]. On the other hand, the general mechanism (Scheme 3) gives little insight into how hydrogen atoms are transferred. Since little attention has been paid to this aspect in the past, and the hydrogen transfer process is closely related to the key alcohol activation step, this introductory discussion is designed to stimulate more focus on these mechanisms in future studies.
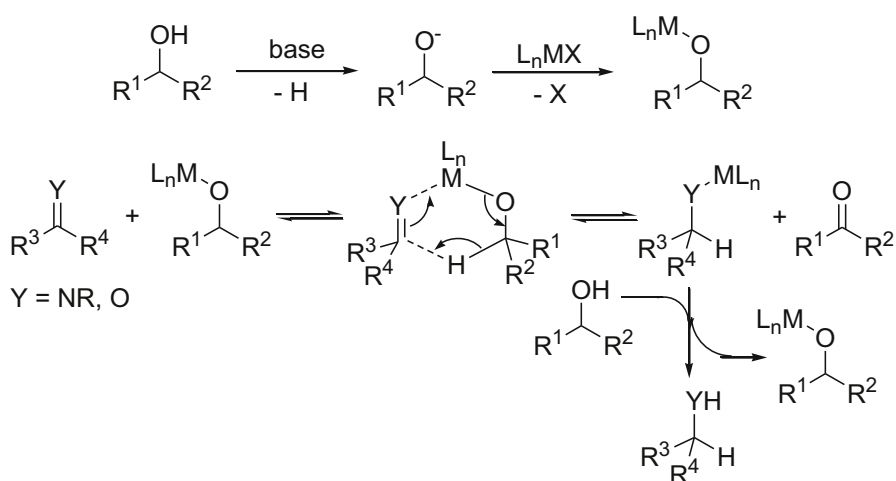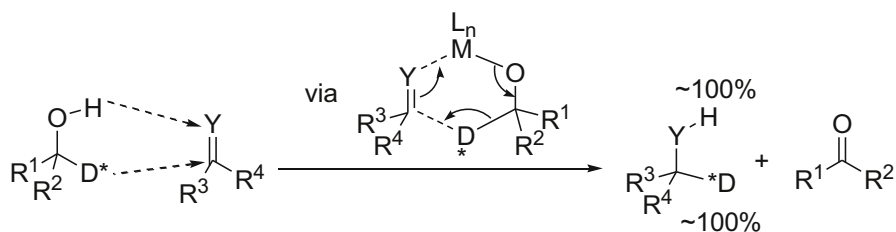

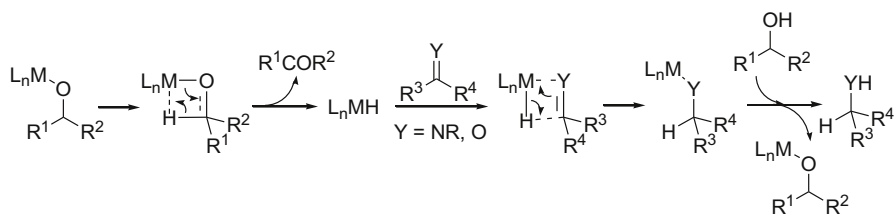**Scheme 5** Direct hydrogen transfer route

As summarized in review papers, there may be several possibilities for hydrogen transfer from alcohols to unsaturated bonds (C=O and C=N bonds in particular) under TM-catalyzed conditions [26, 46–51]. One is the direct hydrogen transfer route, involving a TM-templated concerted process with six-membered cyclic transition states [47, 48]. As shown in Scheme 5, the base first deprotonates the alcohol to facilitate its coordination with the TM pre-catalyst, which then coordinates with the C=Y compound, making both the alcohol and C=Y moieties bind to the metal center in close proximity. The metal acts as a template to provide correct orientation for a concerted hydride shift from the alcohol to the C=Y bond. As a result, both the β-C-H and O-H of the alcohol are transferred selectively to become the β-C-H and Y-H of the product, as can be inferred by using deuterium-labeled alcohols as the hydrogen source and measuring the deuterium content of Y-H and C-H in the product (Scheme 6). The direct hydrogen transfer route is similar to the Meerwein-Pondorf-Verley reduction and Oppenauer oxidation (MPV–O) route of the main group metals (Schemes 39, 40 vide infra) [52–54]. Although the MPV–O route is typical of the main group metals, it cannot be excluded completely in TM-catalyzed reactions [47, 48], especially for TM pre-catalysts, with which it is difficult to form hydridometal species, or under conditions not suitable for formation of hydridometals.

Other possible routes include hydride routes, especially for TM pre-catalysts, which can readily form [MH]/[MH$_2$] species [26, 46–51]. To form [MH]/[MH$_2$] species, coordination of TMs with strong electron-donating ligands, such as phosphines, seems to be indispensable. Nevertheless, most [MH]/[MH$_2$] are still known to be sensitive, short-lived, and prone to react with oxidants such as molecular oxygen. [MH]/[MH$_2$] species are thus usually obtained under anaerobic conditions (such as in a glove box), or prepared/characterized in situ in the presence of ligands. Hence, a borrowing hydrogen or hydrogen autotransfer N-alkylation reaction is typically performed under anaerobic conditions with inert atmosphere protection.

There are two routes for hydride transfer. One is the monohydride route (Scheme 7). It is commonly held that, after alcohol deprotonation by the base and coordination with the TM, the TM center abstracts only the β-C-H of the alcohol to give [MH] species via a four-membered cyclic transition state, which then reduces the C=Y bond via a similar but reverse hydride transfer route. Consequently, if a deuterium-labeled alcohol is used as the hydrogen source (Scheme 8), both the β-C-

Scheme 6 Deuterium labeling of direct hydrogen transfer route

Scheme 7 Monohydride route
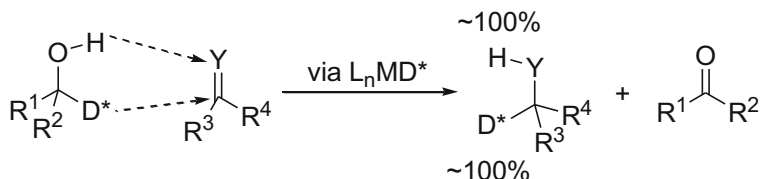
Scheme 8 Deuterium labeling of the monohydride route

D* and O-H of the alcohol can be transferred selectively to become β-C-D* and Y-H in the product, respectively [49, 50]. Since this process is the same with the direct hydrogen transfer (Scheme 6) and TM-free MPV–O (Scheme 40, vide infra) routes, the deuterium labeling method cannot be used to distinguish them.

The other route is the dihydride route, involving sequential abstraction of both the O-H and β-C-H of the alcohol onto the TM center (Scheme 9) [26, 49–51]. It is commonly held that zero-valent TM first inserts into the O–H bond of the alcohol, followed by β-H elimination to give [MH₂] species. [MH₂] then reduces C=Y compounds via a similar but reverse route. As a result, this route is not selective regarding the hydride transfer processes. If a deuterium-labeled alcohol is used, the deuterium contents of Y–H and C–H in the product should both be around 50 % (Scheme 10) [50, 51].

Mechanistically, reactions taking the dihydride route should not require bases. Indeed, several base-free N-alkylation reactions have been reported. Heterogeneous catalysts impregnated with zero-valent TMs may therefore also belong to this class. Besides, zero-valent TM catalyst LₙM(0) and/or [MH₂] may also be generated in situ from the corresponding TM pre-catalysts, such as the frequently used RuCl₂L₃ and PdX₂Lₙ, via reduction by alcohols [49–51]. In such cases, bases are also required to facilitate the generation of LₙM(0) and [MH₂] species. As shown in
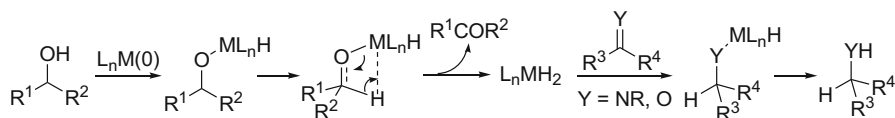
Scheme 9 Dihydride route
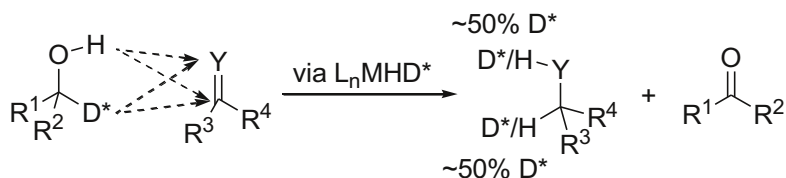
Scheme 10 Deuterium labeling of the dihydride route
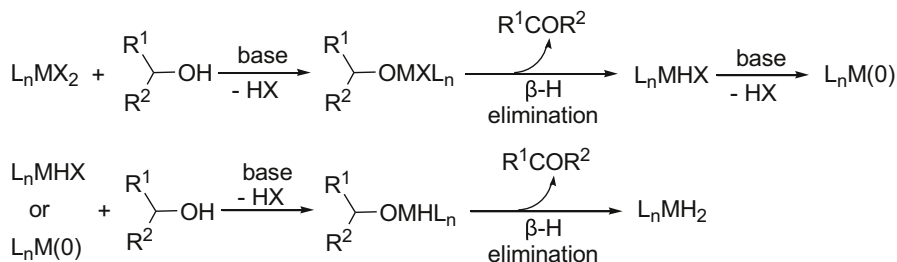
Scheme 11 In situ generation of $L_nM(0)$ and $[MH_2]$ species from transition metal (TM) pre-catalysts

Scheme 11, this transformation is accomplished by a stepwise reduction of the TM precatalyst by the alcohol via formation of monohydride.

2.1.2 Mechanistic Aspects of Dehydrogenative Activation of Alcohols to Carbonyl Intermediates

Since hydroxyl is not a good leaving group, alcohols usually need to be activated for further transformations. In TM-catalyzed *N*-alkylation reactions via the hydrogen autotransfer processes, alcohols are believed to be activated to carbonyl compounds by anaerobic dehydrogenation. However, alcohol dehydrogenation with formation of [MH]/[MH$_2$] species or extrusion of H$_2$ is known as a thermodynamically unfavorable uphill process [55, 56], being in many cases the rate-limiting step of the whole reaction. Meanwhile, substrate and product amines as well as intermediate imines are all known to be good ligands that may complex with TMs, possibly poisoning, or even deactivating, the TM catalysts. Therefore, to accomplish dehydrogenative alcohol activation, the activity of TMs needs to be enhanced. Capricious ligands are hence adopted to improve TM activity and stabilize the [MH]/[MH$_2$] species; exceptions to this are rare.
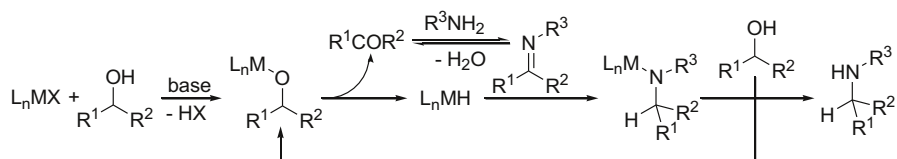
Scheme 12 Possible mechanism of *N*-alkylation reactions via the monohydride route

Based on the general mechanism (Scheme 3), borrowing hydrogen or hydrogen autotransfer catalysts should be able to dehydrogenate alcohols to carbonyl compounds and form [MH]/[MH$_2$] species under inert conditions. As shown in Scheme 12, with the monohydride route, carbonyl compounds and [MH] species are first generated by β–H elimination of the metal alcoholate complex. Imine intermediates formed by simultaneous condensation of the carbonyl intermediates with amines are then reduced by [MH] to give a metal–product complex, and finally the product via proton exchange. This may imply that, with monohydride mechanism, TM catalysts can activate the alcohols to carbonyl compounds followed by formation of imine intermediates, which then serve as the hydrogen acceptor to oxidize [MH] species. By analogy, the monohydride mechanism (Scheme 12) may be most consistent with the general borrowing hydrogen or hydrogen autotransfer mechanism (Scheme 3).

In the dihydride mechanism (Scheme 13), generation of the [MH$_2$] species requires an initial alcohol dehydrogenation process to reduce TM pre-catalysts to L$_n$M(0) with formation of the first carbonyl intermediate, followed by L$_n$M(0) activation of the alcohol to give [MH$_2$] and the second carbonyl intermediate. Consequently, with the dihydride mechanism, TM catalysts can readily activate the alcohols to carbonyl compounds without much difficulty.

In contrast, in the direct hydrogen transfer route, no carbonyl compound is generated simultaneously with, or prior to, the hydrogen transfer step (Scheme 5). Thus, no imine intermediates can be employed as the hydrogen acceptor to accomplish hydrogen transfer from the alcohol. The initial step of alcohol activation to carbonyl compounds is thus an issue to be solved in the catalytic cycle, which may become the rate-limiting step in the whole reaction. Hence, alternative means of alcohol activation should be adopted (Scheme 14). According to recent developments, this may include aerobic N-alkylation reactions using air as the promoter of the reactions, or reactions involving metal oxidants- or hydrogen acceptors-initiated processes.

2.1.3 Computational Mechanistic Studies on TM-Catalyzed N-Alkylation Reactions

Mechanisms of TM-catalyzed N-alkylation reactions have also been investigated in recent years by employing computational methods such as density functional theory (DFT) calculations [57–63]. In 2008, Eisenstein and coworkers [57] performed a DFT calculation on the mechanism of the [Cp*IrCl$_2$]$_2$/K$_2$CO$_3$-catalyzed
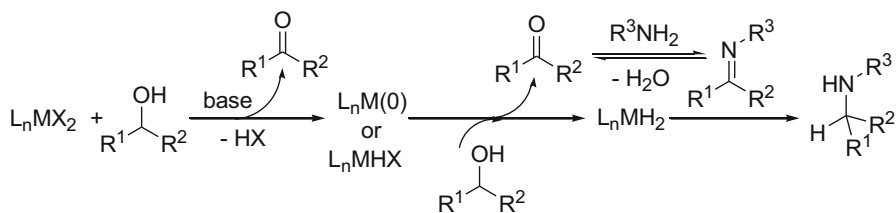
Scheme 13 Possible mechanism of N-alkylation reactions via the dihydride route
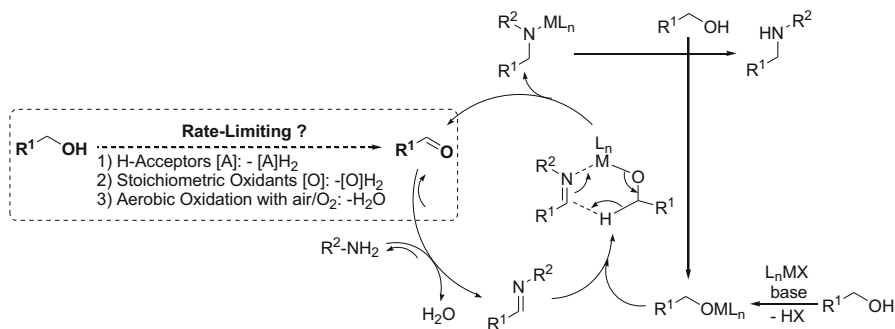
Scheme 14 Possible mechanism of *N*-alkylation reactions via the direct hydrogen transfer route

(Cp* = η⁵-C₅Me₅) *N*-alkylation reaction of amines and alcohols. They found that the reaction favors the product-forming direction because the alcohol dehydrogenation step by β–H elimination has a lower barrier than dehydrogenation of the product amines. Besides, the two hydrogen atoms transferred from the alcohol to the imine intermediate are transferred as one hydride H^- and one proton H^+ (Scheme 15). The hydride goes from the alcohol to the metal, and then from the metal to the imine, which is consistent with the monohydride mechanism (Scheme 12); while the proton goes from the alcohol to the carbonate base and further to the product amine, which differs slightly from the monohydride mechanism (Scheme 12), because the ancillary carbonate ligand was found to coordinate with Ir and thus be involved in the hydrogen transfer step (Scheme 15).

In 2012, Fristrup and Madsen studied the mechanism of the same *N*-alkylation reaction as above by combining experimental and theoretical methods [58]. In contrast to Eisenstein's proposal [57], Fristrup and Madsen's results suggested that both aldehyde and hemiaminal intermediates stay coordinated to the iridium catalyst
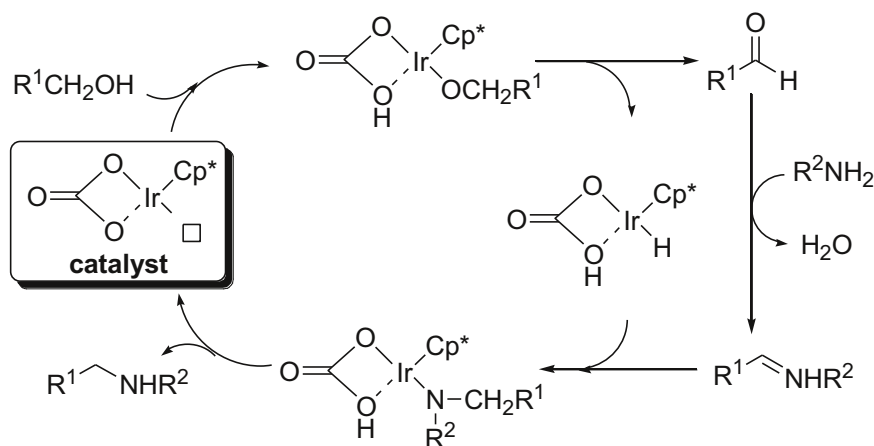
Scheme 15 Proposed mechanism for [Cp*IrCl₂]₂/K₂CO₃-catalyzed *N*-alkylation reaction supported by Eisenstein's density functional theory (DFT) calculation [57]

in the catalytic cycle. Further dehydration to imine and reduction to product amine also take place without breaking the coordination to the catalyst (Scheme 16).

In 2015, Liu and co-workers also re-investigated the DFT calculation of the above [Cp*IrCl$_2$]$_2$/K$_2$CO$_3$-catalyzed N-alkylation reaction [59]. They found the initial alcohol dehydrogenation to aldehyde and the second aldehyde-amine condensation steps are thermodynamically endergonic; whereas the third imine reduction to product amine step is highly exergonic, being the driving force for the whole catalytic cycle. For the alcohol dehydrogenation and imine reduction steps, the most favorable pathways are the inner-sphere hydrogen transfer pathway under the catalysis of Cp*Ir(NHPh)Cl, and the inner-sphere hydrogen transfer pathway with KHCO$_3$ as the proton donor.

In addition to the above computational studies on the mechanism of Ir-catalyzed N-alkylation reactions, in 2015 Martín-Matute and co-workers [60] also investigated a bifunctional iridium complex-catalyzed N-alkylation reaction of amines and alcohols by a combination of experimental and computational methods. The mechanisms of Ru- [61], Cu- [62], and Pd-catalyzed [63] N-alkylation reactions have also been studied by DFT calculations.

2.2 Recent Advances in Homogeneous TM-Catalyzed N-Alkylation Reactions

Homogeneous TM-catalyzed N-alkylation methods for synthesis of amine/amide derivatives are the mainstream of hydrogen autotransfer reactions. Since the seminal reports from the groups of Grigg, Watanabe and Murahashi in the early 1980s [13–15], more and more TM complexes, such as [Rh], [Pd], [Au], [Ag], [Pt], [Os] and [Re], and even the non-noble metals [Ni], [Cu], [Fe], and [Co], have been found to be active catalysts in the last decade [10, 23–34]. Recently, more environmentally benign methods such as reactions in aqueous media, at much lower temperatures, with very low catalyst loadings, or using biomass-derived alcohols, have gradually
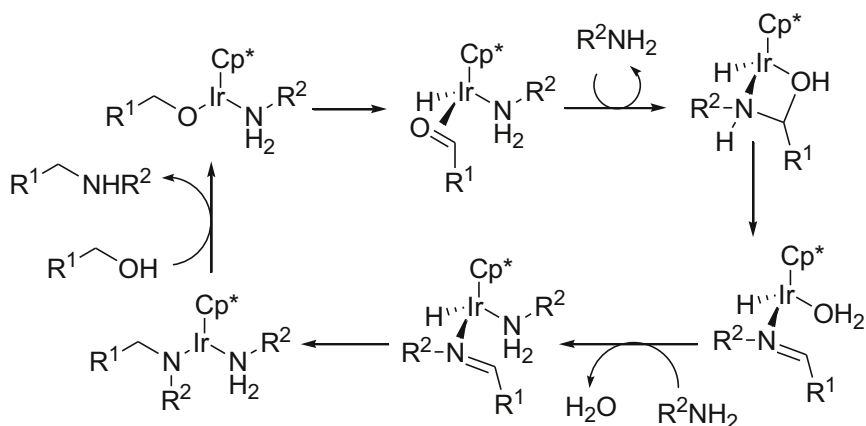
Scheme 16 Revised catalytic cycle for [Cp*IrCl$_2$]$_2$/K$_2$CO$_3$-catalyzed N-alkylation reaction supported by Fristrup and Madsen's DFT calculation [58]

appeared in the field. Applications of *N*-alkylation reactions in the synthesis of bio-active and pharmaceutical molecules have also been reported.

In 2007, Williams and co-workers [64] reported a [Ru(*p*-cymene)Cl$_2$]$_2$/dppf-catalyzed *N*-alkylation of secondary amines with alcohols. Piribedil (**1**), a piperazine dopamine agonist used in the treatment of Parkinson's disease, could be obtained in 87 % yield (Eq. 3). In 2009, by using DPEphos as the ligand instead of dppf, the same group achieved a general *N*-alkylation method for a wide range of amines such as primary and secondary amines, sulfonamides, and amides. *N*-Heterocycles could also be obtained by the reaction of diols and primary amines (Eq. 4) [65, 66]. In 2013, the Williams group extended the method to the synthesis of amines with a boronic ester group. Saccharide sensor **2** could be prepared in 84 % yield (Eq. 5) [67].

$$\tag{3}$$

$$\tag{4}$$

$$\tag{5}$$
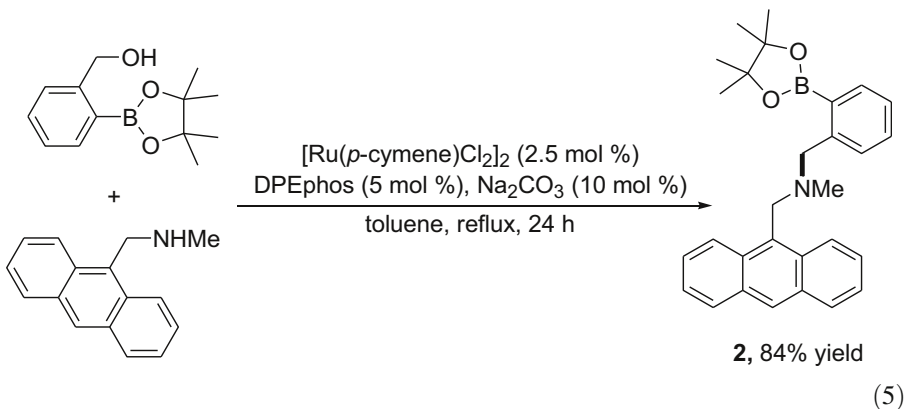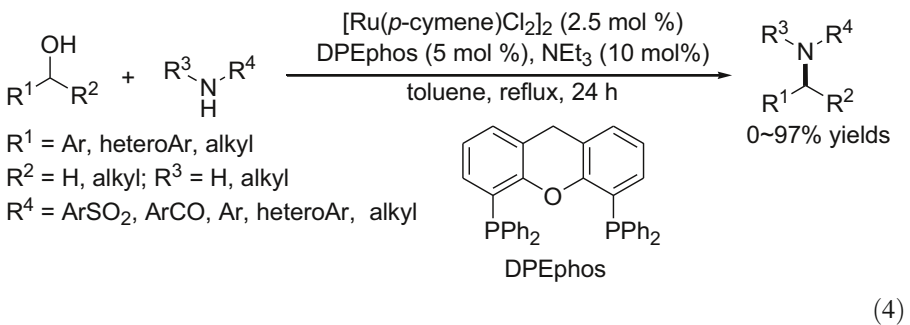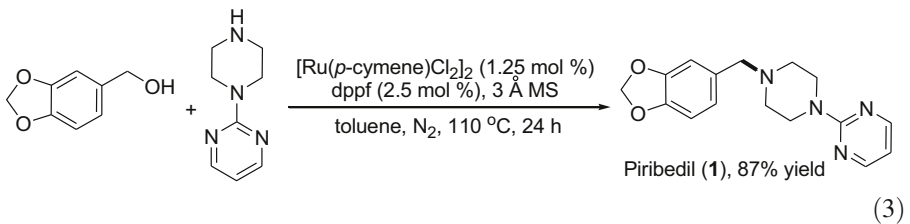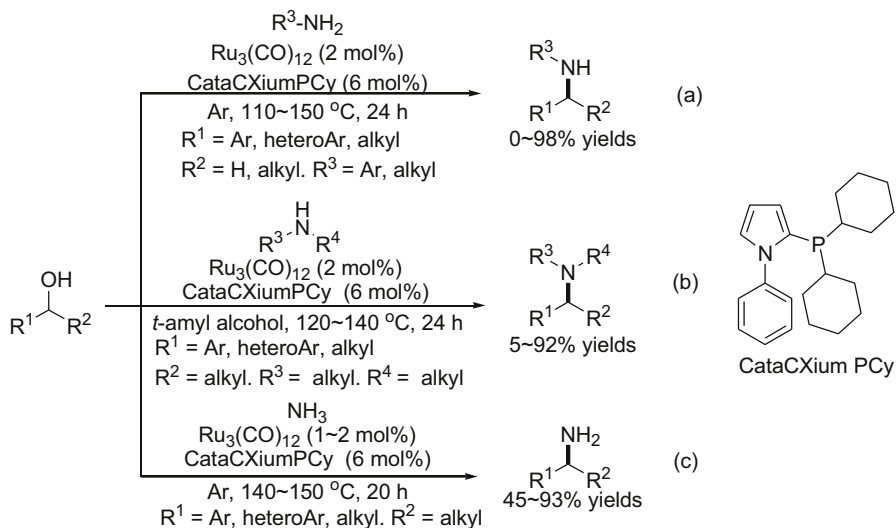
Scheme 17 Ru$_3$(CO)$_{12}$/CataCXiumPCy-ctalyzed *N*-alkylation of primary and secondary amines and ammonia with alcohols

In 2006, Beller and co-workers [68] reported a reaction of primary amines with primary and secondary alcohols using an Ru$_3$(CO)$_{12}$/tri(*o*-tolyl)-phosphine catalyst. In 2007, they developed an improved Ru$_3$(CO)$_{12}$/CataCXiumPCy catalyst, with which a variety of functionalized alcohols and amines could be converted into the corresponding secondary amines in high yields (Scheme 17a) [69]. In 2008, the Beller group extended the method to the reactions of alcohols and secondary amines (Scheme 17b) [70]. In 2010, the Beller group and the Vogt group simultaneously reported the amination of secondary alcohols with ammonia catalyzed by Ru$_3$(CO)$_{12}$/CataCXiumPCy complex (Scheme 17c) [71, 72], which represents further progress after Milstein's first report on the amination of primary alcohols with ammonia using an acridine-based pincer Ru complex (Eq. 6) [73]. In Milstein's method (Eq. 6), the precatalyst **3** might be first reduced by the alcohol to give [RuH] complex **4**, which rapidly converts to the active catalyst [RuH] complex **5** in the presence of ammonia (Scheme 18) [74].

$$(6)$$
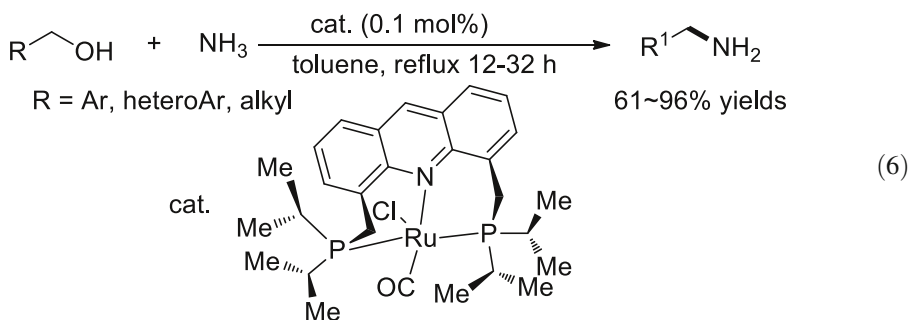
In 2014, Vogt and co-workers reported the selective synthesis of cyclic amides/ amines from amino-alcohols catalyzed by $Ru_3(CO)_{12}$/CataCXiumPCy with catalyst loadings as low as 0.5 mol% (Eq. 7) [75]. Interestingly, upon addition of water, cyclic amines could be produced as the major product. The authors proposed that this may be attributed to water which possibly acts as a weak acid to facilitate the dehydration of the cyclic half-aminals by hydrogen bonding to give imine intermediates.

$$
H_2N \diagup\!\!\!\diagdown\!\!\!\left(\!\!\diagdown\!\!\right)_{n}\!\!OH \xrightarrow[\text{cyclohexane/ } H_2O, \ 140\ ^oC]{\substack{Ru_3(CO)_{12}\ (0.5\ mol\%) \\ \text{CataCXium PCy (3 mol\%)}}} \quad \text{or} \quad \tag{7}
$$

$$n = 1\text{-}3 \qquad\qquad\qquad\qquad\qquad \text{up to } 100\% \text{ selectivity}$$
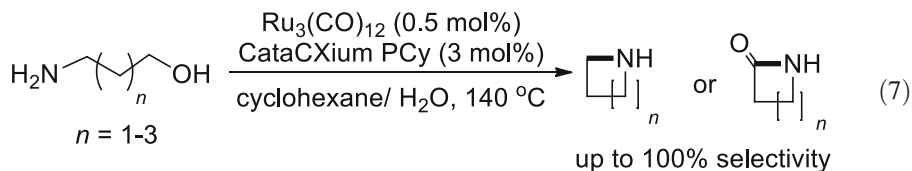
In 2010, Williams, Beller, and co-workers [76] achieved the first homogeneous N-alkylation of indoles with alcohols catalyzed by Shov catalyst with a low catalyst loading (0.2 mol%) (Scheme 19). Unlike Grigg and co-workers' C-3-alkylation of indoles in the presence of KOH (20 mol%) [77], in the former work, a catalytic amount of PTSA (0.025 mol%) was added, which may have led to a change in pH, and thus the selectivity of the reaction.

In 2011, Beller and co-workers reported the direct synthesis of α-amino acid derivatives from the reaction of α-hydroxy amides and esters with anilines, primary and secondary aliphatic amines, and ammonia (Eq. 8) [78]. After screening 17 different ligands, $[Ru_3(CO)_{12}]$ and a bulky phosphine ligand, DCPE gave the best results. In the same year, the authors also reported that $[Ru(CO)ClH(PPh_3)_3]$/ Xantphos is an excellent catalyst for the amination of challenging substrates such as the diamination of isosorbide with ammonia (Eq. 9) [79]. In 2013, Deutsch and co-workers reported a similar $[Ru(CO)ClH(DPEphos)(PPh_3)]$-catalyzed aminnation of alcohols with ammonia [80]. Primary and secondary alcohols, hydroxy esters, and diols are all suitable substrates. Mechanism of the ruthenium-catalyzed direct amination reaction was later investigated by Vogt in 2014, revealing that the initially formed inactive $[RuH_2]$ species could be (re)activated by intermediate imine [81]. Later, the correlation of ligand fluxionality and catalytic performance of the catalyst were investigated by the same group [82].
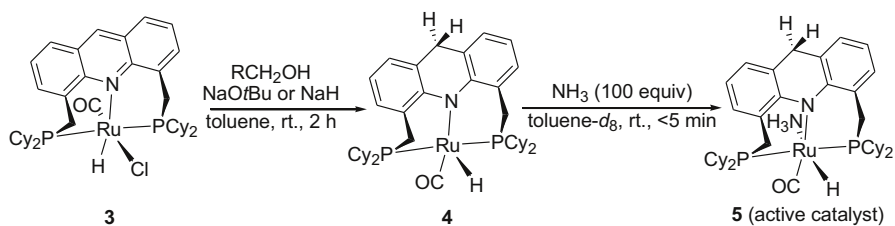
Scheme 18 Possible active Ru complexes in Milstein's method [73, 74]
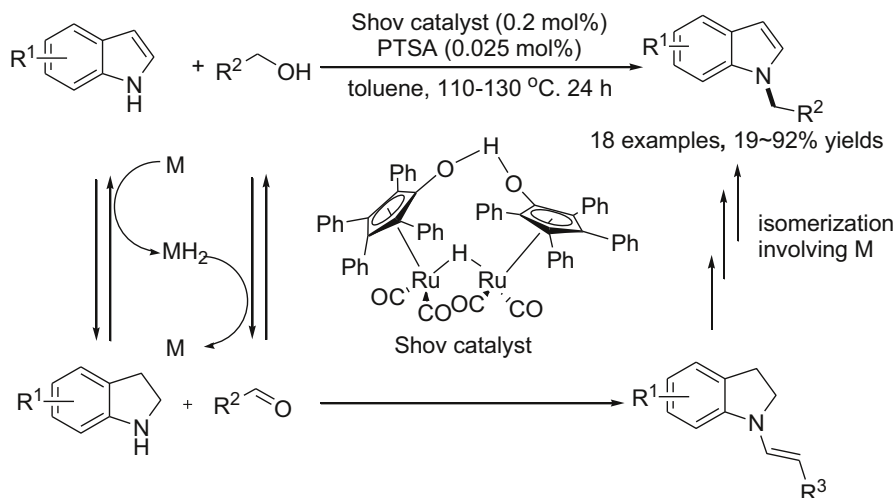
Scheme 19 Possilble mechanism for Ru-catalyzed *N*-alkylation of indoles with alcohols

$$(8)$$

$$(9)$$
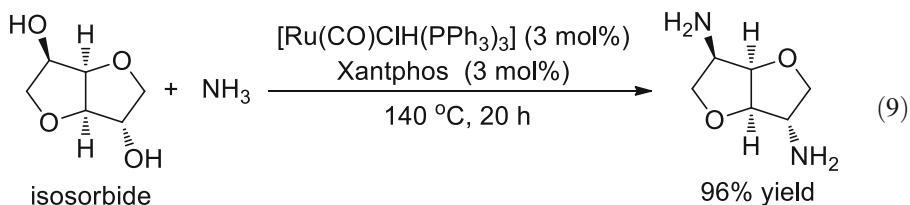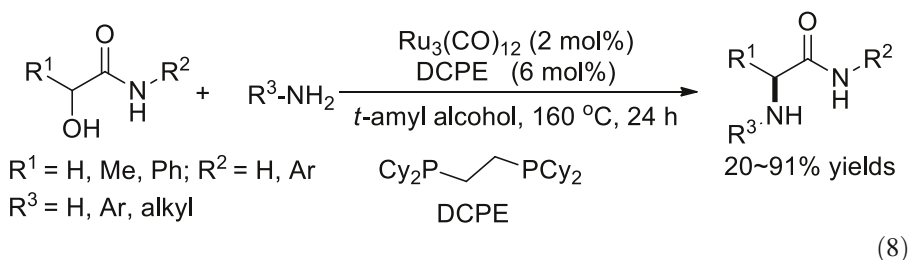
In 2012, Martín-Matute and co-workers [83] reported another pincer ruthenium(II) complex-catalyzed selective *N*-alkylation of (hetero)arylamines with primary alcohols. When the method was extended to aliphatic amines, the authors found that the aliphatic amine moiety could not be oxidized or alkylated. Inspired by this finding, aminoalcohols were later used as the alkyl source for *N*-alkylation of (hetero)aromatic amines. *N*-Arylated diamines were selectively obtained in excellent yield (Eq. 10).

$$(10)$$
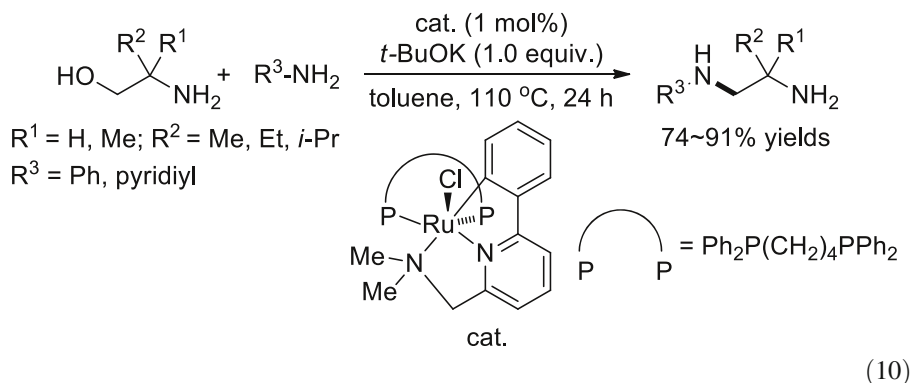
In 2014, Zhang and co-workers [84] reported the $[Ru_3(CO)_{12}]$/binap-catalyzed alkylation of 2-aminobenzonitriles with pyridylmethanols. An important structural unit, 1,2,3,4-tetrahydrobenzo[e][1, 4]diazepin-5-one (**6**), could be achieved by this straightforward one-pot method (Eq. 11).

6a (R = 4Cl-C$_6$H$_4$), 40% yield
6b (R = 3MeO-C$_6$H$_4$), 41% yield

$$(11)$$
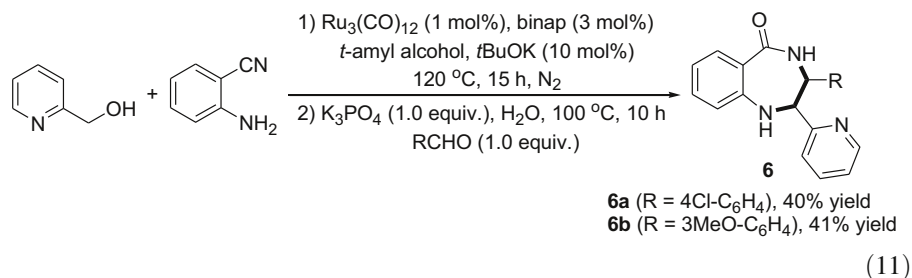
Some highly efficient catalytic systems enabling *N*-alkylation reactions to work under mild conditions even at room temperature have also been developed. In 2014, Enyong and co-workers [85] described ruthenium complex-catalyzed *N*-alkylation of primary and secondary amines with simple alcohols under mild conditions (Eq. 12). The authors found that when the substrate alcohol was used as the solvent, the reactions could be achieved at 40–60 °C and even at room temperature; whereas when using stoichiometric amounts of alcohol, higher temperatures, mostly 110 °C, were required. In 2015, Taddei and co-workers [86] reported a rather mild $[Ru(cod)Cl_2]_n$/PTA/*t*-BuOK-catalyzed *N*-alkylation of aromatic amines with primary alcohols at 55 °C (Eq. 13). This may be the mildest *N*-alkylation reaction catalyzed by ruthenium complexes described so far.

$$R^1 \cdot \overset{H}{\underset{N}{}} R^2 \; + \; R^3 \diagup OH \xrightarrow[\text{3Å MS, N}_2, \text{ rt.~110 °C, 12~61 h}]{\substack{[\text{Ru}(p\text{-cymene})\text{Cl}_2]_2 \,(6\text{~}12\text{mol \%}) \\ \text{L (12~24 mol\%), } t\text{-BuOK (24~48 mol\%)}}} R^3 \diagup \overset{R^2}{\underset{}{N}} \diagdown R^1$$

R^1 = H, Ar, alkyl; R^2 = Ar, alkyl
R^3 = Ar, heteroAr, alkyl

36~99% yields

Ph⌐⌐⌐C(=O)N(H)–Ph   Ligand
    |
   NH$_2$

(12)

$$R \diagup OH \; + \; Ar\text{-}NH_2 \xrightarrow[\text{toulene, 55 °C, 12~48 h}]{\substack{[\text{Ru}(\text{cod})\text{Cl}_2]_n \,(2.5 \text{ mol\%}) \\ \text{PTA (5 mol\%)} \\ \text{KO}t\text{Bu (1.0 equiv.)}}} R \diagup \overset{Ar}{\underset{H}{N}}$$

R = Ar, heteroAr, alkyl

20~99% yields

(PTA)

(13)
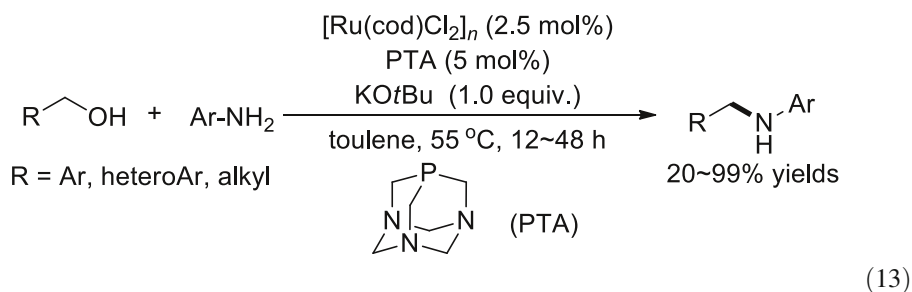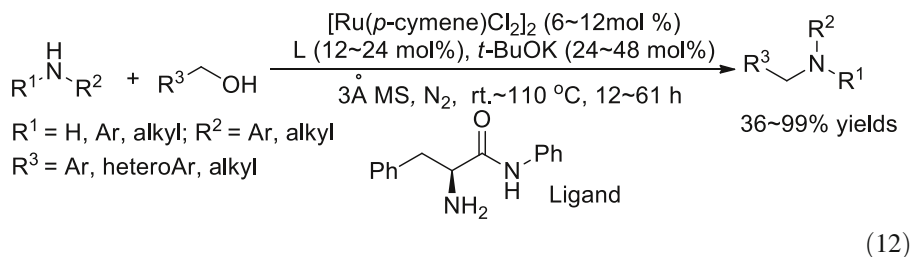
Nitroarenes and nitriles could also be employed as amine precursors. In 2010, Li and co-workers reported a ruthenium complex-catalyzed synthesis of tertiary amines by N-alkylation of nitroarenes with alcohols (Eq. 14) [87]. In this method, large excess amounts of the alcohols (mostly 7.5 equiv.) are necessary to reduce the nitroarenes to anilines prior to N-alkylation. In 2011, Shi and co-workers also developed an amination reaction for secondary amine synthesis from nitro or nitrile compounds (Eq. 15) [88]. In the same year, Deng and co-workers reported a ruthenium-catalyzed method for tertiary-amine synthesis from nitriles and primary alcohols [89]. In 2013, Beller and co-workers reported another N-alkylation reaction of nitrile compounds with secondary alcohols [90].

$$\underset{R^1}{\overset{NO_2}{\diagup}} \; + \; R^2 \diagup OH \xrightarrow[\text{Ar, 150 °C, 16 h}]{\substack{\text{Ru(CO)(H)}_2(\text{PPh}_3)_3 \,(5 \text{ mol\%}) \\ \text{L (7.5mol\%)}}} R^1 \diagup N \underset{R^2}{\overset{R^2}{\diagup}}$$

R^1 = MeO, F, Cl, Br, CO$_2$Et
R^2 = Ar, alkyl

32~91% yields

Ligand

(14)
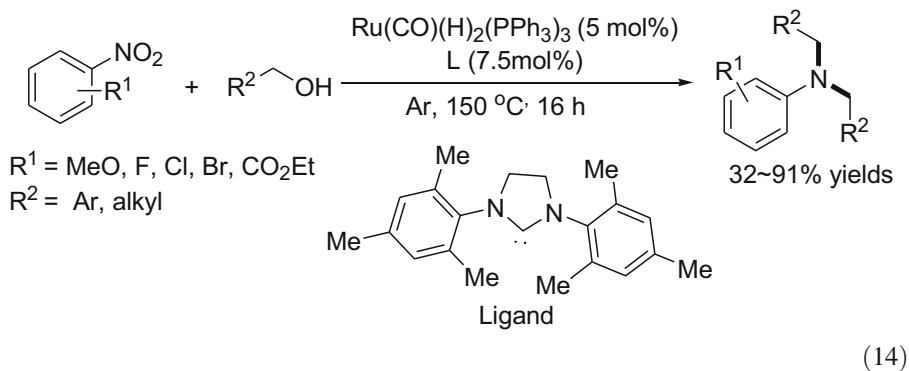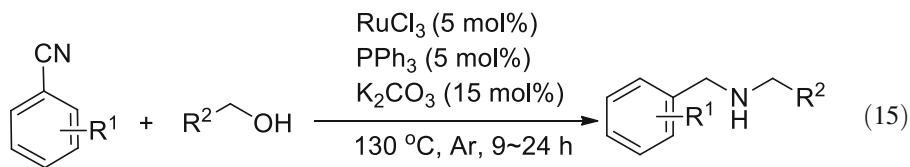
$$R^1 = MeO, Cl \ etc.; \ R^2 = \ aryl, \ alkyl \qquad\qquad 81\text{~}95\% \ yields$$

In 2014, Li and co-workers reported a direct synthesis of *N*-alkylated amides via tandem hydration/*N*-alkylation of nitriles and aldoximes with alcohols catalyzed by [Cp*IrCl₂]₂ with a low catalyst loading (1 mol%) (Eq. 16) [91]. Control experiments revealed that nitriles were initially hydrated by aldoximes to give amides, which then reacted with alcohols to give *N*-alkylated amide products.
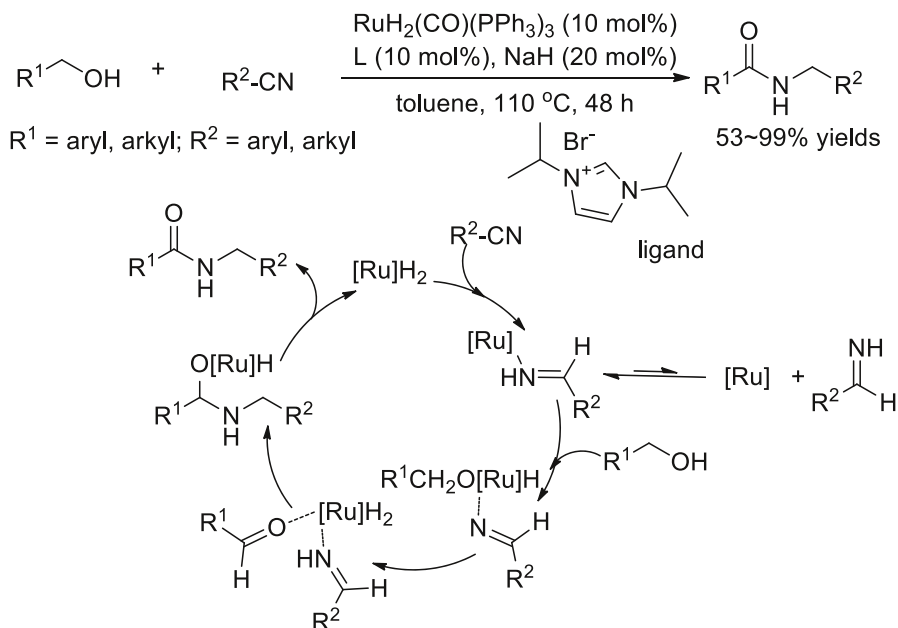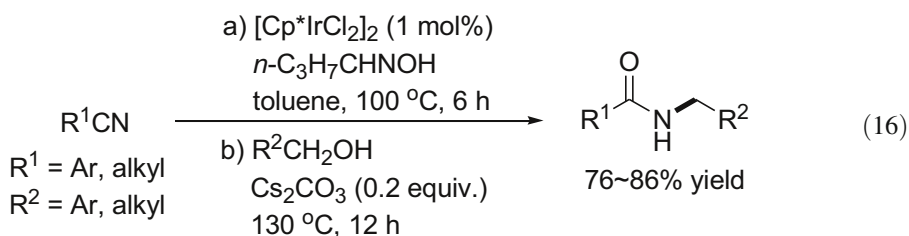
Scheme 20 Proposed catalytic cycle for the reversed and redox-neutral *N*-alkylation reaction of nitriles for amide synthesis

In 2013, Hong and co-workers reported a Ru-catalyzed reversed and redox-neutral *N*-alkylation reaction of nitriles and alcohols to afford *N*-alkylated amides with high atom efficiency (Scheme 20) [92]. Unlike the preceding reactions of alcohols and nitriles [88–91], in this reaction the alcohol serves as the acyl moiety of the amide product rather than the alkyl moiety. This also differs from the Ritter reaction, in which the alcohol serves as the alkyl source [22, 23]. In contrast, in this reaction the cyano moiety of the nitrile was reduced to become the alkyl moiety of the amide product. As shown in Scheme 20, the cyano moiety is initially hydrogenated by the dihydridoruthenium species RuH_2 to form a Ru-imine complex. The alcohol is then dehydrogenated to aldehyde by Ru to give another RuH_2 species, followed by imine reduction by RuH_2 and addition of the generated amine intermediate to aldehyde to give the hemiaminal intermediate. The last
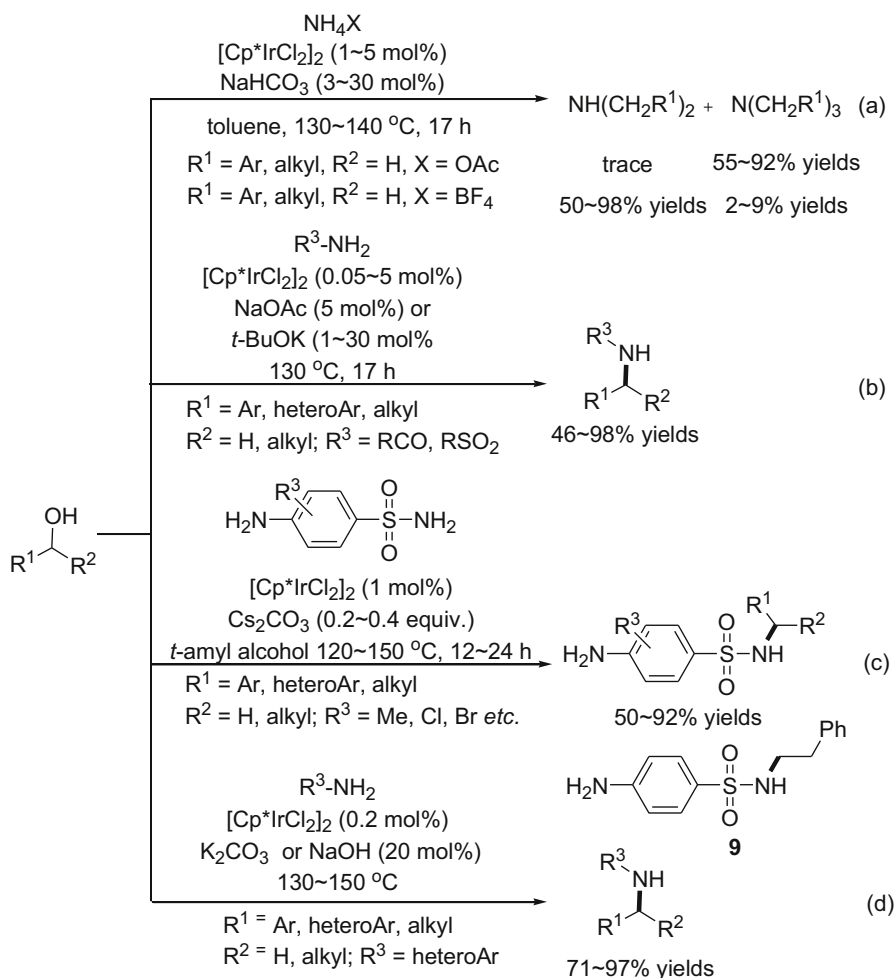
Scheme 21 $[Cp^*IrCl_2]_2$-catalyzed amination of alcohols with ammonium salts, carbamates, amides, sulfonamides and primary heteroarylamines

dehydrogenation of hemiaminal by Ru gives the corresponding *N*-alkylated amide product and regenerates the catalyst. In 2014, the authors extended the method to the synthesis of cyclic imides [93].

In 2010, Bruneau and co-workers described an unprecedented cascade *N*- and C(3)-dialkylation of unactivated cyclic amines with benzylic and aliphatic alcohols using a new (arene)ruthenium (II) complex **7** bearing a phosphinosulfonate ligand as the catalyst (Eq. 17) [94]. In 2012, they achieved a three-component *N*- and C-dialkylation reaction of the easily accessible anilines, diols, and aldehydes through tandem hydrogen transfer reactions in the presence of iridium complex **8** (Eq. 18) [95].

$$(17)$$

$$(18)$$
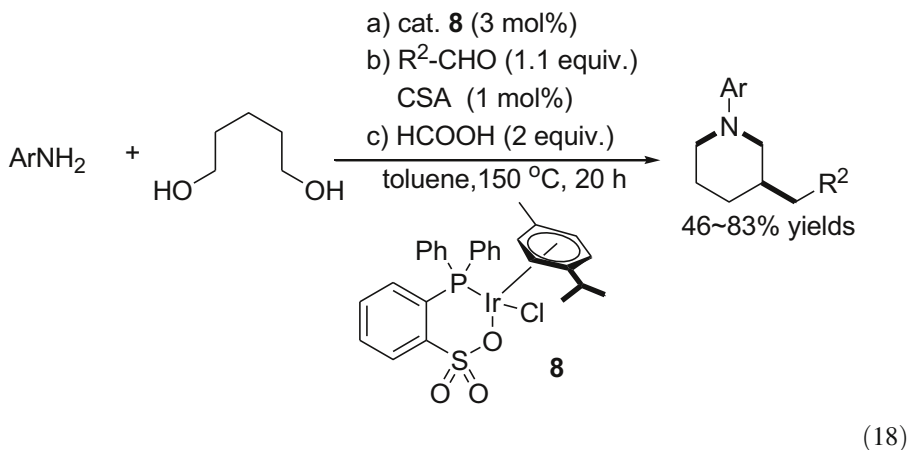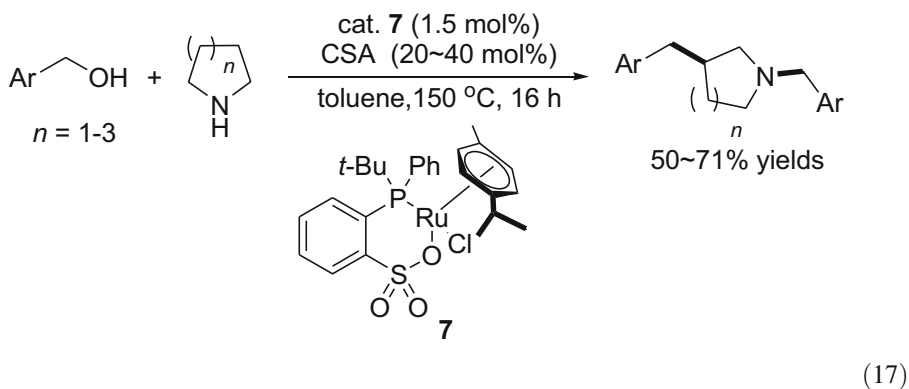
In 2008, Fujita, Yamaguchi and co-workers reported an efficient solvent-free synthesis of secondary and tertiary amines by [Cp*IrCl$_2$]$_2$-catalyzed multi-alkylation of ammonium salts with primary or secondary alcohols [96]. The authors found that the type of ammonium salts greatly affected the selectivity of the reaction (Scheme 21a). Secondary 5- and 6-membered cyclic amines could also be prepared from ammonium tetrafluoroborate and diols by the same method.

In 2009, these authors also reported a similar transformation at 10 mmol scale, which makes the method more practical [97]. In the same year, the same authors again extended the method to N-alkylation of carbamates and amides, and in 2010 to N-alkylation of sulfonamides with catalyst loading as low as 0.05 mol% (Scheme 21b) [98, 99]. In 2014, Trudell and co-workers reported a microwave-mediated $[Cp*IrCl_2]_2$-catalyzed N-alkylation of amides under solvent- and base-free conditions [100]. In 2015, Li and co-workers reported a direct synthesis of amino-(N-alkyl)benzenesulfonamides via N-alkylation of aminobenzenesulfon-amides with alcohols catalyzed by $[Cp*IrCl_2]_2/Cs_2CO_3$ (Scheme 21c) [101]. Notably, biologically active **9**, a histone arginine methyltransferase inhibitor, could be obtained in 80 % yield by this method. In 2012–2013, Li and co-workers also realized the N-alkylation reactions of primary heteroarylamines such as 2-aminothiazoles, 2-aminoimidazoles, 2-aminopyrimidines, 2-aminoquinazolines, and the corresponding secondary amines could be obtained in moderate to excellent yields (Scheme 21d) [102–104].

In 2011, by employing the iridium-catalyzed "borrowing hydrogen" reaction as the key step, Berliner and co-workers achieved the first kilogram-scale synthesis of **10**, a GlyT1 inhibitor for treatment of schizophrenia (Eq. 19) [105]. In a smaller 10 g scale reaction, the catalyst loading could even be reduced to less than 0.05 mol% Ir (S/C >2000), while still affording the product in a good yield of 84 %.

(19)
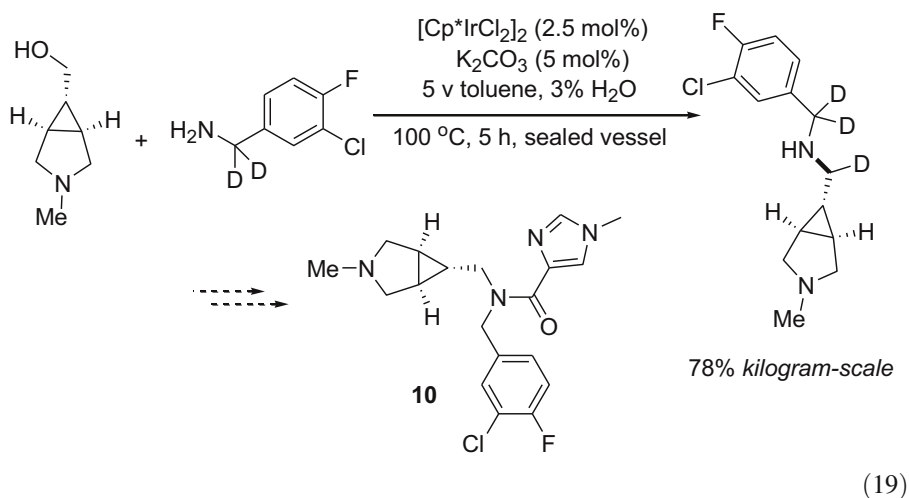
Biomass-based alcohols could also be employed directly as substrates in N-alkylation reactions, making the hydrogen autotransfer method more practical. In 2011, Martín-Matute and co-workers reported a $[Cp*IrCl_2]_2$-catalyzed method for synthesis of secondary aminosugars from primary aminosugars with simple alcohols and primary carbohydrate alcohols (Eq. 20) [106]. In 2009, Stephens, Marr and co-workers reported that a one-pot bio- and chemo-catalytic process could be used for direct conversion of crude glycerol from biodiesel production to valuable secondary amines in a biphasic system without intermediate separation of 1,3-propanediol

[107]. In 2012, Marr and co-workers achieved an amination reaction of pure 1,3-propanediol in the presence of an Ir complex **11** (Eq. 21) [108].

(20)

(21)
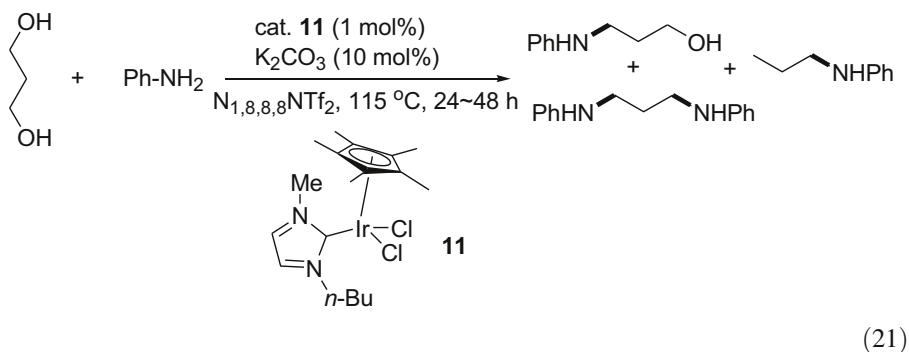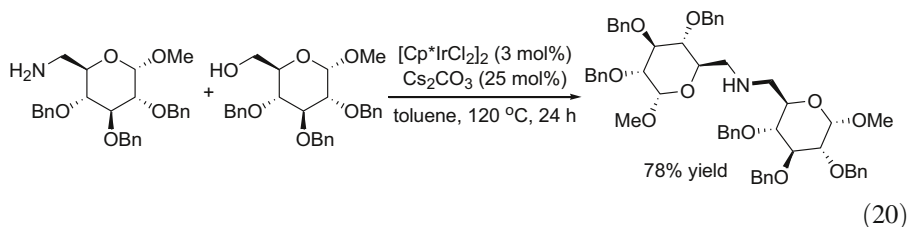
In 2012, Sridharan and co-workers reported a selective C- or *N*-alkylation of 2-aminoacetophenone catalyzed by [Cp*IrCl$_2$]$_2$ under microwave irradiation conditions (Eq. 22) [109]. C-Alkylation takes place in the presence of [Cp*IrCl$_2$]$_2$/KOH at 110 °C, while *N*-alkylation could be achieved using [Cp*IrCl$_2$]$_2$/K$_2$CO$_3$ at 140 °C. By using different bases under different conditions, clean C- or *N*-selectivity could be achieved.

(22)
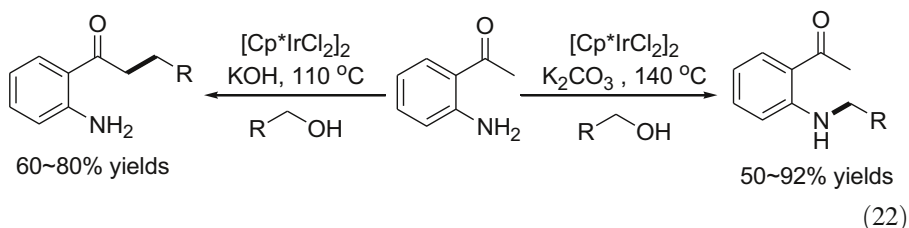
By using certain ligands to improve the activity of the metal catalyst, the *N*-alkylation reactions could also be performed under milder conditions. In 2009, Kempe and co-workers reported that a [Ir(cod)Cl]$_2$/P,N-ligand complex could enable the *N*-alkylation of (hetero)arylamines with alcohols under mild conditions of only 70 °C with a catalyst loading as low as 0.1 mol% (Eq. 23) [110]. In 2010, the same group designed a new P,N-ligand stabilized iridium complex **12** (Scheme 22) for efficient alkylation of anilines with alcohols under mild conditions

(70 °C) with catalyst loadings as low as 0.05 mol% [111]. In 2012, the Kempe group extended the method to the synthesis of symmetrical and unsymmetrical alkylated diamines under mild conditions (70 °C) [112]. For example, 4,4′-sulfonyldianiline (**13**), effective antibiotic medicaments used in the treatment of leprosy or malaria, could be symmetrically and unsymmetrically *N*-alkylated by this method.

$$(23)$$
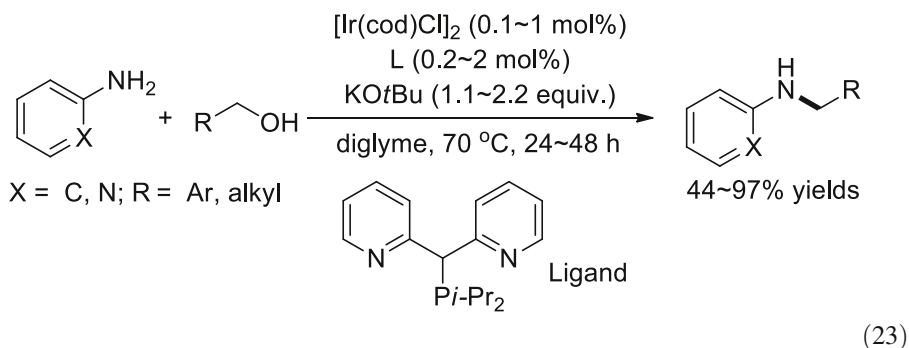
In 2015, Xiao and co-workers reported an iridium complex (**14**)-catalyzed *N*-alkylation of amines with alcohols under mild conditions (100 °C) (Scheme 22) [113]. Anilines, heteroarylamines, *N*-alkyl-*N*-arylamines, and sulfonamides could serve as *N*-nucleophiles. The same method can also be applied to amine-based *N*-alkylation reactions (vide infra).

In 2013, Andersson and co-workers reported an iridium NHC-phosphine complex-catalyzed solvent-free, and selective *N*-alkylation of anilines with alcohols under mild conditions even at room temperature (Eq. 24) [114]. Intramolecular *N*-

$$(23)$$
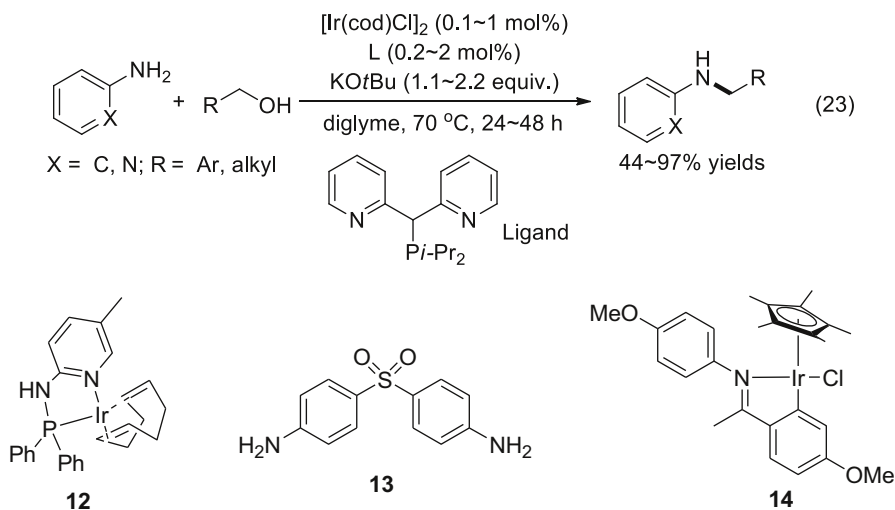
Scheme 22 Iridium complex **12** and **14** and 4′4-sulfonyldianiline **13**

heterocyclization of aminoalcohols could also be achieved to afford indole or 1,2,3,4-tetrahydroquinoline products.

$$
\text{Ar-NH}_2 \ + \ \text{R} \diagdown \text{OH} \quad \xrightarrow[\text{diglyme or neat, rt~50 °C, 24~48 h}]{\substack{\text{cat. (0.5~1 mol\%)} \\ \text{KO}t\text{Bu (50 mol\%)}}} \quad \text{R} \diagdown \text{N} \diagdown \text{Ar}
$$

R = Ar, heteroAr, alkyl.

44~97% yields

cat.

(24)
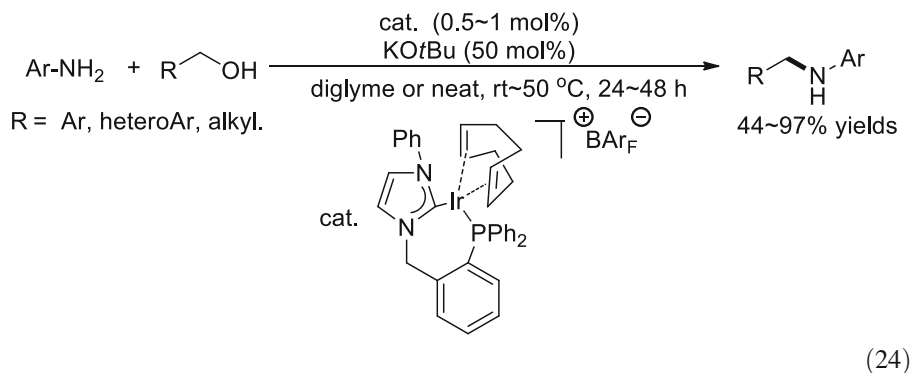
Some water-soluble and water-tolerant iridium catalysts have also been developed in recent years. In 2010, Williams and co-workers found [Cp*IrI$_2$] is a water-tolerant catalyst for *N*-alkylation of primary and secondary amines and sulfonamides in aqueous media [115]. In the same year, Fujita, Yamaguchi and co-workers also reported a water-soluble and air-stable [Cp*Ir(NH$_3$)$_3$][I]$_2$-catalyzed multi-alkylation of aqueous ammonia with alcohols (Eq. 25) [116]. The catalyst could be recycled by an easy procedure that still maintains high activity. Moreover, quinolizidines could also be achieved from the reaction of aqueous ammonia and a water soluble triol employing the same method.

$$
\underset{\text{R}^1 \quad \text{R}^2}{\text{OH}} \ + \ \text{NH}_3 \quad \xrightarrow[\text{140 °C, 24 h}]{\substack{\text{[Cp*Ir(NH}_3)_3][I]_2 \ (0.5\text{-}1.5 \ \text{mol\%})} \\ \text{NaHCO}_3 \ (30 \ \text{mol\%})}} \quad \underset{\text{H}}{\overset{\text{R}^2 \quad \text{R}^1}{\text{R}^1 \diagdown \text{N} \diagdown \text{R}^2}} \ + \ \underset{}{\overset{\text{R}^1}{\text{R}^1 \diagdown \text{N} \diagdown \text{R}^1}}
$$

R^1 = Ar, alkyl; R^2 = H, alky

R^2 =H   ---   65~95% yields

R^2 =alkyl   63~89% yields   ---

[Cp*Ir(NH$_3$)$_3$][I]$_2$ recoverable:1st , 100%; 2nd. 98%; 3rd, 95%

quinolizidine

(25)
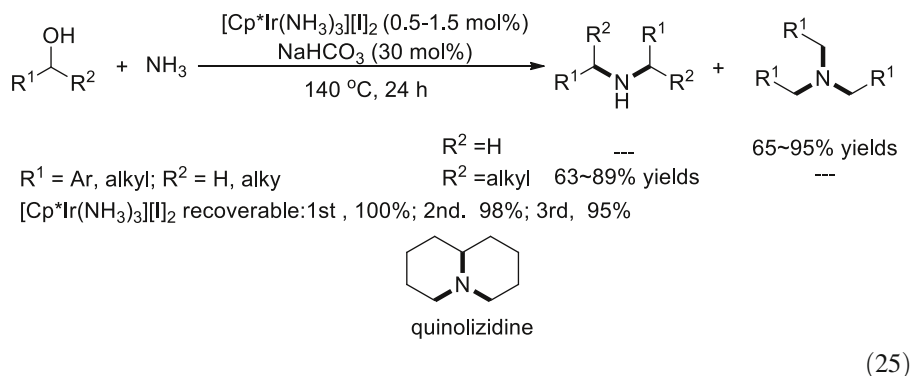
In 2012, Madsen and co-workers reported a [Cp*IrCl$_2$]$_2$-catalyzed method for the synthesis of piperazines from amines and 1,2-diols in toluene or water [117]. In 2013, Trudell and co-workers realized a microwave-assisted [Cp*IrCl$_2$]$_2$-catalyzed synthesis of nicotine and anabasine derivatives in water media (Eq. 26) [118]. In 2014, Li and co-workers reported an iridium complex **15**-catalyzed *N*-alkylation of sulfonamides with alcohols in aqueous media (Eq. 27) [119].

$$n = 1, 2. \quad R^1 = H, MeO. \quad R^2 = Me, Bn, 4\text{-}MeOC_6H_4 \qquad 50\text{-}78\% \text{ yields}$$

(26)

R^1 = aryl, alkyl
R^2 = aryl, heteroAr, alkyl

78-94% yields

(27)
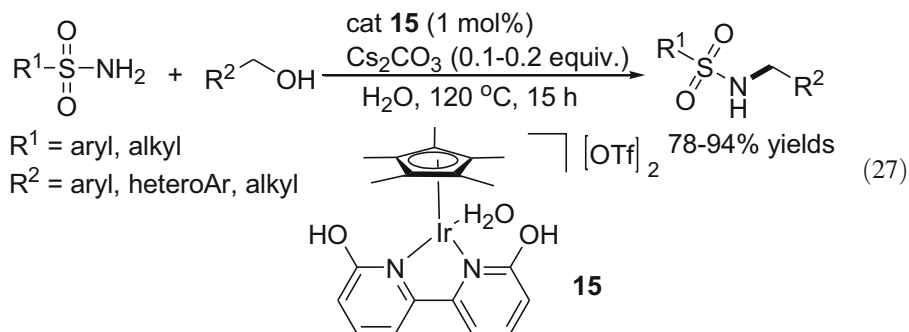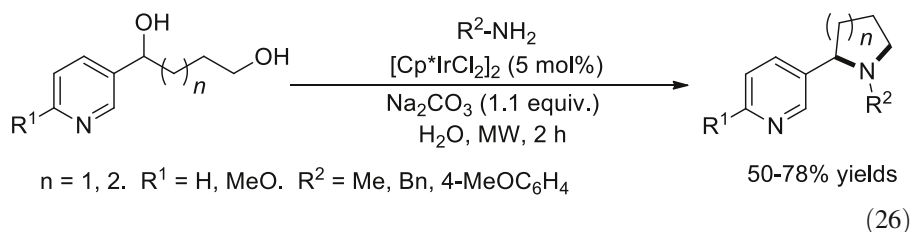
In 2011, Ramón and co-workers reported a $Pd(OAc)_2$-catalyzed N-alkylation of poor nucleophilic heterocyclic amines, carboxamides, and N-(triphenylphosphoranylidene)aniline with alcohols with catalyst loading as low as 0.5 mol% (Eq. 28) [120]. In 2013, Seayad and co-workers reported a powerful $PdCl_2$/dppe-catalyzed N-alkylation of various primary and cyclic secondary amines with primary alcohols at 90–130 °C under neat conditions [121]. Besides, a 10 mmol scale reaction of aniline and benzyl alcohol was performed using 0.1 mol% of the catalyst at 100 °C, with up to 90 % yield of the product and a turnover number (TON) of 900 obtained.

R^1 = Ar, alkyl; R^2 = RSO_2, RCO, Ar, alkyl *etc.*   5~99% yields

(28)
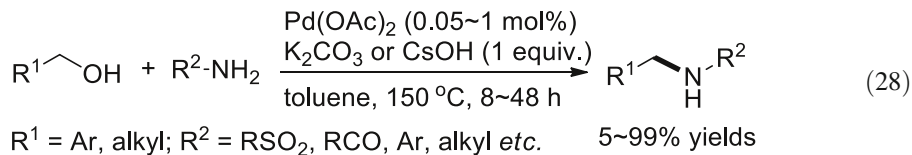
Some N-alkylation reactions catalyzed by other noble metal catalysts have also been reported. In 2011, Gusev and co-workers reported an Osmium complex-catalyzed N-alkylation of amines at 200 °C with a low catalyst loading (0.1 mol%) [122]. In 2014, Zhu and co-workers disclosed a [$ReH_7(PCy_3)_2$]-catalyzed amination of alcohols with anilines under CO atmosphere (Eq. 29) [123]. The authors proposed that coordination of CO with Re might lead to decomposition of $ReH_7(PCy_3)_2$ to a rhenium carbonyl complex, which was believed to be the active

catalyst. In 2014, Cheng reported a [Ph$_3$PAuCl]/AgOTf-catalyzed *N*-alkylation of primary amines with alcohols under a moderate temperature of 100 °C [124].

$$ArNH_2 \quad + \quad \underset{R^1 \quad R^2}{\overset{OH}{\diagdown}} \quad \xrightarrow[\text{CO, 150 °C, 24 h}]{[ReH_7(PCy_3)_2] \ (10 \ mol\%)} \quad \underset{R^1 \quad R^2}{\overset{NHAr}{\diagdown}}$$

R^1 = Ar, alkyl; R^2 = H, Me $\qquad\qquad$ 67~97% yields

(29)
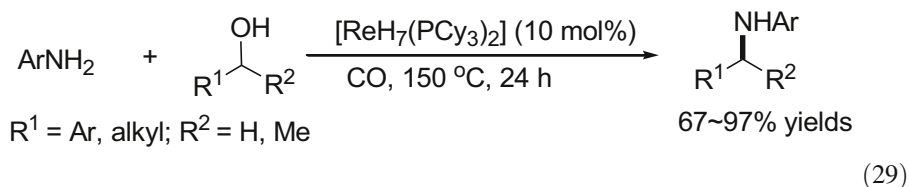
Several non-noble metal-catalyzed *N*-alkylation reactions have also been reported in recent years. In 2010, Ramón, Yus and co-workers reported Cu(OAc)$_2$-catalyzed *N*-alkylation of poor nucleophilic amine derivatives and alcohols (Eq. 30) [125]. Control experiments indicated that a base was indispensable in the reaction to force the alcohol dehydrogenation step, which was later confirmed by DFT calculations reported by Liu, Huang and co-workers [63]. In 2011, Ramón and co-workers reported the results of their own mechanistic studies and proposed two possible catalytic cycles [126]. The main aldehyde-free cycle, depicted with plain arrows, requires the presence of a base. The minor cycle, depicted in dashed arrows, may proceed when an aldehyde exists in the reaction media (Scheme 23). In the same year, Li and co-workers also disclosed a CuCl-catalyzed *N*-alkylation of heteroarylamines [127].

$$R^1 \diagdown OH \quad + \quad R_2\text{-}NH_2 \quad \xrightarrow[\text{Ar, 130~150 °C, 2~10 d}]{\substack{Cu(OAc)_2 \ (1 \ mol\%) \\ \text{base} \ (100 \ mol\%)}} \quad R^1 \diagdown \underset{H}{N} \diagdown R_2$$

base = *t*-BuOK, K$_2$CO$_3$ $\qquad\qquad$ 0~99% yields
R^1 = Ar, heteroAr, alkyl; R^2 = RSO$_2$, RCO, Ar, heteroAr, alkyl

(30)
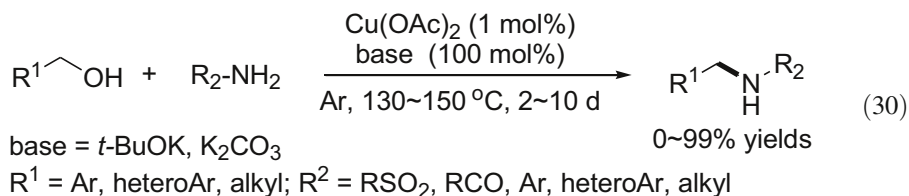
In 2010, Shi, Deng and co-workers reported the first FeCl$_2$/K$_2$CO$_3$-catalyzed *N*-alkylation of sulfonamides with alcohols through the borrowing hydrogen method (Scheme 24) [128]. Tentative mechanism studies were performed to show that the alcohol dehydrogenation step was the rate-determining step.

In 2013, Singh and co-workers also reported an iron(II) phthalocyanine (FePc)-catalyzed *N*-alkylation of heterocyclic amines (Eq. 31) [129]. In most cases, the reactions of benzyl alcohols could give moderate to excellent yields, but aliphatic alcohols gave only poor yields of the products.

$$R^1 \diagup OH \ + \ R^2\text{-}NH_2 \xrightarrow[\text{toulene, 100~120 °C, 12~36 h}]{\substack{\text{FePc (1 mol\%)} \\ \text{NaO}t\text{Bu (200 mol\%)}}} R^1 \diagdown \underset{\underset{H}{N}}{} \diagup R^2$$

R^1 = Ar, heteroAr, alkyl; R^2 = Ar, heteraryl   20~99% yields

(31)
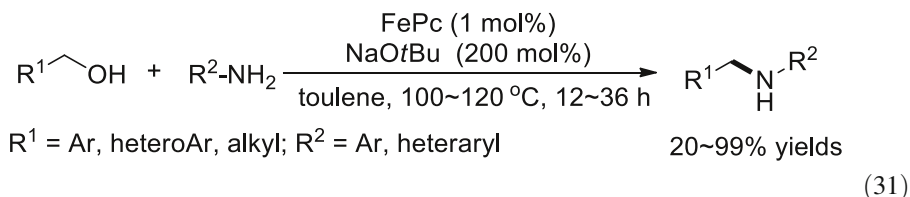
In 2014, Feringa, Barta and co-workers reported an *N*-alkylation reaction of amines with aliphatic alcohols catalyzed by an iron cyclopentadienone complex **16** [130]. A catalytic cycle was proposed based on in situ NMR studies (Scheme 25). Complex **16** was first transformed to the active complex **17** by addition of oxidant Me_3NO. Complex **17** was then reduced to **18** by the alcohol. **16** and **18** acted as the catalysts to dehydrogenate the alcohol and hydrogenate the imine intermediates. In 2015, Zhao and co-workers realized an AgF-assisted amination of secondary alcohols using complex **16** as the catalyst [131]. In the same year, Wills and co-workers demonstrated a similar iron complex for *N*-alkylation of amines with alcohols [132].

In 2015, Kempe and co-workers reported the first cobalt-catalyzed *N*-alkylation of (hetero)arylamines with alcohols under mild conditions (80 °C) with a relatively low catalyst loading (2 mol%) (Eq. 32) [133]. In 2016, Zhang and co-workers developed another pincer cobalt complex **19**, which is an active catalyst for both imination and *N*-alkylation reactions of aromatic and aliphatic amines with alcohols under base-free conditions [134]. By using complex **19**, monoalkylated amine products rather than the imines can be selectively achieved by simply adding 4 Å molecular sieves to the reaction mixture (Eq. 33).

X = C, N
R^1 = F, Cl, Br, I, OMe *etc.*
R^2 = Ar, alkyl

51~96% yields

cat.

(32)
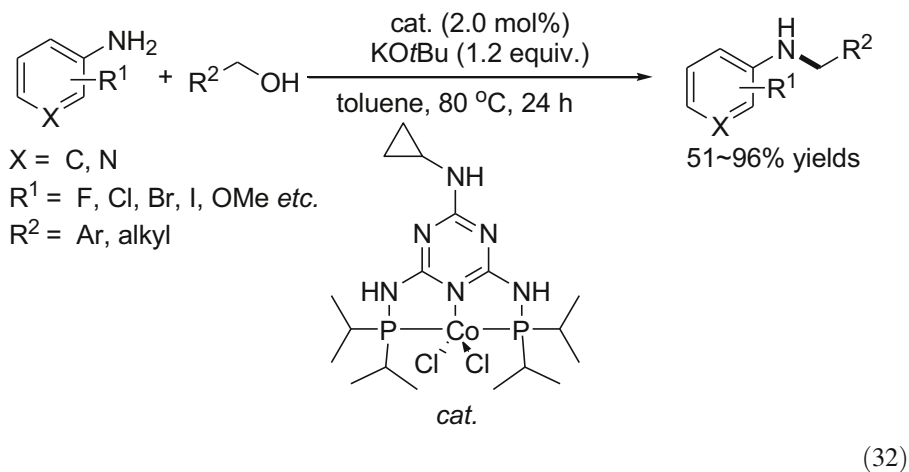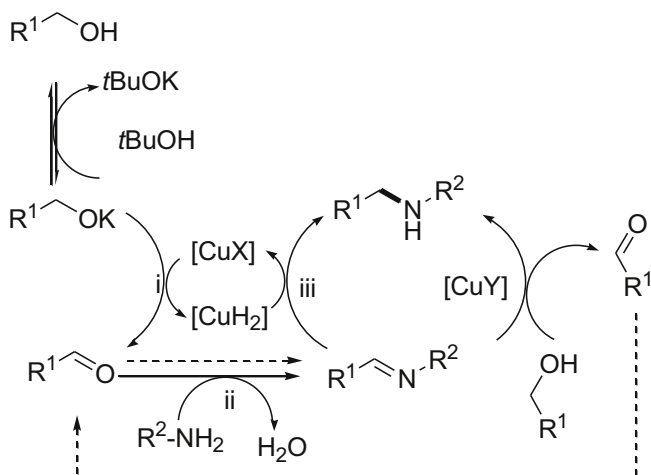
Scheme 23 Tentative catalytic cycles for Cu-catalyzed *N*-alkylation reactions
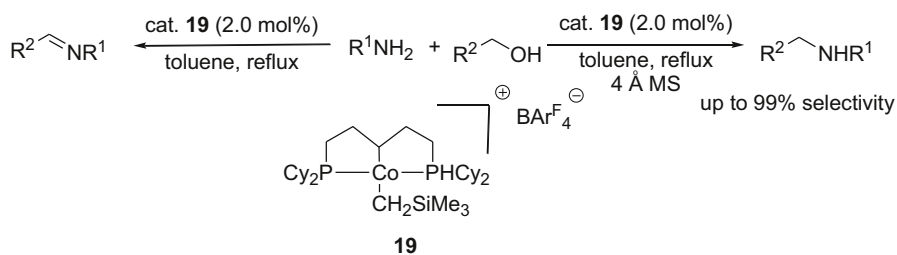
(33)

2.3 Recent Advances in Heterogeneous TM-Catalyzed *N*-Alkylation Reactions

Homogeneous TM catalysts, especially those of noble metals are usually expensive and toxic, and have problems of low availability, low stability, metal residue contaminant in the products, non-recoverability, and, therefore, low potential in large scale and industrial synthesis. In addition, the capricious ligands used are, in
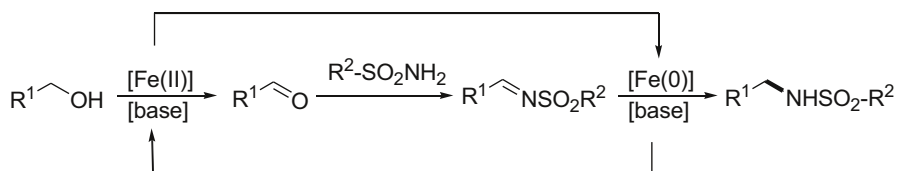
Scheme 24 Proposed mechanism for iron-catalyzed alkylation of sulfonamide with alcohol
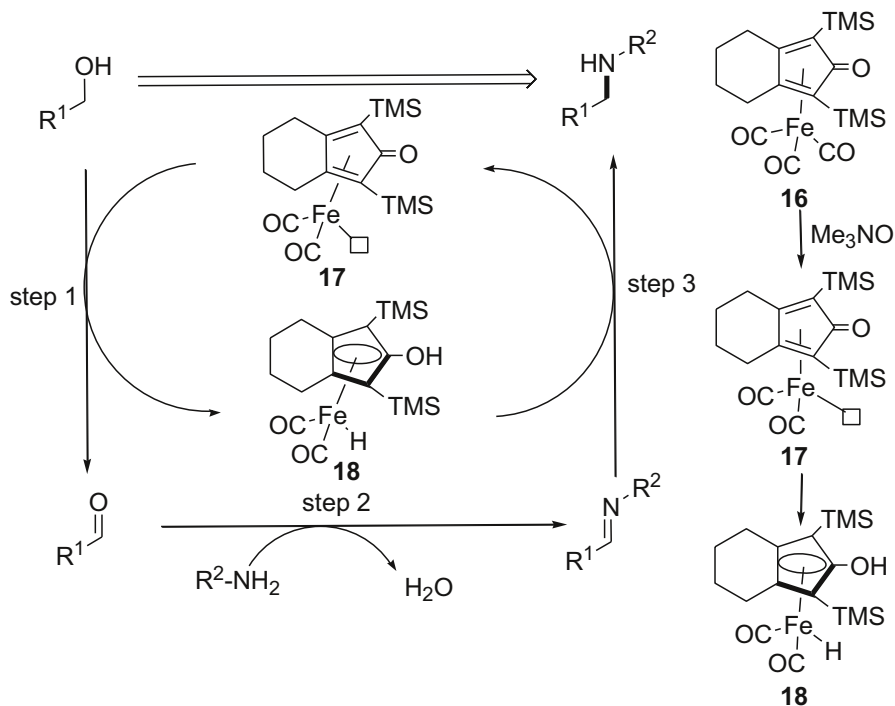
Scheme 25 Proposed mechanism for iron cyclopentadienone complexes-catalyzed *N*-alkylation reactions

many cases, less available and more expensive than the TM pre-catalysts. To solve the problems and reduce the cost, recoverable and reusable heterogeneous catalysts are considered to be promising substitutes for the corresponding homogeneous catalysts. Consequently, various kinds of heterogeneous TM catalysts have also been developed and are used in *N*-alkylation reactions [10–12]. Most of the early heterogeneous methods require harsh conditions and suffer from problems of limited substrate scope, low selectivity, or the need for H_2 [10, 11]. In recent years, more and more active heterogeneous catalysts that can be used under milder or additive-free conditions, with higher catalytic performance and recoverability, have been developed. These include various types of supported Ru, Ir, Pt, Pd, Ag, Cu, and Ni catalysts.

Owing to the high activities of the homogeneous Ru and Ir catalysts in *N*-alkylation reactions, many heterogeneous Ru and Ir catalysts have been developed. In 2009, Mizuno and co-workers reported an effective *N*-alkylation of (hetero)arylamines with benzylic and aliphatic alcohols catalyzed by $Ru(OH)_x/Al_2O_3$ complex without any co-catalysts or additives (Eq. 34) [135]. The catalyst is recoverable and reusable without obvious loss of activity (1st, 89 %; 2nd, 87 %). Later in the same year, the authors reported another additive-free method for synthesis of secondary and tertiary amines from alcohols and urea catalyzed by $Ru(OH)_x/TiO_2$ (Eq. 35)

[136]. The catalyst could be reused at least twice while still maintaining high activity (1st, 92 %; 2nd, 90 %). In 2010, the Mizuno group further extended the method to N-alkylation of other nitrogen sources such as ammonium salt, ammonia, primary amines and secondary amines [137].

$$R^1\diagdown OH \ + \ R^2\text{-}NH_2 \xrightarrow[\text{mesitylene, Ar, 132 }^{\circ}C]{\substack{\text{Ru(OH)}_x/\text{Al}_2\text{O}_3 \text{ (5 mol%)} \\ \text{K}_2\text{CO}_3 \text{ (10~40 mol%)}}} R^1\diagdown N\diagup R^2 \quad (34)$$

60~99% yields
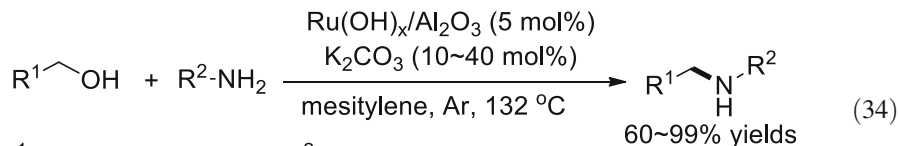
R^1 = Ar, heteroAr, alkyl; R^2 = heteroAr, Ar

Ru(OH)$_x$/Al$_2$O$_3$ recoverable: 1st, 89%; 2nd, 87%

$$\underset{R^1 \diagup R^2}{\overset{OH}{|}} + \underset{H_2N \diagup NH_2}{\overset{O}{||}} \xrightarrow[\text{mesitylene, Ar, 141 }^{\circ}C, 12 h]{\text{Ru(OH)}_x/\text{TiO}_2 \text{ (1.5~2 mol%)}} R^1 \diagdown N \diagup R^2 + R^1 \diagdown N \diagdown R^1$$

R^1 = Ar, alkyl; R^2 = H, alkyl

Ru(OH)$_x$/TiO$_2$ recoverable: 1st, 92%; 2nd, 90%

R^2 = H — — —

R^2 = alkyl 80~98% yields

76~97% yields

$$(35)$$
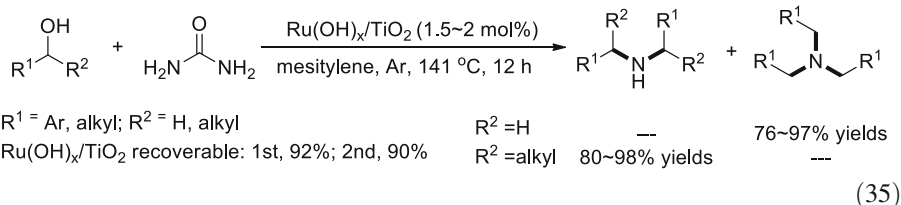
Continuing their work on the previously reported magnetite-catalyzed N-alkylation of aryl amines [138], in 2011 Ramón and co-workers reported Ru(OH)$_3$/Fe$_3$O$_4$-catalyzed N-alkylation reactions of poor nucleophilic amines/amides, such as aromatic and heteroaromatic amines, sulfonamides, sulfinamides, and nitroarenes (Scheme 26) [139]. The catalyst could be easily removed from the reaction mixture by magnet and reused up to ten times, showing the high activity of the catalyst (1st, 99 %; 10th, 93 %).

In 2014, Ramalingam and co-workers reported an additive-free reaction of primary and secondary amines with alcohols catalyzed by a supported ruthenium complex **20**, which was prepared from polystyrene-supported phosphine ligand and Ru(p-cymene)$_2$Cl$_2$]$_2$ (Eqs. 36,37) [140]. The authors found the ratio of the

Ar-NH$_2$

Ar-NO$_2$

ArSO$_2$NH$_2$

t-BuSONH$_2$

$R\diagdown OH$

Ru(OH)$_3$/Fe$_3$O$_4$ (1.3 mol%)
KOH or NaOH (130 mol%)
toluene, 85~130 $^{\circ}$C, 24~72 h

$R\diagdown N\diagup Ar$ (H)

$R\diagdown N\diagup SO_2Ar$ (H)

$R\diagdown N\diagdown SOt\text{-}Bu$ (H)

0~99% yields

R = Ar, heteroAr, arkyl

Ru(OH)$_3$/Fe$_3$O$_4$ recoverable: 1st, 99%; 10th, 93%
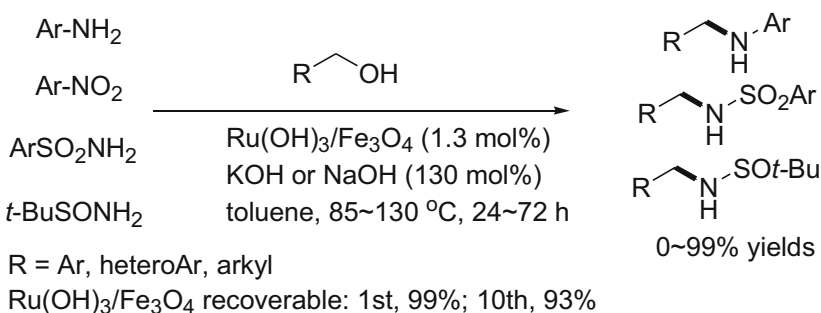
Scheme 26 Ru(OH)$_3$/Fe$_3$O$_4$-catalyzed N-alkylation reactions of poor nucleophilic amines/amides

phosphine ligand and Ru to be crucial to the high activity of the catalyst and low ruthenium leaching. Piribedil (**1**) could also be obtained in high yield by this method (1st, 98 %; 3rd, 97 %). The catalyst was also found effective for *N*-alkylation of piperidine under flow conditions.

(36)

(37)
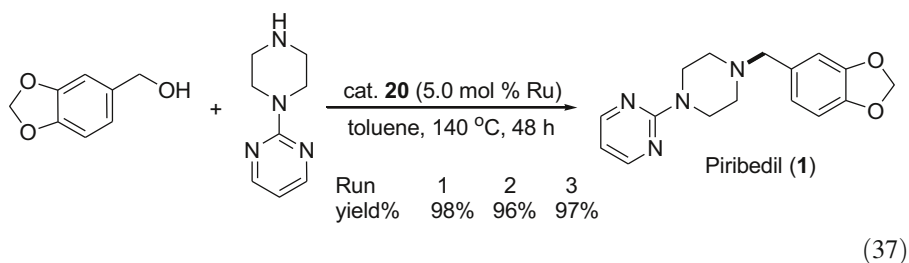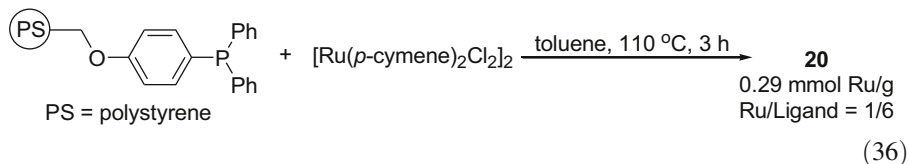
In 2013, Gao, Hou, and co-workers reported a mesoporous silica (SBA-15) supported iridium complex-catalyzed *N*-alkylation of primary amines with benzyl alcohols (Eq. 38) [141]. The catalyst could be recovered easily and reused at least 12 times without notable decrease in catalytic efficiency (1st, 93 %; 12th, 83 %).
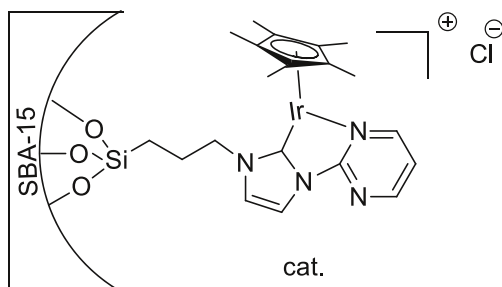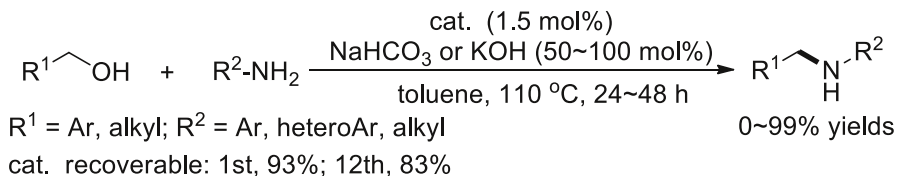
(38)

In 2011, Yu and co-workers reported additive-free *N*-alkylation and *N,N'*-dialkylation reactions of amines and alcohols catalyzed by Pt–Sn/γ-Al$_2$O$_3$ with

catalyst loading as low as 0.25 mol% (Eq. 39) [142]. Later in the same year, the Yu group extended the method to the direct synthesis of diamines by N,N'-dialkylation of amines with diols [143]. The recovered catalyst could be reused three times with the same activity. The same method can also be applied to amine-based N-alkylation reactions (vide infra).
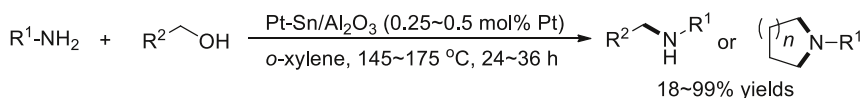
R^1 = Ar, heteroAr, alkyl; R^2 = Ar, heteroAr, alkyl, $(CH_2)_mOH$; n = 1, 2, 3, 4
Pt-Sn/Al$_2$O$_3$ recoverable: 1st, 95%; 3nd, 95%

$$(39)$$

In the same year, Shi and co-workers reported the N-alkylation of anilines, aliphatic amines and indoles with alcohols catalyzed by Pd/Fe$_2$O$_3$ under base- and ligand-free conditions with a low catalyst loading (0.43 mol%) (Eq. 40) [144]. In 2013, Pera-Titus and co-workers reported the N-alkylation of anilines catalyzed by another heterogeneous Pd catalyst Pd/K-OMS-2 (Pd-substituted octahedral molecular sieve) [145].
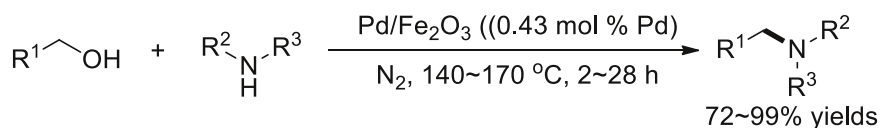
R^1 = Ar, heteroAr, alkyl; R^2 = Ar, heteroAr, alkyl; R^3 = Ar, alkyl

$$(40)$$

In 2015, Seayad and co-workers reported a silica supported palladium complex-catalyzed solvent-free N-alkylation of amines with catalyst loading as low as 0.00196 mol% and TON as high as 469390 (Eq. 41) [146]. The catalyst could be recycled at least four times without obvious loss of activity.
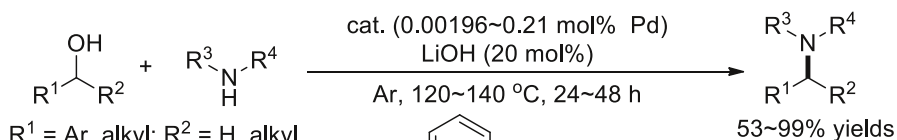
R^1 = Ar, alkyl; R^2 = H, alkyl
R^3 = Ar, alkyl; R^4 = H, alkyl
TON up to 46939
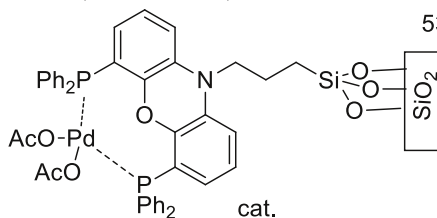
$$(41)$$

In 2010, Cao and co-workers reported the ligand- and base-free N-alkylation of anilines, aliphatic primary amines and pyrrolidine with alcohols catalyzed by very small (VS) Au nano particles: Au/TiO$_2$-VS [147]. The authors reported that 0.0083 mol% of the catalyst is efficient enough to catalyze a 100 mmol reaction of aniline and benzyl alcohol under solvent-free conditions, giving 96 % yield of the product. In 2011, the same group extended the method to reductive N-alkylation of nitrobenzenes with excess alcohols (8.0 equiv.) without external reducing reagents (Eq. 42) [148]. In 2012, the Cao group further extended their method to the synthesis of tertiary and secondary amines from alcohols and urea (Eq. 43) [149]. A 60 mmol scale solvent-free amination reaction of benzyl alcohol and urea gave the product in 92 % yield.

$$R^1 = MeO, F, Cl, Br \; etc.; R^2 = Ar, alkyl \qquad 66\sim99\% \; yields$$

(42)

$$R^1 = Ar, alkyl; R^2 = H, alkyl$$

$$R^2 = H \qquad \text{---} \qquad 80\sim95\% \; yields$$
$$R^2 = alkyl \qquad 80\sim87\% \; yields \qquad \text{---}$$

(43)
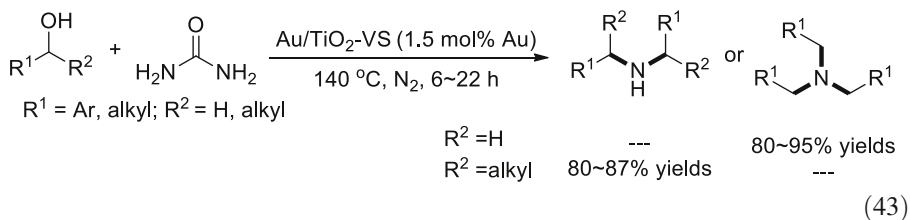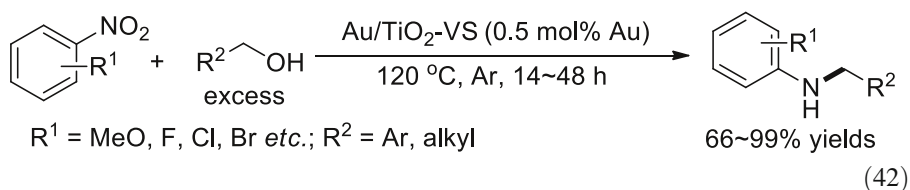
In 2009, Shimizu and co-workers found that Ag/Al$_2$O$_3$-FeCl$_3$ is highly active for the N-alkylation of anilines with benzylic alcohols [150]. The reactions using recovered catalyst led to only a slight decrease in product yields (1st, 94 %; 2nd, 85 %; 3rd, 86 %). In 2012, Jaenicke and co-workers also described the N-alkylation of aniline with linear aliphatic alcohols catalyzed by Ag/Al$_2$O$_3$-Cs$_2$CO$_3$ [151]. The recovered catalyst still exhibited high catalytic activity (1st, 99 %; 3rd, 97 %). In 2011, Shi and co-workers reported an Ag$_6$Mo$_{10}$O$_{33}$-catalyzed N-alkylation of amines, carboxamides, sulfonamides, and aromatic ketones with alcohols (Eq. 44) [152]. No deactivation occurred when the catalyst was recovered and reused twice (1st, 93 %; 2nd, 95 %).

$$R^1\diagup OH + R^2\text{-}NH_2 \xrightarrow[\text{Ar, 160 °C, 12 h}]{\substack{Ag_6Mo_{10}O_{33}\ (40\ mg/2\ mmol)\\KOtBu\ or\ K_2CO_3\ (20\ mol\%)}} R^1\diagdown\underset{H}{N}\diagup R^2$$

70~99% yield
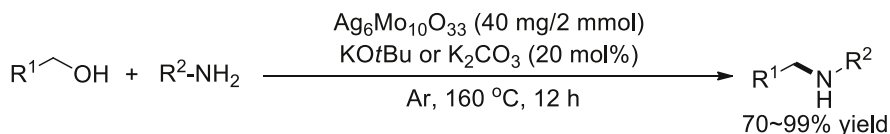
R^1 = Ar, heteroAr, alkyl; R^2 = RSO$_2$, RCO, Ar, heteroAr
Ag$_6$Mo$_{10}$O$_{33}$ recoverable: 1st, 93%; 2nd, 95%

(44)

In addition to above noble metal catalysts, many *N*-alkylation reactions catalyzed by heterogeneous non-noble metal catalysts have also been reported. In 2012, Li and co-workers reported a Ni-Cu/γ-Al$_2$O$_3$-catalyzed *N*-alkylation of amines with alcohols (Eq. 45) [153]. The reactions using recovered catalyst led to slight decrease in product yields (1st, 90 %; 2nd, 84 %).

$$\underset{R^1\diagdown R^2}{\overset{OH}{|}} + R^3\text{-}NH_2 \xrightarrow[\text{o-xylene, Ar, 160 °C, 12 h}]{\substack{Ni\text{-}Cu/Al_2O_3\ (0.1\ g/\ 2\ mmol)\\NaOH\ (40\ mol\%),\ CaCl_2\ (25\ mol\%)}} \underset{R^1\diagdown R^2}{\overset{R^3\diagdown NH}{|}}$$

68-99% yields
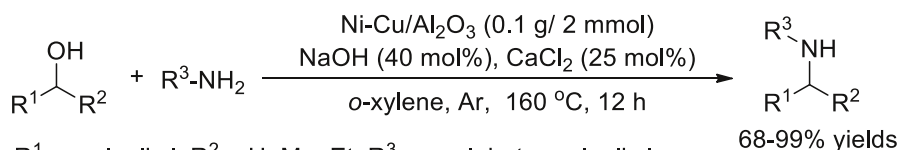
R^1 = aryl, alkyl; R^2 = H, Me, Et; R^3 = aryl, heteraryl, alkyl

(45)

In 2013, Shimizu and co-workers first reported an additive-free Ni/Al$_2$O$_3$-catalyzed synthesis of primary amines from alcohols and ammonia (Scheme 27) [154]. The recovered catalyst could be reused at least twice without losing catalytic activity (1st, 88 %, 3rd, 89 %). Later in 2013, the authors extended the method to amination of alcohols with anilines and aliphatic amines (Scheme 27) [155]. In 2014, the Shimizu group also described a Ni/CaSiO$_3$-catalyzed amination reaction of alcohols with ammonia, anilines and aliphatic amines [156].

In 2013, Shi and co-workers reported a base- and ligand-free *N*-alkylation of ammonia, primary amines and secondary amines with alcohols catalyzed by an air- and moisture-stable NiCuFeO$_x$ catalyst (Scheme 28) [157]. The catalyst can be recovered easily and reused at least 5 times (1st, 94 %; 5th, 82 %). A 10 mmol scale

$$\begin{array}{c} NH_3 \\ R^1\text{-}NH_2 \\ \underset{R^1\diagdown N\diagdown R^2}{\overset{H}{|}} \end{array} + R^3\text{-}OH \xrightarrow[\text{Ar, 140~160 °C}]{Ni/Al_2O_3\ (1\text{~}2\ mol\%)} \begin{array}{c} R^3\text{-}NH_2 \\ R^1\text{-}NH\text{-}R^3 \\ \underset{R^2\diagdown N\diagdown R^3}{\overset{R^1}{|}} \end{array}$$

68~99% yields

R^1 = Ar, heteroAr, alkyl; R^2= alkyl; R^3 = Ar, alkyl
Ni/Al$_2$O$_3$ recoverable: 1st, 88%; 3nd, 89%
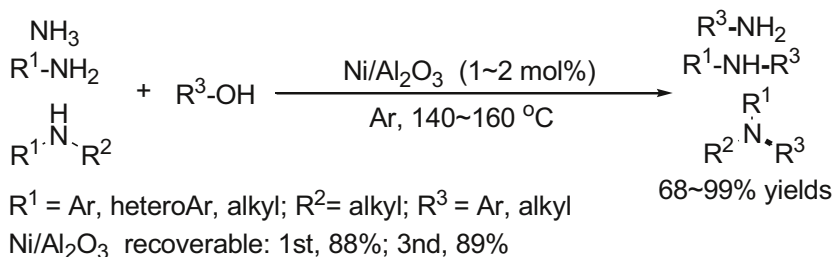
Scheme 27 Ni/Al$_2$O$_3$-catalyzed amination of alcohols with ammonia, anilines, and aliphatic amines
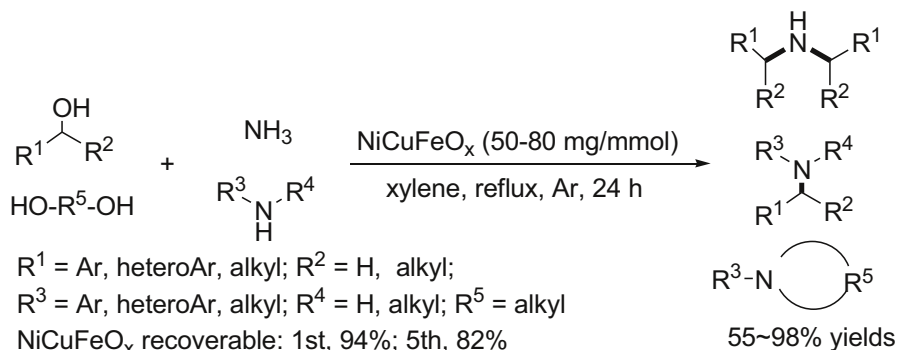
Scheme 28 NiCuFeO$_x$ complex-catalyzed N-alkylation of ammonia and primary and secondary amines with alcohols

solvent-free reaction of aniline and benzyl alcohol afforded the product in 85 % GC yield. In addition, the same method could also be applied to self-N-alkylation of primary amines (vide infra). In 2014, Nandan and coworkers reported a Raney nickel-catalyzed N-alkylation of anilines, primary aliphatic amines, cyclic secondary amines and azole with alcohols [158]. The recovered catalyst showed a very good activity comparable to the fresh catalyst (1st, 91 %; 3rd, 88 %).

In 2009, Mizuno and co-workers reported a base- and ligand-free Cu(OH)$_x$/Al$_2$O$_3$-catalyzed N-alkylation of N-nucleophiles including urea, ammonia, anilines and alkylamines [159]. In 2011, Shimizu and co-workers reported an additive-free Cu$_{0.95}$Ag$_{0.05}$/Al$_2$O$_3$-catalyzed N-alkylation of anilines and aliphatic amines with benzylic and aliphatic alcohols with a low catalyst loading (1 mol%) (Eq. 46) [160]. The recovered catalyst could be reused without losing catalytic activity (1st, 85 %; 2nd, 87 %).

R^1 = Ar, alkyl; R^2 = H, alkyl; R^3 = Ar, alkyl
Cu$_{0.95}$Ag$_{0.05}$/Al$_2$O$_3$ recoverable: 1st, 85%; 2nd, 87%

8~92% yields
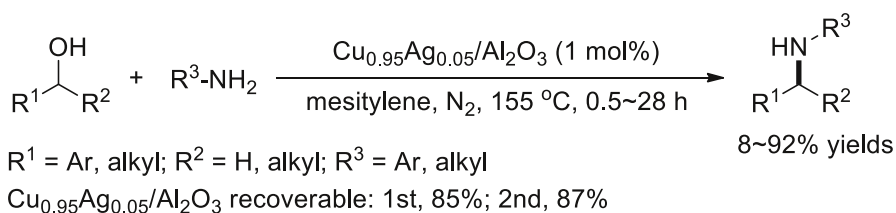
(46)

In 2012, Ravasio and co-workers also reported an additive-free N-alkylation of amines with benzyl and aliphatic alcohols catalyzed by Cu/Al$_2$O$_3$ [161]. In 2014, the authors extended the method to the N-alkylation of anilines with a wide range of alcohols (Eq. 47) [162]. In 2013, Mishra and co-workers reported an additive-free N-alkylation of primary amines with primary and secondary alcohols catalyzed by copper–aluminium hydrotalcite (CuAl-HT) [163].

$R^1 = Ar$, alkyl; $R^2 = H$, alkyl; $R^3 = Ar$, alkyl; $R^4 = H$, alkyl   32.8~99.6% yields

(47)
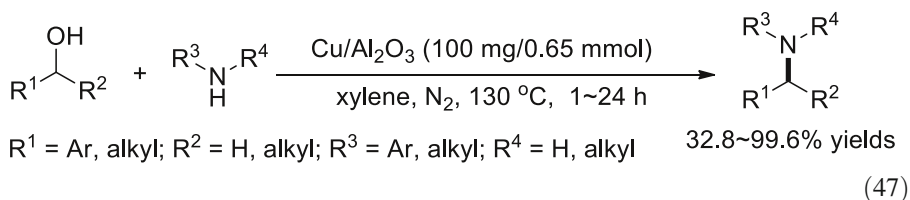
2.4 Miscellaneous Catalytic *N*-Alkylation Reactions

In addition to the homogeneous and heterogeneous TM catalysts discussed above, other catalysts/methods such as nano catalysts, carbon materials, enzymes, chiral catalysts and continuous flow techniques have also been developed successfully and applied in *N*-alkylation reactions of amines/amides with alcohols.

In 2009, Beller and co-workers reported the *N*-alkylation of sulfonamides with benzylic alcohols catalyzed by nano-Ru/Fe$_3$O$_4$ with catalyst loading as low as 0.4 mol% (Eq. 48) [164]. A high 96 % yield of product could still be obtained even when the catalyst was reused 5 times and with TON up to 1100.

$R^1 = Ar$, heteroAr $R^2 = Ar$, heteroAr, alkyl
Ru/Fe$_3$O$_4$ recoverable: 1st, 97%; 5th, 96%. TON up to 1100

(48)
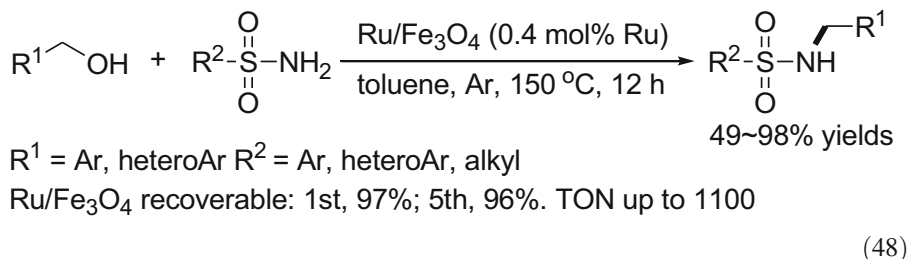
In 2010, Shimizu and co-workers reported a nano-Ag/Al$_2$O$_3$-catalyzed one-step synthesis of *N*-substituted anilines from nitroarenes and stoichiometric benzyl alcohols under H$_2$ atmosphere (Eq. 49) [165], in which H$_2$ was employed to reduce the nitroarenes to anilines.

$R^1 = $ MeO, F, Cl, Br *etc.*; $R^2 = $ Ar,   80~94% yields

(49)
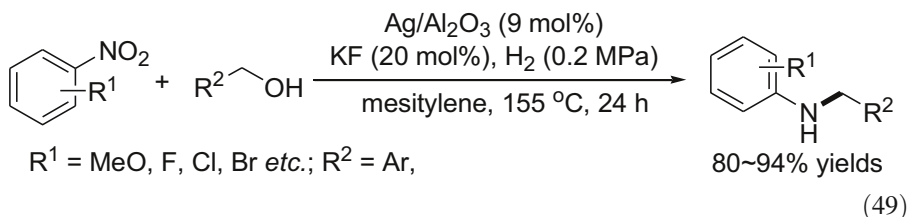
In 2012, Shi and co-workers reported another reductive *N*-alkylation of nitrobenzenes with stoichiometric alcohols (1.0 equiv.) catalyzed by nano-Au/

Ag–Mo nano-rods (Eq. 50) [166]. Unlike Shimizu's work using as H_2 [165], in Shi's work excess glycerol was employed as the reductant.

R^1 = Me, MeO, Cl etc.; R^2 = Ar, alkyl

72-91% yields

$$(50)$$
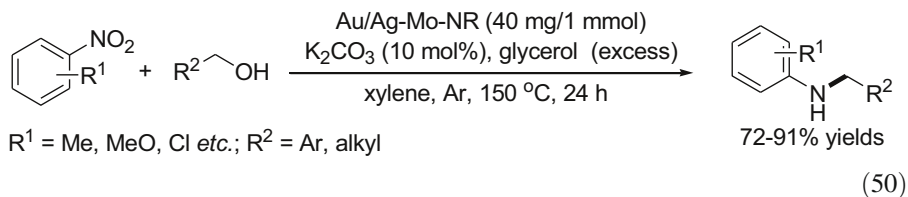
Later in 2012, Corma, Sabater and co-workers reported a nano-Au/CeO$_2$-catalyzed N-alkylation of amines with alcohols [167]. In 2014, De Vos and co-workers reported a nano-Ag/Al$_2$O$_3$/Ga$_2$O$_3$-catalyzed amination of alcohols with a variety of aliphatic and aryl amines under mild conditions [168]. The catalyst remained active for at least three runs (1st, TOF = 1.01/h; 3rd, 1.02/h).

In 2015, Kobayashi and co-workers reported a PI/CB-Au/Pd (PI/CB, polymer-incarcerated metal nanoparticle catalyst with carbon black as a secondary supporter) complex-catalyzed N-alkylation of amides with alcohols (Eq. 51) [169]. The catalyst could be reused 11 times without appreciable loss of catalytic activity (1st, 99 %; 11th, 95 %).

R^1 = Ar, heteroAr, alkyl; R^2 = Ar
PI/CB-Au/Pd recoverable: 1st, 99%; 11th, 95%

44~99% yields

$$(51)$$
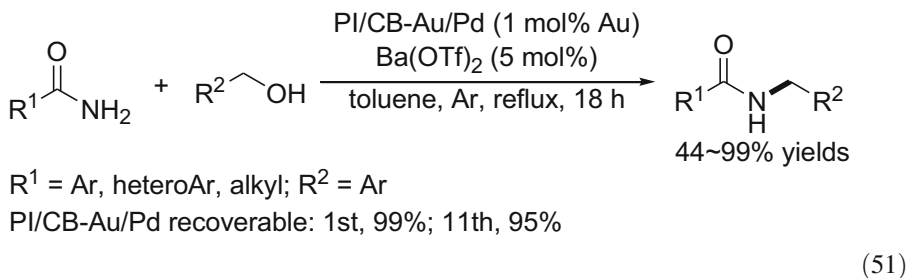
In 2010, Luque and co-workers were the first to report a microwave-assisted N-alkylation of amines with benzylic alcohols catalyzed by nano-Fe-HMS (HMS, hexagonal mesoporous silica) (Eq. 52) [170]. The authors found that base may be crucial in deprotonation/dehydrogenation of the alcohols.

R^1 = Ar; R^2 = Ar, heteroAr, alkyl

70~99% yields

$$(52)$$
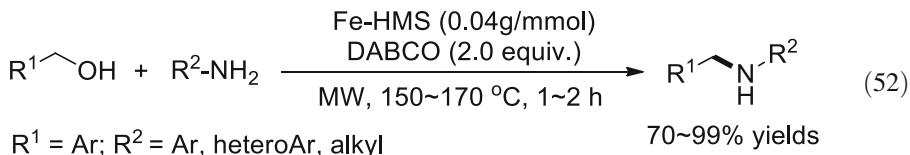
In 2010, Kolaczkowski and co-workers described a continuous flow N-benzylation of morpholine with benzyl alcohol catalyzed by a heterogeneous ruthenium complex with a product yield of 98 %, providing an efficient route for
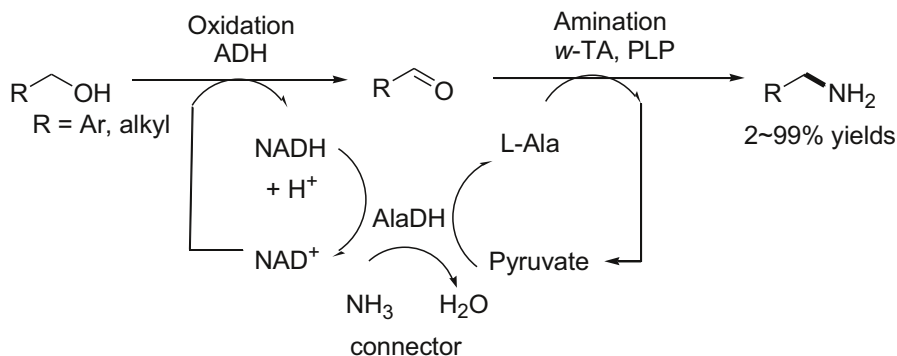
Scheme 29 Proposed mechanism for the artificial multi-enzyme-catalyzed bioamination of primary alcohols

synthesis of *N*-benzyl morpholine [171]. In 2013, Kocsisin and co-workers also reported a Raney nickel-catalyzed *N*-alkylation of amines and pyrrole with alcohols in a continuous flow process [172]. In most cases the effective residence time was less than 1 min.

In 2012, Kroutil and co-workers reported the first amination reaction of primary alcohols with ammonium chloride by an artificial multi-enzyme-catalyzed cascade method (Scheme 29) [173]. The authors assumed that the reaction might proceed by two steps. Initially, the alcohol was oxidized by an alcohol dehydrogenase (ADH), consuming NAD^+ and leading to the formation of the aldehyde and NADH. Then, the aldehyde intermediate was aminated with an amine donor L-alanine by a *w*-transaminase (*w*-TA). Finally, by combining ADH-hT (ADH from *Bacillus stearothermophilus*) with CV-*w*-TA (*w*-TA from *Chromobacterium violaceum*), the amination of various primary alcohols successfully afforded the corresponding primary amines in 2–99 % yields.
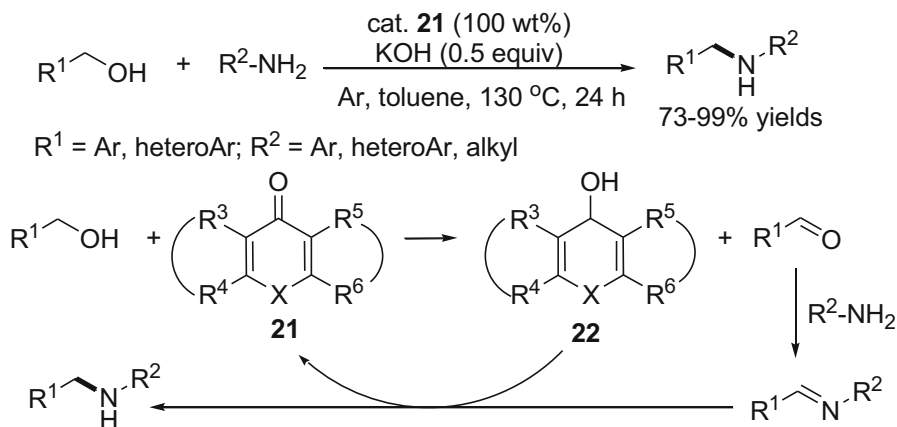
Scheme 30 Tentative mechanism for amination of alcohols catalyzed by carbon material **21**

In 2015, Shi and co-workers reported a carbon material (**21**)-catalyzed amination of (hetero)benzylic alcohols with (hetero)aryl amines and aliphatic amines (Scheme 30) [174]. A tentative mechanism was proposed. First, hydrogen was transferred from the alcohol to the carbon catalyst **21** to give aldehyde intermediate and reduced catalyst **22**. Then, condensation of aldehyde and amine to imine and subsequent reduction by **22** led to the desired N-alkyl amine products and regeneration of carbon catalyst **22**.

The more challenging asymmetric N-alkylation reactions of amines with alcohols was also developed in recent years. In 2009, by employing an Ir-catalyzed N-heterocyclization reaction as the key step, Trudell and co-workers first achieved the enantioselective total synthesis of both enantiomers of noranabasamine with >30 % overall yields and >80 % ee (Eq. 53) [175].

(53)
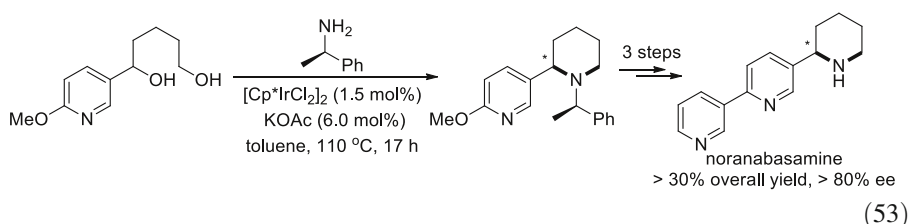
In 2014, Guan and co-workers reported the direct synthesis of α-chiral *tert*-butanesulfinylamines from the reaction of racemic alcohols and Ellman's sulfinamide catalyzed by ruthenium (II) pincer catalyst **23** (Eq. 54) [176], providing an effective method for the synthesis of chiral amine derivatives.

(54)
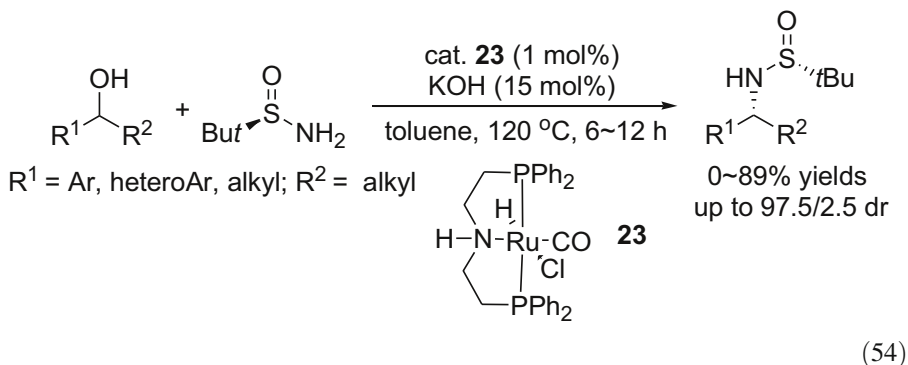
In 2013, Oe and co-workers achieved the first enantioselective synthesis of β-amino alcohols from the reaction of 1,2-diols and secondary amines catalyzed by [Ru(p-cymene)Cl$_2$]$_2$/(S,R)-JOSIPHOS with moderate enantioselectivity (Eq. 55) [177].

R = 2, 4, 6-*i*Pr$_3$C$_6$H$_2$

25

26

R = 2, 4, 6-*i*Pr$_3$C$_6$H$_2$

27
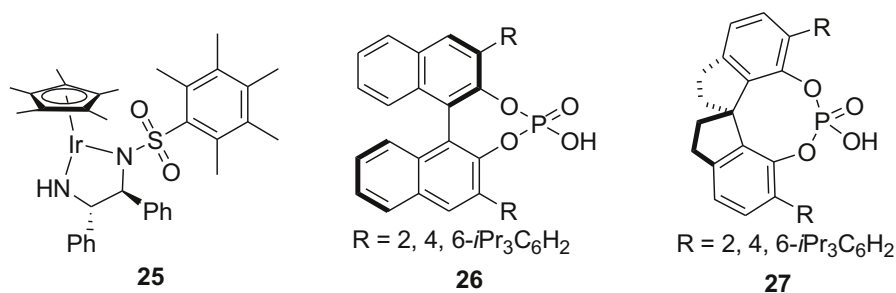
Scheme 31 Iridium complex **22** and chiral phosphoric acids **23** and **25**

R^1 = Ar, alkyl; R^2 = alkyl; R^3 = alkyl

[Ru(*p*-cymene)Cl$_2$]$_2$ (2.5 mol %)
(S,R)-JOSIPHOS (6 mol %)
toluene, 100 °C, 24 h

0~99% yields, 0~77% ee

(S,R)-JOSIPHOS

(55)
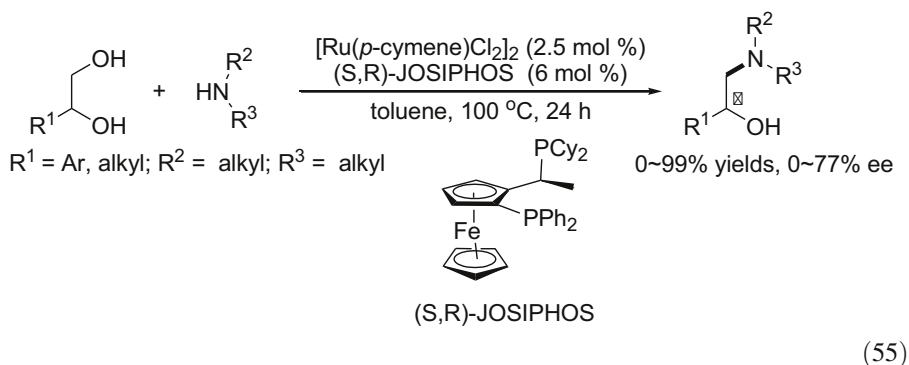
In 2014, by employing the hydrogen autotransfer method, Zhao and co-workers reported the first enantioselective amination of alcohols to chiral secondary arylamines in high yields and high ee up to 97 % (Eq. 56, Scheme 31) [178]. Intramolecular amination could also be achieved to give quinoline **24** with 68 % ee. The authors proposed that the high enantioselectivity might be attributed to the cooperation of the iridium complex **25** and the chiral phosphoric acid **26**.

cat. **25** (5 mol%)
cat. **27** (10 mol%)
4 Å MS, 110 °C, 60~96 h

16~81% yields
dr up to 98/2, er up to 99/1

mixture of
four isomer

[Ir]

[IrH$_2$]

HX
ArNH$_2$

H$_2$O

28

29

30

[IrH$_2$] [Ir]

k$_{fast}$

31

[IrH$_2$] [Ir]

k$_{slow}$

31'
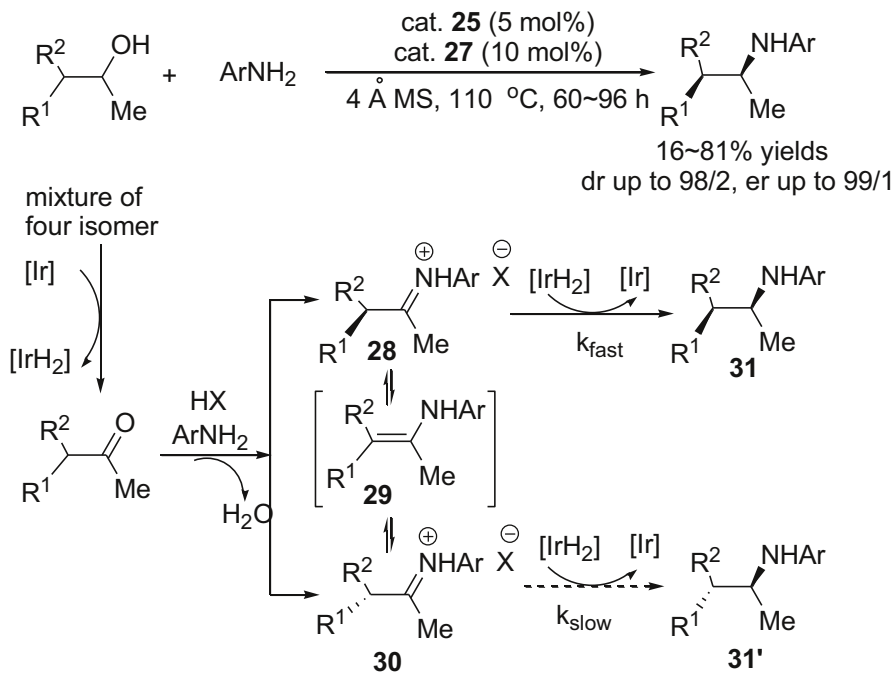
Scheme 32 Proposed mechanism for the dynamic kinetic asymmetric amination of alcohols

cat. **25** (5 mol%)
cat. **26** (5 mol%)
t-amyl alcohol, reflux
4 Å MS, 24 h

R^1 = Ar, alkyl; R^2 = Me, Et

64~98% yields
69~97% ee

(56)

24
73% yield, 68% ee
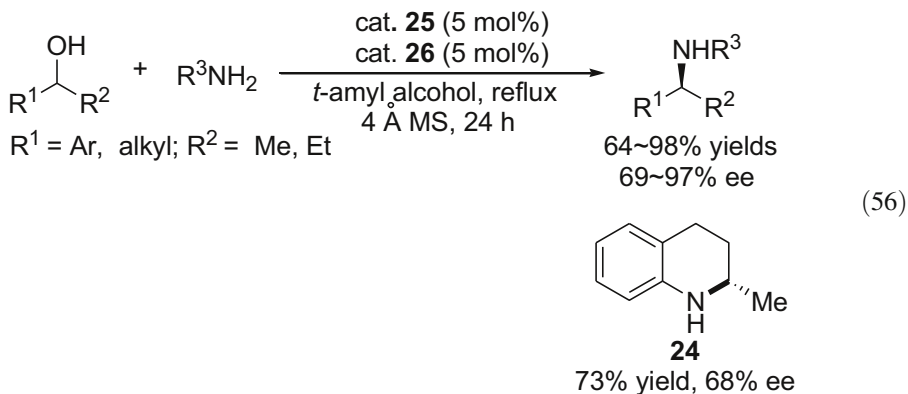
In 2015, Zhao and co-workers described the first dynamic kinetic asymmetric amination of alcohols via borrowing hydrogen methodology under the cooperative catalysis of iridium complex **25** and chiral phosphoric acid **27** (Schemes 31, 32) [179]. The authors proposed that, initially, the two stereocenters in the alcohols were both racemized to ketone by the first oxidation, followed by tautomerization of the iminium intermediates **28** and **30** through enamine intermediate **29**. Then, the
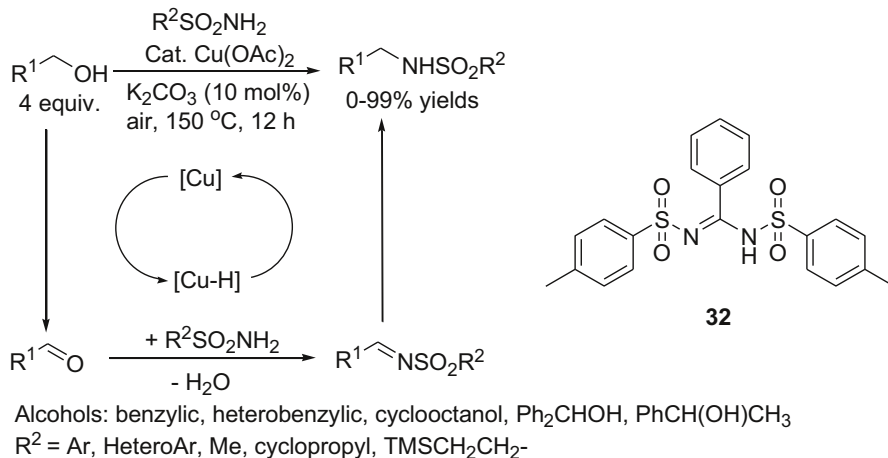
Scheme 33 Proposed mechanism for Cu-catalyzed *N*-alkylation of sulfonamides with alcohols under air
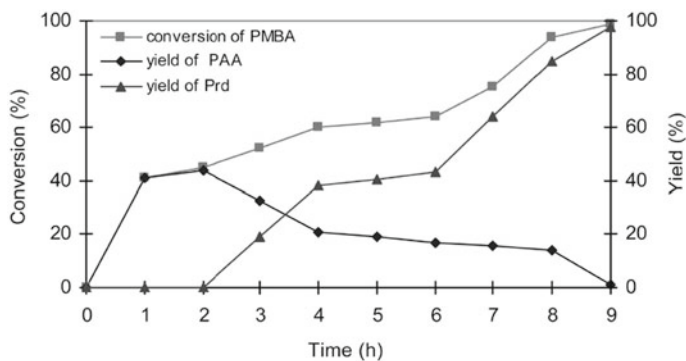
Fig. 1 PAA and *N*-alkylated product over time in the CuAl-HT$_2$/K$_2$CO$_3$-catalyzed amination of PMBA with benzylamine (BA) (160 °C, 9 h). *PAA* p-anisaldehyde, *PMBA* p-methoxybenzyl alcohol, *Prd* product

different reaction rates of the two stereoisomers towards hydrogenation by [IrH$_2$] led to the major product **31**.

2.5 TM-Catalyzed Aerobic *N*-Alkylation Reactions (Reactions Under Air)

In addition to the above *N*-alkylation reactions carried out under inert conditions via anaerobic dehydrogenative activation of alcohols, some TM-catalyzed aerobic *N*-alkylation reactions carried out under air have also been reported in recent years. As they require no inert atmosphere protection, and use air-stable TM catalysts under aerobic conditions, these reactions may be operationally simpler and more practical.

R^1, R^2 = alkyl,aryl, H; R^3, R^4 = alkyl,aryl, H
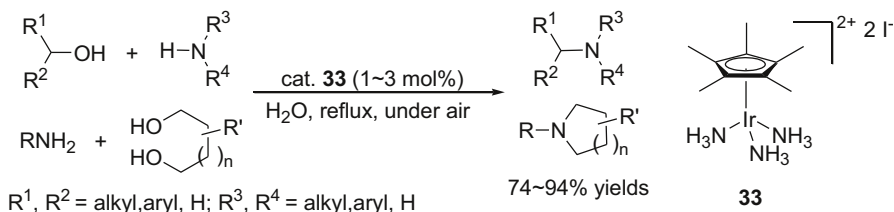
Scheme 34 Cp*Iridium complex (**33**)-catalyzed *N*-alkylation of amines with alcohols under air

In 2009, Shi, Beller and co-workers reported the first homogeneous Cu(OAc)$_2$-catalyzed aerobic *N*-alkylation of sulfonamides with alcohols (Scheme 33) [180, 181]. In condition screening, the authors found the reaction under air was comparatively more efficient (93 % conversion) than those under argon (48 %) or CO$_2$ (51 %). This method is thus a good alternative for *N*-alkylation of sulfonamides for using the cheaper Cu catalyst under aerobic conditions. The substrates seemed to be limited to sulfonamides only. In the cases of secondary alcohols, no base was required and the more Lewis acidic Cu(OTf)$_2$ was found to be a much better catalyst than Cu(OAc)$_2$. According to the mechanistic study, since bissulfonylated amidine **32** could only be generated in situ in reactions performed under air, the authors concluded that **32** should act as the stabilizing ligand to activate the Cu catalyst for dehydrogenation/hydrogenation processes, and, subsequently, the reaction proceeded through the hydrogen autotransfer/borrowing hydrogen mechanism involving [CuH] species (Scheme 33).

In the same year, Likhar and co-workers also reported a heterogeneous copper–aluminium hydrotalcite (CuAl-HT)-catalyzed amination of alcohols under air (Eq. 57) [182]. Benzylic, aliphatic, and secondary alcohols, benzylamines, secondary amines, and anilines could be tolerated in this method. Notably, the CuAl-HT catalyst can be recovered for reuse by simple filtration for at least five cycles without obvious loss of activity (5th cycle, 97 %). In mechanistic studies, the authors observed an initiation period in which the aldehyde intermediate was first generated in considerable amounts (before 2 h) prior to the formation of product, which remained in consideraable amounts until completion of the reaction (Fig. 1). The aldehyde could also be obtained in 98 % yield in a control reaction with the alcohol alone. Since no alkylated amine product was observed in the reaction of aldehyde and amine with CuAl-HT2, the authors concluded that, by an oxidation/imination/reduction sequence, an in situ generated momo(hydrido)copper species generated by a hydrogen transfer process from alcohols to Cu should be responsible for the second hydrogen transfer to imine intermediates to give the products.

aq NH$_3$
R^{1}NH$_2$
R^{1}R^{2}NH   +   HO-R $\xrightarrow[\text{H}_2\text{O, under air}]{\text{PB-Cp*Ir(IPr) (1 mol\% Ir)}}$

NR$_3$
R^{1}NHR (R^{1}NR$_2$)
R^{1}R^{2}NR

61~95% yields

R = benzyl, alkyl
R^1, R^2 = aryl, H; alkyl, H; alkyl, alkyl

34
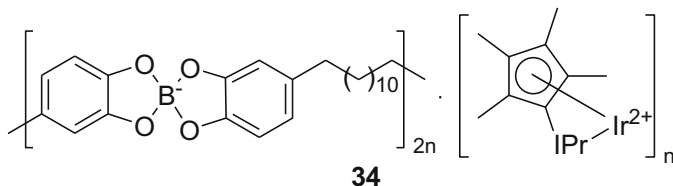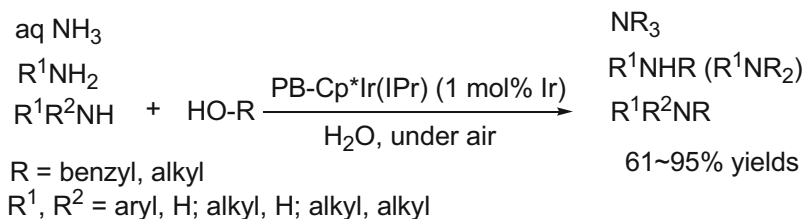
Scheme 35 Boron-iridium heterobimetallic complex (**32**)-catalyzed *N*-alkylation reaction of ammonia and primary, secondary, and cyclic amines with alcohols under air

R^1⌒OH   +   R^{2}NH$_2$ $\xrightarrow[\text{air, 160 °C, 9 h}]{\substack{\text{CuAl-HT (4 mol\% Cu)} \\ \text{K}_2\text{CO}_3 \text{ (1.26 equiv.)}}}$ R^1⌒NHR^2

(1.5 equiv.)

32-98% yields

(57)

Alcohols: benzylic, aliphatic, secondary
Amines: benzylamines, secondary amines, anilines
CuAl-HT recoverable: 1st cycle, 98%; 5th cycle, 97%
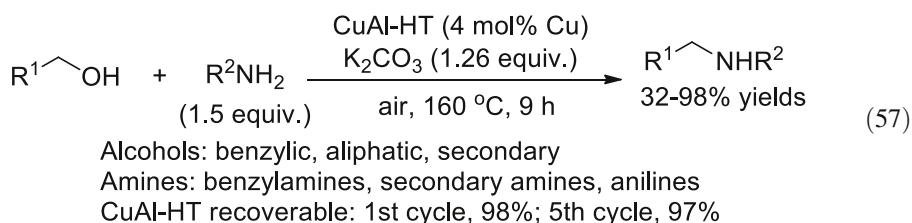
In 2011, Fujita, Yamaguchi and co-workers reported a water-soluble Cp*Iridium complex (**33**)-catalyzed base-free *N*-alkylation of amines with alcohols in water (Scheme 34) [183]. Since the catalyst is air-stable, the reactions could be readily carried out under air. Primary and secondary benzylamines, aliphatic amines, cyclic amines, anilines, as well as benzylic, aliphatic, secondary alcohols can be used to synthesize secondary and tertiary amines. Cyclic amines could also be achieved by *N*-alkylation of amines with diols. The authors also proposed a mechanism with hydrogen transfers from alcohols to form [Ir-H] complexes and finally to the product amines.

Later in the same year, Uozumi, Yamada, and co-workers also reported an in-water dehydrative *N*-alkylation reaction under air using a heterogeneous boron-iridium heterobimetallic Polymeric Catalyst **34** (Scheme 35) [184]. This method is suitable for the reactions of benzylic and aliphatic alcohols with ammonia, and primary, secondary, and cyclic amines. Different to usual hydrogen autotransfer reactions, which require basic conditions, the reactions of benzylic, aliphatic, and secondary amines and ammonia require a pH 4 aqueous buffer solution under microwave conditions. The catalyst can be recovered and reused at least twice without loss of activity.

In the Pd(OAc)$_2$-catalyzed *N*-alkylation reactions reported in 2011 [120], Ramón and co-workers found the reactions of sulfonamides and alcohols under air were

more efficient than those under argon, and Pd(OAc)$_2$ could be used at a very low-loading of 0.05 mol% (Eq. 58).

$$\text{(58)}$$
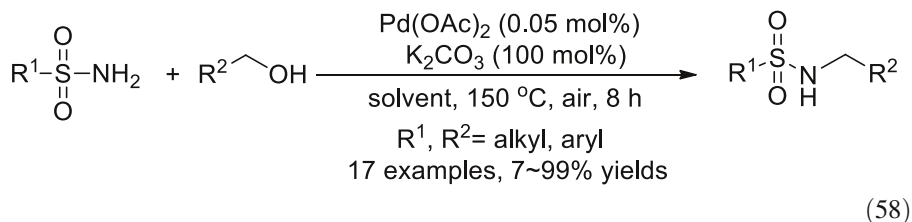
Also in 2011, Xu and co-workers reported a comparatively general TM-catalyzed aerobic N-alkylation reaction of sulfonamides, anilines, heteroarylamines, and carbox-amines with benzylic, heterobenzylic, alkyl and allylic alcohols under air (Eq. 59) [185, 186]. Both ligated and ligand-free TM catalysts such as Rh(PPh$_3$)Cl, Ru, Ir, and Rh halides, and even the noble metal oxides, could be used as catalysts under air. In contrast to previous aerobic N-alkylation reactions that had not investigated air's influence on the reactions [120, 180–184], the authors were the first to observe air's promoting effect on the reaction. Thus, no reaction was observed, or only trace to low yields of the products, could be detected in parallel anaerobic reactions, while under air the same reactions could afford much higher yields of the products. As the authors found out, this is due to TM catalyst deactivation/poisoning by substrate amines/amides, making the alcohol activation process the rate-limiting step of the whole reaction. Air then participated in the reaction as a new way to oxidize the alcohols to the more active aldehydes. Similarly,
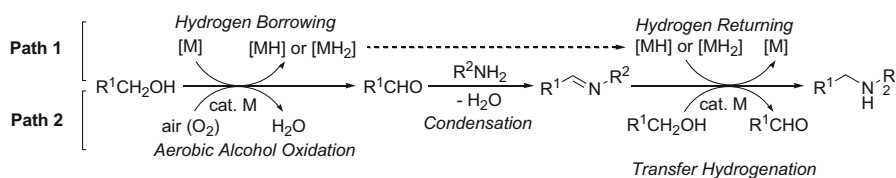
Scheme 36 Possible tandem processes for one-pot/multi-step N-alkylation reactions
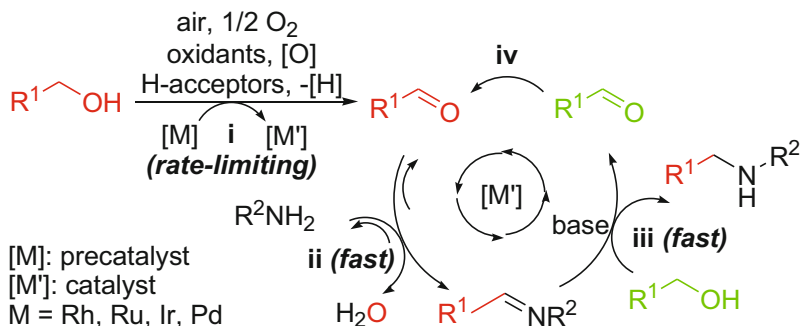
Scheme 37 Proposed mechanism for air-promoted metal-catalyzed aerobic N-alkylation reactions (aerobic relay race mechanism)

if TM oxides, usually used as oxidants in conventional oxidation reactions, including oxidation of alcohols [37–42], were used as catalysts under anaerobic conditions, better results, up to moderate yields of the products, than with other catalysts could be obtained, most likely due to alcohol oxidation by metal oxides. The authors also found that, under the anaerobic conditions typical of the borrowing hydrogen and hydrogen autotransfer reactions, the same TM catalysts could also catalyze N-alkylation reactions, but required much higher temperatures; otherwise, addition of ligands is necessary to promote the originally ineffective reactions to occur to yield the desired products. Obviously these aerobic N-alkylation reactions proceeded via an alternative mechanism other than the typical borrowing hydrogen and hydrogen autotransfer mechanism (Scheme 3).

$$R^1\frown OH \ + \ R^2\text{-}NH_2 \ \xrightarrow[\text{air, }120\sim150\,^{\circ}C,\ 4\sim48\ h]{\substack{M\ (0.5\sim1\ mol\%)\\ \text{base (10}\sim\text{100 mol\%)}}} \ R^1\frown N(H)\text{-}R^2$$

58~99% yields (59)
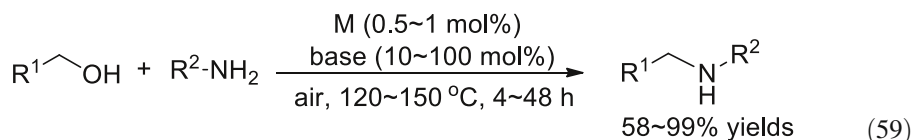
M = Rh(PPh₃)₃Cl, RhCl₃·3H₂O, Rh₂O₃, Rh₂(OAc)₄,
RuCl₃·nH₂O, RuO₂, IrCl₃, IrO₂, MnO₂, etc.
R^1 = aryl, heteroaryl, alkyl, allyl; R^2 = RSO₂, RCO, heteroaryl, aryl

After a detailed and careful study of the individual reactions and the reaction mechanism, Xu and co-workers proposed that, in addition to the known anaerobic dehydrogenation method (Scheme 36, path 1), TM-catalyzed aerobic oxidation of alcohols to aldehydes [36–41] (path 2) should be a good alternative for alcohol activation. Consequently, a new mechanism different from the usual hydrogen autotransfer process was proposed for the air-promoted TM-catalyzed aerobic N-alkylation reactions (Scheme 37). Thus, alcohols were first oxidized by air under TM catalysis to give aldehydes, which then condense with amines/amides to give imine intermediates. Imines were finally reduced by alcohols to product amines via a transfer hydrogenation process [46–51], generating meanwhile, as the authors proved, 1 equiv. of aldehydes as the byproduct. Since the byproduct aldehyde can be recovered to participate in next mechanism cycle, a small amount of air (ca. 10–20 mol% O₂) was adequate to generate the catalytic amount of aldehdye and initiate the whole reaction, resolving the rate-limiting issue in the alcohol activation step. In addition, the latter alcohol (in green), after transferring its hydrogen atoms to the preceding alcohol (in red, in its imine form via aldehyde intermediate), will (also in its imine form via aldehyde intermediate) receive new hydrogen atoms from an even later alcohol in next mechanism cycle, which is analogous to the relay race game with "handing off" of hydrogen atoms. Hence, the authors termed it the "relay race" mechanism.

In fact, the significant role of air in aerobic alkylation reactions had already been observed by the groups of Uozumi [187, 188] and Crabtree [189]. In 2006, Uozumi and co-workers noted that other mechanisms might participate in their aerobic C-alkylation reaction of ketones and alcohols because one reviewer pointed out that metal hydride intermediates are prone to react with molecular oxygen. In 2010, Crabtree and co-workers hypothesized that their C-alkylation reaction of secondary and primary alcohols under air most possibly underwent a procedure involving

participation of air in the reaction, especially the oxidation of primary and secondary alcohols to aldehydes and ketones for next aldol condensation step.

Xu's air-promoted protocol could even be extended to non-noble metal oxides such as MnO_2 [190] and Pd catalysts [191]. In the latter work, the authors also observed the clear coordination between [Pd] and amines, leading to deactivation of the catalyst (Eq. 60) [191]. Therefore, aerobic reactions catalyzed by Pd were also found to be much more efficient and afforded higher yields of the products than the corresponding anaerobic reactions.

$$
\begin{array}{c}
Pd(OAc)_2 \\
+ \\
PyNH_2 \\
(4\ equiv)
\end{array}
\xrightarrow[\text{LC-MS analysis}]{\text{MeOH, air, rt}}
\begin{array}{c}
\underset{\text{minor}}{Pd(OAc)(PyNH)} + \underset{\text{major}}{Pd(PyNH)_2} + \underset{\text{major}}{Pd(OAc)(PyNH)(PyNH_2)} \\
\\
+ \underset{\text{minor}}{Pd(PyNH)_2(PyNH_2)} + \underset{\text{minor}}{Pd(OAc)(PyNH)(PyNH_2)_2}
\end{array}
$$

(60)
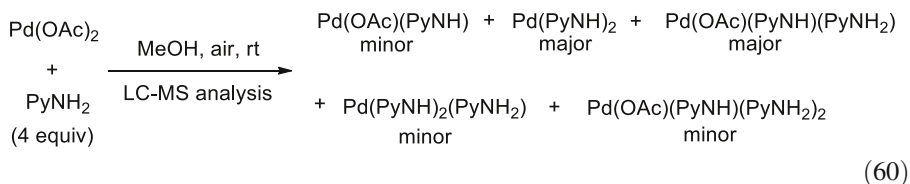
In 2012, Xu and co-workers continued to report a Cu-catalyzed aerobic N-alkylation reaction of sulfonamides, anilines and heteroarylamines with alcohols under air (Eq. 61) [192]. The authors evaluated the effects of the additives on the reaction. They not only observed the promoting effect of air, but also found that aldehyde contamination in substrate alcohols could also lead to more efficient reactions either under either air or under nitrogen. Besides, they observed the successful oxidation of alcohol by Cu(II) under anaerobic conditions (Eq. 62).

$$
R^1{\diagdown}OH + R^2\text{-}NH_2 \xrightarrow[\text{air, 135 °C, 24~36 h}]{\substack{Cu(OAc)_2{\cdot}H_2O\ (1\ mol\%)\\ \text{base (10~20 mol\%)}}} R^1{\diagdown}\underset{H}{N}{\diagup}R^2
$$

R^1 = Aryl, heteroaryl

R^2 = RSO_2, Aryl, heteroaryl

19~95% yields

(61)

$$
PhCH_2OH + Cu(II) \longrightarrow PhCHO + Cu(I)
$$

(62)
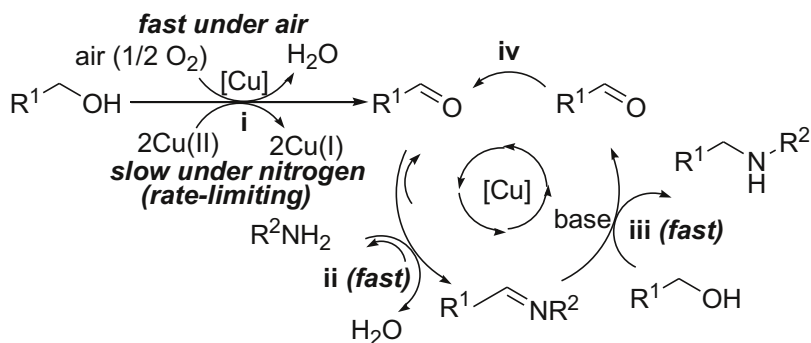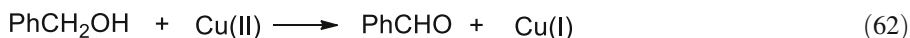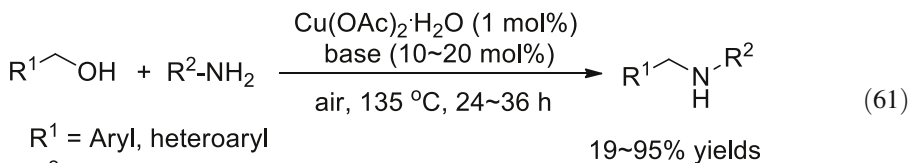
Scheme 38 Proposed mechanism for air-promoted Cu-catalyzed aerobic N-alkylation reactions
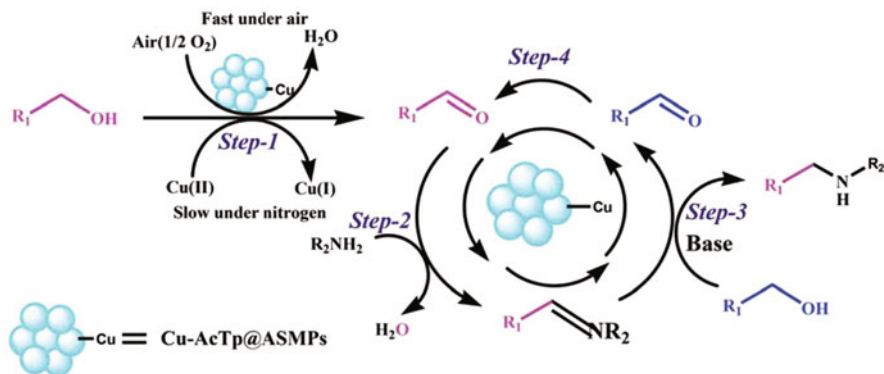
Fig. 2 Proposed mechanism for air-promoted Cu-AcTp@Am–Si-Fe$_3$O$_4$-catalyzed aerobic *N*-alkylation reactions

$$\text{PhCH}_2\text{OH} \;+\; \text{Cu(I)} \;\xcancel{\longrightarrow}\; \text{PhCHO} \;+\; \text{Cu(0)} \tag{63}$$
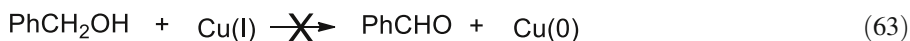
Since no alcohol oxidation was detected with Cu(I) salts under anaerobic conditions (Eq. 63), the authors proposed that the observed catalytic effect of Cu catalyst in anaerobic *N*-alkylation reactions might be attributed to the oxidation of alcohols by Cu(II) to give aldehydes and Cu(I) salts (Eqs. 62, 63), as Cu(II) has also been frequently used as an oxidant in organic reactions. As with the formation of [CuH] species, these authors pointed out that literature reports had indicated that generation of [CuH] species usually requires harsh conditions, such as using strong coordinating phosphine ligands and strong hydride-donating silanes under inert conditions, and that they are prone to be destroyed by molecular oxygen [193–195]. Therefore, the authors proposed a new mechanism for the Cu-catalyzed aerobic *N*-alkylation reactions under air (Scheme 38), in which the alcohol oxidation step is a slow step under inert conditions but a fast process under air. A similar Cu-catalyzed aerobic alkylation method can be extended to C-alkylation reactions of secondary alcohols and methyl ketones with primary alcohols [196].

In 2013, Sharma and co-workers reported another aerobic *N*-alkylation of anilines with benzylic, allylic, and primary and secondary aliphatic alcohols using a magnetite (Fe$_3$O$_4$) silica-based organic-inorganichybrid copper(II) nanocatalyst (Cu-AcTp@Am–Si-Fe$_3$O$_4$) (Eq. 64) [197]. Since Am–Si-Fe$_3$O$_4$ was used as the support for the active Cu catalysts, the Cu-AcTp@Am–Si-Fe$_3$O$_4$ catalyst can be readily recovered using a magnet for separation and reused at least ten times without obvious loss of catalytic activity. The authors also observed the promoting effect of air on the alkylation reaction. Thus, only trace product was observed under anaerobic conditions but a high yield of product could be obtained in reactions under air. Along with other findings, the authors proposed a mechanism following a preceding mechanism proposed for the air-promoted TM-catalyzed aerobic *N*-alkylation reactions (Fig. 2).

$$
\text{R}^1\text{—OH} + \text{R}^2\text{-NH}_2 \xrightarrow[\text{aerobic conditions}]{\substack{\text{cat. Cu-AcTp@Am-Si-Fe}_3\text{O}_4 \\ \text{(recoverable and reusable)}}} \text{R}^1\text{—N(H)—R}^2
$$

Alcohol: benzylic alcohols, allyl alcohols,   82~98% yields
        primary and secondary aliphatic alcohols

$$(64)$$
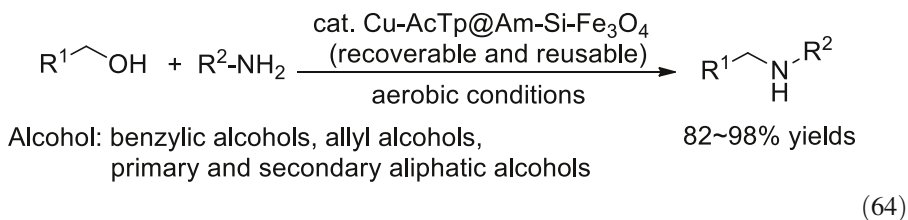
In 2012, Hellgardt, Hii, and coworkers achieved a base-free N-alkylation method for anilines, aliphatic and secondary amines and benzylic, aliphatic and secondary alcohols by using a heterogeneous Au/TiO$_2$ catalyst in a continuous flow reactor (Eq. 65) [198]. By employing the flow chemistry protocol, this provided not only a potentially greater reaction space, but also showed that higher reactivity and selectivity of the reactions can be achieved than using the batch reactors. In addition, the substrates in the reservoir can be stored readily under ambient conditions without the need for specialized inert atmosphere protection, making the method much simpler and more practical.

M_A (main group metals): Na, Mg, Al, K, Cs, etc.
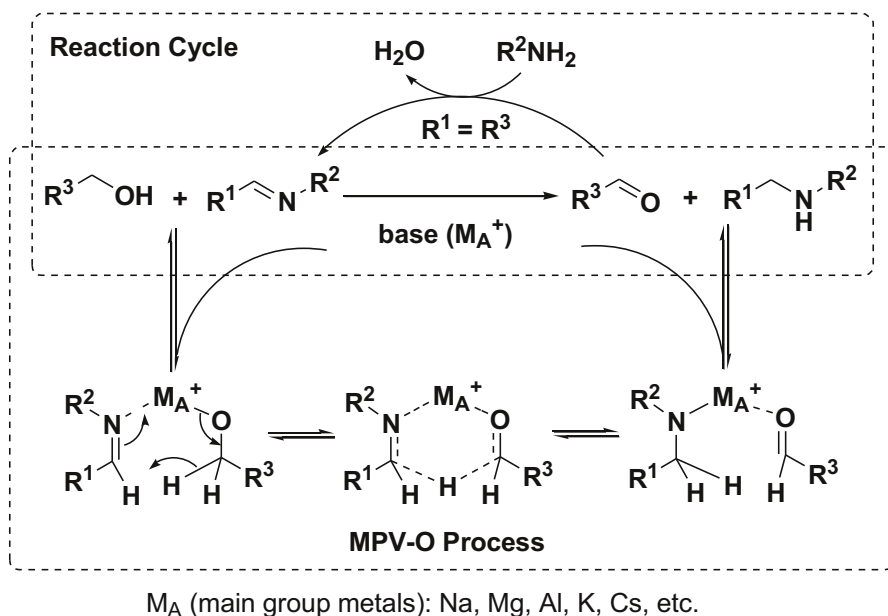
Scheme 39 Possible reaction mechanism for MPV-O N-alkylation reactions
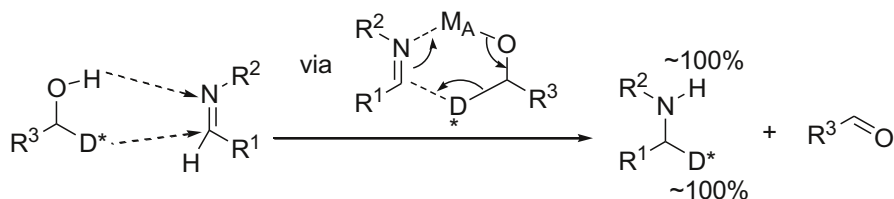
Scheme 40 Deuterium labeling of MPV-O reactions

59~99% GC conversion
93~100% NMR ratio

(65)
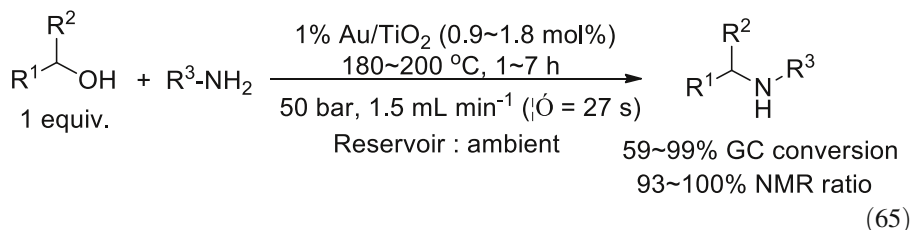
2.6 TM-Free *N*-Alkylation Reactions

TM-free *N*-alkylation reactions were first reported more than 100 years ago [4]. More reports with other methods appeared later [5–9], but these methods require rather harsh reaction conditions. Hence TM-catalyzed methods attracted much more attention and developed rapidly thereafter. It had previously been generally held that TM catalysts and dehydrogenative alcohol activation via formation of [MH]/[MH₂] species was indispensible in alcohol-based dehydrative alkylation reactions. The fact that TM-free catalysts can also be used in the same transformations seems to have been overlooked in recent decades.

2.6.1 Mechanistic Aspects of TM-Free N-Alkylation Reactions

In TM-free *N*-alkylation reactions through hydrogen autotransfer processes, the key step of the reaction mechanism is the transfer hydrogenation of the imine intermediates by alcohols. The Meerwein-Pondorf-Verley reduction of carbonyl compounds by alcohols such as isopropanol, and the Oppenauer oxidation of alcohols by carbonyl compounds such as acetone, namely MPV-O redox reactions, are well known and are widely used for the preparation of given alcohols or carbonyl compounds. It is commonly accepted that MPV-O reactions proceed by hydrogen transfer from the alcohol to the carbonyl moiety via the key six-membered cyclic transition states [52, 53]. It was proposed that, analogous to these MPV-O reactions, transfer hydrogenation of imine intermediates by alcohols most likely proceed via similar MPV-O type six-membered cyclic transition states (Scheme 39, the lower MPV-O Process) [54], in which a key main group metal cation coordinates the imine and alchol moeties in close proximity, to accomplish a concerted hydrogen transfer from the alcohol to the imine C=N bond, affording the

alkylated amine product and the carbonyl byproduct. As shown in Scheme 39 (the upper Reaction Cycle), if byproduct R^3CHO can be recovered to condense with substrate amines as the alkyl source ($R^1=R^3$) to afford new imines, then a TM-free catalytic *N*-alkylation cycle via a hydrogen autotransfer process can be achieved. Consequently, it can be inferred that, if a deuterium-labeled alcohol is used as the hydrogen source (Scheme 40), both the β–C–D* and O–H of the alcohol can be transferred selectively to become β-C-D* and N–H in the product amine. This is also the same as with the direct hydrogen transfer (Scheme 6) and monohydride (Scheme 8) routes in TM-catalyzed reactions, so that it is difficult to distinguish between them using deuterium labeling methods.

As in the alcohol activation step, like the TM-catalyzed direct hydrogen transfer route (Schemes 5, 14), the MPV-O process cannot provide carbonyl compounds directly according to the reaction mechanism (Scheme 39). This may make the alcohol activation reaction the rate-limiting step of the whole process. Most probably for this reason, the early TM-free *N*-alkylation reactions [4–9] were performed under harsh conditions to facilitate the initial formation of aldehydes by high temperature dehydrogenation of the alcohols. Otherwise, alternative ways for alcohol activation should be adopted (vide infra).

2.6.2 Recent Advances in TM-Free N-Alkylation Reactions

In 2013, based on their previous air-promoted TM-catalyzed aerobic *N*-alkylation reactions and the finding of aldehyde contaminant-accelerated reactions, Xu and co-workers further discovered that addition of external aldehydes can be a new way for alcohol activation. Thus, an efficient TM-free aldehyde-catalyzed *N*-alkylation reaction of sulfonamides, sulfinamides, anilines, heteroarylamines with benzylic and heterobenzylic alcohols was developed (Eq. 66) [54]. Since air does not affect the reactions, they could be performed readily in either air or inert atmosphere. The reactions are so efficient that they can be scaled up to at least 50 mmol scale.
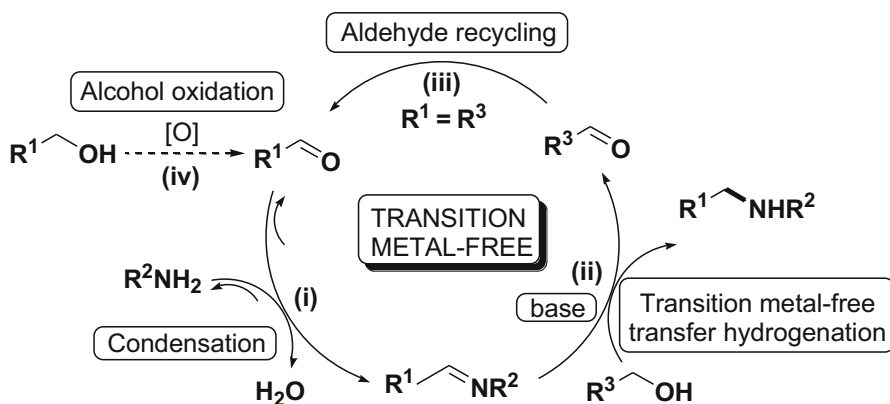
Scheme 41 Proposed mechanism for TM-free aldehyde-catalyzed *N*-alkylation reactions (TM-free relay race mechanism)
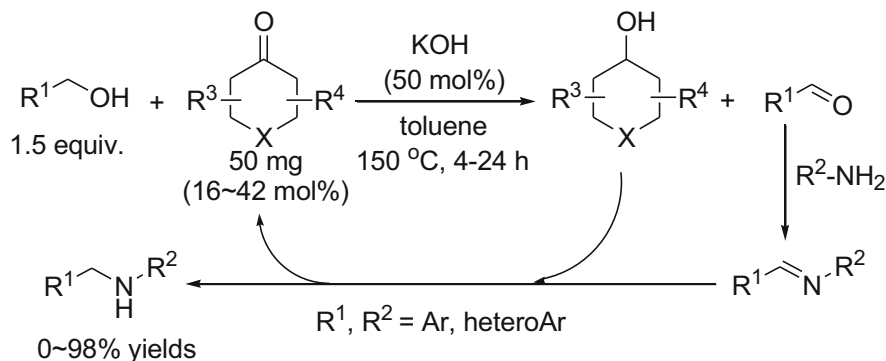
Scheme 42 Proposed mechanism for TM-free conjugated ketones-catalyzed *N*-alkylation reactions
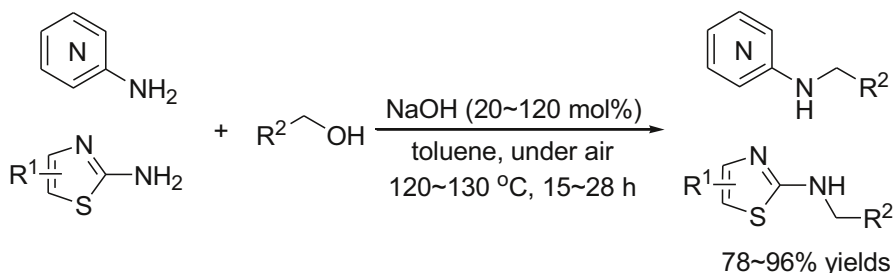
Scheme 43 NaOH-catalyzed *N*-alkylation reaction of heteroaryl amines with alcohols under air

$$R^1 = Ar, heteroAr; R^2 = RSO_2, t\text{-BuSO}, Ar, heteroAr$$
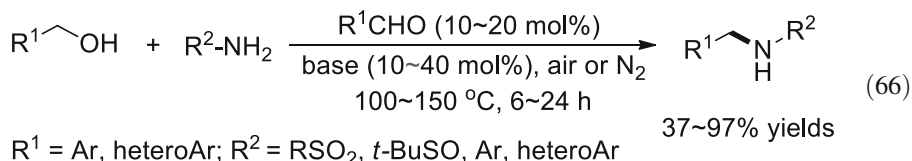
Since no reaction occurred at all in the absence of either the aldehyde catalyst or the base or both of them, as well as other proofs such as control reactions using high purity bases (>99.99 % purity), the authors concluded that the reaction is a true TM-free transformation. In addition to the aldehydes' catalytic effect, the authors proved that imine intermediates and other TM-free oxidants could also be employed to initiate the reaction, which is consistent with, and further supports, the TM-free *N*-alkylation mechanism (Scheme 39). Along with other results of mechanistic studies, the authors proposed a mechanism for the aldehyde-catalyzed *N*-alkylation reaction (Scheme 41). Firstly, the external aldehydes condense with amines/amides to give imine intermediates, which were then reduced by alcohols via a TM-free MPV-O transfer hydrogenation process to give product amines and regenerate byproduct aldehydes as the new alkyl source in next reaction cycle. In the key TM-free transfer
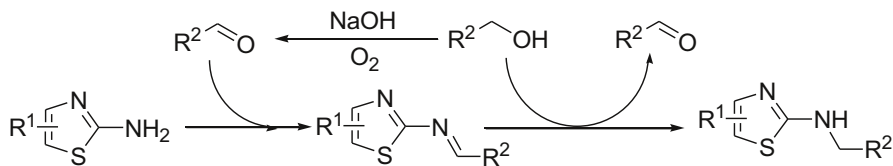
Scheme 44 Proposed mechanism for TM-free NaOH-catalyzed *N*-alkylation reactions
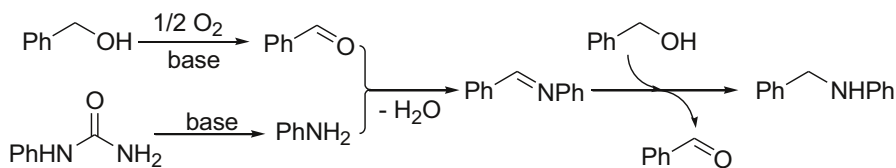
Scheme 45 Possible mechanism for base-mediated synthesis of amines from *N*-arylureas and alcohols under air

hydrogenation step, the existence of imine intermediates and generation of 1 equiv. of aldehyde to the product amine were clearly observed in ^{1}H NMR study of the reaction mixture, showing that aldehyde catalyst can be regenerated quantitatively in the process.

After discovering the catalytic activity of aldehydes, Xu and co-workers later extended the method to TM-free aldehyde-catalyzed C-alkylation of secondary alcohols with primary alcohols [199] and catalyst-free C-alkylation reactions of methyl ketones with alcohols [200]. In 2013, Wu and co-workers also reported a closely related TM-free ketone-initiated C-alkylation of indole and pyrrole with secondary alcohols [201]. Similarly, Shi and co-workers employed conjugated ketones to catalyze the TM-free *N*-alkylation reaction of amines with alcohols in 2015 (Scheme 42) [202], which is mainly suitable for benzylic and heterobenzylic alcohols, and anilines and heteroarylamines. Different ketones showed variant activities in the reaction (the catalysts were added in the same amount of 50 mg regardless of their molecular weights). In mechanistic studies such as the control reactions of the ketone catalyst and the substrate alcohol, up to 92 % ratio of the corresponding alcohol derived from reduction of the ketone catalyst can be detected in addition to formation of aldehdye intermediates derived from substrate alcohol.

In 2013, Adimurthy and co-workers reported a TM-free NaOH-catalyzed *N*-alkylation reaction of 2-aminothiazoles, 2-aminobenzothiazoles, aminopyrimidines, and aminopyridines with benzylic and heterobenzylic alcohols under air (Scheme 43) [203]. In condition optimization, the authors found the model reaction of 2-aminobenzothiazole and 4-chlorobenzylalcohol under air afforded a higher yield of the product (93 %) than the one under nitrogen (90 %). Therefore, along with other results of mechanistic studies and the authors' own previous work on based-catalyzed imine synthesis from alcohols and amines [204], they proposed that alcohol oxidation to aldehyde by air in the presence of bases is the initiation step of
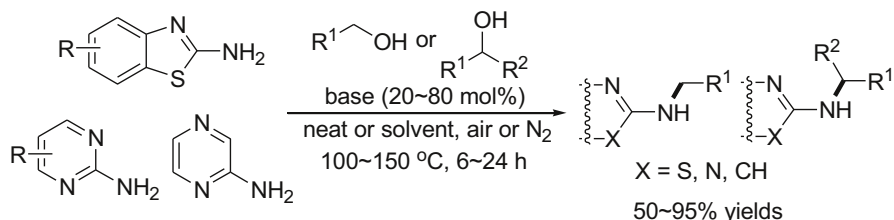
Scheme 46 Autocatalyzed *N*-alkylation of heteroaryl amines with primary and secondary alcohols
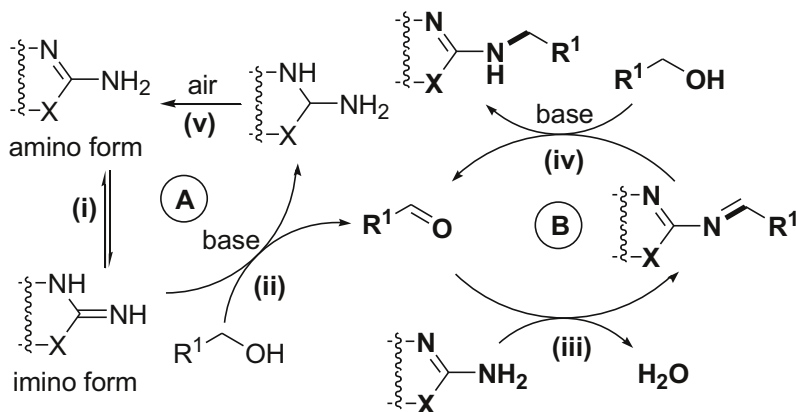
Scheme 47 Proposed mechanism for TM-free substrate heteroarylamine-autocatalyzed *N*-alkylation reactions

the *N*-alkylation reaction, followed by the condensation with amines and reduction of imine intermediate by the alcohol to give the final amine product (Scheme 44).

In 2014, Xia and co-workers also reported a base-catalyzed solvent-free *N*-alkylation of amines with alcohols under air (Eq. 67) [205]. Both aromatic and aliphatic amines and alcohols are suitable substrates. In this method, alcohols are used in large excess amounts (10 equiv.) as both the reactant and solvent, and some reactions have to be heated at high temperatures up to 220 °C. The authors also observed the significant accelerating effects of both aldehyde and imine on the reaction, concluding that they are actual intermediates of the reaction.

R^1, R^2 = aryl, heteroaryl, alkyl, cyclohexyl

20~100% GC conversions
7.3-100% selectivities

(67)
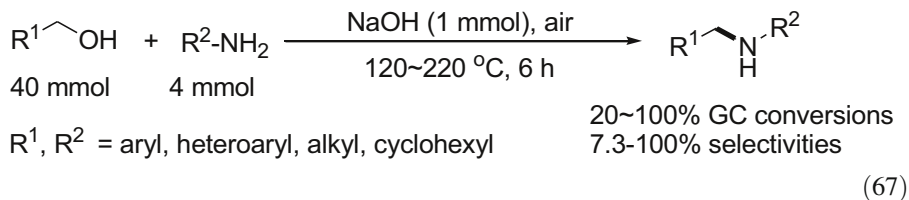
In the same year, Bhanage and co-workers reported a base-mediated synthesis of amines and imines from *N*-arylureas and benzylic alcohols or heteroaryl methanols under air (Eq. 68) [206]. The authors proposed base-mediated *N*-arylurea decomposition and aerobic alcohol oxidation processes for generation of the starting anilines and aldehydes, followed by condensation to imines and transfer hydrogenation by the alcohols to give the final amines (Scheme 45).

$$(68)$$
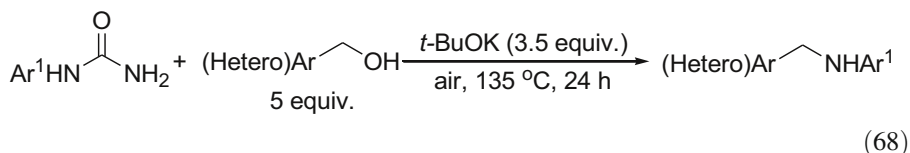
In 2015, Xu and co-workers reported a catalyst-free autocatalyzed *N*-alkylation of certain heteroaryl amines with primary and secondary alcohols (Scheme 46) [207]. Like methyl ketones in catalyst-free C-alkylation reactions [200], the authors hypothesized that certain amines with the typical RC(=X)NH$_2$ structural unit (X=O or N, etc.) may also undergo TM-free MPV-O reactions with alcohols to give the initiating aldehydes in the absence of external catalysts, which may further catalyze the target *N*-alkylation reaction. Indeed, 2-aminobenzothiazoles, 2-aminopyrimidines, and 2-aminopyrazine are active amines under critical catalyst-free conditions (pure aldehyde-free alcohol, strict degassing, and N$_2$ atmosphere protection). The model reaction of 2-aminobenzothiazole and benzyl alcohol gave a high 90 % yield of the product under the critical conditions; whereas the reaction under air slightly improved the product yield to 93 %, revealing that the autocatalyzed *N*-alkylation process
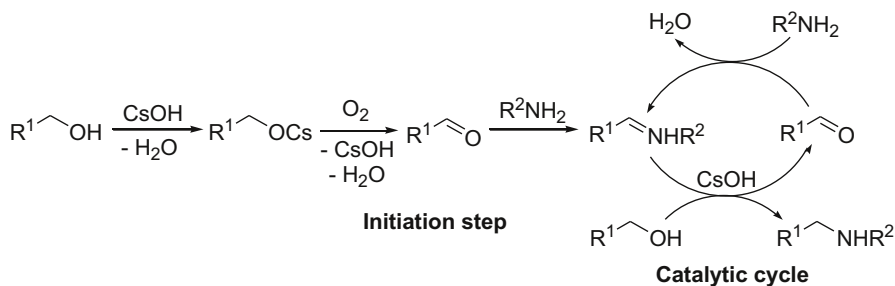
Scheme 48 Proposed mechanism for TM-free O$_2$-induced base-catalyzed *N*-alkylation reactions
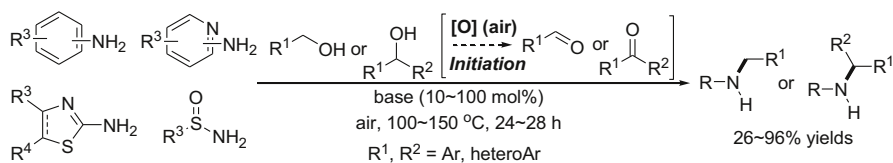
Scheme 49 TM-fee aerobic *N*-alkylation of anilines, certain heteroarylamines, and sulfinamides with alcohols under air
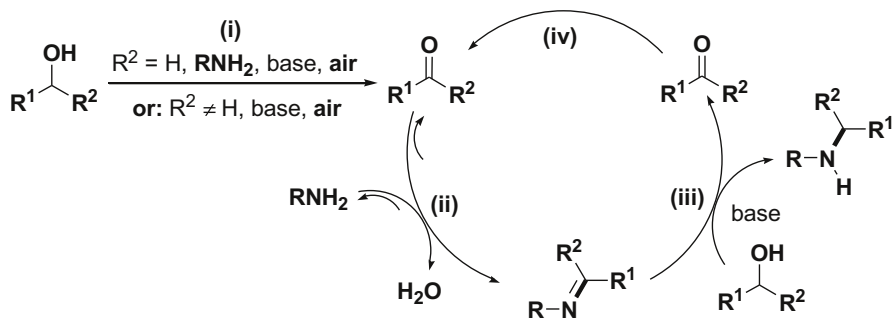
Scheme 50 Proposed mechanism for catalyst-free-like air-initiated *N*-alkylation reactions

contributed to most of the product yield. Since base-mediated aerobic alcohol oxidation by air is not possible under the critical catalyst-free conditions, they concluded that tautomerization of the heteroarylamines and MPV-O reaction of the in situ formed imino tautomer with the alcohols led to the formation of the initiating aldehydes, which then resulted in efficient *N*-alkylation reactions (Scheme 47).

In 2015, Yao, Zhao, and co-workers reported a base-catalyzed *N*-alkylation of anilines and heteroarylamines with benzylic, heterobenzylic, aliphatic alcohols using catalytic amounts of O_2 as the initiator (Eq. 69) [208]. They found air or O_2 play important roles in the reactions because the reactions under O_2 or in open air led to formation of imines in high ratios. The authors further optimized the reaction conditions and found that adding 2–5 mol% O_2 to the reaction vessel was the best, giving high yields and selectivies of the product amines. Therefore, they proposed a mechanism for the *N*-alkylation reaction that was initiated by base-catalyzed aerobic alcohol oxidation by O_2 to the aldehydes (Scheme 48).
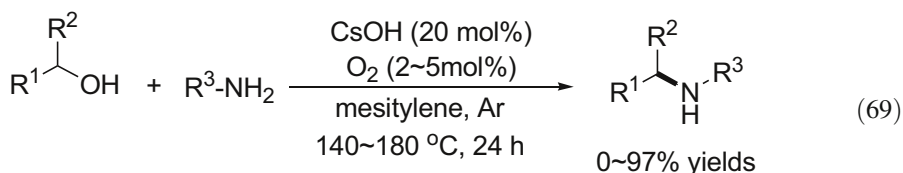
$$\text{R}^1, \text{R}^3 = \text{Ar, heteroAr, R}; \text{R}^2 = \text{H, Ar, R}$$

In 2016, Xu and coworker reported another TM-fee aerobic *N*-alkylation method for anilines, some heteroarylamines, and sulfinamides with alcohols (Scheme 49) [209]. As described in their work, these amines are not effective substrates under anaerobic catalyst-free autocatalyzed conditions, so an oxidant has to be employed to initiate the reaction. Differing from Yao and Zhao's protocol by adding O_2 to an argon atmosphere [208], they found that a catalytic amount of air is active enough to initiate the reaction. In addition to primary alcohols, secondary alcohols can also be used as the alkyl source. In mechanistic studies, the authors observed that primary and secondary alcohols underwent different initiation processes, i.e., primary alcohols require the presence of the amine to facilitate the aerobic oxidation to
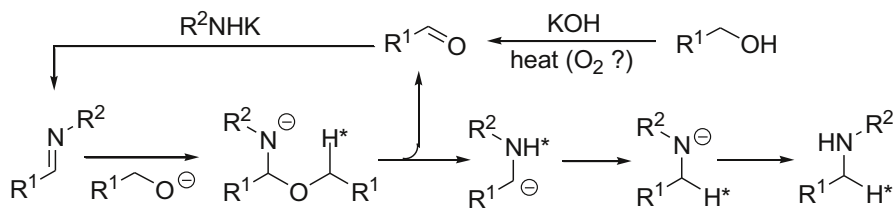
Scheme 51 Proposed mechanism for TM-free base-mediated *N*-alkylation reactions

aldehydes, while secondary alcohols can be transformed directly to ketones by air in the presence of a base (Scheme 50).

In 2015, Kang and coworkers reported another TM-free base-mediated *N*-alkylation reaction of sulfonamides and alcohols under argon (Eqs. 70, 71, 72) [210]. The authors found that the stronger base KOH is a better base for the reaction, and large excess alcohol was used as both reactant and solvent (Eq. 70); whereas, if corresponding basic salt potassium sulfonamides were employed instead, KOH can be used in catalytic amounts (Eq. 71). The reactions of anilines, heteroarylamines, and heterobenzylic and aliphatic alcohols also yielded corresponding alkylated amines efficiently in the presence of excess alcohols and 3 equiv. of base (Eq. 72). Since potassium sulfonamides were used as the reactant, and the reaction conditions are rather different (much stronger basicity) to previous aldehyde-catalyzed methods using only catalytic amounts of weak base K_2CO_3 [54], and no imine intermediates were detected in the present reactions, the authors excluded the possibility of an aldehyde-catalyzed mechanism and the MPV-O transfer hydrogenation process [52–54], and proposed a new mechanism (Scheme 51) involving the addition of potassium alcoholate to the imine intermediates to give hemiaminal intermediates. As to the initial aldehyde formation step, the authors proposed that oxidation of the alcohols by trace O_2 in the reaction systems might be a possible means of aldehyde generation [although alcohols with aldehyde contaminants (<0.1 %) were used, and trace amounts of H_2 were detected by GC in control reactions under the argon atmosphere as described in the work].

Scheme 52 General mechanism for amine-based hydrogen autotransfer reactions
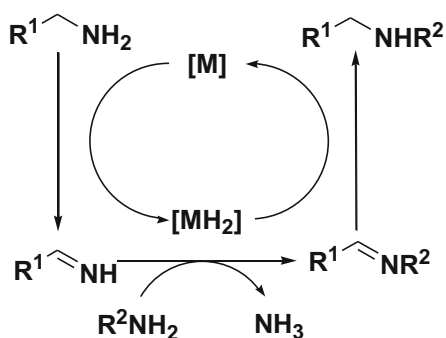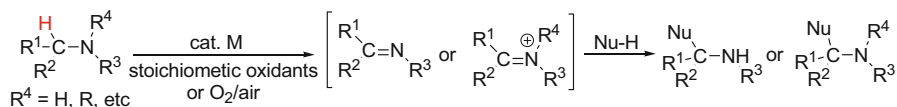
Scheme 53 General reaction routes for cross-dehydrogenative-coupling (CDC) reactions

$$Ph\!-\!\!\!\!\overset{}{\frown}\!\!\!\!OH + p\text{-TolSO}_2\text{NH}_2 \xrightarrow[\text{Ar, 130 °C, 10 h}]{\text{base (130 mol\%)}} Ph\!-\!\!\!\!\overset{}{\frown}\!\!\!\!\overset{\text{SO}_2p\text{-Tol}}{\underset{\text{H}}{N}}$$

10 equiv.

0–95% yields

(70)

$$R^1\!-\!\!\!\!\overset{}{\frown}\!\!\!\!OH + R^2\text{SO}_2\text{NHK} \xrightarrow[\text{Ar, 130 °C}]{\text{KOH (5~50 mol\%)}} R^1\!-\!\!\!\!\overset{}{\frown}\!\!\!\!\overset{\text{SO}_2R^2}{\underset{\text{H}}{N}}$$

10 equiv.

R^1 = Ar, HeteroAr; R^2 = Ar, HeteroAr, Me

81~99% yields

(71)

$$R^1\!-\!\!\!\!\overset{}{\frown}\!\!\!\!OH + R^2\text{-NH}_2 \xrightarrow[\text{Ar, 130~160 °C}]{\text{KOH or NaH (3 equiv.)}} R^1\!-\!\!\!\!\overset{}{\frown}\!\!\!\!\overset{R^2}{\underset{\text{H}}{N}}$$

10 equiv.

R^1 = Ar, HeteroAr, R; R^2 = Ar, HeteroAr

41~99% yields

(72)
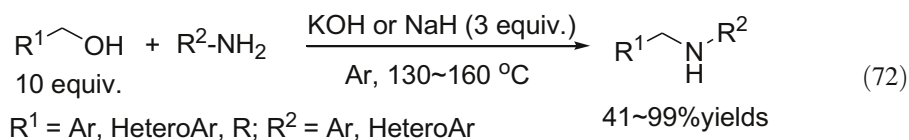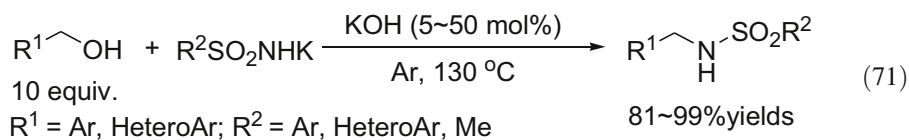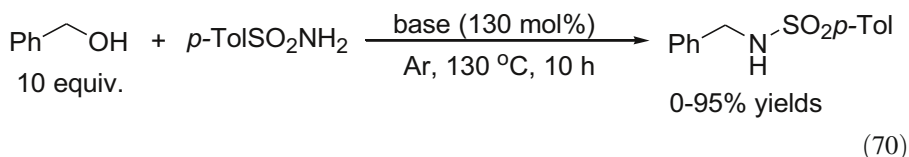
3 Hydrogen Autotransfer *N*-Alkylation Reactions Using Amines as the Alkylating Reagents

Like alcohols, amines could also be used as alkylating reagents to react with another amine to give *N*-alkylated amine products [10, 26], librating NH$_3$ as the byproduct instead of H$_2$O as in the case of alcohols. It is also held that amine activation proceeds via a hydrogen autotransfer process similar to that of alcohol activation. As shown in Scheme 52, the primary amine is first dehydrogenated, and then condenses with another amine to give different imine intermediates sequentially, which are reduced to give product amines. In addition to primary amines, secondary and tertiary amines could also be used as alkylating reagents.

It should be pointed out that this type of amine activation by anaerobic dehydrogenation resembles the cross-dehydrogenative-coupling (CDC) reactions [42, 43], in which the amine substrates, usually the secondary and tertiary amines, were also dehydrogenated/oxidized to give imines or iminium intermediates under oxidative conditions as the substrate activation protocol (Scheme 53). The difference is, in CDC reactions, no condensation/deamination reactions occur, and

the reaction proceeds via addition of nucleophiles, usually not an *N*-nucleophile, to give addition products.

Since the first homogeneous catalytic self-*N*-alkylation of amines reported by the groups of Laine and Concilio independently in the beginning of 1980s [211–213], more TM catalysts such as [Ru], [Ir], [Os], [Rh] and [Pt] have also been developed in the past two decades [10, 26]. More recently, effective cross-*N*-alkylation of two different amines, with low catalyst loadings, or those at lower temperatures were also reported.

In 2007, Beller and co-workers described the first additive-free homogeneous *N*-alkylation of (hetero)aryl amines with aliphatic amines catalyzed by the Shvo complex with a low catalyst loading (1 mol%) (Eq. 73) [214]. The reactions of some challenging substrates, such as cyclic secondary amines, furan-, thiophene-, and indole-substituted amines, could also afford the corresponding products with good yields by this method.

$$R^1 = Ar, alkyl; R^2 = H, alkyl; R^3 = aryl, heteroAr$$

$$(73)$$
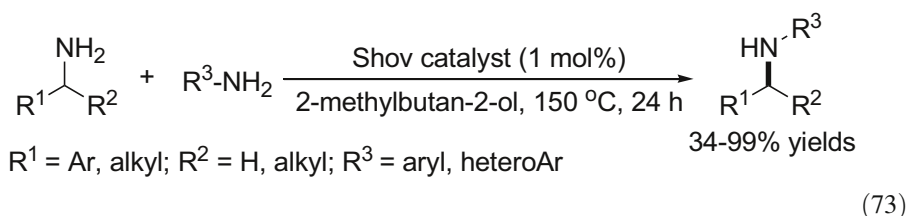
In 2008, the Beller group extended the method to the *N*-alkylation of aryl amines with secondary amines and tertiary amines (Eq. 74) [215]. In the same year, they further applied the method to the *N*-alkylation of *tert*-alkylamines with aliphatic amines [216]. In 2011, the Beller group also reported the synthesis of primary amines by the reaction of secondary and tertiary amines with ammonia catalyzed by Shov catalyst (Eq. 75) [217].

$$(74)$$

$$(75)$$
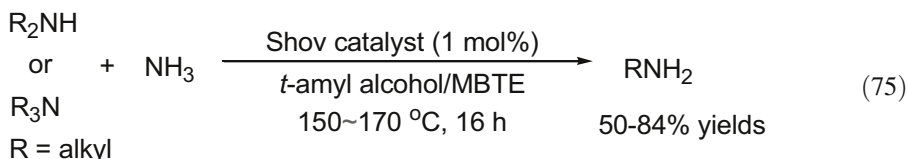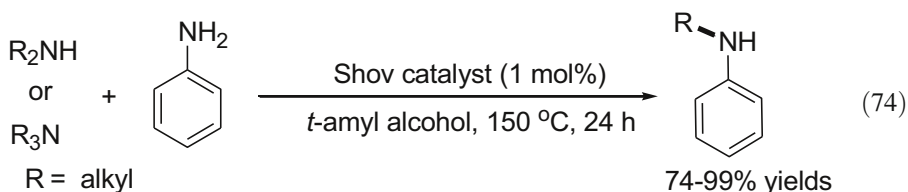
In 2008, Peris and coworkers developed an iridium complex (**35**)-catalyzed *N*-alkylation of anilines with alkyl amines (Eq. 76) [218]. The authors have previously

found that iridium complex **35** has similar activity with Shvo complex in the same year [219].

$$\text{Ar-NH}_2 \;+\; \text{R-NH}_2 \xrightarrow[\text{toluene, 150 °C, 24 h}]{\substack{\text{cat. } \mathbf{35}\ (5\ \text{mol\%}) \\ \text{AgOTf (15 mol\%)}}} \text{R-NH-Ar}$$

R = alkyl

50~95% yields

(76)

35
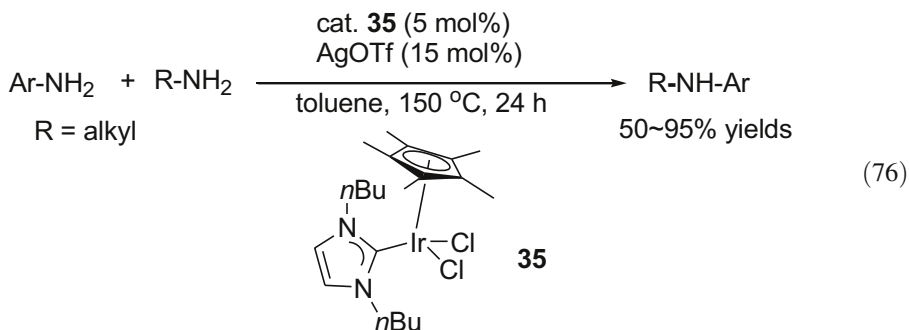
In 2009, Williams and co-workers described the [Cp*IrI$_2$]$_2$-catalyzed *N*-alkylation of anilines, benzylic and aliphatic primary amines with diisopropylamine (Eq. 77) [220]. Although both substrate amines could be oxidized to give different imines and possibly different product amines, excellent selectivity could still be obtained. For example, the reaction of diisopropylamine and benzylamine gave exclusively *N*-isopropyl-*N*-benzylamine without any tertiary amine and dibenzylamine byproducts.

$$\text{RNH}_2 \;+\; i\text{-Pr}_2\text{NH} \xrightarrow[\text{xylene, 155 °C, 10 h}]{\text{[Cp*IrI}_2\text{]}_2\ (1\ \text{mol\%})} \text{RNH}i\text{-Pr}$$

R = Ar, arkyl

26~99% yields

(77)
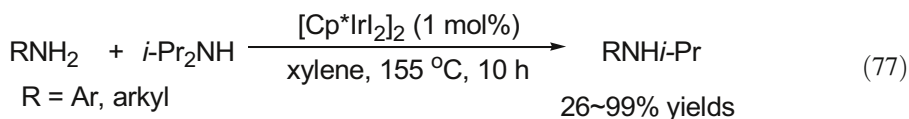
The aforementioned cyclometallated iridium complex **14** developed by Xiao and co-workers was also effective for *N*-alkylation of anilines and even benzohydrazide with diisopropylamine under mild conditions (Eq. 78) [113].

$$\text{RNH}_2 \;+\; i\text{-Pr}_2\text{NH} \xrightarrow[\text{TFE, 100 °C, 24 h}]{\substack{\text{cat. } \mathbf{14}\ (1\ \text{mol\%}) \\ \text{K}_2\text{CO}_3\ (5\ \text{mol\%})}} \text{RNH}i\text{-Pr}$$

R = Ar, PhCONH

48~99% yields

(78)

14
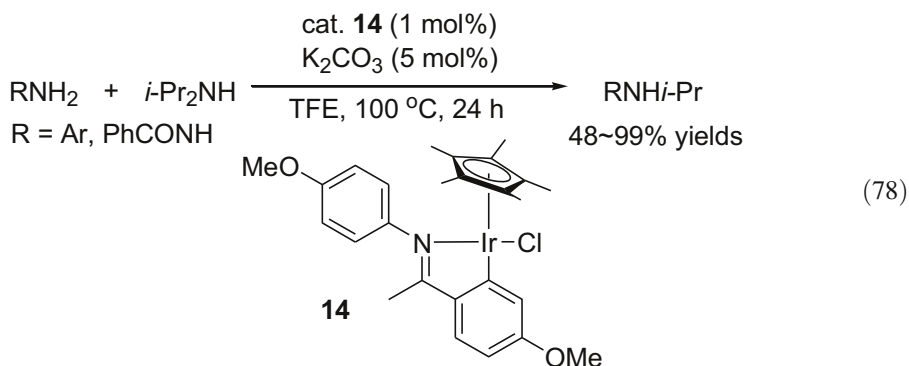
In addition to homogeneous TM catalysts, some heterogeneous TM catalysts, nano catalysts and even biomimetic and electrolytic catalysts have also been applied

successfully in the *N*-alkylation of amines using amines as the alkylating reagents. In 2011, Shimizu and co-workers reported a nano-Pd1/Al$_2$O$_3$-1.8-catalyzed cross-coupling of amines (Eq. 79) [221]. The recovered catalyst showed a very close catalytic activity with the fresh one (1st, 86 %, 2nd, 85 %). In the same year, Porcheddu and co-workers reported a microwave-assisted Pd/C-catalyzed *N*-alkylation of anilines with tertiary amines [222].

$$R^1{\diagdown}NH_2 \ + \ R^2{\diagdown}N(H){\diagup}R^3 \ \xrightarrow[\text{\textit{o}-xylene, reflux, 1~20 h}]{\text{Pd1/Al}_2\text{O}_3\text{-1.8 (1 mol\%)}} \ R^1{\diagup}N(R^3){\diagdown}R^2$$

R^1 = Ar, heteroAr, alkyl; R^2 = alkyl; R^3 = alkyl   44~85% yields
Pd1/Al$_2$O$_3$ recoverable: 1st, 86%; 2nd, 85%

(79)
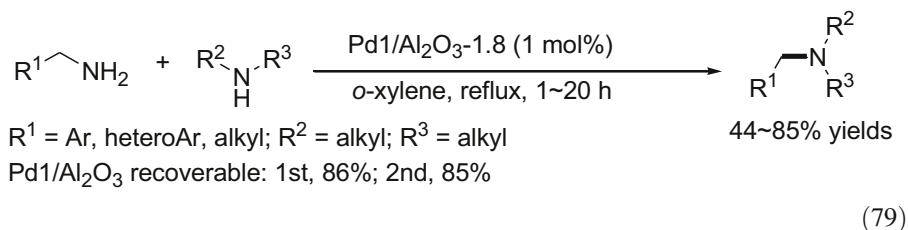
The aforementioned Pt–Sn/γ-Al$_2$O$_3$ catalyst developed by Yu and co-workers in 2011 was also effective for self-coupling of aliphatic primary amines with catalyst loading as low as 0.25 mol% (Eq. 80) [142]. In 2012, Shimizu and co-workers found nano-NaPt/SiO$_2$ and nano-SPt/SiO$_2$ are both effective catalysts for the *N*-alkylation of anilines, secondary and branched primary amines [223, 224]. In 2013, Shi and co-workers accidentally found that NiCuFeO$_x$ complex could catalyze the self-*N*-alkylation of primary amines [157].

$$R{\diagdown}NH_2 \ \xrightarrow[\text{\textit{o}-xylene, 145 °C, 24~36 h}]{\text{Pt-Sn/Al}_2\text{O}_3\text{ (0.25~0.5 mol\%)}} \ R{\diagdown}N(H){\diagdown}R$$

R = Ar, alkyl   87~95% yields   (80)
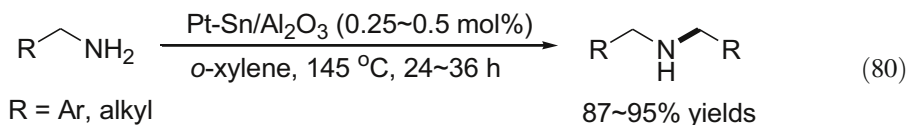
In 2009, Largeron and co-workers reported a biomimetic electrolytic synthesis of secondary benzylic amines at room temperature (Scheme 54) [224]. An initial
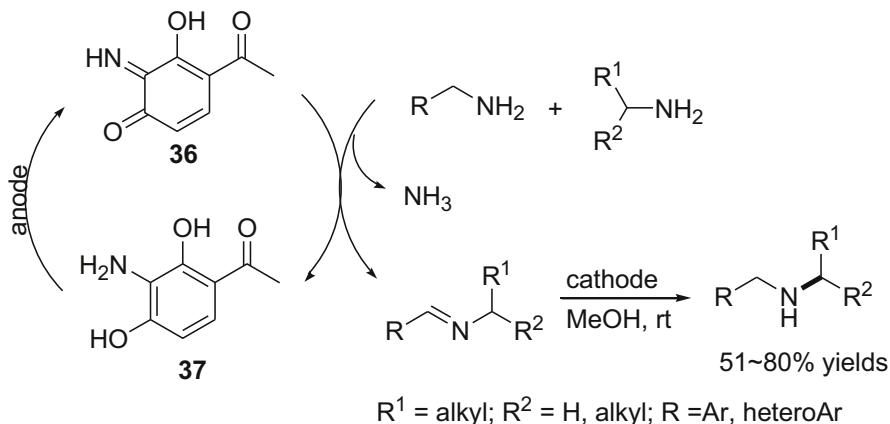
Scheme 54 Proposed mechanism for biomimetic electrolytic synthesis of secondary amines

electrochemical oxidation of the benzylic amines by *o*-iminoquinone **36** and a subsequent condensation gave imine intermediates, which were then reduced to give the desired secondary amines along with the reoxidation of **37** to **36**.

4 Conclusion and Outlook

In summary, owing to their green and environmentally benign features, alcohols have been used widely as the alkylating reagents in the synthesis of amine and amide derivatives through dehydrogenative/oxidative activation to the more active carbonyl compounds and transfer of hydrogens to the products. Like alcohols, amines can also be used in a similar way as the alkylating reagents. This field developed rapidly in the past decades, being one of the hottest topics in the fields of organometallic catalysis, green chemistry, and even the pharmaceutical and industrial chemistry. More recently, in addition to TM-catalyzed anaerobic dehydrogenation methods, air-participated TM-catalyzed aerobic oxidative reactions using air-stable catalysts, nano and carbon materials, and biocatalysts have also been found to be new ways for alcohol activation and new catalysts. Some catalysts are so efficient that either bio-derived alcohols can be used as the alkylating reagents or the reactions can be performed under rather mild conditions at relatively lower temperatures (below 100 °C) or in an aqueous media. Meanwhile, new TM-free organocatalytic methods, including the use of aldehydes, substrate or external ketones, substrate amines, and the combination of air and base have also been developed as simple but efficient, economical and practical methods for *N*-alkylation of amines and amides with alcohols, and also represent meaningful advances to the early TM-free *N*-alkylation methods performed under harsh conditions [5–9]. Moreover, the recent development of asymmetric *N*-alkylation reactions for the successful synthesis of chiral amines and direct application of the *N*-alkylation method in pharmaceutical synthesis have also revealed the great potential of *N*-alkylation reactions. With the development of the new catalysts, new methods, and new protocols for alcohol activation, new concepts such as substrate-participated autocatalysis have also appeared in the field.

However, problems and bottlenecks still remain. Unlike the alcohols, new methods for using amines as alkylating reagents are still rare. This may be due to limited methods for amine activation. Like the newly developed aerobic oxidative activation of alcohols, advances in amines' cross-dehydrogenative coupling (CDC) reactions [42, 43] and amine oxidation reactions [226–229] may provide new possibilities for amine-based alkylation reactions. Besides, present mild and asymmetric reactions are still catalyzed by homogeneous metal complexes, so that developing efficient and recoverable heterogeneous methods would thus be another meaningful advance in the field. Moreover, most of the TM-free methods seemed to have limited scope for substrates, otherwise harsh conditions have to be applied. Therefore, developing new TM-free methods with relatively broad substrate scope and/or under mild reaction conditions remains a meaningful research topic in this field. Computational mechanistic studies of these TM-free reactions in order to acquire deeper insight and theoretical understanding of the reaction mechanism may

also help to develop new TM-free methods avoiding the use of expensive homogeneous catalysts and tedious preparation of heterogenous catalysts. In addition, mechanism elucidation in *N*-alkylation reactions by the hydrogen autotransfer processes remains a challenge, since: (1) there are mainly two mechanistic types in the reactions of amines/amides with alcohols (i.e., the direct nucleophilic substitution reactions and the hydrogen autotransfer processes), (2) there are at least four possible routes for hydrogen transfer from alcohols to products (direct hydrogen transfer, monohydride route, dihydride route, and MPV-O process), (3) similarities exist among the four routes of the hydrogen autotransfer reactions so that it is difficult to distinguish them as well as the reaction mechanism, and (4) mechanisms of specific reactions may vary depending on the substrates, catalysts, reaction conditions, even the settled conditions for mechanistic studies (e.g., in the sect. 2.1.3, the DFT studies of Ir-catalyzed *N*-alkylation reactions by different groups showed slightly different results). Mechanistic studies of the *N*-alkylation reaction are significant to this research also because they may afford new/deeper insights into the nature of the reactions, and provide new research opportunities and even conceptual and technical advances in the field. In a word, although there have been many meaningful advances in the field in recent decades, there still remains much room for improvement and extension of research. *N*-alkylation reactions by hydrogen autotransfer processes may have entered a new stage of development deserving of more attention and effort.

References

1. Salvatore RN, Yoon CH, Jung KW (2001) Synthesis of secondary amines. Tetrahedron 57(37):7781–7785
2. Hofmann AW (1850) Researches regarding the molecular constitution of the volatile organic bases. Phil Trans R Soc Lond 140:93–141
3. McMurry J (2008) Organic chemistry, 7th edn. Thomson, Brooks/Cole, Boston
4. Nef JU (1901) Dissociationsvorgänge bei den einatomigen alkoholen, aethern und salzen. Liebigs Ann Chem 318(2–3):137–230
5. Lazier WA, Adkins H (1924) The alkylation of primary amines with aluminum alkoxides to give secondary amines free from tertiary amines. J Am Chem Soc 46(3):741–746
6. Sprinzak Y (1956) Reduction and benzylation by means of benzyl alcohol. II. *N*-benzylation. The preparation of secondary aromatic benzylamines. J Am Chem Soc 78(13):3207–3208
7. Miyano S (1965) Syntheses of *N*-(2-Pyridylmethyl)aniline and its derivatives. Chem Pharm Bull 13(9):1135–1137
8. Zvezdina EA, Pozharskii AF, Sokolov VI (1970) Imidazole derivatives containing potentially labile groupings attached to an *N*-atom. Chem Heterocycl Compd 6(3):389–391
9. Miyano S, Nakao M (1972) *N*-Alkylation of aromatic amines by means of alcohol. IV. Syntheses of *N*-alkylanilines and related compounds. Chem Pharm Bull 20(6):1328–1331
10. Guillena G, Ramón DJ, Yus M (2010) Hydrogen autotransfer in the *N*-alkylation of amines and related compounds using alcohols and amines as electrophiles. Chem Rev 110(3):1611–1641
11. Roundhill DM (1992) Transition metal and enzyme catalyzed reactions involving reactions with ammonia and amines. Chem Rev 92(1):1–27

12. Shimizu KI (2015) Heterogeneous catalysis for the direct synthesis of chemicals by borrowing hydrogen methodology. Catal Sci Technol 5(3):1412–1427
13. Grigg R, Mitchell TRB, Sutthivaiyakit S, Tongpenyai N (1981) Transition metal-catalysed N-alkylation of amines by alcohols. J Chem Soc, Chem Commun 12:611–612
14. Watanabe Y, Tsuji Y, Ohsugi Y (1981) The ruthenium catalyzed N-alkylation and N-heterocyclization of aniline using alcohols and aldehydes. Tetrahedron Lett 22(28):2667–2670
15. Murahashi S-I, Kondo K, Hakata T (1982) Ruthenium catalyzed synthesis of secondary or tertiary amines from amines and alcohols. Tetrahedron Lett 23(2):229–232
16. Muzart J (2005) Palladium-catalysed reactions of alcohols. Part B: formation of C-C and C-N bonds from unsaturated alcohols. Tetrahedron 61(17):4179–4212
17. Detz RJ, Hiemstra H, van Maarseveen JH (2009) Catalyzed propargylic substitution. Eur J Org Chem 36:6263–6276
18. Emer E, Sinisi R, Cozzi PG et al (2011) Direct nucleophilic SN1-type reactions of alcohols. Eur J Org Chem 4:647–666
19. Bandini M, Cera G, Chiarucci M (2012) Catalytic enantioselective alkylations with allylic alcohols. Synthesis 4:504–512
20. Chen L, Yin XP, Zhou J et al (2014) Catalytic functionalization of tertiary alcohols to fully substituted carbon centres. Org Biomol Chem 12(32):6033–6048
21. Plaut H, Ritter JJ (1951) A new reaction of nitriles. VI. Unsaturated amides1. J Am Chem Soc 73(9):4076–4077
22. Guérinot A, Reymond S, Cossy J (2012) Ritter reaction: recent catalytic developments. Eur J Org Chem 1:19–28
23. Hamid MHSE, Slatford P, Williams JMJ (2007) Borrowing hydrogen in the activation of alcohols. Adv Synth Catal 349(10):1555–1575
24. Nixon TD, Whittlesey MK, Williams JMJ (2009) Transition metal catalysed reactions of alcohols using borrowing hydrogen methodology. Dalton Trans 5:753–762
25. Watson AJA, Williams JMJ (2010) The give and take of alcohol activation. Science 329:635–636
26. Dobereiner GE, Crabtree RH (2010) Dehydrogenation as a substrate-activating strategy in homogeneous transition-metal catalysis. Chem Rev 110(2):681–703
27. Suzuki T (2011) Organic synthesis involving iridium-catalyzed oxidation. Chem Rev 111(3):1825–1845
28. Bähn S, Imm S, Beller M et al (2011) The catalytic amination of alcohols. ChemCatChem 3(12):1853–1864
29. Yang Q, Wang Q, Yu Z (2015) Substitution of alcohols by N-nucleophiles via transition metal-catalyzed dehydrogenation. Chem Soc Rev 44(8):2305–2329
30. Marr AC (2012) Organometallic hydrogen transfer and dehydrogenation catalysts for the conversion of bio-renewable alcohols. Catal Sci Technol 2(2):279–287
31. Hollmann D (2014) Advances in asymmetric borrowing hydrogen catalysis. ChemSusChem 7(9):2411–2413
32. Leonard J, Blacker AJ, Marsden SP et al (2015) A survey of the borrowing hydrogen approach to the synthesis of some pharmaceutically relevant intermediates. Org Pro Res Deve 19(10):1400–1410
33. K-I Fujita, Yamaguchi R (2005) Cp*Ir complex-catalyzed hydrogen transfer reactions directed toward environmentally benign organic synthesis. Synlett 4:560–571
34. Yamaguchi R, K-I Fujita, Zhu M (2010) Recent progress of new catalytic synthetic methods for nitrogen heterocycles based on hydrogen transfer reactions. Heterocycles 81(5):1093–1140
35. Xu Q, Li Q (2013) Recent advances of transition metal-catalyzed aerobic dehydrative reactions of alcohols and amines and related researches. Chin J Org Chem 33(1):18–35
36. Sheldon RA, Arends IW, Dijksman A et al (2002) Green, catalytic oxidations of alcohols. Acc Chem Res 35(9):774–781
37. Hashmi ASK (2007) Gold-catalyzed organic reactions. Chem Rev 107(7):3180–3211
38. Naota T, Takaya H, Murahashi SI (1998) Ruthenium-catalyzed reactions for organic synthesis. Chem Rev 98(7):2599–2660
39. Sigman MS, Jensen DR (2006) Ligand-modulated palladium-catalyzed aerobic alcohol oxidations. Acc Chem Res 39(3):221–229
40. Stahl SS (2004) Palladium oxidase catalysis: selective oxidation of organic chemicals by direct dioxygen-coupled turnover. Angew Chem Int Ed 43(26):3400–3420

41. Zhan BZ, Thompson A (2004) Recent developments in the aerobic oxidation of alcohols. Tetrahedron 60(13):2917–2935
42. Li CJ (2008) Cross-dehydrogenative coupling (CDC): exploring C–C bond formations beyond functional group transformations. Acc Chem Res 42(2):335–344
43. Scheuermann CJ (2010) Beyond traditional cross couplings: the scope of the cross dehydrogenative coupling reaction. Chem Asian J 5(3):436–451
44. Blackburn L, Taylor RJK (2001) In situ oxidation-imine formation-reduction routes from alcohols to amines. Org Lett 3(11):1637–1639
45. Guérin C, Bellosta V, Cossy J et al (2011) Mild nonepimerizing N-alkylation of amines by alcohols without transition metals. Org Lett 13(13):3534–3537
46. Zassinovich G, Mestroni G, Gladiali S (1992) Asymmetric hydrogen transfer reactions promoted by homogeneous transition metal catalysts. Chem Rev 92(5):1051–1069
47. Palmer MJ, Wills M (1999) Asymmetric transfer hydrogenation of C=O and C=N bonds. Tetrahedron Asymmetry 10(11):2045–2061
48. Gladiali S, Alberico E (2006) Asymmetric transfer hydrogenation: chiral ligands and applications. Chem Soc Rev 35(3):226–236
49. Bäckvall JE (2002) Transition metal hydrides as active intermediates in hydrogen transfer reactions. J Organomet Chem 652(1):105–111
50. Samec JS, Bäckvall JE, Andersson PG et al (2006) Mechanistic aspects of transition metal-catalyzed hydrogen transfer reactions. Chem Soc Rev 35(3):237–248
51. Muzart J (2015) Pd-Catalyzed Hydrogen-Transfer Reactions from Alcohols to C=C, C=O, and C=N Bonds. Eur J Org Chem 2015(26):5693–5707
52. Cha JS (2006) Recent developments in Meerwein-Ponndorf-Verley and related reactions for the reduction of organic functional groups using aluminum, boron, and other metal reagents: a review. Org Pro Res Deve 10(5):1032–1053
53. De Graauw CF, Peters JA, Huskens J et al (1994) Meerwein-Ponndorf-Verley reductions and Oppenauer oxidations: an integrated approach. Synthesis 10:1007–1017
54. Xu Q, Li Q, Zhu X et al (2013) Green and scalable aldehyde-catalyzed transition metal-free dehydrative N-alkylation of amides and amines with alcohols. Adv Syn Catal 355(1):73–80
55. Crabtree RH (2011) An organometallic future in green and energy chemistry? Organometallics 30(1):17–19
56. Gunanathan C, Ben-David Y, Milstein D (2007) Direct synthesis of amides from alcohols and amines with liberation of H$_2$. Science 317(5839):790–792
57. Balcells D, Crabtree RH, Eisenstein O et al (2008) Mechanism of homogeneous iridium-catalyzed alkylation of amines with alcohols from a DFT study. Organometallics 27(11):2529–2535
58. Fristrup P, Tursky M, Madsen R (2012) Mechanistic investigation of the iridium-catalysed alkylation of amines with alcohols. Org Biomol Chem 10(13):2569–2577
59. Zhao G-M, Liu H-L, Huang X-R et al (2015) Mechanistic study on the Cp* iridium-catalyzed N-alkylation of amines with alcohols. RSC Adv 5(29):22996–23008
60. Bartoszewicz A, González Miera G, Martín-Matute B et al (2015) Mechanistic studies on the alkylation of amines with alcohols catalyzed by a bifunctional iridium complex. ACS Catal 5(6):3704–3716
61. Nova A, Crabtree RH, Eisenstein O et al (2010) An experimental-theoretical study of the factors that affect the switch between ruthenium-catalyzed dehydrogenative amide formation versus amine alkylation. Organometallics 29(23):6548–6558
62. Zhao G-M, Liu H-L, Huang X-R et al (2014) DFT study on mechanism of N-alkylation of amino derivatives with primary alcohols catalyzed by copper(II) acetate. ACS Catal 4(7):2231–2240
63. Zhao G-M, Liu H-L, Huang X-R et al (2015) DFT study on the homogeneous palladium-catalyzed N-alkylation of amines with alcohols. ACS Catal 5(10):5728–5740
64. Hamid MHSA, Williams JMJ (2007) Ruthenium-catalysed synthesis of tertiary amines from alcohols. Tetrahedron Lett 48(47):8263–8265
65. Hamid MHSA, Allen CL, Williams JMJ et al (2009) Ruthenium-catalyzed N-alkylation of amines and sulfonamides using borrowing hydrogen methodology. J Am Chem Soc 131(5):1766–1774
66. Watson AJ, Maxwell AC, Williams JM (2011) Borrowing hydrogen methodology for amine synthesis under solvent-free microwave conditions. J Org Chem 76(7):2328–2331
67. Ma WMJ, James TD, Williams JMJ (2013) Synthesis of amines with pendant boronic Esters by borrowing hydrogen catalysis. Org Lett 15(18):4850–4853

68. Tillack A, Hollmann D, Beller M et al (2006) A novel ruthenium-catalyzed amination of primary and secondary alcohols. Tetrahedron Lett 47(50):8881–8885
69. Hollmann D, Tillack A, Beller M et al (2007) An improved ruthenium catalyst for the environmentally benign amination of primary and secondary alcohols. Chem-Asian J 2(3):403–410
70. Tillack A, Hollmann D, Beller M et al (2008) Salt-free synthesis of tertiary amines by ruthenium-catalyzed amination of alcohols. Eur J Org Chem 28:4745–4750
71. Imm S, Bahn S, Beller M et al (2010) An efficient and general synthesis of primary amines by ruthenium-catalyzed amination of secondary alcohols with ammonia. Angew Chem Int Ed 49(44):8126–8129
72. Pingen D, Muller C, Vogt D (2010) Direct amination of secondary alcohols using ammonia. Angew Chem Int Ed 49(44):8130–8133
73. Gunanathan C, Milstein D (2008) Selective synthesis of primary amines directly from alcohols and ammonia. Angew Chem Int Ed 47(45):8661–8664
74. Ye X, Plessow PN, Hofmann P (2014) Alcohol amination with ammonia catalyzed by an acridine-based ruthenium pincer complex: a mechanistic study. J Am Chem Soc 136(16):5923–5929
75. Pingen D, Vogt D (2014) Amino-alcohol cyclization: selective synthesis of lactams and cyclic amines from amino-alcohols. Catal Sci Technol 4(1):47–52
76. Bahn S, Williams JMJ, Beller M (2010) Selective ruthenium-catalyzed *N*-alkylation of indoles by using alcohols. Chem-Eur J 16(12):3590–3593
77. Whitney S, Grigg R, Keep A (2007) [Cp* IrCl$_2$]$_2$-catalyzed indirect functionalization of alcohols: novel strategies for the synthesis of substituted indoles. Org Lett 9(17):3299–3302
78. Zhang M, Imm S, Beller M et al (2011) Synthesis of alpha-amino acid amides: ruthenium-catalyzed amination of alpha-hydroxy amides. Angew Chem Int Ed 50(47):11197–11201
79. Imm S, Bahn S, Beller M et al (2011) Improved ruthenium-catalyzed amination of alcohols with ammonia: synthesis of diamines and amino esters. Angew Chem Int Ed 50(33):7599–7603
80. Baumann W, Spannenberg A, Deutsch J (2013) Utilization of common ligands for the ruthenium-catalyzed amination of alcohols. Chem-Eur J 19(52):17702–17706
81. Pingen D, Lutz M, Vogt D (2014) Mechanistic study on the ruthenium-catalyzed direct amination of alcohols. Organometallics 33(7):1623–1629
82. Pingen D, Lebl T, Vogt D et al (2014) Catalytic activity and fluxional behavior of complexes based on RuHCl(CO)(PPh$_3$)$_3$ and Xantphos-type ligands. Organometallics 33(11):2798–2805
83. Agrawal S, Lenormand M, Martín-Matute B (2012) Selective alkylation of (hetero)aromatic amines with alcohols catalyzed by a ruthenium pincer complex. Org Lett 14(6):1456–1459
84. Chen M, Zhang M, Jiang H et al (2014) Ruthenium-catalyzed *N*-alkylation for the synthesis of 2-*N*-pyridylmethyl benzonitriles and an exploration of its synthetic utility. ChemCatChem 6(10):2993–2997
85. Enyong AB, Moasser B (2014) Ruthenium-catalyzed *N*-alkylation of amines with alcohols under mild conditions using the borrowing hydrogen methodology. J Org Chem 79(16):7553–7563
86. Jumde VR, Gonsalvi L, Taddei M et al (2015) A ruthenium-based catalytic system for a mild borrowing-hydrogen process Eur J Org Chem 2015(8):1829–1833
87. Feng C, Deng G, Li C-J et al (2010) Ruthenium-catalyzed tertiary amine formation from nitroarenes and alcohols. Org Lett 12(21):4888–4891
88. Cui X, Shi F, Deng Y et al (2011) Ruthenium-catalyzed nitro and nitrile compounds coupling with alcohols: alternative route for *N*-substituted amine synthesis. Chem-Eur J 17(9):2587–2591
89. Liu S, Chen R, Deng GJ (2011) Ruthenium-catalyzed formation of tertiary amines from nitriles and alcohols. Chem Lett 40(5):489–491
90. Werkmeister S, Bornschein C, Beller M et al (2013) Ruthenium-catalyzed transfer hydrogenation of nitriles: reduction and subsequent *N*-monoalkylation to secondary amines. Eur J Org Chem 18:3671–3674
91. Wang N, Zou X, Li F et al (2014) The direct synthesis of *N*-alkylated amides via a tandem hydration/*N*-alkylation reaction from nitriles, aldoximes and alcohols. Chem Commun 50(61):8303–8305
92. Kang B, Fu Z, Hong SH (2013) Ruthenium-catalyzed redox-neutral and single-step amide synthesis from alcohol and nitrile with complete atom economy. J Am Chem Soc 135(32):11704–11707
93. Kim J, Hong SH (2014) Synthesis of cyclic imides from nitriles and diols using hydrogen transfer as a substrate-activating strategy. Org Lett 16(17):4404–4407

94. Sundararaju B, Tang Z, Bruneau C et al (2010) Ruthenium-catalyzed cascade *N*- and C(3)-di-alkylation of cyclic amines with alcohols involving hydrogen autotransfer processes. Adv Synth Catal 352(18):3141–3146

95. Yuan K, Jiang F, Bruneau C et al (2012) Iridium-catalyzed oxidant-free dehydrogenative C-H bond functionalization: selective preparation of *N*-arylpiperidines through tandem hydrogen transfers. Angew Chem Int Ed 51(35):8876–8880

96. Yamaguchi R, Kawagoe S, K-I Fujita et al (2008) Selective synthesis of secondary and tertiary amines by Cp*iridium-catalyzed multialkylation of ammonium salts with alcohols. Org Lett 10(2):181–184

97. K-I Fujita, Yamaguchi R, Mingwen Z et al (2009) A new atom-economical and selective synthesis of secondary and tertiary alkylamines by means of Cp*iridium complex catalyzed multiple *N*-alkylation of ammonium salts with alcohols without solvent. Synthesis 2009(07):1220–1223

98. K-I Fujita, Komatsubara A, Yamaguchi R (2009) *N*-alkylation of carbamates and amides with alcohols catalyzed by a Cp*Ir complex. Tetrahedron 65(18):3624–3628

99. Zhu M, K-I Fujita, Yamaguchi R (2010) Simple and versatile catalytic system for *N*-alkylation of sulfonamides with various alcohols. Org Lett 12(6):1336–1339

100. Apsunde T, Trudell M (2014) Solvent-free, base-free microwave-mediated iridium-catalyzed *N*-alkylation of amides with alcohols. Synthesis 46(02):230–234

101. Lu L, Ma J, Li F et al (2015) Effective recognition of different types of amino groups: from aminobenzenesulfonamides to amino-(*N*-alkyl)benzenesulfonamides via iridium-catalyzed *N*-alkylation with alcohols. Org Lett 17(10):2350–2353

102. Li F, Shan H, Chen L (2012) Direct *N*-alkylation of amino-azoles with alcohols catalyzed by an iridium complex/base system. Chem Commun 48(4):603–605

103. Li F, Kang Q (2012) Shan H (2012) Regioselective *N*-alkylation of 2-aminoimidazoles with alcohols to 2-(*N*-alkylamino)imidazoles catalyzed by the [Cp*IrCl₂]₂/K₂CO₃ System. Eur J Org Chem 26:5085–5092

104. Li F, Chen L, Kang Q (2013) Regioselective *N*-alkylation with alcohols for the preparation of 2-(*N*-alkylamino)quinazolines and 2-(*N*-alkylamino)pyrimidines. New J Chem 37(3):624–631

105. Berliner MA, Dubant SPA, Makowski T (2011) Use of an iridium-catalyzed redox-neutral alcohol-amine coupling on kilogram scale for the synthesis of a GlyT1 inhibitor. Org Proc Res Deve 15(5):1052–1062

106. Cumpstey I, Agrawal S, Martín-Matute B et al (2011) Iridium-catalysed condensation of alcohols and amines as a method for aminosugar synthesis. Chem Commun 47(27):7827–7829

107. Liu S, Stephens G, Marr AC et al (2009) Adding value to renewables: a one pot process combining microbial cells and hydrogen transfer catalysis to utilise waste glycerol from biodiesel production. Chem Commun 45(17):2308–2310

108. Lacroix SD, Pennycook A, Marr AC et al (2012) Amination and dehydration of 1,3-propanediol by hydrogen transfer: reactions of a bio-renewable platform chemical. Catal Sci Technol 2(2):288–290

109. Bhat S, Sridharan V (2012) Iridium catalysed chemoselective alkylation of 2′-aminoacetophenone with primary benzyl type alcohols under microwave conditions. Chem Commun 48(39):4701–4703

110. Blank B, Michlik S, Kempe R (2009) Selective iridium-catalyzed alkylation of (hetero)aromatic amines and diamines with alcohols under mild reaction conditions. Chem-Eur J 15(15):3790–3799

111. Michlik S, Kempe R (2010) New iridium catalysts for the efficient alkylation of anilines by alcohols under mild conditions. Chem-Eur J 16(44):13193–13198

112. Michlik S, Hille T, Kempe R (2012) The iridium-catalyzed synthesis of symmetrically and unsymmetrically alkylated diamines under mild reaction conditions. Adv Synth Catal 354(5):847–862

113. Zou Q, Wang C, Xiao J et al (2015) Alkylation of amines with alcohols and amines by a single catalyst under mild conditions. Chem-Eur J 21(27):9656–9661

114. Li JQ, Andersson PG (2013) Room temperature and solvent-free iridium-catalyzed selective alkylation of anilines with alcohols. Chem Commun 49(55):6131–6133

115. Saidi O, Blacker AJ, Williams JMJ (2010) Borrowing hydrogen in water and ionic liquids: iridium-catalyzed alkylation of amines with alcohols. Org Proc Res Deve 14(4):1046–1049

116. Kawahara R, K-I Fujita, Yamaguchi R (2010) Multialkylation of aqueous ammonia with alcohols catalyzed by water-soluble Cp*Ir-ammine complexes. J Am Chem Soc 132(43):15108–15111

117. Lorentz-Petersen LLR, Nordstrøm LU (2012) Madsen R (2012) Iridium-catalyzed condensation of amines and vicinal diols to substituted piperazines. Eur J Org Chem 34:6752–6759

118. Trudell M, Apsunde T (2013) Microwave-assisted iridium-catalyzed synthesis of nicotine and anabasine derivatives. Synthesis 45(15):2120–2124
119. Qu P, Sun C, Li F et al (2014) The N-alkylation of sulfonamides with alcohols in water catalyzed by the water-soluble iridium complex {Cp*Ir[6,6′-(OH)₂bpy](H₂O)}[OTf]₂. Adv Synth Catal 356(2–3):447–459
120. Ramón D, Martínez-Asencio A, Yus M (2011) Palladium(II) acetate as catalyst for the N-alkylation of aromatic amines, sulfonamides, and related nitrogenated compounds with alcohols by a hydrogen autotransfer process. Synthesis 22:3730–3740
121. Dang TT, Ramalingam B, Seayad AM et al (2013) An efficient palladium-catalyzed N-alkylation of amines using primary and secondary alcohols. ACS Catal 3(11):2536–2540
122. Bertoli M, Choualeb A, Gusev DG et al (2011) PNP pincer osmium polyhydrides for catalytic dehydrogenation of primary alcohols. Dalton Trans 40(35):8941–8949
123. Abdukader A, Jin H, Zhu C et al (2014) Rhenium-catalyzed amination of alcohols by hydrogen transfer process. Tetrahedron Lett 55(30):4172–4174
124. Yang H, Mao R, Cheng G et al (2014) An efficient homogeneous gold(I) catalyst for N-alkylation of amines with alcohols by hydrogen autotransfer. Tetrahedron 70(46):8829–8835
125. Martínez-Asencio A, Ramón DJ, Yus M (2010) N-Alkylation of poor nucleophilic amine and sulfonamide derivatives with alcohols by a hydrogen autotransfer process catalyzed by copper(II) acetate. Tetrahedron Lett 51(2):325–327
126. Martínez-Asencio A, Ramón DJ, Yus M (2011) N-alkylation of poor nucleophilic amines and derivatives with alcohols by a hydrogen autotransfer process catalyzed by copper(II) acetate: scope and mechanistic considerations. Tetrahedron 67(17):3140–3149
127. Li F, Shan H, Kang Q et al (2011) Regioselective N-alkylation of 2-aminobenzothiazoles with benzylic alcohols. Chem Commun 47(17):5058–5060
128. Cui X, Shi F, Deng Y et al (2010) Fe(II)-catalyzed N-alkylation of sulfonamides with benzylic alcohols. Tetrahedron Lett 51(15):2048–2051
129. Bala M, Verma PK, Singh B (2013) Iron phthalocyanine as an efficient and versatile catalyst for N-alkylation of heterocyclic amines with alcohols: one-pot synthesis of 2-substituted benzimidazoles, benzothiazoles and benzoxazoles. Green Chem 15(6):1687–1693
130. Yan T, Feringa BL, Barta K (2014) Iron catalysed direct alkylation of amines with alcohols. Nat Commun 5:5602. doi:10.1038/ncomms6602
131. Pan H-J, Ng TW, Zhao Y (2015) Iron-catalyzed amination of alcohols assisted by Lewis acid. Chem Commun 51(59):11907–11910
132. Rawlings AJ, Diorazio LJ, Wills M (2015) C–N bond formation between alcohols and amines using an iron cyclopentadienone catalyst. Org Lett 17(5):1086–1089
133. Rösler S, Ertl M, Kempe R et al (2015) Cobalt-catalyzed alkylation of aromatic amines by alcohols. Angew Chem Inl Ed 54(50):15046–15050
134. Zhang G, Yin Z, Zheng S (2016) Cobalt-catalyzed N-alkylation of amines with alcohols. Org Lett 18(2):300–303
135. Kim JW, Yamaguchi K, Mizuno N (2009) Heterogeneously catalyzed selective N-alkylation of aromatic and heteroaromatic amines with alcohols by a supported ruthenium hydroxide. J Catal 263(1):205–208
136. He J, Kim JW, Mizuno N et al (2009) Efficient catalytic synthesis of tertiary and secondary amines from alcohols and urea. Angew Chem Int Ed 48(52):9888–9891
137. Yamaguchi K, He J, Mizuno N et al (2010) The "borrowing hydrogen strategy" by supported ruthenium hydroxide catalysts: synthetic scope of symmetrically and unsymmetrically substituted amines. Chem-Eur J 16(24):7199–7207
138. Martínez R, Ramón DJ, Yus M (2009) Selective N-monoalkylation of aromatic amines with benzylic alcohols by a hydrogen autotransfer process catalyzed by unmodified magnetite. Org Biomol Chem 7(10):2176–2181
139. Cano R, Ramón DJ, Yus M (2011) Impregnated ruthenium on magnetite as a recyclable catalyst for the N-alkylation of amines, sulfonamides, sulfinamides, and nitroarenes using alcohols as electrophiles by a hydrogen autotransfer process. J Org Chem 76(14):5547–5557
140. Pei Shan S, Seayad AM, Ramalingam B et al (2014) Reusable supported ruthenium catalysts for the alkylation of amines by using primary alcohols. ChemCatChem 6(3):808–814
141. Wang D, Gao Z-W, Hou X-F et al (2013) An efficient and recyclable catalyst for N-alkylation of amines and β-alkylation of secondary alcohols with primary alcohols: SBA-15 supported N-heterocyclic carbene iridium complex. Adv Synth Catal 355(6):1117–1125

142. He W, Wang L, Yu Z et al (2011) Pt-Sn/γ-Al$_2$O$_3$-catalyzed highly efficient direct synthesis of secondary and tertiary amines and imines. Chem-Eur J 17(47):13308–13317

143. Wang L, He W, Yu Z et al (2011) Heterogeneous bimetallic Pt–Sn/γ-Al$_2$O$_3$ catalyzed direct synthesis of diamines from N-alkylation of amines with diols through a borrowing hydrogen strategy. Tetrahedron Lett 52(52):7103–7107

144. Zhang Y, Shi F, Deng Y et al (2011) Palladium catalyzed N-alkylation of amines with alcohols. Tetrahedron Lett 52(12):1334–1338

145. Ousmane M, Perrussel G, Pera-Titus M et al (2014) Highly selective direct amination of primary alcohols over a Pd/K-OMS-2 catalyst. J Catal 309:439–452

146. Dang TT, Ramalingam B, Seayad AM et al (2015) An efficient heterogenized palladium catalyst for N-alkylation of amines and alpha-alkylation of ketones using alcohols. RSC Adv 5(53):42399–42406

147. He L, Cao Y, Fan KN et al (2010) Efficient and clean gold-catalyzed one-pot selective N-alkylation of amines with alcohols. Chem-Eur J 16(47):13965–13969

148. Tang CH, Cao Y, Fan KN et al (2011) Direct one-pot reductive N-alkylation of nitroarenes by using alcohols with supported gold catalysts. Chem-Eur J 17(26):7172–7177

149. He L, Fan KN, Cao Y et al (2012) Highly efficient heterogeneous gold-catalyzed direct synthesis of tertiary and secondary amines from alcohols and urea. ChemSusChem 5(4):621–624

150. Shimizu K, Nishimura M, Satsuma A (2009) γ-Alumina-supported silver cluster for N-benzylation of anilines with alcohols. ChemCatChem 1(4):497–503

151. Liu H, Chuah G-K, Jaenicke S (2012) N-alkylation of amines with alcohols over alumina-entrapped Ag catalysts using the "borrowing hydrogen" methodology. J Catal 292:130–137

152. Cui X, Shi F, Deng Y et al (2011) Organic ligand-free alkylation of amines, carboxamides, sulfonamides, and ketones by using alcohols catalyzed by heterogeneous Ag/Mo oxides. Chem- Eur J 17(3):1021–1028

153. Sun J, Jin X, Li R et al (2012) Ni–Cu/γ-Al$_2$O$_3$ catalyzed N-alkylation of amines with alcohols. Catal Commun 24:30–33

154. K-I Shimizu, Kon K, Onodera W et al (2013) Heterogeneous Ni catalyst for direct synthesis of primary amines from alcohols and ammonia. ACS Catal 3(1):112–117

155. K-I Shimizu, Imaiida N, Kon K et al (2013) Heterogeneous Ni catalysts for N-alkylation of amines with alcohols. ACS Catal 3(5):998–1005

156. K-I Shimizu, Kanno S, Kon K et al (2014) N-alkylation of ammonia and amines with alcohols catalyzed by Ni-loaded CaSiO$_3$. Catal Today 232:134–138

157. Cui X, Deng Y, Shi F et al (2013) Development of a general non-noble metal catalyst for the benign amination of alcohols with amines and ammonia. Chem-Eur J 19(11):3665–3675

158. Mehta A, Thaker A, Nandan SR et al (2014) Reinvestigating Raney nickel mediated selective alkylation of amines with alcohols via hydrogen autotransfer methodology. Appl Catal A: Gen 478:241–251

159. He J, Yamaguchi K, Mizuno N (2010) Selective synthesis of secondary amines via N-alkylation of primary amines and ammonia with alcohols by supported copper hydroxide catalysts. Chem Lett 39(11):1182–1183

160. K-I Shimizu, Shimura K, Nishimura M et al (2011) Silver cluster-promoted heterogeneous copper catalyst for N-alkylation of amines with alcohols. RSC Adv 1(7):1310–1317

161. Santoro F, Psaro R, Ravasio N et al (2012) Reductive amination of ketones or amination of alcohols over heterogeneous Cu catalysts: matching the catalyst support with the N-alkylating agent. ChemCatChem 4(9):1249–1254

162. Santoro F, Psaro R, Ravasio N et al (2014) N-Alkylation of amines through hydrogen borrowing over a heterogeneous Cu catalyst. RSC Adv 4(6):2596–2600

163. Dixit M, Mishra M, Joshi PA et al (2013) Clean borrowing hydrogen methodology using hydrotalcite supported copper catalyst. Catal Commun 33:80–83

164. Shi F, Tse MK, Beller M et al (2009) Green and efficient synthesis of sulfonamides catalyzed by nano-Ru/Fe3O4. J Am Chem Soc 131(5):1775–1779

165. K-I Shimizu, Miyamoto Y, Satsuma A (2010) Silica-supported silver nanoparticles with surface oxygen species as a reusable catalyst for alkylation of arenes. ChemCatChem 2(1):84–91

166. Cui X, Shi F, Deng Y et al (2012) Au/Ag-Mo nano-rods catalyzed reductive coupling of nitrobenzenes and alcohols using glycerol as the hydrogen source. Chem Commun 48(75):9391–9393

167. Corma A, Navas J, Sabater MJ (2012) Coupling of two multistep catalytic cycles for the one-pot synthesis of propargylamines from alcohols and primary amines on a nanoparticulated gold catalyst. Chem-Eur J 18(44):14150–14156

168. Geukens I, Vermoortele F, De Vos DE et al (2014) Ag nanoparticles on mixed Al_2O_3-Ga_2O_3 supports as catalysts for the N-alkylation of amines with alcohols. Appl Catal A: Gen 469:373–379

169. Choo GCY, Miyamura H, Kobayashi S (2015) Synergistic cascade catalysis by metal nanoparticles and Lewis acids in hydrogen autotransfer. Chem Sci 6(3):1719–1727

170. Gonzalez-Arellano C, Luque R, Gai PL et al (2010) Highly active and selective supported iron oxide nanoparticles in microwave-assisted N-alkylations of amines with alcohols. Green Chem 12(7):1281–1287

171. Lamb GW, Al Badran FA, Williams JMJ et al (2010) Production of pharmaceuticals: amines from alcohols in a continuous flow fixed bed catalytic reactor. Chem Eng Res Des 88(12):1533–1540

172. Sipos G, Kocsis L, Jones RV et al (2013) Important industrial procedures revisited in flow: very efficient oxidation and N-alkylation reactions with high atom-economy. J Flow Chem 3(2):51–58

173. Sattler JH, Fuchs M, Kroutil W et al (2012) Redox self-sufficient biocatalyst network for the amination of primary alcohols. Angew Chem Int Ed 51(36):9156–9159

174. Yang H, Deng Y, Shi F et al (2015) Carbon-catalysed reductive hydrogen atom transfer reactions. Nat Commun 6:6478. doi:10.1038/ncomms7478

175. Miao L, DiMaggio SC, Trudell ML et al (2009) Enantioselective syntheses of both enantiomers of noranabasamine. Org Lett 11(7):1579–1582

176. Oldenhuis NJ, Dong VM, Guan Z (2014) From racemic alcohols to enantiopure amines: Ru-catalyzed diastereoselective amination. J Am Chem Soc 136(36):12548–12551

177. Eka Putra A, Oe Y, Ohta T (2013) Ruthenium-catalyzed enantioselective synthesis of β-amino alcohols from 1,2-diols by "borrowing hydrogen". Eur J Org Chem 2013(27):6146–6151

178. Zhang Y, Lim CS, Zhao Y et al (2014) Catalytic enantioselective amination of alcohols by the use of borrowing hydrogen methodology: cooperative catalysis by iridium and a chiral phosphoric acid. Angew Chem Int Ed 53(5):1399–1403

179. Rong Z-Q, Zhang Y, Zhao Y et al (2015) Dynamic kinetic asymmetric amination of alcohols: from a mixture of four isomers to diastereo- and enantiopure α-branched amines. J Am Chem Soc 137(15):4944–4947

180. Shi F, Tse MK, Beller M et al (2009) Copper-catalyzed alkylation of sulfonamides with alcohols. Angew Chem Int Ed 48(32):5912–5915

181. Cui X, Shi F, Beller M et al (2009) Copper-catalyzed N-alkylation of sulfonamides with benzylic alcohols: catalysis and mechanistic studies. Adv Synth Catal 351(17):2949–2958

182. Likhar PR, Arundhathi R, Kantam ML et al (2009) Amination of alcohols catalyzed by copper-aluminium hydrotalcite: a green synthesis of amines. Eur J Org Chem 2009(31):5383–5389

183. Kawahara R, K-I Fujita, Yamaguchi R (2011) N-alkylation of amines with alcohols catalyzed by a water-soluble Cp* iridium complex: an efficient method for the synthesis of amines in aqueous media. Adv Synth Catal 353(7):1161–1168

184. Ohta H, Uozumi Y, Yamada YM et al (2011) In-water dehydrative alkylation of ammonia and amines with alcohols by a polymeric bimetallic catalyst. Org Lett 13(15):3892–3895

185. Feng SL, Liu CZ, Xu Q et al (2011) Rhodium-catalyzed aerobic N-alkylation of sulfonamides with alcohols. Chin Chem Lett 22(9):1021–1024

186. Liu C, Liao S, Xu Q et al (2011) Discovery and mechanistic studies of a general air-promoted metal-catalyzed aerobic N-alkylation reaction of amides and amines with alcohols. J Org Chem 76(14):5759–5773

187. Yamada YM, Uozumi Y (2006) A solid-phase self-organized catalyst of nanopalladium with main-chain viologen polymers: α-alkylation of ketones with primary alcohols. Org Lett 8(7):1375–1378

188. Yamada YM, Uozumi Y (2007) Development of a convoluted polymeric nanopalladium catalyst: α-alkylation of ketones and ring-opening alkylation of cyclic 1, 3-diketones with primary alcohols. Tetrahedron 63(35):8492–8498

189. Allen LJ, Crabtree RH (2010) Green alcohol couplings without transition metal catalysts: base-mediated β-alkylation of alcohols in aerobic conditions. Green Chem 12(8):1362–1364

190. Yu X, Liu C, Xu Q et al (2011) Manganese dioxide catalyzed N-alkylation of sulfonamides and amines with alcohols under air. Org Lett 13(23):6184–6187

191. Yu X, Jiang L, Xu Q et al (2012) Palladium-catalyzed N-alkylation of amides and amines with alcohols employing the aerobic relay race methodology. Chin J Chem 30(10):2322–2332

192. Li Q, Fan S, Xu Q et al (2012) Copper-catalyzed *N*-alkylation of amides and amines with alcohols employing the aerobic relay race methodology. Org Biomol Chem 10(15):2966–2972
193. Deutsch C, Krause N, Lipshutz BH (2008) CuH-catalyzed reactions. Chem Rev 108(8):2916–2927
194. Rendler S, Oestreich M (2007) Polishing a diamond in the rough:"Cu–H" catalysis with silanes. Angew Chem In. Ed 46(4):498–504
195. Lipshutz BH (2009) Rediscovering organocopper chemistry through copper hydride. It's all about the ligand. Synlett 2009(04):509–524
196. Liao S, Yu K, Xu Q et al (2012) Copper-catalyzed C-alkylation of secondary alcohols and methyl ketones with alcohols employing the aerobic relay race methodology. Org Biomol Chem 10(15):2973–2978
197. Sharma RK, Monga Y, Gaba G et al (2013) Magnetite (Fe_3O_4) silica based organic–inorganic hybrid copper (ii) nanocatalyst: a platform for aerobic *N*-alkylation of amines. Green Chem 15(10):2800–2809
198. Zotova N, Hellgardt K, Hii KKM et al (2012) Catalysis in flow: Au-catalysed alkylation of amines by alcohols. Green Chem 14(1):226–232
199. Xu Q, Chen J, Liu Q et al (2013) Aldehyde-catalyzed transition metal-free dehydrative β-alkylation of methyl carbinols with alcohols. Adv Synth Catal 355(4):697–704
200. Xu Q, Chen J, Tian H et al (2014) Catalyst-free dehydrative α-alkylation of ketones with alcohols: green and selective autocatalyzed synthesis of alcohols and ketones. Angew Chem Int Ed 53(1):225–229
201. Han X, Wu J (2013) Redox chain reaction-indole and pyrrole alkylation with unactivated secondary alcohols. Angew Chem Int Ed 52(17):4637–4640
202. Dai X, Deng Y, Shi F et al (2015) A conjugated ketone as a catalyst in alcohol amination reactions under transition-metal and hetero-atom free conditions. RSC Adv 5(54):43589–43593
203. Donthiri RR, Pappula V, Adimurthy S et al (2013) Sodium hydroxide catalyzed *N*-alkylation of (hetero)aromatic primary amines and N1, C5-dialkylation of 4-phenyl-2-aminothiazoles with benzyl alcohols. J Org Chem 78(13):6775–6781
204. Donthiri RR, Patil RD, Adimurthy S et al (2012) NaOH-catalyzed imine synthesis: aerobic oxidative coupling of alcohols and amines. Eur J Org Chem 24:4457–4460
205. Lu XH, Sun YW, Xia QH et al (2014) Solid base catalyzed highly efficient *N*-alkylation of amines with alcohols in a solvent-free system. Catal Commun 55:78–82
206. Yadav DKT, Bhanage B (2014) Base-mediated synthesis of imines and amines from *N*-phenylureas and alcohols. Synlett 25:1611–1615
207. Li S, Li X, Xu Q et al (2015) Structure-dependent tautomerization induced catalyst-free autocatalyzed *N*-alkylation of heteroaryl amines with alcohols. Green Chem 17(6):3260–3265
208. Wang C, Yao Y, Zhao Y et al (2015) Insight into O2-promoted base-catalyzed *N*-alkylation of amines with alcohols. Eur J Org Chem 13:2972–2977
209. Li X, Li S, Xu Q et al (2016) Efficient and practical catalyst-free-like dehydrative *N*-alkylation of amines and sulfinamides with alcohols initiated by aerobic oxidation of alcohols under air. Tetrahedron 72(2):264–272
210. Li QQ, Xiao ZF, Kang YB (2015) Direct alkylation of amines with alcohols catalyzed by base. Org Lett 17(21):5328–5331
211. Shvo Y, Laine RM (1980) Homogeneous catalytic activation of C–N bonds. Alkyl exchange between tertiary amines. J Chem Soc, Chem Commun 16:753–754
212. Bui The K, Concilio C, Porzi G (1981) A facile synthesis of symmetrical secondary amines from primary amines promoted by the homogeneous catalyst RuCl$_2$(Ph$_3$P)$_3$. J Organomet Chem 208(2):249–251
213. Bui The K, Concilio C, Porzi G (1981) Cyclization of alpha, omega aliphatic diamines and conversion of primary amines to symmetrical tertiary amines by a homogeneous ruthenium catalyst. J Org Chem 46(8):1759–1760
214. Hollmann D, Bahn S, Beller M et al (2007) A general ruthenium-catalyzed synthesis of aromatic amines. Angew Chem Int Ed 46(43):8291–8294
215. Hollmann D, Bahn S, Beller M et al (2008) *N*-dealkylation of aliphatic amines and selective synthesis of monoalkylated aryl amines. Chem Commun 44(27):3199–3201
216. Bähn S, Hollmann D, Beller M et al (2008) Ruthenium-catalyzed synthesis of secondary alkylamines: selective alkylation with aliphatic amines. Adv Synth Catal 350(13):2099–2103
217. Bahn S, Imm S, Beller M et al (2011) Synthesis of primary amines from secondary and tertiary amines: ruthenium-catalyzed amination using ammonia. Chem-Eur J 17(17):4705–4708

218. Prades A, Corberan R, Peris E et al (2008) [IrCl$_2$Cp*(NHC)] complexes as highly versatile efficient catalysts for the cross-coupling of alcohols and amines. Chem-Eur J 14(36):11474–11479

219. Corberán R, Peris (2008) An unusual example of base-free catalyzed reduction of C=O and C=NR bonds by transfer hydrogenation and some useful implications. Organometallics 27(8):1954–1958

220. Saidi O, Marsden SP, Williams JM et al (2009) Selective amine cross-coupling using iridium-catalyzed "borrowing hydrogen" methodology. Angew Chem Int Ed 48(40):7375–7378

221. K-I Shimizu, Shimura K, Ohshima K et al (2011) Selective cross-coupling of amines by alumina-supported palladium nanocluster catalysts. Green Chem 13(11):3096–3100

222. Lubinu MC, De Luca L, Porcheddu A et al (2011) Microwave-promoted selective mono-N-alkylation of anilines with tertiary amines by heterogeneous catalysis. Chem-Eur J 17(1):82–85

223. K-I Shimizu, Shimura K, Kato K et al (2012) Electronic effect of Na promotion for selective mono-N-alkylation of aniline with di-iso-propylamine by Pt/SiO$_2$ catalysts. J Mol Catal A: Chem 353–354:171–177

224. K-I Shimizu, Shimura K, Tamagawa N et al (2012) Sulfur promoted Pt/SiO$_2$ catalyzed cross-coupling of anilines and amines. Appl Catal A: Gen 417–418:37–42

225. Largeron M, Fleury M-B (2009) A biomimetic electrocatalytic system for the atom-economical chemoselective synthesis of secondary amines. Org Lett 11(4):883–886

226. Schümperli MT, Hammond C, Hermans I (2012) Developments in the aerobic oxidation of amines. ACS Catal 2(6):1108–1117

227. Largeron M, Fleury MB (2013) Bioinspired oxidation catalysts. Science 339(6115):43–44

228. Largeron M (2013) Protocols for the catalytic oxidation of primary amines to imines. Eur J Org Chem 2013(24):5225–5235

229. Chen B, Wang L, Gao S (2015) Recent advances in aerobic oxidation of alcohols and amines to imines. ACS Catal 5(10):5851–5876

CrossMark

R E V I E W

Ruthenium-Catalyzed Transfer Hydrogenation for C–C Bond Formation: Hydrohydroxyalkylation and Hydroaminoalkylation via Reactant Redox Pairs

Felix Perez[1] · Susumu Oda[1] · Laina M. Geary[1,2] ·
Michael J. Krische[1]

Abstract Merging the chemistry of transfer hydrogenation and carbonyl or imine addition, a broad new family of redox-neutral or reductive hydrohydroxyalkylations and hydroaminomethylations have been developed. In these processes, hydrogen redistribution between alcohols and π-unsaturated reactants is accompanied by C–C bond formation, enabling direct conversion of lower alcohols to higher alcohols. Similarly, hydrogen redistribution between amines to π-unsaturated reactants results in direct conversion of lower amines to higher amines. Alternatively, equivalent products of hydrohydroxyalkylation and hydroaminomethylation may be generated through the reaction of carbonyl compounds or imines with π-unsaturated reactants under the conditions of 2-propanol-mediated reductive coupling. Finally, using vicinally dioxygenated reactants, that is, diol, ketols, or diones, successive transfer hydrogenative coupling occurs to generate 2 C-C bonds, resulting in products of formal [4+2] cycloaddition.

Keywords Ruthenium · Transfer Hydrogenation · Enantioselective · Borrowing Hydrogen · C-C Bond Formation

1 Catalytic Hydrogenation—A Brief Historical Perspective

The first metal-catalyzed additions of elemental hydrogen to π-unsaturated reactants were reported by James F. Boyce of the Nathaniel Kellogg Fairbank Soap Company in connection with the processing of vegetable oils [1]. Subsequently, Paul Sabatier of the University of Toulouse developed general protocols for the hydrogenation of alkenes employing heterogeneous nickel catalysts [2]. Foreshadowing the merger hydrogenation and carbonyl addition described in the present account, Paul Sabatier and Victor Grignard jointly received the Nobel Prize in Chemistry in 1912 [3]. Following Sabatier's pioneering work, numerous noble metal catalysts for heterogeneous hydrogenation emerged. Among these, the platinum oxide catalyst developed by Roger Adams in 1922 is still one of the most active and readily prepared catalysts for heterogeneous hydrogenation [4].
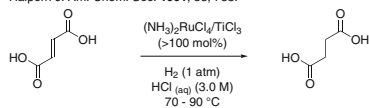
The first examples of homogeneous hydrogenation were reported by Melvin Calvin at the University of California at Berkeley in 1938 [5]. Calvin showed that under one atmosphere of hydrogen, copper acetate catalyzed the reduction of 1,4-benzoquinone to 1,4-hydroquinone in quinoline solution at 100 °C. It was not until 1961 that Halpern's group at the University of British Columbia performed the first homogeneous hydrogenation of an olefin [6]. In Halpern's system, ruthenium catalysts were used to reduce activated alkenes such as maleic acid. In 1962, Vaska subsequently found that IrCl(CO)(PPh$_3$)$_2$ reacts reversibly with elemental hydrogen to form isolable dihydrides [7]. This result solidified the conceptual foundation of catalytic hydrogenation by establishing hydrogen "oxidative addition" as a key mechanistic feature.

Finally, in 1965, Wilkinson's group at Imperial College reported the homogeneous hydrogenation of unactivated alkenes and alkynes catalyzed by RhCl(PPh$_3$)$_3$ [8, 9]. This finding ultimately led William S. Knowles of Monsanto Company in St. Louis to discover the first enantioselective hydrogenation in 1968 [10]. Knowles' discovery was made possible by Horner and Mislow's disclosure of methods for the preparation of nonracemic *P*-stereogenic phosphines [11, 12]. In Knowles' initially reported asymmetric hydrogenation, a maximum enantiomeric excess of 15 % was obtained. Subsequent work by Kagan in 1971 using chiral *bis*(phosphines) derived from tartaric acid (i.e., "DIOP") gave up to 72 % enantiomeric excess [13]. Using a *P*-stereogenic *bis*(phosphine) known as DiPAMP, chemists at Monsanto performed the first industrial catalytic asymmetric synthesis for the production of L-DOPA, a treatment for Parkinson's disease. Lastly, in 1980 Ryoji Noyori reported the synthesis of BINAP and demonstrated the broad utility of this ligand in asymmetric hydrogenation [14, 15].
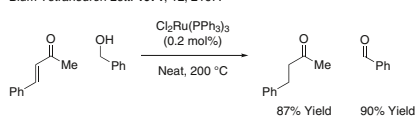
The purpose of this review is to provide a comprehensive summary of ruthenium-catalyzed C–C couplings induced via alcohol-mediated transfer hydrogenation [16–20]. These studies build on several important milestones in the area of ruthenium-catalyzed hydrogenation and transfer hydrogenation (Scheme 1). In 1971, one decade after the seminal work of Halpern on ruthenium-catalyzed hydrogenation [6], transfer hydrogenations employing ruthenium catalysts were described [21]. The ruthenium-catalyzed acceptorless dehydrogenation of alcohols was reported by Robinson in 1977 [22] and ruthenium-catalyzed oxidative esterifications were reported by Shvo in 1981 [23, 24]. These studies were followed by the first highly
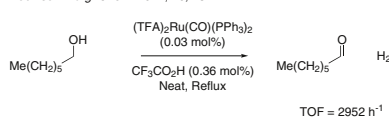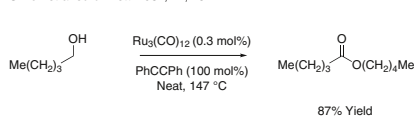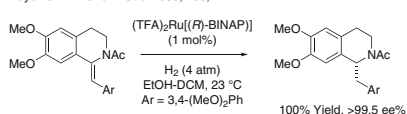
Scheme 1 Selected milestones in homogeneous ruthenium-catalyzed hydrogenation and transfer hydrogenation. [a]BINAP = 2,2′-bis-(diphenylphosphino)-1,1′-binaphthalene. TsDPEN = N-p-Tosyl-1,2-diphenylethylenediamine

enantioselective ruthenium-catalyzed hydrogenations and transfer hydrogenations, reported by Noyori in 1986 and 1995, respectively [25, 26]. As documented in this account, ruthenium-catalyzed transfer hydrogenation now serves as the basis for C–C bond constructions that directly convert lower alcohols to higher alcohols [16–20]. This body of work was preceded by studies on metal-catalyzed carbonyl reductive couplings mediated by elemental hydrogen, as initially described in 2002 by the present author [27], and as documented in the review literature [28, 29].

## 2 Conversion of Primary Alcohols to Secondary Alcohols

In 2007, our laboratory reported the first transfer hydrogenative couplings of alcohols with π-unsaturated reactants using iridium-based catalysts [30]. In 2008, the first ruthenium-catalyzed reactions of this type were developed (Scheme 2). Specifically, it was found that exposure of alcohols to 1,3-dienes in the presence of catalysts derived from HClRu(CO)(PPh$_3$)$_3$ and various phosphine ligands results in hydrogen transfer to furnish aldehyde-allylruthenium pairs that combine to form homoallylic alcohols as single regioisomers [31]. The coupling of isoprene to d$_2$-benzyl alcohol results in transfer of a benzylic deuteride to the allylic methyl (19 % ^{2}H) and allylic methine (32 % ^{2}H). These data are consistent with reversible hydrometallation of the less-substituted olefin to form a secondary σ-allyl. Conversion to the more stable primary σ-allyl haptomer occurs in advance of carbonyl addition, which proceeds through the indicated closed six-centered transition state with allylic inversion to deliver the product of carbonyl allylation.

Remarkably, while the primary alcohol reactants readily dehydrogenate, the secondary homoallylic alcohol products resist further oxidation due to chelation of homoallylic olefin to ruthenium to generate a coordinatively saturated complex.
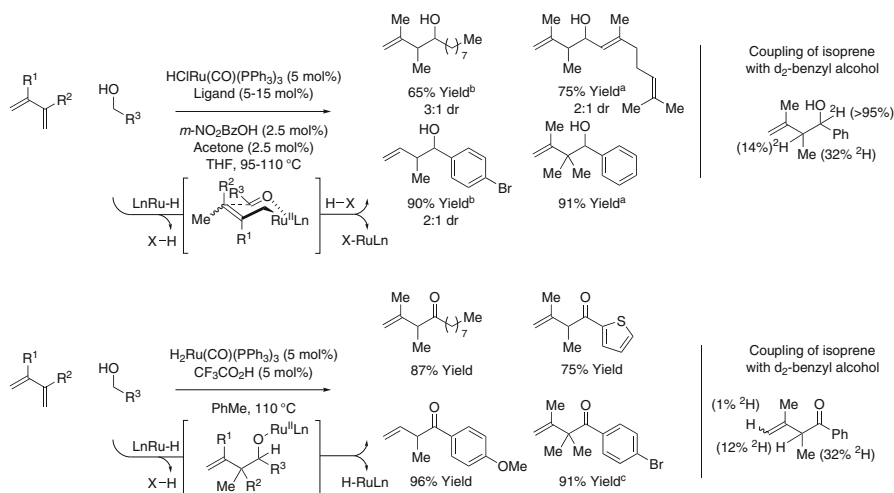
Scheme 2 Ruthenium-catalyzed C–C coupling of primary alcohols with 1,3-dienes to form homoallylic alcohols or β,γ-enones. Yields are of material isolated by flash chromatography on silica gel.
[a]Ligand = (p-MeOPh)₃P, [b]Ligand = rac-BINAP, 2,2'-bis-(diphenylphosphino)-1,1'-binaphthalene.
[c]120 °C

Indeed, in the coupling of isoprene to d_2-benzyl alcohol, deuterium is completely retained at the carbinol position, suggesting that the product is completely unreactive toward alcohol dehydrogenation. However, the ruthenium catalyst (F_3CCO_2) $(H)Ru(CO)(PPh_3)_2$, which is generated in situ through the acid-base reaction of $H_2Ru(CO)(PPh_3)_3$ and F_3CCO_2H (TFA), possesses a higher degree of coordinative unsaturation, enabling β-hydride elimination at the stage of the homoallylic ruthenium alkoxide to form the β,γ-unsaturated enones (Scheme 2) [32]. Notably, both transformations, diene hydrohydroxyalkylation or hydroacylation, may be conducted from the alcohol or aldehyde (not shown) oxidation level of the reactant [31, 32].

Initial studies aimed at directing relative and absolute stereochemistry in alcohol-mediated diene hydrohydroxyalkylation relied on the use of 2-trialkylsilyl-butadienes [33]. Hydrometallation of 2-trialkylsilyl-substituted dienes gives rise to crotylmetal species that exist as single geometrical isomers due to allylic strain [34–36]. In the event, using the chiral ruthenium catalyst generated in situ from $HClRu(CO)(PPh_3)_3$ and (R)-DM-SEGPHOS, the indicated 2-trialkylsilyl-butadiene couples with reactant alcohols to furnish the branched products of hydrohydroxyalkylation with complete syn-diastereoselectivity and uniformly high levels of enantioselectivity (Scheme 3).

Direct diastereo- and enantioselective hydrohydroxyalkylations of butadiene, an abundant petrochemical feedstock, required the use of a ruthenium catalyst modified by a chiral phosphate counterion derived from H_8-BINOL. The anion is attached to the metal center through the acid–base reaction of $H_2Ru(CO)(PPh_3)_3$ with the indicated chiral phosphoric acid. With the chiral counterion as the sole chiral inducing element, primary benzylic alcohols hydrohydroxyalkylate butadiene with good levels of anti-diastereo- and enantioselectivity (Scheme 3) [37].
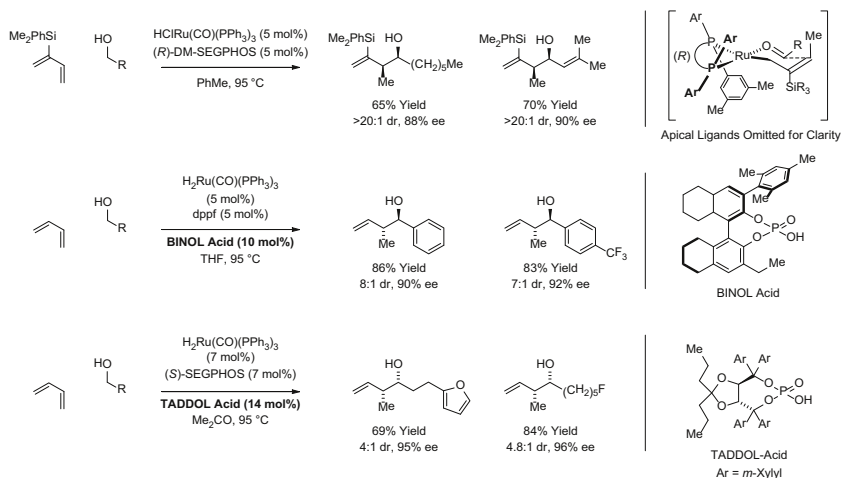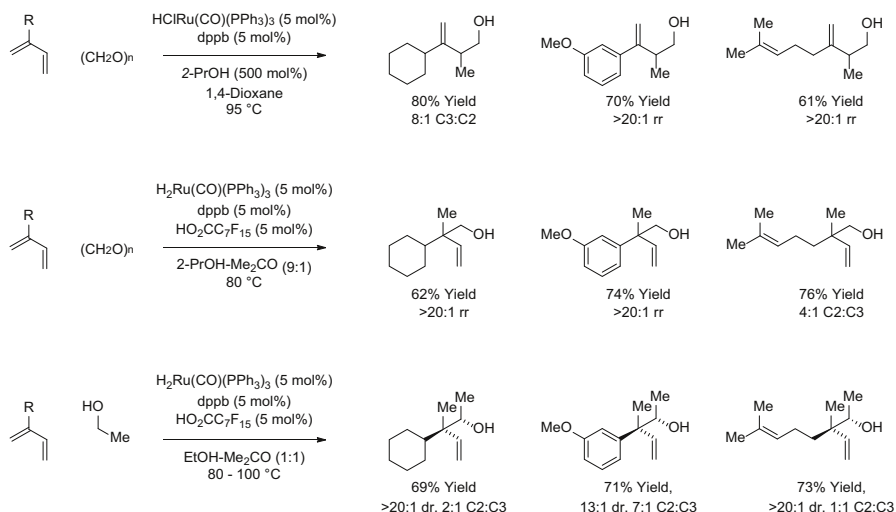
Scheme 3 Diastereo- and enantioselective alcohol-mediated hydrohydroxyalkylation of butadienes. Yields are of material isolated by flash chromatography on silica gel. Diastereoselectivity was determined through ^{1}H NMR analysis of crude reaction mixtures. Enantiomeric excess was determined by chiral stationary phase HPLC analysis. DM-SEGPHOS = 5,5′-*bis*-[di(3,5-xylyl)phosphino]-4,4′-bi-1,3-benzodioxole. dppf = 1,1-*bis*-(diphenylphosphino)ferrocene. SEGPHOS = 5,5′-*bis*-(diphenylphosphino)-4,4′-bi-1,3-benzodioxole

The corresponding *syn*-diastereomers are formed upon use of the ruthenium catalyst generated in situ from RuH$_2$(CO)(PPh$_3$)$_3$, (S)-SEGPHOS, and the indicated TADDOL-derived phosphoric acid (Scheme 3) [38]. It is postulated that the s-*cis*-conformer of butadiene hydrometalates to form a (Z)-σ-crotylruthenium intermediate. The relatively Lewis basic TADDOL-derived phosphate counterion preserves the kinetic selectivity of diene hydrometallation by attenuating the degree of coordinative unsaturation, decelerating isomerization to the (E)-σ-crotylruthenium haptomer with respect to carbonyl addition. Additionally, computational studies suggest a formyl hydrogen bond between the transient aldehyde and the phosphate oxo-moiety assists in stabilizing the (Z)-σ-crotylruthenium intermediate [36].

A divergence in regioselectivity is observed upon the use of neutral vs. cationic ruthenium complexes in alcohol-mediated hydrohydroxyalkylations of 2-substituted dienes. For example, in 2-propanol-mediated reductive couplings of 2-substituted dienes with paraformaldehyde (Scheme 4) [39–41], neutral ruthenium complexes favor coupling at the C3 position [40], whereas ruthenium catalysts with greater cationic character favor coupling at the C2 position, resulting in formation of an all-carbon quaternary center [39]. An erosion in C2-regioselectivity is observed when cationic ruthenium catalysts are applied in reactions of higher carbonyl partners with 2-substituted dienes, as illustrated in couplings with ethanol (Scheme 4) [42].

The collective data, including deuterium labeling experiments [39, 40], are consistent with the following mechanistic interpretation (Scheme 5). Hydroruthenation to form allylruthenium complex **A** is kinetically preferred. For neutral ruthenium catalysts, hydrometallation is less reversible and strongly favors formation of allylruthenium complex **A**. Hence, formation of C3-coupling products

Scheme 4 Divergent regioselectivity in 2-propanol-mediated reductive couplings of dienes with paraformaldehyde and redox neutral couplings of ethanol. Yields are of material isolated by flash chromatography on silica gel. Diastereoselectivity was determined through ^{1}H NMR analysis of crude reaction mixtures. dppb = *bis*-(diphenylphosphino)butane
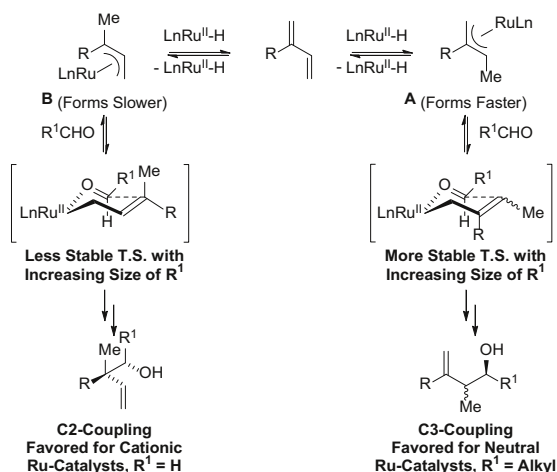
Scheme 5 Divergent regioselectivity in the hydrohydroxyalkylation of 2-substituted dienes

is preferred. For cationic ruthenium complexes, hydrometallation becomes highly reversible, enabling access to both allylruthenium complex **A** and allylruthenium complex **B**. It now appears that a Curtin–Hammett scenario is operative. For small aldehyde partners (R^1=H), the transition state leading to C2-adducts is lower in energy. However, as the aldehyde increases in size (R^1=Me), the formation of a
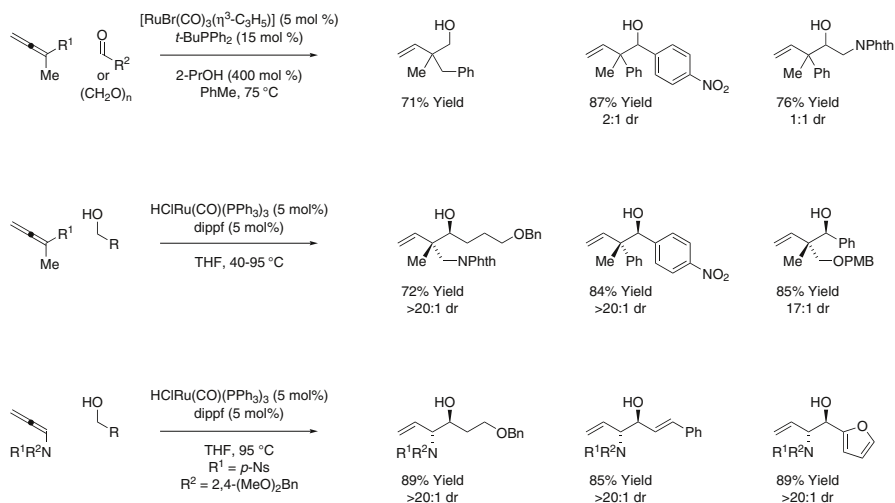
Scheme 6 Alcohol-mediated hydrohydroxyalkylation of allenes. Yields are of material isolated by flash chromatography on silica gel. Diastereoselectivity was determined through ¹H NMR analysis of crude reaction mixtures. dippf = *bis*-(diisopropylphosphino)ferrocene

more congested C–C bond raises the energy of the transition state for formation of C3-adducts, eroding regioselectivity.

Hydrogen transfer from primary alcohols to allenes represents an alternate means of accessing allylruthenium-carbonyl pairs that deliver products of hydrohydroxyalkylation (Scheme 6) [43–47]. Interestingly, whereas 2-propanol-mediated reductive couplings of 1,1-disubstituted allenes display poor levels of diastereoselectivity [43], related redox-neutral couplings with primary alcohols deliver branched homoallylic allylic alcohols bearing all-carbon quaternary centers with good to complete control of relative stereochemistry [45]. In reactions conducted from the alcohol oxidation level, diastereoselectivities are highly concentration-dependent. At lower concentrations, higher diastereoselectivities are observed. These data suggest a Curtin–Hammett scenario wherein turn-over limiting carbonyl addition preferentially consumes the (*E*)-σ-allylruthenium haptomer via stereospecific carbonyl addition from an equilibrating mixture of transient (*Z*)- and (*E*)-σ-allylruthenium isomers. At lower concentration, the (*E*)-isomer can be replenished via isomerization of the (*Z*)-σ-allylruthenium isomer. These conditions have been applied to the coupling of allenes with fluorinated alcohols (not shown) [47].

In the case of *mono*-substituted allenes, the steric demand of an appropriately defined substituent can direct exclusive formation of (*E*)-σ-allylruthenium intermediates that participate in stereospecific carbonyl addition to deliver single diastereomers. For example, hydrogen transfer from primary alcohols to allenamides provides geometrically defined (amino)allylruthenium-aldehyde pairs that combine to form vicinal *anti*-aminoalcohols as single diastereomers (Scheme 6) [45]. Identical products are accessible as single diastereomers via 2-propanol-mediated reductive coupling of allenamides and aldehydes (not shown) [44].
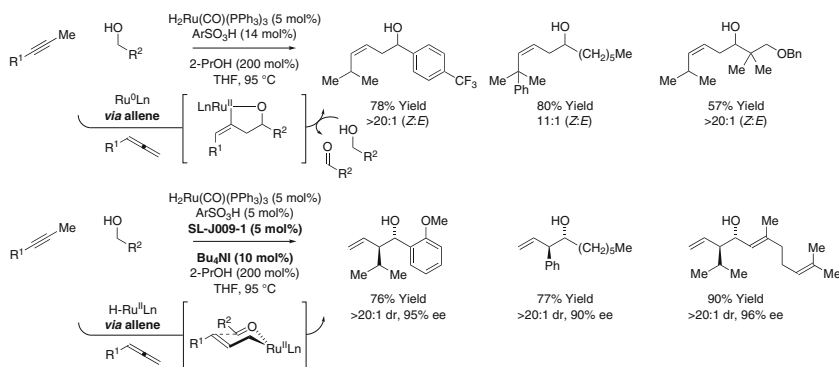
Scheme 7 Alkynes as latent allenes in alcohol-mediated hydrohydroxyalkylation to form linear or branched homoallylic alcohols. Yields are of material isolated by flash chromatography on silica gel. Diastereoselectivity was determined through ^{1}H NMR analysis of crude reaction mixtures. Enantiomeric excess was determined by chiral stationary phase HPLC analysis. SL-J009-1 = (R)-1-[(SP)-2-(dicyclohexylphosphino)ferrocenyl]ethyldi-*tert*-butylphosphine. Ar = 2,4,6-triisopropylphenyl

Isomerization of alkynes to allenes under the conditions of ruthenium catalyzed hydrohydroxyalkylation enables transformations that are otherwise inaccessible, including the conversion of primary alcohols to (Z)-homoallylic secondary alcohols (Scheme 7) [48]. Isomerization is promoted through the use of cationic ruthenium catalysts generated through the acid–base reaction of $H_2Ru(CO)(PPh_3)_3$ and 2,4,6-$(2-Pr)_3PhSO_3H$. As corroborated by deuterium labeling studies, the cationic ruthenium complex appears to exist in equilibrium with zero-valent species that promote isomerization via propargyl C-H oxidative addition. Allene-aldehyde oxidative coupling mediated by ruthenium(0) then forms an oxaruthenacycle, which upon transfer hydrogenolysis delivers the (Z)-homoallylic alcohols with good to complete levels of stereocontrol. Oxidative coupling pathways are suppressed upon introduction of iodide ion and a chelating phosphine ligand, the Josiphos ligands SL-J009-1 or SL-J002-1, yet alkyne-to-allene isomerization pathways persist. Under these conditions, the transient allenes accept hydrogen from primary alcohols to form chiral allylruthenium-aldehyde pairs that deliver enantiomerically enriched branched homoallylic alcohols as single diastereomers [49]. In this way, alkynes serve as chiral allylmetal equivalents [50–57].

A third mechanism for the coupling of primary alcohols with alkynes becomes operative when these conditions are applied to the propargyl ether, $MeC\equiv CCH_2$-OTIPS (TIPS = triisopropylsilyl) (Scheme 8) [58]. Unlike closely related ruthenium-catalyzed alkyne-alcohol C–C couplings, deuterium labeling studies corroborate a novel 1,2-hydride shift mechanism that converts metal-bound alkynes to vinyl carbenes that protonate to form siloxy-π-allylruthenium nucleophiles in the absence of intervening allenes. Due to the negative inductive effect of the siloxy moiety, carbonyl addition occurs through a closed transition structure from the σ-allylruthenium haptomer where ruthenium resides at the oxygen-bearing carbon. Using a Josiphos (SL-J009-1)-modified ruthenium(II) catalyst, the resulting products of siloxy-crotylation form as single regioisomers with complete levels of
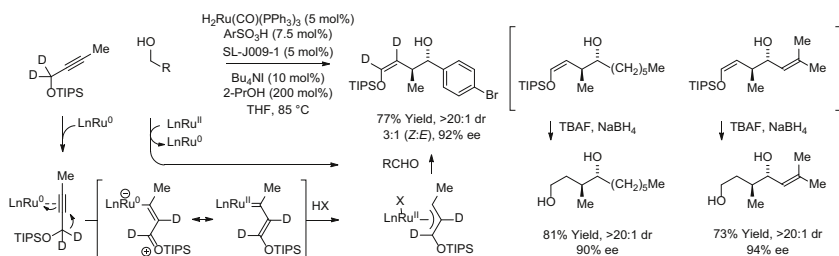
Scheme 8 *anti*-Diastereo- and enantioselective siloxy-crotylation in the transfer hydrogenative coupling of primary alcohols with alkynes via hydride-shift enabled π-allyl formation. Yields are of material isolated by flash chromatography on silica gel. Diastereoselectivity was determined through ^{1}H NMR analysis of crude reaction mixtures. Enantiomeric excess was determined by chiral stationary phase HPLC analysis. SL-J009-1 = (R)-1-[(S_P)-2-(dicyclohexylphosphino)ferrocenyl]ethyldi-*tert*-butylphosphine
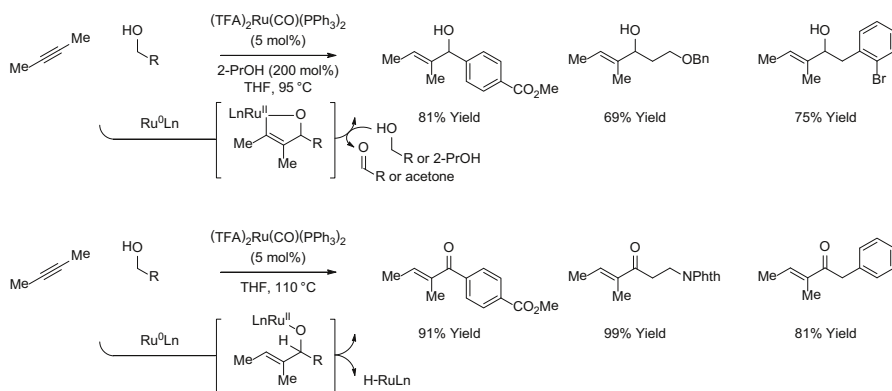
Scheme 9 Transfer hydrogenative couplings of 2-butyne to form allylic alcohols and conjugated enones. Yields are of material isolated by flash chromatography on silica gel

anti-diastereoselectivity and high levels of enantioselectivity. Although mixtures of enol geometrical isomers are produced, the (Z)- and (E)-selectivity is inconsequential as fluoride-assisted cleavage of the enol in the presence of NaBH₄ converts both isomers to the same 1,4-diol.

Remarkably, a fourth mechanism for the coupling of primary alcohols with alkynes is evident in couplings that form allylic alcohols [59] or conjugated enones (Scheme 9) [60]. These processes are catalyzed by (TFA)$_2$Ru(CO)(PPh$_3$)$_2$ in the absence of added phosphine ligand. It is postulated that coordinative unsaturation, the presence of a π-acidic carbonyl ligand and the reducing environment provided by 2-propanol, promote equilibration between ruthenium(II) and ruthenium(0) complexes. Thus, while the experimental data cannot exclude hydrometalative pathways involving vinylruthenium-aldehyde pairs, another possible mechanism involves ruthenium(0)-mediated alkyne-carbonyl oxidative coupling to form a ruthenacyclopentene that suffers alcohol-mediated transfer hydrogenolysis to release the allylic alcohol and regenerate the zero valent catalyst. Under more

forcing conditions (higher temperatures, longer reaction times) and in the absence of 2-propanol, the initially formed allylic alcohols undergo further dehydrogenation to form the conjugated enones. Resubjection of the allylic alcohols to the reaction conditions results in formation of the enone, suggesting β-hydride elimination may not occur at the stage of the intermediate ruthenacycle.

Hydrogen transfer from primary alcohols to 1,3-enynes delivers allenylruthenium-aldehyde pairs that combine to form products of carbonyl propargylation (Scheme 10) [61–63]. Initially developed conditions provided products of α-methyl-propargylation as diastereomeric mixtures [61]. Identical products of propargylation are generated upon 2-propanol-mediated 1,3-enyne-aldehyde reductive coupling. In subsequent work, it was found that *anti*-diastereoselectivity improves upon use of sterically demanding reactants [62]. More recently, the chiral ruthenium complex formed in situ from $(TFA)_2Ru(CO)(PPh_3)_2$ and (R)-BINAP was found to catalyze the C–C coupling of primary alcohols with the 1,3-enyne, $TMSC \equiv CC(Me) = CH_2$, to form secondary homopropargyl alcohols bearing *gem*-dimethyl groups [63]. These conditions deliver products of C–C coupling with uniformly high levels of enantioselectivity and are applicable to aliphatic, allylic, and benzylic alcohols. One may view these protocols as an alternative to the use of stoichiometric allenylmetal reagents in carbonyl propargylation [64, 65].
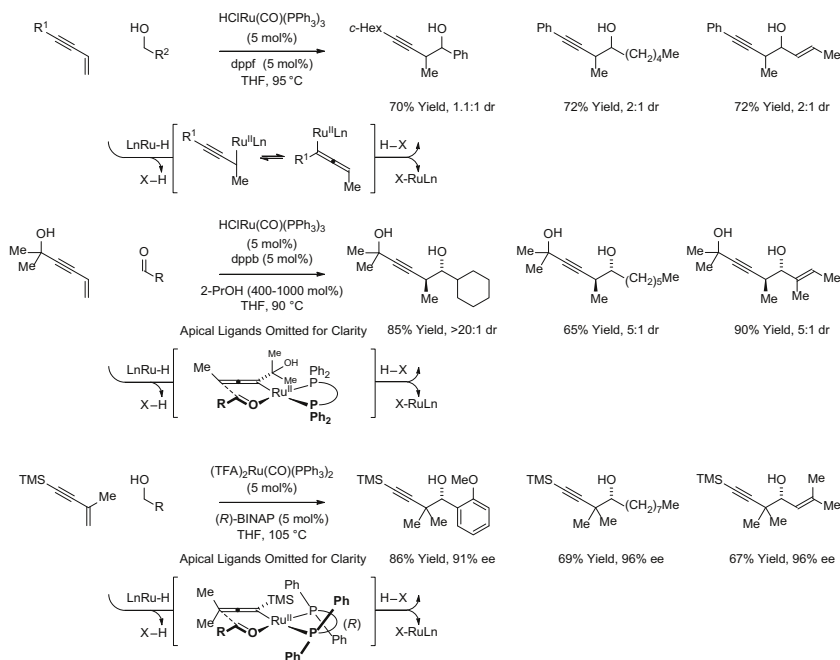
Scheme 10 Carbonyl propargylation via 1,3-enyne hydrohydroxyalkylation. Yields are of material isolated by flash chromatography on silica gel. Diastereoselectivity was determined through ^{1}H NMR analysis of crude reaction mixtures. Enantiomeric excess was determined by chiral stationary phase HPLC analysis. dppb = *bis*-(diphenylphosphino)butane. dppf = 1,1-*bis*-(diphenylphosphino)ferrocene. BINAP = 2,2′-*bis*-(diphenylphosphino)-1,1′-binaphthalene

3 Conversion of Secondary Alcohols to Tertiary Alcohols

In 2012, it was found that ruthenium(0) complexes catalyze the C–C coupling of activated secondary alcohols with feedstock dienes such isoprene and myrcene to furnish products of carbinol C-H prenylation and geranylation, respectively (Scheme 11) [66–68]. Mechanistic studies corroborate a catalytic mechanism involving diene-carbonyl oxidative coupling to form an oxaruthenacycle. The transfer of hydrogen from the secondary alcohol reactant mediates transfer hydrogenolysis to release the products of C–C coupling and regenerate the activated ketone to close the catalytic cycle. The regioselectivity of C–C bond formation for the diene C4-position is unique among diene-carbonyl reductive couplings [41, 69]. Beyond α-hydroxy esters [66], these conditions are applicable to 3-hydroxy-2-oxindoles [67] and secondary alcohols substituted by certain heteroaromatic moieties [68]. In the latter case, the putative oxaruthenacycle
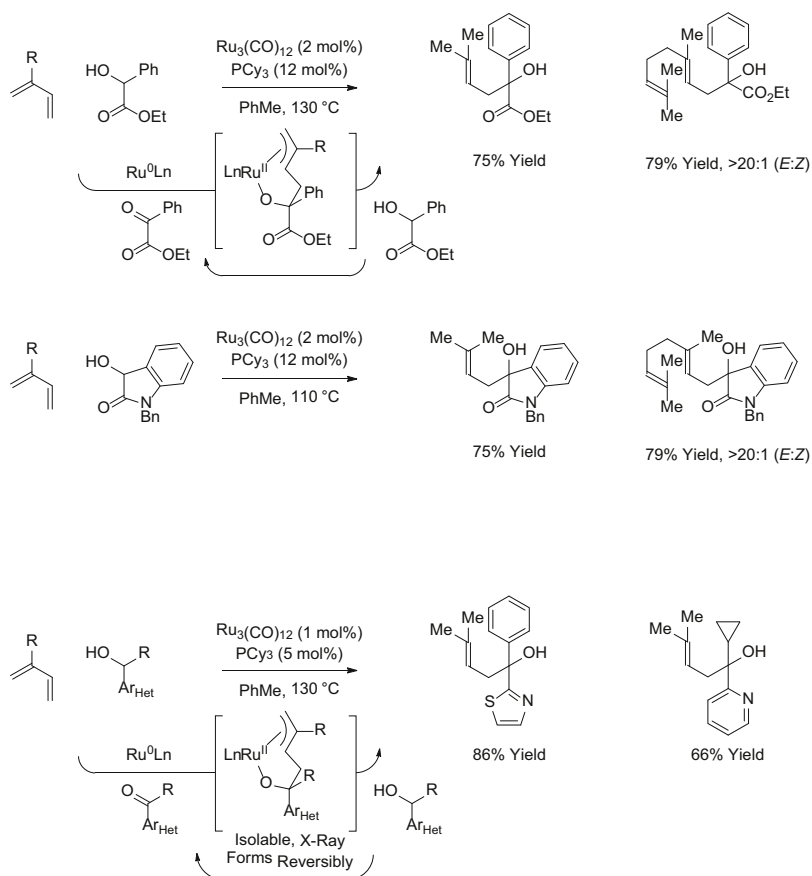

Scheme 11 Conversion of secondary to tertiary alcohols via ruthenium(0)-catalyzed C–C bond forming transfer hydrogenation with conjugated dienes. Yields are of material isolated by flash chromatography on silica gel. PCy₃ = tricyclohexylphosphine

intermediate was isolated, characterized, and reversible metalacycle formation was demonstrated through experiments involving diene exchange.

The transient 1,2-dicarbonyl motifs required for oxidative coupling are also accessible from vicinal diols. For example, in the presence of the ruthenium(0) catalyst derived from $Ru_3(CO)_{12}$ and PCy_3, vicinal diols and alkynes react to form α-hydroxy β,γ-unsaturated ketones as single geometrical isomers (Scheme 12) [70]. Here, it was found that carboxylic acid cocatalysts dramatically increase rate and conversion. A catalytic mechanism that accounts for the effect of the carboxylic acid cocatalysts is as follows. A mononuclear ruthenium(0) complex [71] promotes alkyne-dione oxidative coupling to form the indicated oxaruthenacycle [72, 73]. Direct protonation of the oxaruthenacycle by the diol or ketol is postulated to be slow compared to protonolytic cleavage of the oxaruthenacycle by the carboxylic acid. The resulting ruthenium carboxylate exchanges with the diol or ketol to form a ruthenium alkoxide, which upon β-hydride elimination releases the ketol or dione, respectively, and a vinylruthenium hydride. C–H reductive elimination furnishes the product of C–C coupling and returns ruthenium to its zero-valent form. Conventional diol-alkyne transfer hydrogenation provides the initial quantities of dione required for entry into the catalytic cycle [23, 24, 74].

Intermolecular catalytic reductive couplings of α-olefins with unactivated aldehydes and ketones remains an unmet challenge [75–77]. In a significant step toward this goal, it was found that ruthenium(0) catalysts promote the transfer hydrogenative C–C coupling of 3-hydroxy-2-oxindoles with α-olefins, including feedstocks such as ethylene, propylene and styrene, to furnish the branched adducts as single regio- and diastereomers [78]. In the absence of carboxylic acid cocatalyst, only trace quantities of product were formed (Scheme 13).
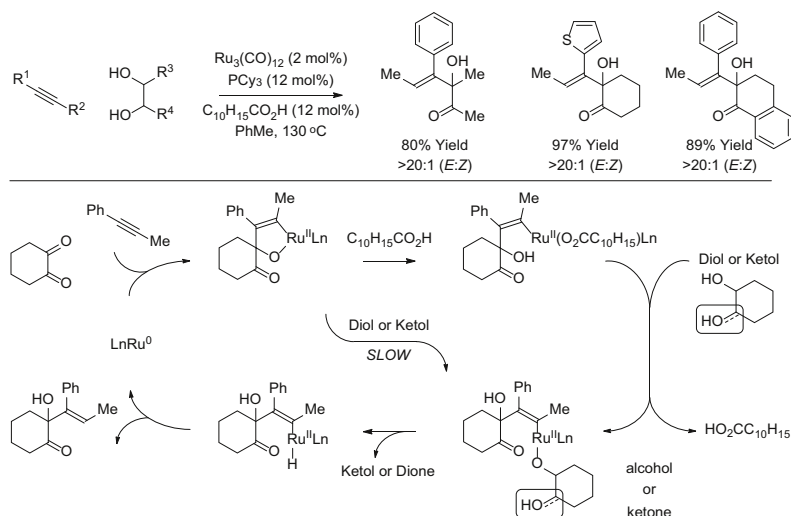
Scheme 12 Ruthenium(0)-catalyzed C–C coupling of diols with alkynes via transfer hydrogenation. Yields are of material isolated by flash chromatography on silica gel. $C_{10}H_{15}CO_2H =$ 1-adamantanecarboxylic acid. $PCy_3 =$ tricyclohexylphosphine
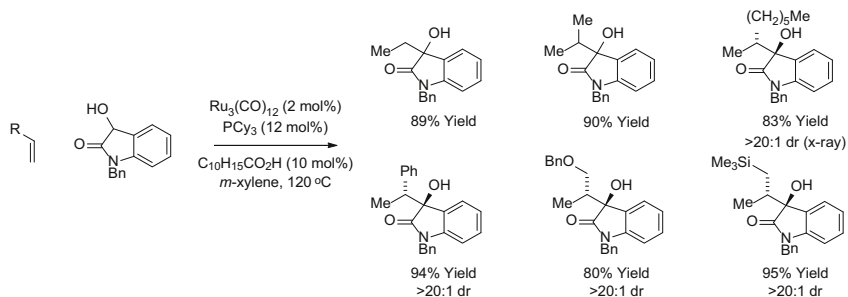
Scheme 13 Ruthenium(0)-catalyzed C–C coupling of diols with α-olefins via transfer hydrogenation. Yields are of material isolated by flash chromatography on silica gel. $C_{10}H_{15}CO_2H =$ 1-adamantanecarboxylic acid. $PCy_3 =$ tricyclohexylphosphine

4 Transfer Hydrogenative Cycloaddition

Intermolecular hydrogen transfer reactions that result in the formation of rings represent a new class of metal-catalyzed cycloadditions [79, 80]. Ruthenium-catalyzed C–C bond forming transfer hydrogenation contributes a new dimension to this emerging area. Using a ruthenium(0) catalyst, diols react with acrylates to form spiro-γ-butyrolactones (Scheme 14) [81]. Ethyl 2-(hydroxymethyl)acrylate reacts with diols by way of transient oxaruthenacycles that engage in E1cB elimination to
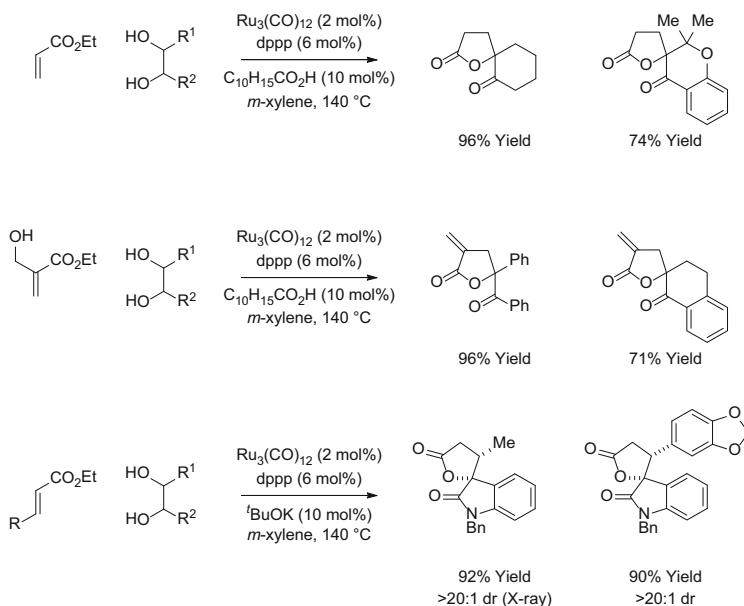
**Scheme 14** Ruthenium(0)-catalyzed C–C coupling of acrylic esters with diols and α-hydroxycarbonyl compounds via transfer hydrogenation. Yields are of material isolated by flash chromatography on silica gel. $C_{10}H_{15}CO_2H =$ 1-adamantanecarboxylic acid. dppp = *bis*-(diphenylphosphino)propane

furnish α-methylene-spiro-γ-butyrolactones [81]. As illustrated in couplings with 3-hydroxy-2-oxindoles, β-substituted acrylic esters provides spiro-γ-butyrolactones as single diastereomers [81]. Remarkably, the cycloadditions may be conducted in oxidative, redox-neutral, or reductive modes using diols, ketols, or diones, respectively, as reactants. To illustrate, ethyl acrylate reacts with hydrobenzoin, benzoin or benzil to form an identical γ-lactone. For the latter reaction involving benzil, 2-propanol (300 mol %) is employed as terminal reductant (Scheme 15).

In the presence of a ruthenium(0) catalyst, vicinal diols transfer hydrogen to conjugated dienes to furnish diones that engage in diene-carbonyl oxidative coupling. The resulting oxaruthenacycles incorporate an allylruthenium moiety that engages the pendant ketone in intramolecular allylruthenation to form products of formal [4+2] cycloaddition as single diastereomers (Scheme 16) [82, 83]. The cycloadducts are readily transformed to the 9–12 membered 1,6-diketones upon exposure to iodosobenzene diacetate [83]. Alternatively, the cycloadducts can be dehydrated to form products of benzannulation [84]. Two-directional benzannulation is especially powerful. For example, exposure of the indicated pyracylene-based tetraol to butadiene in the presence of the ruthenium(0) catalyst delivers the double [4+2] cycloadduct, which is directly dehydrated to form the indeno[1,2,3-cd]-fluoranthene in a single "one-pot" operation.

Exposure of 3,4-benzannulated 1,5-diynes (benzo-endiynes) to α-ketols in the presence of ruthenium(0) catalysts derived from $Ru_3(CO)_{12}$ and RuPhos results in successive redox-triggered C–C coupling to generate products of [4+2] cycloaddition (Scheme 17) [85]. Here, redox-neutral couplings using α-ketols are essential, as diols require a sacrificial hydrogen acceptor, which contributes to partial reduction of the diyne reactant. Regioselective cycloaddition is achieved using nonsymmetric diynes with alkyne termini substituted by *n*-propyl and *t*-butyl groups. This strategy for cycloaddition has been extended to the reaction of *ortho*-acetylenic benzaldehydes with α-ketols [86]. Using ruthenium(0) catalysts modified by CyJohnPhos, the indicated products of [4+2] cycloaddition form as single regio- and diastereomers. This methodology enables convergent construction of ring systems characteristic of type II polyketides, specifically those of the angucycline class [87–89].
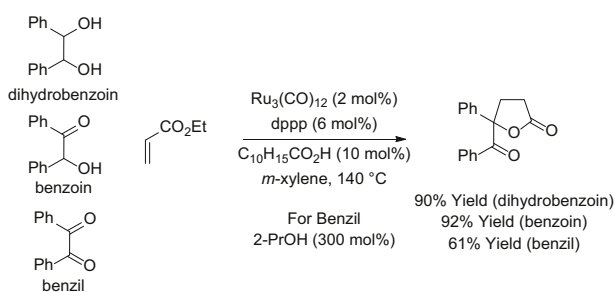
Scheme 15 Redox level-independent cycloaddition to form a γ-lactone. Yields are of material isolated by flash chromatography on silica gel. $C_{10}H_{15}CO_2H$ = 1-adamantanecarboxylic acid. dppp = *bis*-(diphenylphosphino)propane
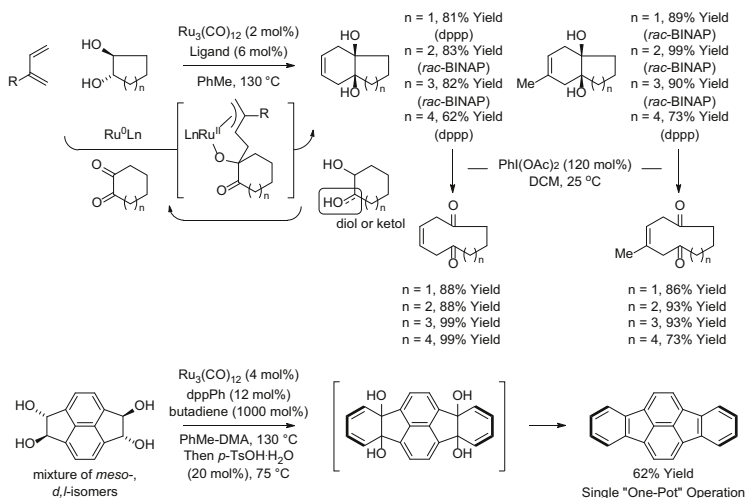
Scheme 16 Transfer hydrogenative diene-diol [4+2] cycloaddition. Yields are of material isolated by flash chromatography on silica gel. dppp = *bis*-(diphenylphosphino)propane. BINAP = 2,2′-*bis*-(diphenylphosphino)-1,1′-binaphthalene. dppPh = *bis*-(1,2-diphenylphosphino)benzene
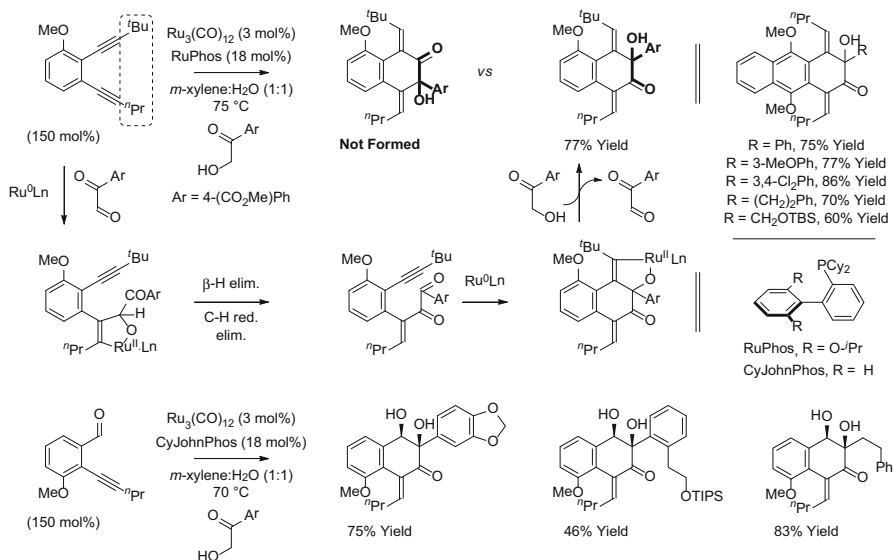
Scheme 17 Transfer hydrogenative cycloaddition of α-ketols with benzannulated 1,5-diynes or *ortho*-acetylenic benzaldehydes. Yields are of material isolated by flash chromatography on silica gel

5 Hydroaminoalkylation

Since the initial discovery of metal-catalyzed hydroaminoalkylation (Maspero [90] and Nugent [91]) in the early 1980s, significant advances in the field of hydroaminoalkylation using early transition metal catalysts have been made. In contrast, the development of corresponding late transition metal-catalyzed amine C-H functionalizations has proven challenging [92–94]. Indeed, with the exception of the present authors work [95–99], all other late-transition metal-catalyzed hydroaminoalkylations require pyridyl-directing groups in combination with *mono*-olefin reactants [100–108]. In a significant departure from prior art, it was found that ruthenium-catalyzed hydrogen transfer from 4-aminobutanol to 1-substituted-1,3-dienes results in the generation of dihydropyrrole-allylruthenium pairs, which combine to form products of hydroaminoalkylation with good to complete control of *anti*-diastereoselectivity (Scheme 18) [95]. As corroborated by deuterium labeling experiments, kinetically preferred hydrometallation of the terminal olefin of the 1-substituted-1,3-diene delivers a 1,1-disubstituted π-allylruthenium complex that isomerizes to the more stable monosubstituted π-allylruthenium complex. Imine addition then occurs with allylic inversion through a closed transition structure. Using a carboxylic acid cocatalyst, pyrrolidine itself can be engaged in direct ruthenium-catalyzed diene hydroaminoalkylations. Finally, 2-propanol-mediated reductive coupling of butadiene with the dihydropyrrole trimer provides the identical product of diene hydroaminoalkylation. All three reaction types proceed through a common set of reactive intermediates, as shown in the indicated stereochemical model (Scheme 18).

Carbonylative hydroaminomethylation (hydroformylation-reductive amination) [109–115] has only been reported for mono-olefin reactants, as hydroformylation of dienes and allenes suffers from poor regioselectivity and "over-hydroformylation"
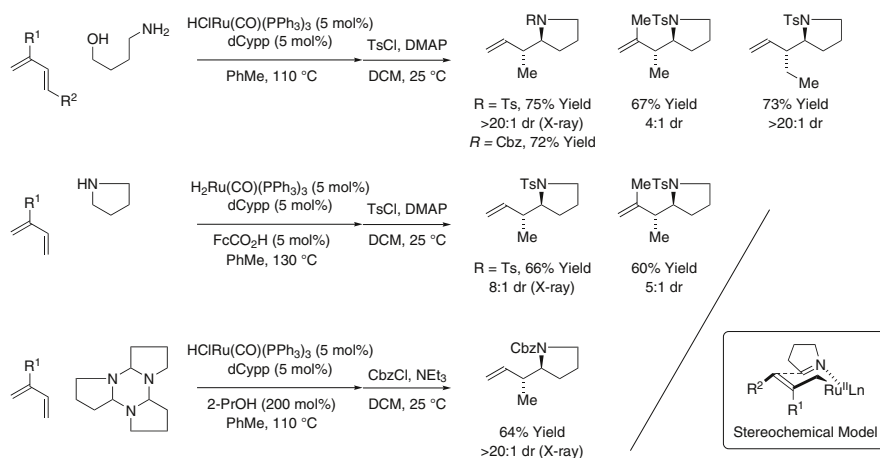
Scheme 18 Transfer hydrogenative imine addition and hydroaminoalkylation. Yields are of material isolated by flash chromatography on silica gel. dCypp = *bis*-(dicyclohexylphosphino)propane. FcCO₂H = ferrocene carboxylic acid
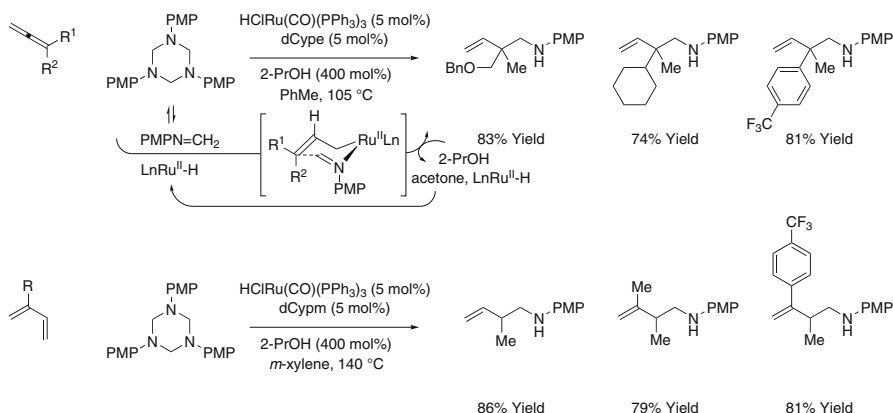
Scheme 19 Regioselective hydroaminomethylation of allenes and dienes via 2-propanol-mediated reductive coupling with formaldimines. Yields are of material isolated by flash chromatography on silica gel. dCypm = *bis*-(dicyclohexylphosphino)methane, dCype = *bis*-(dicyclohexylphosphino)ethane
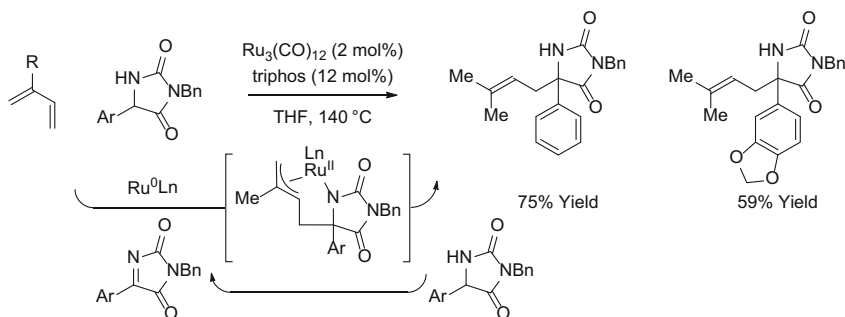
Scheme 20 Regioselective ruthenium(0)-catalyzed hydroaminoalkylation of isoprene with hydantoins. Yields are of material isolated by flash chromatography on silica gel. triphos = *bis*-(diphenylphosphinoethyl)phenylphosphine

to form dialdehyde products. In contrast, 2-propanol-mediated reductive couplings of allenes or dienes with formaldimines (generated in situ from saturated 1,3,5-triazines) are efficient and selective processes (Scheme 19) [96–97]. Specifically, ruthenium-catalyzed transfer hydrogenation of allenes in the presence of 1,3,5-*tris*(4-methoxyphenyl)-hexahydro-1,3,5-triazine provides products of hydroaminomethylation as single regioisomers [96]. Under similar conditions, butadiene and related 2-substituted dienes engage in regioselective reductive C–C coupling to furnish products of hydroaminomethylation [97]. Here, higher temperatures (140 °C) are required to suppress the competing aza-Diels–Alder reaction of formaldimine. Regioselective 2-propanol-mediated reductive coupling of dienes with iminoacetates also have been described (not shown) [98].

Whereas ruthenium(II) catalysts promote hydroaminoalkylation through hydrometalative pathways, ruthenium(0) catalysts derived from Ru$_3$(CO)$_{12}$ and triphos enable catalytic mechanism involving diene-imine oxidative coupling (Scheme 20) [99]. Presently, transformations of this type are restricted to the

hydroaminoalkylation of isoprene with aryl substituted hydantoins. The catalytic mechanism involves hydrogenolytic cleavage of the azaruthenacyclopentane intermediate through hydrogen transfer from the hydantoin reactant, which releases product and regenerates the requisite imine for oxidative coupling.

6 Conclusions and Outlook

Since the seminal work of Sabatier and Grignard, hydrogenation and carbonyl addition have found longstanding use as methods for chemical synthesis. Merging the chemistry of transfer hydrogenation and carbonyl or imine addition, we have developed a broad, new family of reductive and redox-neutral hydrohydroxyalkylations and hydroaminomethylations—processes in which the transfer or redistribution of hydrogen is accompanied by C–C bond formation. We have just begun to exploit the potential of this novel reactivity mode, yet already one may see that carbonyl additions traditionally employing stoichiometric organometallic reagents can now be conducted catalytically via hydrogen transfer. Perhaps most importantly, this new reactivity has enabled transformations that have no counterpart in the current lexicon of synthetic methods.

References

1. James F. Boyce is credited with the hydrogenation of vegetable oils prior to Sabatier's seminal work. To our knowledge, the earliest written record of Boyce's work is a patent filed in 1911: Boyce, J "Process of producing an edible compound." US1061254 A, May 6, 1913
2. Sabatier P, Senderens J-B (1897) Action du Nickel sur l'Éthyléne. Synthéses de l'Éthane. C R Acad Sci Paris 124:1358–1360
3. Kagan HB (2012) Victor Grignard and Paul Sabatier: two showcase laureates of the Nobel Prize for Chemistry. Angew Chem Int Ed 51:7376–7382
4. Voorhees V, Adams R (1922) The use of the oxides of platinum for the catalytic reduction of organic compounds. J Am Chem Soc 44:1397–1405
5. Calvin M, Polyani M (1938) Homogeneous catalytic hydrogenation. Trans Faraday Soc 34:1181–1191
6. Halpern J, Harrod JF, James BR (1961) Homogeneous catalytic hydrogenation of olefinic compounds. J Am Chem Soc 83:753–754
7. Vaska L, DiLuzio JW (1962) Activation of hydrogen by a transition metal complex at normal conditions leading to a stable molecular dihydride. J Am Chem Soc 84:679–680
8. Jardine FH, Osborn JA, Wilkinson G, Young JF (1965) Homogeneous catalytic hydrogenation and hydroformylation of acetylenic compounds. Chem Ind 560–561
9. Young JF, Osborn JA, Jardine FH, Wilkinson G (1965) Hydride intermediates in homogeneous hydrogenation reactions of olefins and acetylenes using rhodium catalysts. Chem Commun 131–132
10. Knowles WS, Sabacky MJ (1968) Catalytic asymmetric hydrogenation employing a soluble, optically active, rhodium complex. Chem Commun 1445–1446
11. Horner L, Winkler H, Rapp A, Mentrup A, Hoffmann H, Beck P (1961) Phosphororganische verbindungen optisch aktive tertiare phosphine aus optisch aktiven quartaren phosphoniumsalzen. Tetrahedron Lett 2:161–166
12. Korpiun O, Mislow K (1967) New route to the preparation and configurational correlation of optically active phosphine oxides. J Am Chem Soc 89:4784–4786

13. Dang TP, Kagan HB (1971) The asymmetric synthesis of hydratropic acid and amino-acids by homogeneous hydrogenation. J Chem Soc D Chem Commun 481–481

14. Miyashita A, Yasuda A, Takaya H, Toriumi K, Ito T, Souchi T, Noyori R (1980) Synthesis of 2,2′-bis(diphenylphosphino)-1,1-binapthyl (BINAP), an atropisomeric chiral bis(triaryl)phosphine, and its use in the rhodium(I)-catalyzed asymmetric hydrogenation of α-(acylamino)acrylic acids. J Am Chem Soc 102:7932–7934

15. Noyori R, Takaya H (1990) BINAP: an efficient chiral element for asymmetric catalysis. Acc Chem Res 23:345–350

16. Shibahara F, Krische MJ (2008) Formation of C–C bonds via ruthenium-catalyzed transfer hydrogenation: carbonyl addition from the alcohol or aldehyde oxidation level. Chem Lett 37:1102–1107

17. Bower JF, Krische MJ (2011) Formation of C–C bonds via iridium-catalyzed hydrogenation and transfer hydrogenation. Top Organomet Chem 34:107–138

18. Hassan A, Krische MJ (2011) Unlocking hydrogenation for C–C bond formation: a brief overview of enantioselective methods. Org Process Res Dev 15:1236–1242

19. Moran J, Krische MJ (2012) Formation of C–C bonds via ruthenium-catalyzed transfer hydrogenation. Pure Appl Chem 84:1729–1739

20. Ketcham JM, Shin I, Montgomery TP, Krische MJ (2014) Catalytic enantioselective C–H functionalization of alcohols by redox-triggered carbonyl addition: borrowing hydrogen, returning carbon. Angew Chem Int Ed 53:9142–9150

21. Sasson Y, Blum J (1971) Homogenous catalytic transfer-hydrogenation of α, β-unsaturated carbonyl compounds by dichlorotris(triphenylphosphine)ruthenium(II). Tetrahedron Lett 12:2167–2170

22. Dobson A, Robinson SD (1977) Complexes of the platinum metals. 7. homogeneous ruthenium and osmium catalysts for the dehydrogenation of primary and secondary alcohols. Inorg Chem 16:137–142

23. Blum Y, Reshef D, Shvo Y (1981) H-Transfer catalysis with $Ru_3(CO)_{12}$. Tetrahedron Lett 22:1541–1544

24. Shvo Y, Blum Y, Reshef D, Menzin M (1982) Catalytic oxidative coupling of diols by $Ru_3(CO)_{12}$. J Organomet Chem 226:C21–C24

25. Noyori R, Ohta M, Hsiao Y, Kitamura M, Ohta T, Takaya H (1986) Asymmetric synthesis of isoquinoline alkaloids by homogeneous catalysis. J Am Chem Soc 108:7117–7119

26. Hashiguchi S, Fujii A, Takehara J, Ikariya T, Noyori R (1995) Asymmetric transfer hydrogenation of aromatic ketones catalyzed by chiral ruthenium(II) complexes. J Am Chem Soc 117:7562–7563

27. Jang H-Y, Huddleston RR, Krische MJ (2002) Reductive generation of enolates from enones using elemental hydrogen: catalytic C–C bond formation under hydrogenative conditions. J Am Chem Soc 124:15156–15157

28. Iida H, Krische MJ (2007) Catalytic reductive coupling of alkenes and alkynes to carbonyl compounds and imines mediated by hydrogen. Top Curr Chem 279:77–104

29. Skucas E, Ngai M-Y, Komanduri V, Krische MJ (2007) Enantiomerically enriched allylic alcohols and allylic amines via C–C bond forming hydrogenation: asymmetric carbonyl and imine vinylation. Acc Chem Res 40:1394–1401

30. Bower JF, Skucas E, Patman RL, Krische MJ (2007) Catalytic C–C coupling via transfer hydrogenation: reverse prenylation, crotylation and allylation from the alcohol or aldehyde oxidation level. J Am Chem Soc 129:15134–15135

31. Shibahara F, Bower JF, Krische MJ (2008) Ruthenium-catalyzed C–C bond forming transfer hydrogenation: carbonyl allylation from the alcohol or aldehyde oxidation level employing acyclic 1,3-dienes as surrogates to preformed allyl metal reagents. J Am Chem Soc 130:6338–6339

32. Shibahara F, Bower JF, Krische MJ (2008) Diene hydroacylation from the alcohol or aldehyde oxidation level via ruthenium-catalyzed C–C bond-forming transfer hydrogenation: synthesis of β, γ-unsaturated ketones. J Am Chem Soc 130:14120–14122

33. Zbieg JR, Moran J, Krische MJ (2011) Diastereo- and enantioselective ruthenium-catalyzed hydrohydroxyalkylation of 2-Silyl-butadienes: carbonyl syn-crotylation from the alcohol oxidation level. J Am Chem Soc 133:10582–10586

34. Sato F, Kusakabe M, Kobayashi Y (1984) Highly diastereofacial selective addition of nucleophiles to 2-alkyl-3-trimethylsilylalk-3-enyl carbonyl compounds. Stereoselective preparation of β-methyl-homoallyl alcohols and β-hydroxy-α-methyl ketones. J Chem Soc Chem Commun 1130–1132

35. Helm MD, Mayer P, Knochel P (2008) Preparation of silyl substituted crotylzinc reagents and their highly diastereoselective addition to carbonyl compounds. Chem Commun 1916–1917
36. Grayson MN, Krische MJ, Houk KN (2015) Ruthenium-catalyzed asymmetric hydrohydroxyalkylation of butadiene: the role of the formyl hydrogen bond in stereochemical control. J Am Chem Soc 137:8838–8850
37. Zbieg JR, Yamaguchi E, McInturff EL, Krische MJ (2012) Enantioselective C–H crotylation of primary alcohols via hydrohydroxyalkylation of butadiene. Science 336:324–327
38. McInturff EL, Yamaguchi E, Krische MJ (2012) Chiral anion dependent inversion of diastereo- and enantioselectivity in carbonyl crotylation via ruthenium-catalyzed butadiene hydrohydroxyalkylation. J Am Chem Soc 134:20628–20631
39. Smejkal T, Han H, Breit B, Krische MJ (2009) All carbon quaternary centers via ruthenium-catalyzed hydroxymethylation of 2-substituted butadienes mediated by formaldehyde: beyond hydroformylation. J Am Chem Soc 131:10366–10367
40. Köpfer A, Sam B, Breit B, Krische MJ (2013) Regiodivergent reductive coupling of 2-substituted dienes to formaldehyde employing ruthenium or nickel catalysts: hydrohydroxymethylation via transfer hydrogenation. Chem Sci 4:1876–1880
41. Sam B, Breit B, Krische MJ (2015) Paraformaldehyde and methanol as C1-feedstocks in metal-catalyzed C–C couplings of π-unsaturated reactants: beyond hydroformylation. Angew Chem Int Ed 54:3267–3274
42. Han H, Krische MJ (2010) Direct ruthenium-catalyzed C–C coupling of ethanol: diene hydro-hydroxyethylation to form all carbon quaternary centers. Org Lett 12:2844–2846
43. Ngai M-Y, Skucas E, Krische MJ (2008) Ruthenium-catalyzed C–C bond formation via transfer hydrogenation: branch-selective reductive coupling of allenes to paraformaldehyde and higher aldehydes. Org Lett 10:2705–2708
44. Skucas E, Zbieg JR, Krische MJ (2009) anti-aminoallylation of aldehydes via ruthenium-catalyzed transfer hydrogenative coupling of sulfonamido-allenes: 1,2-aminoalcohols. J Am Chem Soc 131:5054–5055
45. Zbieg JR, McInturff EL, Krische MJ (2010) Allenamide hydro-hydroxyalkylation: 1,2-aminoalcohols via ruthenium-catalyzed carbonyl anti-aminoallylation. Org Lett 12:2514–2516
46. Zbieg JR, McInturff EL, Leung JC, Krische MJ (2011) Amplification of anti-diastereoselectivity via Curtin–Hammett effects in ruthenium-catalyzed hydrohydroxyalkylation of 1,1-disubstituted allenes: diastereoselective formation of all-carbon quaternary centers. J Am Chem Soc 133:1141–1144
47. Sam B, Luong T, Krische MJ (2015) Ruthenium-catalyzed C–C coupling of fluorinated alcohols with allenes: dehydrogenation at the energetic limit of β-hydride elimination. Angew Chem Int Ed 54:5465–5469
48. Park BY, Nguyen KD, Chaulagain MR, Komanduri V, Krische MJ (2014) Alkynes as allylmetal equivalents in redox-triggered C–C couplings to primary alcohols: (Z)-homoallylic alcohols via ruthenium-catalyzed propargyl C–H oxidative addition. J Am Chem Soc 136:11902–11905
49. Liang T, Nguyen KD, Zhang W, Krische MJ (2015) Enantioselective ruthenium-catalyzed carbonyl allylation via alkyne-alcohol C–C bond forming transfer hydrogenation: allene hydrometallation vs. oxidative coupling. J Am Chem Soc 137:3161–3164
50. Ramachandran PV (2002) Pinane-based versatile allyl boranes. Aldrichimica Acta 35:23–35
51. Kennedy JWJ, Hall DG (2003) Recent advances in the activation of boron and silicon reagents for stereocontrolled allylation reactions. Angew Chem Int Ed 42:4732–4739
52. Denmark SE, Fu J (2003) Catalytic enantioselective addition of allylic organometallic reagents to aldehydes and ketones. Chem Rev 103:2763–2794
53. Yu C-M, Youn J, Jung H-K (2006) Regulation of stereoselectivity and reactivity in the inter- and intramolecular allylic transfer reactions. Bull Korean Chem Soc 27:463–472
54. Marek I, Sklute G (2007) Creation of quaternary stereocenters in carbonyl allylation reactions. Chem Commun 1683–1691
55. Hall DG (2007) Lewis and Brønsted acid-catalyzed allylboration of carbonyl compounds: from discovery to mechanism and applications. Synlett 1644–1655
56. Lachance H, Hall DG (2008) Allylboration of carbonyl compounds. Org React 73:1–573
57. Yus M, González-Gómez JC, Foubelo F (2011) Catalytic enantioselective allylation of carbonyl compounds and imines. Chem Rev 111:7774–7854

58. Liang T, Zhang W, Chen T-Y, Nguyen KD, Krische MJ (2015) Ruthenium-catalyzed diastereo- and enantioselective coupling of propargyl ethers with alcohols: siloxy-crotylation via hydride shift enabled conversion of alkynes to π-allyls. J Am Chem Soc 137:13066–13071

59. Patman RL, Chaulagain MR, Williams VM, Krische MJ (2009) Direct vinylation of alcohols or aldehydes employing alkynes as vinyl donors: a ruthenium-catalyzed C–C bond forming transfer hydrogenation. J Am Chem Soc 131:2066–2067

60. Williams VM, Leung JC, Patman RL, Krische MJ (2009) Hydroacylation of 2-butyne from the alcohol or aldehyde oxidation level via ruthenium-catalyzed C–C bond forming transfer hydrogenation. Tetrahedron 65:5024–5029

61. Patman RL, Williams VM, Bower JF, Krische MJ (2008) Carbonyl propargylation from the alcohol or aldehyde oxidation level employing 1,3-enynes as surrogates to preformed allenylmetal reagents: a ruthenium-catalyzed C–C bond forming transfer hydrogenation. Angew Chem Int Ed 47:5220–5223

62. Geary LM, Leung JC, Krische MJ (2012) Ruthenium-catalyzed reductive coupling of 1,3-enynes and aldehydes via transfer hydrogenation: *anti*-diastereoselective carbonyl propargylation. Chem Eur J 18:16823–16827

63. Nguyen KD, Herkommer D, Krische MJ (2016) Ruthenium-BINAP-catalyzed alcohol C-H *tert*-prenylation via 1,3-enyne transfer hydrogenation: beyond stoichiometric carbanions in enantioselective carbonyl propargylation. J Am Chem Soc 138:5238–5241

64. Ding C-H, Lou X-L (2011) Catalytic asymmetric propargylation. Chem Rev 111:1914–1937

65. Wisniewska HM, Jarvo ER (2013) Enantioselective propargylation and allenylation reactions of ketones and imines. J Org Chem 78:11629–11636

66. Leung JC, Geary LM, Chen T-Y, Zbieg JR, Krische MJ (2012) Direct, redox neutral prenylation and geranylation of secondary carbinol C–H bonds: C4 regioselectivity in ruthenium-catalyzed C–C couplings of dienes to α-hydroxy esters. J Am Chem Soc 134:15700–15703

67. Chen T-Y, Krische MJ (2013) Regioselective ruthenium-catalyzed hydrohydroxyalkylation of dienes with 3-hydroxy-2-oxindoles: prenylation, geranylation and beyond. Org Lett 15:2994–2997

68. Park BY, Montgomery TP, Garza VJ, Krische MJ (2013) Ruthenium-catalyzed hydrohydroxyalkylation of isoprene with heteroaromatic secondary alcohols: isolation and reversible formation of the putative metallacycle intermediate. J Am Chem Soc 135:16320–16323

69. Kimura M, Tamaru Y (2007) Nickel-catalyzed reductive coupling of dienes and carbonyl compounds. Top Curr Chem 279:173–207

70. McInturff EL, Nguyen KD, Krische MJ (2014) Redox-triggered C–C coupling of diols and alkynes: synthesis of β, γ-unsaturated α-hydroxyketones and furans by ruthenium-catalyzed hydrohydroxyalkylation. Angew Chem Int Ed 53:3232–3235

71. Ru₃(CO)₁₂ reacts with dppe in benzene solvent to provide Ru(CO)₃(dppe): Sanchez-Delgado RA, Bradley JS, Wilkinson G (1976) Further studies on the homogeneous hydroformylation of alkenes by use of ruthenium complex catalysts. J Chem Soc Dalton Trans 399–404

72. Chatani N, Tobisu M, Asaumi T, Fukumoto Y, Murai S (1999) Ruthenium carbonyl-catalyzed [2+2+1]-cycloaddition of ketones, olefins, and carbon monoxide, leading to functionalized γ-butyrolactones. J Am Chem Soc 121:7160–7161

73. Tobisu M, Chatani N, Asaumi T, Amako K, Ie Y, Fukumoto Y, Murai S (2000) Ru₃(CO)₁₂-catalyzed intermolecular cyclocoupling of ketones, alkenes or alkynes, and carbon monoxide. [2+2+1] cycloaddition strategy for the synthesis of functionalized γ-butyrolactones. J Am Chem Soc 122:12663–12674

74. Meijer RH, Ligthart GBWL, Meuldijk J, Vekemans JAJM, Hulshof LA, Mills AM, Kooijman H, Spek AL (2004) Triruthenium dodecacarbonyl/triphenylphosphine-catalyzed dehydrogenation of primary and secondary alcohols. Tetrahedron 60:1065–1072

75. Crowe WE, Rachita MJ (1995) Titanium-catalyzed reductive cyclization of δ, ε-unsaturated ketones and aldehydes. J Am Chem Soc 117:6787–6788

76. Kablaoui NM, Buchwald SL (1996) Development of a method for the reductive cyclization of enones by a titanium catalyst. J Am Chem Soc 118:3182–3191

77. Kablaoui NM, Buchwald SL (1995) Reductive cyclization of enones by a titanium catalyst. J Am Chem Soc 117:6785–6786

78. Yamaguchi E, Mowat J, Luong T, Krische MJ (2013) Regio- and diastereoselective C–C coupling of α-olefins and styrenes to 3-hydroxy-2-oxindoles by Ru-catalyzed hydrohydroxyalkylation. Angew Chem Int Ed 52:8428–8431

79. Lautens M, Klute W, Tam W (1996) Transition metal-mediated cycloaddition reactions. Chem Rev 96:49–92

80. Nandakumar A, Midya SP, Landge VG, Balaraman E (2015) Transition-metal-catalyzed hydrogen-transfer annulations: access to heterocyclic scaffolds. Angew Chem Int Ed 54:11022–11034

81. McInturff EL, Mowat J, Waldeck AR, Krische MJ (2013) Ruthenium-catalyzed hydrohydrox-yalkylation of acrylates with diols and α-hydroxycarbonyl compounds to form spiro- and α-methylene-γ-butyrolactones. J Am Chem Soc 135:17230–17235

82. Geary LM, Glasspoole BW, Kim MM, Krische MJ (2013) Successive C–C coupling of dienes to vicinally dioxygenated hydrocarbons: ruthenium-catalyzed [4+2] cycloaddition across the diol, Hydroxycarbonyl or dione oxidation levels. J Am Chem Soc 135:3796–3799

83. Kasun ZA, Geary LM, Krische MJ (2014) Ring expansion of cyclic 1,2-diols to form medium sized rings via ruthenium-catalyzed transfer hydrogenative [4+2] cycloaddition. Chem Commun 50:7545–7547

84. Geary LM, Chen TY, Montgomery TP, Krische MJ (2014) Benzannulation via ruthenium-catalyzed diol-diene [4+2] cycloaddition: one- and two-directional syntheses of fluoranthenes and acenes. J Am Chem Soc 136:5920–5922

85. Saxena A, Perez F, Krische MJ (2015) Ruthenium(0)-catalyzed endiyne-α-ketol [4+2] cycload-dition: convergent assembly of type II polyketide substructures. J Am Chem Soc 137:5883–5886

86. Saxena A, Perez F, Krische MJ (2016) Ruthenium(0)-catalyzed [4+2] cycloaddition of acetylenic aldehydes with α-ketols: convergent construction of angucycline ring systems. Angew Chem Int Ed 55:1493–1497

87. Krohn K, Rohr J (1997) Angucyclines: total syntheses, new structures, and biosynthetic studies of an emerging new class of antibiotics. Top Curr Chem 188:127–195

88. Carreño MC, Urbano A (2005) Recent advances in the synthesis of angucyclines. Synlett 36(1):1–25

89. Kharel MK, Pahari P, Shepherd MD, Tibrewal N, Nybo SE, Shaaban KA, Rohr J (2012) Angucyclines: biosynthesis, mode-of-action, new natural products, and synthesis. Nat Prod Rep 29:264–325

90. Clerici MG, Maspero F (1980) Catalytic C-alkylation of secondary amines with alkenes. Synthesis 305–306

91. Nugent WA, Ovenall DW, Holmes SJ (1983) Catalytic C–H activation in early transition-metal dialkylamides and alkoxides. Organometallics 2:161–162

92. Campos KR (2007) Direct sp^3 C–H bond activation adjacent to nitrogen in heterocycles. Chem Soc Rev 36:1069–1084

93. Roesky PW (2009) Catalytic hydroaminoalkylation. Angew Chem Int Ed 48:4892–4894

94. Chong E, Garcia P, Schafer LL (2014) Hydroaminoalkylation: early-transition-metal-catalyzed α-alkylation of amines. Synthesis 46:2884–2896

95. Chen T-Y, Tsutsumi R, Montgomery TP, Volchkov I, Krische MJ (2015) Ruthenium-catalyzed C–C coupling of amino alcohols with dienes via transfer hydrogenation: redox-triggered imine addition and related hydroaminoalkylations. J Am Chem Soc 137:1798–1801

96. Oda S, Sam B, Krische MJ (2015) Hydroaminomethylation beyond carbonylation: allene-imine reductive coupling by ruthenium-catalyzed transfer hydrogenation. Angew Chem Int Ed 54:8525–8528

97. Oda S, Franke J, Krische MJ (2016) Diene hydroaminomethylation via ruthenium-catalyzed C–C bond forming transfer hydrogenation: beyond carbonylation. Chem Sci 7:136–141

98. Zhu S, Lu X, Luo Y, Zhang W, Jiang H, Yan M, Zeng W (2013) Ruthenium(II)-catalyzed regioselective reductive coupling of α-imino esters with dienes. Org Lett 15:1440–1443

99. Schmitt DC, Lee J, Dechert-Schmitt A-MR, Yamaguchi E, Krische MJ (2013) Ruthenium-catalyzed hydroaminoalkylation of isoprene via transfer hydrogenation: byproduct-free prenylation of hydantoins. Chem Commun 49:6096–6098

100. Jun C-H (1998) Chelation-assisted alkylation of benzylamine derivatives by Ru^0 catalyst. Chem Commun 1405–1406

101. Chatani N, Asaumi T, Yorimitsu S, Ikeda T, Kakiuchi F, Murai S (2001) $Ru_3(CO)_{12}$-catalyzed coupling reaction of sp^3 C–H bonds adjacent to a nitrogen atom in alkylamines with alkenes. J Am Chem Soc 123:10935–10941

102. Bergman SD, Storr TE, Prokopcová H, Aelvoet K, Diels G, Meerpoel L, Maes BUW (2012) The role of the alcohol and carboxylic acid in directed ruthenium-catalyzed $C(sp^3)$-H α-alkylation of cyclic amines. Chem Eur J 18:10393–10398

103. Schinkel M, Wang L, Bielefeld K, Ackermann L (2014) Ruthenium(II)-catalyzed C(sp^3)-H α-alkylation of pyrrolidines. Org Lett 16:1876–1879

104. Kulago AA, Van Steijvoort BF, Mitchell EA, Meerpoel L, Maes BUW (2014) Directed ruthenium-catalyzed C(sp^3)-H α-alkylation of cyclic amines using dioxolane-protected alkenones. Adv Synth Catal 356:1610–1618

105. Tsuchikama K, Kasagawa M, Endo K, Shibata T (2009) Cationic Ir(I)-catalyzed sp^3 C–H bond alkenylation of amides with alkynes. Org Lett 11:1821–1823

106. Pan S, Endo K, Shibata T (2011) Ir(I)-catalyzed enantioselective secondary sp^3 C–H bond activation of 2-(Alkylamino)pyridines with alkenes. Org Lett 13:4692–4695

107. Pan S, Matsuo Y, Endo K, Shibata T (2012) Cationic iridium-catalyzed enantioselective activation of secondary sp^3 C–H bond adjacent to nitrogen atom. Tetrahedron 68:9009–9015

108. Lahm G, Opatz T (2014) Unique regioselectivity in the C(sp^3)-H α-alkylation of amines: the benzoxazole moiety as a removable directing group. Org Lett 16:4201–4203

109. Eilbracht P, Bärfacker L, Buss C, Hollmann C, Kitsos-Rzychon BE, Kranemann CL, Rische T, Roggenbuck R, Schmidt A (1999) Tandem reaction sequences under hydroformylation conditions: new synthetic applications of transition metal catalysis. Chem Rev 99:3329–3366

110. Breit B, Seiche W (2001) Recent advances on chemo-, regio- and stereoselective hydroformylation. Synthesis 1–36

111. Eilbracht P, Schmidt AM (2006) Synthetic applications of tandem reaction sequences involving hydroformylation. Top Organomet Chem 18:65–95

112. Crozet D, Urrutigoïty M, Kalck P (2011) Recent advances in amine synthesis by catalytic hydroaminomethylation of alkenes. Chem Cat Chem 3:1102–1118

113. Behr A, Vorholt AJ (2012) Hydroformylation and related reactions of renewable resources. Top Organomet Chem 39:103–128

114. Raoufmoghaddam S (2014) Recent advances in catalytic C–N bond formation: a comparison of cascade hydroaminomethylation and reductive amination reactions with the corresponding hydroamidomethylation and reductive amidation reactions. Org Biomol Chem 12:7179–7193

115. Wu X-F, Fang X, Wu L, Jackstell R, Neumann H, Beller M (2014) Transition-metal-catalyzed carbonylation reactions of olefins and alkynes: a personal account. Acc Chem Res 47:1041–1053